

A CONSTITUTIVE MODEL FOR CREEP  
OF  
A FROZEN SAND

By

© Mohammed G. Rahman

A Thesis  
Submitted to the Faculty of Graduate Studies  
in Partial Fulfillment of the Requirements for the Degree of  
Doctor of Philosophy

Department of Civil Engineering  
The University of Manitoba  
Winnipeg, Manitoba  
June, 1988

Permission has been granted to the National Library of Canada to microfilm this thesis and to lend or sell copies of the film.

The author (copyright owner) has reserved other publication rights, and neither the thesis nor extensive extracts from it may be printed or otherwise reproduced without his/her written permission.

L'autorisation a été accordée à la Bibliothèque nationale du Canada de microfilmer cette thèse et de prêter ou de vendre des exemplaires du film.

L'auteur (titulaire du droit d'auteur) se réserve les autres droits de publication; ni la thèse ni de longs extraits de celle-ci ne doivent être imprimés ou autrement reproduits sans son autorisation écrite.

ISBN 0-315-48052-1

A CONSTITUTIVE MODEL FOR CREEP OF A FROZEN SAND

BY

MOHAMMED G. RAHMAN

A thesis submitted to the Faculty of Graduate Studies of  
the University of Manitoba in partial fulfillment of the requirements  
of the degree of

DOCTOR OF PHILOSOPHY

© 1988

Permission has been granted to the LIBRARY OF THE UNIVERSITY OF MANITOBA to lend or sell copies of this thesis, to the NATIONAL LIBRARY OF CANADA to microfilm this thesis and to lend or sell copies of the film, and UNIVERSITY MICROFILMS to publish an abstract of this thesis.

The author reserves other publication rights, and neither the thesis nor extensive extracts from it may be printed or otherwise reproduced without the author's written permission.

to my family

## ABSTRACT

The stress-strain characteristics of frozen sands is nonlinear and time dependent. This thesis develops a constitutive creep model based on time and stress dependent deformation parameters. The general stress state is separated into mean normal and deviatoric components. The associated deformations are volumetric and shear strains. The bulk creep function relates the mean normal stress and the volumetric strain, and the shear creep function relates the deviatoric stress and the shear strain.

Triaxial compression creep tests were carried out on a quartz-carbonate sand at a temperature of  $-30^{\circ}\text{C}$  to develop the creep functions. Isotropic compression creep tests were performed to model the bulk creep function as a function of time and mean normal stress. Constant mean normal stress triaxial compression tests were performed to model the shear creep function as a function of time, mean normal stress and deviatoric stress. The two creep functions were then coupled to provide a constitutive creep model applicable to a general stress state.

An assesment of the models developed was made by carrying out a multi-stage constant cell pressure triaxial tests and comparing the values of the axial deformation calculated using the aforementioned constitutive model, with the measured values. The theoretical attenuated axial deformation agreed well with the observed values. The

correlation coefficient was found to be 0.85. The agreement between the predicted and experimental axial strain versus time curves was quite good considering the scatter that was inherent in all test data and the basic assumption made in reconstructing the strain time curves.

A series of short-term constant mean normal stress triaxial compression creep tests were performed to determine whether the onset of dilation was a stress or strain phenomenon. The results from the tests suggested that the onset of dilation was neither singly a strain nor a stress phenomenon but was influenced by both.

A new failure criterion based on the onset of dilation during the creep process was suggested.

The interaction of rigid particles and ice was studied by observing the penetration of rigid steel spheres into ice. The penetration rate was found to be constant under a constant hemispherical stress and was independent of the size of the spheres. A relationship between penetration rate and hemispherical stress was determined.

## ACKNOWLEDGEMENTS

This research was carried out under the direct supervision of Dr. L. Domaschuk, Department of Civil Engineering, University of Manitoba. His encouragement, constant interest and helpful criticisms during the investigation and preparation of this thesis are gratefully acknowledged. The author sincerely appreciates the academic freedom which he offered during the investigation.

The author also wishes to thank Dr. D. H. Shields, Dr. E. Z. Lajtai and Dr. A. Shah who as members of the authors advisory committee provided useful ideas. As an external examiner, Dr. V. R. Parameswaran of Northwestern University, Evanston, Illinois, provided useful comments and suggestions which are greatly appreciated.

The author wishes to thank Mr. E. Lemke, Mr. N. Piamsalee, Mr. J. Clark, Mr. S. Meyerhoff, Mr. D. Fedorowich and Mr. B. Turnbull for their assistance during the investigation.

Financial support provided by the National Science and Engineering Research Council and the Civil Engineering department is gratefully acknowledged.

Finally, last but not least, the author wishes to thank his wife Nigar and sons Asef and Atef for their continued support, patience and understanding throughout this long period.

## TABLE OF CONTENTS

TITLE	i
ABSTRACT	ii
ACKNOWLEDGEMENTS	iv
TABLE OF CONTENTS	v
LIST OF FIGURES	ix
LIST OF TABLES	xvi
LIST OF SYMBOLS	xvii
<b>CHAPTER 1 INTRODUCTION</b>	<b>1</b>
1.1 GENERAL	1
1.2 IDENTIFICATION OF THE PROBLEM	3
1.3 OBJECTIVES	4
1.4 SCOPE OF INVESTIVATION	5
<b>CHAPTER 2 REVIEW OF MECHANICS OF ICE AND FROZEN SOIL</b>	<b>8</b>
2.1 MECHANICS OF ICE	9
2.1.1 Structure of Ice in Frozen Soil	9
2.1.2 Deformational Mechanisms of Ice	12
2.1.2.1 Strength of Ice	16
2.1.2.2 Deformation of Ice	21
2.1.3 Quantitative Models of Strength and Deformation of Ice	28
2.2 MECHANICS OF FROZEN SOIL	31
2.2.1 Structure of Frozen Soil	31
2.2.2 Deformational Mechanisms of Frozen Soil	39
2.2.3 Strength of Frozen Soil	41
2.2.3.1 Effect of Mineral Particle Concentration	41
2.2.3.2 Effect of Confining Pressure	41
2.2.3.3 Effect of Temperature	45
2.2.3.4 Effect of Strain Rate	45
2.2.4 Deformation of Frozen Soil	46
2.2.4.1 Effect of Stress Level	50
2.2.4.2 Effect of Temperature	52



2.2.4.3	Effect of Confining Stress	56
2.2.5	Quantitative Models of Strength and Deformation of Frozen Soil	56
2.3	STRESS-STRAIN RELATIONSHIP	71
2.3.1	Deformation Parameters	71
2.3.1.1	E and $\epsilon$ from Triaxial Tests	72
2.3.1.2	Direct Determination of K and G	73
2.3.2	Mean Normal and Deviatoric Components of Stresses and strains	74
CHAPTER 3	LABORATORY INVESTIGATION	80
3.1	SCOPE OF INVESTIGATION	81
3.2	SAMPLE PREPARATION	82
3.2.1	Frozen Sand Sample	82
3.2.1.1	Sand Deposition	83
3.2.1.2	Saturation	83
3.2.1.3	Freezing	84
3.3	TESTING EQUIPMENTS	85
3.3.1	Triaxial Cell	85
3.4	SAMPLE TRIMMING AND SETTING-IN PROCEDURE	87
CHAPTER 4	BULK CREEP FUNCTION	94
4.1	INTRODUCTION	95
4.2	TEST PROCEDURE	96
4.3	TEST RESULTS AND DISCUSSIONS	97
4.3.1	Volumetric Stress-strain Relationship	97
4.3.2	Influence of Time and Mean Normal Stress on Volumetric Strain Rate	99
4.3.3	Solution for Bulk Creep Function	100
CHAPTER 5	SHEAR CREEP FUNCTION	114
5.1	INTRODUCTION	115
5.2	TEST PROCEDURE	116
5.2.1	Constant Mean Normal stress Multi-stage Triaxial Tests	116
5.3	TEST RESULTS	118
5.3.1	MST1	118
5.3.2	MST2	120

5.3.3	MST3	120
5.3.4	MST4	121
5.3.5	MST5	122
5.4	CREEP RATES	123
5.4.1	Introduction	123
5.4.2	Axial Creep Rates	124
5.4.3	Time to Attenuation	125
5.5	FAILURE CRITERION	126
5.5.1	Failure Stress	126
5.5.2	Failure Strain	127
5.6	SHEAR CREEP FUNCTION	129
5.6.1	Resultant Deviatoric Stress-Strain Curve	129
5.6.2	Shear Creep Function	130
CHAPTER 6	VERIFICATION OF MODEL	197
6.1	INTRODUCTION	198
6.2	CONSTANT CELL PRESSURE TRIAXIAL CREEP TEST	198
6.2.1	Test Procedure	198
6.2.2	Test Results	200
6.3	VERIFICATION OF THE MODEL	201
CHAPTER 7	DILATION AND FAILURE	223
7.1	INTRODUCTION	224
7.2	TEST PROCEDURE	225
7.2.1	Constant Mean Normal Stress Multi-stage Short Term Triaxial Creep Test	225
7.3	TEST RESULTS	225
7.3.1	MST6	225
7.3.2	MST7	226
7.3.3	MST8	226
7.3.4	MST9	227
7.4	DISCUSSION OF TEST RESULTS	227
7.4.1	Failure Mechanisms	228
CHAPTER 8	INTERACTION OF RIGID PARTICLES AND ICE	242
8.1	INTRODUCTION	243

8.2	TEST PROGRAM	243
8.2.1	Ice Sample Preparation	244
8.2.2	Loading Procedure	244
8.3	TEST RESULTS	245
8.3.1	Constant Sphere Diameter Tests	245
8.3.2	Constant Hemispherical Stress Tests	247
8.3.3	Viscosity	248
CHAPTER 9	CONCLUSIONS AND RECOMMENDATIONS	258
9.1	CONCLUSIONS	259
9.1.1	Creep Behaviour under Isotropic Stress	259
9.1.2	Creep Behaviour under Deviatoric Stress	261
9.1.3	Verification of the Creep Models	262
9.1.4	Comparison of Long and Short-term Tests	263
9.1.5	Interaction of ice and Rigid Particles	263
9.2	RECOMMENDATIONS	265
REFERENCES		266
APPENDIX		275

## LIST OF FIGURES

FIGURE		PAGE
2.1	Phase diagram for Ice (after Whalley et al. 1968)	10
2.2	Deformation-mechanism map for polycrystalline ice of 1 mm grain size (after Shoji and Higashi, 1978)	15
2.3	Effect of strain rate on the uniaxial compressive strength of frozen soils	17
2.4	Typical stress-strain curves for granular ice at $-9.5^{\circ}\text{C}$ (after Gold and Krausz, 1971)	18
2.5	Effect of sand concentration on the strength of a sand-ice system (after Goughnour and Andersland, 1968)	20
2.6	Typical creep curves for ice	22
2.7	Logarithm of strain-rate as a function of temperature for polycrystalline ice (after Barnes et al., 1971)	26
2.8	Strain rate versus grain size ratio of polycrystalline ice of various authors (after Sego, 1980)	27
2.9	Normalized secondary creep rate as a function of volume fraction of sand (after Hooke et al., 1972)	29
2.10	Components of the Andrade equation	32
2.11	Two dimensional schematic of the proposed structure of the frozen sand system (after Ting, 1981)	36
2.12	Cooling and freezing curve of sand with moisture content of 19.6 percent using the refrigerant at $-10^{\circ}\text{C}$ (after Vyalov, 1975)	38
2.13	Results of axial compression tests with frozen Ottawa sand. (a) Stress-strain curve at different confining pressure. (b) Mohr's envelopes for frozen Ottawa sand (after Sayles, 1973)	43
2.14	Schematic representation of the whole failure envelop for frozen Ottawa sand (after Chamberlain et al. 1972, and Sayles, 1973)	44

2.15	Average strength versus temperature for a frozen silt in uniaxial compression and tension tests (after Haynes and Karalius, 1977)	47
2.16	Typical stress-strain curves for a frozen sand at different strain rates and tested at $-10^{\circ}\text{C}$ (after Bragg and Andersland, 1980)	48
2.17	Compressive strength versus strain rate for a frozen sand at different temperatures (after Bragg and Andersland, 1980)	48
2.18	Effect of strain rate on the triaxial strength of frozen soils (after Sayles, 1973)	49
2.19	True axial creep rate as a function of reciprocal of temperature (after Andersland and Akili, 1967)	51
2.20	Creep rate as a function of time (after Rein et al., 1975)	53
2.21	Log of minimum strain rate versus reciprocal of axial stress (after Yalin et al. 1983)	55
2.22	Log of time to failure versus reciprocal of axial stress (after Yalin et al. 1983)	55
2.23	Creep curves for Ottawa sand at constant axial stress and different confining pressure (after Sayles, 1973)	57
2.24	Mohr's envelopes for creep strength of Ottawa sand at $-3.85^{\circ}\text{C}$ (after Sayles, 1973)	69
2.25	Nomenclature for stress system	77
3.1	Grain size distribution of the sand	89
3.2	Plexiglass mold (not to scale)	90
3.3	Schematic diagram of saturation process of the sand samples	91
3.4	Schematic diagram of the triaxial cell	93
3.5	Triaxial cell details (not to scale)	94
4.1	True volumetric strain versus cumulative time	104
4.2	True volumetric strain versus time	105
4.3	True volumetric strain versus mean normal stress	106

4.4	Volumetric strain rate versus time	107
4.5	Time to attenuation versus mean normal stress	108
4.6	True volumetric strain versus mean normal stress at various time	109
4.7	Ratio $\sigma_m/\epsilon_v$ versus mean normal stress	110
4.8	Parameter $\beta$ versus time	111
4.9	Bulk creep function versus mean normal stress	112
4.10	Bulk creep function versus time	113
5.1	True volumetric and true axial strain versus accumulated time (MST1)	142
5.2	True volumetric and true axial strain versus time (MST1)	143
5.3	True volumetric and true axial strain versus accumulated time (MST2)	144
5.4	True volumetric and true axial strain versus time (MS2)	145
5.5	True volumetric and true axial strain versus accumulated time (MST3)	146
5.6	True volumetric and true axial strain versus time (MST3)	147
5.7	True volumetric and true axial strain versus accumulated time (MST4)	148
5.8	True volumetric and true axial strain versus time (MST4)	149
5.9	True volumetric and true axial strain versus accumulated time (MST5)	150
5.10	True volumetric and true axial strain versus time (MST5)	151
5.11	Axial strain rate versus time (after Rein et al., 1975)	152
5.12	Axial strain rate versus time for silt (after Yalin and Carbee, 1984)	153
5.13	Axial strain rate versus time for polycrystalline ice (Mellor, 1979)	154

5.14	Axial creep rate versus time (MST1)	155
5.15	Axial creep rate versus time (MST2)	156
5.16	Axial creep rate versus time (MST3)	157
5.17	Axial creep rate versus time (MST4)	158
5.18	Axial creep rate versus time (MST5)	159
5.19	Axial creep rate versus time for $\sigma_m=140$ kPa	160
5.20	Axial creep rate versus time for $\sigma_m=280$ kPa	161
5.21	Axial creep rate versus time for $\sigma_m=280$ kPa	162
5.22	Axial creep rate versus time for $\sigma_m=70$ kPa	163
5.23	Axial creep rate versus time for $\sigma_m=420$ kPa	164
5.24	Axial creep rate versus time for $S_d=196$ kPa	165
5.25	Axial creep rate versus time for $S_d=392$ kPa	166
5.26	Time to attenuation versus mean normal stress	167
5.27	Resultant deviatoric stress at failure versus mean normal stress	168
5.28	Axial strain at failure versus mean normal stress	169
5.29	Resultant deviatoric strain versus accumulated time (MST1)	170
5.30	Resultant deviatoric strain versus accumulated time (MST2)	171
5.31	Resultant deviatoric strain versus accumulated time (MST3)	172
5.32	Resultant deviatoric strain versus accumulated time (MST4)	173
5.33	Resultant deviatoric strain versus accumulated time (MST5)	174
5.34	Resultant deviatoric stress versus resultant deviatoric strain (MST1)	175
5.35	Resultant deviatoric stress versus resultant deviatoric strain (MST2)	176
5.36	Resultant deviatoric stress versus resultant	

	deviatoric strain (MST3)	177
5.37	Resultant deviatoric stress versus resultant deviatoric strain (MST4)	178
5.38	Resultant deviatoric stress versus resultant deviatoric strain (MST5)	179
5.39	Tangent shear modulus versus ratio $\sigma_m/S_a$ (MST1)	180
5.40	Tangent shear modulus versus ratio $\sigma_m/S_a$ (MST3)	181
5.41	Tangent shear modulus versus ratio $\sigma_m/S_a$ (MST4)	182
5.42	Tangent shear modulus versus ratio $\sigma_m/S_a$ (MST5)	183
5.43	Ratio $(\sigma_m/S_a)/G$ versus ratio $\sigma_m/S_a$ (MST1)	184
5.44	Ratio $(\sigma_m/S_a)/G$ versus ratio $\sigma_m/S_a$ (MST3)	185
5.45	Ratio $(\sigma_m/S_a)/G$ versus ratio $\sigma_m/S_a$ (MST4)	186
5.46	Ratio $(\sigma_m/S_a)/G$ versus ratio $\sigma_m/S_a$ (MST5)	187
5.47	Parameter 'a' versus time	188
5.48	Parameter 'b' versus time	189
5.49	Parameter 'b' at time $t=1$ hour versus mean normal stress	190
5.50	Shear creep function versus time (MST1)	191
5.51	Shear creep function versus time (MST3)	192
5.52	Shear creep function versus time (MST4)	193
5.53	Shear creep function versus time (MST5)	194
5.54	Shear creep function versus mean normal stress	195
5.55	Shear creep function versus resultant deviatoric stress	196
6.1	True volumetric and true axial strain versus accumulated time (MST10)	210
6.2	True volumetric and true axial strain versus accumulated time (MST12)	211
6.3	True volumetric and true axial strain versus accumulated time (MST13)	212
6.4	Axial creep strain versus time	213



6.5	Axial creep strain versus time, $(\sigma_1 - \sigma_3) = 120$ kPa	214
6.6	Axial creep strain versus time, $(\sigma_1 - \sigma_3) = 140$ kPa	215
6.7	Axial creep strain versus time, $(\sigma_1 - \sigma_3) = 160$ kPa	216
6.8	Axial creep strain versus time, $(\sigma_1 - \sigma_3) = 180$ kPa	217
6.9	Axial creep strain versus time, $(\sigma_1 - \sigma_3) = 200$ kPa	218
6.10	Deviatoric stress versus attenuated true axial strain (MST10)	219
6.11	Deviatoric stress versus attenuated true axial strain (MST12)	220
6.12	Deviatoric stress versus attenuated true axial strain (MST13)	221
6.13	Observed axial strain versus predicted axial strain	222
7.1	True volumetric and true axial strain versus accumulated time (MST6)	235
7.2	True volumetric and true axial strain versus accumulated time (MST7)	236
7.3	True volumetric and true axial strain versus accumulated time (MST8)	237
7.4	True volumetric and true axial strain versus accumulated time (MST9)	238
7.5	Resultant deviatoric stress at failure versus mean normal stress	239
7.6	Axial strain at failure versus mean normal stress	240
7.7	Axial strain at failure versus ratio $\sigma_m/S_a$ at failure	241
8.1	Ice sample with steel sphere at the centre	250
8.2	Penetration of steel spheres versus accumulated time (Tests - Series 1, Phase 1 & Phase 2)	251
8.3	Penetration rate versus hemispherical stress	252
8.4	Penetration rate versus hemispherical stress (log-log scale)	253
8.5	Penetration of steel spheres versus time (Tests - Series 2)	254

8.6	Penetration rate versus hemispherical stress (Tests - Series 1 & 2)	255
8.7	Viscosity of polycrystalline ice versus hemispherical stress	256
8.8	Viscosity of polycrystalline ice versus hemispherical stress (semi-log scale)	257

## LIST OF TABLES

TABLE		PAGE
5.1	Physical Properties of Frozen Sand Samples	139
5.2	Summary of Stress Condition for the Constant Mean Normal Stress Tests	140
5.3	Details of Stress Application (MST1)	141
5.4	Details of Stress Application (MST2)	142
5.5	Details of Stress Application (MST3)	143
5.6	Details of Stress Application (MST4)	144
5.7	Details of Stress Application (MST5)	145
6.1	Physical Properties of Frozen Sand Samples	205
6.2	Details of Stress Application (MST10)	206
6.3	Details of Stress Application (MST11)	207
6.4	Details of Stress Application (MST12)	208
6.5	Details of Stress Application (MST13)	209
7.1	Physical Properties of Frozen Sand Samples	230
7.2	Details of Stress Application (MST6)	231
7.3	Details of Stress Application (MST7)	232
7.4	Details of Stress Application (MST8)	233
7.5	Details of Stress Application (MST9)	234

## LIST OF COMMONLY USED SYMBOLS

- A constant in equation (2.4)
- a constant in equation (5.10)
- B temperature dependent soil parameter
- b constant in equation (5.10)
- c constant in equations (2.1), (2.8), (5.16) and (8.2)
- c dimensionless shape parameter
- c cohesion
- $c_{\infty}$  temperature dependent adhesion at time,  $t=\infty$
- E elastic modulus
- E activation energy
- $F(\gamma)$  constant dependent on activation energy and temperature
- $f(0)$  temperature dependent parameter
- f strength parameter  $f=(1+\sin\phi)/(1-\sin\phi)$
- G shear modulus
- $G_{\infty}$  shear creep function
- K constant in equation (2.9)
- K fitting constant
- K bulk modulus
- K soil parameter in equation (2.13)
- $K_{\infty}$  bulk creep function
- $K_1$  parameter dependent on temperature and stress
- $K_2$  parameter dependent on temperature and stress
- $K_0$  initial tangent bulk modulus
- $K_{\infty}$  attenuated bulk modulus

$L_0$  initial length of specimen  
 $L_t$  length of specimen at time,  $t$   
 $m$  creep exponent  
 $m$  constant in equations (2.4) and (2.8)  
 $m$  soil parameter in equation (2.13) and (4.9)  
 $m_1$  constant in equation (5.16)  
 $n$  creep exponent  
 $n$  constant in equations (2.8), (2.13), (2.16), (4.9) and (8.3)  
 $n_0$  material constant in equation (2.16)  
 $n(T)$  material constant  
 $n_1$  parameter dependent on stress and temperature  
 $n_2$  parameter dependent on stress and temperature  
 $Q$  activation energy based on strength test  
 $R$  universal gas constant  
 $S$  penetration rate  
 $S_a$  resultant deviatoric stress  
 $S_{i,j}$  deviatoric stress tensor  
 $S_1$  deviatoric stress tensor in the direction of  $\sigma_1$   
 $S_2$  deviatoric stress tensor in the direction of  $\sigma_2$   
 $S_3$  deviatoric stress tensor in the direction of  $\sigma_3$   
 $T$  absolute temperature  $^{\circ}K$   
 $t$  time elapsed after load application  
 $t_f$  time to failure  
 $t_m$  time to reach minimum creep rate  
 $t^*$  stress and temperature dependent constant  
 $U$  activation energy  
 $w$  soil parameter in equation (2.13)

$\alpha$  constant in equation (5.16)  
 $\alpha_0$  value of  $\alpha$  at  $\sigma_m=0$   
 $\beta$  reciprocal of the ultimate value of  $\epsilon_v$   
 $\beta$  fitting constant  
 $\beta$  constant in equation (2.9)  
 $\beta$  time dependent constant in equation (2.29)  
 $\beta_1$  material constant in equation (5.16)  
 $\beta_2$  material constant in equation (6.9)  
 $\epsilon$  axial strain  
 $\epsilon_c$  creep strain  
 $\epsilon_d$  resultant deviatoric strain  
 $\epsilon_{ij}$  strain tensor  
 $\epsilon_{ie}$  pseudo instantaneous elastic strain  
 $\epsilon_{ip}$  pseudo instantaneous plastic strain  
 $\epsilon_k$  arbitrary small strain  
 $\epsilon_{kk}$  volumetric strain tensor  
 $\epsilon_0$  instantaneous strain  
 $\epsilon_{oct}$  octahedral normal strain  
 $\epsilon_m$  strain at minimum creep strain rate  
 $\epsilon_t$  strain at time,  $t$   
 $\epsilon_v$  true volumetric strain  
 $\epsilon_1$  true axial strain  
 $\epsilon_2$  true lateral strain in the direction of  $\sigma_2$   
 $\epsilon_3$  true lateral strain in the direction of  $\sigma_3$   
 $\dot{\epsilon}$  axial strain rate  
 $\dot{\epsilon}_1$  axial strain rate  
 $\dot{\epsilon}_c$  creep proof strain rate

$\dot{\epsilon}_e$  equivalent creep rate  
 $\dot{\epsilon}_f$  strain rate at failure  
 $\dot{\epsilon}_m$  minimum creep rate  
 $\dot{\epsilon}_0$  strain rate at initial time,  $t=0$   
 $\dot{\epsilon}_p$  plastic strain rate  
 $\dot{\epsilon}_v$  volumetric strain rate  
 $\nu$  Poisson's ratio  
 $\phi$  angle of internal friction  
 $\phi_\infty$  angle of internal friction at  $t=\infty$   
 $\sigma$  axial stress  
 $\sigma$  hemispherical stress in equation (8.2)  
 $\sigma$  deviatoric stress in equation (2.1)  
 $\sigma_c$  critical creep strength  
 $\sigma_c$  creep proof stress  
 $\sigma_{cu}$  value of critical stress at critical strain rate  
 $\sigma_e$  equivalent stress  
 $\sigma_{ij}$  stress tensor  
 $\sigma_k$  temperature dependent deformation modulus  
 $\sigma_m$  mean normal stress  
 $\sigma_m$  isotropic stress  
 $\sigma_n(\tau)$  a function of temperature  
 $\sigma_1$  major principal stress  
 $\sigma_2$  intermediate principal stress  
 $\sigma_3$  minor principal stress  
 $\theta$  negative temperature  
 $\theta_0$  reference temperature  
 $\delta_{ij}$  kronecker delta

# **CHAPTER ONE**

## **INTRODUCTION**



## CHAPTER 1

### INTRODUCTION

#### 1.1 GENERAL

Frozen soil is a particulate composite material composed of four different constituents: solid mineral or organic grains, ice, unfrozen water, and gases. The most important characteristic by which it differs from unfrozen soil and other particulate materials is that, the matrix which is composed of ice and unfrozen water may change significantly with temperature and pressure. Knowledge of time-dependent stress-strain-strength behaviour of frozen soil is important in design and construction involving naturally occurring and artificially frozen ground. Frozen ground in Canada and other parts of the world has received increasing attention due to the increased development in the permafrost regions of the north.

In the last decade, the Arctic ocean has become of great interest to the petroleum companies, because of the large deposits of oil and natural gases discovered beneath the ocean bottom. The petroleum companies active in the exploration have identified the excessive deformability characteristics of ocean bottom permafrost as one of the major geotechnical problems they face. The ocean bottom permafrost is ice-rich and exists at temperatures that range between 0°C and -3°C and is known in the literature as warm permafrost.

Ice-rich frozen soil exhibits large creep strains under a constant stress and to date there is a limited understanding of its behaviour, and there is no reliable model for predicting its behaviour. The creep behaviour is important in the design and construction of structures bearing on either onshore or offshore permafrost, as well as in the use of artificially frozen soil for soil stabilization.

Most of the existing creep theories used to describe the creep behaviour of frozen soils have their roots in the theories originally developed for the plastic and creep deformation of metals. As such they do not include the effects of superimposed hydrostatic stress and consider deformations to be small. The creep theories of metals have been developed using two basic approaches; one is the phenomenological theory and the other is the physical theory. The physical theory, which is based on the established laws of physics is rather complex and has found little use in engineering application. The phenomenological theory, better known as engineering theory is based on the micro-mechanistic behaviour, and provides semi-empirical solutions to engineering problems. In the study of the creep of frozen soils most of the recent research has been centered on engineering theory rather than on the physical theory. There are exceptions such as the studies by Goughnour and Andersland (1968), Chamberlain et al. (1972), Sayles (1973), Vyalov (1973) and Ladanyi (1981) which attempted to take the physical phenomenon into account in the development of empirical solutions.

Most of the existing theories attempted to correlate strain rate with stress, temperature, and some other material properties. Very little effort has been made to evaluate the deformation parameters which relate the stresses and strains. The axial stress-strain data obtained from standard triaxial tests does not represent the true deformation characteristics, because this approach considers only the changes in major principal stress and does not reflect the actual stress conditions in the soil mass. The deformability characteristics of frozen soils can perhaps be characterized by bulk and shear creep functions because they can be associated with separate physical components of frozen soil behaviour and can be solved for independently.

## 1.2 IDENTIFICATION OF THE PROBLEM

The existing creep theories, as discussed in Section 1.1, fail to differentiate between the fundamental behaviour of metal and particulate material like frozen soil. The following specific problems have been identified after review of the literature.

1. The present creep theories do not take superimposed hydrostatic stress into account in their formulation.
2. The present creep theories are based on the notion of no volume change during the creep deformation.

3. The present theories are based on uniaxial tests and the results are then extended to the general state of stress by using equivalent stress and strain relationships.
4. The present theories are based on relatively short term tests using high stresses and the results are extrapolated to predict long term behaviour at low stresses.
5. The deformation parameters relating stresses and strains are not given due importance in formulating the theories.
6. The physical phenomenon of interaction between ice and soil particles is not fully appreciated.

### 1.3 OBJECTIVES

The general objective of the investigation was to provide a better qualitative understanding of the creep behaviour of frozen soil and to study those aspects, as described in Section 1.2, of creep behaviour that have not been previously investigated so as to generate a more general creep model than the models that are in use today. The specific objectives were :

1. To investigate the influence of the hydrostatic or mean normal stress on the creep behaviour of frozen soil.

2. To measure the volume changes that accompany creep and assess the significance of those volume changes on the creep behaviour.
3. To perform long term creep tests using low stresses which are ordinarily exerted by foundations, as well as high stresses.
4. To obtain solutions for bulk and shear creep functions of a quartz carbonate sand and to generate a constitutive equation and creep model embracing these functions.
5. To examine the interaction between soil particles and ice in an attempt to understand the creep mechanism in frozen soil.
6. To assess the validity of the model by performing standard triaxial compression tests and comparing observed deformations with those predicted by the model.

#### 1.4 SCOPE OF INVESTIGATION

An extensive review of literature on the mechanics of ice and frozen soil was carried out. The review of mechanics of ice included structure of ice in frozen soil, deformation mechanism of ice and quantitative models of strength and deformation of ice. The review of mechanics of frozen soil included structure of frozen soil,

deformational mechanism of frozen soil, effect of mineral particle concentration, confining pressure, temperature and strain rate on strength and deformation of frozen soil. Deformation parameters which relate the stress and strains of nonlinear materials were also reviewed to analyze the stress-strain characteristics of frozen sand.

The approach followed in this study was based on the separation of the stress system into mean normal and deviatoric components. The creep behaviour under changes in hydrostatic stress was studied and the bulk creep function was evaluated based on the data obtained from isotropic compression tests. The creep behaviour under changes in deviatoric stress was studied using triaxial compression tests in which the mean normal stress was kept constant so that all the strains were the result of changes in the deviatoric component of stress only. The shear creep function was evaluated based on the data obtained from the constant mean normal stress triaxial compression tests. The deformation of frozen sand depends to some extent on the interaction of the ice and sand particles. This interaction was studied by applying loads to steel spheres embedded in polycrystalline ice.

In carrying out the experimental investigation, the program was divided into four groups — 1) multi-stage isotropic consolidation tests, 2) constant mean normal stress multi-stage triaxial tests, 3) constant cell pressure multi-stage triaxial tests and 4) penetration of rigid steel spheres into polycrystalline ice. The sample preparation technique, setting-in procedure and the description of the triaxial equipment are given in Chapter 3. The detailed test procedures are

given in the chapters dealing with each test. The bulk creep function is developed in Chapter 4 and the shear creep function in Chapter 5. A new creep failure criteria is proposed in Chapter 5. Chapter 6 deals with the verification of the model for bulk and shear creep function. The mechanisms of creep deformations are examined in Chapter 7 by comparing the short and long-term test results. The interaction of ice and rigid particle are presented in Chapter 8. Finally the conclusions and recommendations for futher study are given in Chapter 9.

**CHAPTER TWO**  
**REVIEW OF MECHANICS OF ICE**  
**AND FROZEN SOIL**



## CHAPTER 2

### REVIEW OF MECHANICS OF ICE AND FROZEN SOIL

#### 2.1 MECHANICS OF ICE

##### 2.1.1 Structure of Ice in Frozen Soil

Ice is an important structural component of frozen soil. There are nine different forms of ice as shown in Figure 2.1. The hexagonal structure identified as  $I_h$  in Figure 2.1 is the only one which is known to be thermodynamically stable at temperatures between  $0^{\circ}\text{C}$  and  $-130^{\circ}\text{C}$  and at atmospheric pressure. The oxygen atoms in ice  $I_h$  are arranged in a tetrahedral pattern, each oxygen atom being surrounded by four equally spaced oxygen atoms at the vertices of the tetrahedron. The tetrahedral coordination of the oxygen atoms gives rise to a crystal structure possessing hexagonal symmetry. The molecules form layers of puckered parallel planes known as the basal planes. The normal to the basal plane is referred to as the  $c$ -axis of the crystal. There are two hydrogen atoms adjacent to each oxygen atom, but only one hydrogen atom between each pair of oxygen atoms and each molecule is oriented so as to direct its hydrogen atoms towards two of the four neighboring atoms. A unit cell in the crystal structure contains four molecules which correspond to a density of  $0.917 \text{ Mg/m}^3$  at  $0^{\circ}\text{C}$ . The basal plane is the demonstrated glide plane of the lattice, and shear applied parallel to

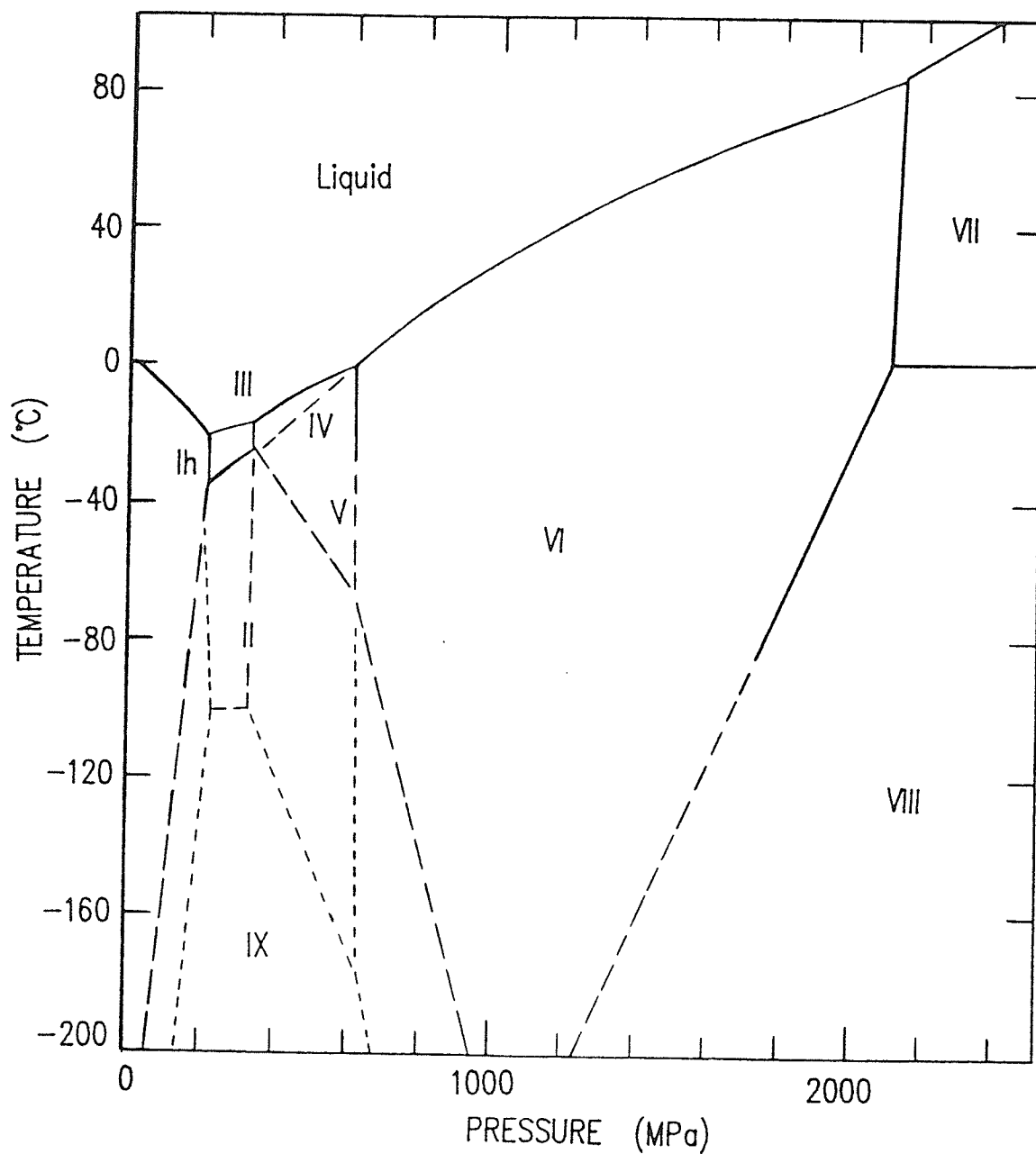


Figure 2.1 Phase diagram for Ice (after Whalley et al. 1968)

this plane gives a strain rate about two orders of magnitude higher than that resulting from shear normal to the basal plane (Mellor, 1979). Higashi (1969) stated that the stress required for nonbasal slip is 10 times greater than that for basal slip. However it has been shown that when attempts are made to produce slip in nonbasal plane directions, ice often fractures before slip occurs (Gold, 1970).

A special property of ice Ih is the mobility of the hydrogen atom in its crystal lattice which changes position under the influence of external disturbances, such as changes in pressure and temperature. The mobility of the hydrogen atom decreases with a lowering of temperature and acquires an organized and stable structure at  $-78^{\circ}\text{C}$  (Tsytovich, 1975).

The temperature at which crystallization starts spontaneously could be as low as  $-40^{\circ}\text{C}$  for pure water. The condition of supercooling alone is not a sufficient cause for a system to begin crystallization. Before crystals can grow there must exist in the solution a number of minute centres of crystallization. These centres are either the existing ice crystals or some impurities.

Typical natural ice exists in polycrystalline form. The ice, which is an inevitable component of frozen soils, represents a monomineralic cryohydrate materials with highly unique physicommechanical properties that sharply differ from those of other crystalline materials (Tsytovich, 1975). Ice in frozen soil is polycrystalline in nature. The structure of this ice will depend on

soil properties such as grain size, pore size, permeability, specific surface area, surface activity, degree of saturation, amount of impurities and the freezing process.

The axes of the constituent crystals of the polycrystalline ice are randomly oriented and when such ice is stressed the compliance of individual grains varies, depending partly on how the basal planes are oriented relative to the stress field. Under a constant deviatoric stress, recrystallization can take place so as to bring basal planes into closer coincidence with resolved shears, and consequently the crystal orientation ceases to be random and this process is accompanied by strain softening of the sample.

### 2.1.2 Deformational Mechanisms of Ice

Ice is present in nature at a very high homologous temperature. The effect of temperature in the typical range of 0°C to -20°C is very important because of its strong influence on the unfrozen water content and consequently on the mechanical behaviour of the soil. Polycrystalline ice possesses a unique combination of strength and deformation properties because of the nonsymmetrical behaviour of each of its crystals under stress. Ice exhibits a very time dependent deformational behaviour. It creeps under a very low deviatoric stress and the actual limiting long term strength still remains undetermined. In addition the level of applied stress or the strain rate has appreciable influence on the mechanical behaviour. At sufficiently

high or low levels of either, brittle or ductile failure, respectively, can occur.

Plastic strains in a volume element of a polycrystalline ice are not homogeneous. This inhomogeneous distribution of strains leads to initiation of fracture. Plastic flow occurs by shearing by the process of slip. Slip always occurs by the displacement of blocks of crystals in specific crystallographic directions called slip directions. It usually takes place on particular lattice planes called slip planes or glide planes. Since all atoms on the slip plane do not vibrate in phase with one another, the shearing force that is necessary for atomic displacements will vary from point to point on the same plane. Consequently, slip cannot occur simultaneously with the entire slip plane moving, but it occurs consecutively, beginning in a minute region on the glide plane and spreading outwards. The boundary between the regions where slip has and has not occurred is called a dislocation. It is commonly represented by a line on this plane and is called a dislocation line. The element initially containing very few dislocations is able to be strained plastically and the dislocation density increases with strain. Consequently, dislocations multiply when they move.

Polycrystalline ice, which is of particular interest to this study is composed of grains which are randomly oriented with respect to one another. In general, because of the random orientation of the grains, plastic deformation cannot spread easily from one grain to its adjacent grains. Furthermore, the deformation of any one grain cannot

occur independently of its neighbours because, this exerts a constraint effect on the deformation in order that the continuity be maintained at the grain boundary. Due to increase in applied stress, cracking occurs as a result of dislocation pileups at the grain boundaries and stress concentration within the crystals due to defects or impurities. These cracks are transcrystalline and intercrystalline in nature and usually involve one or two grains at a time (Gold, 1966(b), 1970, Hawkes and Mellor, 1972). The propagation of a crack is a brittle phenomenon but the overall appearance is ductile. Hawkes and Mellor (1972) reported that initial cracking occurred at between 2 and 4 MPa at  $-7^{\circ}\text{C}$  for polycrystalline snow ice, while Gold (1977), reported that cracking activity started at a stress of about 1 MPa. Gold (1960, 1970) observed formations of microcracks, within a crystal of the aggregate, which were either parallel or perpendicular to the basal plane of the grain. He found the cracks would start to appear only at a certain stress level in compression. They would thus increase during transient creep, but came to a stop if the stress was not exceeded.

Plastic deformation in polycrystalline ice can also occur due to grain boundary sliding, grain boundary migration, phase boundary sliding, or pressure melting at points of high stresses. A deformational mechanism postulated as a function of stress level, temperature and strain rate was developed by Shoji and Higashi, 1978, and is shown in Figure 2.2.

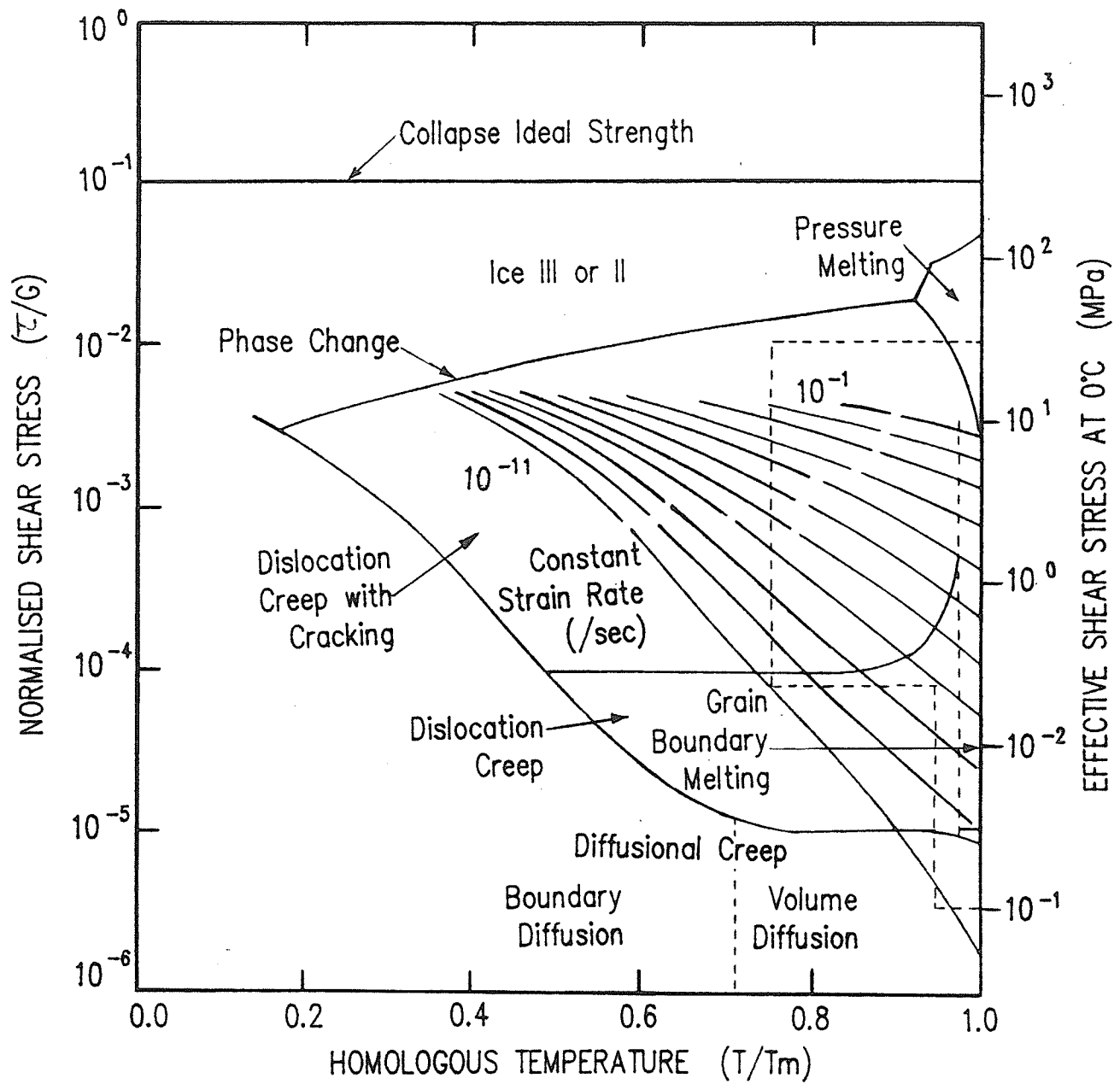


Figure 2.2 Deformation mechanism map for polycrystalline ice of 1mm grain size (after Shoji and Higashi, 1978)

### 2.1.2.1 Strength of Ice

The strength of a material is usually defined in terms of the maximum stress that can be sustained by the material without failure, when it is loaded at either constant strain rate or constant stress. For ice, this maximum stress is strongly dependent on the strain rate and temperature. Other minor factors such as end restraint conditions, sample shape, structure, grain size and impurities also affect the strength. However, these factors often cause scatter in the test results and make it more difficult to compare results from various sources. It is generally observed that the compressive strength increases with strain rate in the ductile range of the behaviour, but then it reaches a peak and drops to a lower constant value above a strain rate characterized as the ductile/brittle transition (Gold, 1970). Results from stress controlled compression tests on polycrystalline ice at various temperatures, such as those reported by Hawkes and Mellor (1972) shown in Figure 2.3, show strong dependence of uniaxial compressive strength on the applied strain rate.

The uniaxial compressive strength of ice generally increases with a decrease in temperature. The rate of increase depends on the applied strain rate, the other variables remaining constant. Based on the tests by Goughnour and Andersland (1968), the uniaxial compressive strength of ice increases at the rate of 0.14 MPa/°C between -4°C and -12°C at an applied strain rate of  $4.4 \times 10^{-6}$ /sec.

Figure 2.4 shows a typical stress-strain curve for snow ice at -9.5°C subjected to unconfined compressive stress at strain rates



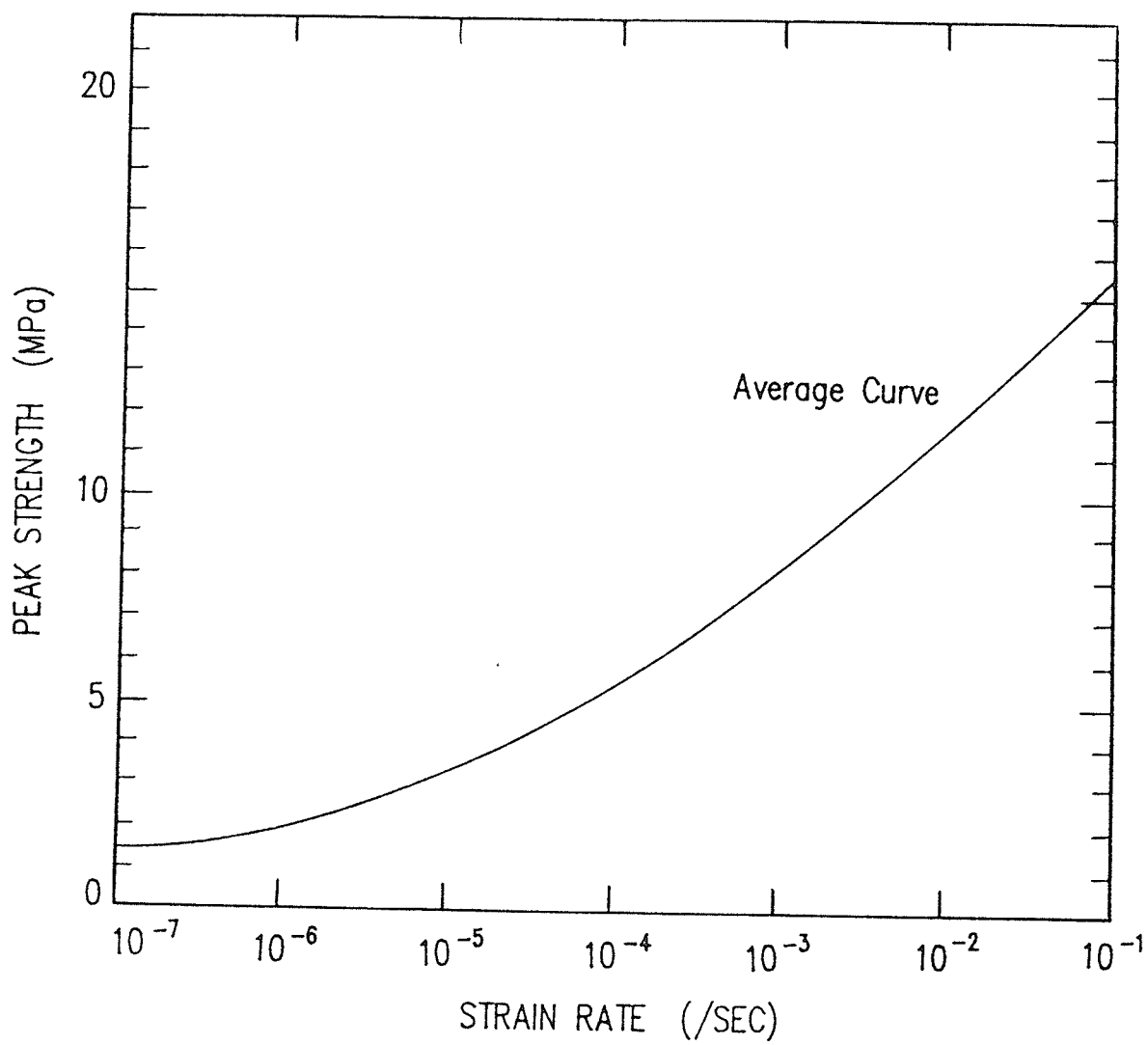


Figure 2.3 Uniaxial compressive strength of ice at  $-9.5^{\circ}\text{C}$   
(after Ting, 1981)

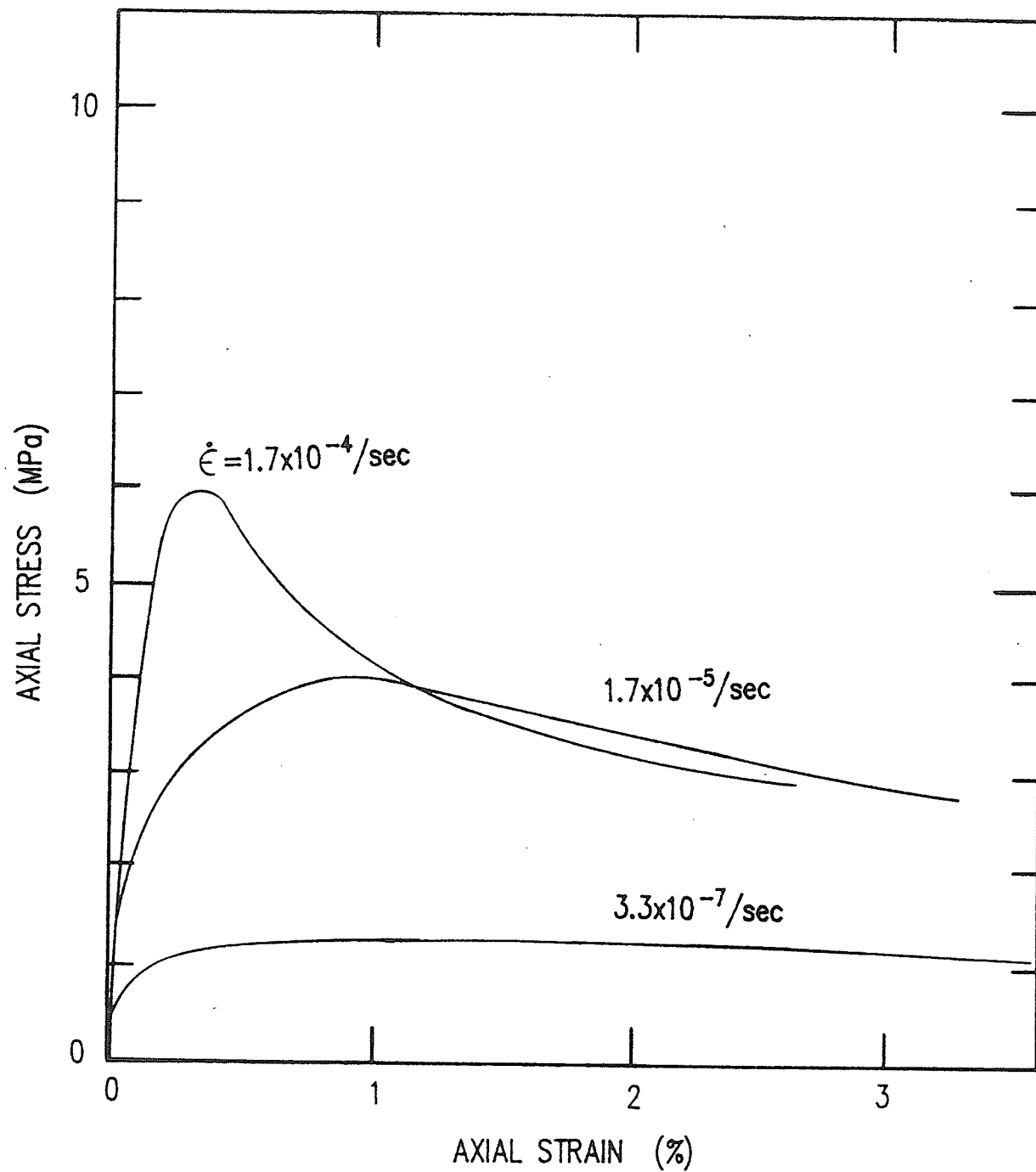


Figure 2.4 Typical stress-strain curves for granular ice at  $-9.5^{\circ}\text{C}$   
 (after Gold and Krausz, 1971)

varying from  $10^{-7}$ /sec to  $10^{-4}$ /sec. It is observed that the peak stress occurred at a much lower strain at the higher strain rate and subsequently at the lowest strain rate the stress-strain curves show a smooth transition to a fairly low asymptotic stress with the strain (Gold and Krausz, 1971).

The strength of ice increases with an increase in the concentration of foreign particles. Goughnour and Andersland (1968) observed that peak strength of ice embedded with Ottawa sand increased with an increase in sand concentration as shown in Figure 2.5. The rate of increase in strength rises sharply at a concentration of 42 percent of sand by volume. This was also confirmed by Hooke et al. (1972). This sharp increase is attributed to the interaction of the sand grains.

While most of the strength tests reported in the literature have used uniaxial loading, Sayles (1973), Smith and Cheatham (1975) and Jones (1978) have used triaxial tests and considered the effect of confining stress on the strength. They found an increase in strength with confining stress. Jones (1978) reported that this increase occurred only up to a limiting confining stress of 40 MPa. Strength decreased with further confinement. He suggested that the decrease was due to localized pressure melting. Global pressure melting occurs at a confining stress of about 110 Mpa at  $-10^{\circ}\text{C}$ .

The tensile strength of ice is almost independent of temperature and strain rate for strain rates above  $10^{-5}$ /sec (Tsytoovich,

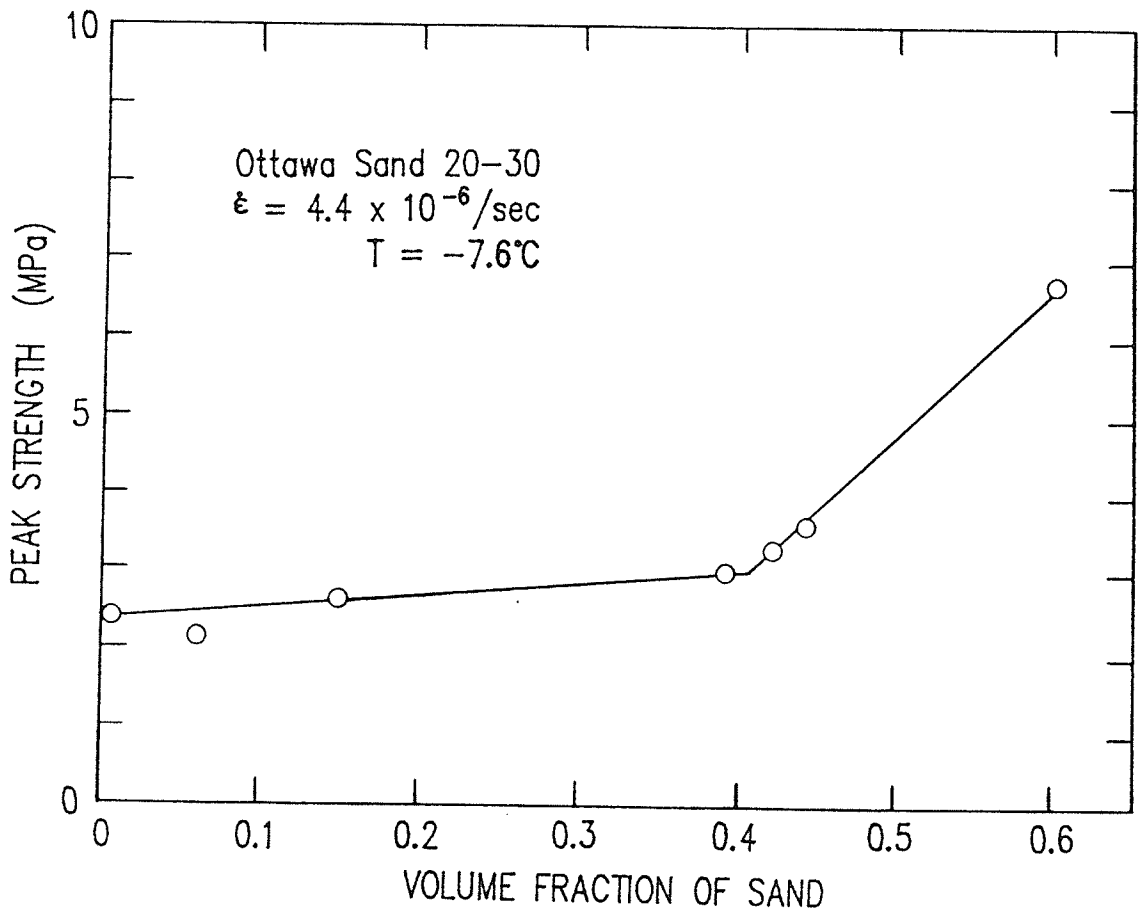


Figure 2.5 Effect of sand concentration on the strength of a sand-ice system (after Goughnour and Andersland, 1968)

1975). In such cases ice fails by brittle fracture with little evidence of internal cracking prior to fracture and separation.

It is generally agreed that the strength of any material increases with an increase in the rate of loading, but the deformation mechanism of ice changes from ductile to brittle at a strain rate known as the transition strain rate and the strength drops abruptly and takes on an asymptotic value. The numerical value of this strain rate again depends on the same factors affecting the strength. At high confining pressure this transition point is suppressed and only ductile behaviour results. Nevertheless, a ductile/brittle transition zone at a strain rate of  $10^{-3}$ /sec has been reported by researchers using uniaxial compressive stress tests (Gold and Krauz, 1971, Jones, 1978).

#### 2.1.2.2 Deformation of Ice

Most of the information on the deformation properties of ice is derived from uniaxial testing either in compression or in tension. Ice exhibits significant elastic, instantaneous permanent, and time-dependent permanent and recoverable deformation under load. The time-dependent permanent deformation contributes a significant portion to the total deformation. If the tests are carried out to sufficiently large strains they display the responses as illustrated in Figure 2.6 where the strain is plotted, on linear scale, as a function of time. The complete strain-time curve displays instantaneous elastic strain,  $\epsilon_0$ , decelerating "primary creep", I, transitional "secondary creep", II, and accelerating "tertiary creep", III.

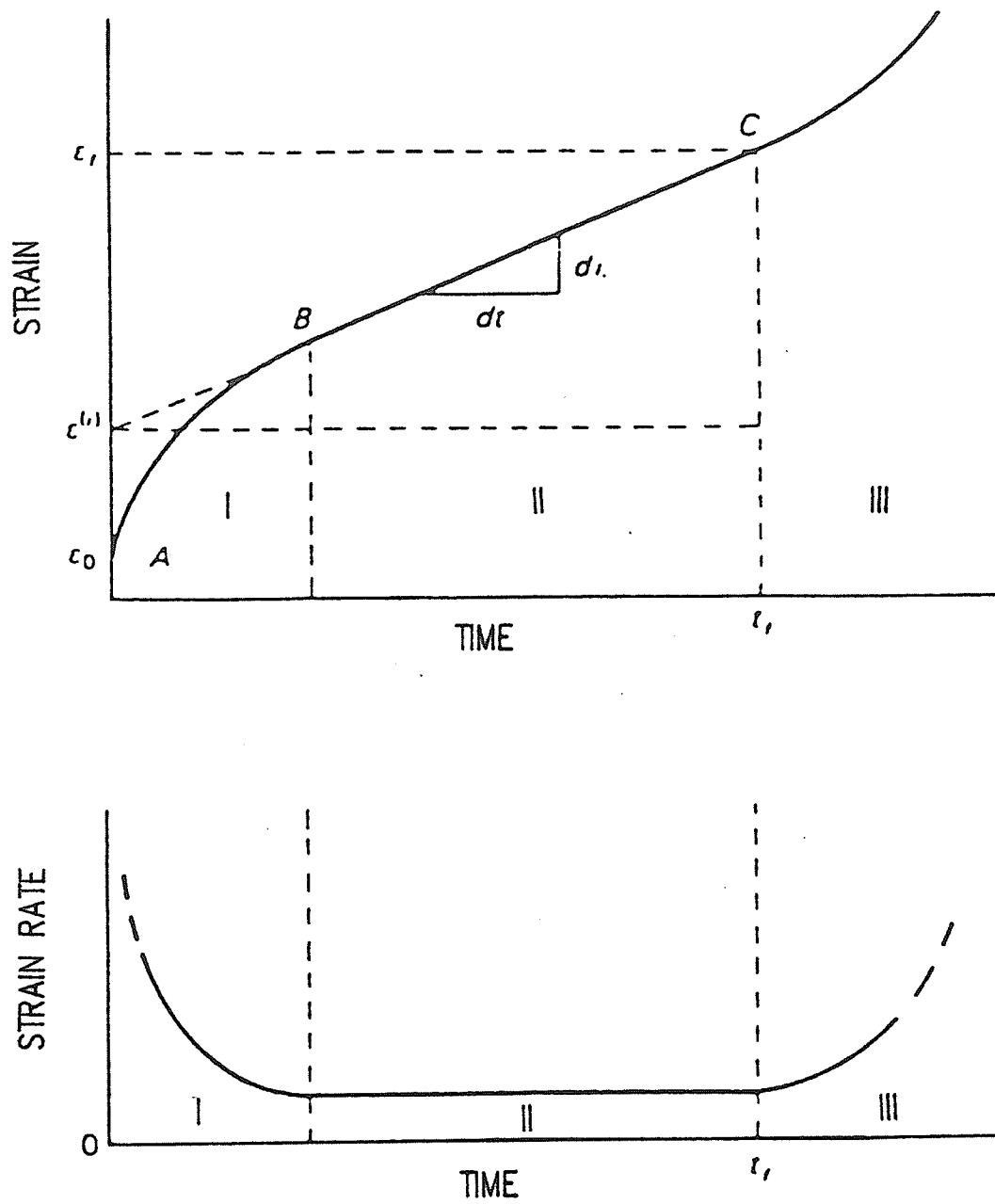


Figure 2.6 Typical creep curves for ice  
 (a) Strain-Time curve  
 (b) Strain rate-Time curve

Instantaneous elastic strain is dependent on the Young's modulus of ice. In most of the tests, the stress is applied abruptly at zero time producing an infinite strain rate. It was reported by Mellor (1979) that relatively high stresses applied instantaneously could damage the specimen permanently by developing internal cracks. In a typical creep test, the instantaneous elastic strain is relatively small, in the order of 0.01 percent with a stress of 1 MPa and proportionately less at lower stresses.

Primary creep is a viscoelastic response consisting of a recoverable "delayed elastic" strain and irreversible viscous strain. This stage is characterized by a progressive decrease in the rate of irreversible strain approaching zero as a limit. The primary creep is accompanied by reorientation and recrystallization of the ice with a decrease in sizes of the crystals, consequently increasing the density of ice. If the stress is removed abruptly during the course of the creep test, abrupt recovery of the instantaneous elastic strain and gradual recovery of the delayed elastic strain will occur.

Secondary creep is characterized by a constant rate of deformation. This is accompanied by the closing of microcracks, the decrease in the porosity and the formation of new microcracks. After a certain time equilibrium is reached between the healing of the existing structural defects and the generation of new defects.

Tertiary creep is characterized by the acceleration of the rate of deformation. This stage is accompanied by the development of

microscopic cracks, the appearance of new microscopic cracks at a steadily increasing rate with their transition to macroscopic cracks. This would result in recrystallization and reorientation of the crystals with their basal planes parallel to the shear direction causing a substantial decrease in the shear strength of the ice. Tertiary creep at large strains has not been well studied. However, a reasonable supposition states that acceleration gradually ceases so that strain rate tends asymptotically to a limit (Mellor, 1979).

Almost all the mechanisms of deformation such as microcracking, point and line defect motion, grain boundary sliding, dislocation buildup, crystal orientation and recrystallization exhibit time dependence. Of these deformational mechanisms, some tend to harden while others tend to soften the structure of ice crystals. It is clear from the above that several deformational mechanisms appear to control the creep of ice during the entire time period from initial loading to final rupture.

The creep of ice depends on stress, temperature and sample quality. Most of the previous work in the literature centered on the relationship between minimum creep rate,  $\dot{\epsilon}_m$ , and applied stress,  $\sigma$ . Mellor (1979) reported a relationship expressed in the form of  $\dot{\epsilon}_m = A\sigma^n$ , where the exponent  $n$  is between 3 and 4, and  $A$  is a temperature dependent constant. The above expression is good for a stress range of 0.2 to 2 MPa. At higher stress  $n$  increases with stress level.

Studies, on the effect of temperature on the creep behaviour of



ice by different researchers, have shown that the creep rate of ice is temperature sensitive at temperatures above  $-10^{\circ}\text{C}$ . The strain rate decreases with the decrease in temperature as shown in Figure 2.7. Barnes et al. (1971) concluded that for low stresses, microcreep mechanisms such as point and line defect movement dominated below  $-10^{\circ}\text{C}$ , while above this, grain boundary mechanism dominated. Pressure melting and recrystallization become significant at a temperature higher than  $-3^{\circ}\text{C}$ .

The effect of grain size of ice on creep has been studied by Jacka (1984), Duval and leGac (1981), Jones and Chew (1981), Baker (1978) and Goodman (1978). Jacka stated that ice crystal size had little or no effect on the minimum flow rate of isotropic polycrystalline ice. It may, however, affect the primary or transient flow rate and thus the time to reach minimum strain rate. As a consequence of dynamic recrystallization during the creep process the mean crystal sizes increase or decrease to an equilibrium size apparently dependent on stress and temperature. Baker (1978) indicated that the strain rate increased markedly with decrease in grain size. Duval and LeGac (1981) and Jones and Chew (1981) disagreed with the results of Baker. Combined plots (Figure 2.8) of Duval et al., Jones et al., Baker and Segó show wide discrepancy in measured strain rate for a given grain size while results of each supports their own conclusions.

The particulate impurities in ice has appreciable influence on its deformation behaviour. Hooke et al. (1972) observed that the creep

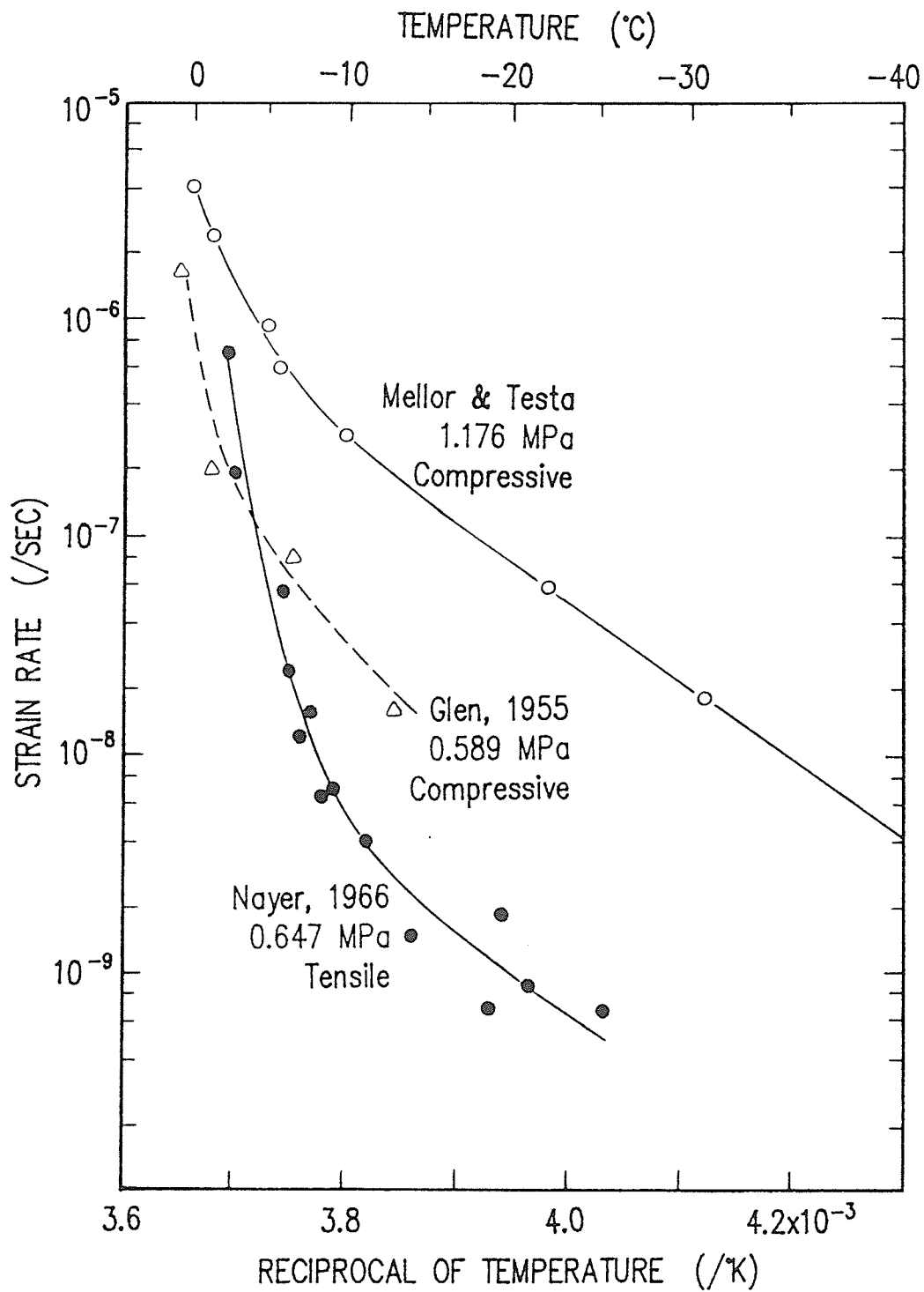


Figure 2.7 Logarithm of strain-rate as a function of temperature for polycrystalline ice (after Barnes et al., 1971)

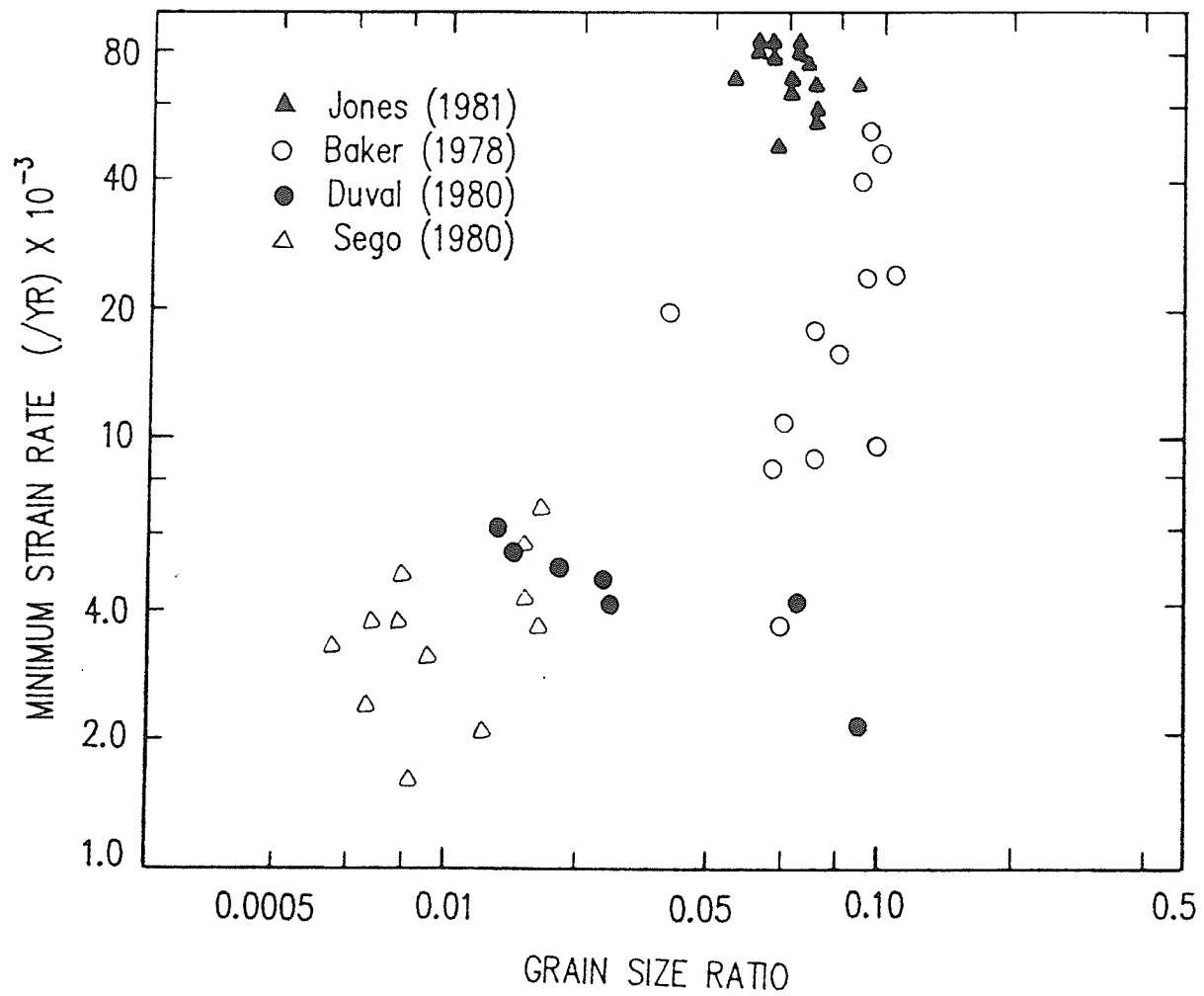


Figure 2.8 Strain rate versus grain size ratio of various authors.

of the ice-sand mixture decreased as the amount of sand increased. The plot of minimum strain rate versus volume of sand fraction in Figure 2.9 indicates that the minimum strain rate decreases with an increase in sand content. This confirms the results obtained by Goughnour and Andersland (1968) presented in Figure 2.5 where the peak strength increased with an increase in volume of sand.

### 2.1.3 Quantitative Models of Strength and Deformation of Ice

Strength and deformation properties of ice have been studied extensively by various researchers during the last two decades. Large scatter in strength and deformation data is found for nominally identical samples tested under similar test conditions. The scatter in the test results may be attributed to the ice sample, testing apparatus and testing environment.

One of the earliest theories which relates the steady state strain rate, temperature and stress level of ice is the Rate Process Theory formulated by Eyring (1936). Weertman (1973), Langdon (1973) and Gold (1973) have modified the Rate Process Theory equation and wrote it in simpler form :

$$\dot{\epsilon} = c\sigma^n \exp\left(-\frac{E}{RT}\right) \quad (2.1)$$

where  $\dot{\epsilon}$  = steady state strain rate

n, c = constants

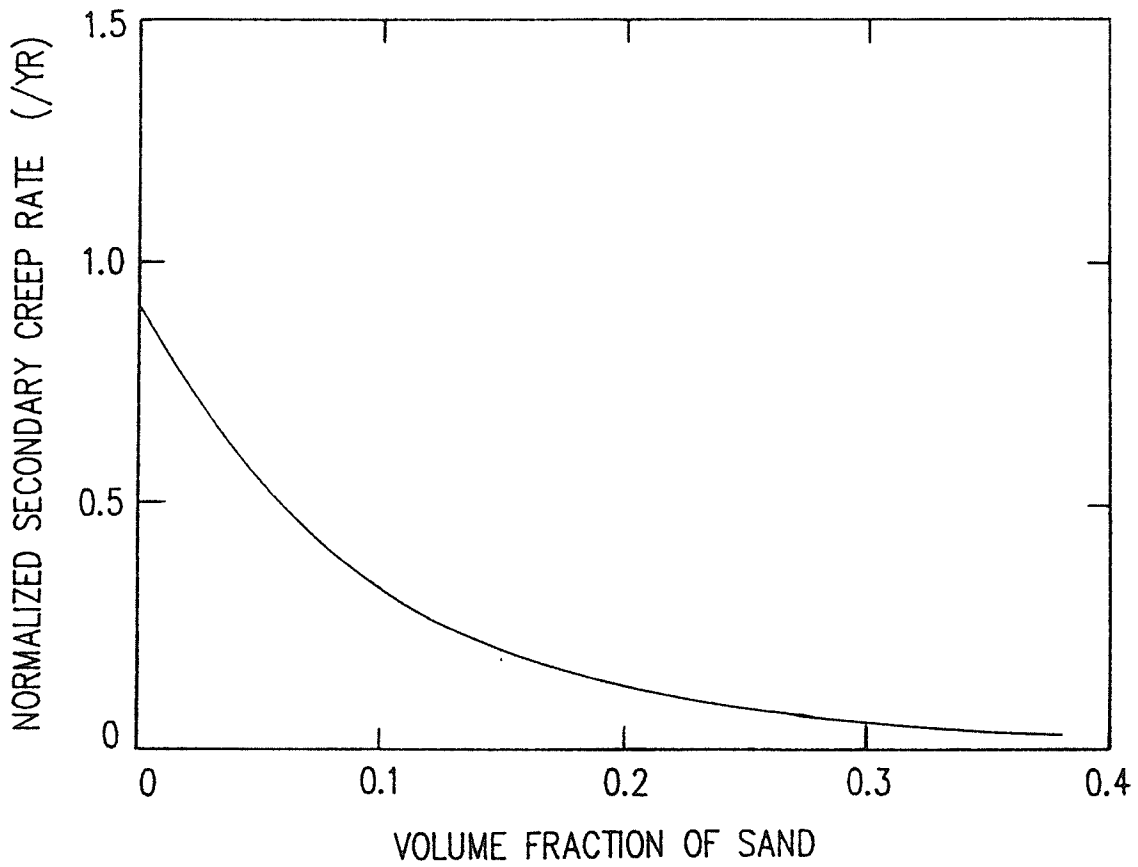


Figure 2.9 Normalized secondary creep rate as a function of volume fraction of sand (after Hooke et al., 1972)

$\sigma$  = deviatoric stress level

E = activation energy

R = universal gas constant (8.31 J/°K mole)

T = temperature (°K)

Based on the modified Rate Process Theory equation (2.1) was rewritten by Muguruma (1969) in terms of stress :

$$\sigma = c' \dot{\epsilon}^{1/n} \exp\left(\frac{Q}{nRT}\right) \quad (2.2)$$

where the value of n varies from 1.3 to 6.7 and Q varies from 42 to 75 K Joules/Mole, as reported by various researchers and summarized by Weertman (1973). Although equations 2.1 and 2.2 are identical, the parameters  $\sigma$  and  $\dot{\epsilon}$  in equation 2.1 are defined as the applied stress and steady state creep rate whereas in equation 2.2 they are defined as peak strength and applied strain rate. The constant c' in equation 2.2 is equal to inverse of c in equation 2.1.

Andrade (1910) put forward an empirical relationship between creep strain and time based on the viscous flow of metal. This is expressed in the form :

$$\epsilon = \epsilon_0 + \beta t^{1/3} + Kt \quad (2.3)$$

$$\beta t^{1/3} \ll 1$$

where t = time after load application

$\epsilon$  = sample strain at time t

$\beta$  = fitting constants

$K$  = steady state creep rate

$\epsilon_0$  = instantaneous strain

Andrade's equation was verified by Glen (1955) and Barnes et al. (1971) for ice and Ting and Martin (1979) for frozen soil who found that it could predict the primary creep reasonably better than the secondary and tertiary creep. The components of Andrade's equation are shown graphically in Figure 2.10.

Assur (1979) proposed an empirical model, as described by equation (2.4), which can describe the entire creep curve including primary, secondary and tertiary stages.

$$\dot{\epsilon} = A \exp(\beta t) t^{-m} \quad (2.4)$$

where  $\epsilon$  is the strain rate,  $t$  is the time,  $A$ ,  $\beta$  and  $m$  are constants. Although this model describes the entire creep curve, it does not take into account the effect of temperature and stress level. It is obvious from the literature that a general model, which takes into account all the variables affecting the strength and deformation properties, is yet to be developed.

## 2.2 MECHANICS OF FROZEN SOIL

### 2.2.1 Structure of Frozen Soil

The basic constituents of frozen soils are solid mineral

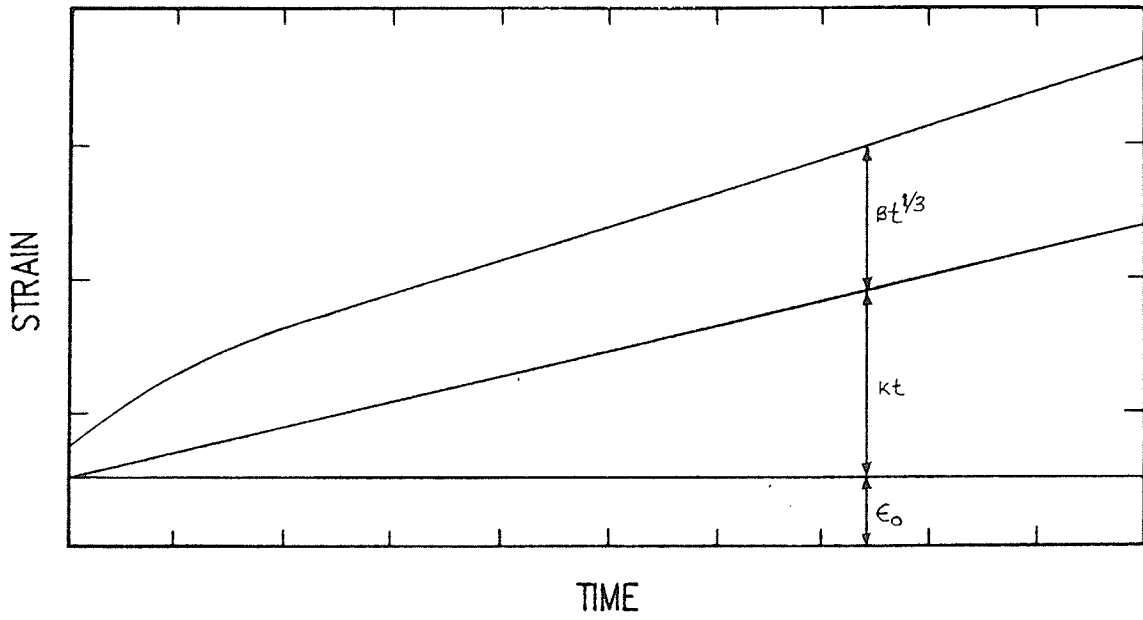


Figure 2.10 Components of the Andrade equation



particles, viscoplastic ice inclusions, unfrozen water and gaseous inclusions. All of these constituents are related to one another in ways that depend on the properties of the individual phases and on the levels of external disturbances.

The solid mineral particles of frozen soils exert an essential influence on the properties of the frozen soil, which depend not only on the sizes and shapes of the particles, but also on the physicochemical nature of their surfaces. The nature of the surfaces is generally determined by the mineralogical composition of the particles and the composition of cations that they have absorbed. The shapes of the mineral particles also have a large influence on the load transfer mechanism within the frozen soil system. If the particles are flat the external forces remain untransformed, while they may reach enormous values in the case of sharp-angular mineral particles. Tsyrovich (1975) found that an external pressure of 0.2 MPa could cause an internal stress of 117 MPa due to particle shape and orientation. Such a high pressure can occur only within the elastic range of deformation and eventually decrease with time because of the increase in contact area.

The size of the mineral particles also has an appreciable influence on the behaviour of frozen soils. The specific surface area increases with a decrease in grain size of the mineral. The unfrozen water, which influences the mechanical behaviour, increases with an increase in specific surface area and consequently with decrease in grain size. Mineralogical composition also affects the behaviour depending on the interaction of the mineral particle with the pore ice.

Tensile and shear adhesion tests by Jellinek (1962,1967) on ice which had been frozen to various surfaces with varying roughness, showed that cohesive type breaks, within the ice crystals, were observed in tension tests, independent of surface roughness. Adhesive type breaks at the interface between the ice and the solid were observed in shear tests, with strength as a function of surface roughness, temperature and rate of shear strain. The strength of adhesion increased with an increase in surface roughness and a decrease in temperature, but below  $-13^{\circ}\text{C}$  the adhesive strength was independent temperature and surface roughness.

Ice is responsible in large measure for the mechanical properties of frozen soil. With variations in thermodynamic conditions such as temperature and pressure, the properties of ice such as structure, viscosity etc. may undergo considerable variations. These changes result in instability of the properties of both the ice and the frozen soil. The pore ice is polycrystalline with a random crystal orientation. Under ordinary condition its response to deviatoric stress is governed by the motion of dislocations and/or microfracture.

It is generally agreed that a film of unfrozen, liquid-like water exists around soil particles in the frozen soil. According to Tsytoovich (1975) this liquid-like layer consists of strongly bound water and loosely bound water. Because of the very large electro-molecular forces of the surface, the strongly bound water in the vicinity of the solid particle cannot form hexagonal crystal lattices even at very low temperatures. The loosely bound water

freezes at temperatures below 0°C. The thinner the layers of loosely bound water, the stronger will be the effect of soil mineral particle surfaces on the freezing process and the lower will be the freezing temperature. The amount of unfrozen water present in the frozen soil at a certain temperature can be related to the specific surface area of the mineral particle (Anderson and Tice, 1972). A recent investigation showed that in a frozen clay, unfrozen film may exist down to a temperature of -110°C (Ladanyi, 1985). From the above discussion one can conclude that with an increase in specific surface area, the unfrozen water content increases at a constant temperature. Consequently with an increase in surface area as the particle size gets smaller, the thickness of bound water decreases requiring more energy to freeze the water.

The gaseous components of frozen soil are water vapour and gases. Their role in the frozen soil is to produce porosity which affects the compressibility characteristics of frozen soil.

Ting et al. (1983) proposed a conceptual frozen sand structure (Figure 2.11), based on an extensive literature review, having the following characteristics :

- in coarse grained frozen soils, solid contacts exists between most particles
- continuous unfrozen water exists at the ice-to-soil solids interface and at grain boundaries in the ice phase
- ice in frozen soil is polycrystalline in nature and the

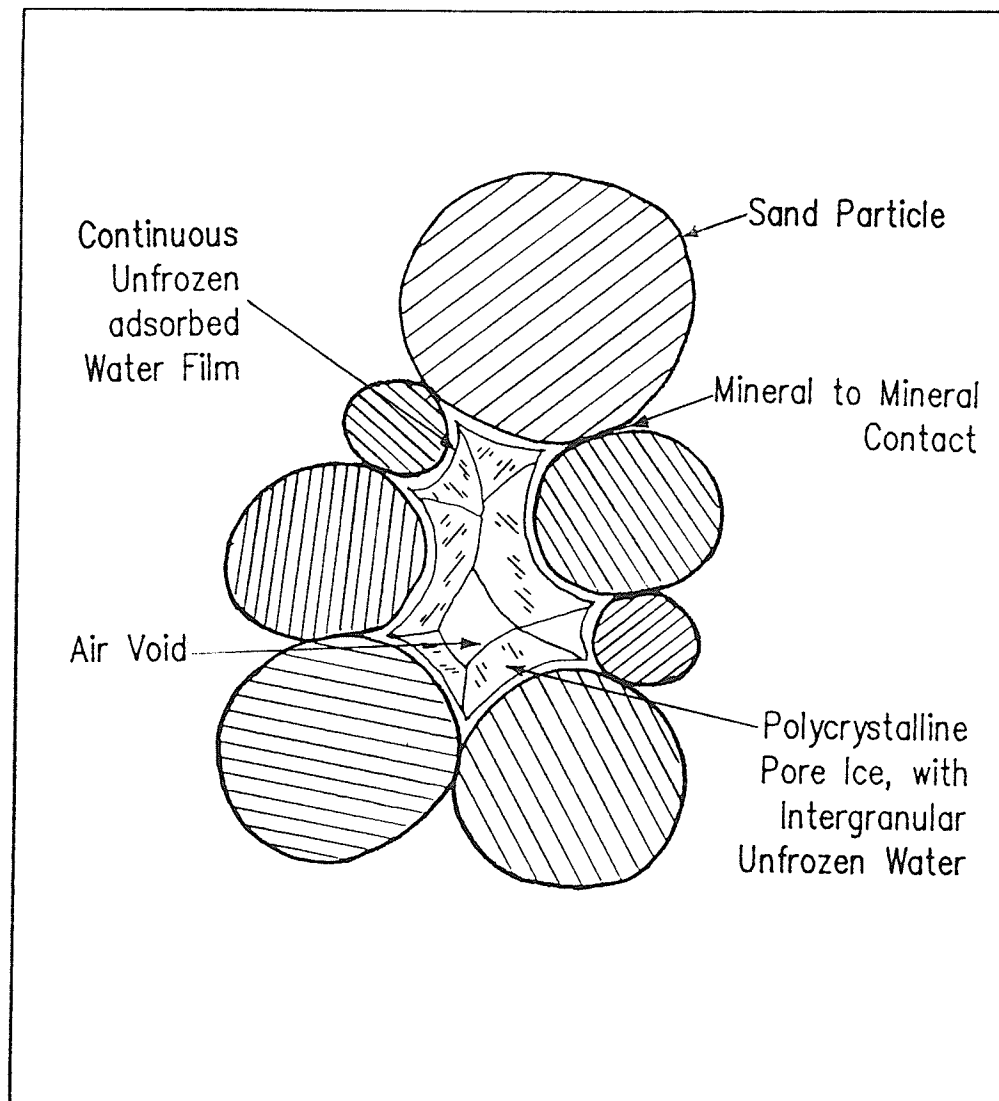


Figure 2.11 Two dimensional schematic of the proposed structure of the frozen sand system (after Ting, 1981)

number of ice grains in a pore is equal to the number of particles adjacent to the pore.

The freezing process has an appreciable influence on the structure of pore ice and thereby on the frozen soil. It is generally agreed that a layer of unfrozen water exists around the soil particles in frozen soil. This layer is mobile, continuous and capable of mass transport. It is understood that ice nucleates in the presence of silicate particles adjacent to the unfrozen adsorbed water film rather than directly on the particle surface. Corte (1962) observed in the case of soil freezing upward, the freezing front could carry soil particle floating on the heaving ice surface. This is possible if an unfrozen water film surrounds the soil particles.

The freezing curve of water saturated Lyubertsy quartz sand is shown in Figure 2.12 (Vyalov, 1975). The first segment, I, corresponds to initial supercooling of the sample without formation of any ice. The supercooling temperature depends on the material type. For this sand it was about  $-3^{\circ}\text{C}$ . As soon as the pore water begins to freeze, a significant amount of latent heat of ice formation is released and the temperature of the soil rises to very close to  $0^{\circ}\text{C}$  as shown by stage II. At this temperature all the free water present in the sand freezes, the time of freezing depends on moisture content, freezing rate and the dimension of the sample. This is shown by the part III of the curve. When all the free water in the sample turns into ice, cooling of the sample starts as shown by the part IV. If the temperature is raised as shown by the segment V, the temperature varies

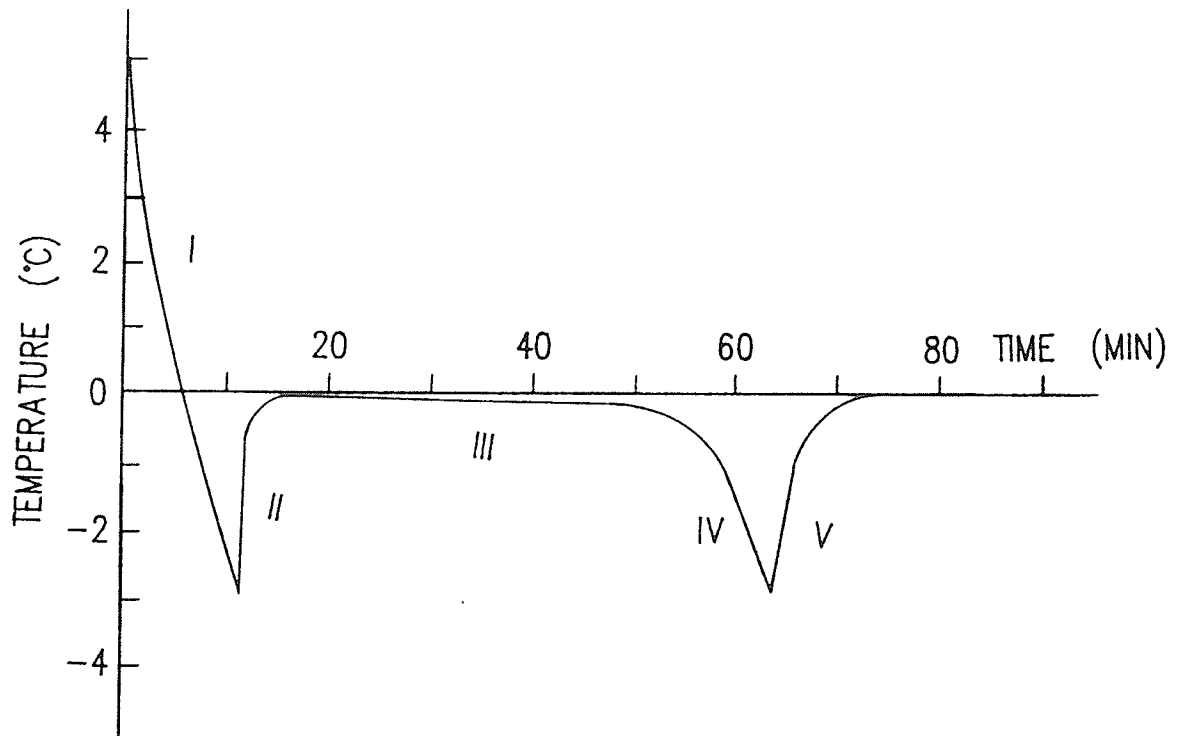


Figure 2.12 Cooling and freezing curve of sand with moisture content of 19.6 percent , refrigerant at  $-10^{\circ}\text{C}$  (after Vyalov, 1975)

linearly at first, but then in curvilinear fashion. For sands the curvature starts approximately at temperatures ranging between  $-0.5$  and  $-1^{\circ}\text{C}$ . This shows that the absorption of the latent heat of ice formation begins even before the thawing temperature of the soil has been reached.

The rate of freezing plays an important role in determining the structure of ice and frozen soil, and consequently the mechanical behaviour. It is observed that the first freezing causes the air voids to become entrapped whereas slow unidirectional freezing drives the air void ahead of the freezing front.

#### 2.2.2 Deformational Mechanisms of Frozen Soil

The rheological characteristics of frozen soil are a direct result of the presence of ice as a matrix which undergoes plastic flow under a load practically of any magnitude, causing reorientation of crystals. The presence of a viscous film of unfrozen water initiates and furthers the rheological process when any additional load is applied.

The strong development of rheological processes in frozen soils is due to the peculiarity of their internal bonds. There are three basic types of internal bonds identified in frozen soils : i) purely molecular bond ii) ice cement bond and iii) structural bond. Purely molecular bond depends on the area of direct contact, distance between

mineral particles, their compactness and the physicochemical nature of the particles. Ice cement bond, which is responsible for the strength and deformation properties of frozen soil, depends on the temperature, ice content, structure of the ice and their position with respect to the applied force, unfrozen water, gas inclusions and cavities in the ice. Structural bonds depend on the conditions of formation and the subsequent existence of the frozen soil. The greater the inhomogeneity of frozen soil, the greater will be the number of structural and constitutional defects in it.

The strength and deformation properties of frozen soil differ from those of other solids in that the application of external load to a frozen soil always gives rise to irreversible restructuring, which causes stress relaxation and creep deformation under a very small load. Much of these behaviours can be attributed to the presence of pore ice. Three basic mechanisms of deformation of pore ice are identified : i) flow of ice in slow shear parallel to the basal plane of the crystals without any change in the structure of the ice, ii) microcracking, recrystallization, intergranular shifting and breakup into fragments with randomized orientation, iii) melting of ice under very high shear stresses due to the heat of friction along cleavage planes. Based on the discussion in the previous sections on the behaviour of frozen soils and ice, some qualitative and quantitative models for the observed behaviour are presented.



## 2.2.3 Strength of Frozen Soil

### 2.2.3.1 Effect of Mineral Particle Concentration

The ratio of mineral particles to ice affects the behaviour of frozen soils. Ice with some impurities has lower strength than pure ice. This is supported by the work of Goughnour and Andersland (1968) and Hooke et al. (1972). They observed that polycrystalline ice with sand particles of 1 to 3 percent by volume had about 10 percent lower peak strength than pure ice. This is attributed to the fact that the sand particles decrease the ice crystal size which is more prone to grain boundary slipping and even act as a site for primary dislocation. The peak strength starts increasing with the increase in sand ice ratio (Hooke et al., 1972). Goughnour and Andersland (1968) reported that the influence of interparticle friction and dilatancy became apparent when the sand concentration was increased beyond 42 percent. Kaplar (1971) showed that the peak strength started increasing rapidly when the sand concentration was increased beyond 40 percent. The strength increase occurred as the sand remain ice saturated (Kaplar, 1973, Baker, 1979). Sayles and Carbee (1980) had shown that at silt concentration of less than 50 percent the strength was governed by ice matrix at low strains while at higher particle concentrations the stress-strain curve showed an increasingly strain hardening character.

### 2.2.3.2 Effect of Confining pressure

The strength of frozen sand consists of cohesion of the ice matrix and the frictional resistance of the sand grains. It has been found, however, that these sources of strength may be independent of

each other depending on the strain rate. For Ottawa sand if the strain rate is greater than 0.02/min, the ice matrix attains peak strength first at a strain less than 1.0 percent and then the soil skeleton resistance becomes a function of confining pressure and attains a peak strength at a strain of 10 percent (Sayles, 1973). This is shown in Figure 2.13a. The first yield point is considered to be the yielding of ice matrix while the second one corresponds to the sand-ice composite. Failure envelope based on the two peaks are presented in Figure 2.13b. Chamberlain et al. (1972) observed that at low confining pressure the shear strength increased for Ottawa sand but decreased for silt. He suggested that the strengthening of the Ottawa sand was due to particle interlocking and interparticle friction and while the low strength for silt was due to the presence of unfrozen water film. In the intermediate pressure range, both the Ottawa sand and the silt exhibited decreasing shear strength with increasing confining pressure. This was due to the onset of pressure melting caused by stress concentration and the suppression of dilation due to high pressure. In the high pressure region, about 100 MPa, both the Ottawa sand and the silt showed an increase in shear strength due to increase in confining pressure. In this pressure range ice/water phase transformation occurred and began to start behaving as unfrozen soil. This can be represented by a schematic diagram shown in Figure 14. Very similar results of a study of the effects of high confining pressures on the strength of frozen Ottawa sand were obtained by Simonsen (1974) and Sego (1984). Parameswaran and Jones (1981) found that yield and peak strength increased with increasing confining pressure up to 35 to 40 MPa, beyond which pressure melting causes decrease in strength.

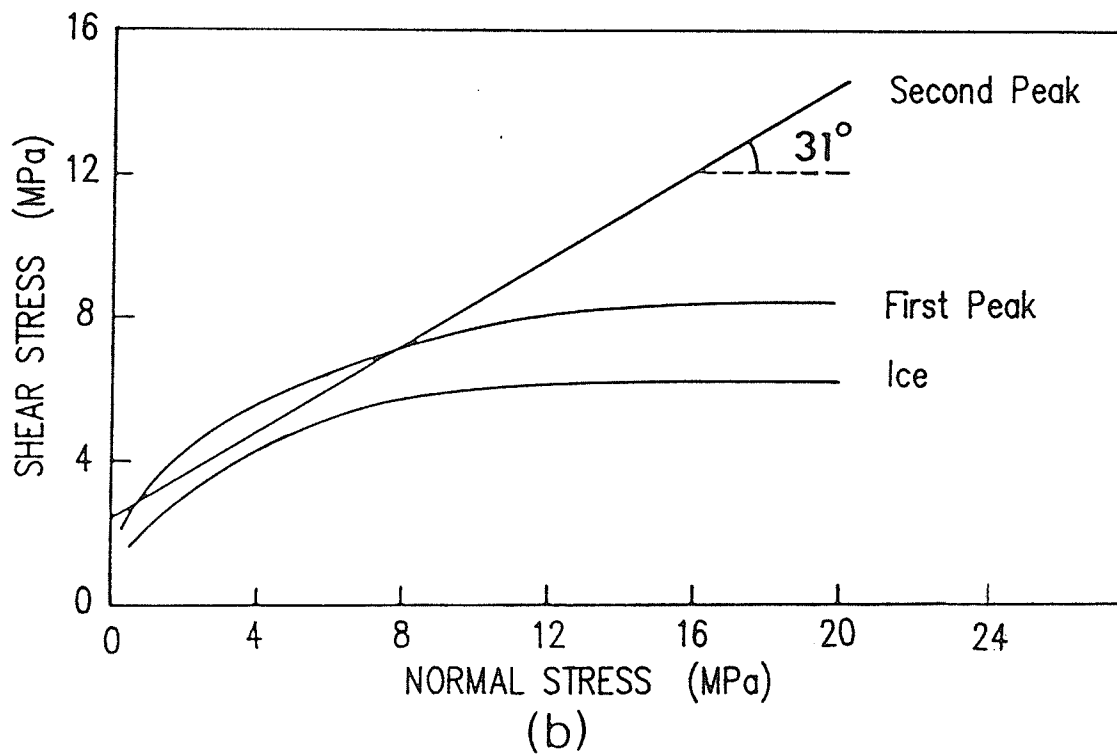
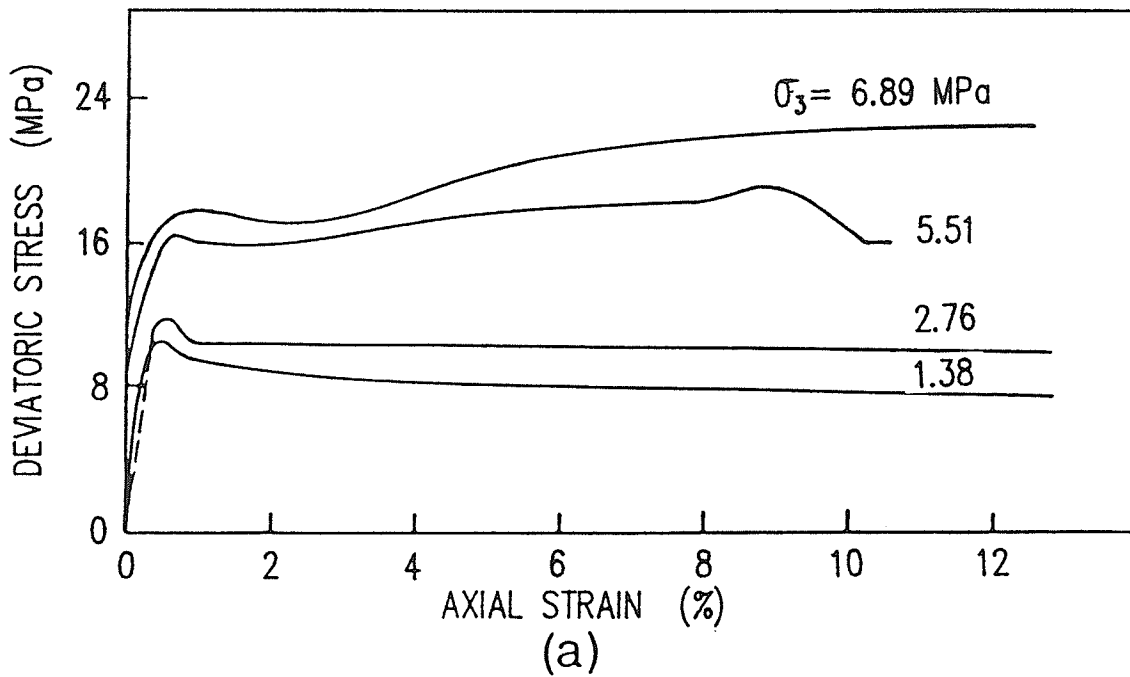


Figure 2.13 Results of axial compression tests with frozen Ottawa sand  
 (a) Stress-strain curve at different confining pressure  
 (b) Mohr's envelopes  
 (after Sayles, 1973)

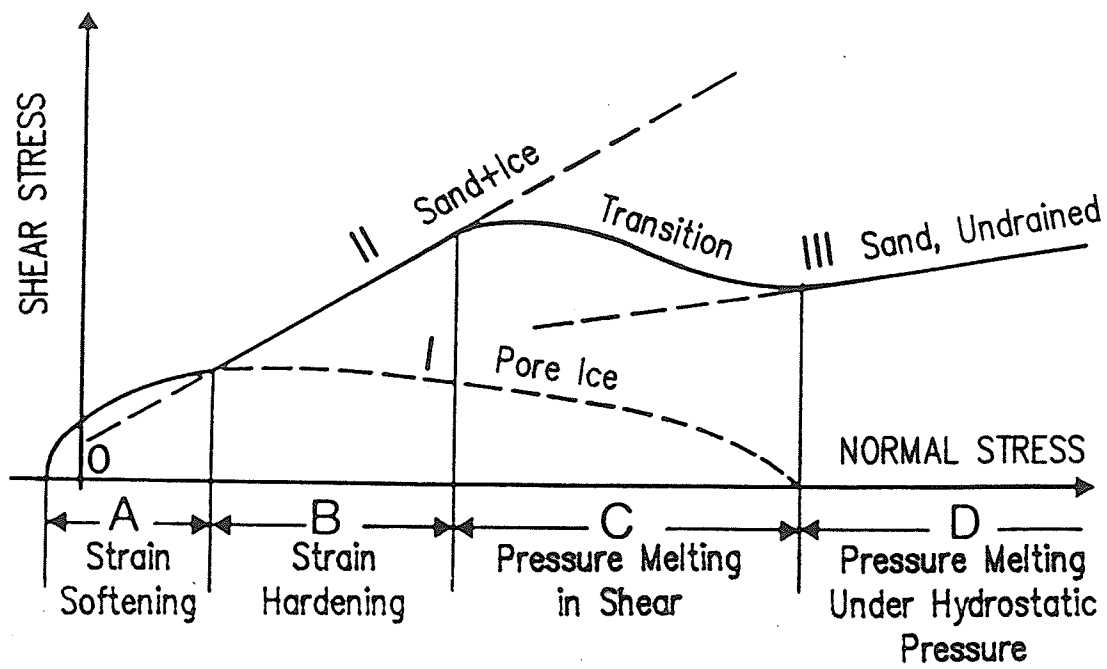


Figure 2.14 Schematic representation of the whole failure envelope for frozen Ottawa sand (after Chamberlain et al., 1972, and Sayles, 1973)

### 2.2.3.3 Effect of Temperature

Temperature has a marked influence on the behaviour of frozen soil. Any change in temperature alters the constitution of the frozen soil by changing the amount of unfrozen water content and influencing the strength of intergranular ice. Haynes and Karalius (1977) (Figure 2.15) observed that the uniaxial compressive strength increased with the lowering of temperature. The strength increase was dependent on the strain rate having higher strength with higher strain rate. The strain rate and temperature had very little effect on the tensile strength at temperatures lower than about  $-5^{\circ}\text{C}$  whereas the tensile strength increase was noticed between  $0^{\circ}\text{C}$  and  $-5^{\circ}\text{C}$ . Triaxial tests performed by Smith and Cheatham (1975) showed that with the increase in confining stress, the temperature dependence of strength decreased.

Andersland and AlNouri (1970) and Andersland and Douglas (1970) had tried to express the strength variation of frozen soils with temperature by means of Rate Process Theory and found the theory to be useful only if very high values of apparent activation energy are substituted into the equation.

Vyalov et al. (1962), Parameswaren (1980) and Bragg and Andersland (1980) have used power law to express variations of strength with temperature. A procedure for determining the parameters for the power law was given by Ladanyi (1972).

### 2.2.3.4 Effect of Strain Rate

Parameswaran (1980), Bragg and Andersland (1980) studied the

effect of strain rate on the uniaxial compressive strength of frozen sand. Figure 2.16 shows the stress-strain curve for a frozen sand at different strain rates at  $-10^{\circ}\text{C}$ . This shows that the peak strength increased with an increase in strain rate. Figure 2.17 plots the compressive strength against strain rates. The compressive strength increased with an increase in strain rate upto  $10^{-5}/\text{sec}$ . The strain rate higher than  $10^{-5}/\text{sec}$  had no effect on the compressive strength. Triaxial tests on the Ottawa sand by Sayles (1973) showed (Figure 2.18) that strain dependence of strength did not change appreciably as the confining pressure was increased.

#### 2.2.4 Deformation of Frozen Soil

Deformation behaviour of frozen soil depends on the pore ice which normally binds the grains together and fills most of the void spaces. Frozen soil, like ice, undergoes time-dependent deformation or creep under constant stress. Experimental evidence from literature shows that upon application of a deviatoric stress, the frozen soil shows an elastic deformation followed by a stage of decelerating creep which gradually stabilizes and eventually starts accelerating depending on the stress level. Similar to that of ice, the entire creep process of the frozen soil can be described as primary creep or decelerating creep, secondary or steady state creep and tertiary or accelerating creep.

An external load causes stress concentration at the point of

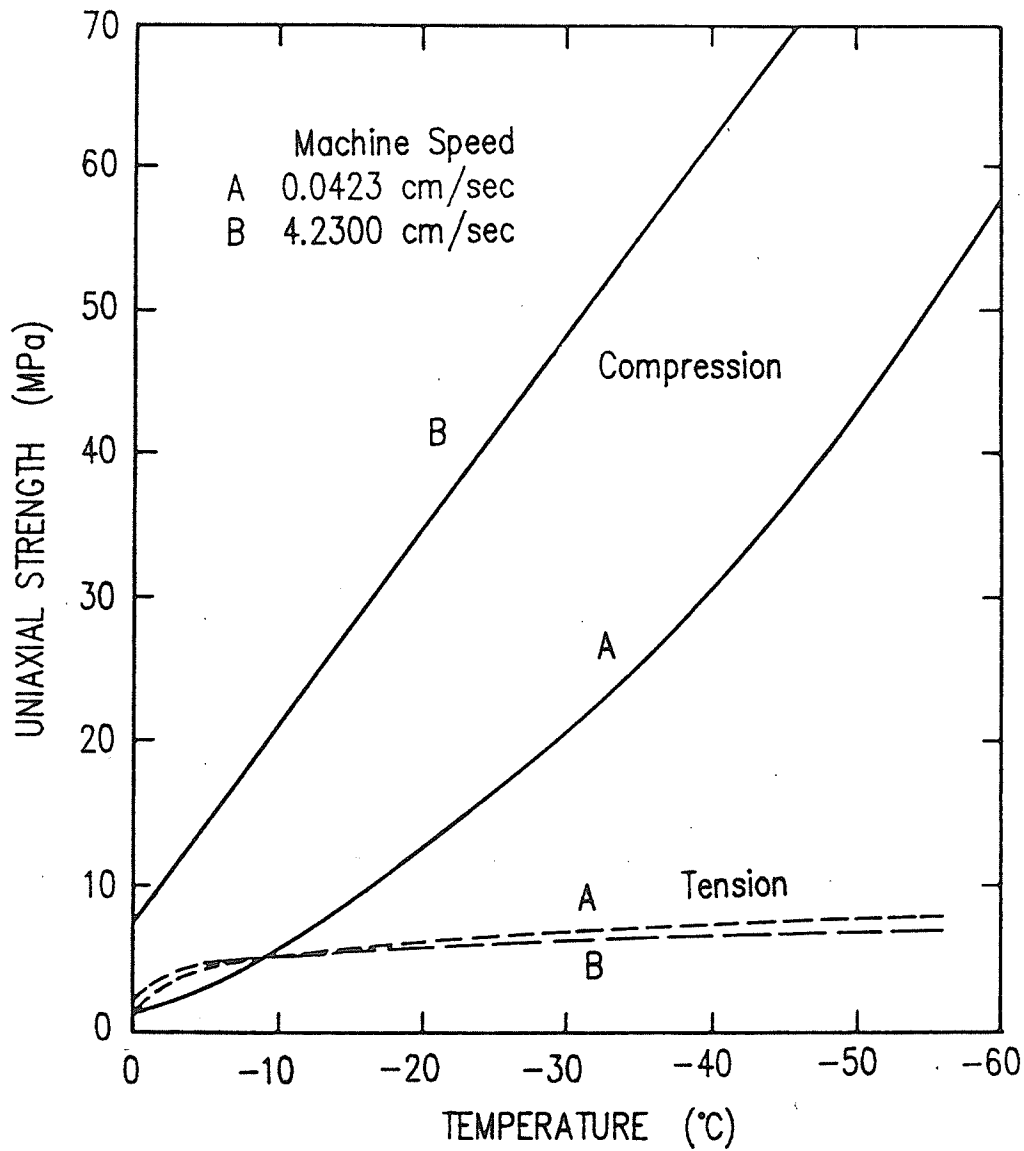


Figure 2.15 Average strength versus temperature for a frozen silt in uniaxial compression and tension tests (after Haynes and Karalius, 1977)

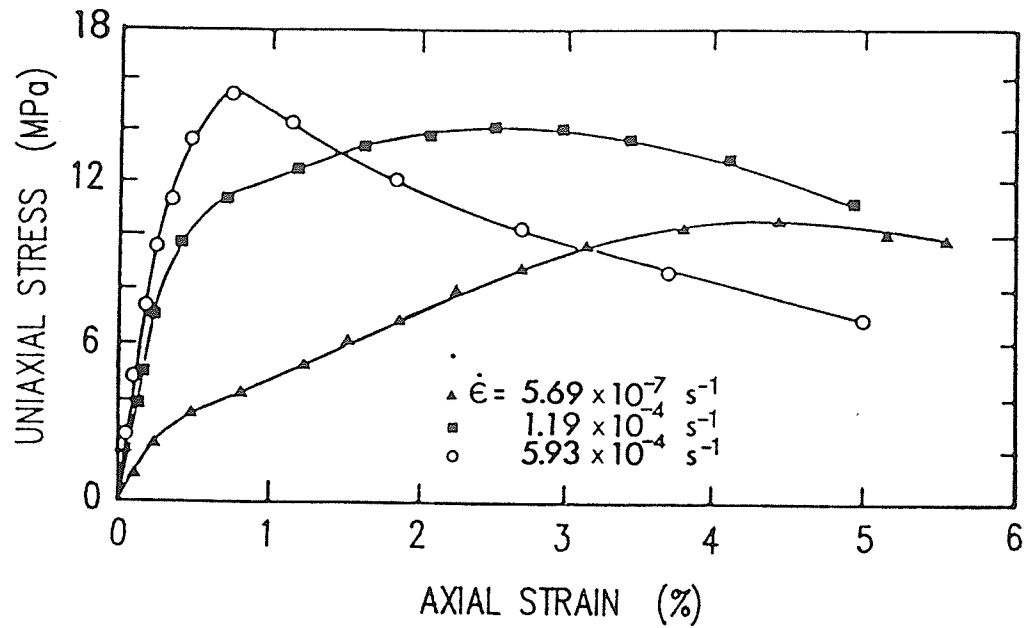


Figure 2.16 Typical stress-strain curve for frozen sand at different strain rates and tested at  $-10^{\circ}\text{C}$  (after Bragg and Andersland, 1980)

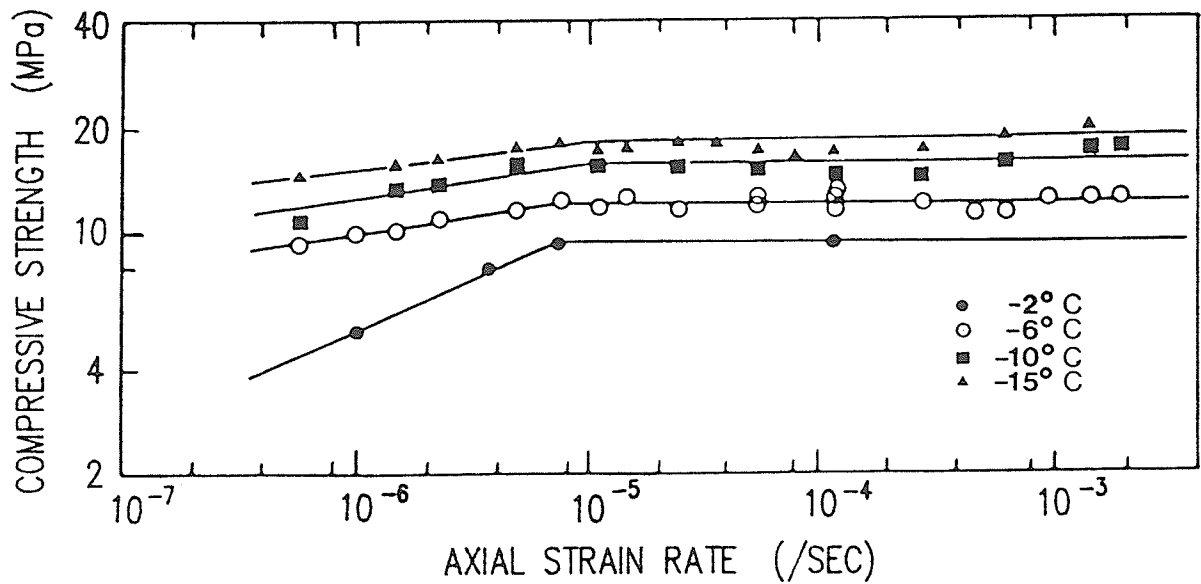


Figure 2.17 Compressive strength versus strain rate for a frozen sand at different temperature (after Bragg and Andersland, 1980)



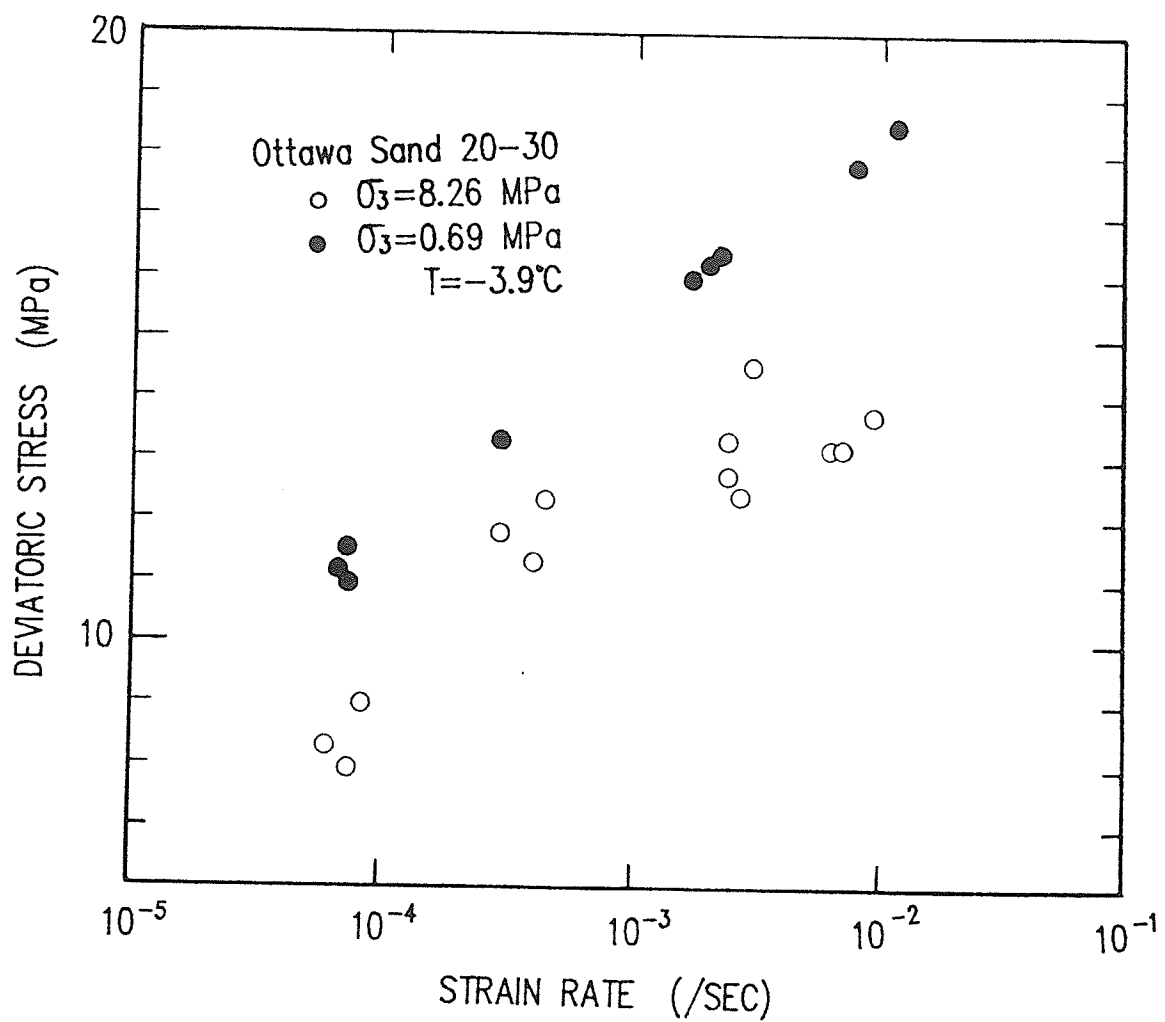


Figure 2.18 Effect of strain rate on the triaxial strength of frozen soils (after Sayles, 1973)

contact of the grains and develops stresses many times higher than the average stress calculated on the basis of the applied load. This causes plastic flow and melting of ice, and dynamic equilibrium is disturbed. The pore water caused by the melting of ice moves to lower stress points and refreezes. At the same time, ice cementation bond in the weaker spots yields and reorientation of the ice crystals and mineral particles takes place which tend to orient their basal planes parallel to the slide direction. This process, accompanied by reduction of shearing strength, denser packing of the mineral particles, increase in intermolecular bonds, build up of new ice cementation bonds, causes both strengthening and weakening. If the strengthening exceeds weakening, the deformation process is damped, but if weakening overcomes strengthening, prolonged and accelerating creep occurs.

#### 2.2.4.1 Effect of stress Level

Depending upon the stress level the deformation of frozen soil includes instantaneous axial deformation followed by regions of primary, secondary and tertiary creep. Vyalov (1962) stated that at low stresses strengthening of frozen soil led to damped creep deformations whereas at higher stresses structural weakening led to increasing creep rate and subsequent failure. Plot of axial stress versus the reciprocal of temperature (Andersland and Akili, 1967, Figure 2.19) provided a graphical means for predicting creep rates for selected stresses and temperatures. Damped creep occurs below the region which has a creep rate of  $10^{-7}$ /sec. Strain rate versus time

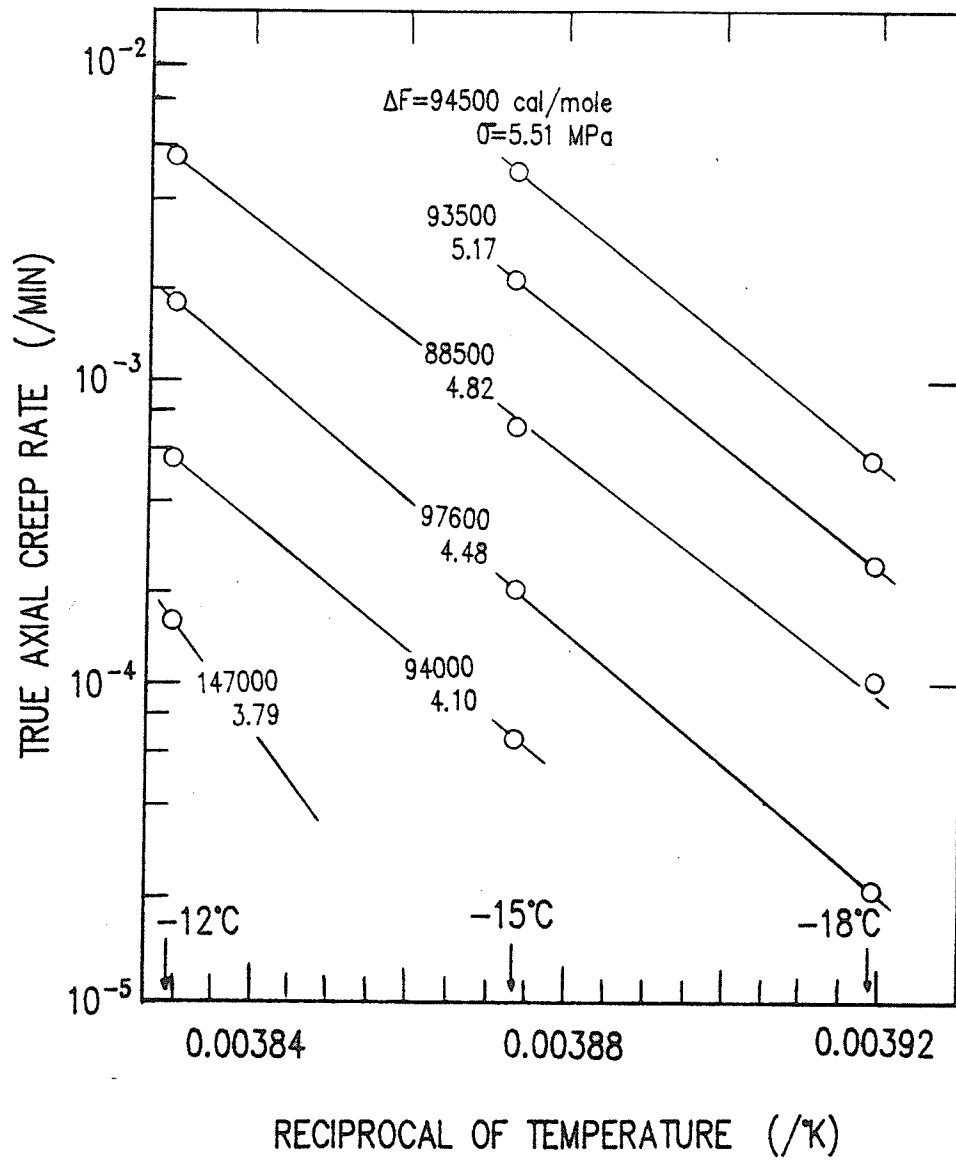


Figure 2.19 True axial creep rate as a function of reciprocal of temperature (after Andersland and Akili, 1967)

for various stress level are plotted in Figure 2.20 using data obtained by Rein et al. (1975) from unconfined compression tests on Ottawa sand at -8.5°C. This shows that at each stress level the strain rate reached a minimum value before further acceleration. Assur (1980), Mellor and Cole (1982) and Martin et al. (1981) reported that creep failure occurred when creep rate reached its minimum creep rate. It is observed from the above plot that the time to minimum creep rate increases with the decrease in stress level. Based on Vyalov's power law equation Ting (1983) expressed the minimum creep rate as:

$$\dot{\epsilon}_m = \dot{\epsilon}_c \left( \frac{\sigma_1}{\sigma_c} \right)^n \quad (2.5)$$

in which  $\dot{\epsilon}_m$  = minimum creep rate  
 $\dot{\epsilon}_c$  = arbitrary normalizing strain rate at stress level,  $\sigma_c$   
 $\sigma_1$  = applied stress  
 $n$  = material property

Rein et al. (1975) suggested that possibly for every material there was a stress level below which damped creep behaviour might be present. This stress level might possibly be defined as the limiting long term strength of the material.

#### 2.2.4.2 Effect of Temperature

The creep behaviour of frozen soil is extremely sensitive to temperature. The ice and unfrozen water ratio in the frozen soil matrix is not a constant but changes with temperature and consequently

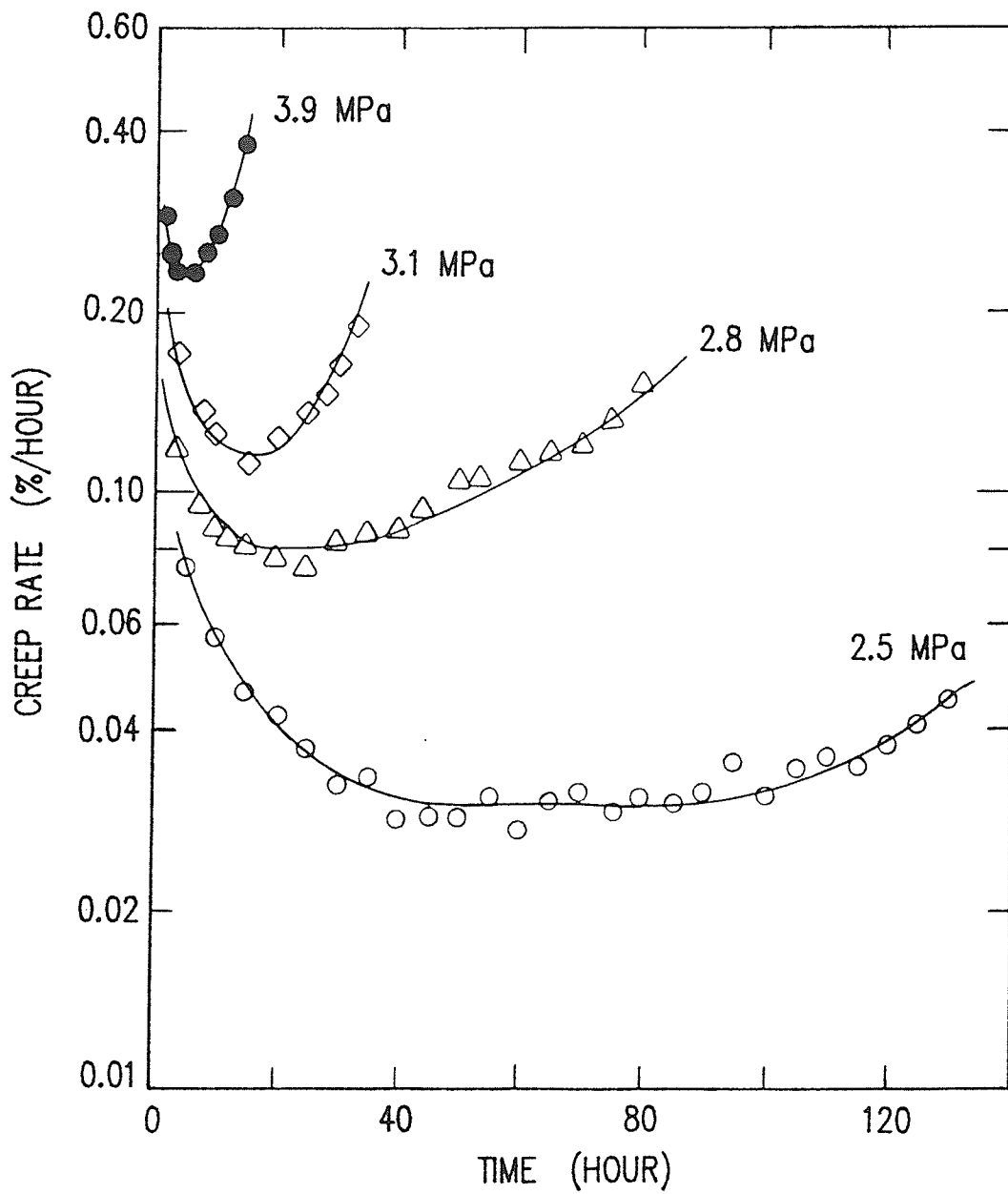


Figure 2.20 Creep rate as a function of time (after Rein et al., 1975)

changes the matrix of the frozen soil and thereby its behaviour. The plot of minimum strain rate in log scale against the reciprocal of applied stress at various temperature in Figure 2.21 (Yalin and Carbee, 1983) shows that as the temperature decreases the applied stress increases for the same minimum strain rate. From Figure 2.22, time to failure against reciprocal of stress, it is observed that time to failure increases with the decrease in temperature with the stress remaining constant. They have expressed the relationship as :

$$\dot{\epsilon}_m = \dot{\epsilon}_c \exp\left(-K \left( \frac{1}{\sigma} - \frac{1}{\sigma_c} \right)\right) \quad (2.6)$$

$$\dot{\epsilon}_m = c t_m^{-n} \quad (2.7)$$

where  $\dot{\epsilon}_c$  = critical creep rate

$\sigma_c$  = critical creep strength

$\dot{\epsilon}_m$  = minimum creep rate

$t_m$  = time to reach minimum creep strain

$c, n$  = material constant

$K$  = function of temperature =  $125.7 \theta^{1.1}$  for silt

Martin et al. (1981) observed similar behaviour when testing Manchester fine sand under uniaxial compression. It is evident from all these that the frozen soil is far more temperature sensitive than ice. This extreme sensitivity to temperature results in experimental problems and comparison of results from various sources.

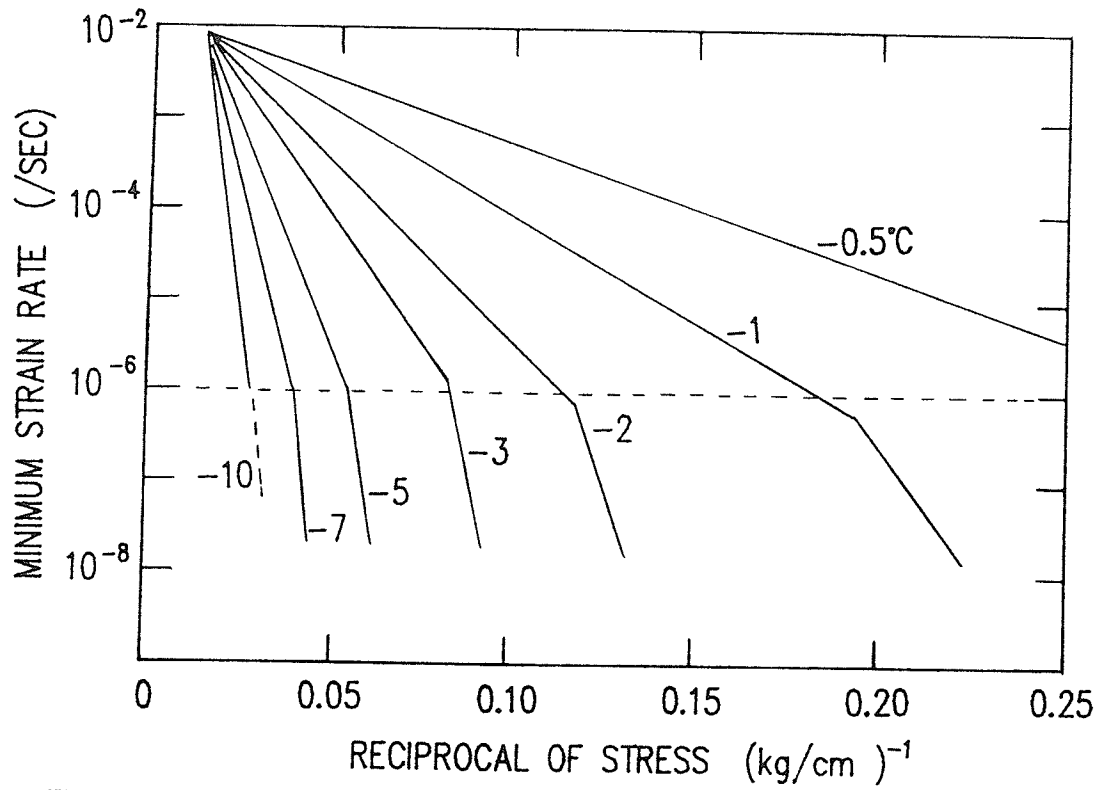


Figure 2.21 Log of minimum strain rate versus reciprocal of axial stress (after Yalin et al., 1983)

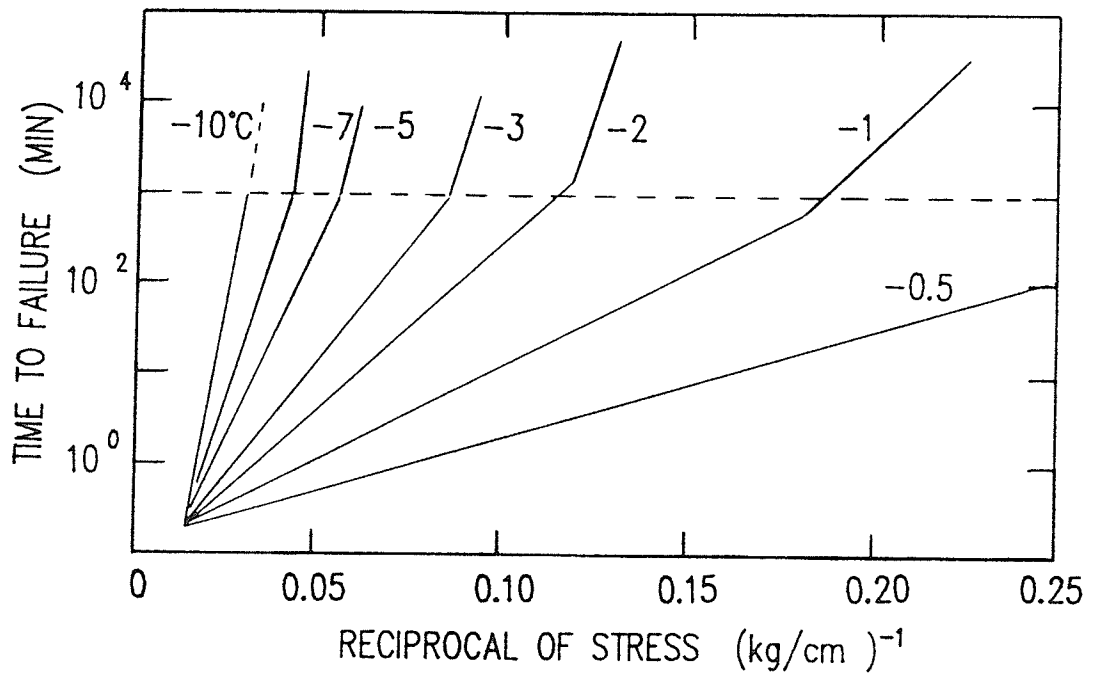


Figure 2.22 Log of time to failure versus reciprocal of axial stress (after Yalin et al., 1983)

#### 2.2.4.3 Effect of Confining Stress

Consistent with other structured materials, the strength of frozen soil increases with increase in confining pressure and thereby the creep rate under any deviatoric stress decreases. A set of creep curves for Ottawa sand at constant axial stress and different confining pressures are shown in Figure 2.23 (Sayles, 1973). It is evident from the curves that for the same deviatoric stress of 4.13MPa damped creep occurs at the confining pressure of 5.5 MPa whereas accelerated creep occurs at the confining pressure of 1.38 MPa.

Alkire and Andersland (1973) and Andersland and AlNouri (1970) studied the effect of confining pressure on the creep behaviour of Ottawa sand. They related the strain rate with the deviatoric stress and the octahedral stress by the following equation.

$$\dot{\epsilon} = c \exp(n(\sigma - \sigma_3)) \exp(-m\sigma_{oct}) \quad (2.8)$$

where  $\sigma_{oct} = (1/3)(\sigma_1 + \sigma_2 + \sigma_3)$  and  $c$ ,  $m$  and  $n$  are constants.

#### 2.2.5 Quantitative Models of Strength and Deformation of Frozen Sand

All existing creep theories of frozen soils had their roots in theories originally developed for metals of which strains are usually taken to be small and upon which a superimposed hydrostatic stress hardly has any effect.



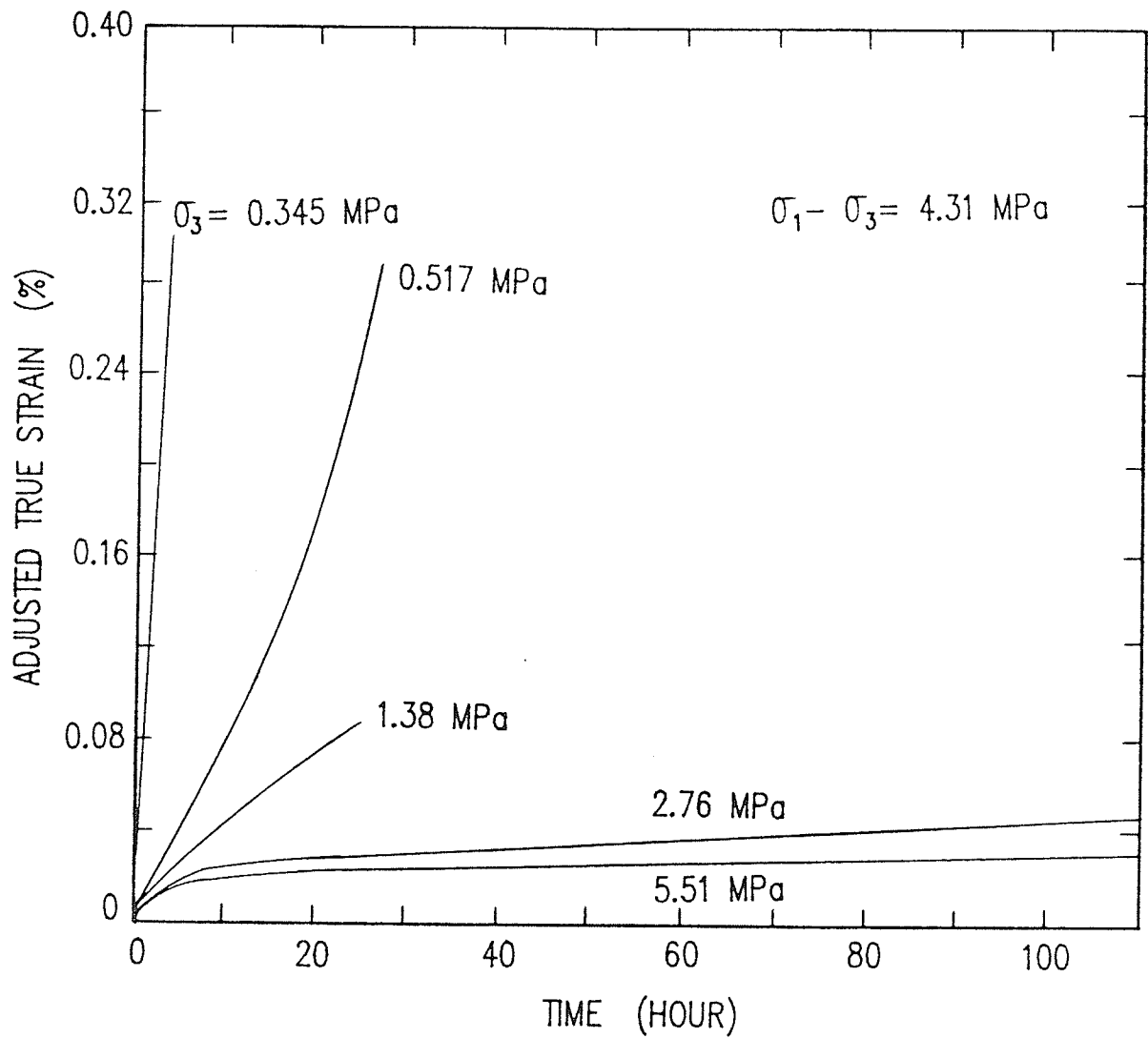


Figure 2.23 Creep curves for frozen Ottawa sand at constant axial stress and different confining pressure (after Sayles, 1973)

Andrade (1910) demonstrated that the tensile creep, of several pure metals and a selection of alloys, under constant load could best be represented by :

$$L = L_0(1+\beta t^{1/3}) \exp(kt) \quad (2.9)$$

where  $L$  is the length of the specimen at time  $t$  under a constant stress and  $L_0$  is the initial length immediately before loading. Andrade found that the constant  $k$  and  $\beta$  increased in roughly analogous fashion with stress and temperature.

Bailey (1929) and Norton (1929) expressed the creep law in the form of simple power law :

$$\dot{\epsilon} = \frac{1}{\gamma} \left( \frac{\sigma}{\sigma_n(T)} \right)^{n(T)} \quad (2.10)$$

where  $\dot{\epsilon}$  = creep rate

$\sigma_n(T)$  = a suitable function of temperature

$\gamma$  = a fixed standard time unit introduced to give the creep

stress  $\sigma_n$  the dimension of stress

$n$  = a creep exponent ( $n \geq 1$ )

Odqvist and Hult (1962), based on the power law, generalized the creep equation, for uniaxial and multiaxial states of stress, of nondamped creep behaviour of metals. They expressed the steady state creep rate in terms of equivalent strain rate and stress assuming the validity of Von Mises plasticity rule and the volume constancy for all

plastic deformation including creep deformation.

$$\dot{\epsilon}_e = \epsilon_c \left( \frac{\sigma_e}{\sigma_c} \right)^n \quad (2.11)$$

where  $\dot{\epsilon}_e$  = equivalent strain rate

$\sigma_e$  = equivalent stress

$\epsilon_c$  &  $\sigma_c$  = temperature dependent creep parameter

$n$  = creep exponent

For axially symmetric state the equivalent stress is replaced by  $(\sigma_1 - \sigma_3)$ .

Vyalov (1962) proposed a primary creep model representing the total strain as the sum of the initial strain,  $\epsilon_0$ , and the time dependent strain,  $\epsilon(t)$ .

$$\epsilon = \epsilon_0 + \epsilon(t) \quad (2.12)$$

For negligible initial strain,  $\epsilon_0$ , the total strain may be approximated to :

$$\epsilon = \epsilon(t) = \left( \frac{\sigma t^\lambda}{w(\theta + \theta_0)^k} \right)^{1/m} \quad (2.13)$$

where  $\theta$  = negative temperature ( $^{\circ}\text{C}$ )

$\theta_0$  = reference temperature usually  $-1^{\circ}\text{C}$

$w, k, \lambda, m$  = soil parameters

The strain rate may be written by differentiating the equation (2.13) with respect to time :

$$\dot{\epsilon} = \frac{\lambda}{m} \left( \frac{\sigma}{w(\theta + \theta_0)^k} \right)^{1/m} t^{(\lambda - m)/m} \quad (2.14)$$

The equation (2.14) confirms that the strain rate decreases with time and hence the equation (2.13) is indeed a primary creep model.

Vyalov (1978) proposed another equation for frozen soil in the prefailure state where he has taken into account of the effect of mean normal stress.

$$\epsilon_{\infty} = \left( \frac{c_{\infty}}{B} \right)^{1/m} \left( \frac{\sigma_m t^{\alpha}}{c_{\infty} + \sigma_m + \tan \phi_{\infty}} \right) \quad (2.15)$$

where  $c_{\infty}$  = temperature dependent adhesion at  $t = \infty$

$\phi$  = internal friction angle at  $t = \infty$

$m$  = creep exponent

$B = w(1 + \theta)^k$  = temperature dependent experimental parameter

$\alpha$  = material characteristic

Odqvist (1966) proposed a creep model as given by equation (2.16) for multiaxial states of stress based on the total deformation theory which is particularly suitable to describe behaviour of material in the secondary stage of creep, taking account of primary creep with

its total amount as correction.

$$\frac{d\varepsilon_{ij}}{dt} = -\frac{3}{2} \left( \frac{d\sigma_e}{dt} \left( \frac{\sigma_e}{\sigma_c} \right)^{n-1} \frac{S_{ij}}{\sigma_e} \right) + \left( \frac{\sigma_e}{\sigma_c} \right)^{n-1} \frac{S_{ij}}{\sigma_e} \quad (2.16)$$

where  $\sigma_e$  = equivalent stress

$\sigma_c$  = proof stress

$S_{ij}$  = stress deviator tensor

$\sigma_c, n, n$  = material constant

$\frac{d\varepsilon_{ij}}{dt}$  = creep rate tensor

The above equation (2.16) is founded on the following hypotheses :

- i) material is incompressible
- ii) creep rate is independent of superimposed hydrostatic pressure
- iii) existence of a flow potential
- iv) material is isotropic
- v) Norton's law holds in the special case of uniaxial stress

Ladanyi (1972) proposed a secondary creep model adapted from the theory of Odqvist (1966) and Hult (1962). At constant temperature and stress Ladanyi expressed strain as :

$$\varepsilon = \varepsilon_{ie} + \varepsilon_{ip} + \varepsilon_c \quad (2.17)$$

where  $\epsilon_{ie}$  = pseudo-instantaneous elastic strain  
 $\epsilon_{ip}$  = pseudo-instantaneous plastic strain  
 $\epsilon_c$  = creep strain

The pseudo-instantaneous elastic and plastic strains are the functions of stress and temperature. The creep strain rate may be described by :

$$\frac{d\epsilon_c}{dt} = G(\sigma, T) = \epsilon_c \left( \frac{\sigma}{\sigma_c(T)} \right)^{n(T)} \quad (2.18)$$

where  $\epsilon_c$  = arbitrary strain rate corresponding  $\sigma_c(T)$  (proof stress)  
 $n$  = material constant  
 $\sigma$  = applied stress

The equation (2.17) for a given material at a constant temperature is replaced by :

$$\epsilon = \frac{\sigma}{E} + \epsilon_k \left( \frac{\sigma}{\sigma_c} \right)^k + t \dot{\epsilon}_c \left( \frac{\sigma}{\sigma_c} \right)^n \quad (2.19)$$

where the first term in the equation (2.19) represents pseudo-instantaneous elastic strain, the second term plastic strain and the third term creep strain. Experimental evidence in frozen soils shows that for a time interval greater than about 24 hours the two instantaneous strain terms together constitute less than 10 percent of the total creep strain (Vyalov, 1959).

For a period longer than about one day it may be sufficient for practical purposes to retain only the third term in the equation (2.19), i.e.

$$\varepsilon = t \dot{\varepsilon}_c \left( \frac{\sigma}{\sigma_c} \right)^n \quad (2.20)$$

Ladanyi expressed the equation (2.20) in terms of strain rate and mean normal stress in the case of multiaxial state of stress :

$$\varepsilon = \dot{\varepsilon}_c \left( \frac{(f+2)(\sigma_1 - \sigma_3) - 3(f-1)\sigma_m}{3\sigma_{cu}f(\theta)} \right)^n \quad (2.21)$$

where

$$f(\theta) = \left( 1 + \frac{\theta}{\theta_c} \right)^w$$

$$f = \frac{1 + \sin\phi}{1 - \sin\phi}$$

$$\sigma_m = \frac{1}{3}(\sigma_1 + \sigma_2 + \sigma_3)$$

$\dot{\varepsilon}_c$  = arbitrary strain rate

$\sigma_{cu}$  = value of  $\sigma_c$  at  $\varepsilon_c$  in compression test

The equation (2.21) assumes full mobilization of internal friction over the whole region of pre-failure state which leads to a non-zero strain rate at zero stress difference. Therefore the application of the equation (2.21) should be limited either to strain close to failure or to those contained within a narrow range of mobilization of internal friction.

Odqvist (1966) and Hult (1962) in effect regarded a metal in

stationary creep as an incompressible generalized Newtonian fluid whose viscosity function obeys the power law; when solving boundary value problem they often added the assumption of small deformations so that the stretching tensor (rate of strain) could be replaced by time derivative of the infinitesimal strain tensor. Although Ladanyi made adhoc modifications to account for the effect of hydrostatic pressure, he implicitly adopted the assumption of small deformations when employed the infinitesimal strain tensor and its time derivative in all his formulations.

Andersland and AlNouri (1970) proposed a creep equation based on exponential form serving the same general purpose as equation (2.21) :

$$\dot{\epsilon}_c = \frac{A \exp(N(\sigma_1 - \sigma_3))}{F(T) \exp(m\sigma_m)} \quad (2.22)$$

where  $F(T) = \exp(L/T)$

$L = U/R$

$U =$  activation energy

$T =$  absolute temperature

$R =$  universal gas constant

and  $A$ ,  $N$  and  $m$  are experimental parameters.

Goughnour and Andesland (1968) proposed a constitutive equation to model the entire creep phenomenon including the accelerating or tertiary creep :



$$\dot{\epsilon}_p = \frac{K_1}{\sqrt{t}} \exp(-n_1\sqrt{t}) + K_2 \exp(n_2 t) \quad (2.23)$$

where all the four soil parameters  $n_1$ ,  $n_2$ ,  $K_1$ , and  $K_2$  are functions of both stress and temperature and  $\epsilon_p$  is the plastic strain rate. The first term represents strain hardening and the second term represents strain softening which is dependent on the adsorbed strain energy. They observed that the influence of the hardening term became negligible with increasing axial strain. Goughnour and Andersland reported excellent correlations between their model and data obtained on Ottawa sand

Ting (1983) proposed a simple empirical tertiary creep model for frozen sand, based on the model proposed by Assur (1979) for polycrystalline ice, of the form :

$$\dot{\epsilon} = A \exp(\beta t) t^{-m} \quad (2.24)$$

where  $A$ ,  $\beta$  and  $m$  are experimentally determined constant defined as :

$$\beta = \frac{\ln(\dot{\epsilon}_0/\dot{\epsilon}_m)}{t_m \ln(t_m/t_0) + (t_0 - t_m)} \quad (2.25)$$

$$m = \beta t_m \quad (2.26)$$

$$A = \frac{\dot{\epsilon}_0 t_0^m}{\exp(\beta t_0)} \quad (2.27)$$

where  $\dot{\epsilon}_m$  = minimum strain rate

$t_m$  = time to minimum strain rate

$\epsilon_m$  = strain at minimum strain rate

$\epsilon_0$  = strain at some initial nonzero time  $t_0=1$  min

$\dot{\epsilon}_0$  = strain rate at initial time  $t_0$

Ting reported excellent correlation between his model and data on Manchester fine sand.

Gardner (1984), based on the constitutive equation proposed by Assur (1979) for polycrystalline ice, proposed a new equation which gave a good estimate of both creep strain and strain rate for the whole creep curve with an excellent fit up to inflection point. This equation is expressed as :

$$\frac{\epsilon_c}{\epsilon_m - \epsilon_0} = \left(\frac{t}{t_m}\right)^c \exp\left[\left(\sqrt{c} - c\right)\left(\frac{t}{t_m} - 1\right)\right] \quad (2.28)$$

where  $c$  is the dimensionless parameter describing the shape of the curve and  $\epsilon_m$  is the strain at  $t_m$  which is the time to reach minimum creep rate.  $\epsilon_0$  is the initial strain and  $\epsilon_c$  is the creep strain.

Yalin and Carbee (1983) proposed an equation of the following form which they claimed could describe the entire creep curve.

$$\epsilon(t) = \epsilon_0 + \frac{\epsilon_c}{e^{\beta} t_m^{\beta-1}} \left(\frac{t}{t_m}\right)^{1-\beta} \exp(\beta t/t_m) \left[ \frac{1}{(1-\beta)} - \frac{\beta t/t_m}{(1-\beta)(2-\beta)} + \frac{(\beta t/t_m)^2}{(1-\beta)(2-\beta)(3-\beta)} \right] \quad (2.29)$$

where  $\epsilon_0$  = instantaneous strain

$\beta = 0.33$  when  $t_m < 30$  min.

$\beta = 0.23t_m^{0.11}$  when  $t_m \geq 30$  min.

$t_m$  = time to reach minimum strain rate

$\epsilon_x = \dot{\epsilon}_m t_m^n$ .

Although the creep models in the literature can describe a variety of creep behaviour, there is no comprehensive theory which considers creep rupture and eventual failure of the specimen during creep. In most cases long term strength models, which take into account the ruptures and failures, are described separately in the literature.

It is known that frozen soil flows, even under small stresses, if we consider this process on geologic time scale. The limiting long term strength for all practical purposes may be defined as the strength below which creep rupture or excessive deformation do not occur and reduction of strength with time become insignificant.

Vyalov (1962, 1966, 1973) described the long term strength of frozen soil by :

$$\sigma_{\epsilon} = \frac{\beta}{\ln[(t_x + t^*)/B]} \approx \frac{\beta}{\ln(t_x/B)} \quad (2.30)$$

where  $\beta$  and  $B$  = temperature dependent soil parameters

$t_x$  = time to failure

$\sigma_{\epsilon}$  = long term strength

$$t^* = B \exp(\beta/\sigma_1)$$

$\sigma_1$  = instantaneous reference strength

Andersland and AlNouri (1976) observed that the confining pressure had little influence on the ultimate shear strength of frozen clay and that the long term angle of internal friction was found to be zero. An increase in shear strength occurred with the increase in normal stress for sand-ice system giving a long term value of  $\phi=25.1^\circ$ . This value of  $\phi$  was less than that would be expected for dry Ottawa sand with the same density. Parameswaran and Jones (1981) found that the angle of internal friction in frozen sand under confining pressure up to 90 MPa was only  $12.4^\circ$ ; compared to  $37^\circ$  in unfrozen sand.

Sayles (1973) and Rogensack and Morgenstern (1978) suggested that the envelope for the frozen sand approached that of the unfrozen sand with time. Figure 2.24 shows that 3.2 hour and 22 hour envelopes are curved while 60 hour envelope is a straight line. The curved envelope for the shorter period of time indicates that the strength and the friction between the ice crystals dominate the strength of soil mass. The 60 hour straight line envelope suggests that the frictional resistance of the sand grains dominates the strength of the sand over long period. Sayles emphasized that for all practical purposes Mohr-Coulomb's expression (equation, 2.31) could be used for long term strength of sand with low ice contents.

$$\tau = c + \sigma_n \tan \phi \quad (2.31)$$

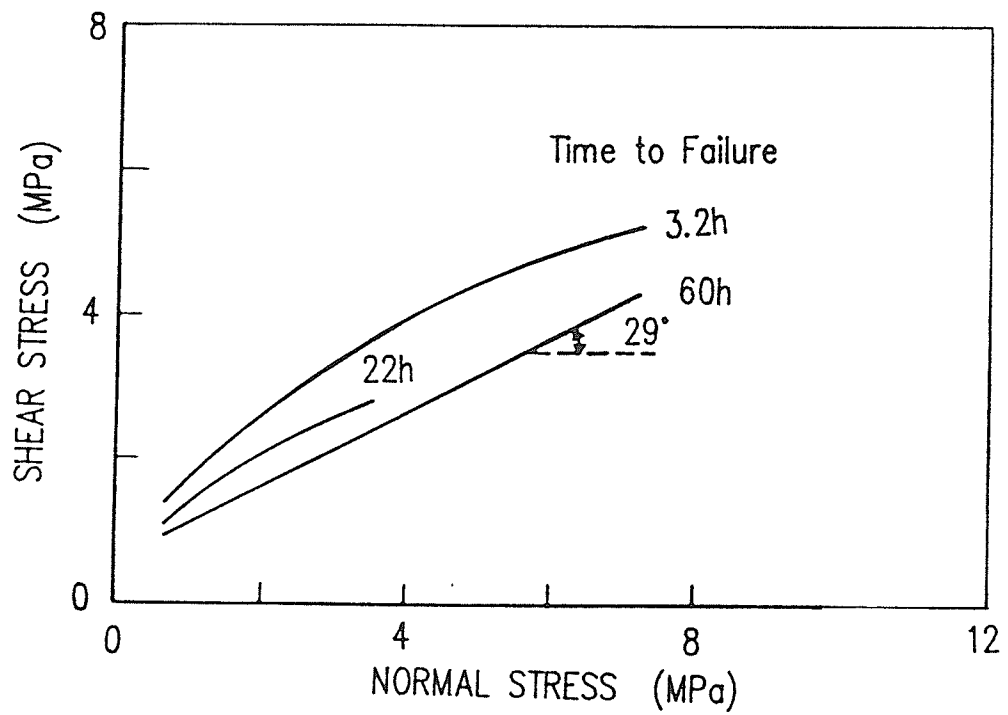


Figure 2.24 Mohr's envelopes for creep strength of Ottawa sand at  $-3.85^{\circ}\text{C}$  (after Sayles, 1973)

where  $c$  = cohesion

$\sigma_n$  = normal stress

$\phi$  = angle of internal friction

Assuming the long term angle of internal friction for frozen sand is approximately equal to the friction angle of unfrozen sand, the strength of frozen sand according to equation (2.31) decreases with time due to a decrease in apparent cohesion.

Ladanyi (1972) expressed the strength at failure by :

$$(\sigma_1 - \sigma_3)_f = \sigma_{fu}(t, 0) + \sigma_3(f-1)(\dot{\epsilon}_f / \dot{\epsilon}_c)^{1/n} \quad (2.32)$$

where  $\sigma_1$  = major principal stress

$\sigma_3$  = minor principal stress

$\sigma_{fu} = \sigma_{cu0}(\dot{\epsilon}_f / \dot{\epsilon}_c)^{1/n} f(0)$

$\dot{\epsilon}_f$  = strain rate at failure

$\dot{\epsilon}_c$  = arbitrary strain rate

$$f = \frac{1 + \sin \phi}{1 - \sin \phi}$$

This equation implies a time dependent angle of friction if  $\epsilon_f$  is kept constant or  $\epsilon_f$  increases linearly with time, if the angle of friction is made independent of time. A simpler form may be obtained if only the strength and not the whole stress-strain behaviour is made dependent on normal pressure.

## 2.3 STRESS-STRAIN RELATIONSHIP

### 2.3.1 Deformation Parameters

The internal mechanical response of a material can be expressed in terms of stress and strains. The parameters which relate stresses and strains are generally defined as deformation parameters. For elastic, isotropic and homogeneous materials, it is necessary to know only two parameters, which may be either Young's modulus,  $E$ , and Poisson's ratio,  $\nu$ , or bulk modulus,  $K$ , and shear modulus,  $G$ , to express stress-strain relationships. Since the behaviour of frozen soil is nonlinear and dependent on time, temperature, stress state, ice and unfrozen water content and other sample variations, the deformation parameters,  $E$  and  $\nu$ , or  $K$  and  $G$ , are functions of these variables. Because of the complexity of the problem, previous researchers in the past have chosen to express axial strain as a function of the above variables and very little effort has been made to evaluate any of the deformation parameters for the frozen soils. For the unfrozen soils, extensive investigations have been carried out to study mainly the dependency of deformation parameters on the state of stress. Most of the literature on deformation parameters for frozen soils is drawn from the unfrozen soil mechanics to demonstrate how the deformation parameters are evaluated for nonlinear materials. The solutions available in the literature for the stress dependent deformation parameters may be broadly classified into the following categories :

- i)  $E$  and  $\nu$  from triaxial compression tests

## ii) Direct determination of K and G

A brief review of each of the above methods is presented in the following sections.

### 2.3.1.1 E and $\nu$ from Triaxial Tests

Clough and Woodward (1967), based on the standard triaxial test, expressed the Young's modulus, E, and Poisson's ratio,  $\nu$ , by the following :

$$E = \frac{(\sigma_1 - \sigma_3)_i - (\sigma_1 - \sigma_3)_{i-1}}{(\epsilon_1)_i - (\epsilon_1)_{i-1}} \quad (2.33)$$

$$\nu = \frac{-1 + \sqrt{1 - 8((E/2K) - 1)}}{4} \quad (2.34)$$

where  $(\sigma_1 - \sigma_3)$  = principal stress difference

$\epsilon_1$  = axial strain

i = stage of increment of loading

K = bulk modulus assumed constant during loading

Skermer (1973) used the following expression in the finite element analysis of E. L. Infernillo dam.

$$E = \frac{d}{d\epsilon_1} (\sigma_1 - \sigma_3) \quad (2.35)$$

$$\nu = \frac{1}{2} \left( 1 - \frac{d\epsilon_v}{d\epsilon_1} \right) \quad (2.36)$$



where  $\frac{d}{d\varepsilon_1} (\sigma_1 - \sigma_3)$  = instantaneous slope of the curve  $(\sigma_1 - \sigma_3)$  vs  $\varepsilon_1$

$\frac{d\varepsilon_v}{d\varepsilon_1}$  = instantaneous slope of the vol. vs axial strain curve

Duncan and Chaung (1970) and Clough and Duncan (1971) had shown that the tangent modulus,  $E$ , and Poisson's ratio,  $\nu$ , could be approximated by some hyperbolic function where all the parameters were determined by triaxial tests.

#### 2.3.1.2 Direct Determination of $K$ and $G$

Newmark (1960) stated that it was often convenient to divide a general state of stress into two components : a) a state of hydrostatic stress accounting for the entire volumetric stress and strain and b) a deviator stress tensor accounting for shearing stress and strain.

Domaschuk and Wade (1969) proposed a method of obtaining  $K$  and  $G$ , by using isotropic compression test for  $K$ , and constant mean normal stress triaxial test for  $G$ . The basis of this approach is to separate the response under isotropic compression and under shearing stress. Data from triaxial tests on unfrozen soil (Konder and Zelasko, 1963), in which the mean normal stress was held constant, revealed that the stress-strain behaviour was nonlinear and was dependent on the magnitude of the mean normal stress.

Gill (1969), Liu (1970), and Stewart (1970) extended the

approach proposed by Domaschuk and Wade and obtained solutions for K and G for unfrozen Winnipeg clay. This approach was further developed by Valliappan (1974) for the Lake Agasis clay. Hanrahan (1985) followed the same approach of separating the stress system and obtained solutions for K and G for unfrozen soils.

The author's study is a continuation of the same approach with the objective of obtaining a generalized solution for K and G of the frozen sand. The parameters K and G are the functions of stress state, time, temperature, ice and unfrozen water content in addition to sample variation, grain size and other impurities. Because, K and G for frozen sand depend mainly on the creep behaviour, the parameters, henceforth will be defined as bulk creep function,  $K_c$ , and shear creep function,  $G_c$ . The theoretical considerations which form the basis of the direct determination of  $K_c$  and  $G_c$  are presented in the following sections.

### 2.3.2 Mean Normal and Deviatoric Components Stresses and Strains

The stress-strain relationship of a homogeneous, isotropic material exhibiting small strains when subjected to a general state of stress, can be expressed in terms of the bulk and shear moduli with tensor notations as follows :

$$\sigma_{ij} = K \epsilon_{kk} \delta_{ij} + 2G \left( \epsilon_{ij} - \frac{1}{3} \epsilon_{kk} \delta_{ij} \right) \quad (2.37)$$

where  $\sigma_{ij}$  = stress tensor  
 $\epsilon_{ij}$  = strain tensor  
 $\epsilon_{kk}$  = volumetric strain tensor  
 $\delta_{ij}$  = Kronecker delta  
 $K$  = bulk modulus  
 $G$  = shear modulus

Equation (2.37) can be separated into two components — one in terms of mean normal components and the other in terms of deviatoric components. The equation in terms of mean normal components is given by :

$$\sigma_{ii} = 3K\epsilon_{ii} \quad (2.38)$$

The equation in terms of deviatoric components is given by :

$$S_{ij} = 2G\left(\epsilon_{ij} - \frac{1}{3}\epsilon_{kk}\delta_{ij}\right) \quad (2.39)$$

where  $S_{ij}$  = deviatoric stress tensor  
 $(\epsilon_{ij} - (1/3)\epsilon_{kk}\delta_{ij})$  = deviatoric strain tensor

The deviatoric stress tensor can be expressed by :

$$S_{ij} = \sigma_{ij} - (1/3)\sigma_{kk}\delta_{ij} \quad (2.40)$$

in which  $(1/3)\sigma_{kk}$  is the mean normal stress.

The deviatoric stress tensor is a second order symmetric tensor and it is important to note that the first invariant of deviatoric stress tensor is always zero. The principal directions of the deviatoric stress tensor are the same as for the original stress tensor.

The general state of stress at a point may be represented by the three principal stresses and their direction cosines. The magnitude and direction of each of these principal stresses can be represented by vectors acting on the face of a cube of an element of soil, as shown in Figure 2.25. These principal stresses can be separated into components of mean normal stress and deviatoric stress. The mean normal stress,  $\sigma_m$ , which imposes a uniform stress on the element (Figure 2.25b), is the average of the three principal stresses. Subtracting the mean normal stress from each of the principal stress gives the deviatoric stress components  $S_1$ ,  $S_2$  and  $S_3$  as shown in Figure 2.25c. The three deviatoric stress components can be combined and represented by their resultant,  $S_d$ . The components of stresses,  $\sigma_m$  and  $S_d$ , are given by :

$$\sigma_m = \frac{\sigma_1 + \sigma_2 + \sigma_3}{3} \quad (2.41)$$

$$S_d^2 = S_1^2 + S_2^2 + S_3^2 \quad (2.42)$$

in which  $S_1 = \sigma_1 - \sigma_m$

$$S_2 = \sigma_2 - \sigma_m$$

$$S_3 = \sigma_3 - \sigma_m$$

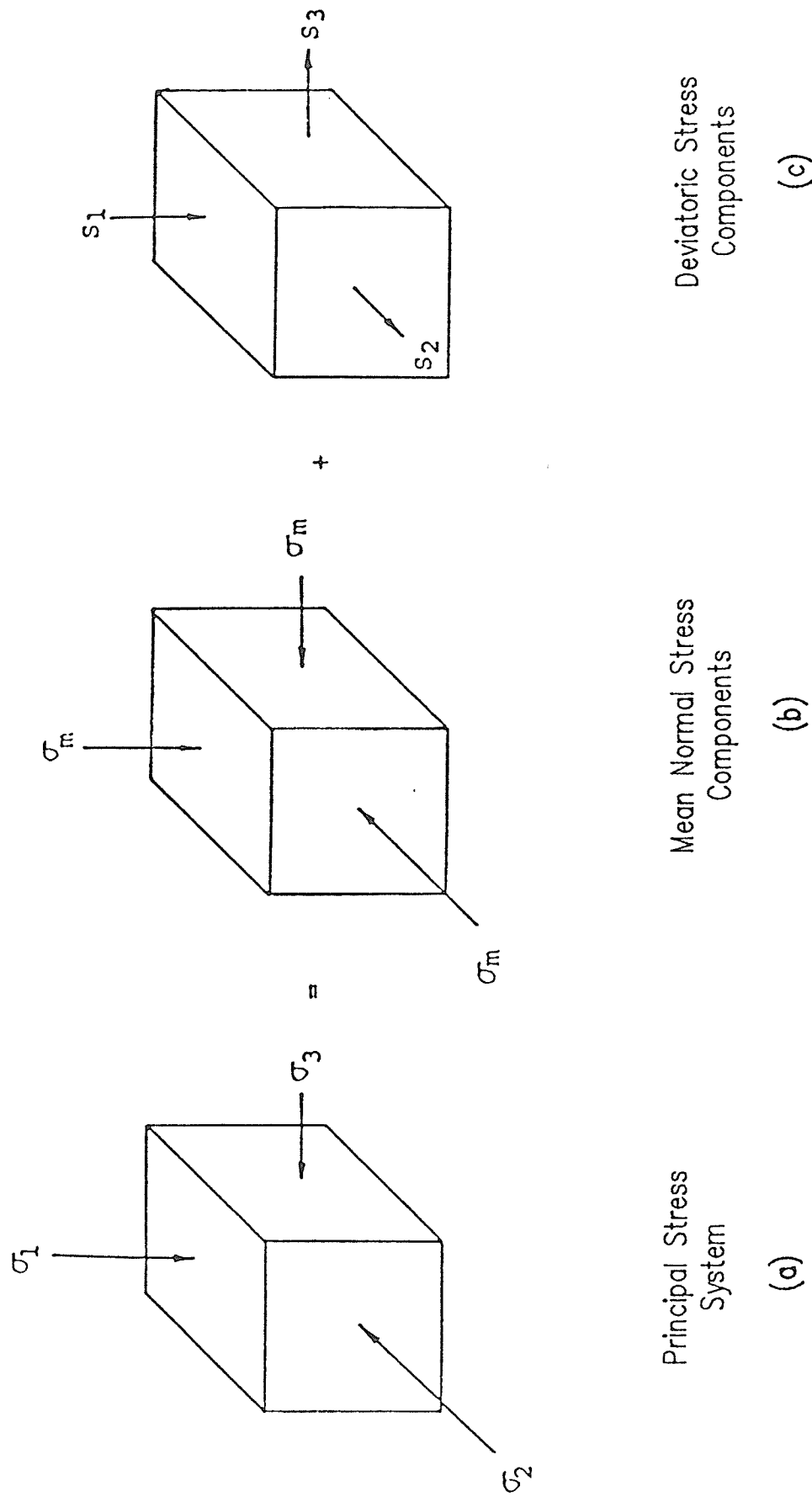


Figure 2.25 Nomenclature for stress system

The general state of strain in an element can be represented by the three components of principal strain and their direction cosines. This state of strain can further be separated into the volumetric strain associated with the mean normal stress and the deviatoric strain associated with the deviatoric components of the stress. As in the case of stress system, the mean normal strain,  $\epsilon_m$ , and the resultant deviatoric strain,  $\epsilon_d$ , are given by :

$$\epsilon_m = \frac{\epsilon_1 + \epsilon_2 + \epsilon_3}{3} \quad (2.43)$$

$$\epsilon_d = 2\sqrt{((\epsilon_1 - \epsilon_m)^2 + (\epsilon_2 - \epsilon_m)^2 + (\epsilon_3 - \epsilon_m)^2)} \quad (2.44)$$

In terms of mean normal stress and mean normal strain the equation (2.38) becomes :

$$\sigma_m = 3K\epsilon_m \quad (2.45)$$

The resultant deviatoric stress and strain components are related by the shear modulus,  $G$ , in accordance with the equation (2.46).

$$S_d = G\epsilon_d \quad (2.46)$$

Thus the stress-strain system at a point may be separated into two separate components, each associated with a distinct component of behaviour. For elastic solids there exists unique relationships between the parameters,  $K$  and  $G$ , and the parameters,  $E$  and  $\nu$ . It is

found in the literature that the experimental investigation to evaluate the parameters,  $E$  and  $\nu$  is not unique but varies with the application of stress system. The advantage, however, of using  $G$  and  $K$  rather than  $E$  and  $\nu$  is that the former moduli may be evaluated independently and may be more readily related to the stress system.

The parameters,  $G$  and  $K$  are simple, single valued quantities for a linear elastic material. For real materials, especially for the frozen sand, they are complex quantities which must be evaluated from the appropriate laboratory tests. In this study the elastic bulk modulus,  $K$ , will be replaced by bulk creep function,  $K_c$ , as a function of time, temperature, mean normal stress and ice content :

$$K_c = f(t, T, \sigma_m, i_c) \quad (2.47)$$

and the elastic shear modulus,  $G$ , by shear creep function,  $G_c$ , as a function of time, temperature, mean normal stress, resultant deviatoric stress and ice content :

$$G_c = f(t, T, \sigma_m, S_d, i_c) \quad 2.48)$$

**CHAPTER THREE**  
**LABORATORY INVESTIGATION**



## CHAPTER 3

### LABORATORY INVESTIGATION

#### 3.1 SCOPE OF INVESTIGATION

An understanding of the behaviour of frozen soils, under the changes of isotropic stress and deviatoric stress, is essential to the formulation of a valid constitutive law which establishes the relationship between the stresses and strains in the soil mass. The main objectives of the investigation were to obtain deformation moduli of frozen soils in functional form which would relate stresses, strains and time, and to understand the mechanics of frozen soil behaviour.

The testing program consisted of multi-stage isotropic creep tests, constant mean-normal-stress triaxial creep tests, and stress controlled constant cell pressure triaxial creep tests. A multi-stage isotropic creep test with isotropic pressures ranging from 50 to 300 kPa, was performed in order to establish a functional relationship for the bulk creep function. A total of 9 multi-stage constant mean-normal-stress triaxial compression creep tests were performed with mean normal stresses varying between 70 and 420 kPa, to establish a functional relationship for the shear creep function. A total of 4 multi-stage stress controlled constant cell pressure triaxial creep tests were performed to verify the model developed on the basis of the

isotropic and constant mean-normal-stress triaxial tests. The details of the tests are given in subsequent chapters.

A strict sample preparation technique as outlined in the following sections was followed using a quartz-carbonate sand in order to obtain as identical sample as possible. Low pressure ranges were used to simulate conditions normally observed in the field.

## 3.2 SAMPLE PREPARATION

### 3.2.1 Frozen Sand Sample

The frozen sand samples used in the investigation were prepared in the laboratory. A specific sample preparation technique outlined in the following sections was followed in an attempt to achieve samples with identical densities and water/ice contents.

The soil used was uniform, quartz-carbonate medium-grain sand with a uniformity coefficient ( $D_{60}/D_{10}$ ) of 2.0. The grain size distribution of the sand is shown in Figure 3.1. The sand had a specific gravity of 2.70.

Sample preparation involved three stages, namely, i) sand deposition, ii) saturation, and iii) freezing. These stages are described in the following sections.

### 3.2.1.1 Sand Deposition

A plexiglass split mold with two end caps, 76 mm in diameter and 200 mm in height (Figure 3.2) was first assembled and the inside of the mold was properly greased to avoid any bond between the sample and the mold. Care was taken to clean and place all the O-rings and seals in place to ensure air and water tight joints and connections. A saturated porous stone was set up, under water, on the base plate. The sand was poured into the mold through a free fall device at a constant rate, while maintaining a constant height of fall of 25 mm. The sand was filled to a height of 15 mm from the top of the mold. A porous stone was placed on top of the sand and the top cap was put into place. An approximately constant density with a maximum variation of 7 percent between samples was achieved and the technique was reproducible. The dry density ranged between 15.2 and 15.8 kN/m<sup>3</sup>.

### 3.2.1.2 Saturation

A schematic set-up of the saturation process is shown in Figure 3.3. All connections were checked and the water lines were saturated by circulating water through them. Deaired distilled water was used in the saturation process. Each sample was saturated under a vacuum pressure of 55 kPa applied at the top, with access to distilled water through a porous stone at the bottom. The water was supplied at a constant rate of 2 ml/min by adjusting the valve every 10 minutes. A burette, on line, was used to check the flow of water into the sample. This process allowed sufficient time to draw almost all the air from

within the specimen under a vacuum pressure of 55 kPa. This process of specimen saturation was achieved through experience and trial by the author and others who helped to develop the process.

At least 0.5 litres of additional water was circulated through the specimen to ensure further removal of any air bubbles entrapped in the sample. The whole process took about five hours. At the end of saturation, the water supply valve was closed and the suction was released very slowly. The top cap was removed and the water level in the mold was lowered to the top surface of the porous stone. The relative level of the porous stone to the base was recorded to determine if any heaving occurred during the freezing process. The top cap was then put into place.

#### 3.2.1.3 Freezing

It is well known that when a saturated soil sample is frozen, it increases in volume by about 9 percent of the volume of water present in the sample. After saturation and replacing the top cap, a thin access tube was attached to the fixture at the top cap to allow dissipation of any pressure built-up by the release of gas from within the sample. The whole assembly of the mold was placed in a wooden box with a circular opening at the bottom to allow the mold to protrude by about 20 mm at the bottom. The box was then filled with vermiculite which insulated all of the mold except the bottom 20 mm of the mold. The assembly consisting of the box and the mold was placed in a chest freezer in which the temperature was maintained at  $-20^{\circ}\text{C}$ . The samples

were frozen unidirectionally from the bottom to the top in a period of about 48 hours.

The average freezing rate was 3.5 mm per hour. No ice lensing was observed in any of the samples when examined later. Some excess ice, due to the expulsion of water during the freezing process, formed at the top of the samples and was subsequently removed by trimming.

### 3.3 TESTING EQUIPMENT

#### 3.3.1 Triaxial Cell

Double-walled aluminum triaxial cells similar to that used by Mitchell and Burn (1971) and Baker et al. (1981) were modified and used in all the tests. A schematic of the set-up including the volume change measurement device is shown in Figure 3.4. A schematic of the double-walled cell is shown in Figure 3.5.

The triaxial cell consisted of two aluminum cylinders sitting axisymmetrically on a base. The sample was placed inside the inner cylinder on a pedestal. The cylinders were capped separately so that the inner cylinder with the cap was contained wholly within the outer cylinder. A volume change measurement device was connected with the inner cylinder. During the test both the inner and outer cylinders were filled with antifreeze. Any change in volume of the sample inside the inner cylinder was reflected in the level of antifreeze in the

volume change measurement device. O-rings as shown in Figure 3.5 were provided to seal various components of the cell. Copper cooling coil, wrapped around the inner cell, was used to circulate cooling fluid to minimize temperature variations in the sample due to the variations in the room temperature during the defrosting cycle.

During testing, the cell pressure was supplied by a pressurized bottle of dry nitrogen gas through a high precision, two stage regulator. Equal pressure was maintained in both the inner and outer cylinders through a T-connection in the pressure line as shown in Figure 3.4. The cell pressure was monitored by a pressure transducer and was double checked with a pressure gauge fitted to the pressure regulator.

A thermistor of the type OMEGA 44203 was mounted in the inner cell to monitor the temperature of the inner cell fluid. The thermistor was calibrated against a precision thermometer, accurate to one-hundredth of a degree in Celcius scale. Each thermistor was connected with the electronic readout device for regular monitoring during the test.

A Volume change measurement device was designed to measure the volume displacement of the inner cell fluid by using a double-walled burette sometimes called a back pressure burette. A burette was preferred to an electronic device because of its simplicity, accuracy and reliability.

The assembly of the triaxial cell was calibrated for creep due to axial load using a dummy cylindrical steel block sample and the antifreeze was calibrated for volume change with isotropic cell pressure.

#### 3.4 SAMPLE TRIMMING AND SETTING-IN PROCEDURE

The mold containing the frozen sample was taken out of the freezer and carried to the cold room which was maintained at a temperature of  $-30^{\circ}\text{C}$ . The sample was then removed from the plexiglass mold, placed in a steel split mold and was trimmed to the required length using a band saw. The trimmed end was then smoothed, the sample was removed from the split steel mold and was weighed. Trimmings were collected for determining the ice content of the sample.

Two dry porous stones were placed on the pedestal of the triaxial cell. The trimmed sample was placed with the trimmed end down, on the porous stones. A top cap was placed on the top end porous stone which was built in during the sample preparation.

The sample was then placed in a rubber membrane and O-rings were used to seal the ends. The inner cell was put in place and bolted at the bottom with the base plate. The cooling coil was connected to the fixture at the base plate. The top cap of the inner cell was replaced and bolted with the top end flange. The outer cylinder was placed and bolted in with the base plate. The piston was then inserted

into the top cap of the inner cylinder.

Both the inner cell and the outer cell were filled with antifreeze which was brought to the test temperature at least 24 hours prior to the filling. The filling of the inner cell was completed when the antifreeze started bleeding through a port on the top cap of the inner cell. The bleed valve was plugged with a brass nut. The top cap of the outer cell was then replaced and bolted on to the top flange of the outer cell. The rest of the outer cell was then filled until it started bleeding through a valve at the top of the outer cell cap.

A small amount of pressure, about 10 kPa, was applied to check for any leakage in the system. If no leakage was found, the system was ready for loading.



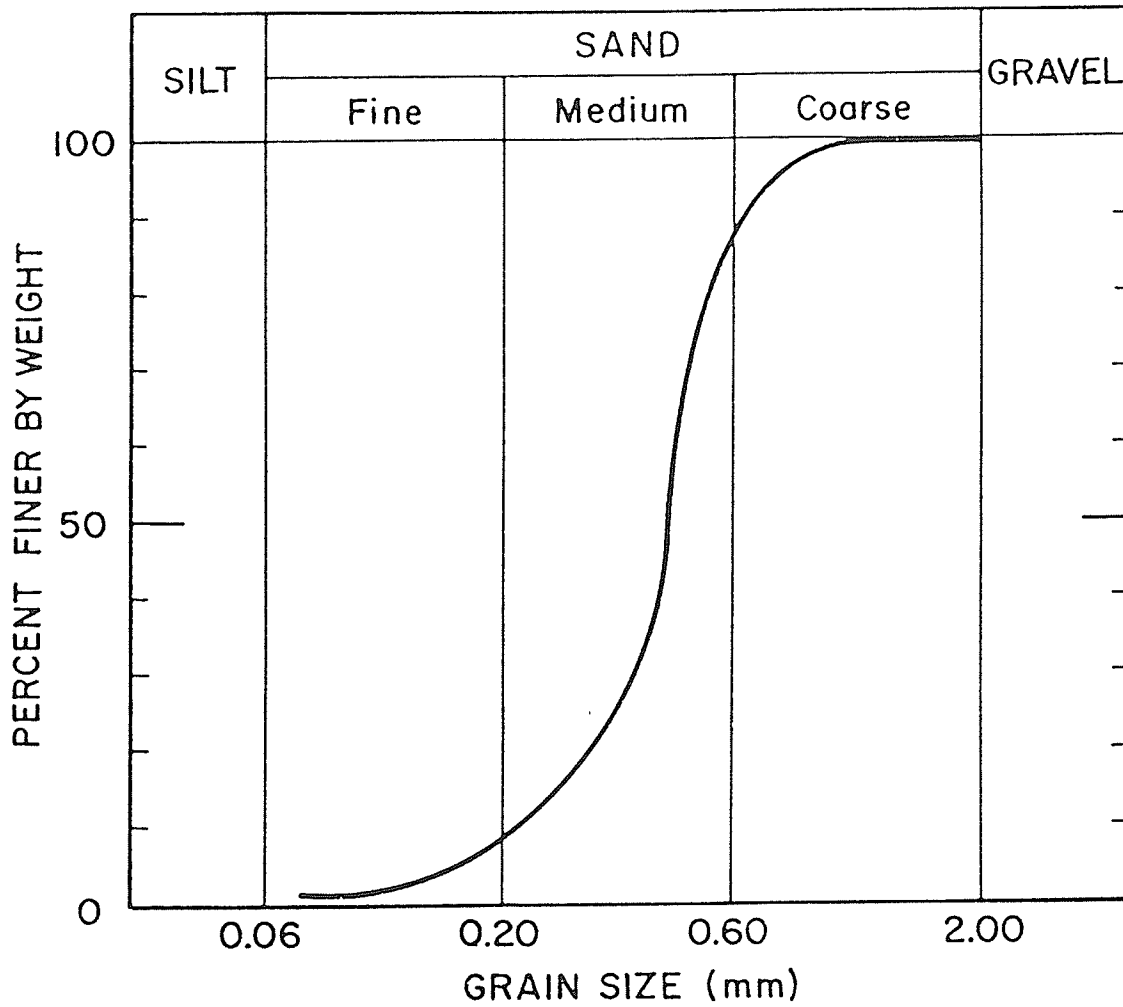


Figure 3.1 Grain size distribution of the sand

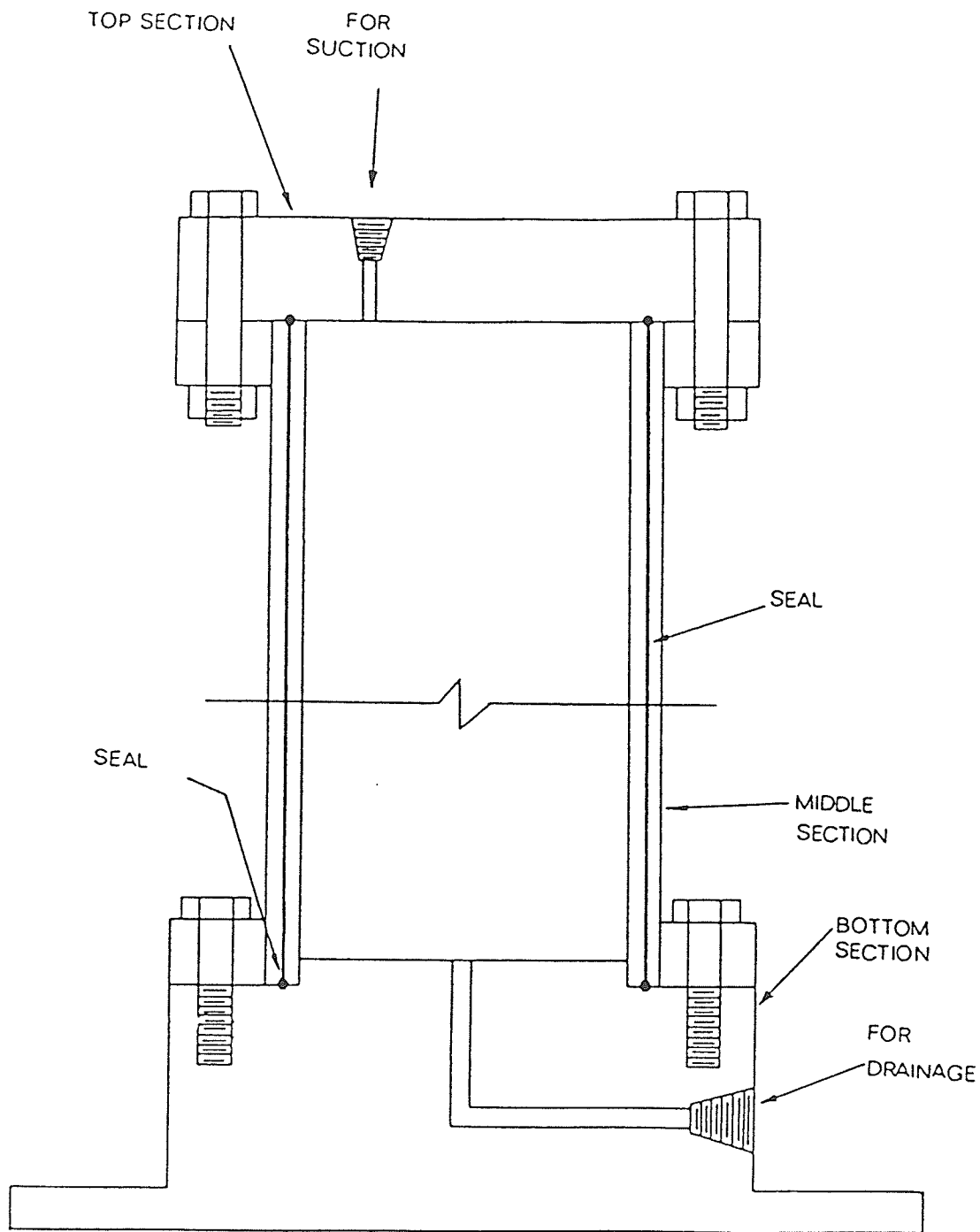


Figure 3.2 Plexiglass mold (not to scale)

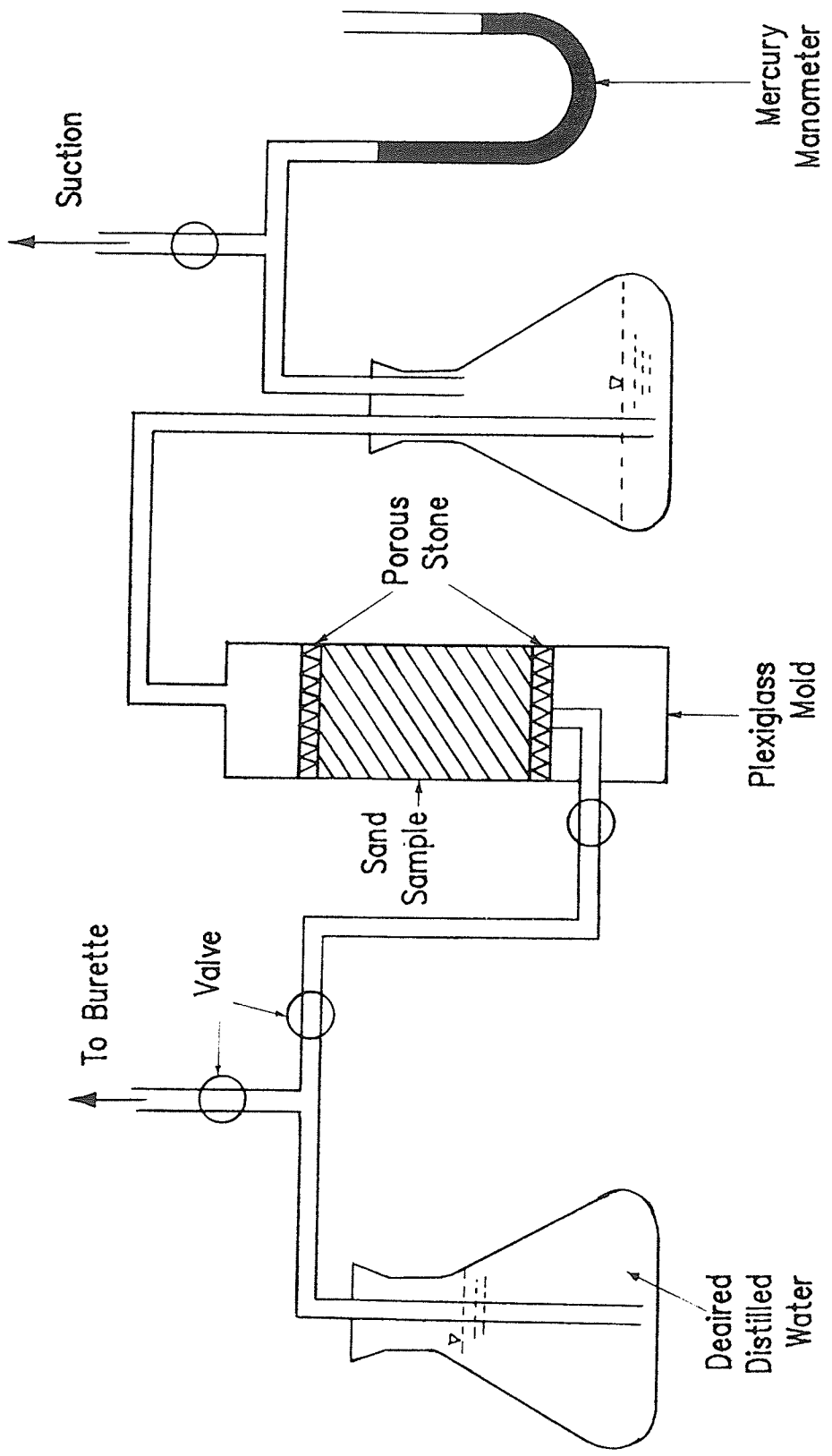


Figure 3.3 Schematic diagram of saturation process of the sand sample

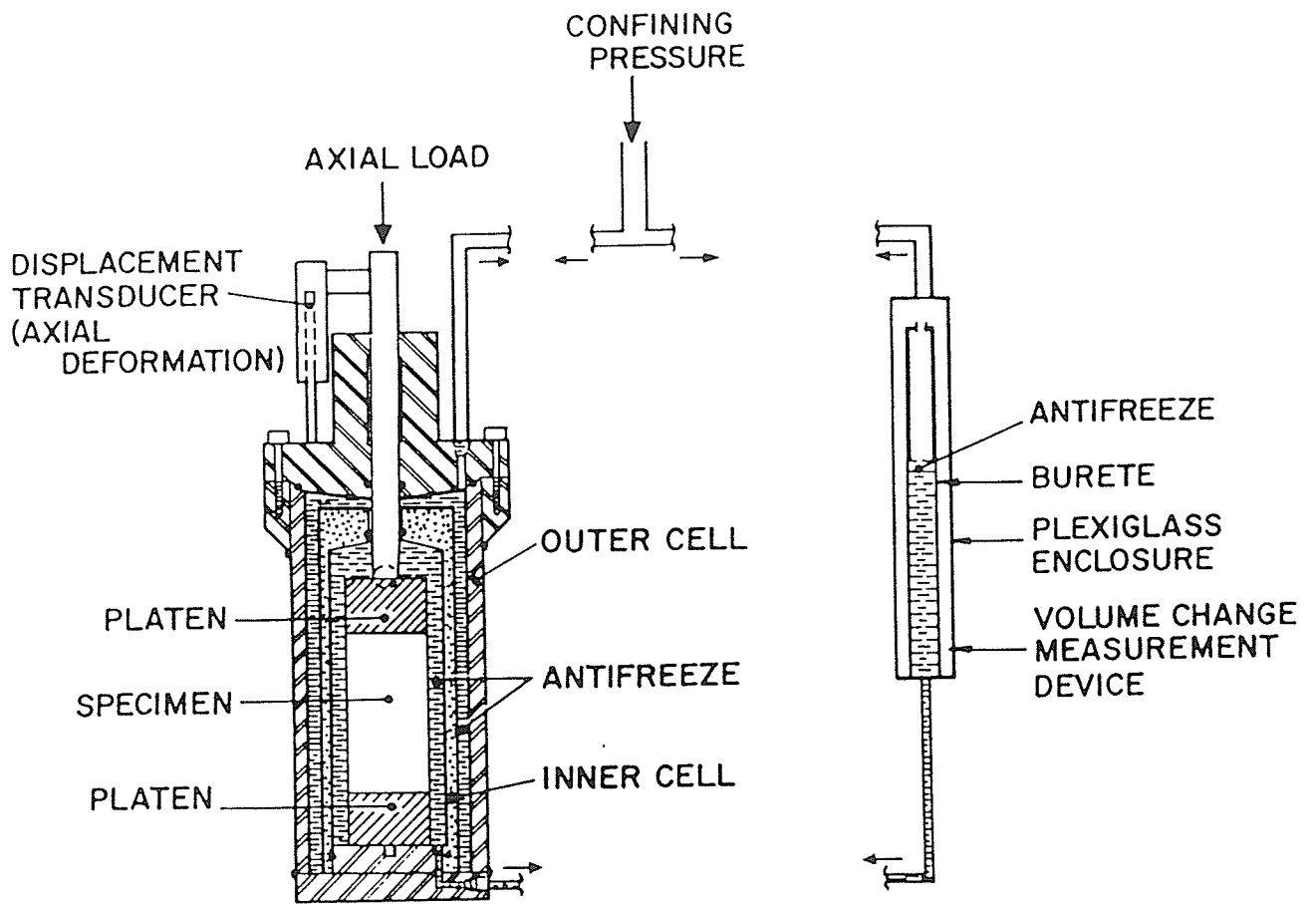


Figure 3.4 Schematic diagram of the triaxial cell

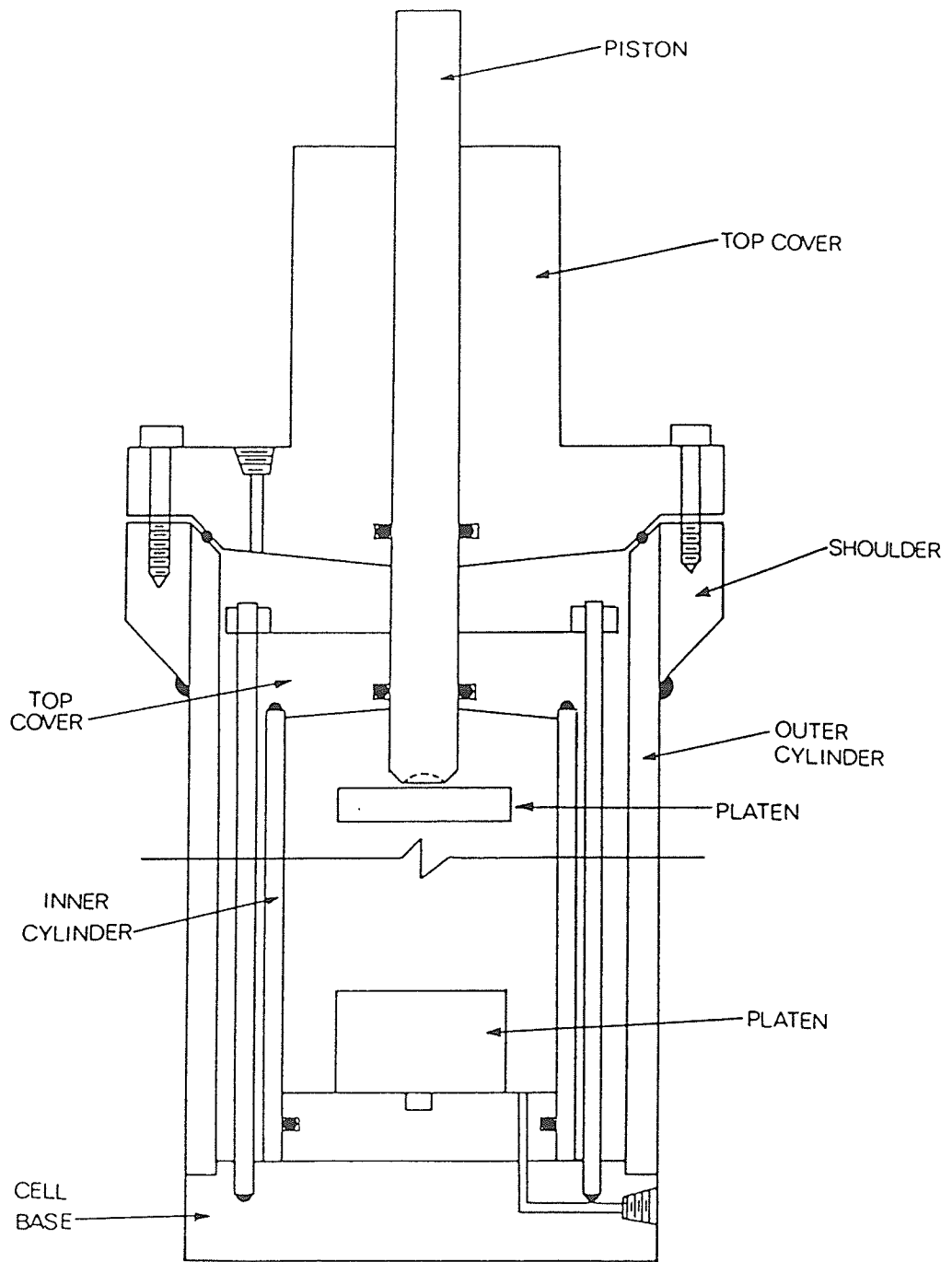


Figure 3.5 Triaxial cell details (not to scale)

# **CHAPTER FOUR**

## **BULK CREEP FUNCTION**

## CHAPTER 4

### BULK CREEP FUNCTION

#### 4.1 INTRODUCTION

As mentioned in Chapter 3, formulation of a valid constitutive law for a frozen soil and a better prediction of the relationship between stress and displacement in the frozen soil mass require an understanding of the behaviour of the frozen soil under isotropic stress changes. The stress-strain data obtained from isotropic compression tests are particularly useful in the direct determination of bulk creep function. The bulk creep function,  $K_c$ , as given by equations 2.45 and 2.47, relates the isotropic stress,  $\sigma_m$ , and the associated volume change,  $\epsilon_v$ , of a frozen soil element. Since the relationship is nonlinear, the bulk creep function is defined as :

$$\frac{d\sigma_m}{d\epsilon_m} = K_c = \lim_{\Delta\epsilon_v \rightarrow 0} \left( \frac{\Delta\sigma_m}{\Delta\epsilon_v} \right) \quad (4.1)$$

The bulk creep function depends on many factors, such as, temperature, time, stress level, ice content, unfrozen water content and mineralogical composition of the soil. In the investigation, the index properties of the frozen sand sample and the temperature were held constant and the bulk creep function was investigated as a function of mean normal stress and time.

## 4.2 TEST PROCEDURE

A single multi-stage isotropic consolidation test, IC1, was conducted to determine the relationship between isotropic stress and volumetric creep strain. After the sample was set up, as outlined in Chapter 3, a 24-hour period was allowed before any load application, to bring the sample and the system into temperature equilibrium. The cell pressure was applied by bottled nitrogen gas and the pressure was monitored by a pressure transducer and double checked by a pressure gauge mounted on the high precision two stage regulator. Equal pressure was maintained in both the fluid in the inner cell and in the outer cell so that the inner cell was not subjected to any volume change due to changes in the cell pressure. The volume change of the sample was measured by measuring the change in volume of the fluid in the inner cell using a burette.

The test was started with a stress increment of 50 kPa. Volume change and axial deformation of the sample were recorded at frequent intervals. The stress was held constant until the volumetric strain approached an asymptotic value which occurred after about 300 hours. The isotropic stress was then increased to 100 kPa and subsequently to 150, 200, and 300 kPa. Each stress level was maintained until the volumetric deformation appeared to be close to its asymptotic value for that particular stress level. Because complete attenuation takes an inordinate length of time to achieve, it was considered to be



impractical to wait until there was no further change in volume. Generally it was assumed that complete attenuation occurred if the volumetric strain was of the order of  $10^{-9}$ /sec. The stress steps of 100, 150, 200, and 300 kPa were maintained for 216.5, 527.5, 1247.5 and 2159.5 hours respectively. The test took almost 200 days to complete.

### 4.3 TEST RESULTS AND DISCUSSIONS

#### 4.3.1 Volumetric Stress-strain Relationship

Plots of cumulative true volumetric strain versus cumulative time are presented in Figure 4.1 along with the magnitude of isotropic stress at each increment. The true volumetric strain differs from conventional engineering volumetric strain in that each increment of strain is based on the actual volume at the time of the increment, instead of the original volume. The true volumetric strain is given by:

$$\epsilon_v = \int_{V_0}^{V_t} \frac{dV}{V} = \ln \frac{V_t}{V_0} \quad (4.2)$$

in which  $dV$  = change in volume

$V_t$  = volume of the sample at time  $t$

$V_0$  = volume of the sample at time  $t=0$

Individual plots of true volumetric strain versus time for each stress increment are shown in Figure 4.2. The final volumetric strain

for one stress increment was plotted as the initial volumetric strain for the subsequent stress increment and thus the volumetric strains shown are cumulative.

From the plots of Figure 4.1 and 4.2 it was observed that typically for each application, there was an instantaneous volumetric strain followed by time-dependent volumetric strain, the rate of which decreased with time. The time for attenuation (negligible strain rate) increased from about 300 hours for the initial stress increment to about 2000 hours for the final stress increment. The cumulative attenuated volumetric strains varied from about 0.8 to 2.9 percent for the 50 to 300 kPa isotropic stress range.

The cumulative instantaneous and attenuated volumetric strains are shown in Figure 4.3 which is a plot of volumetric strains versus the isotropic or mean normal stress. It is seen that practically all of the instantaneous strain, (95%), occurred during the first stress application with only a slight, approximately linear, increase in volumetric strain with stress level. When the sample was unloaded at the end of the isotropic compression test, the recovery was immeasurable, indicating that all the strains were of inelastic compression.

The relationship between the attenuated volumetric strains and the mean normal stress was approximately linear for the stress range investigated. A significance of this relationship is that its slope provides an ultimate or attenuated, pseudo-elastic bulk modulus,  $K_{\infty}$ .

For the test conditions the attenuated bulk modulus was determined to be:

$$K_{\infty} = 10,250 \text{ kPa} \quad (4.3)$$

The difference between the instantaneous and attenuated volumetric strain represents creep strains which are seen to increase with stress level.

#### 4.3.2 Influence of Time and Mean Normal Stress on Volumetric Strain Rate

The variation in volumetric strain rate with time for each increment of mean normal stress is shown in Figure 4.4. For each stress level the relationship between strain rate and time consisted of a curve which is asymptotic to the ordinate and the abscissa. At time  $t=0$  the strain rate approaches infinity reflecting the instantaneous response of the soil to a stress change. At time  $t=\infty$  the volumetric strain rate approaches zero reflecting the attenuation of volumetric creep.

The relative positions of the curves indicate that generally the creep rate increased with an increase in mean normal stress for elapsed time greater than about 250 hours. The mean normal stress also had a major influence on the "attenuated time",  $t_{\infty}$ , and the magnitude of the attenuated volumetric strain. A plot of mean normal stress versus attenuated-time is shown in Figure 4.5. It is seen that the

attenuation time increased exponentially with stress.

#### 4.3.3 Solution for Bulk Creep Function

The bulk creep function relates mean normal stress to volumetric strain and as defined earlier, is the instantaneous slope of the volumetric stress-strain curve. The volumetric stress-strain curves could not be obtained directly from the multi-stage isotropic creep tests in which the stress at every step was maintained constant and deformations were recorded with time and the results were obtained in the form of volumetric strain versus time for various mean normal stresses. Therefore it became necessary to obtain the volumetric strain versus mean normal stress relationship for various times from the data obtained in the multi-stage isotropic creep tests. The relationship between mean normal stress and volumetric strain after various elapsed times are shown in Figure 4.6. These curves were constructed from the data obtained from the multi-stage isotropic consolidation test as presented in Figures 4.1 and 4.2. The total strain at any particular time was assumed to be the sum of all the instantaneous strains and the creep strains which the sample had undergone prior to the time under consideration. The curves in Figure 4.6 are straight lines in the transformed plot of  $\sigma_m/\epsilon_v$  versus  $\sigma_m$  as shown in Figure 4.7 and therefore can be represented by equation (4.4) as follows:

$$\frac{\sigma_m}{\epsilon_v} = K_{cm} = K_o + \beta\sigma_m \quad (4.4)$$

in which  $\epsilon_v$  = accumulated true volumetric strain  
 $\sigma_m$  = mean normal stress (isotropic stress)  
 $K_{\infty}$  = secant bulk creep function  
 $K_0$  = intercept on  $\sigma_m/\epsilon_v$  axis  
 $\beta$  = slope of the straight lines

The intercept on the  $\sigma_m/\epsilon_v$  axis provides the initial value  $K_0$  of the bulk creep function in the relationship between the secant bulk creep function,  $K_{\infty}$ , and the mean normal stress. Thus it represents a minimum value of the secant bulk creep function i.e. for  $\sigma_m=0$ . Its value was 10250 kPa which is the same as the attenuated bulk creep function,  $K_{\infty}$ . This is to be expected since  $K_{\infty}$  also represents the minimum value of the bulk creep function based on attenuated volumetric strains. Thus in Figure 4.7, the relationship between  $K_{\infty}$  and  $\sigma_m$  is a horizontal line for  $t=\infty$  which is consistent with equation (4.3).

The parameter  $\beta$  was plotted as a function of time in Figure 4.8 and the relationship was represented by the following equation.

$$\beta = ne^{-mt} \quad (4.5)$$

in which  $m$  &  $n$  = material constants

$t$  = time (hour)

For the tests these constants were:

$$n = 180$$

$$m = 0.0045$$

Thus the equation for the secant bulk creep function may be written as:

$$K_{cs} = K_0 + ne^{-mt} \sigma_m \quad (4.6)$$

Equation (4.6) for the test data can be rewritten as:

$$K_{cs} = 10250 + 180 e^{-0.0045t} \sigma_m \quad (4.7)$$

To obtain an expression for the tangent bulk creep function,  $K_{ct}$ , equation (4.4) is rewritten as:

$$\epsilon_v = \frac{\sigma_m}{K_0 + \beta\sigma_m} \quad (4.8)$$

The first derivative of equation (4.8) provides the inverse of the tangent bulk creep function,  $K_{ct}$ , as follows:

$$\frac{1}{K_{ct}} = \frac{d\epsilon_v}{d\sigma_m} = \frac{K_0}{(K_0 + \beta\sigma_m)^2} \quad (4.9)$$

or

$$K_{ct} = \frac{(K_0 + \beta\sigma_m)^2}{K_0} \quad (4.10)$$

Substituting the expression for  $\beta$  (equation 4.5) into equation (4.10), the equation for the tangent bulk creep function,  $K_{ct}$ , becomes:

$$K_{ct} = K_0 \left( 1 + \frac{1}{K_0} ne^{-mt}\sigma_m \right)^2 \quad (4.11)$$

which for the test data becomes:

$$K_{ct} = 10,250 (1 + 1.756 \times 10^{-2} e^{-0.0045t\sigma_m})^2 \quad (4.12)$$

Time,  $t$ , and mean normal stress,  $\sigma_m$ , in equation (4.12) are expressed in hour and kPa respectively. According to equation (4.12), the tangent bulk creep function,  $K_{ct}$ , increases exponentially with an increase in the mean normal stress. This is illustrated by a plot of  $K_{ct}$  versus  $\sigma_m$  for selected elapsed times in Figure 4.9. On the other hand, as shown in Figure 4.10, the tangent bulk creep function decreases exponentially with time for a constant mean normal stress. At time  $t=\infty$ , the second term of the equation reduces to zero and  $K_{ct}$  is equal to  $K_0$  which is also equal to  $K_\infty$ .

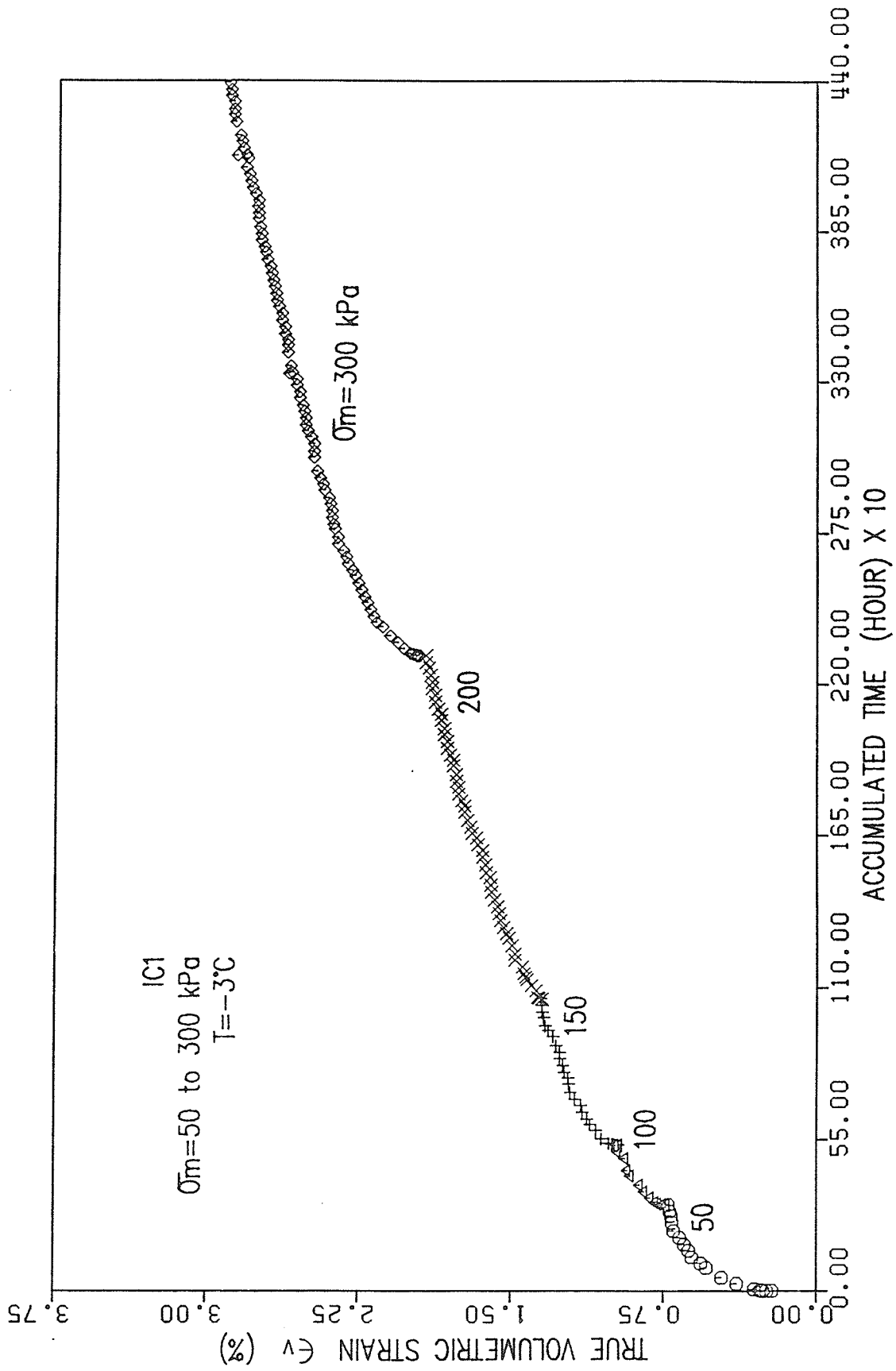


Figure 4.1 True volumetric strain as a function of accumulated time



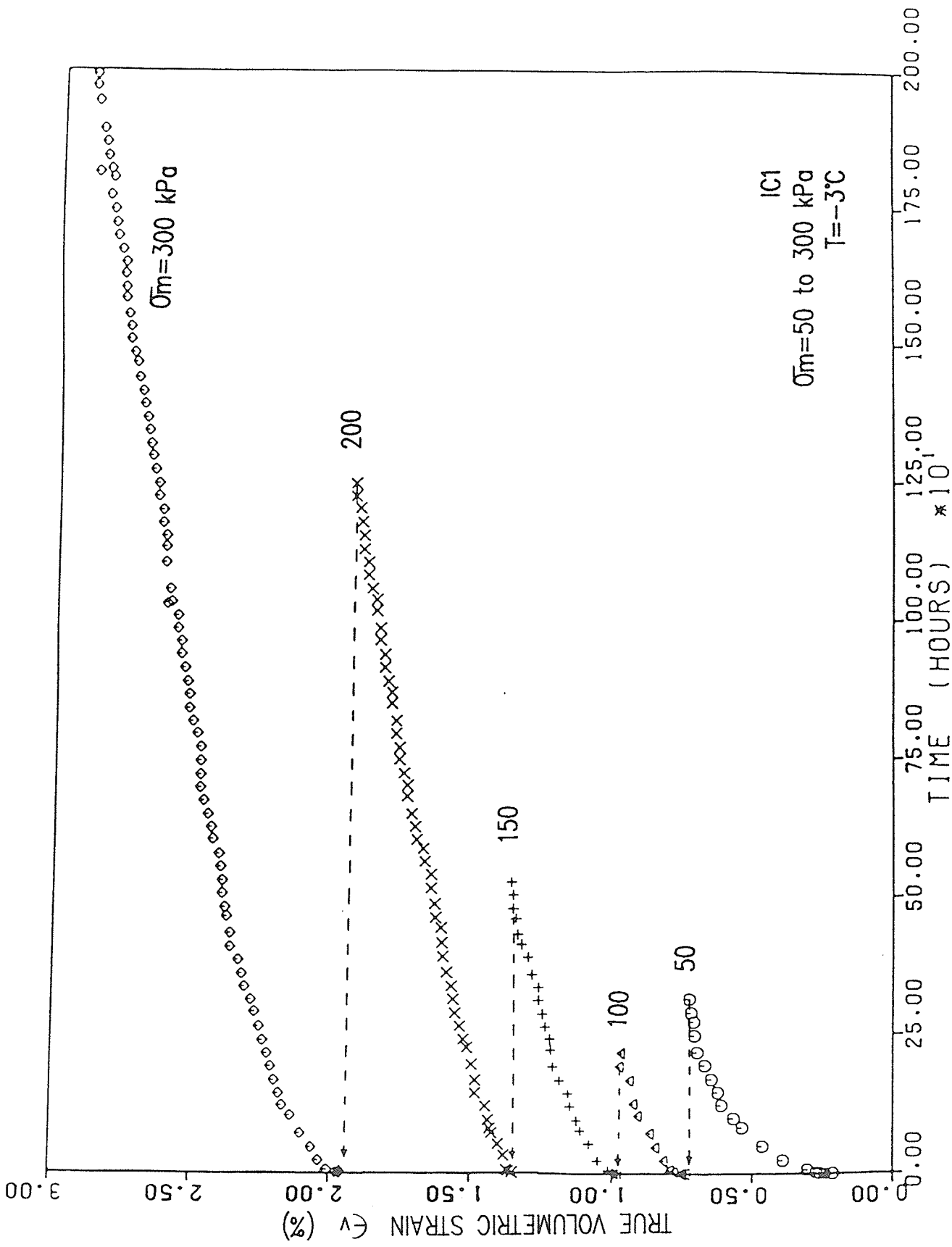


Figure 4.2 True volumetric strain versus time

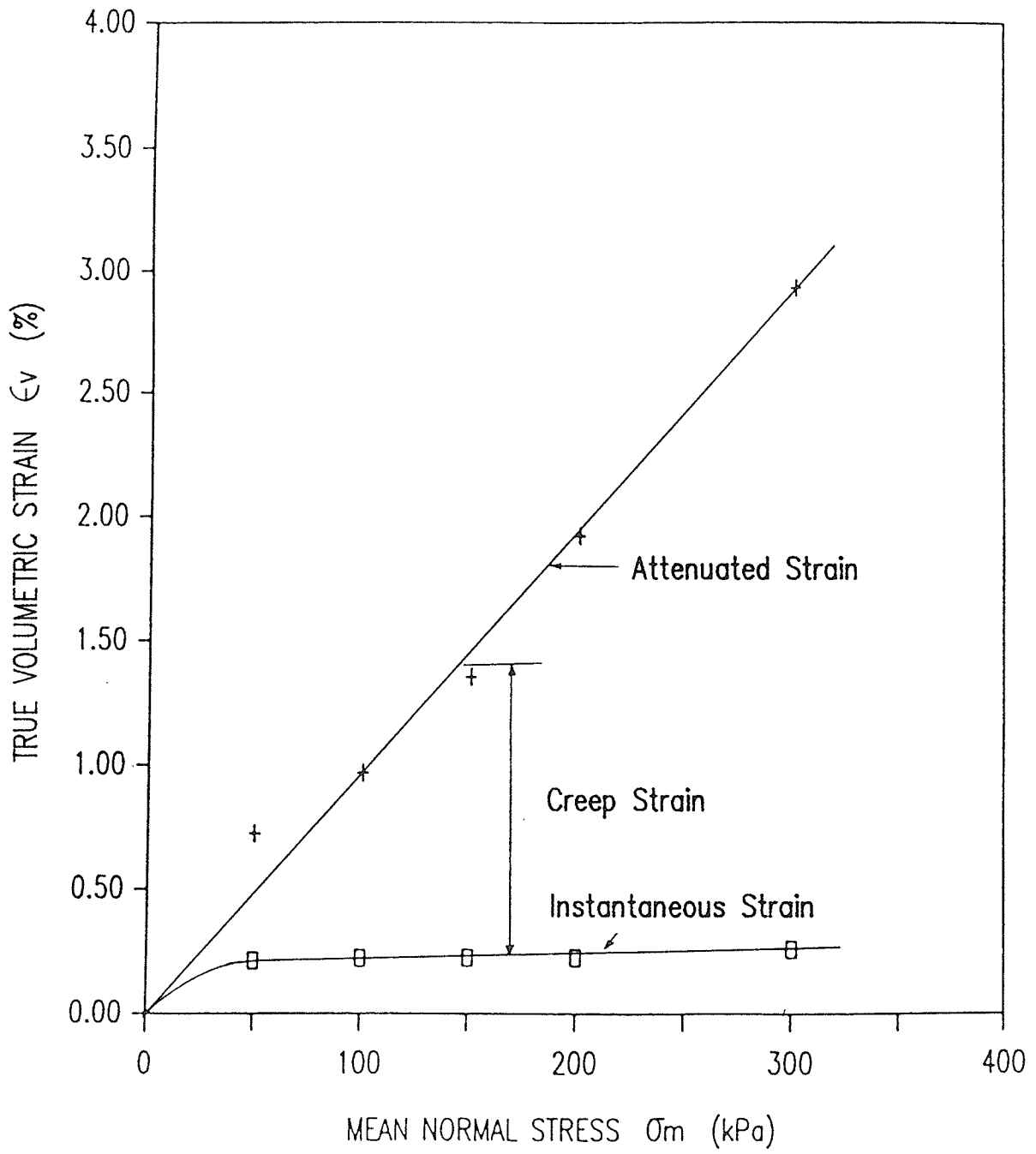


Figure 4.3 True volumetric strain versus mean normal stress

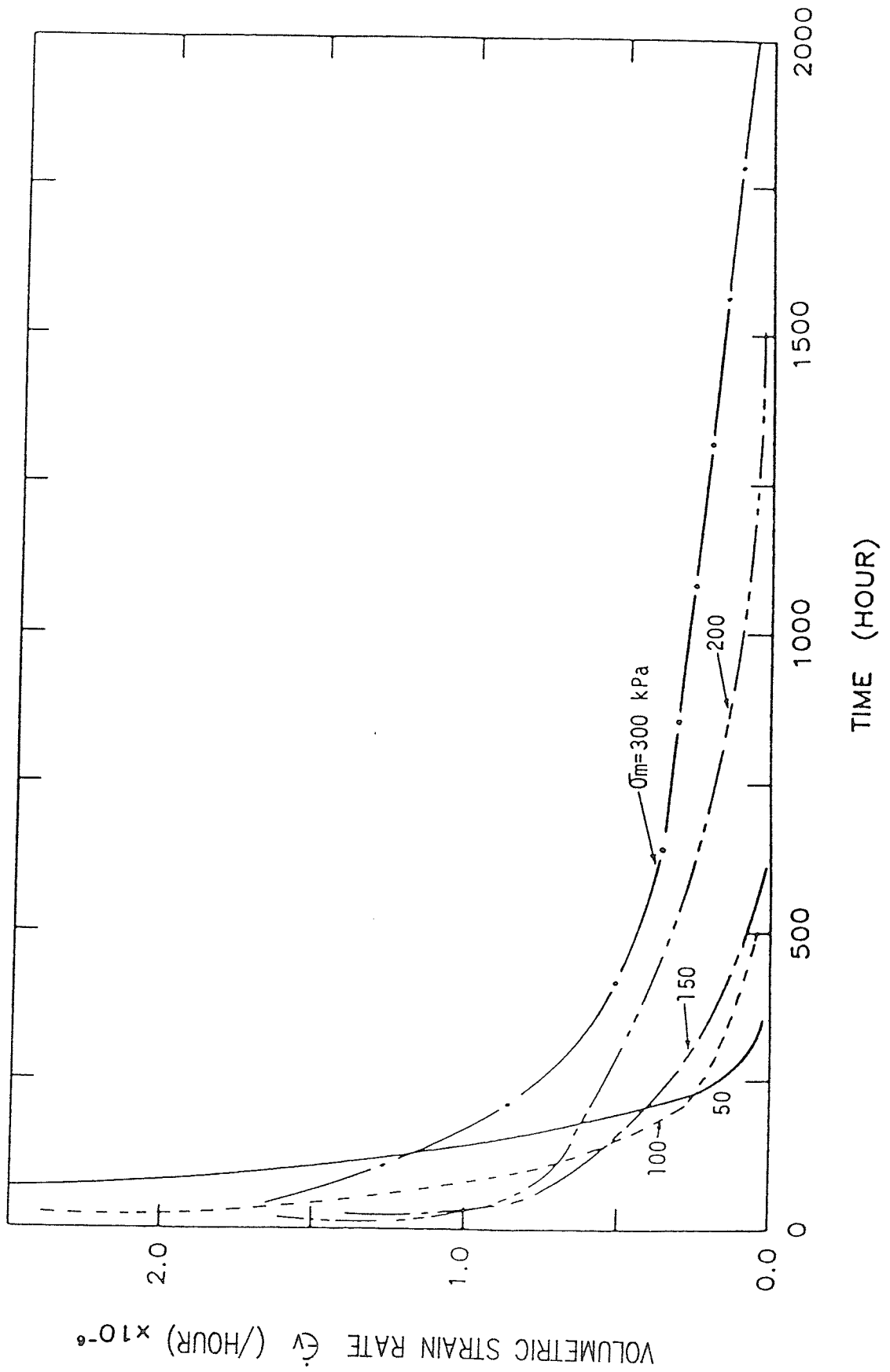


Figure 4.4 Volumetric strain rate versus time

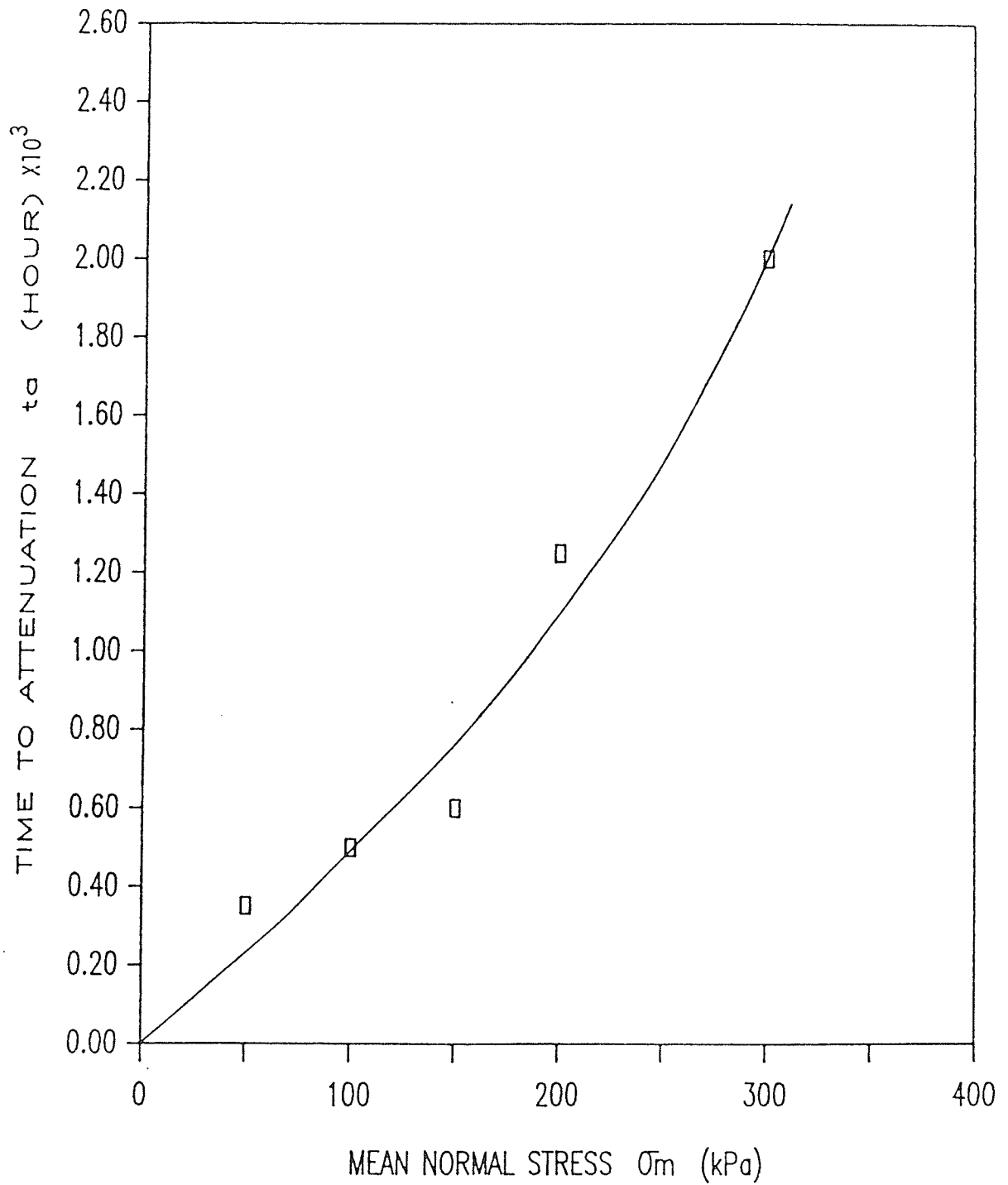


Figure 4.5 Time to attenuation versus mean normal stress

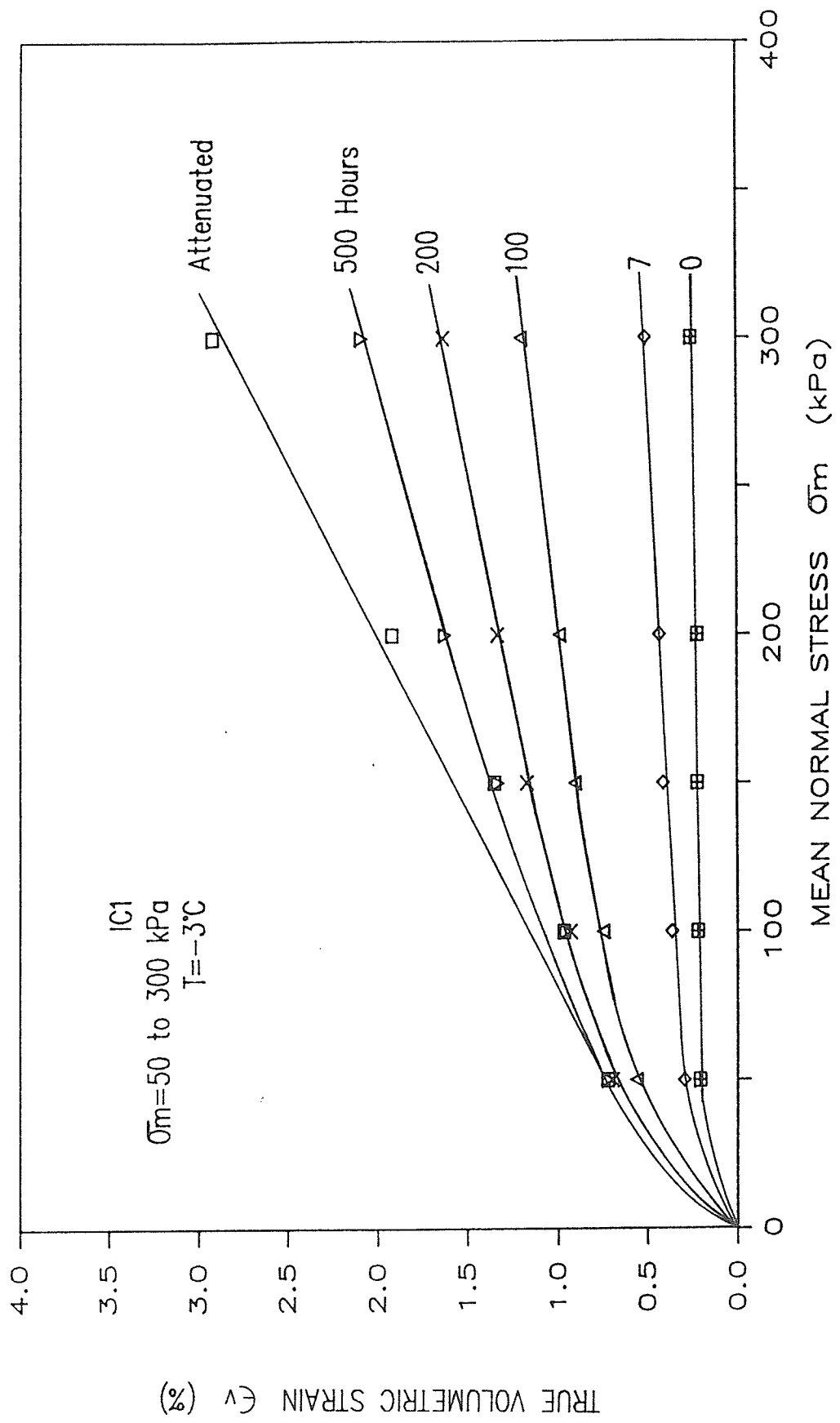


Figure 4.6 True volumetric strain versus mean normal stress

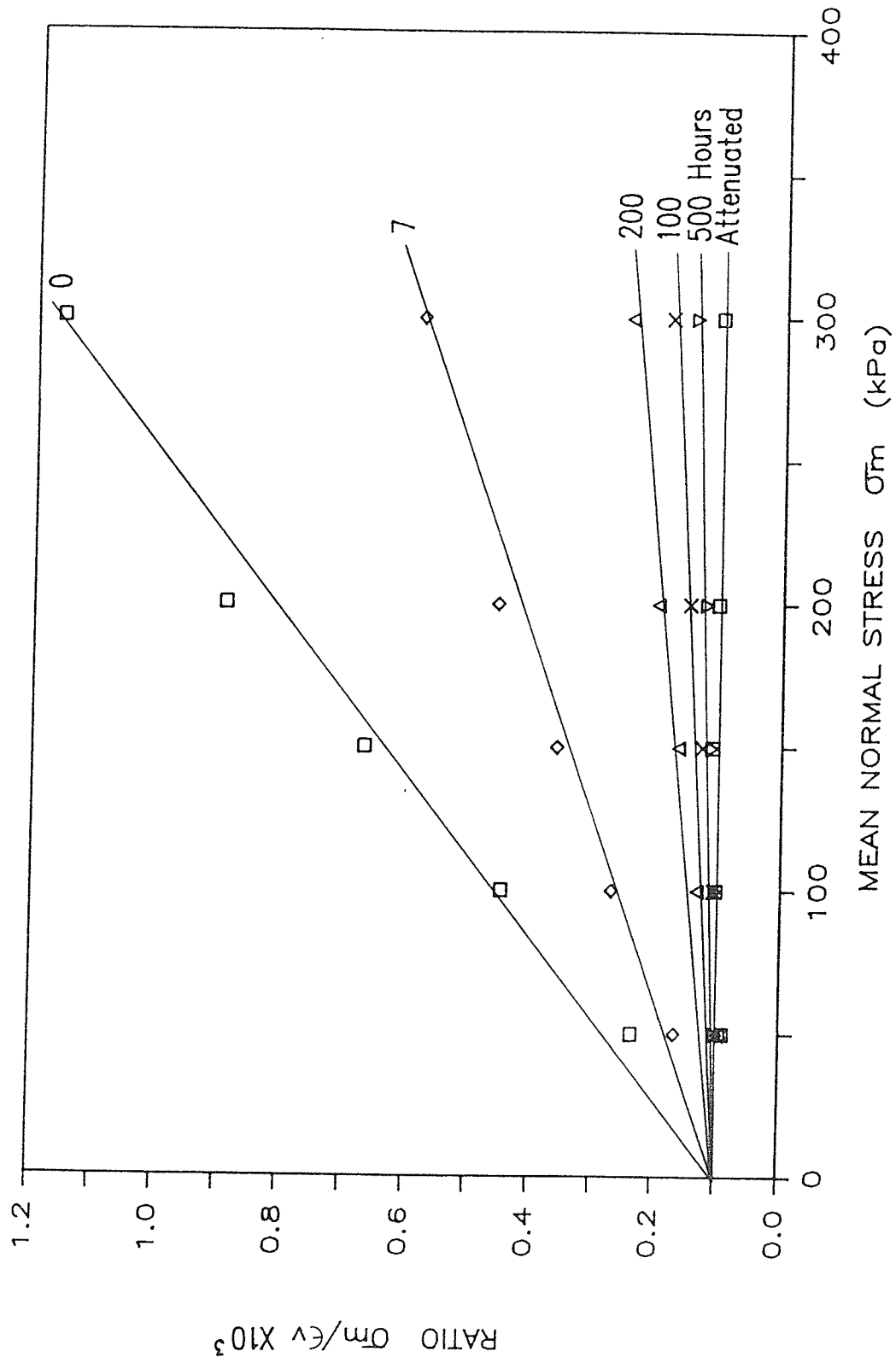


Figure 4.7 Ratio  $\sigma_m/\epsilon_v$  versus mean normal stress

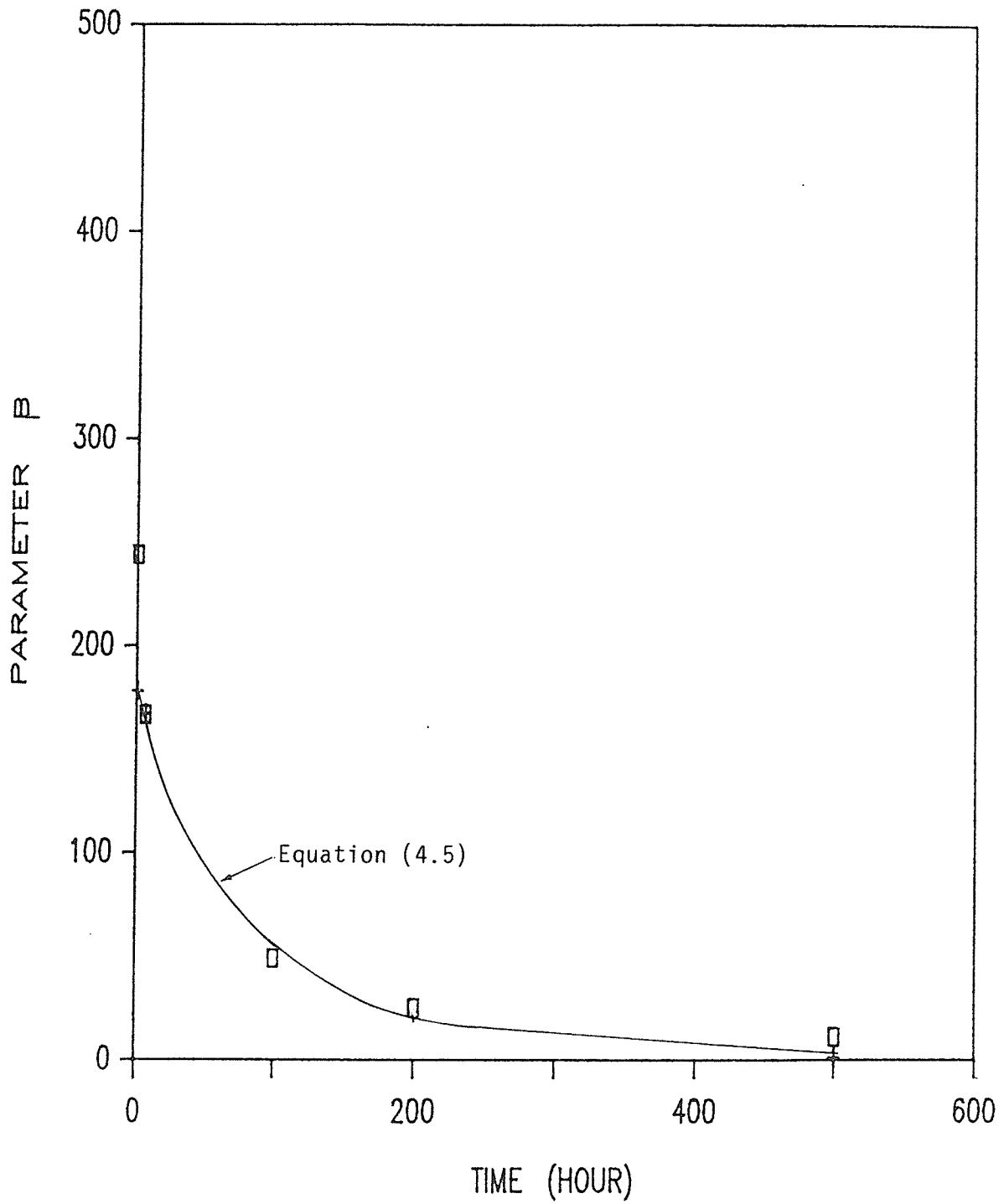


Figure 4.8 Parameter  $\beta$  versus time

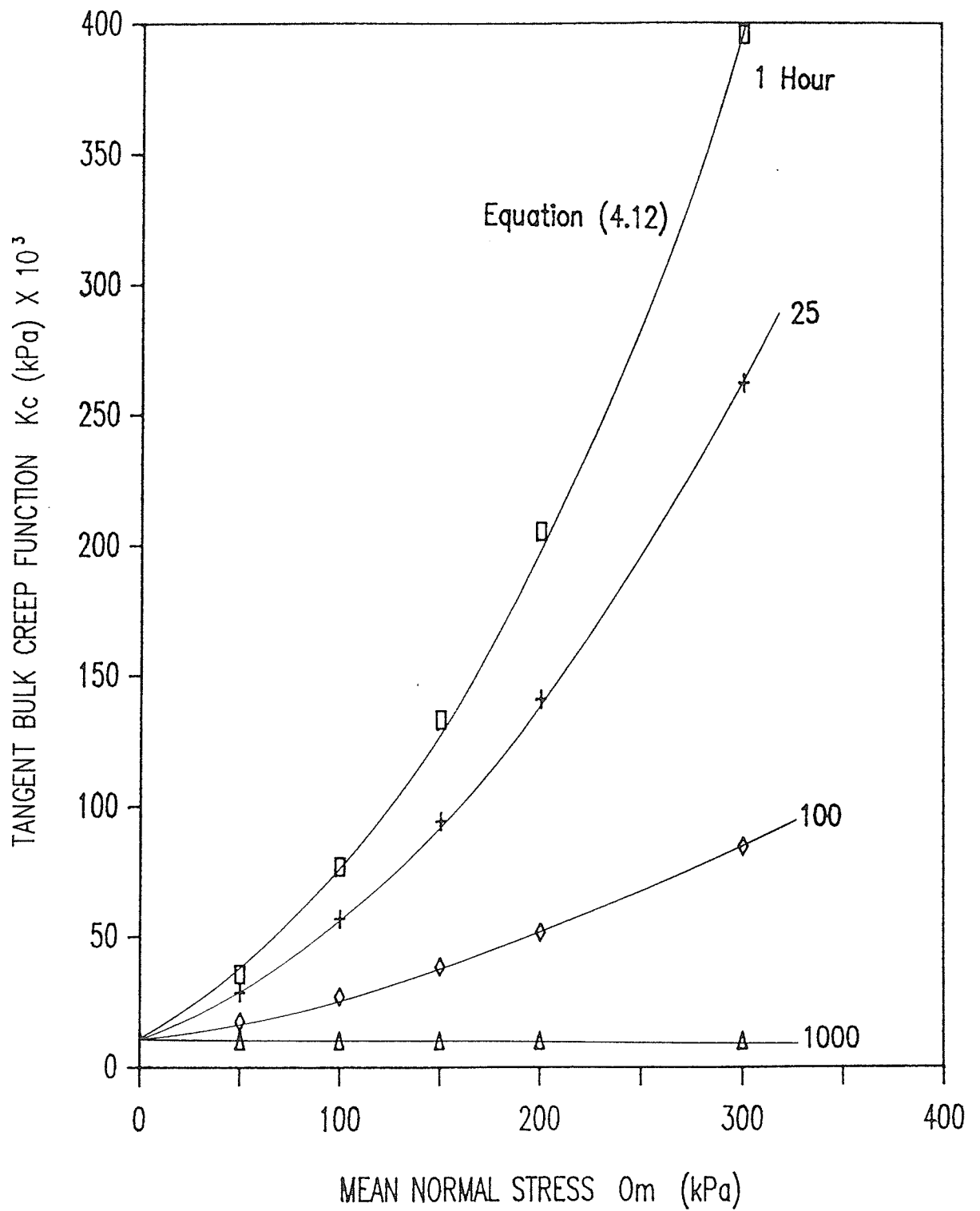


Figure 4.9 Bulk creep function versus mean normal stress



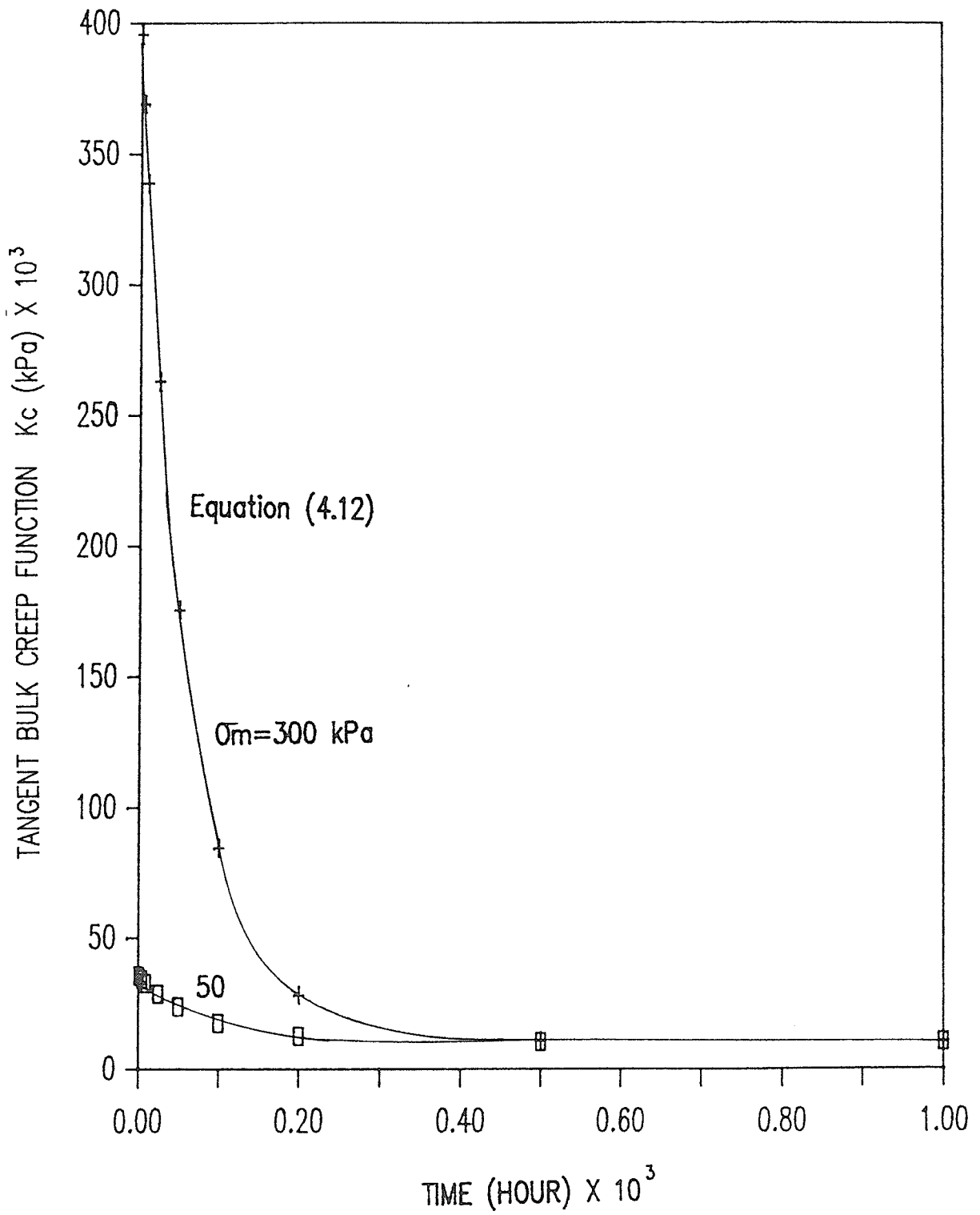


Figure 4.10 Bulk creep function versus time

**CHAPTER FIVE**  
**SHEAR CREEP FUNCTION**

## CHAPTER 5

### SHEAR CREEP FUNCTION

#### 5.1 INTRODUCTION

The shear creep function,  $G_c$ , as defined by equation 2.48, relates the resultant shear stress and the associated resultant creep shear strain. Since the relationship is nonlinear, the shear creep function is defined as the instantaneous slope of the resultant shear stress-strain curve and is represented by:

$$\frac{dS_d}{d\varepsilon_d} = G_c = \lim_{\Delta S_d \rightarrow 0} \left( \frac{\Delta S_d}{\Delta \varepsilon_d} \right) \quad (5.1)$$

For frozen soil the shear creep function depends on a number of factors, such as, mean normal stress, resultant deviatoric stress, time, temperature and material properties which include mineralogy, grain size, ice content, unfrozen water content, gases and air voids. The shear creep function may be determined by pure shear, torsion or constant mean normal stress triaxial compression tests. In the present investigation constant mean normal stress triaxial compression tests were used to evaluate the shear creep function of a quartz carbonate sand. The investigation included the influence of mean normal stress, resultant deviatoric stress, and duration of loading on the shear creep function.

Very few studies have been carried out to evaluate the shear modulus of frozen soils, but extensive studies have been made in the determination of the dynamic shear modulus and cyclic stress-strain characteristics of unfrozen soils. Constant mean normal stress triaxial compression tests have been successfully used for the evaluation of static shear modulus of unfrozen soils by Valliappan (1974), Liu (1970), Domaschuk (1969), and Gill (1969).

The development of an expression for the shear creep function including the test procedure for constant mean normal stress triaxial tests is presented in this chapter.

## 5.2 TEST PROCEDURE

### 5.2.1 Constant Mean Normal Stress Multi-stage Triaxial Tests

The constant mean normal stress multi-stage triaxial tests were conducted to determine the relationship between shear stress and strain. After the sample was set up as outlined in Chapter 3, a 24-hour period was allowed before load application to bring the sample and the system into temperature equilibrium. The physical properties of the frozen sand samples are given in Table 5.1. The cell pressure was applied by bottled nitrogen gas and the pressure was monitored by a pressure transducer and double checked by a pressure gauge mounted on the high precision two-stage regulator. A constant axial stress was applied to the sample through a hanger and lever arm system.

As in the multi-stage isotropic test, the cell was hooked up with a temperature controlled bath maintained at  $-3^{\circ}\text{C}$ . A thermistor mounted on the inner cell measured the temperature of the cell fluid. The axial deformation of the sample was monitored by means of a displacement transducer (LVDT) mounted on the load piston of the cell. The volume change of the sample was measured by measuring the change in volume of the fluid in the inner cell using a burette.

Each test was carried out at a pre-chosen mean normal stress using a stepwise increase in deviatoric stress. Firstly the sample was isotropically consolidated under the pre-chosen mean normal stress. Volume changes and axial deformations were recorded with time. The deviatoric stress was then applied by appropriately decreasing the confining pressure and increasing the axial stress so as to maintain the mean normal stress constant. The decrement of confining pressure, increment of axial stress and the resultant deviatoric stresses are given in Table 5.2. Each deviatoric stress level was maintained until the axial strain remained essentially constant for about two days or until the axial strain rate became less than  $2 \times 10^{-5}$  percent per hour which was chosen arbitrarily. After this, a new stress step was applied and generally this procedure of increasing the deviatoric stress was repeated until the sample failed or the cell pressure was lowered to 0 kPa. Axial deformations, volume changes and thermistor readings were recorded at frequent time intervals.

In order to maintain a constant mean normal stress, it was

necessary to know the cross-sectional area of the sample at all stages of the test. In this respect the cross-sectional area was calculated on the assumption that the sample retained its cylindrical shape throughout the test. The axial load adjustments were made at the start of each stress step and also during the stress step when the deformation, and hence the change in area, was significant. Each of the multi-stage tests is dealt with in sections 5.3.1 through 5.3.5.

### 5.3 TEST RESULTS

The volumetric and axial deformations were converted to true volumetric and true axial strains respectively. True volumetric strain was defined in Section 4.3.1. The true axial strain differs from conventional engineering strain in that each increment of strain is based on the actual length at the time of the increment instead of the original length. The true axial strain is given by :

$$\epsilon = \int_{L_0}^{L_t} \frac{dL}{L} = \ln \frac{L_t}{L_0} \quad (5.2)$$

in which  $dL$  = change in length

$L_t$  = length of the sample at time  $t$

$L_0$  = length of the sample at time,  $t=0$

#### 5.3.1 MST1

In this test the mean normal stress was 140 kPa and the increment of resultant deviatoric stress component,  $S_d$ , was 49 kPa. Seven stepwise increments of deviatoric stress were applied. Details of the stress applications are given in Table 5.3 and the axial and volumetric deformations are given in the Appendix.

The cumulative true axial and true volumetric strains versus time for the entire test are shown in Figure 5.1 and for each individual stress application in Figure 5.2. The sample underwent attenuating axial creep when subjected to resultant deviatoric stress steps of 49, 98, 147, 196 kPa. Inadvertently the stress step of  $S_d=245$  kPa was not maintained long enough to positively identify the creep rate as attenuating or accelerating. The first definite indication of axial accelerating creep occurred during the stress step,  $S_d=294$  kPa, at time  $t=750$  hours. This stress was maintained for a total of 1154 hours and then the next stress step,  $S_d=343$  kPa, was applied. The axial creep rate continued to accelerate under the added stress. The rate of axial creep increased substantially.

The volumetric strains indicated that the sample continued to decrease in volume until the stress step reached  $S_d=245$  kPa, and remained essentially unchanged at this stress level and then increased in volume when the stress level was increased to  $S_d=294$  kPa. The onset of dilation corresponded with the stress level at which accelerating axial creep first occurred.

### 5.3.2 MST2

In this test the mean normal stress was 280 kPa and the increment of resultant deviatoric stress was 98 kPa. Five stepwise increments of deviatoric stress were applied. Details of the stress applications are given in Table 5.4 and the axial and volumetric deformations are given in the Appendix.

The cumulative true axial and true volumetric strains versus time for the entire test are shown in Figure 5.3 and for each individual stress application in Figure 5.4. The sample underwent attenuating axial creep up to a stress level of  $S_a=392$  kPa, accelerating creep occurred at the next stress step of  $S_a=490$  kPa, and the test was terminated at this stress level. The volumetric strain indicated that dilatancy also first occurred at  $S_a=490$  kPa. During the stress level of  $S_a=294$  kPa, there was a breakdown in the cold room refrigeration unit and the sample temperature rose to  $-1^{\circ}\text{C}$ . This resulted in a sharp increase in both the axial and volumetric strains. When the sample temperature was restored to  $-3^{\circ}\text{C}$ , the axial and volumetric strains continued at rates comparable to those that preceded the breakdown.

### 5.3.3 MST3

For this test the mean normal stress was 280 kPa which was same as in the test MST2, but the increment of resultant deviatoric stress,



$S_a$ , was doubled to 196 kPa to see whether or not the magnitude of the deviatoric stress step had any influence on the results. Two stepwise increments of deviatoric stress were applied. Details of the stress applications are given in Table 5.5 and the axial and volumetric deformations are given in the Appendix. This test was conducted simultaneously with Test, MST2, and was therefore subjected to the same cold room temperature variations associated with the breakdown of the refrigeration unit.

The cumulative true axial and true volumetric strains versus time for the entire test are shown in Figure 5.5 and for each individual stress step in Figure 5.6. The sample underwent attenuating creep during the first increment of  $S_a=196$  kPa. The accelerating creep first occurred during the second increment at a stress level of  $S_a=392$  kPa and the test was terminated at this stress level. The volumetric strain data indicated that the dilatancy first occurred at the same stress level,  $S_a=392$  kPa. It was observed from a comparison of tests MST2 and MST3 that the increase in  $S_a$  from 98 kPa to 196 kPa reduced the stress level at which accelerating axial creep and dilation first occurred from 490 kPa to 392 kPa. This appears to be reasonable because the higher stress increment caused a higher axial strain rate and the sample did not get enough time to adjust to the new stress level.

#### 5.3.4 MST4

In this test the mean normal stress was 70 kPa and the incremental resultant deviatoric stress was 49 kPa. Three stepwise increments of deviatoric stress were applied. Details of the stress applications are given in Table 5.6 and the axial and volumetric deformations are given in the Appendix.

The cumulative true axial and true volumetric strains were plotted against time for the entire test in Figure 5.7 and for each individual stress application in Figure 5.8. The sample underwent attenuating creep under stress levels of  $S_d=49$  and 98 ka, and accelerating creep occurred at a stress level of 147 kPa. The volumetric strain data indicated that dilatancy also first occurred at  $S_d=147$  kPa and the test was terminated at this stress level.

#### 5.3.5 MST5

In this test the mean normal stress was 420 kPa and the incremental resultant deviatoric stress,  $S_d$ , was 196 kPa. Three stepwise increments of deviatoric stress were applied. Details of the stress applications are given in Table 5.7 and the axial and volumetric deformations are given in the Appendix.

The cumulative true axial and true volumetric strains versus time for the entire test are shown in Figure 5.9 and for each individual stress application in Figure 5.10. The sample underwent attenuating axial creep up to the stress level of  $S_d=392$  kPa and

accelerating axial creep occurred at the next stress step of  $S_a=588$  kPa. The volumetric strain data indicated that dilatancy also first occurred at the same stress level of  $S_a=588$  kPa. The test was terminated at this stress level.

## 5.4 CREEP RATES

### 5.4.1 Introduction

The axial creep rate of a frozen soil depends on the deviatoric stress in a constant stress test. The strain rate versus time curves for various stress levels in unconfined compression tests for the Ottawa sand as reported by Rein et al. (1975) are presented in Figure 5.11 and those for a frozen silt as reported by Yalin (1984) are presented in Figure 5.12. It was observed that the strain rates in all the plots reached a minimum and thereafter increased.

The strain rate versus time curves for polycrystalline ice as reported by Mellor and Cole (1982) are presented in Figure 5.13. The nature of the plots were the same as those of the sand and the silt presented by Rein et al. (1975), and Yalin and Carbee (1984) respectively in that the strain rate passed through a minimum.

It is observed that the stress in each case was high enough so that the strain rate passed through a minimum and the researchers were only interested in finding the time to reach the minimum strain rate.

#### 5.4.2 Axial Creep Rates

Axial creep rates versus time for the tests presented in Section 5.3 are shown plotted in Figures 5.14 through 5.18 for the individual tests. The mean normal stress and the deviatoric stress for each test are indicated in the figures. Smooth curves were drawn through the data points. It was observed that in most instances the creep rate tended to decrease towards zero and only in three instances did the creep rate pass through a minimum and then accelerate. In these three instances the ratio of the resultant deviatoric stress to the mean normal stress ranged from 1.75 to 2.1. However there were two tests in which the aforementioned stress ratios were 2.1 and 1.4 and the creep rate continued to decrease with time within the test time period.

To investigate the effects of resultant deviatoric stresses on the axial creep rate, the axial creep rate versus time curves having the same mean normal stress but different resultant deviatoric stresses were superimposed on single plots as shown in Figures 5.19 through 5.23. It was observed in all the figures that for a constant mean normal stress, the higher the resultant deviatoric stresses the higher the creep rate at any given time.

To determine the effects of the mean normal stress on creep rates, tests conducted at the same deviatoric stress and with the same

increment of deviatoric stress but at different mean normal stresses were selected. Tests MST3 and MST5, with resultant deviatoric stress,  $S_d=196$  kPa, increment of resultant deviatoric stress,  $S_d=196$  kPa, and constant mean normal stresses,  $\sigma_m=280$  and  $420$  kPa respectively, were selected. The creep rate versus time relationship for these two tests are shown in Figures 5.24 and 5.25. It is observed in Figure 5.24 that for attenuating creep there was no significant difference in creep rates for a difference in mean normal stresses of  $140$  kPa. For resultant deviatoric stress,  $S_d=392$  kPa, as observed in Figure 5.25 the creep rate passed through a minimum and then accelerated for  $\sigma_m=280$  kPa whereas the creep rate tended to become zero for  $\sigma_m=420$  kPa. This suggests that the strength increased with an increase in the mean normal stress.

#### 5.4.3 Time to Attenuation

It is observed in Figures 5.19 through 5.23 that the mean normal stress had some influence on the time to complete attenuation. Tests MST3 and MST5, conducted at the same resultant deviatoric stress of  $196$  kPa with the same increment of resultant deviatoric stress,  $S_d=196$  kPa, but at different mean normal stresses of  $280$  and  $420$  kPa respectively, were selected to determine the effects of mean normal stress on time to complete attenuation. Time to complete attenuation, for the resultant deviatoric stress of  $196$  kPa, versus mean normal stress were shown plotted in Figure 5.26. It was observed that the time to complete attenuation increased exponentially with an increase in the mean normal stress.

## 5.5 FAILURE CRITERION

### 5.5.1 Failure Stress

It was observed from the Figure 5.1 through 5.10 that during shear deformation the samples initially underwent volume reduction and then dilation. It can be assumed that the beginning of dilation coincided with the initiation of cracks in the sample and any further increase in stress would cause the cracks to continue to grow with time. Generally the beginning of dilation coincided with acceleration of the axial creep rate, which supports the concept of fracture development.

A plot of resultant deviatoric stress at which dilation first occurred, versus mean normal stress, is shown in Figure 5.27 and the values are presented in tabular form in Table 5.8. The relationship in

TABLE 5.8

Resultant deviatoric stress at failure and mean normal stress

Test	$\sigma_m$ (kPa)	$Sd_z$ (kPa)
MST1	140	294
MST2	280	392
MST3	280	490
MST4	70	147
MST5	420	588

fact can serve as a failure criterion in which failure is defined as

the onset of tertiary creep. For the tests conducted the relationship was found to be linear and can be expressed as:

$$S_{d\epsilon} = S_{d_0} + m\sigma_m \quad (5.3)$$

in which  $S_{d_0}$  is the intercept corresponding to  $\sigma_m=0$ , and the parameter,  $m$ , is the rate at which the failure resultant deviatoric stress,  $S_{d\epsilon}$ , increases with the mean normal stress. For the given soil, temperature, and stress range,  $S_{d_0}=100$  kPa and  $m=1.3$  and equation (5.3) becomes:

$$S_{d\epsilon} = 100 + 1.3 \sigma_m \quad (\text{kPa}) \quad (5.4)$$

From equation (5.4) it is obvious that the mean normal stress has a very profound effect on failure stress as defined herein. An increase in strength of frozen sand with an increase in confining pressure was observed by Sayles (1973), Chamberlain et al (1972), Alkire and Andersland (1973), Smith and Cheatham (1975), Parameswaran and Jones (1981), and Jones and Parameswaran (1983).

The concept of a threshold stress that defines the onset of accelerating creep was supported by Man (1984) in his theoretical formulation to determine long term strength of frozen soils. Man stated that for viscoelastic material, there is always a stress, at a particular temperature, below which the material behaves as a solid and exhibits attenuating creep and above which, the material behaves as a fluid and undergoes stationary creep.

### 5.5.2 Failure Strain

The creep failure strain has been expressed in the literature as a function of minimum creep strain rate,  $\dot{\epsilon}_m$ , and time to reach minimum creep strain rate,  $t_m$ , (Ting, 1983 ; Yalin and Carbee, 1984) and the form of the equation was as follows :

$$\epsilon_f = \dot{\epsilon}_m t_m^n \quad (5.5)$$

To satisfy the above relationship the sample must pass through a minimum strain rate in a constant stress creep test which means that the applied stress must be large enough to produce tertiary creep. In the studies mentioned above, the applied stresses were of sufficient magnitude to produce tertiary creep. In defining the minimum strain rate and the time to reach the minimum strain rate, Ting (1983) suggested the existence of an approximately constant strain at the minimum strain rate. Mellor and Cole (1982) plotted strain rate against axial strain for polycrystalline ice and found that the minimum strain rate occurred at about 1 percent of axial strain. This implies that the failure phenomenon is strain dependent rather than stress dependent. In the writer's investigation it was found that the total axial strain at failure, i.e the start of dilation varied with the stress and ranged between 1 and 2 percent. Figure 5.28 shows the axial strain at failure plotted against the mean normal stress. The axial strains at failure increased with an increase in mean normal stress. This can be explained by noting that ductile fractures generally occur



by the formation and subsequent growth of and coalescence of voids and cavities. If the cavity nucleation can be delayed or suppressed by increasing the mean normal stress, an increase in strength can be achieved. In the case of frozen sand an increase in mean normal stress may have had the effect of delaying (from the point of view of strain) the development and growth of fractures.

## 5.6 SHEAR CREEP FUNCTION

### 5.6.1 Resultant Deviatoric Stress-Strain Curve

The resultant deviatoric stress as defined by equation (2.42) reduces to the following form for the case of triaxial compression tests.

$$S_d = \sqrt{\frac{2}{3}}(\sigma_1 - \sigma_3) \quad (5.6)$$

in which  $\sigma_2 = \sigma_3$  and

$$\sigma_m = \frac{\sigma_1 + 2\sigma_3}{3}$$

As well the resultant deviatoric strain as defined by equation (2.44) reduces to the following form :

$$\epsilon_d = \frac{2\sqrt{2}}{\sqrt{3}} (\epsilon_1 - \epsilon_3) \quad (5.7)$$

in which  $\epsilon_2 = \epsilon_3$

$$\epsilon_m = \frac{\epsilon_1 + 2\epsilon_3}{3}$$

In the evaluation of resultant deviatoric strain, the axial strain,  $\epsilon_1$ , was measured during the experimental investigation and the lateral strain  $\epsilon_3$ , was calculated from the measured sample volume change and axial strain assuming that the sample remained cylindrical during deformation. For small strains it may be assumed that

$$\epsilon_v = \epsilon_1 + \epsilon_2 + \epsilon_3 \quad (5.8)$$

or 
$$\epsilon_v = \epsilon_1 + 2\epsilon_3 \quad (5.9)$$

The resultant deviatoric strain versus time curves for various resultant deviatoric stresses and mean normal stresses are presented in Figures 5.29 through 5.33. From these data, resultant deviatoric stress versus resultant deviatoric strain after various elapsed times were plotted and are shown in Figures 5.34 through 5.38. The total resultant deviatoric strain at any particular time was assumed to be the sum of all the instantaneous strains and the creep strains which the sample had undergone prior to the time under consideration. Figures 5.34 through 5.38 indicated that the deviatoric stress-strain relationship for the chosen time were nonlinear. The curves for  $t=500$  hours, were of hyperbolic form while all others were of a power form.

### 5.6.2 Shear Creep Function

As defined earlier, the shear creep function is the instantaneous slope of the resultant deviatoric stress-strain curve, at a given time. The instantaneous slope of the stress-strain curve was determined graphically at selected points and plotted against the ratio of mean normal stress to the resultant deviatoric stress in Figures 5.39 through 5.42. The curves can be represented by the following hyperbolic equation:

$$G_c = \frac{\sigma_m/S_d}{a + b (\sigma_m/S_d)} \quad (5.10)$$

in which  $G_c$  = shear creep function

$\sigma_m$  = mean normal stress

$S_d$  = resultant deviatoric stress

$a$  &  $b$  = constants

The equation (5.10) can be rearranged in the following form:

$$\frac{\sigma_m/S_d}{G_c} = a + b \frac{\sigma_m}{S_d} \quad (5.11)$$

The hyperbolic curves defined by equation (5.10) linearized in the transformed plot,  $(\sigma_m/S_d)/G_c$  versus  $(\sigma_m/S_d)$ , as shown in Figures 5.43 through 5.46.

The parameter,  $a$ , which varied with time was found to linearize on a log-log scale as shown in Figure 5.47. The scatter of the points due to various mean normal stress was so small that the relationship could be represented by a single straight line with the following equation:

$$a = ct^\alpha \quad (5.12)$$

in which  $c$  = value of 'a' at an arbitrarily chosen time  $t=1$  hour

$t$  = time

$\alpha$  = slope of the straight line

The parameter,  $b$ , is shown plotted against time on a log-log scale in Figure 5.48. The straight lines obtained was represented by the following equation:

$$b = mt^n \quad (5.13)$$

in which  $n$  = slope of the straight lines

$t$  = time

$m$  = value of 'b' at time  $t=1$  hour

It was observed that the slope,  $n$ , was independent of the mean normal stress whereas the factor  $m$  was dependent on the mean normal stress. The values of  $m$  were plotted against the mean normal stresses on a log-log scale in Figure 5.49 and the straight line obtained was

represented by the following equation:

$$m = m_1 \sigma_m^\beta \quad (5.14)$$

in which  $m_1$  = value of  $m$  at  $\sigma_m=1$  kPa

$\beta$  = slope of the straight line

$\sigma_m$  = mean normal stress

Substituting equation (5.14) in equation (5.13), the parameter  $b$ , can be represented by the following equation:

$$b = m_1 \sigma_m^\beta t^n \quad (5.15)$$

Substituting equation (5.12) for 'a' and equation (5.15) for 'b' in equation (5.10), the equation for the shear creep function can be written as:

$$G_c = \left( m_1 \sigma_m^\beta t^n + ct^\alpha \frac{S_c}{\sigma_m} \right)^{-1} \quad (5.16)$$

which for the tests conducted becomes:

$$G_c = \left( 3 \times 10^{-5} \sigma_m^{-0.205} t^{0.147} + 1 \times 10^{-5} t^{0.23} \frac{S_c}{\sigma_m} \right)^{-1} \quad (5.17)$$

According to equation (5.17), the shear creep function,  $G_c$ , decreases exponentially with an increase in time after the load application. This is illustrated by plots of  $G_c$  versus time in Figures

5.50 through 5.53 for various deviatoric stresses and for various mean normal stresses, in which the values predicted by the equation are represented by the solid lines and the data points by the symbols. The shear creep function,  $G_e$ , increases hyperbolically with an increase in mean normal stress. This is shown by plots of  $G_e$  versus mean normal stress for various times in Figure 5.54. On the other hand, as shown in Figure 5.55, the shear creep function decreases exponentially with an increase in deviatoric stress for a constant time.

TABLE 5.1

## Physical Properties of Frozen Sand Sample

Sample	Dry Unit Weight KN/m <sup>3</sup>	Water Content %	Porosity %	Water Saturation %	Sample Test Temp. °C
MST1	15.2	26.6	43.2	92.5	-3
MST2	15.2	25.3	43.6	88.5	-3
MST3	15.6	24.4	41.1	94.5	-3
MST4	15.7	25.0	41.7	94.1	-3
MST5	15.8	24.1	40.6	90.0	-3

TABLE 5.2

Summary of Stress Conditions for the Constant Mean Normal Stress Tests

Test	$\sigma_m$ (kPa)	$\sigma_3$ (kPa)	$\sigma_1$ (kPa)	$S_d$ (kPa)
MST1	140	-20	+40	49.0
MST2	280	-40	+80	98.0
MST3	280	-80	+160	196.0
MST4	70	-20	+40	49.0
MST5	420	-80	+160	196.0



TABLE 5.3

## Details of Stress Application

test MST1  $\sigma_m=140$  kPa

$\sigma_1$ (kPa)	$\sigma_3$ (kPa)	$S_a$ (kPa)	Duration of Stress Application (Hours)
140	140	0	21
180	120	49	3
220	100	98	69
260	80	147	95
300	60	196	94
340	40	245	95
380	20	294	1154
420	0	343	862

TABLE 5.4

## Details of Stress Application

Test MST2  $\sigma_m=280$  kPa

$\sigma_1$ (kPa)	$\sigma_3$ (kPa)	$S_d$ (kPa)	Duration of Stress Application (Hour)
280	280	0	596
360	240	98	475
440	200	196	504
520	160	294	1006
600	120	392	1393
680	80	490	984

TABLE 5.5

Details of Stress Application

Test MST3  $\sigma_m=280$  kPa

$\sigma_1$ (kPa)	$\sigma_3$ (kPa)	$S_a$ (kPa)	Duration of Stress Application (Hour)
280	280	0	570
440	200	196	410
600	120	392	1848

TABLE 5.6

## Details of Stress Application

Test MST4  $\sigma_m=70$  kPa

$\sigma_1$ (kPa)	$\sigma_3$ (kPa)	$S_a$ (kPa)	Duration of Stress Application (Hour)
70	70	0	960
110	50	49	815
150	30	98	1852
190	10	147	1808

TABLE 5.7

Details of Stress Application

Test MST5  $\sigma_m=420$  kPa

$\sigma_1$ (kPa)	$\sigma_3$ (kPa)	$S_d$ (kPa)	Duration of Stress Application (Hour)
420	420	0	1152
580	340	196	817
740	260	392	1029
900	180	588	2144

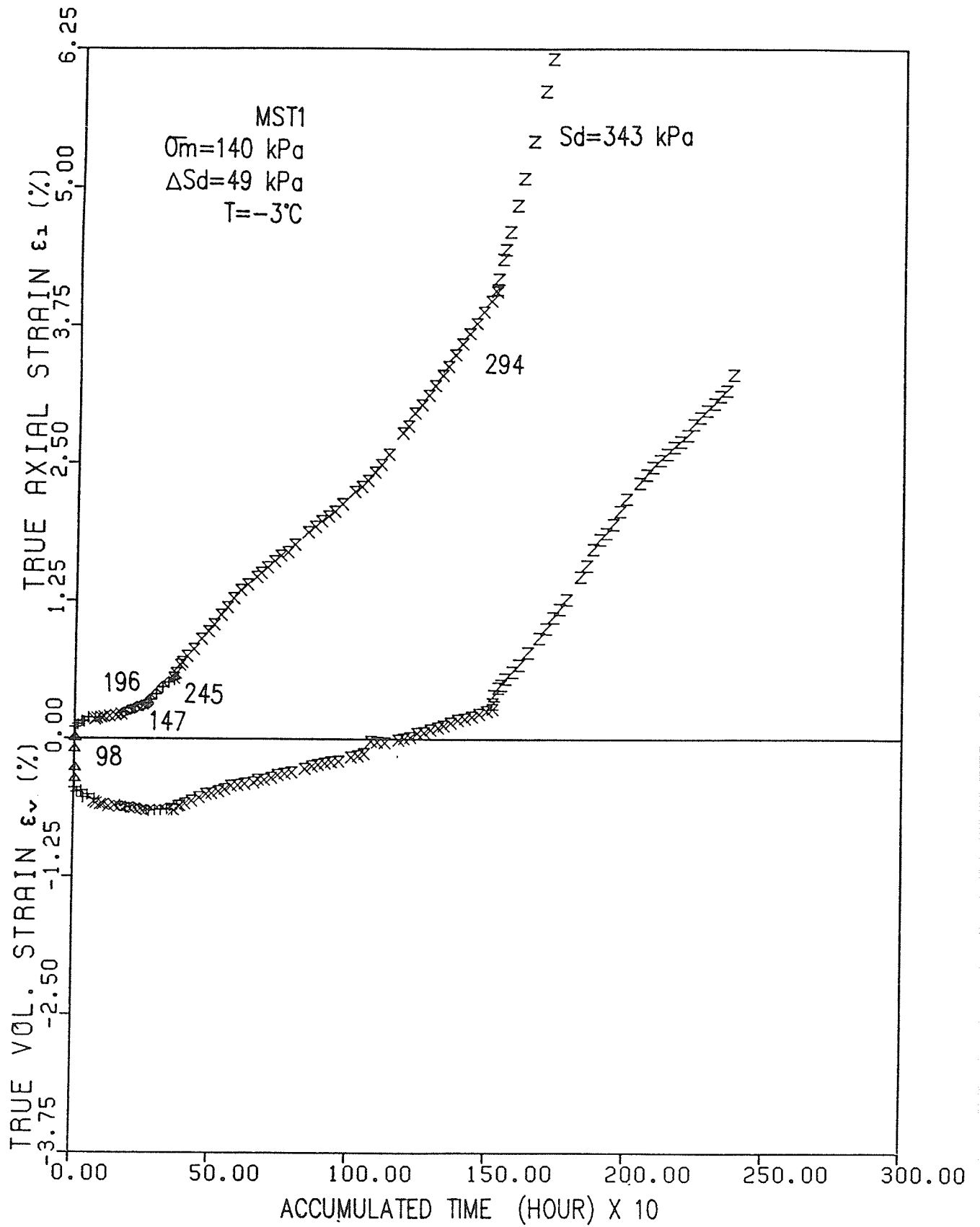


Figure 5.1 True volumetric and true axial strain versus accumulated time (MST1)

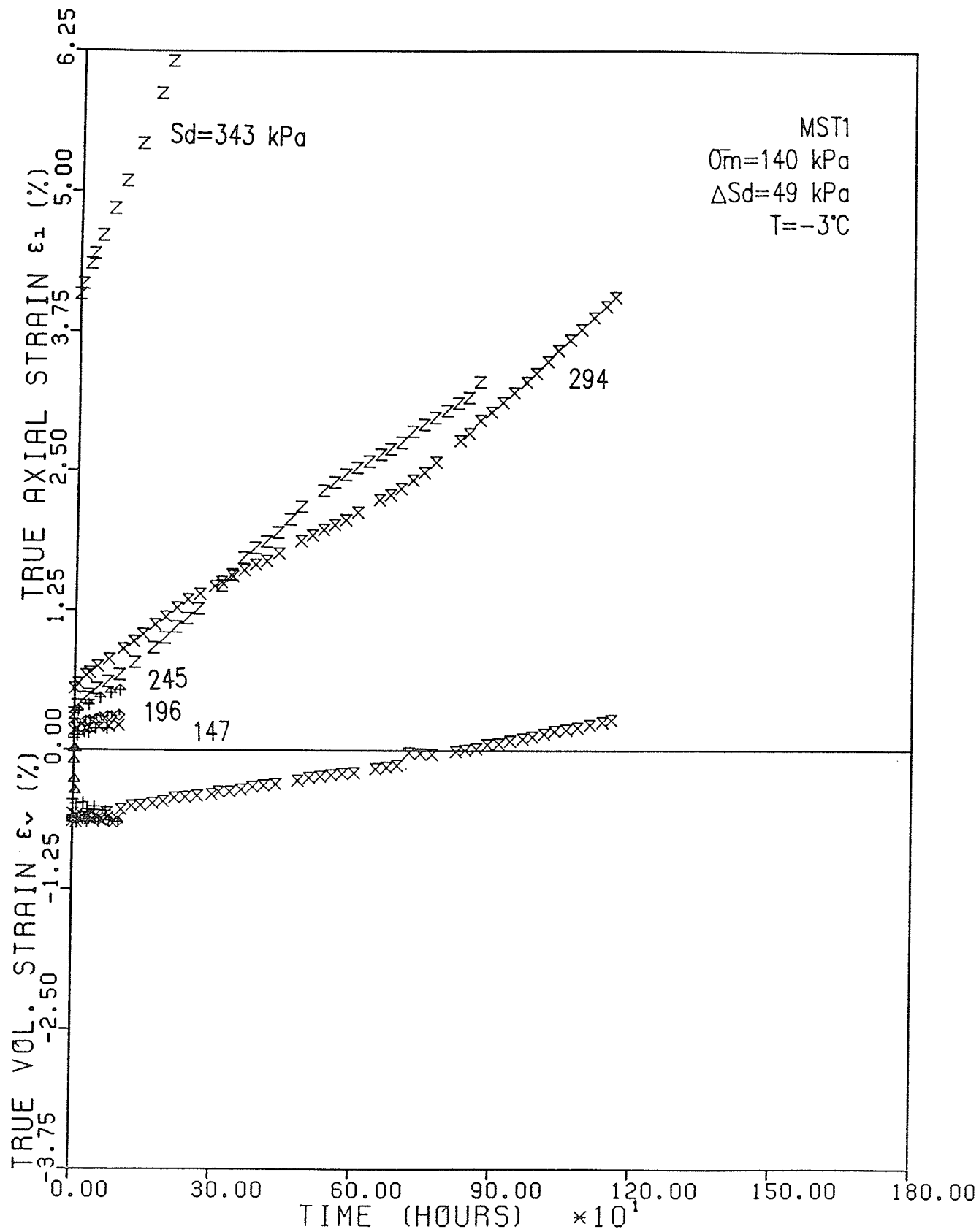


Figure 5.2 True volumetric and true axial strain versus time (MST1)

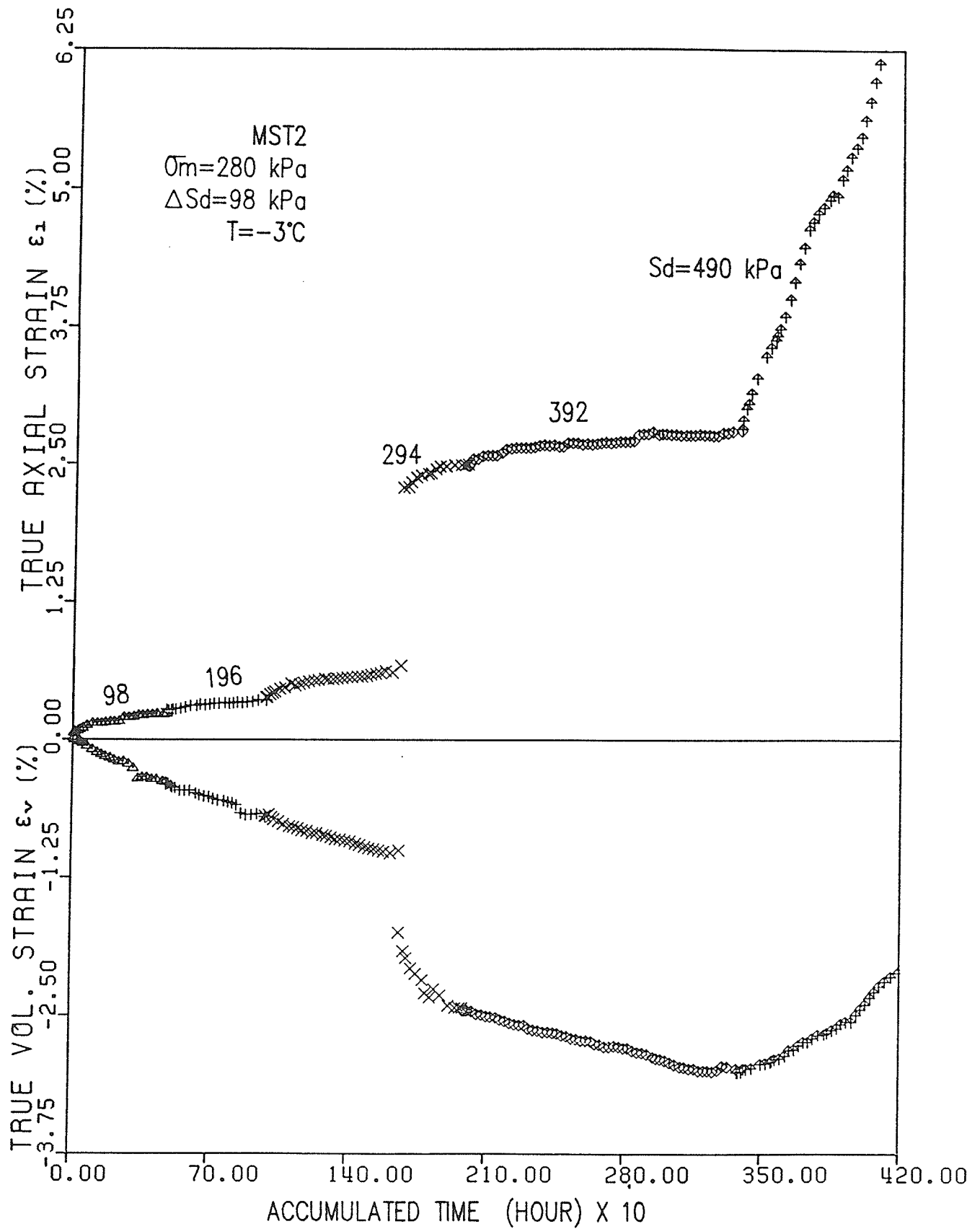


Figure 5.3 True volumetric and true axial strain versus accumulated time (MST2)



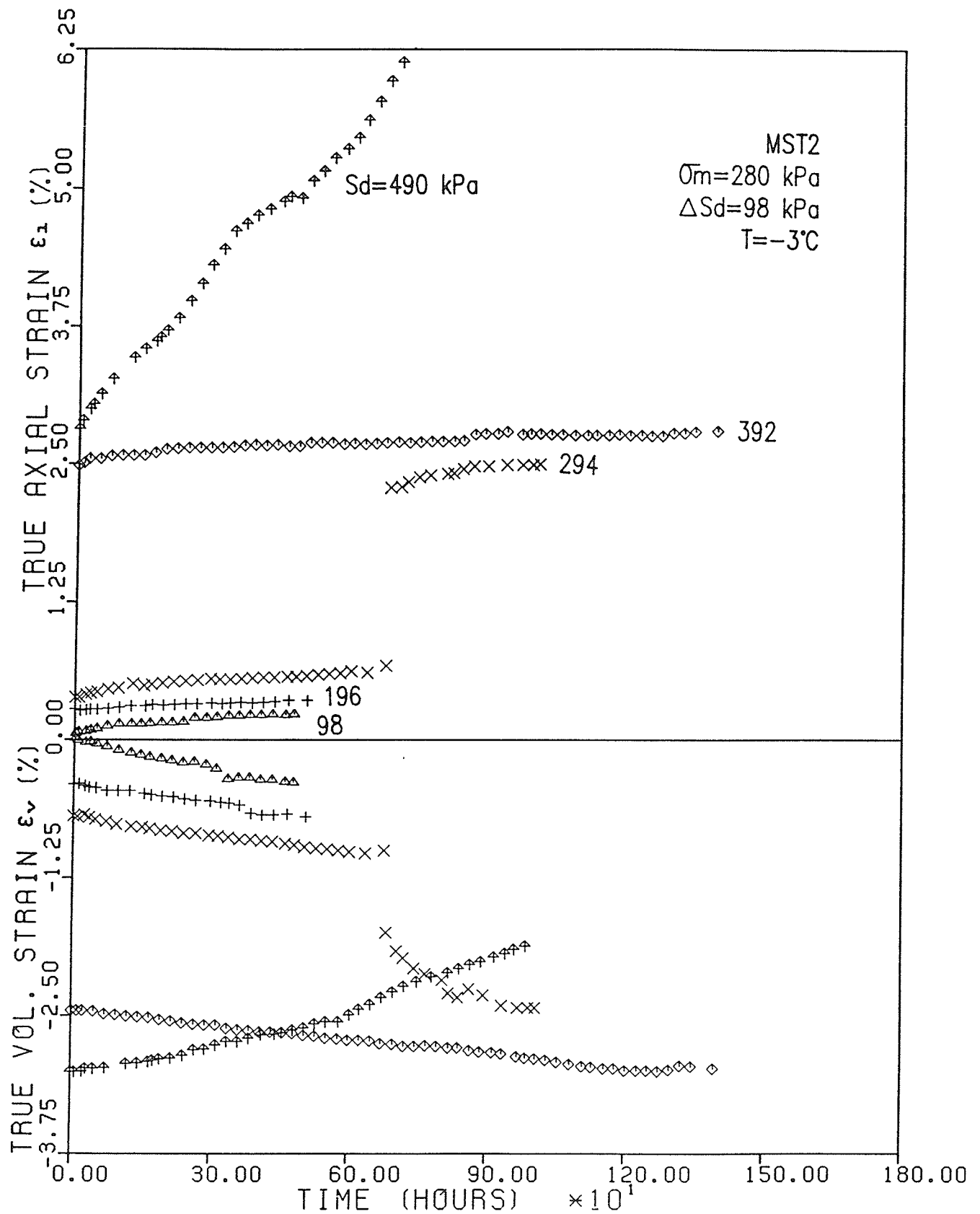


Figure 5.4 True volumetric and true axial strain versus time (MST2)

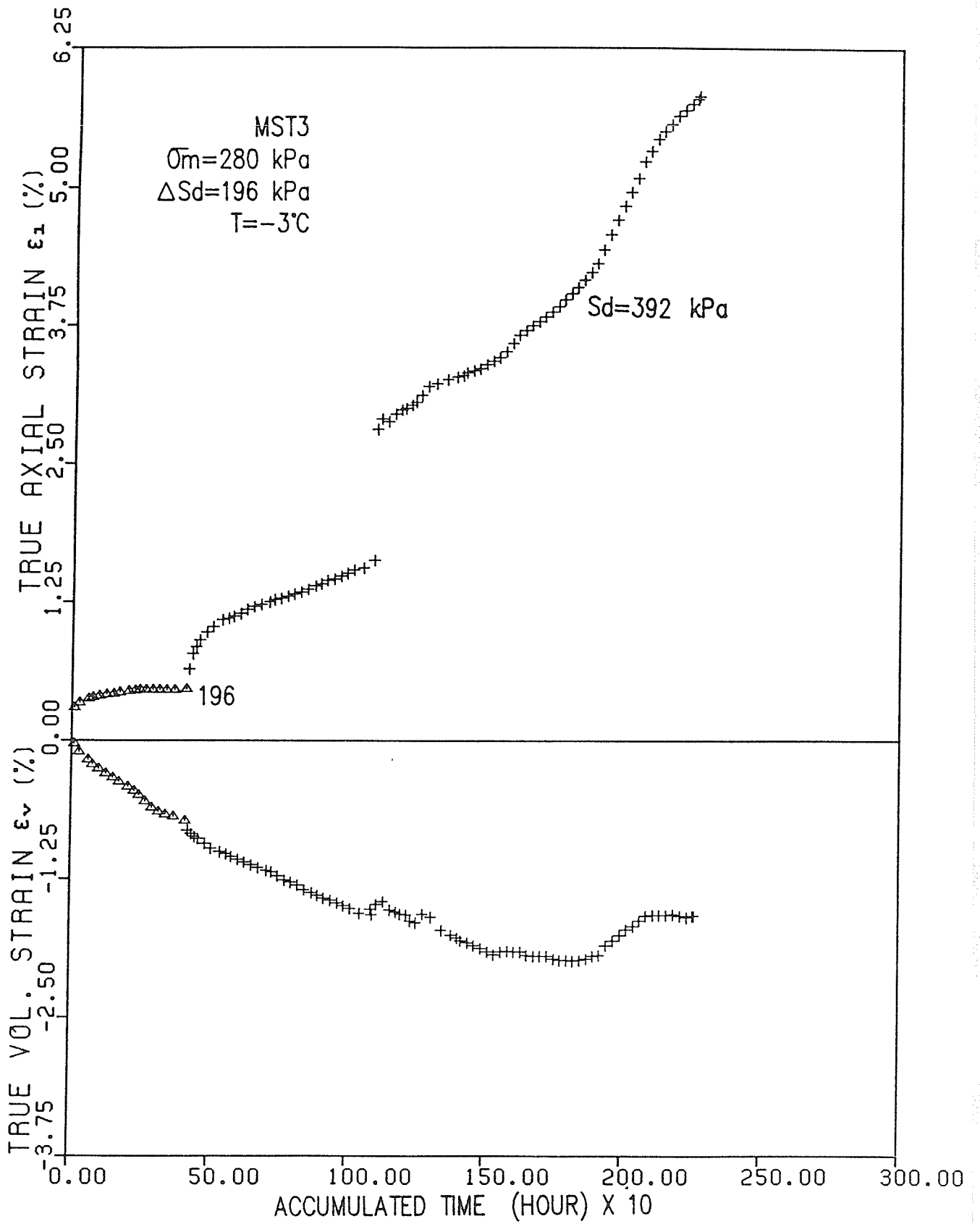


Figure 5.5 True volumetric and true axial strain versus accumulated time (MST3)

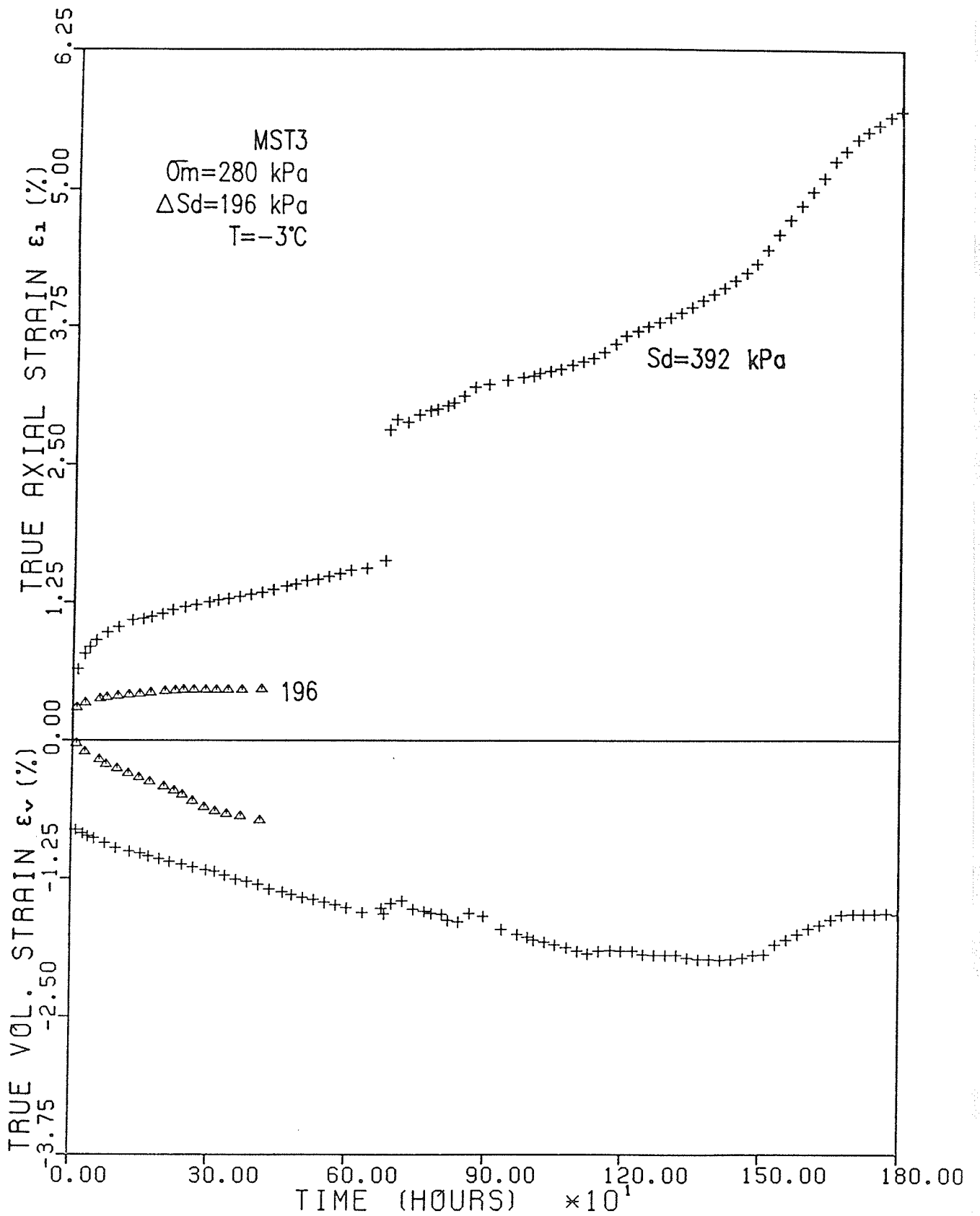


Figure 5.6 True volumetric and true axial strain versus time (MST3)

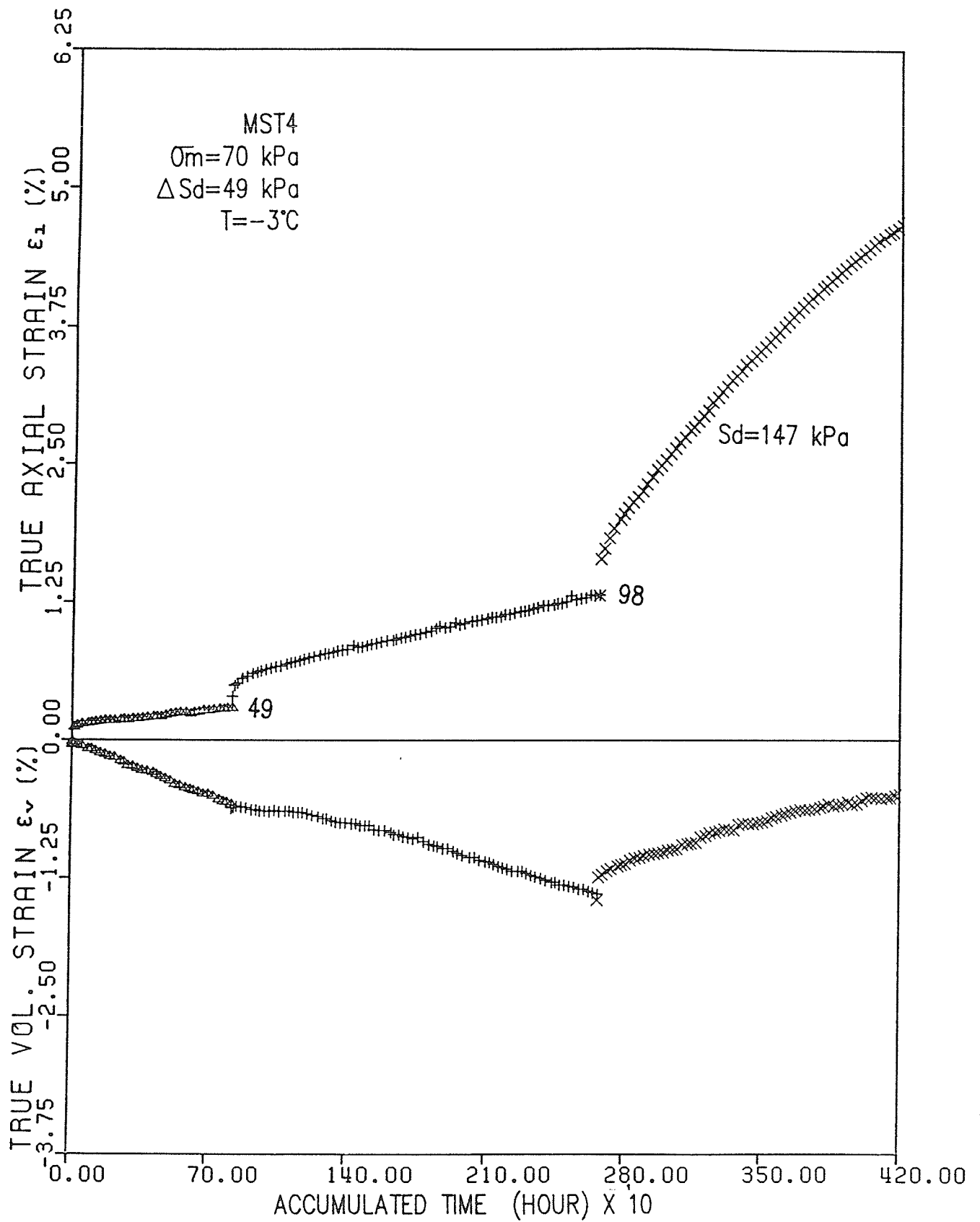


Figure 5.7 True volumetric and true axial strain versus accumulated time (MST4)

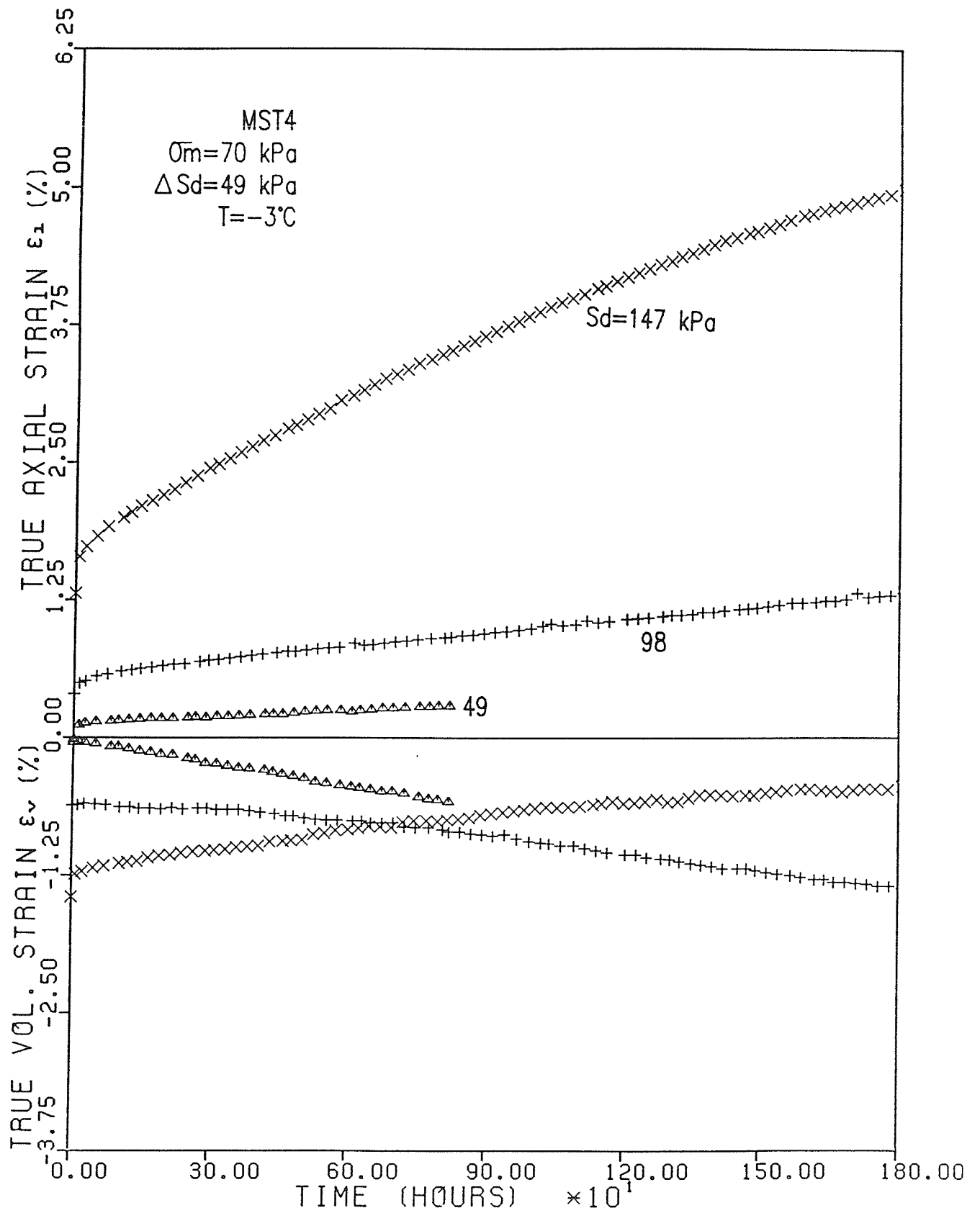


Figure 5.8 True volumetric and true axial strain versus time (MST4)

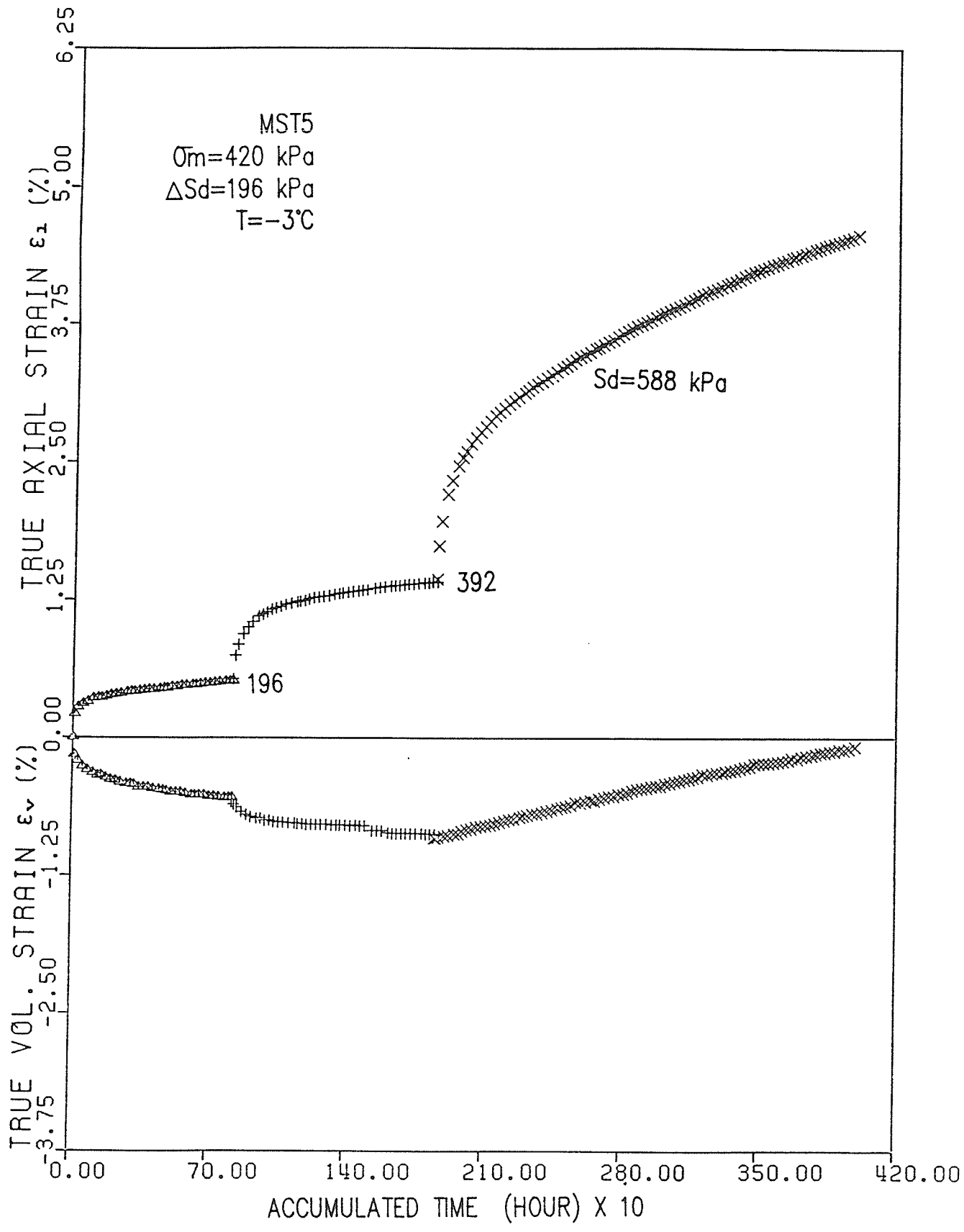


Figure 5.9 True volumetric and true axial strain versus accumulated time (MST5)

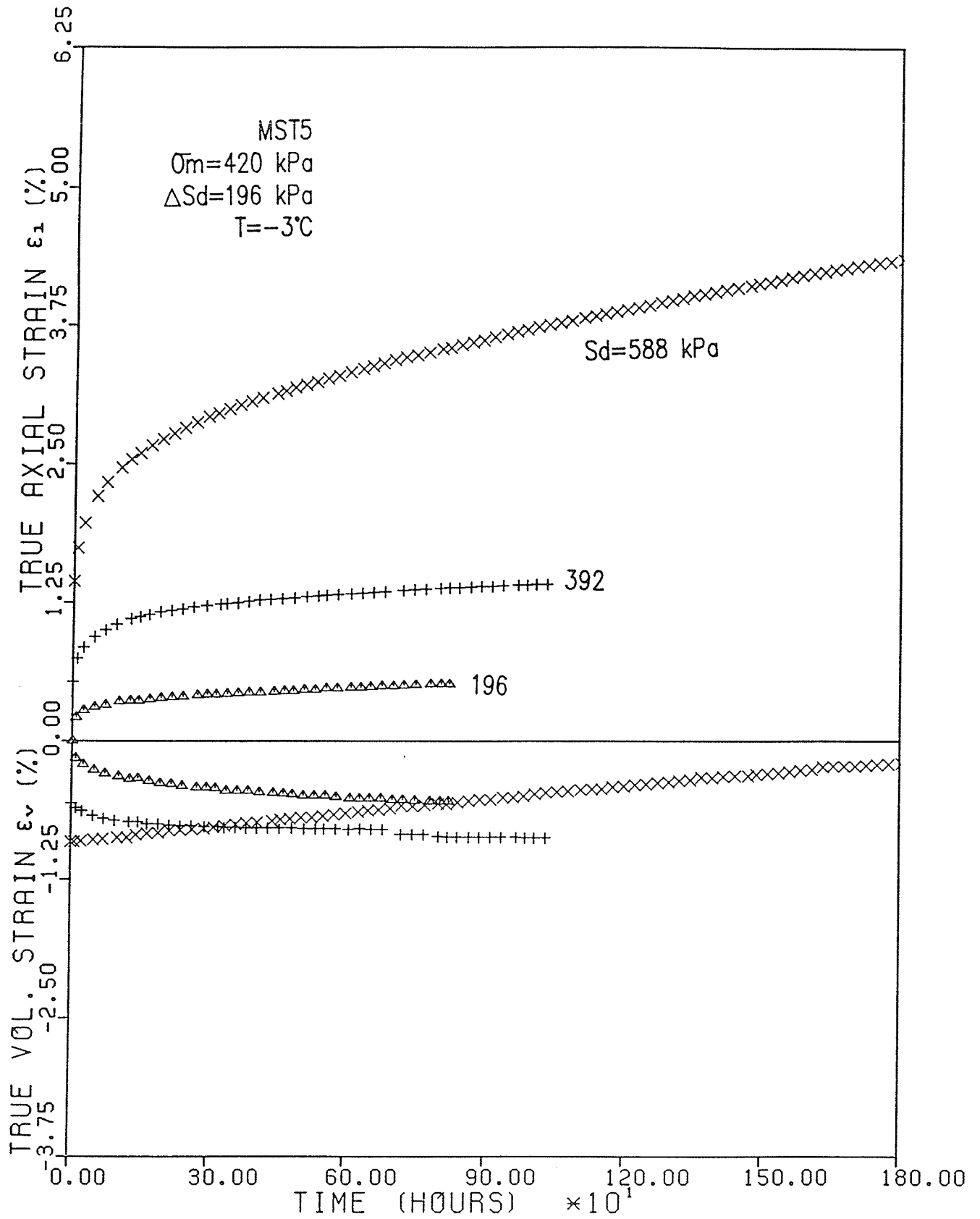


Figure 5.10 True volumetric and true axial strain versus time (MST5)

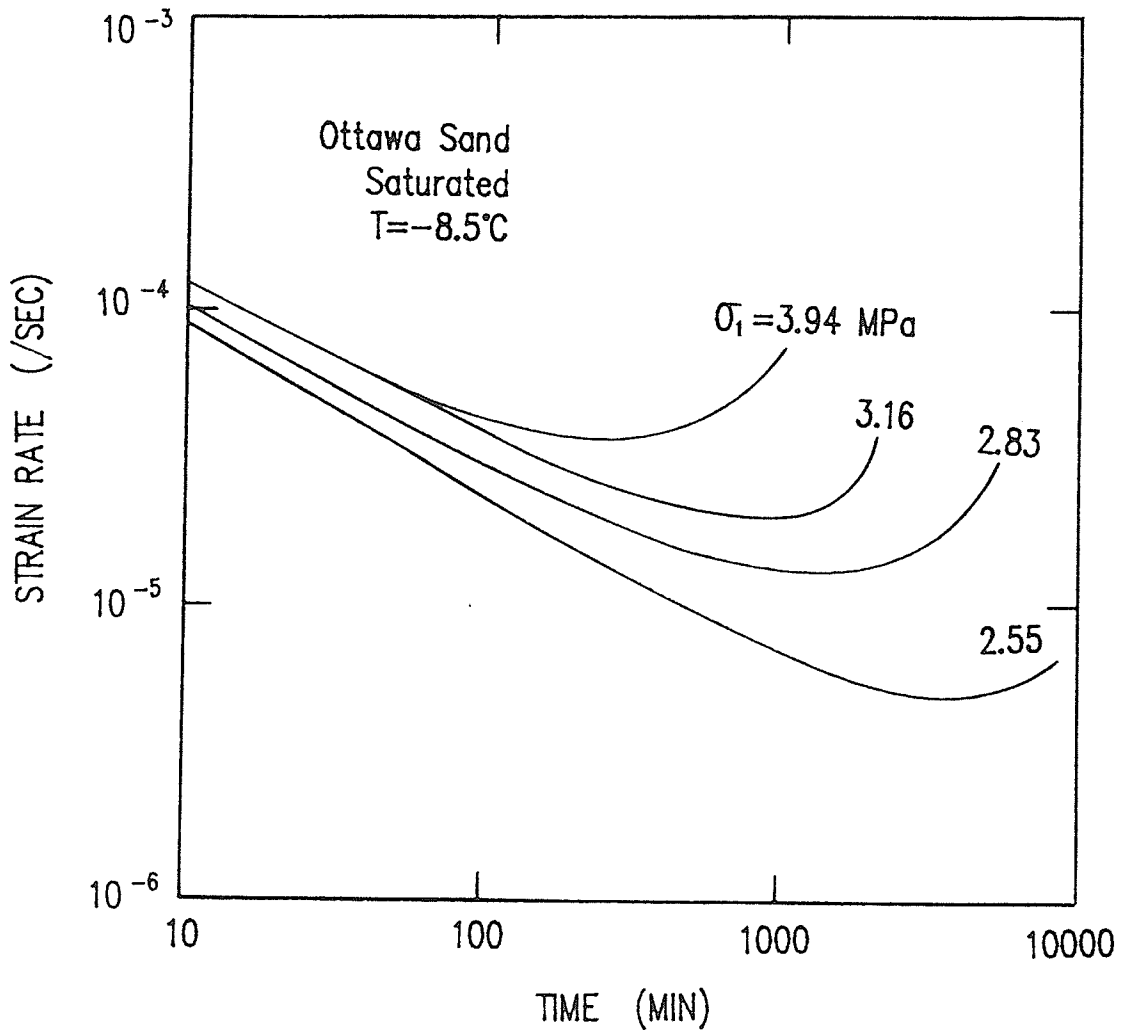


Figure 5.11 Axial strain rate versus time (after Rein et al., 1975)



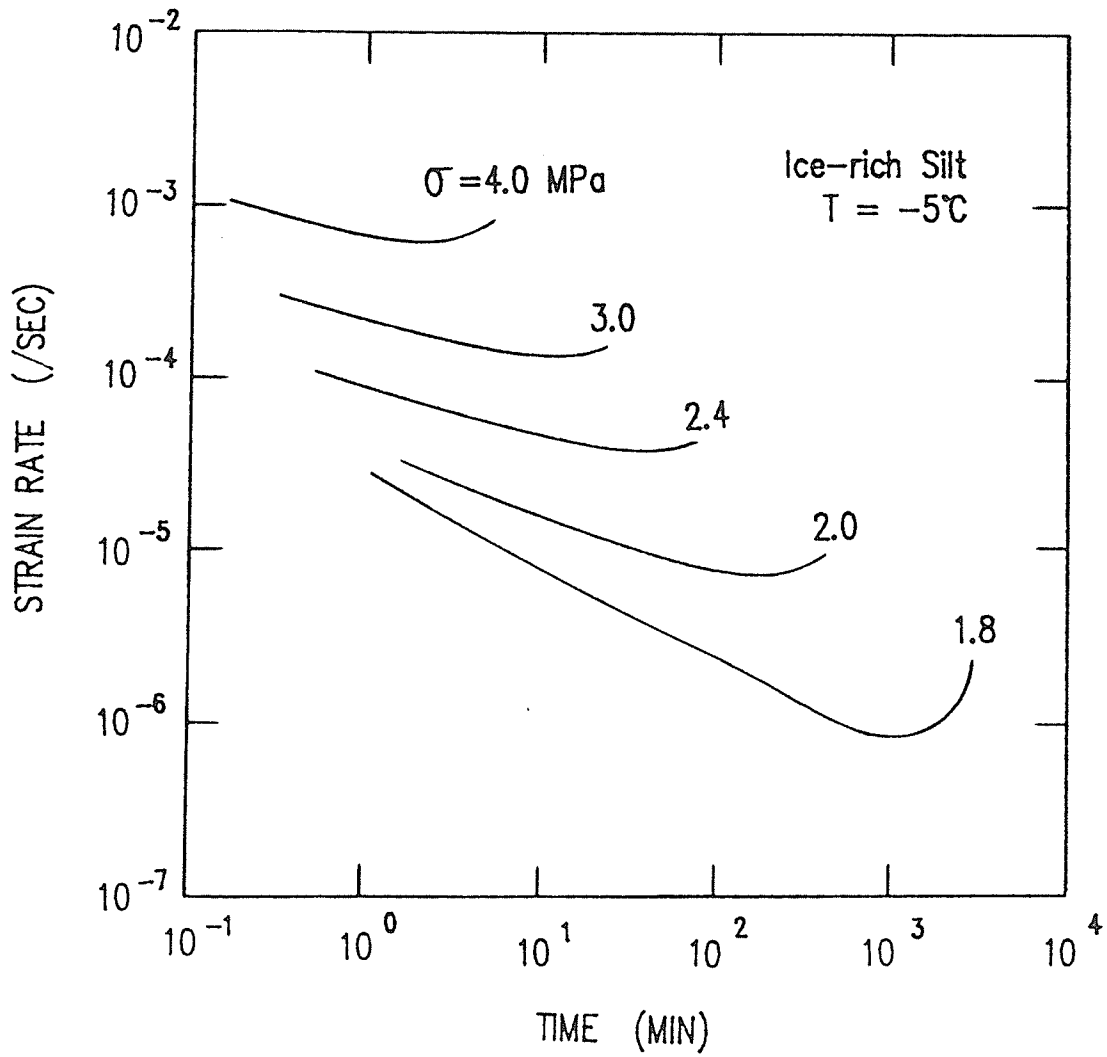


Figure 5.12 Axial strain rate versus time for silt (after Yalin and Carbee, 1984)

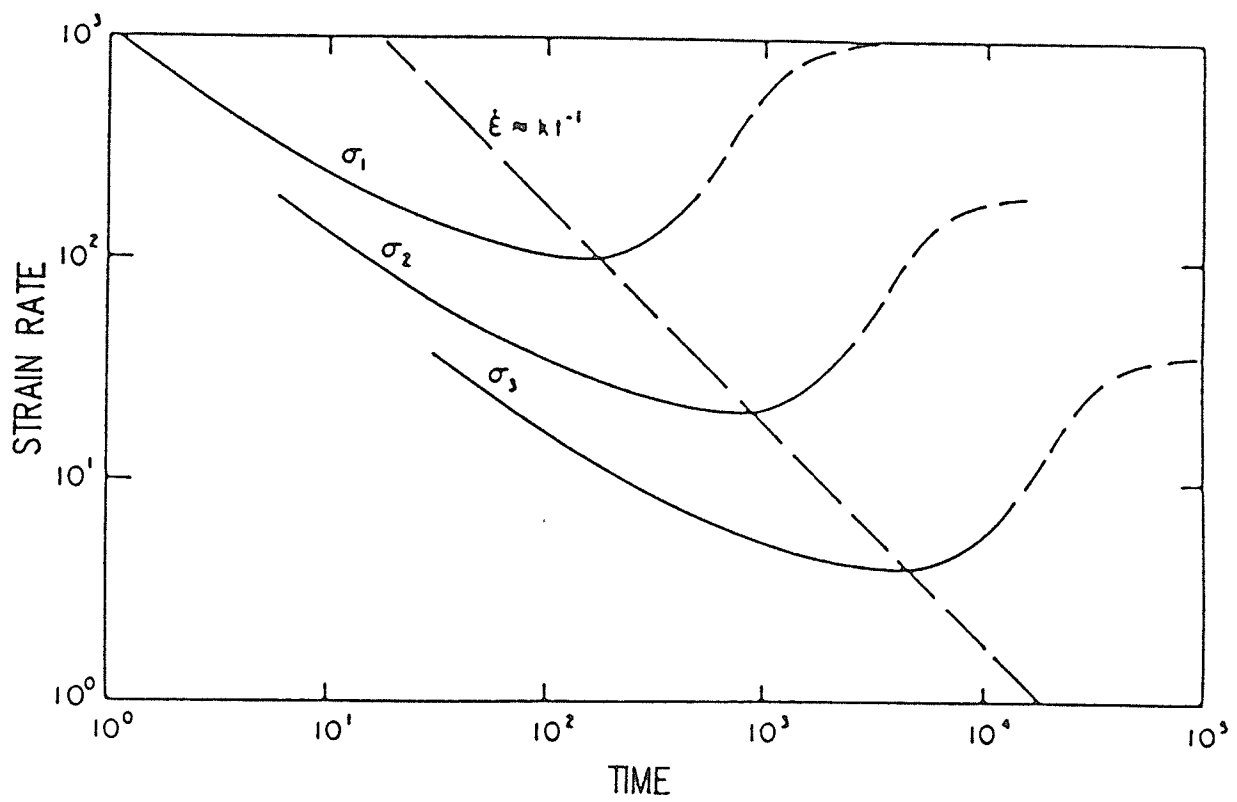


Figure 5.13 Axial strain rate versus time for polycrystalline ice (Mellor, 1979)

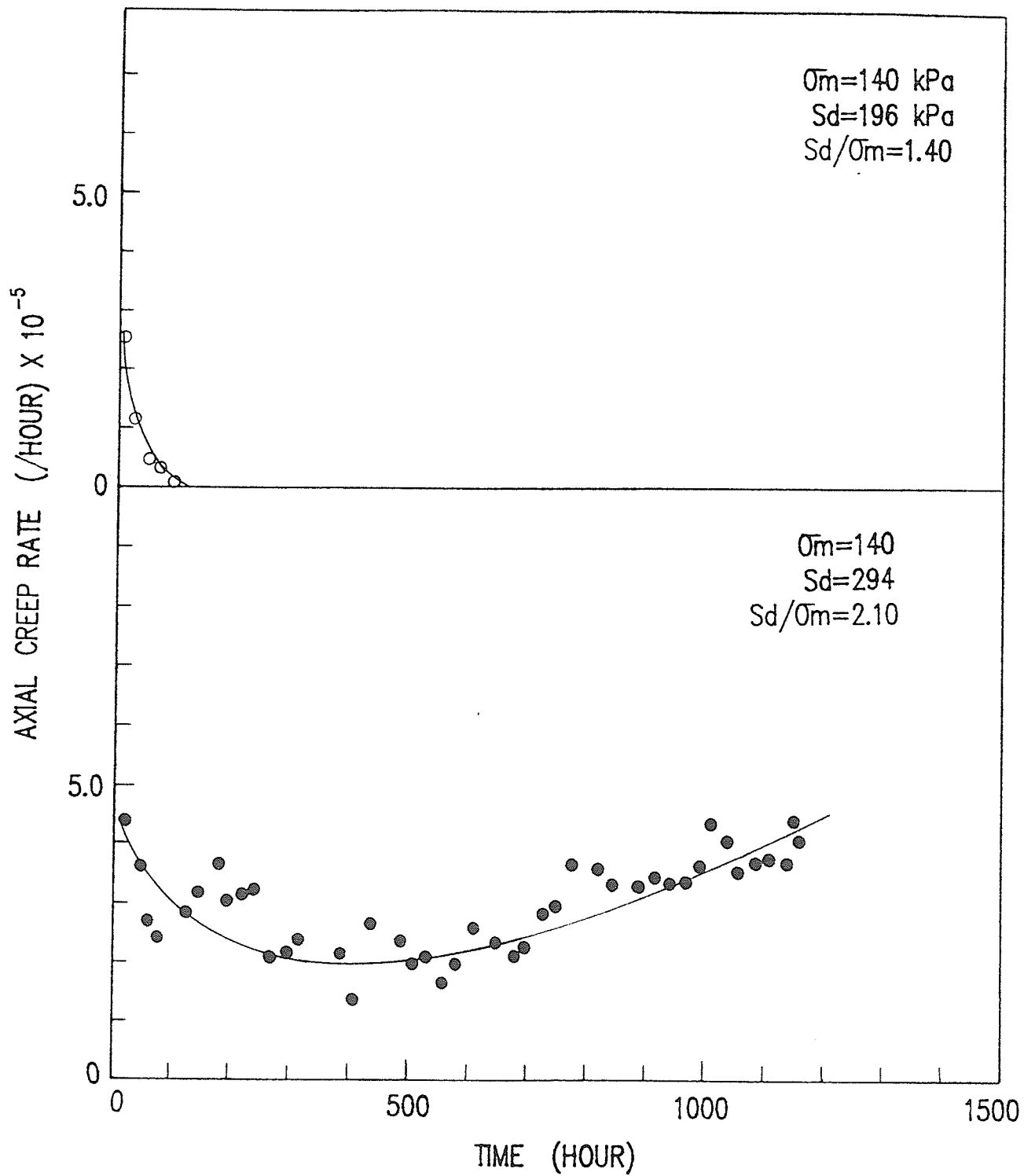


Figure 5.14 Axial creep rate versus time (MST1)

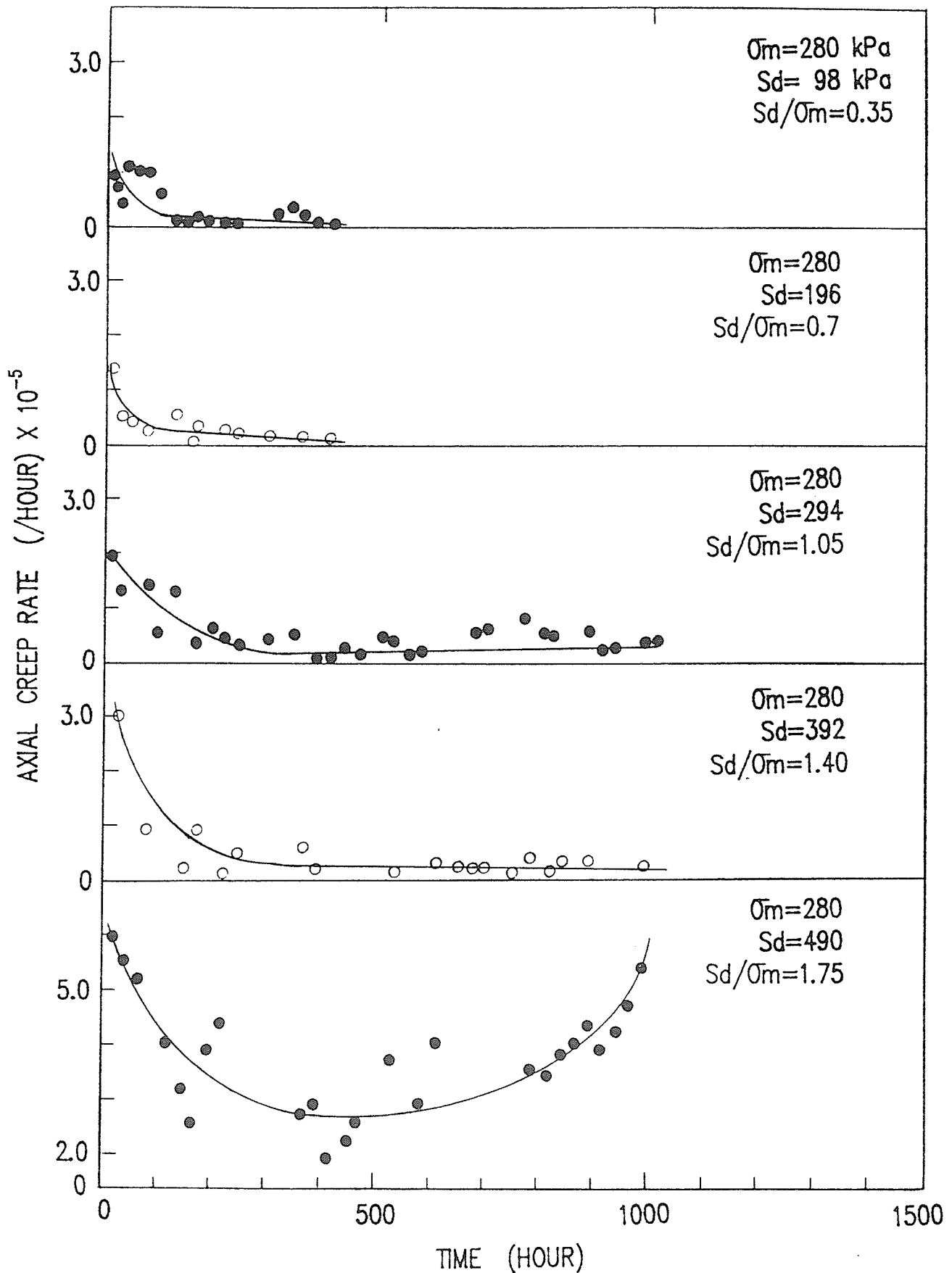


Figure 5.15 Axial creep rate versus time (MST2)

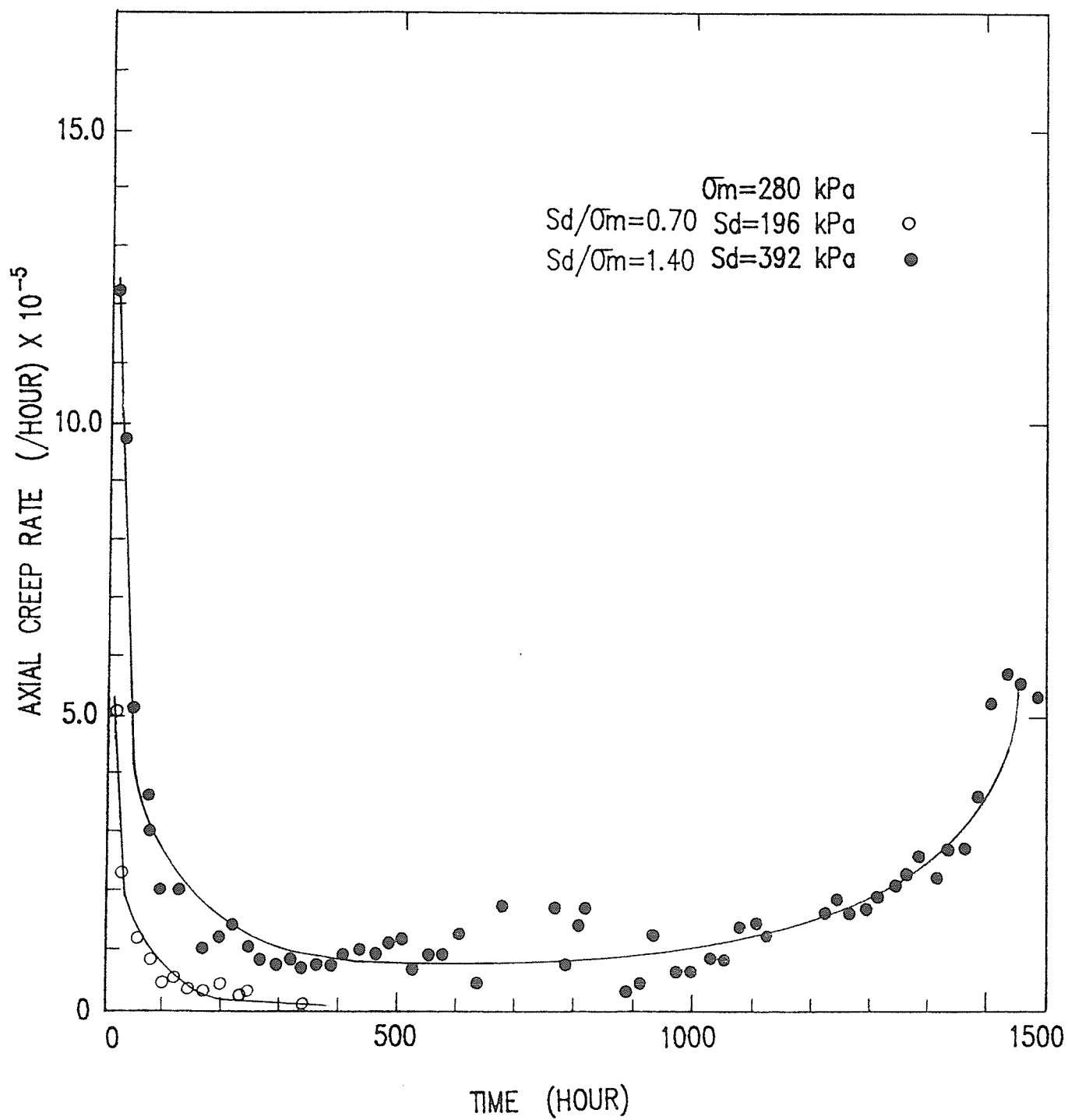


Figure 5.16 Axial creep rate versus time (MST3)

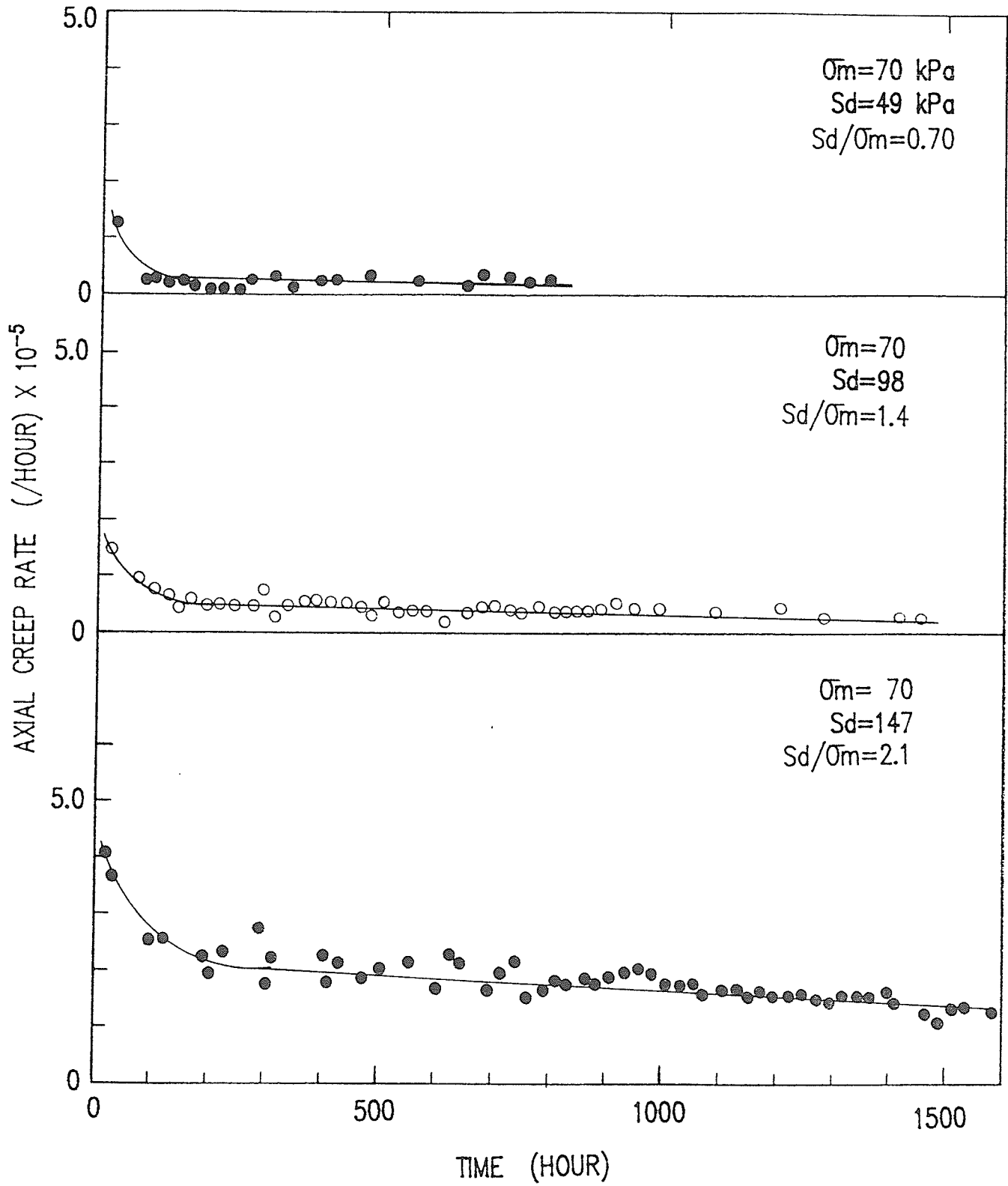


Figure 5.17 Axial creep rate versus time (MST4)

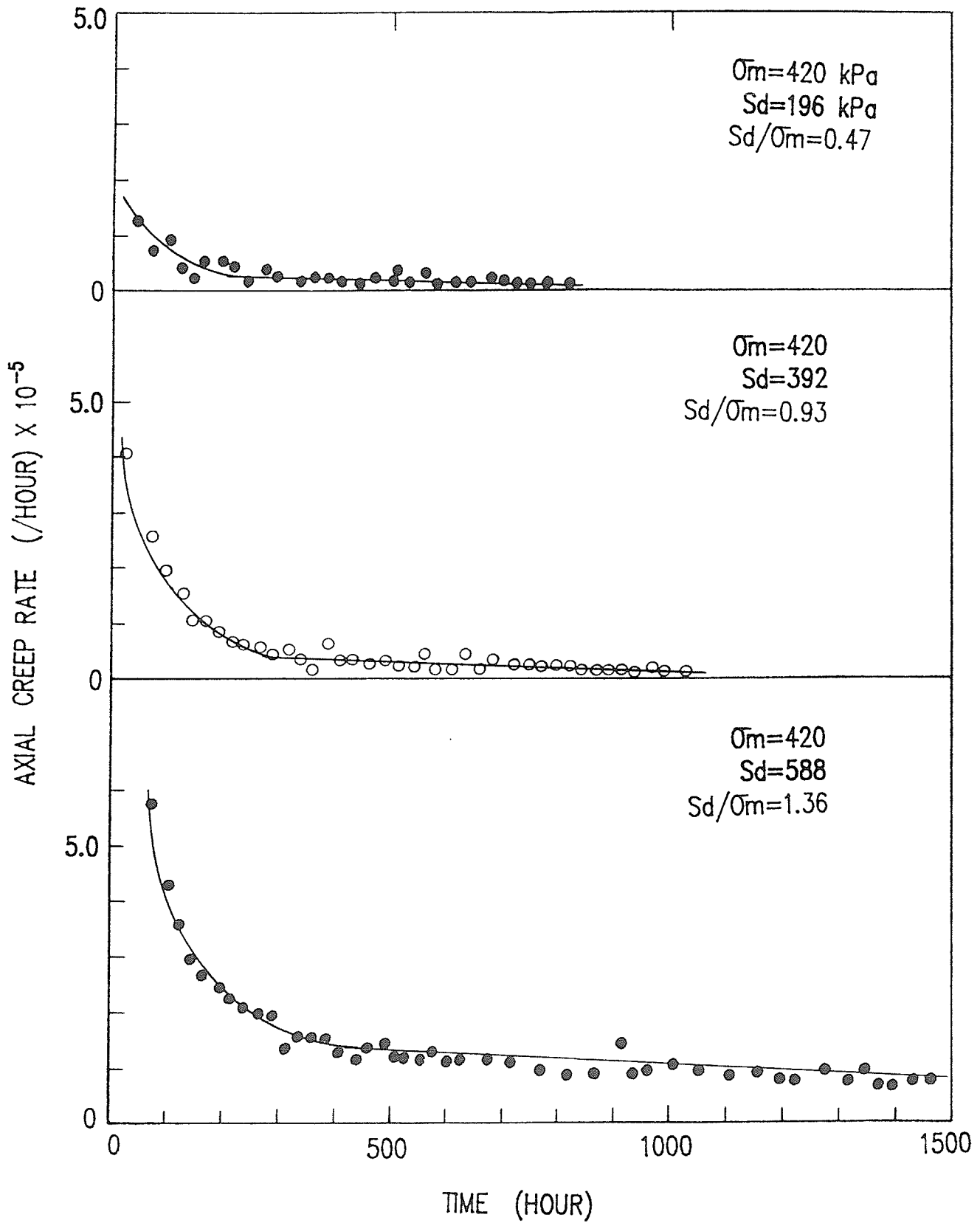


Figure 5.18 Axial creep rate versus time (MST5)

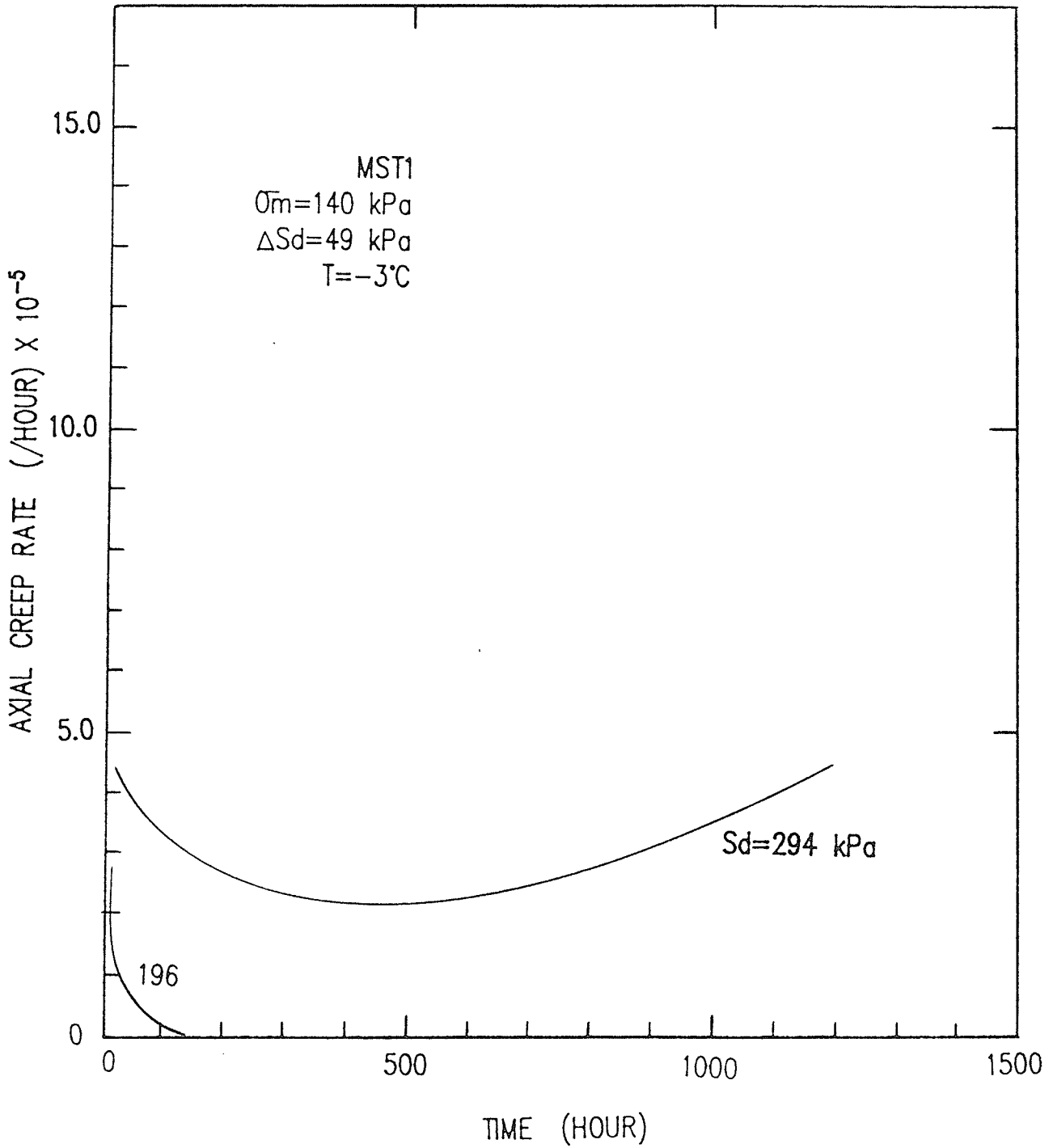


Figure 5.19 Axial creep rate versus time for  $\bar{\sigma}_m = 140 \text{ kPa}$



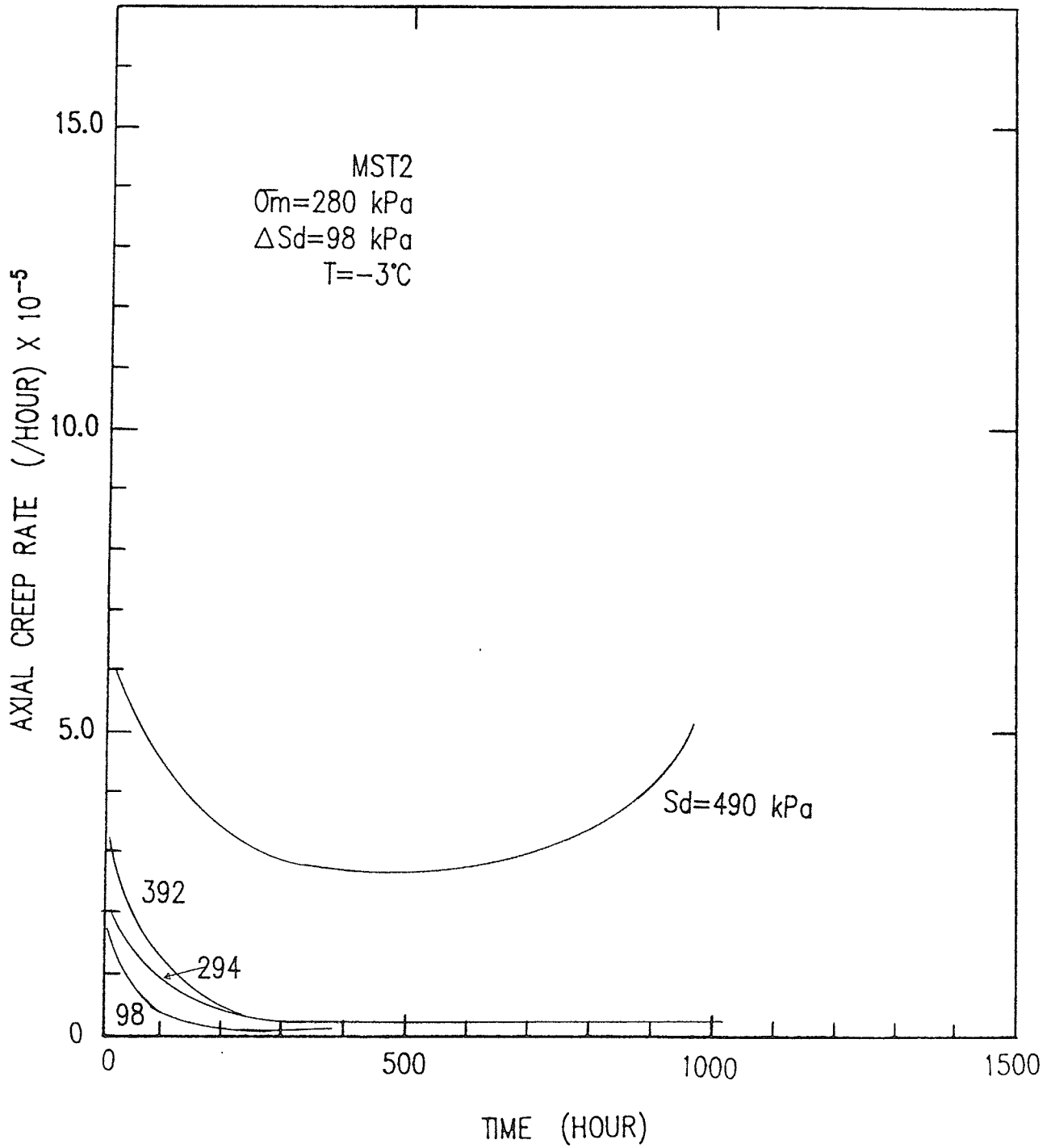


Figure 5.20 Axial creep rate versus time for  $\bar{\sigma}_m = 280 \text{ kPa}$

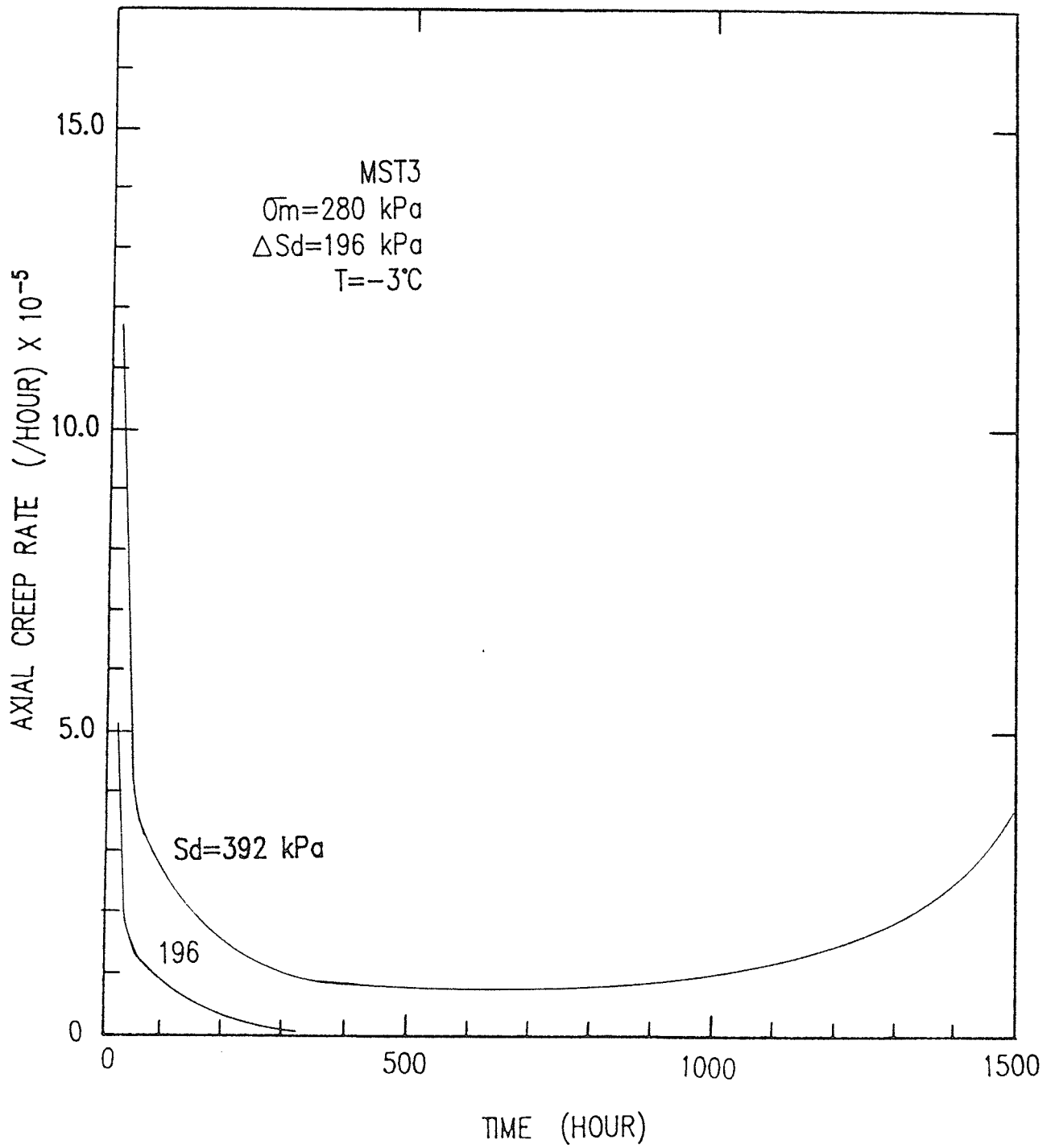


Figure 5.21 Axial creep rate versus time for  $\bar{\sigma}_m = 280 \text{ kPa}$

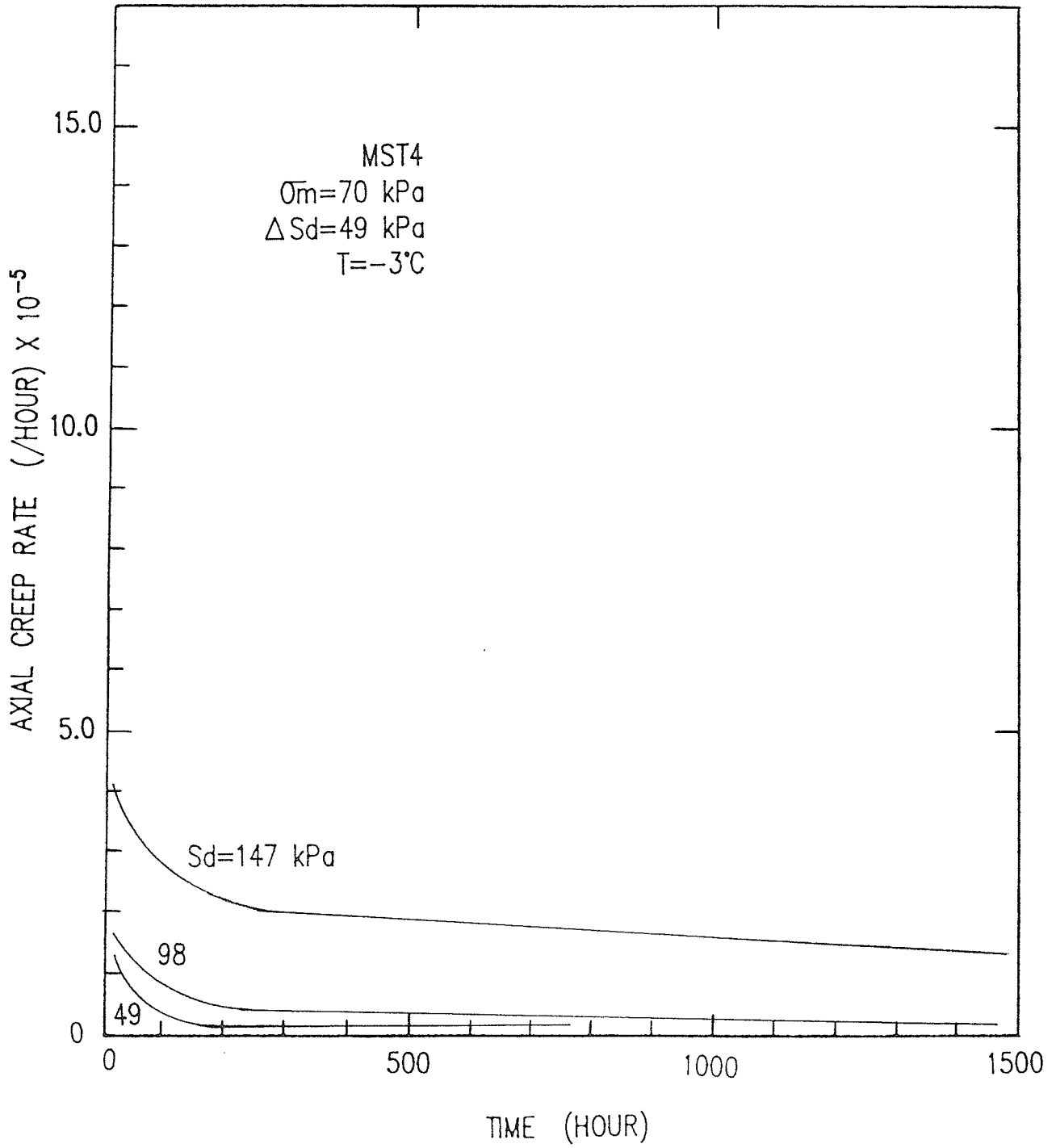


Figure 5.22 Axial creep rate versus time for  $\bar{\sigma}_m = 70 \text{ kPa}$

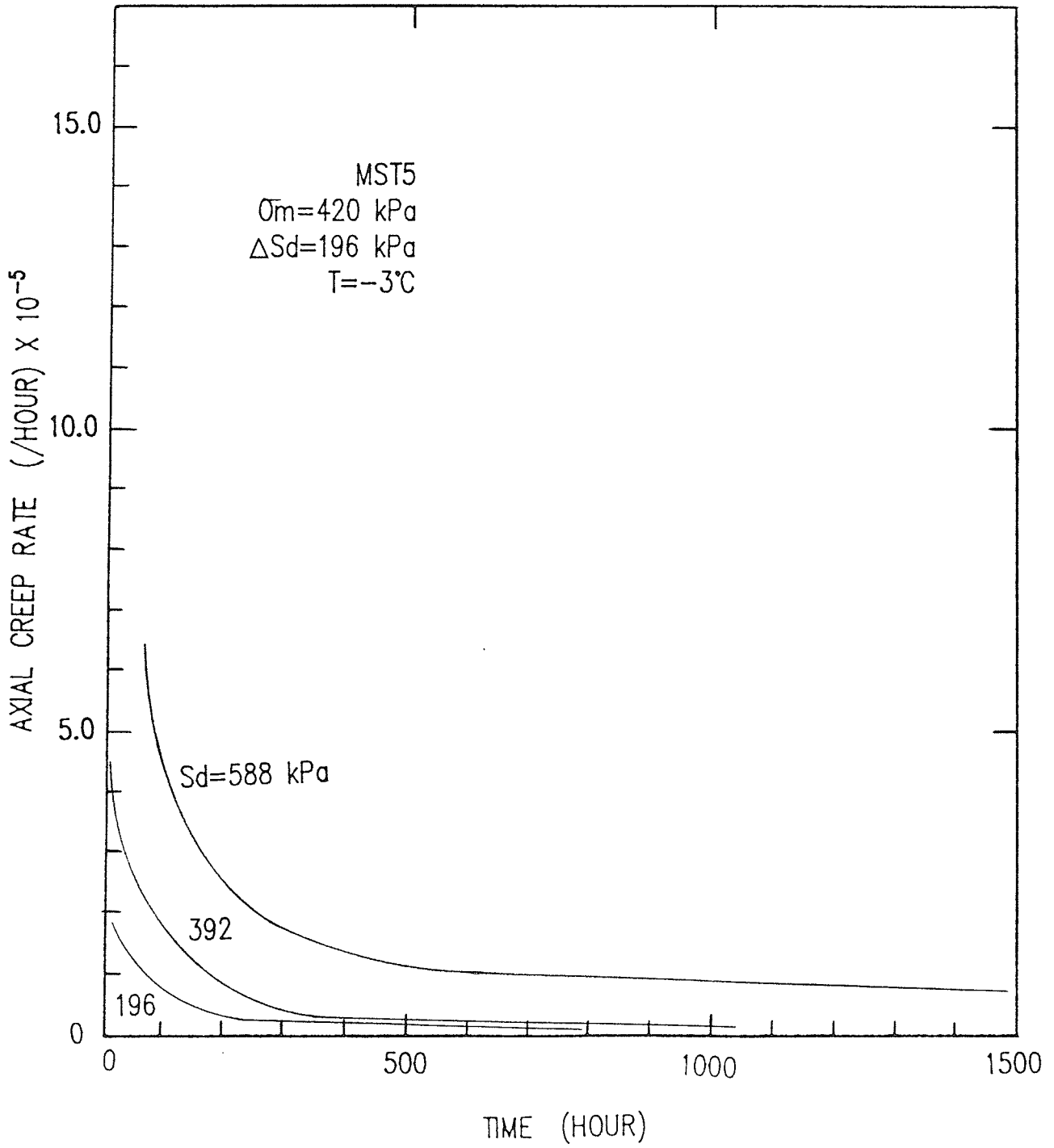


Figure 5.23 Axial creep rate versus time for  $\bar{\sigma}_m = 420 \text{ kPa}$

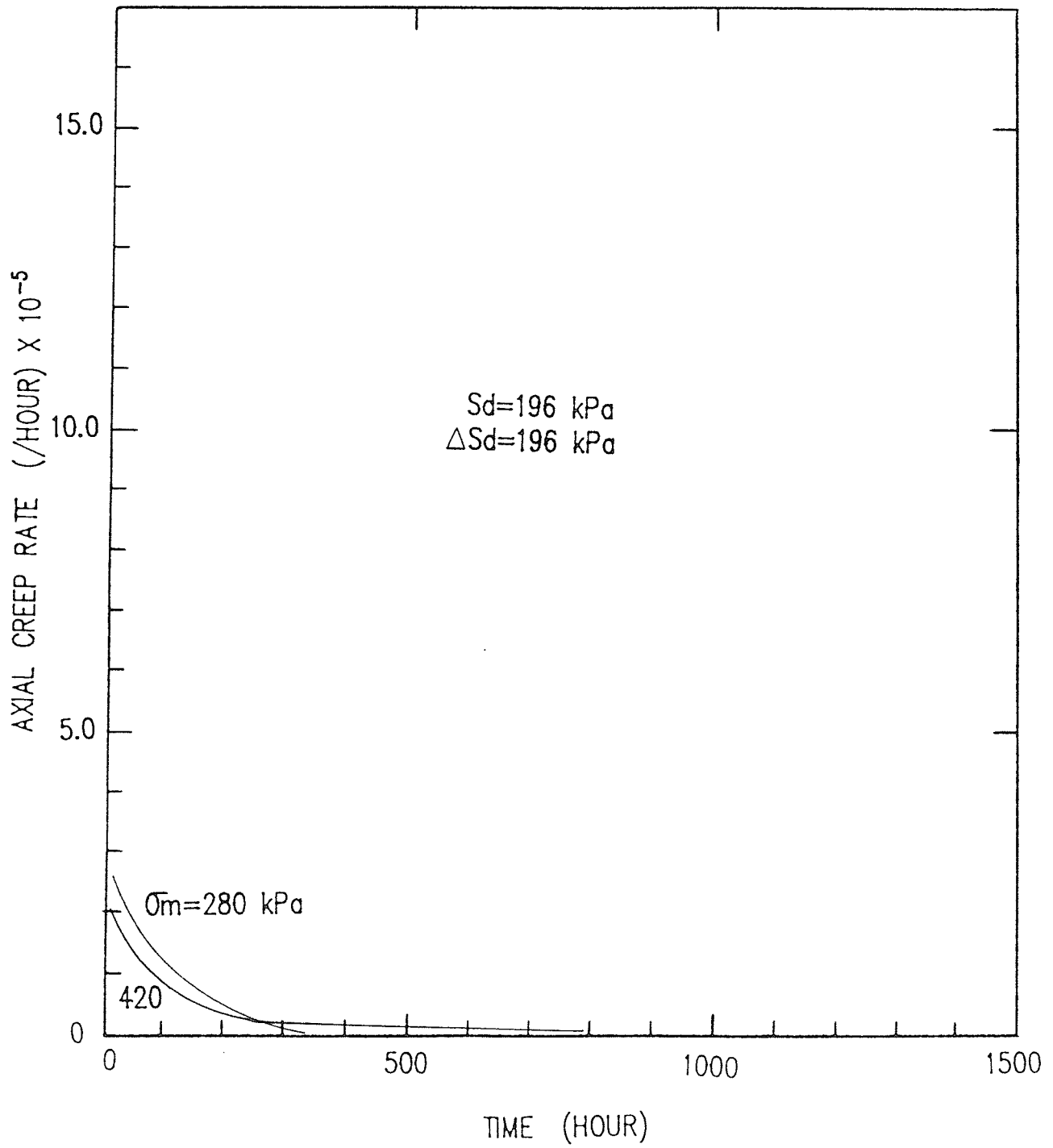


Figure 5.24 Axial creep rate versus time for  $S_d=196 \text{ kPa}$

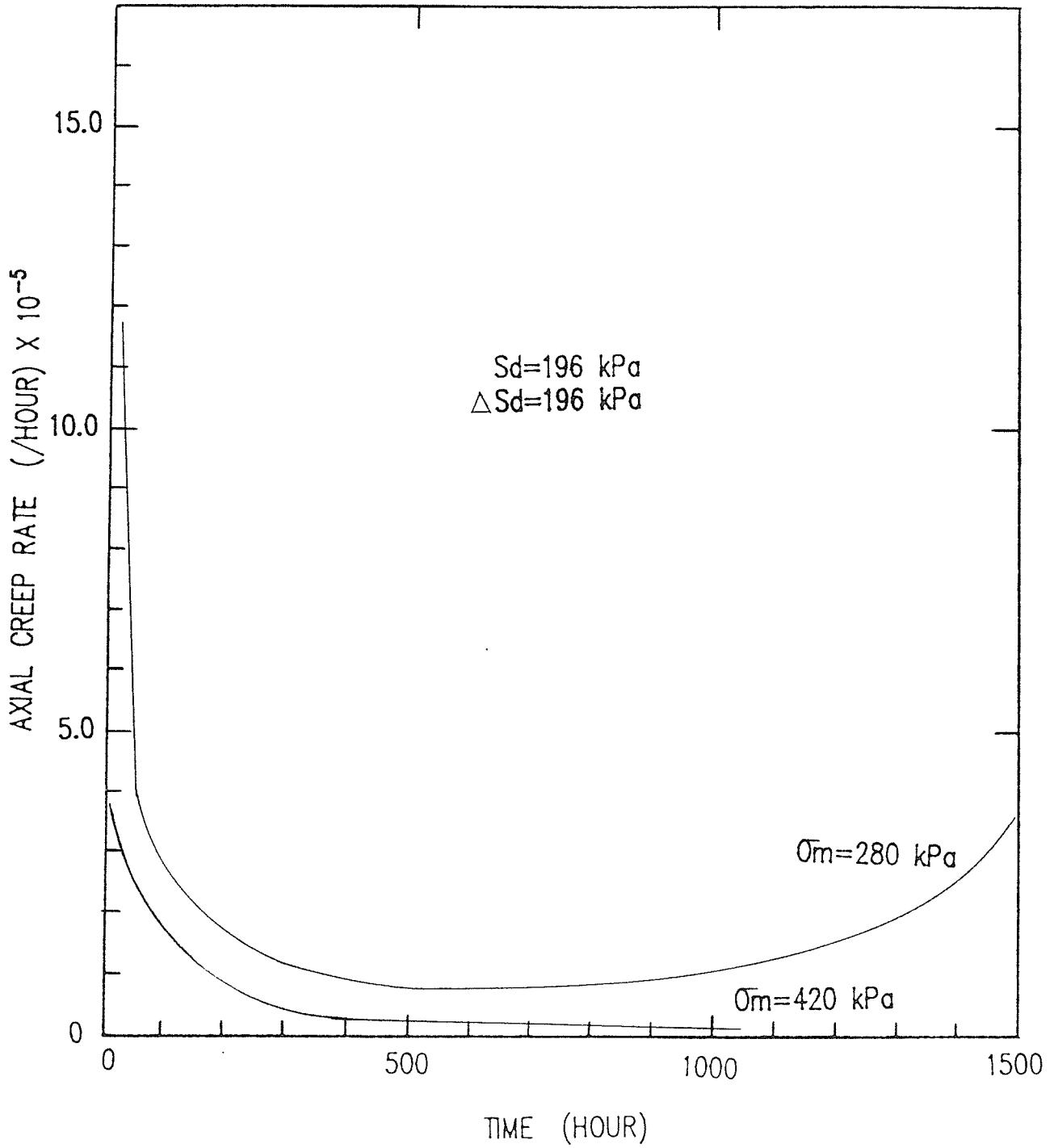


Figure 5.25 Axial creep rate versus time for  $S_d=392 \text{ kPa}$

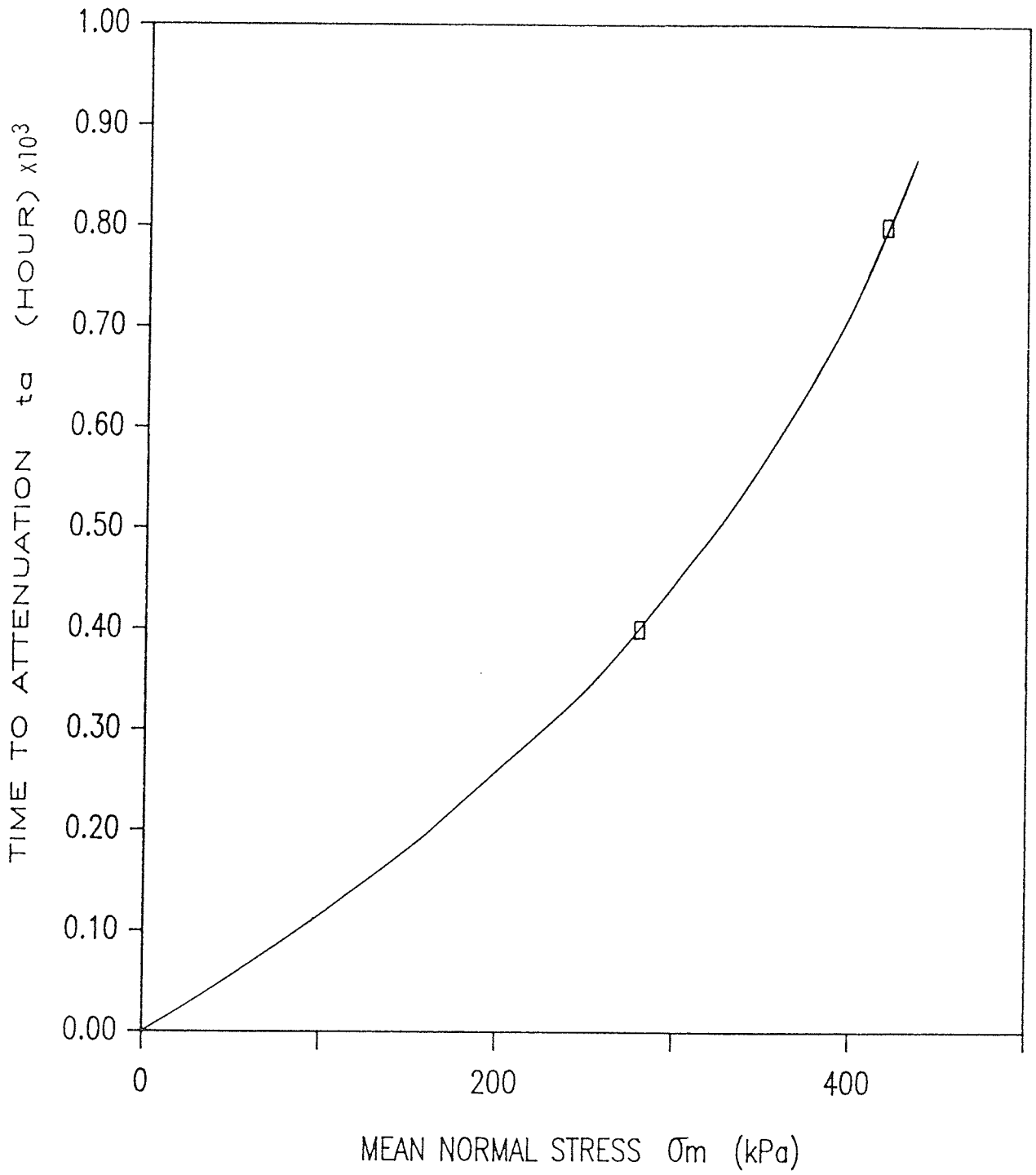


Figure 5.26 Time to attenuation versus mean normal stress

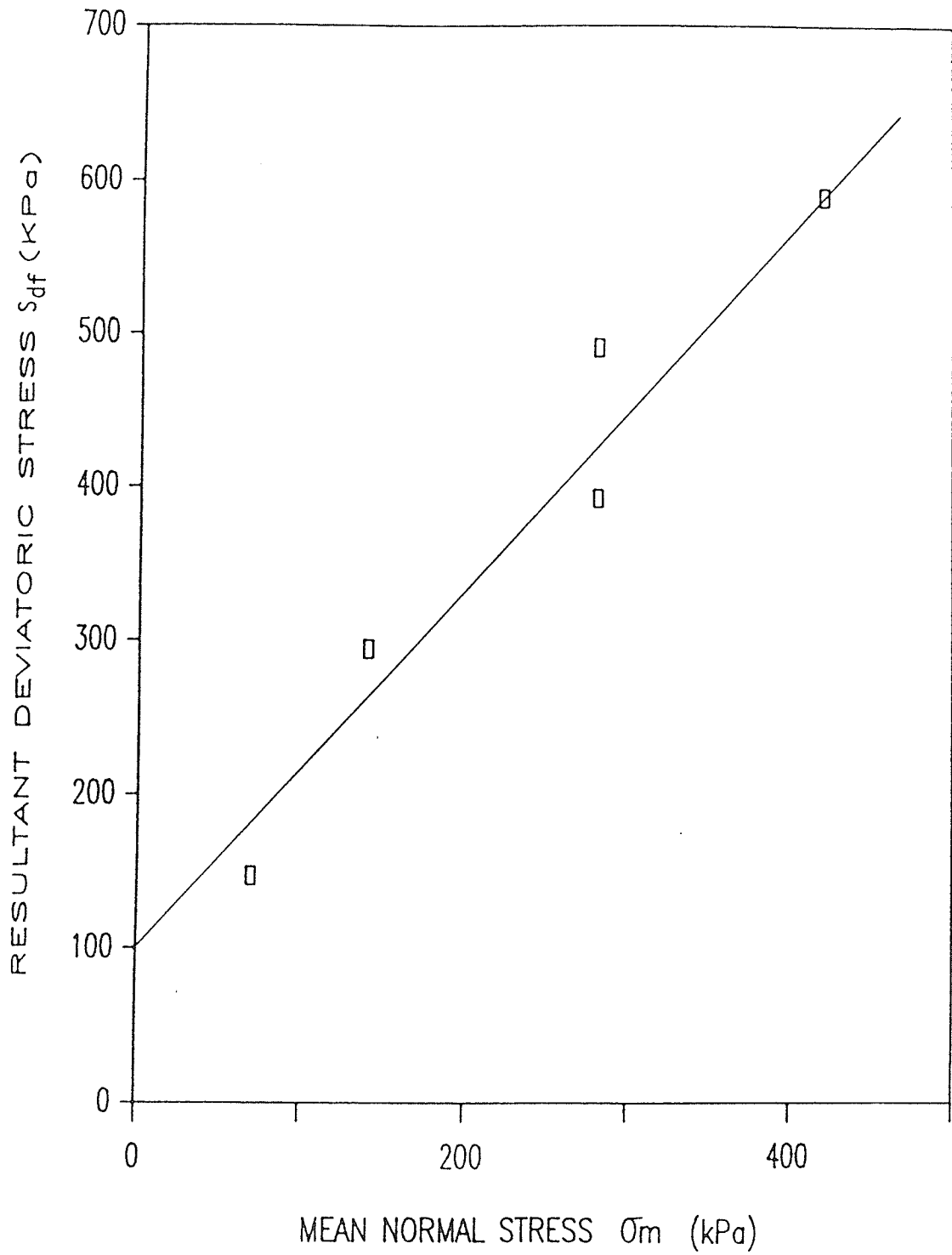


Figure 5.27 Resultant deviatoric stress at failure versus mean normal stress



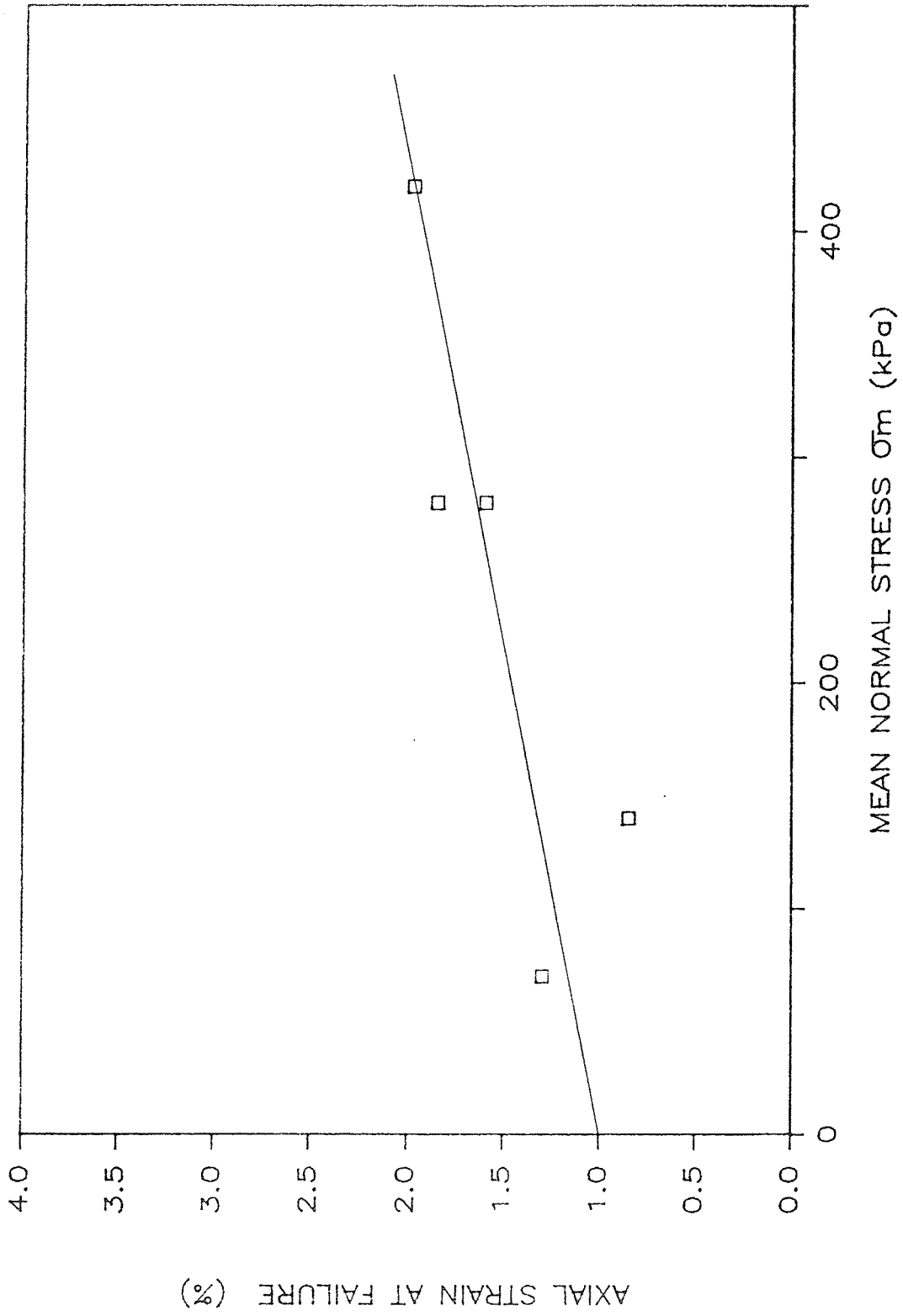


Figure 5.28 Axial strain at failure versus mean normal stress

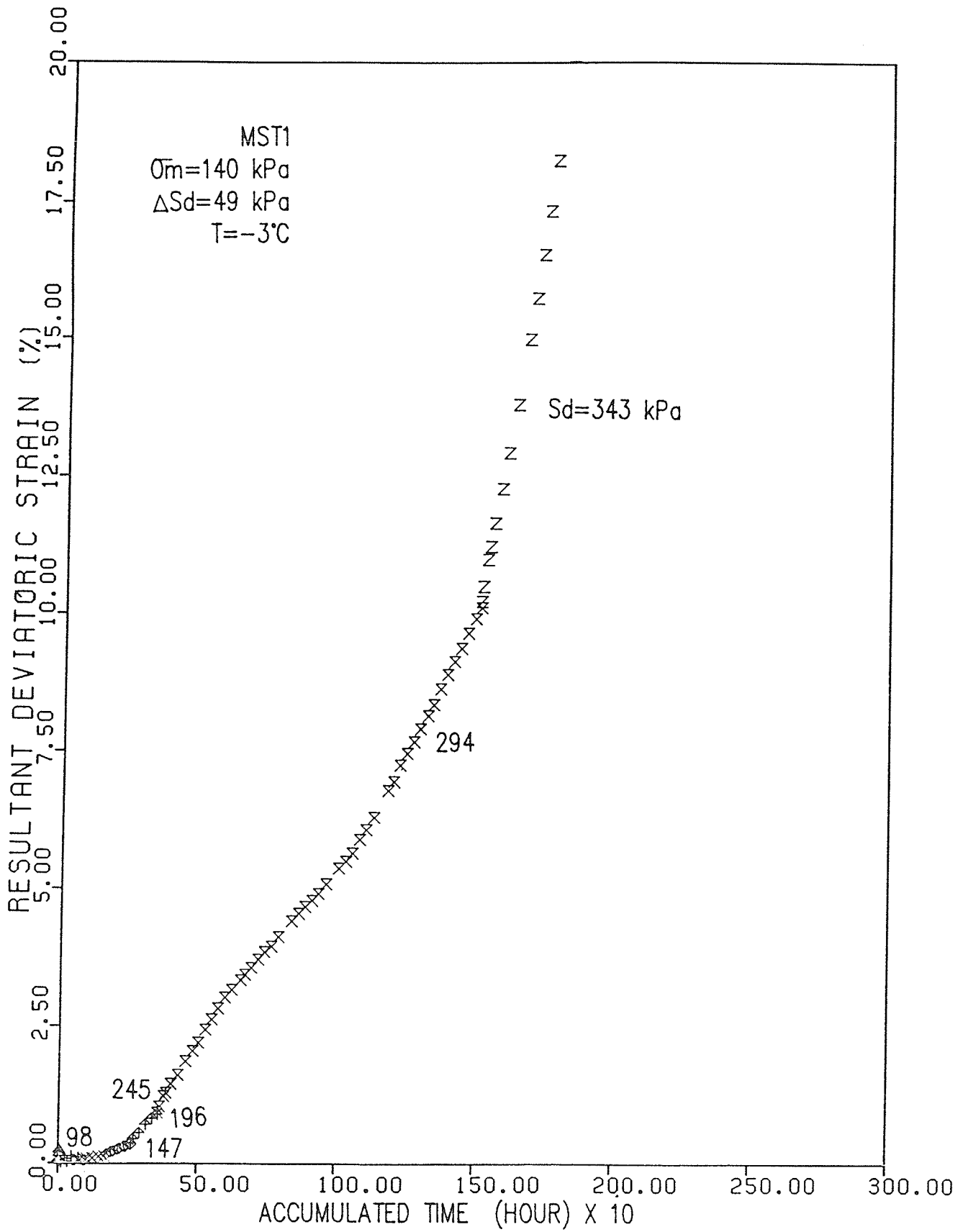


Figure 5.29 Resultant deviatoric strain versus accumulated time (MST1)

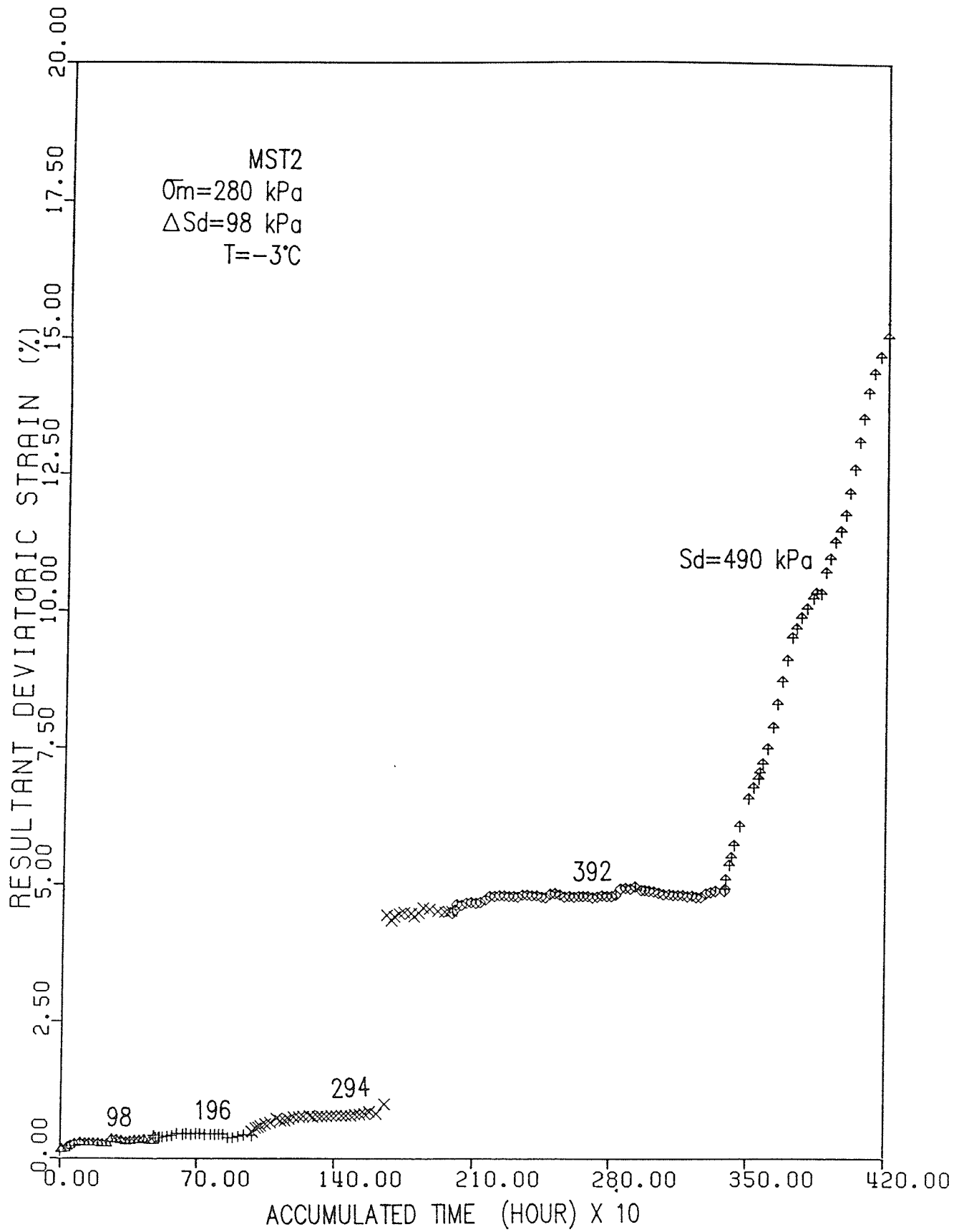


Figure 5.30 Resultant deviatoric strain versus accumulated time (MST2)

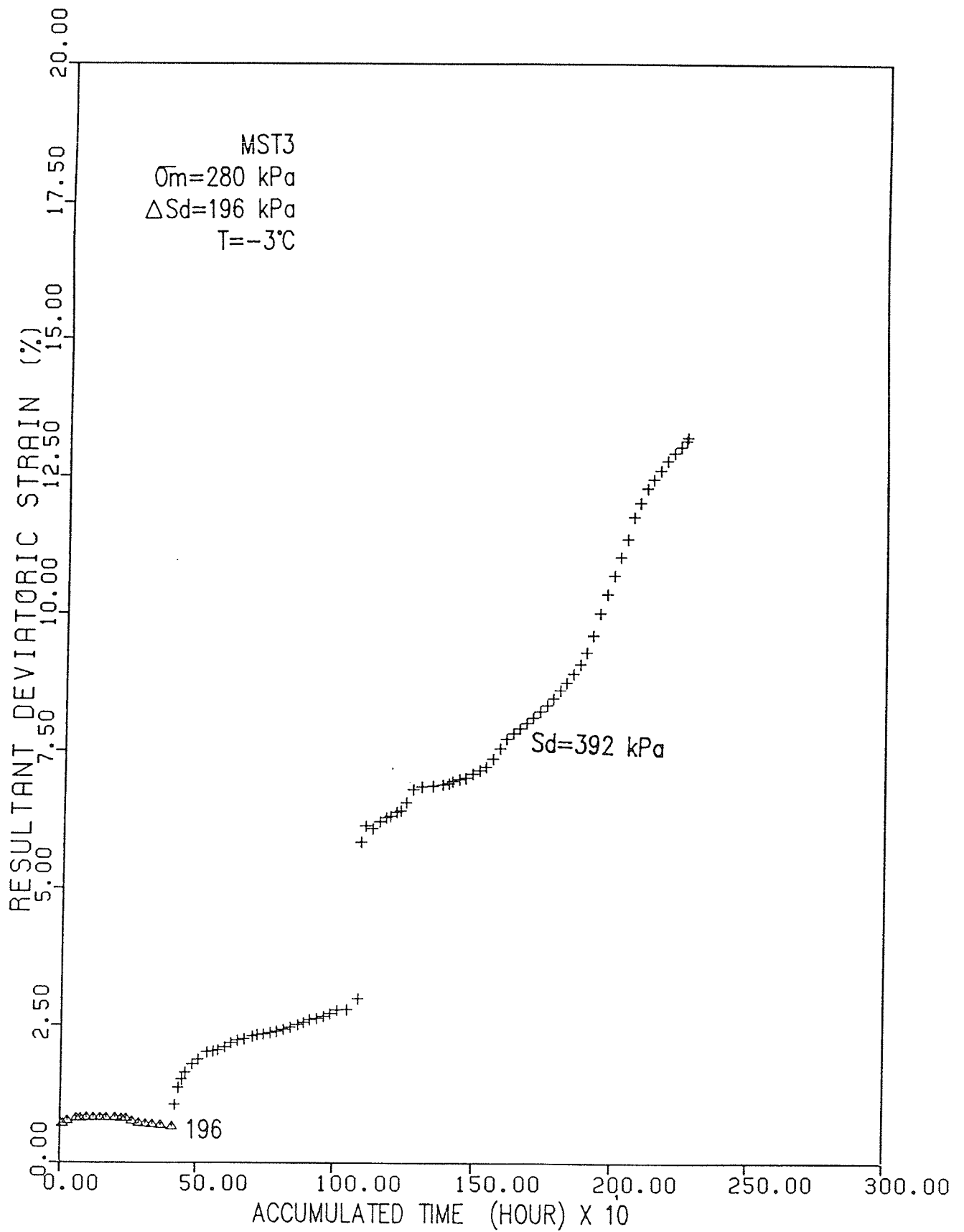


Figure 5.31 Resultant deviatoric strain versus accumulated time (MST3)

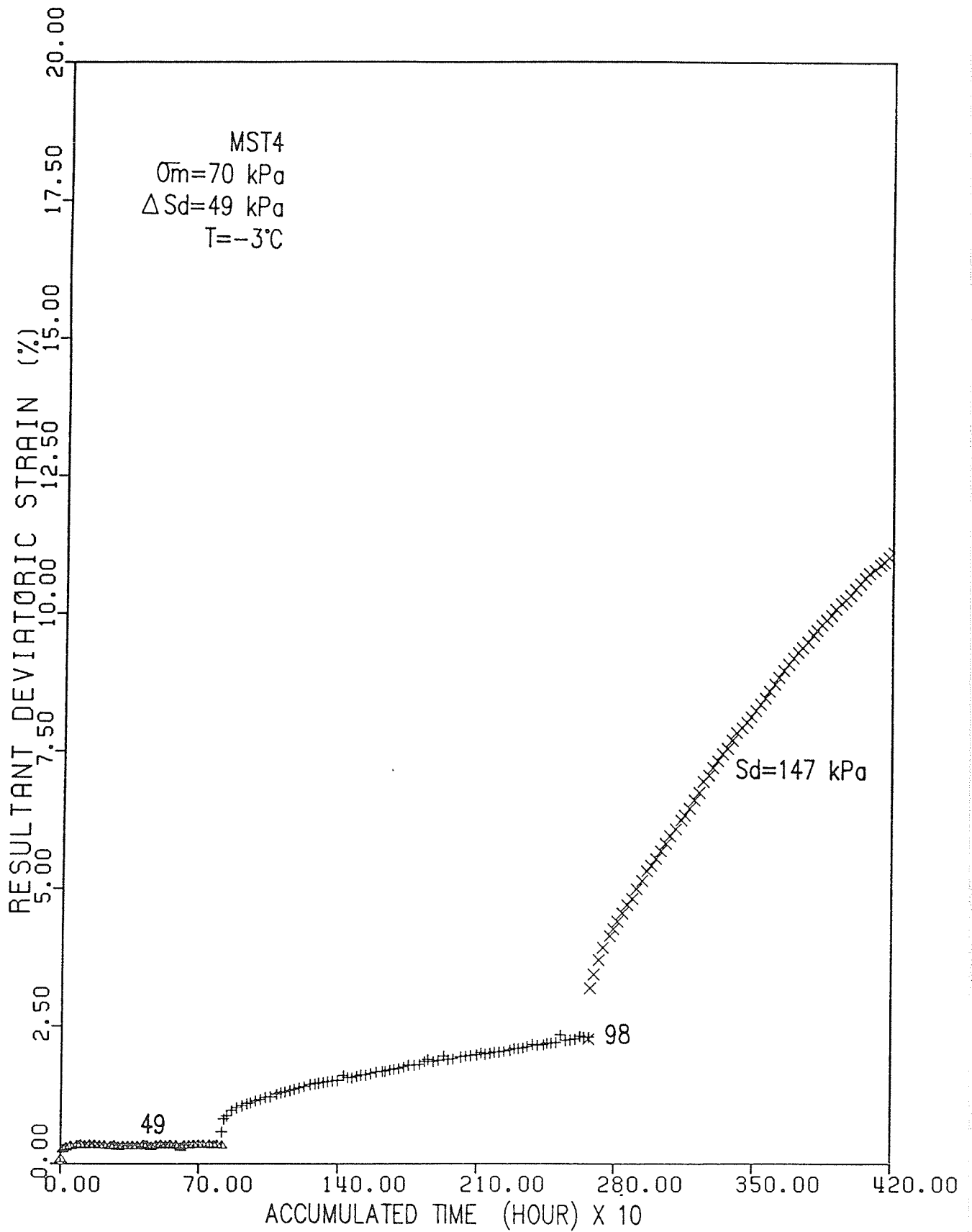


Figure 5.32 Resultant deviatoric strain versus accumulated time (MST4)

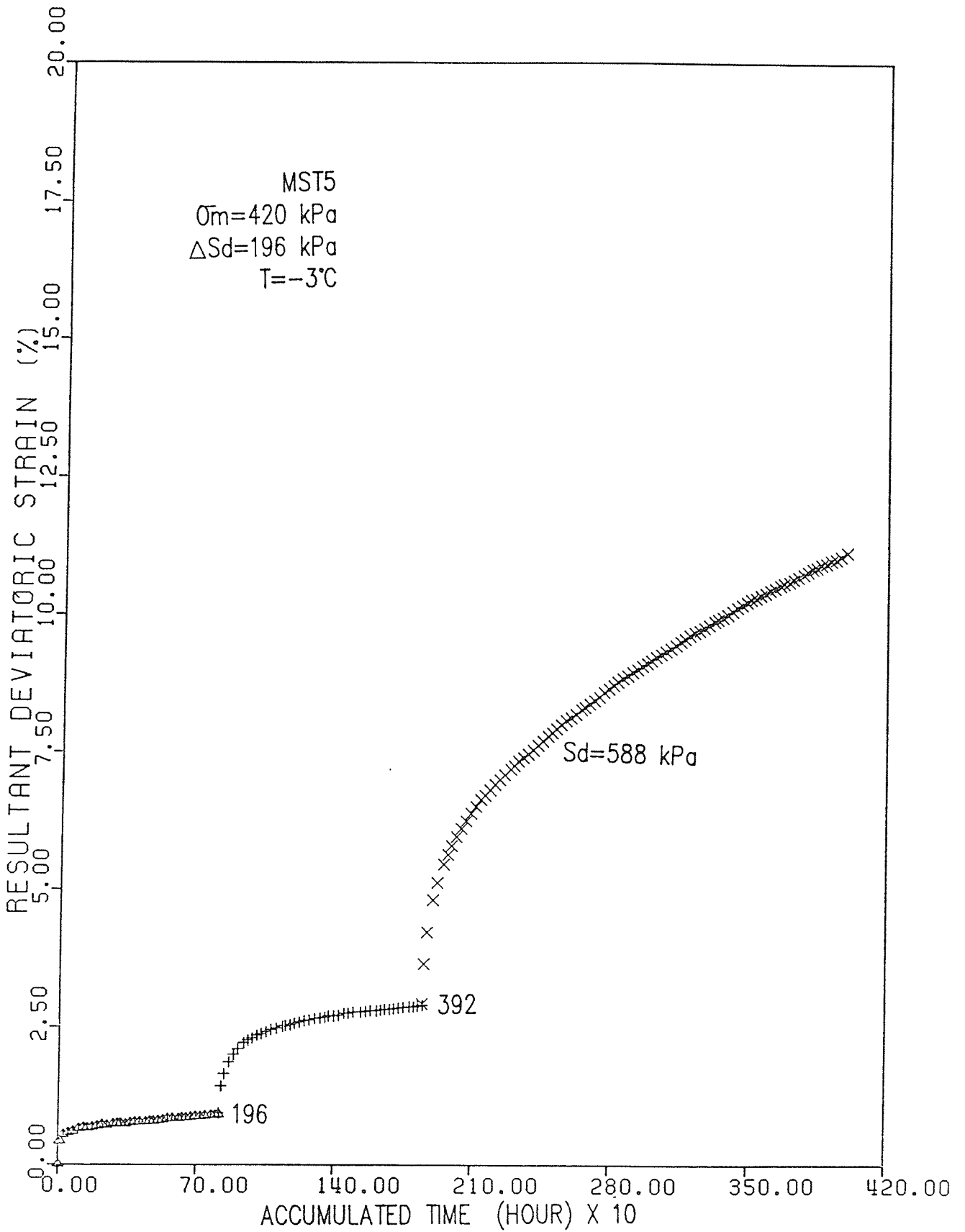


Figure 5.33 Resultant deviatoric strain versus accumulated time (MST5)

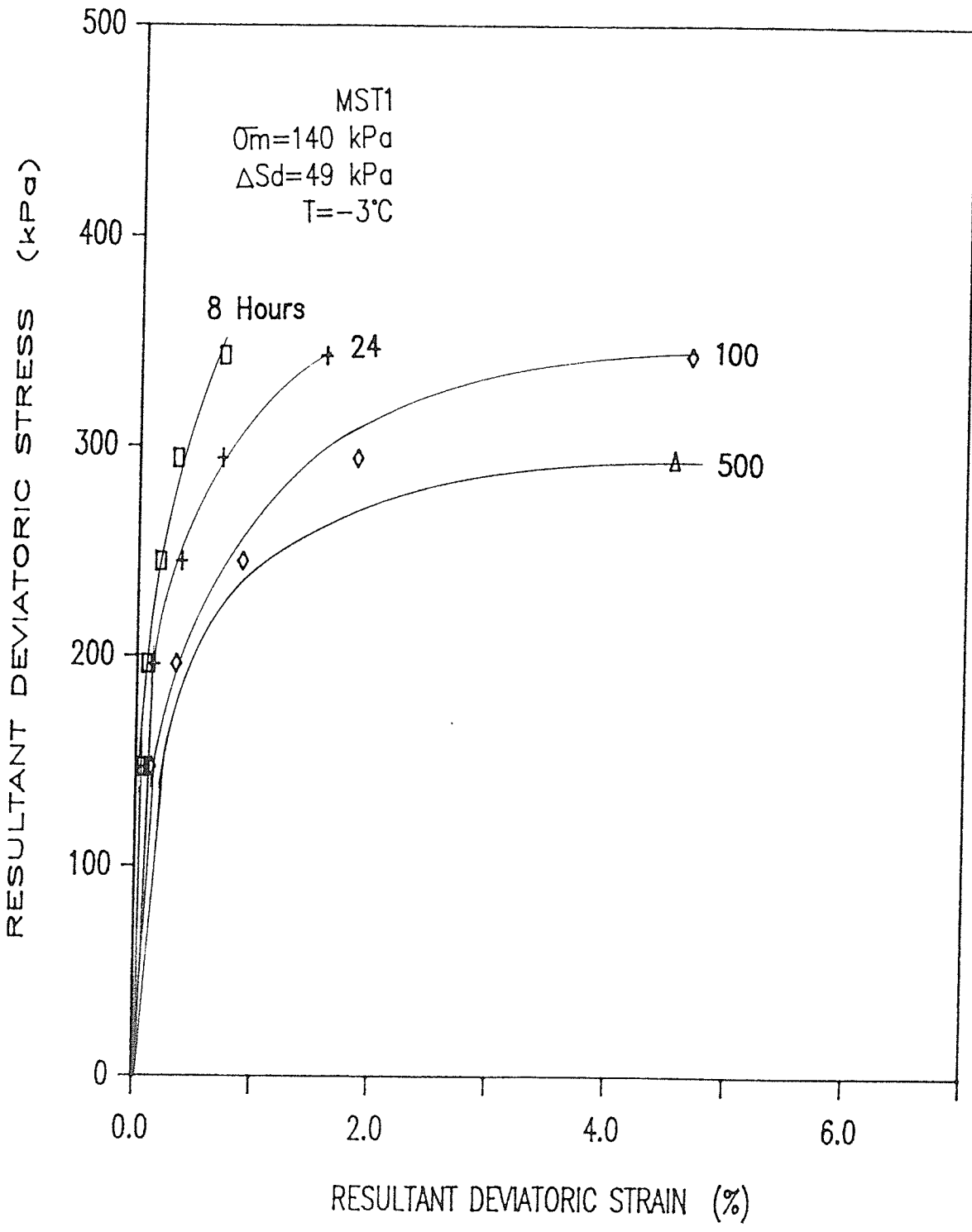


Figure 5.34 Resultant deviatoric stress versus resultant deviatoric strain (MST1)

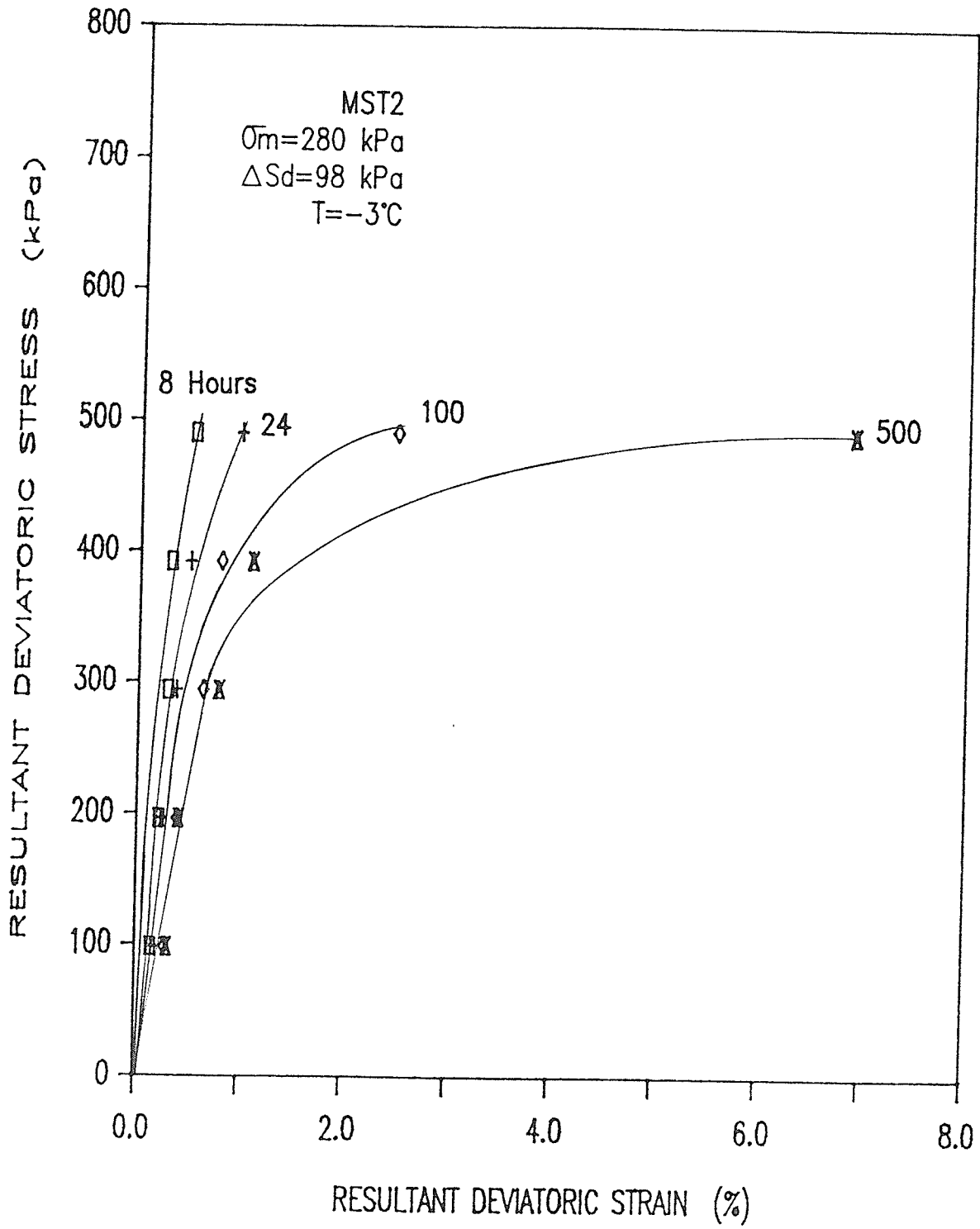


Figure 5.35 Resultant deviatoric stress versus resultant deviatoric strain (MST2)



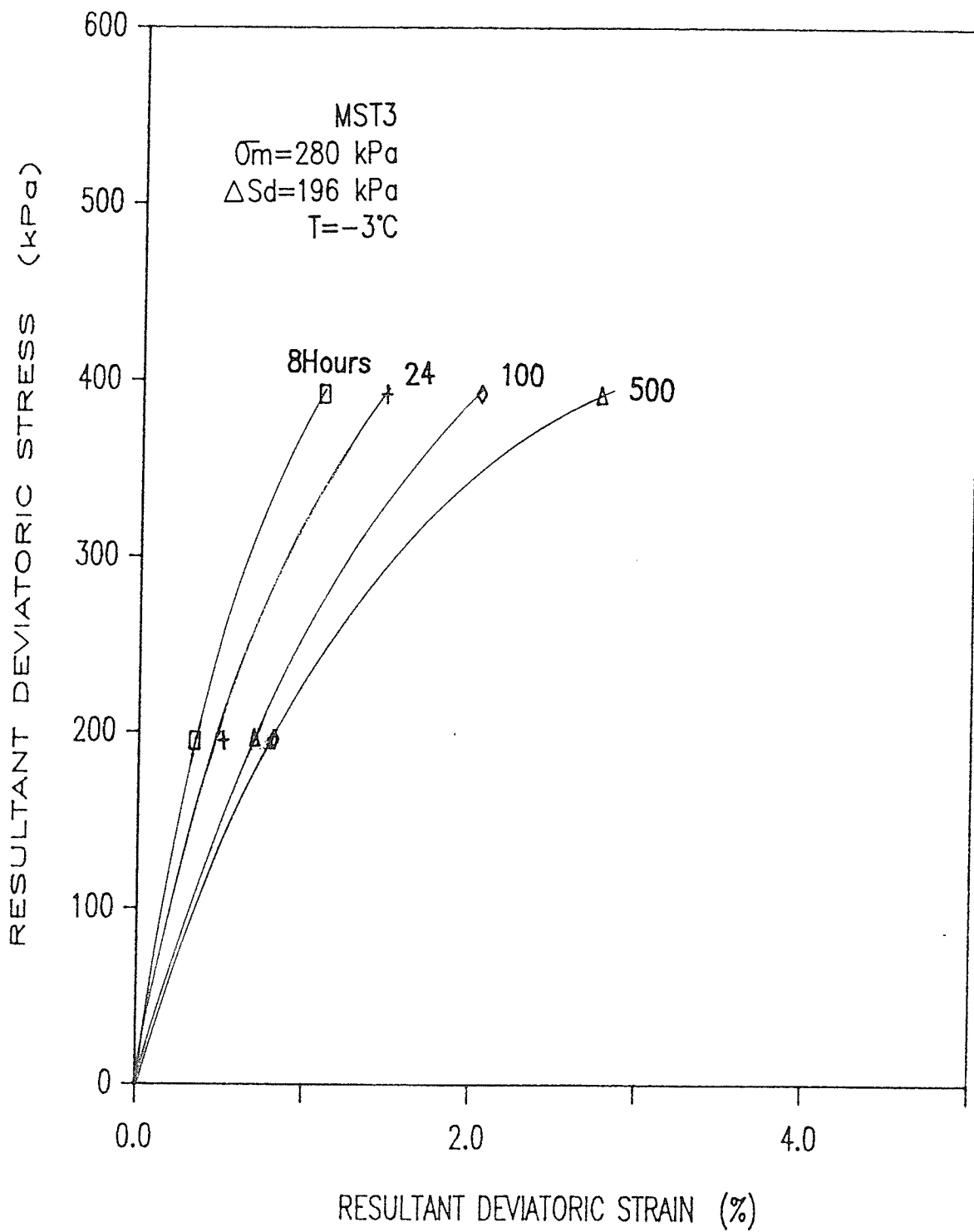


Figure 5.36 Resultant deviatoric stress versus resultant deviatoric strain (MST3)

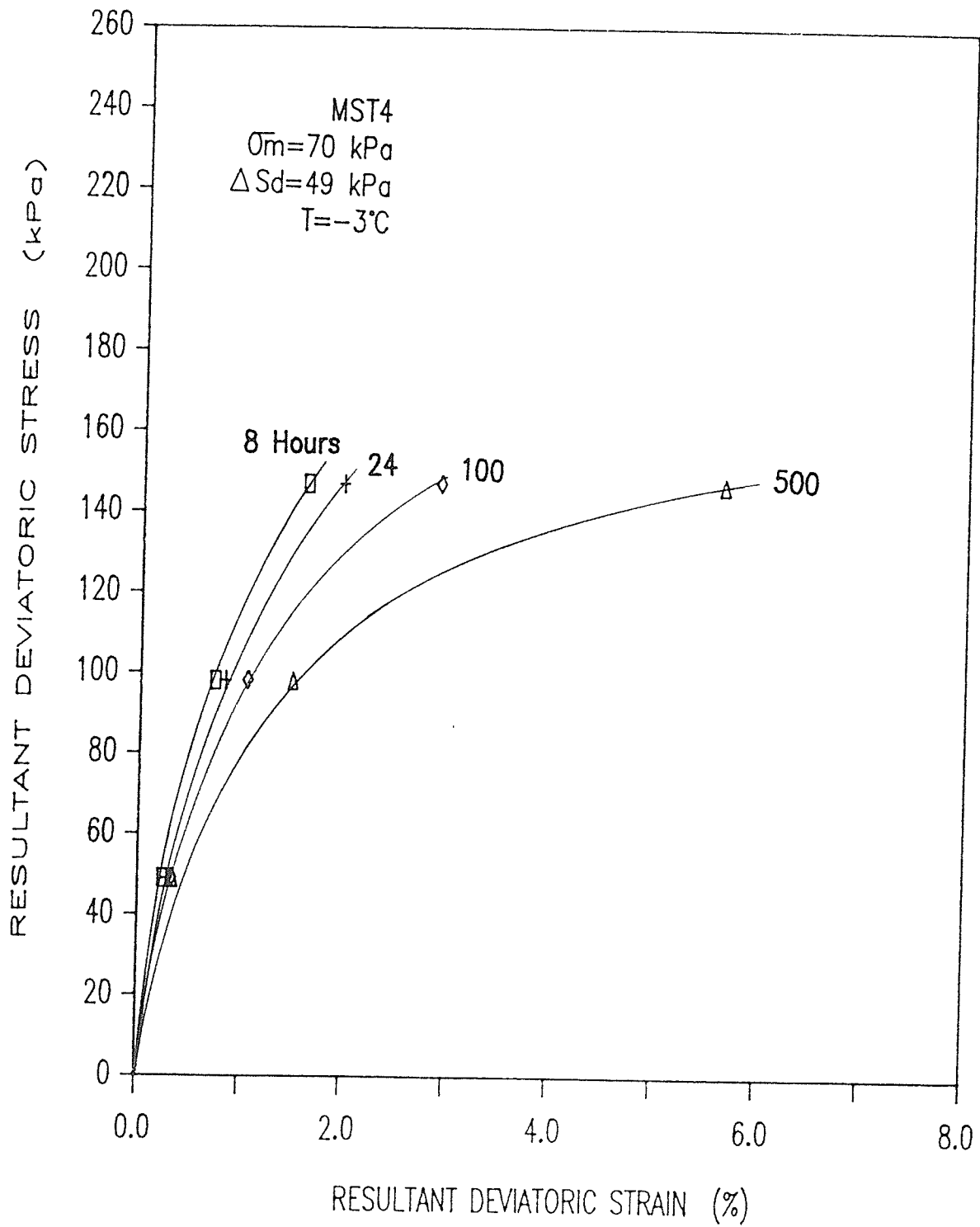


Figure 5.37 Resultant deviatoric stress versus resultant deviatoric strain (MST4)

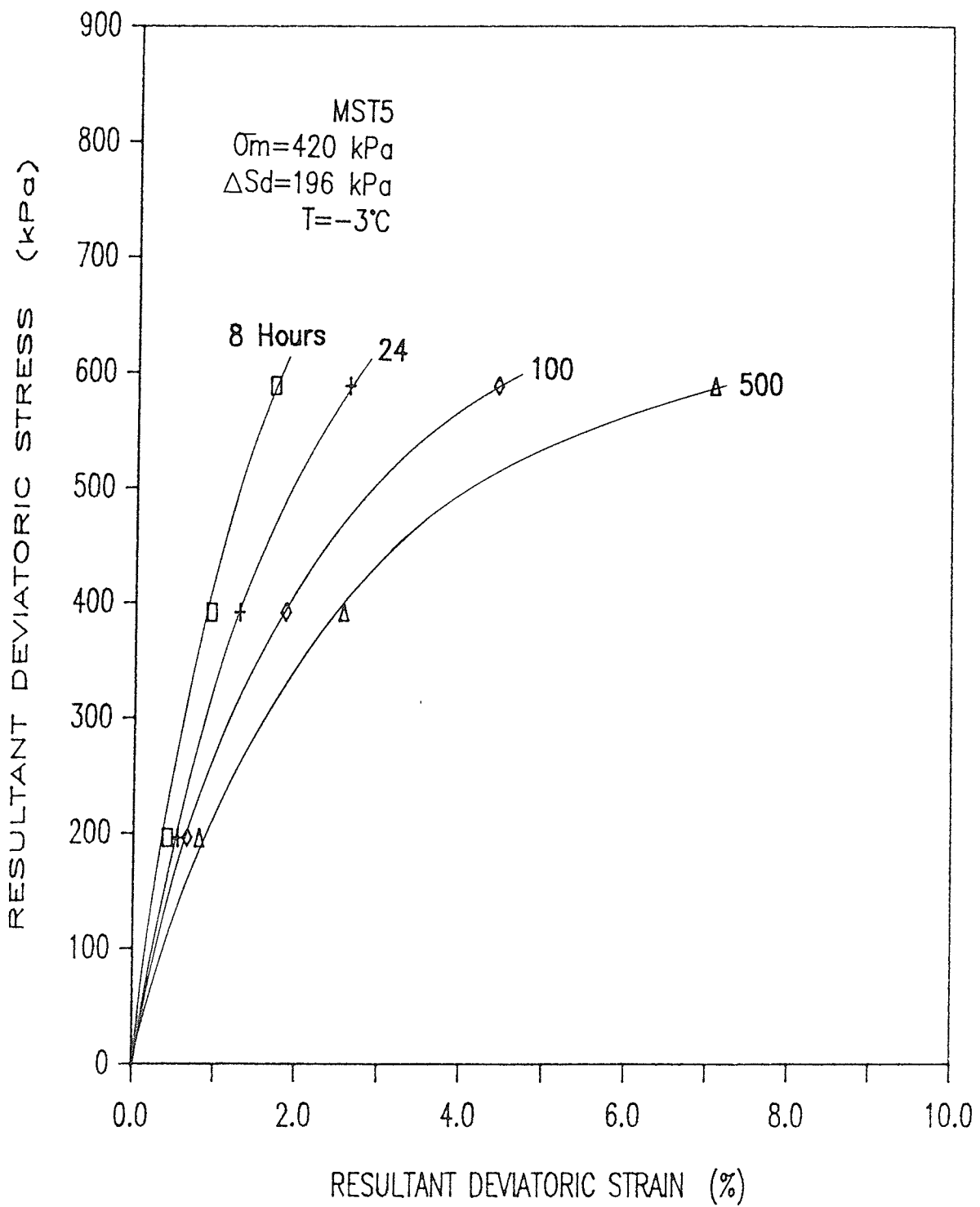


Figure 5.38 Resultant deviatoric stress versus resultant deviatoric strain (MST5)

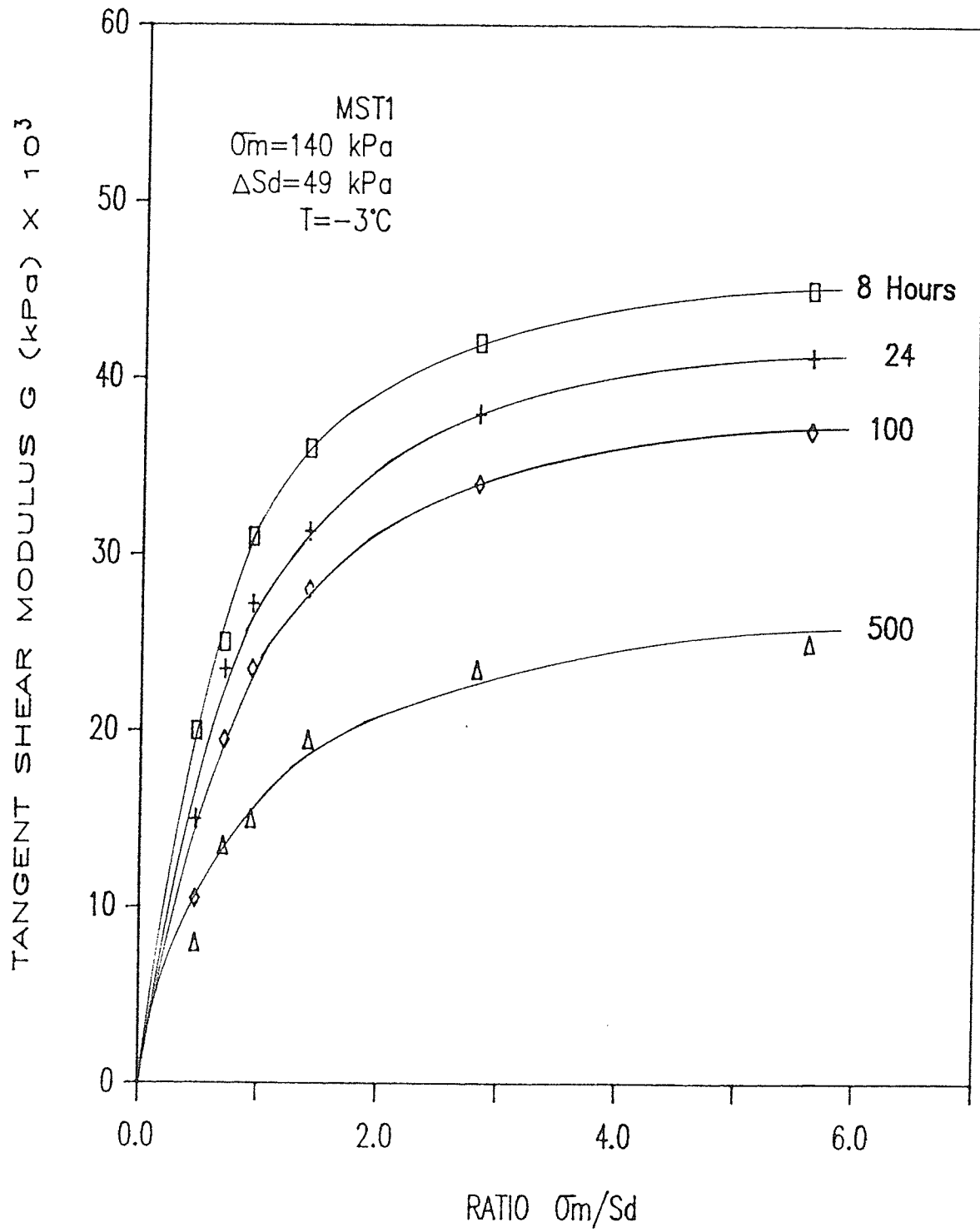


Figure 5.39 Tangent shear modulus versus ratio,  $\bar{\sigma}_m/S_d$  (MST1)

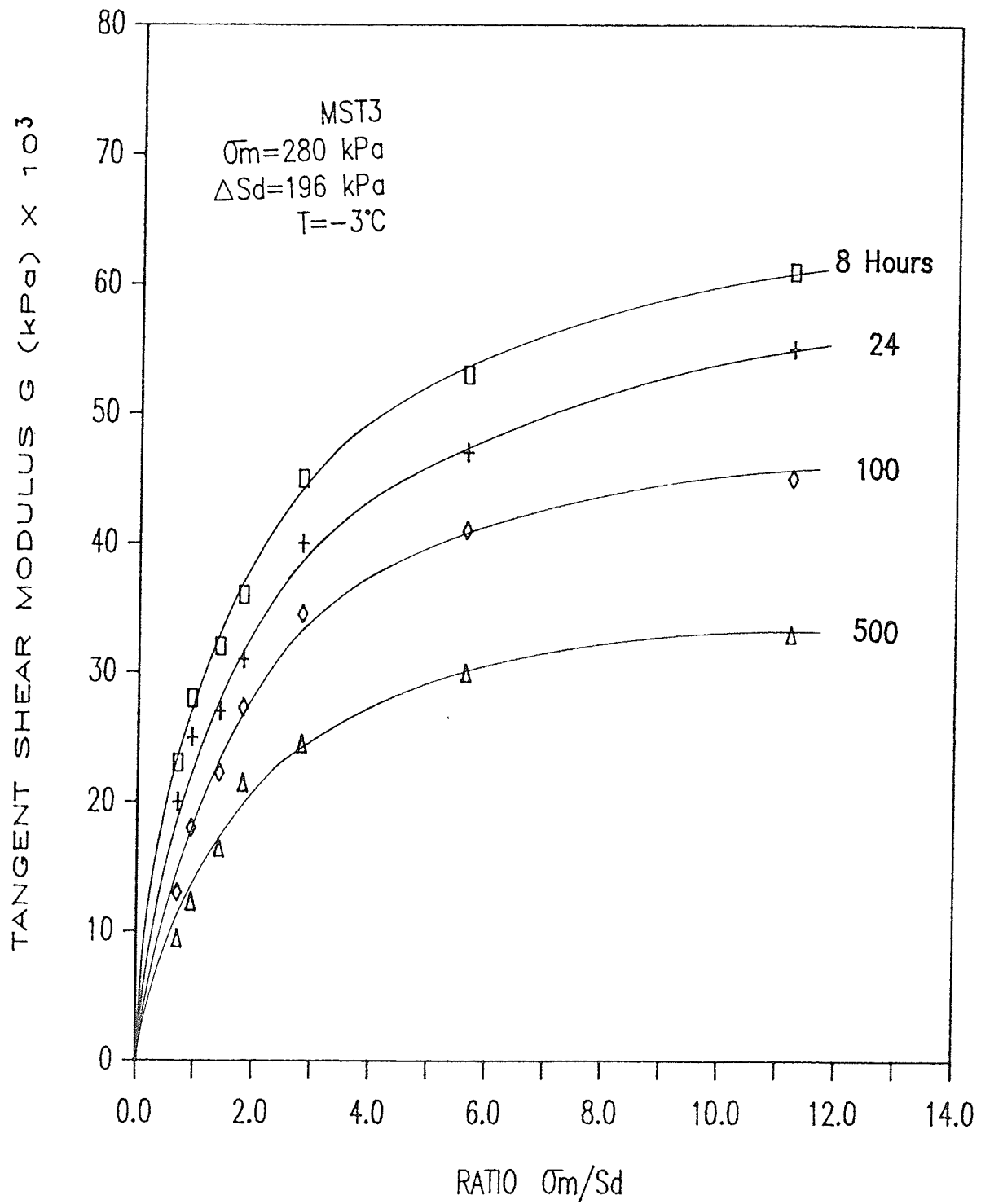


Figure 5.40 Tangent shear modulus versus ratio,  $\bar{\sigma}_m/S_d$  (MST3)

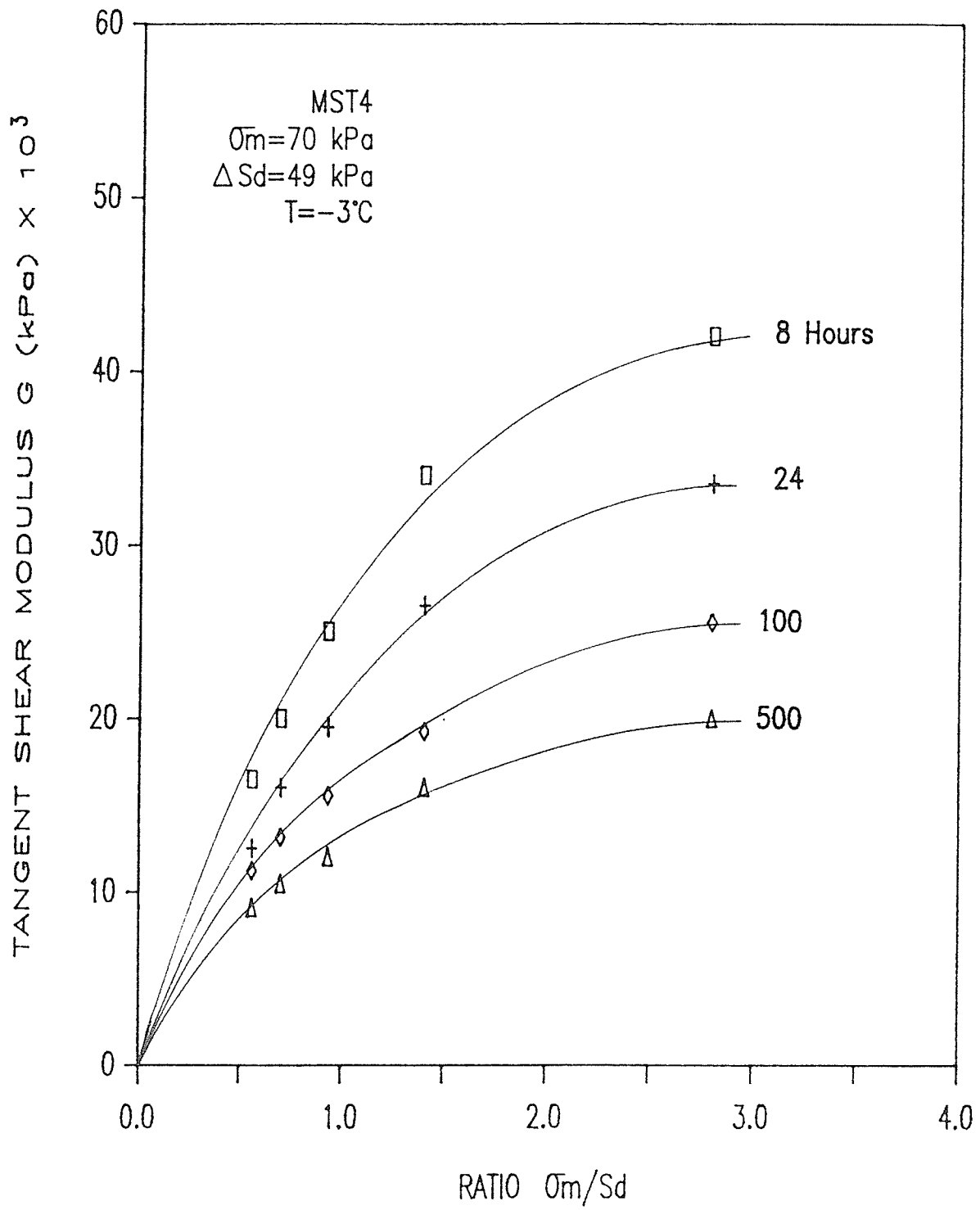


Figure 5.41 Tangent shear modulus versus ratio,  $\bar{\sigma}_m/S_d$  (MST4)

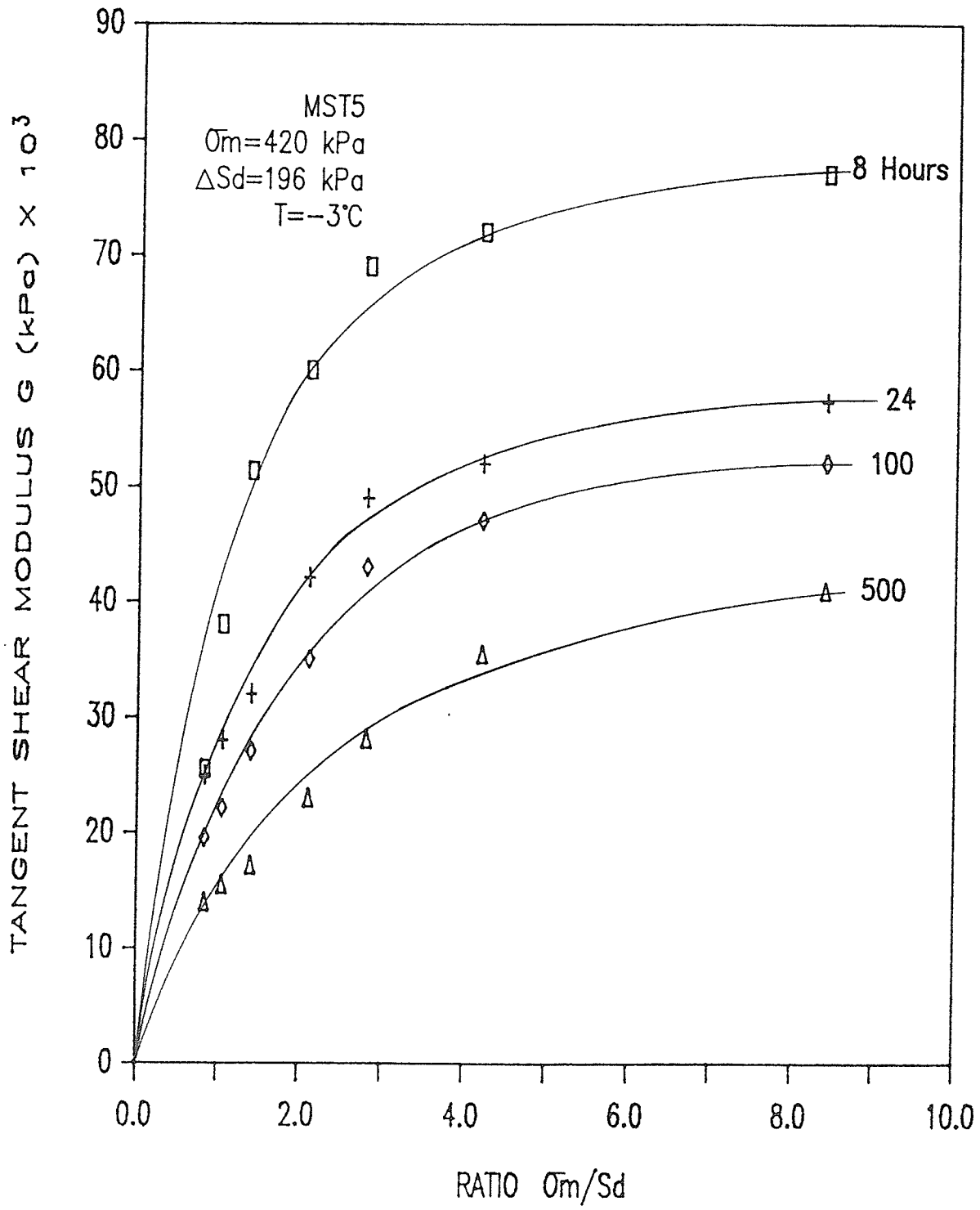


Figure 5.42 Tangent shear modulus versus ratio,  $\bar{\sigma}_m/\sigma_d$  (MST5)

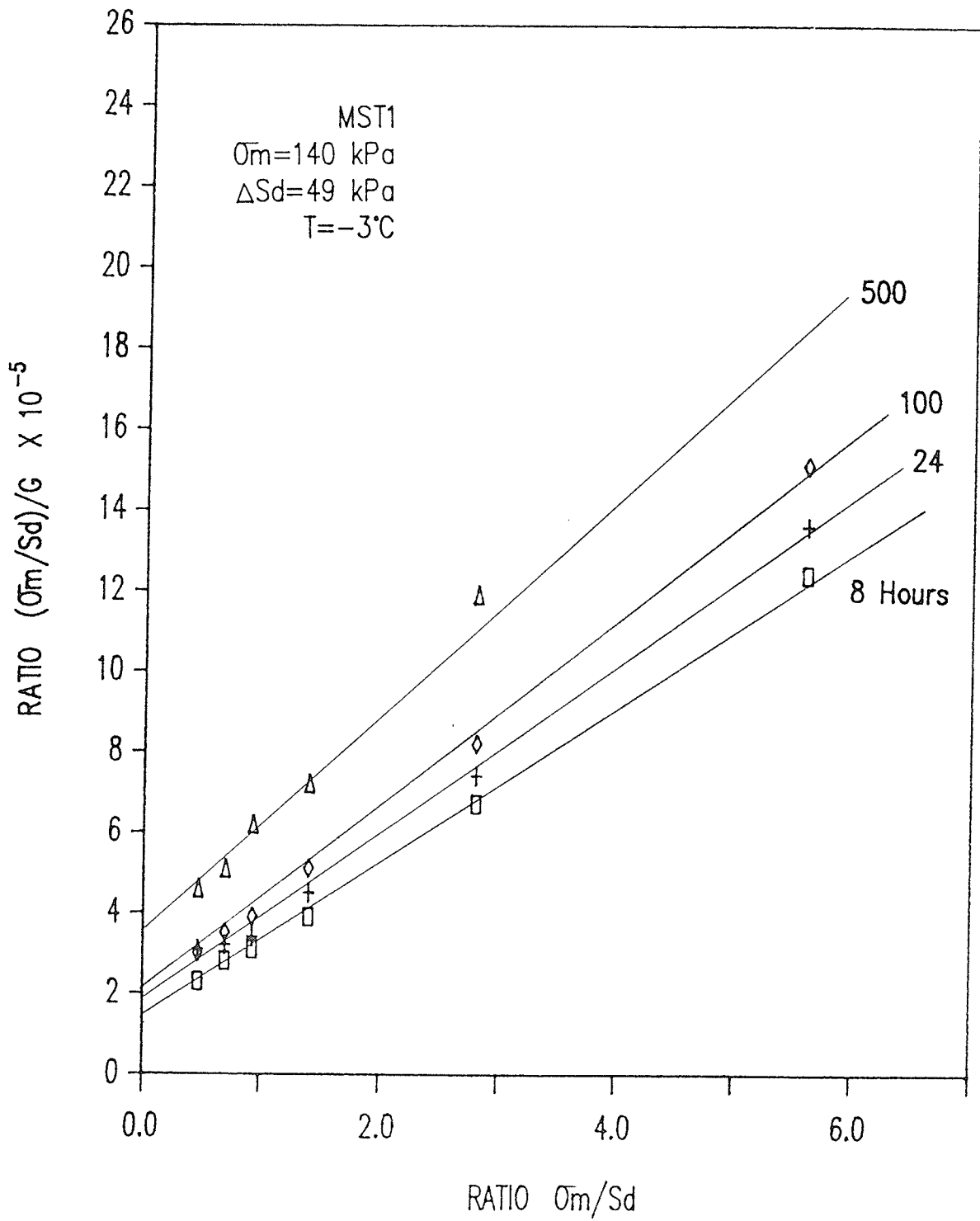


Figure 5.43 Ratio  $(\bar{\sigma}_m/S_d)/G$  Versus  $\bar{\sigma}_m/S_d$  (MST1)



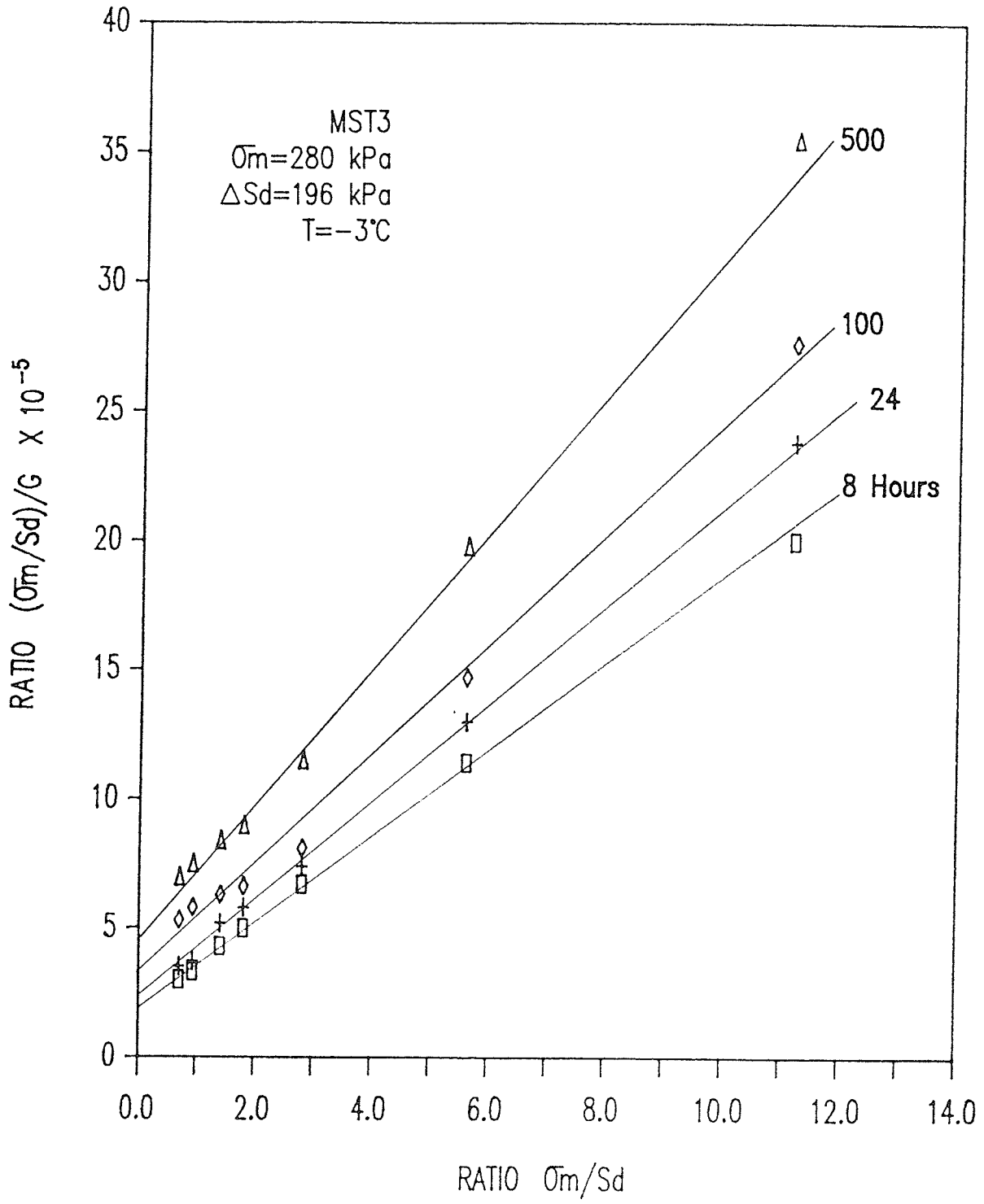


Figure 5.44 Ratio  $(\sigma_m/S_d)/G$  Versus  $\sigma_m/S_d$  (MST3)

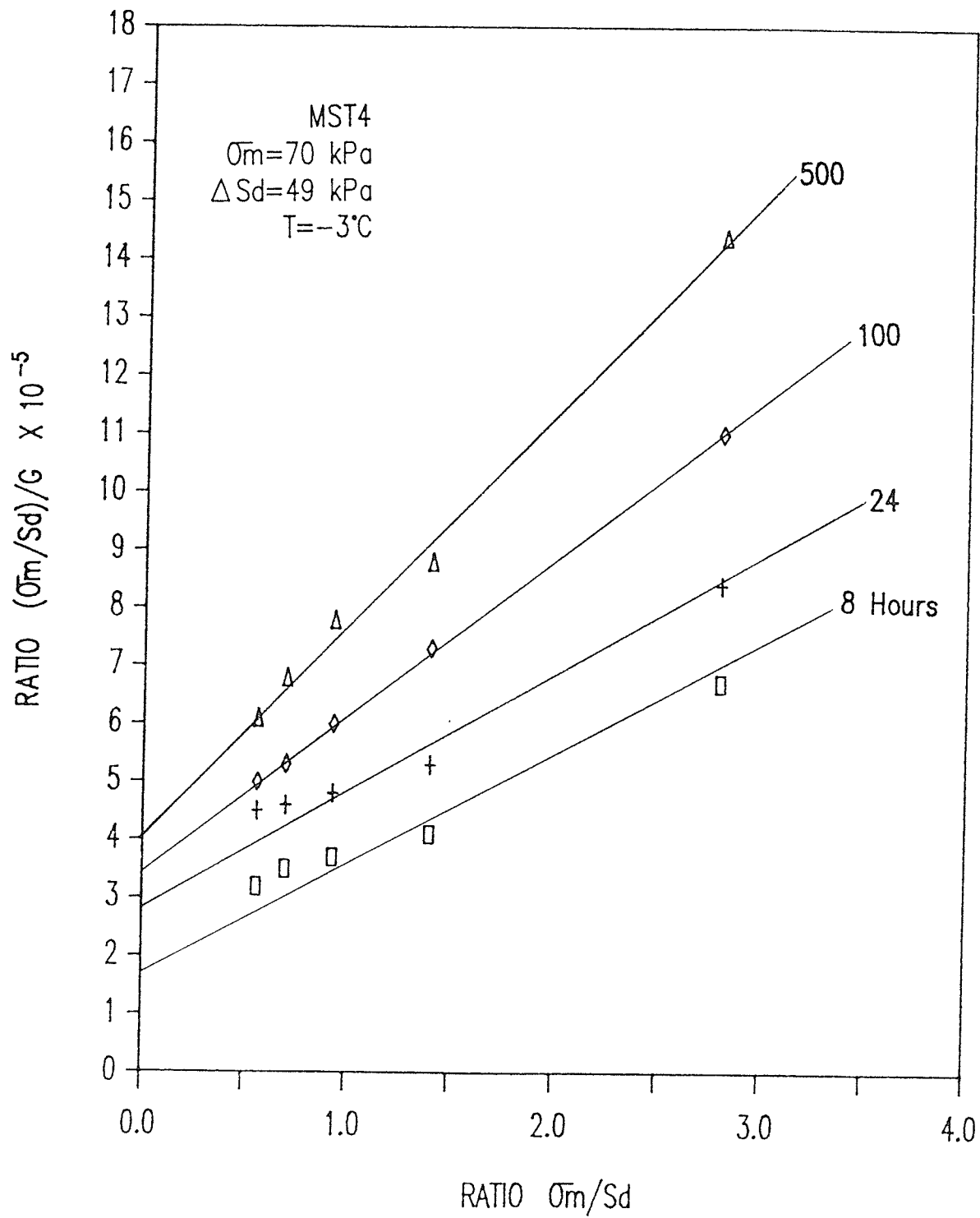


Figure 5.45 Ratio  $(\bar{\sigma}_m/S_d)/G$  Versus  $\bar{\sigma}_m/S_d$  (MST4)

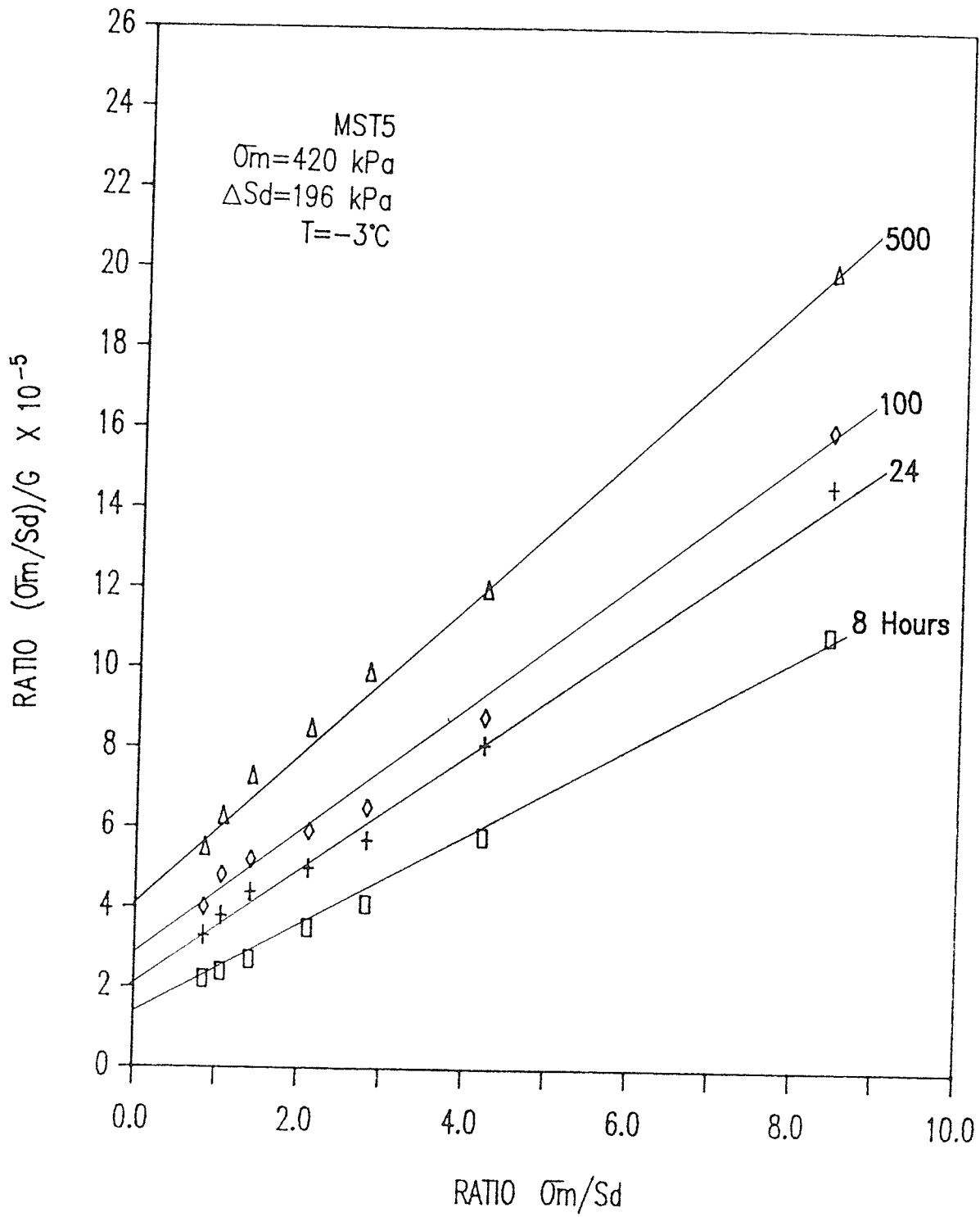


Figure 5.46 Ratio  $(\bar{\sigma}_m/S_d)/G$  Versus  $\bar{\sigma}_m/S_d$  (MST5)

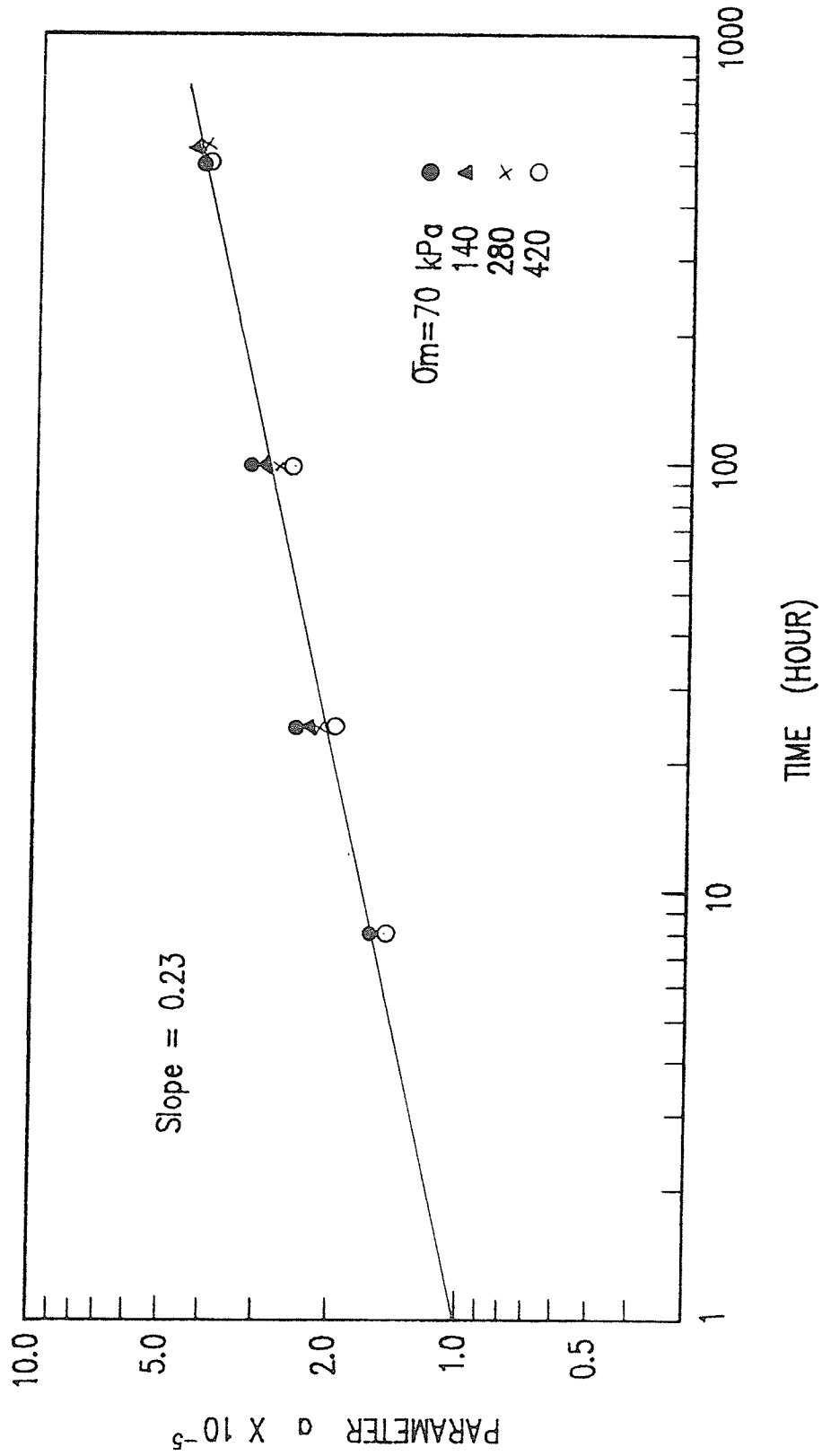


Figure 5.47 Parameter 'a' versus time

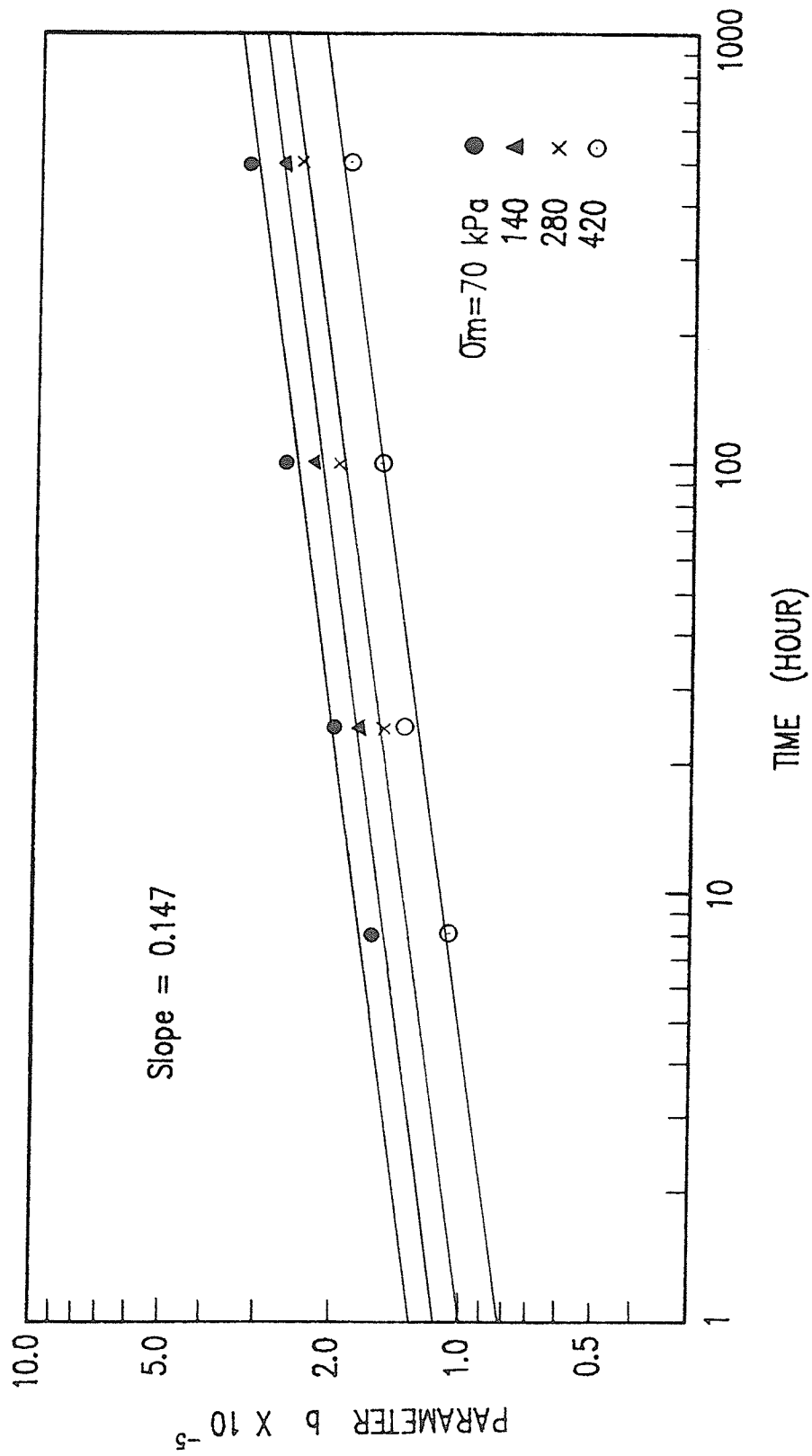


Figure 5.48 Parameter 'b' versus time

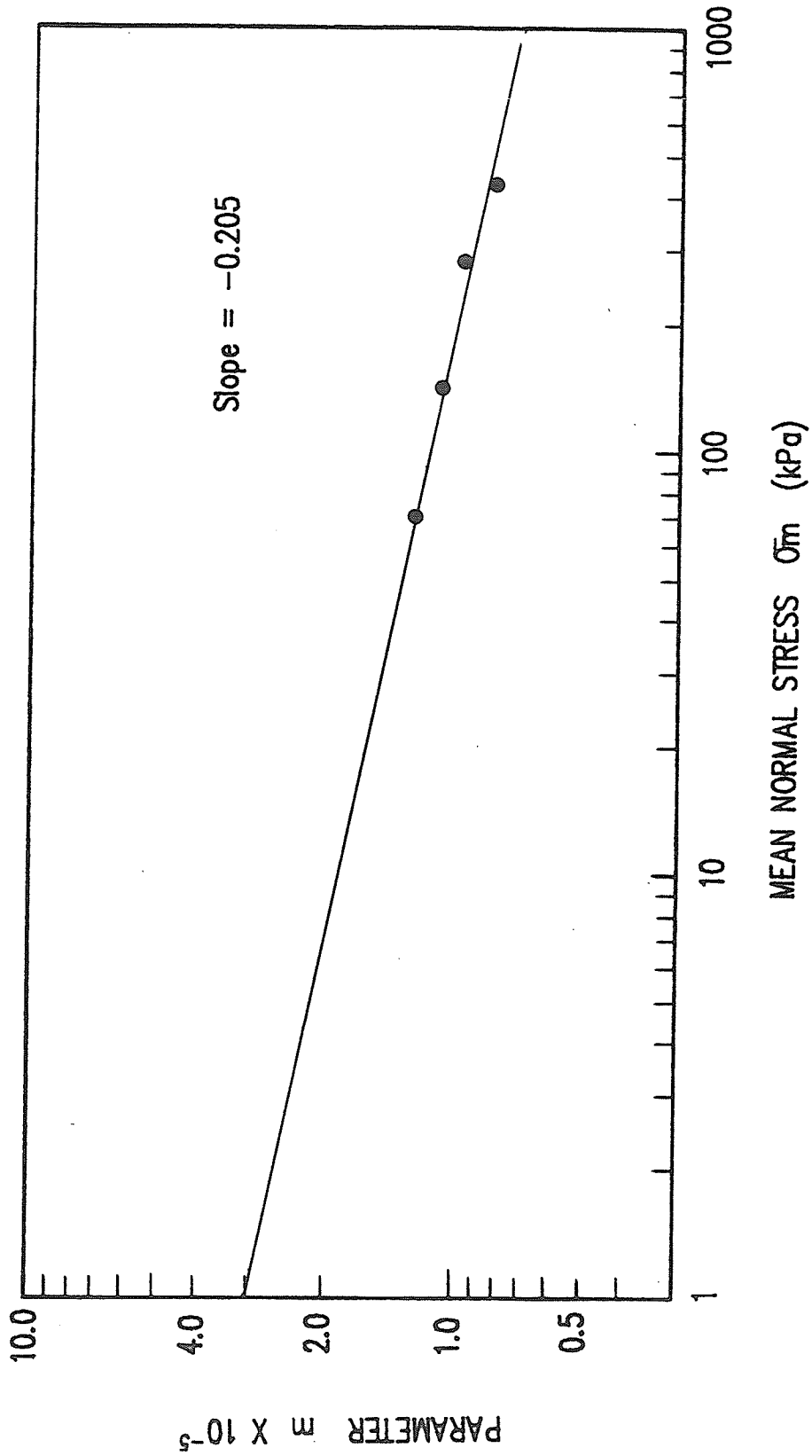


Figure 5.49 Parameter  $m$  versus mean normal stress

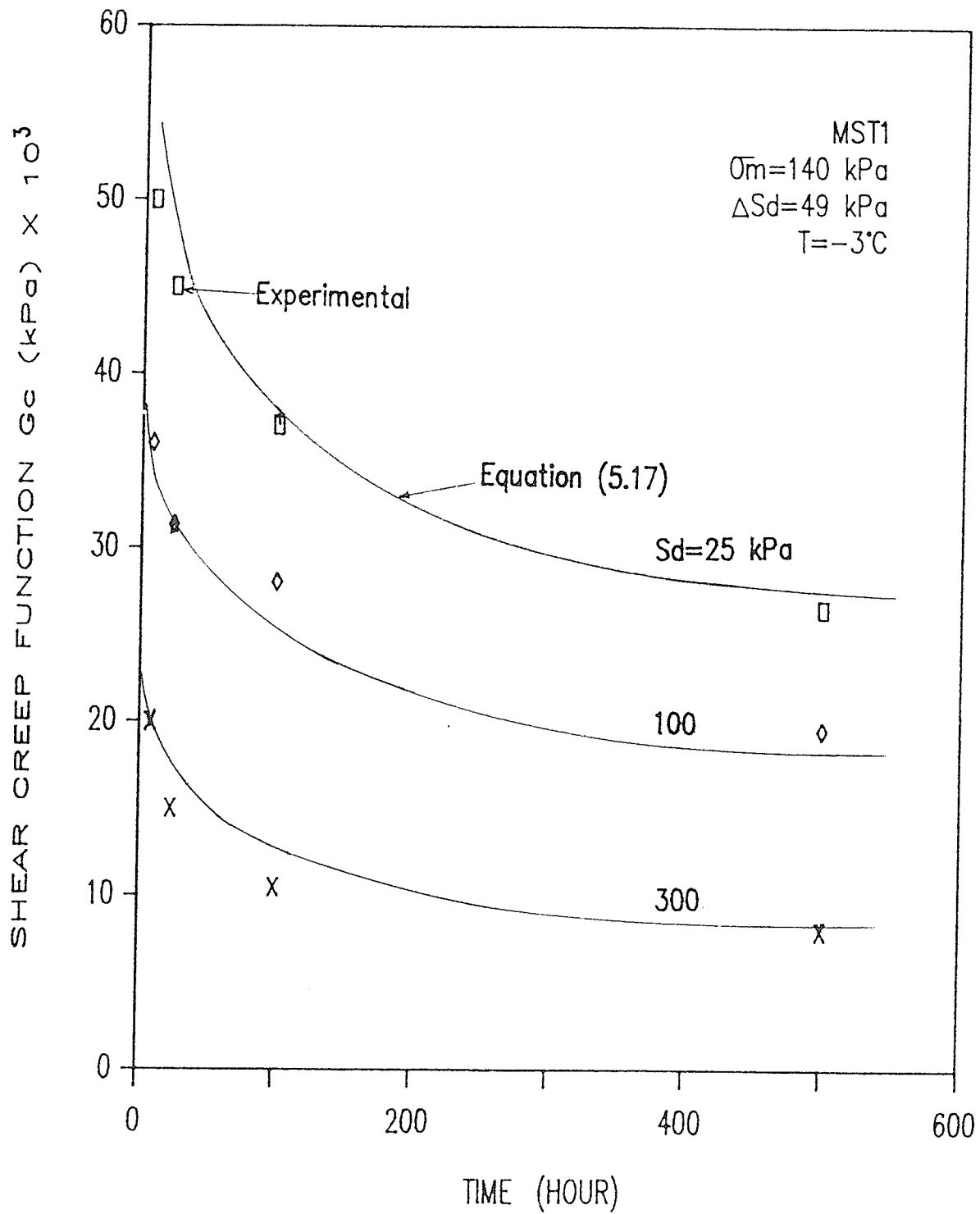


Figure 5.50 Shear creep function versus time (MST1)

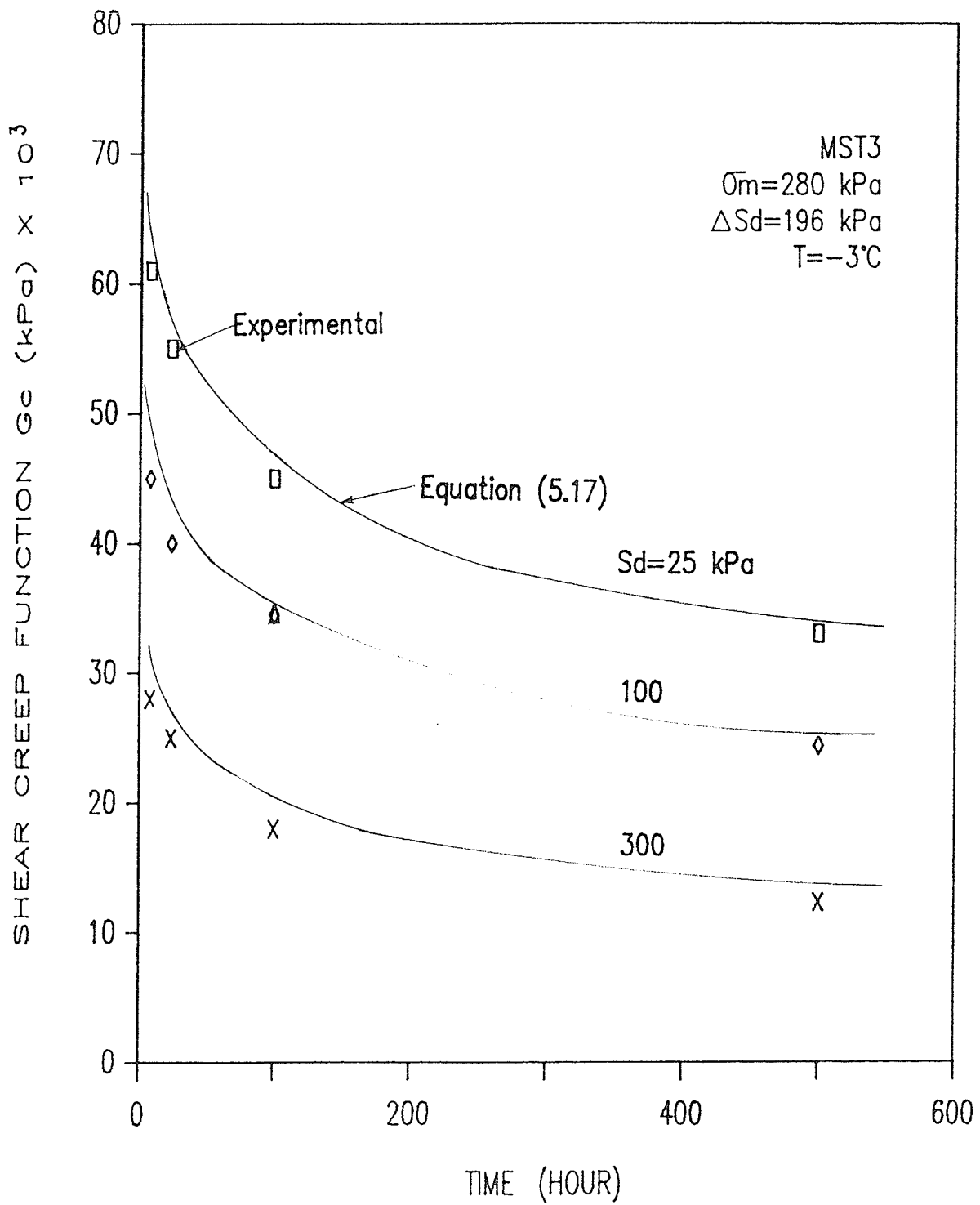


Figure 5.51 Shear creep function versus time (MST3)



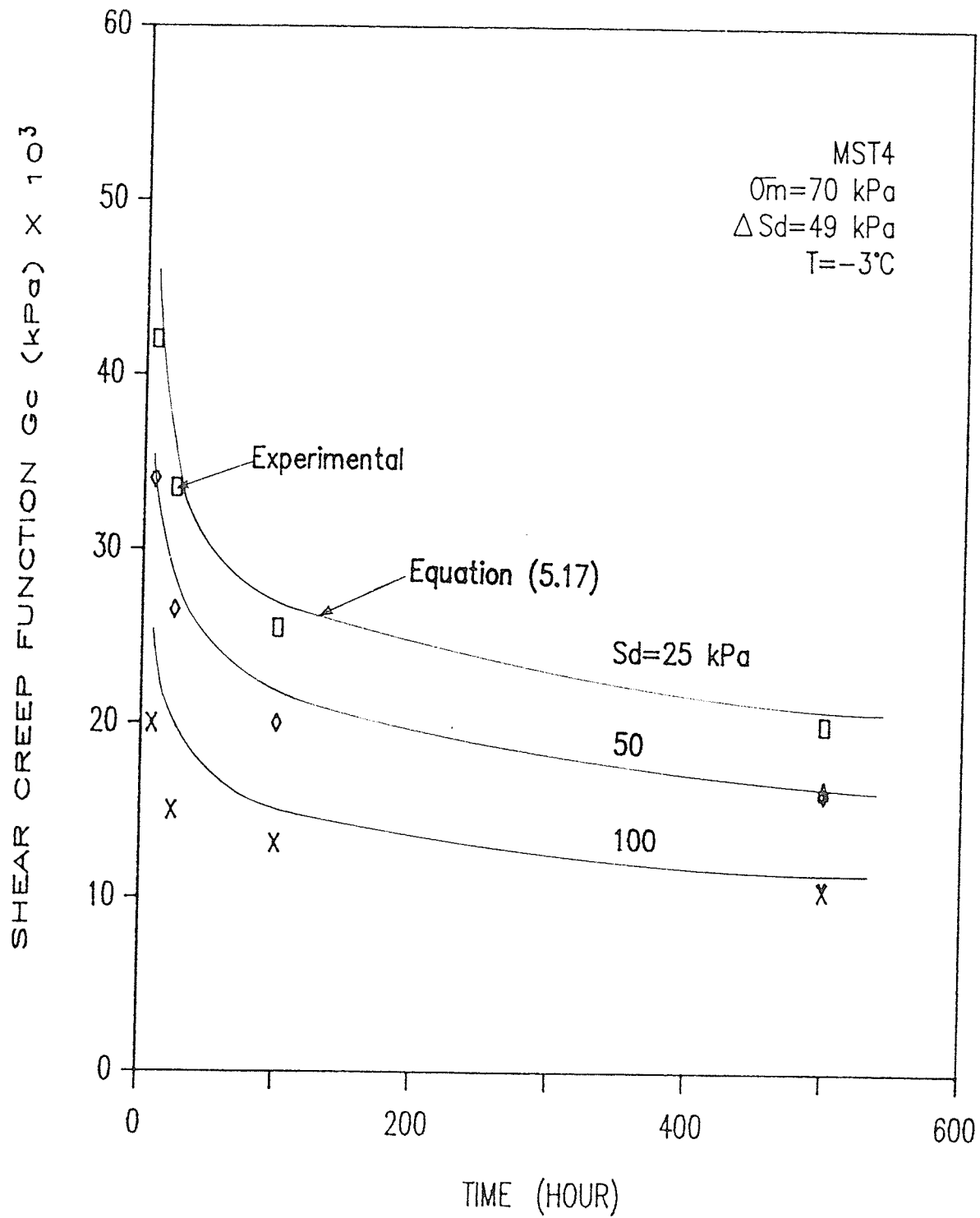


Figure 5.52 Shear creep function versus time (MST4)

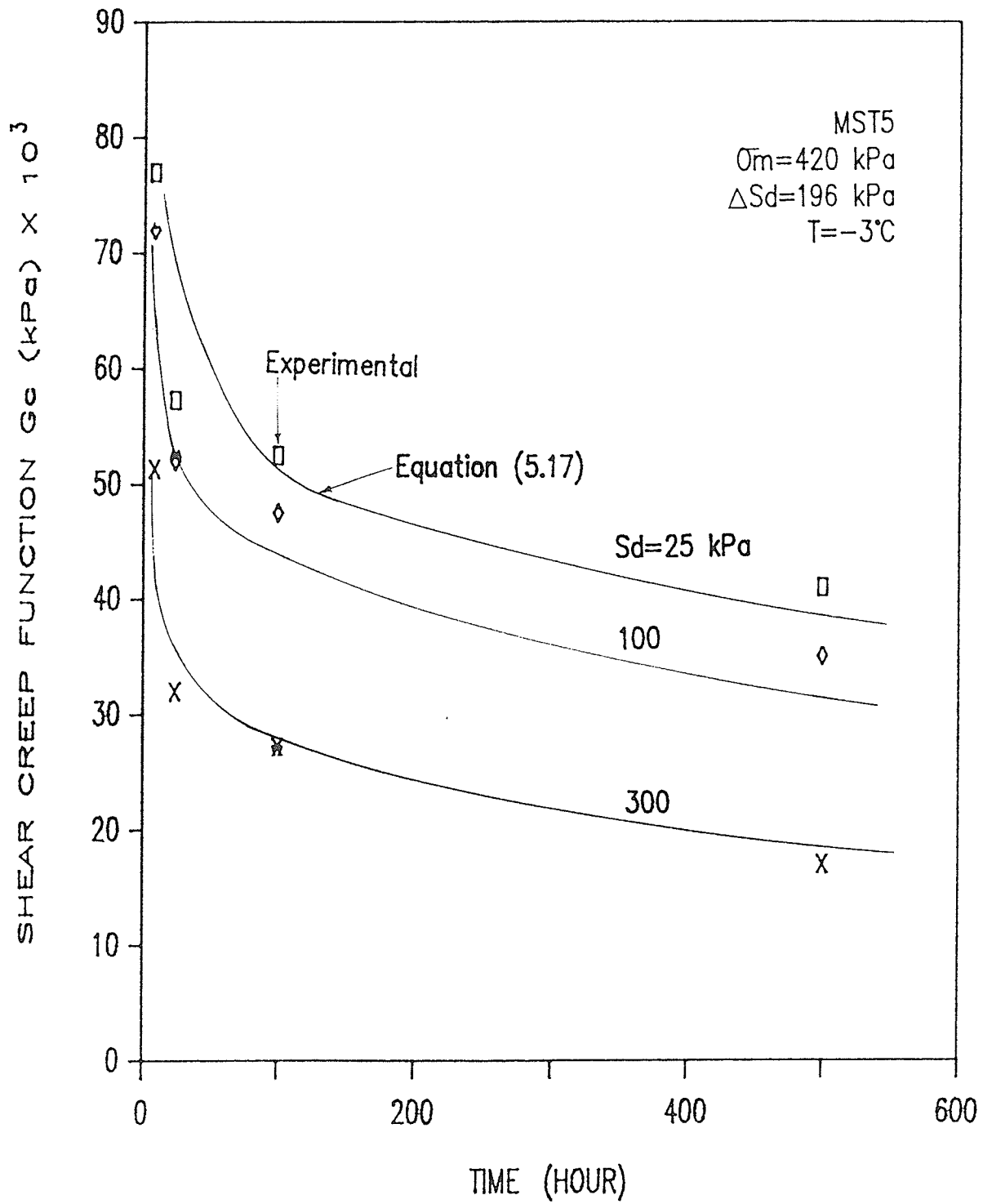


Figure 5.53 Shear creep function versus time (MST5)

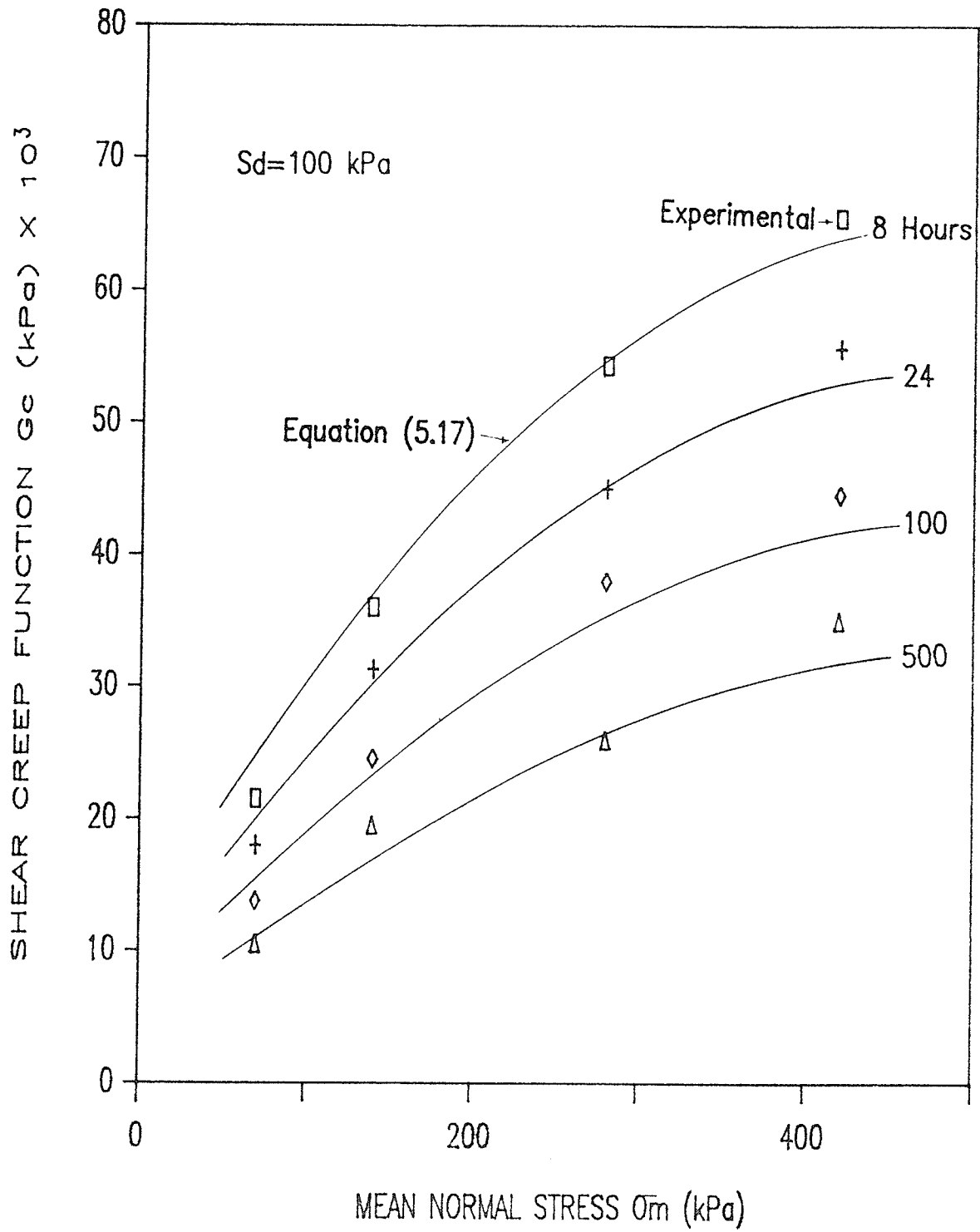


Figure 5.54 Shear creep function versus mean normal stress

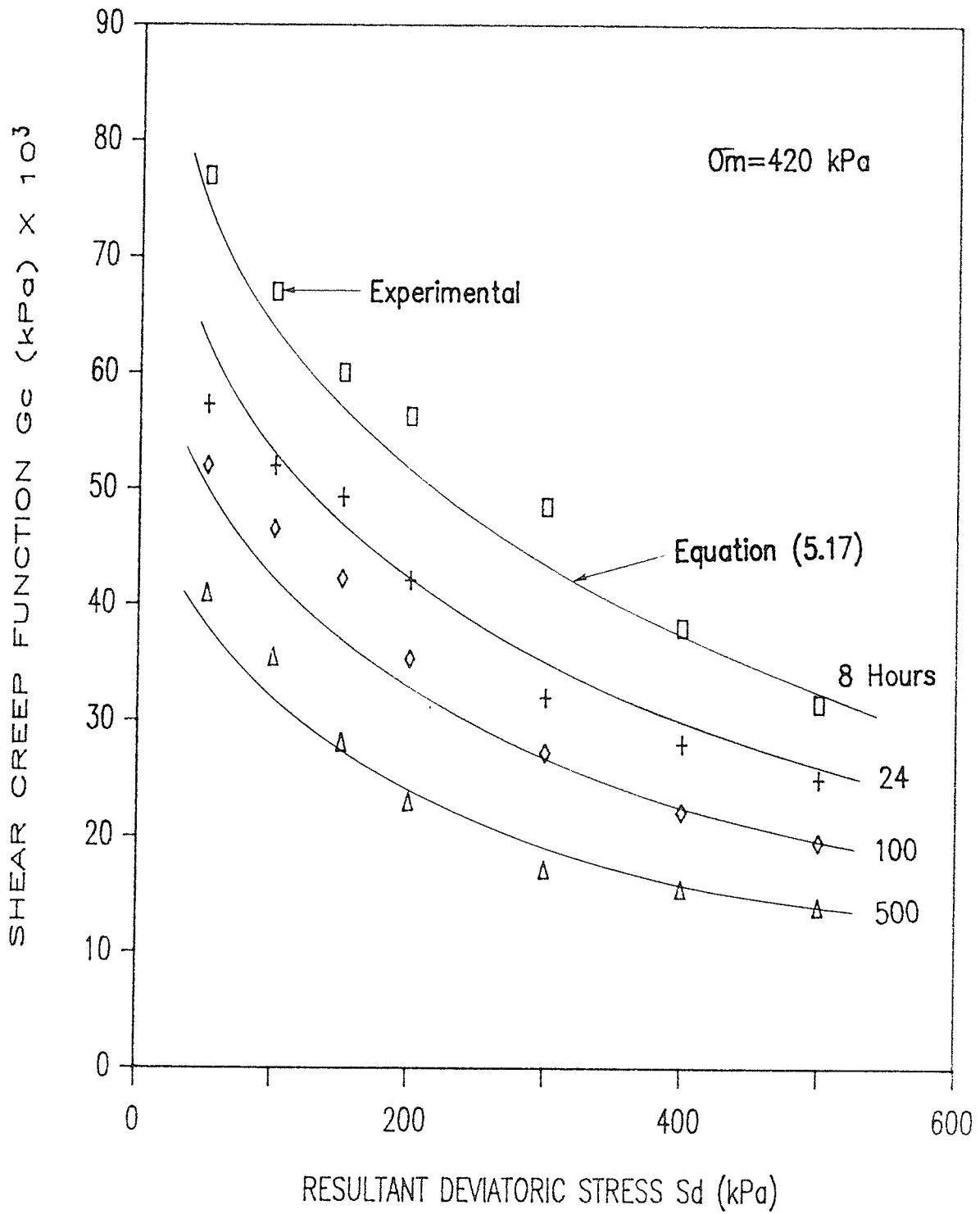


Figure 5.55 Shear creep function versus resultant deviatoric stress

# **CHAPTER SIX**

## **VERIFICATION OF THE MODELS**

## CHAPTER 6

### VERIFICATION OF THE MODELS

#### 6.1 INTRODUCTION

In preceding Chapters 4 and 5, the models for bulk creep function and shear creep function were developed. The model for bulk creep function was based on isotropic consolidation tests and the model for shear creep function was based on constant mean normal stress triaxial compression tests. The purpose was to develop a constitutive creep equation that could be used to predict deformation under a general stress state. To test the model, four constant cell pressure triaxial compression tests (in which changes in mean normal stress and deviator stress occur simultaneously) were carried out and a comparison was made between the observed deformations, and those calculated on the basis of the model. The basic constitutive creep equation (eqn. 2.37) was used to calculate the axial strain of the sample and this was compared to the measured axial strain. In this chapter the constant cell pressure triaxial tests are described, the results and the comparisons are presented.

#### 6.2 CONSTANT CELL PRESSURE, MULTI-STAGE TRIAXIAL CREEP TESTS

##### 6.2.1 Test Procedure

Four constant cell pressure multi-stage triaxial creep tests, MST10, MST11, MST12 and MST13 were performed. The samples for the tests were prepared according to the procedure described in Section 3.2. The physical properties including dry unit weight, water content, porosity and saturation level of the samples are given in Table 6.1. The samples in all four tests were consolidated under an isotropic stress of 70 kPa. Following consolidation the samples were subjected to shear. The cell pressure was held constant and the axial stress was increased in steps. Details of stress application are given in Tables 6.2 through 6.5. Each stress step was maintained constant until the axial strain attenuated. The axial and volumetric deformations were recorded at frequent intervals and are given in the Appendix.

During the tests there were two breakdowns in the refrigeration system of the cold room for about 5 hours in each case and the temperature rose to almost 0°C. In order to avoid excessive sample deformations at this high temperature, the axial loads were removed during the breakdowns. The deformations were not excessive in any of the samples during the first breakdown because the tests were at the initial stage and the axial loads were small. Test MST11 was dismantled after the first breakdown and the sample was checked for any ice lensing, disintegration and other sample variations which may have been caused by the rise in temperature. The physical examination of the sample indicated no disintegration, segregation or any ice lensing. Therefore, tests MST10 and MST12 were continued further and test MST11 was replaced by test MST13.

### 6.2.2 Test Results

The true axial and true volumetric strains are shown plotted against cumulative time for test MST10, in Figures 6.1. The deviator stress,  $(\sigma_1 - \sigma_3)$ , for each increment is shown on the plot. The axial strain attenuated at every deviatoric stress step although, it is not very evident from the plots because of the scale. This test was continued for more than 400 days. The first breakdown occurred during stress increment,  $(\sigma_1 - \sigma_3) = 40$  kPa. There was no excessive deformation during this breakdown. The second breakdown occurred during  $(\sigma_1 - \sigma_2) = 200$  kPa. This resulted in a sharp increase in the axial strain and a sharp drop in the volumetric strain. When the sample temperature was restored to  $-30^\circ\text{C}$ , the axial and volumetric strains continued at rates comparable to those that preceded the breakdown.

The true axial and true volumetric strains versus cumulative time for test MST12, are shown plotted in Figure 6.2. The deviatoric stress for each increment is shown on the plot. The sample underwent attenuating creep during each stress step. The test was conducted simultaneously with test, MST10, and was therefore subjected to the same cold room-temperature variations associated with the breakdown of the refrigeration unit. Sudden changes in axial and volumetric strains accompanied the rapid rise in temperature.

The true axial and true volumetric strains versus cumulative time for test MST13, are shown plotted in Figure 6.3. As before the



deviator stress for each loading step is shown on the plot. There was only one breakdown during this test, because this test was set up after the first breakdown. The breakdown occurred during the stress step of  $(\sigma_1 - \sigma_3) = 200$  kPa. Both the axial and volumetric strain increased sharply during the breakdown. When the sample temperature was restored to  $-30^\circ\text{C}$  both the axial and volumetric strains continued at rates comparable to those that preceded the breakdown.

### 6.3 VERIFICATION OF THE MODEL

The creep model based on the bulk creep function and the shear creep function developed in chapters 4 and 5 was applied to the measured axial deformations observed in constant cell pressure triaxial creep tests. Both the deviatoric and mean normal stresses changed at every loading step and therefore the deformations which occurred were the result of simultaneous changes in linear and shear strains. For the triaxial test equation (2.37) can be written as:

$$\sigma_{11} = K_c \epsilon_v + 2G_c (\epsilon_{11} - 1/3 \epsilon_v) \quad (6.1)$$

in which  $\sigma_{11}$  = axial stress

$\epsilon_v$  = volumetric strain

$\epsilon_{11}$  = axial strain

Rearranging equation (6.1), the expression for  $\epsilon_{11}$  becomes:

$$\epsilon_{11} = \frac{1}{2G_c} (\sigma_{11} - K_c \epsilon_v + \frac{2}{3} G_c \epsilon_v) \quad (6.2)$$

Since  $K_c$  and  $G_c$  are time dependent, solutions can be obtained for  $\epsilon_{11}$  as a function of time. However, the solutions developed for  $K_c$  (4.12) and  $G_c$  (5.17), are for constant stress and variable time. As such they are used to generate strain, as a function of time, for a given stress state. Therefore equation (6.2) is directly applicable to single stage loading. Unfortunately a multi-stage triaxial test was performed to test the constitutive model rather than a series of tests at different stress levels. However, it is possible to make a comparison between predicted and observed axial strains, in an approximate manner at least, by reconstructing strain-time curves for each stress increment, by assuming that for a given stress increment and a given elapsed time the total strain is the cumulative sum of all strains that occurred during an equal elapsed time interval for each and every stress increment up to and including the increment under consideration. This is illustrated in Figure 6.4. The cumulative strain at time  $t$  due to stress,  $\sigma_3$ , applied as a single step is assumed to be the cumulative sum of the instantaneous and creep strains  $a_1, a_c, b_1, b_c$  and  $c_1, c_c$  which occurred during an equal elapsed time  $t$  under the incremental stresses. This reconstructed strain-time curve can then be compared to one generated by equation (6.2) for the same stress state. This was done for five stress increments of the multi-stage triaxial test MST10. The stress increments chosen were consecutive and were started at a level  $(\sigma_1 - \sigma_3) = 120$  kPa which was large enough to produce significant strains.

The predicted and the reconstructed strain-time curves are shown in Figure 6.5 through 6.9. The agreement between the predicted and reconstructed is quite good considering the scatter that was inherent in all test data and the basic assumption made in reconstructing the strain-time curves. No definite conclusion can be made regarding the predictive reliability of the constitutive creep model but, on the basis of the comparison made, it can be said that the model shows some promise.

As another test of the predictive accuracy of the model, the cumulative attenuated axial strains, at the end of each stress increment, during each constant cell pressure triaxial compression test, were compared to those computed using equation (6.2) in conjunction with the attenuated values of  $K_e$  and  $G_e$ . The computed and observed attenuated axial strains for the three constant cell pressure triaxial compression tests are shown plotted against deviatoric stress,  $(\sigma_1 - \sigma_3)$ , in Figures 6.10 through 6.12. It was observed in Figure 6.10 that in test, MST10, the observed axial strains were lower at low deviatoric stresses but higher at higher deviatoric stresses than the predicted values of the axial strains. In tests, MST12 and MST13, as observed in Figures 6.11 and 6.12, the predicted axial strains were slightly lower than those of the observed values at all stress levels. At higher deviatoric stresses the differences between the predicted and the observed values of axial strains tended to diminish in all the tests. The observed axial strains are plotted against predicted axial strains in Figure 6.13. The correlation coefficient was found to be 0.85.

The comparisons indicate that the creep constitutive equation developed by separating isotropic and deviatoric components of stress provided reasonably good agreement between predicted and observed strains when applied to triaxial test results in which isotropic and deviatoric components of stress were increased simultaneously.

TABLE 6.1

## Physical Properties of Frozen Sand Sample

Sample	Dry Unit Weight (KN/m <sup>3</sup> )	Water Content (%)	Porosity (%)	Water Saturation (%)	Sample Test Temp. (°C)
MST10	16.0	25.1	42.5	92.0	-3
MST11	15.2	23.1	40.5	91.5	-3
MST12	15.1	24.2	41.3	90.3	-3
MST13	15.3	23.5	42.0	91.7	-3

TABLE 6.2

## Details of Stress Application

Test MST10  $\sigma_3=70$  kPa

$(\sigma_1 - \sigma_3)$ (kPa)	$S_a$ (kPa)	$\sigma_m$ (kPa)	Duration of Stress Application (Hour)
0	0.0	70.0	407
20	16.3	76.7	226
40	32.7	83.3	503
60	49.0	90.0	117
80	65.3	96.7	144
100	81.6	103.3	144
120	98.0	110.0	312
140	114.3	116.7	503
160	130.6	123.3	1549
180	147.0	130.0	720
200	163.3	136.7	1223
240	195.9	150.0	719
280	228.6	163.3	807
320	261.3	176.7	1319
360	294.0	190.0	959
400	326.6	203.3	240

TABLE 6.3

## Details of Stress Application

Test MST11  $\sigma_3=70$  kPa

$(\sigma_1 - \sigma_3)$ (kPa)	$S_d$ (kPa)	$\sigma_m$ (kPa)	Duration of Stress Application (Hour)
0	0.0	70.0	407
20	16.3	76.7	226
40	32.7	83.3	439

TABLE 6.4

## Details of Stress Application

Test MST12  $\sigma_3=70$  kPa

$(\sigma_1 - \sigma_3)$ (kPa)	$S_d$ (kPa)	$\sigma_m$ (kPa)	Duration of Stress Application (Hour)
0	0.0	70.0	407
20	16.3	76.7	226
40	32.7	83.3	503
60	49.0	90.0	117
80	65.3	96.7	144
100	81.6	103.3	144
120	98.0	110.0	312
140	114.3	116.7	167
160	130.6	123.3	359
180	147.0	130.0	506
200	163.3	136.7	1749
220	179.6	143.3	1293
240	195.9	150.0	719
280	228.6	163.3	807
320	261.3	176.7	1319
360	294.0	190.0	959
400	326.6	203.3	240



TABLE 6.5

## Details of Stress Application

Test MST13  $\sigma_3=70$  kPa

$(\sigma_1 - \sigma_3)$ (kPa)	$S_a$ (kPa)	$\sigma_m$ (kPa)	Duration of Stress Application (Hour)
0	0.0	70.0	335
80	65.3	96.7	312
100	81.6	103.3	167
120	98.0	110.0	335
140	114.3	116.7	503
160	130.6	123.3	1082
180	147.0	130.0	720
200	163.3	136.7	1223
240	195.9	150.0	719
280	228.6	163.3	807
320	261.3	176.7	1319
400	326.6	203.3	959
480	391.9	230.0	240

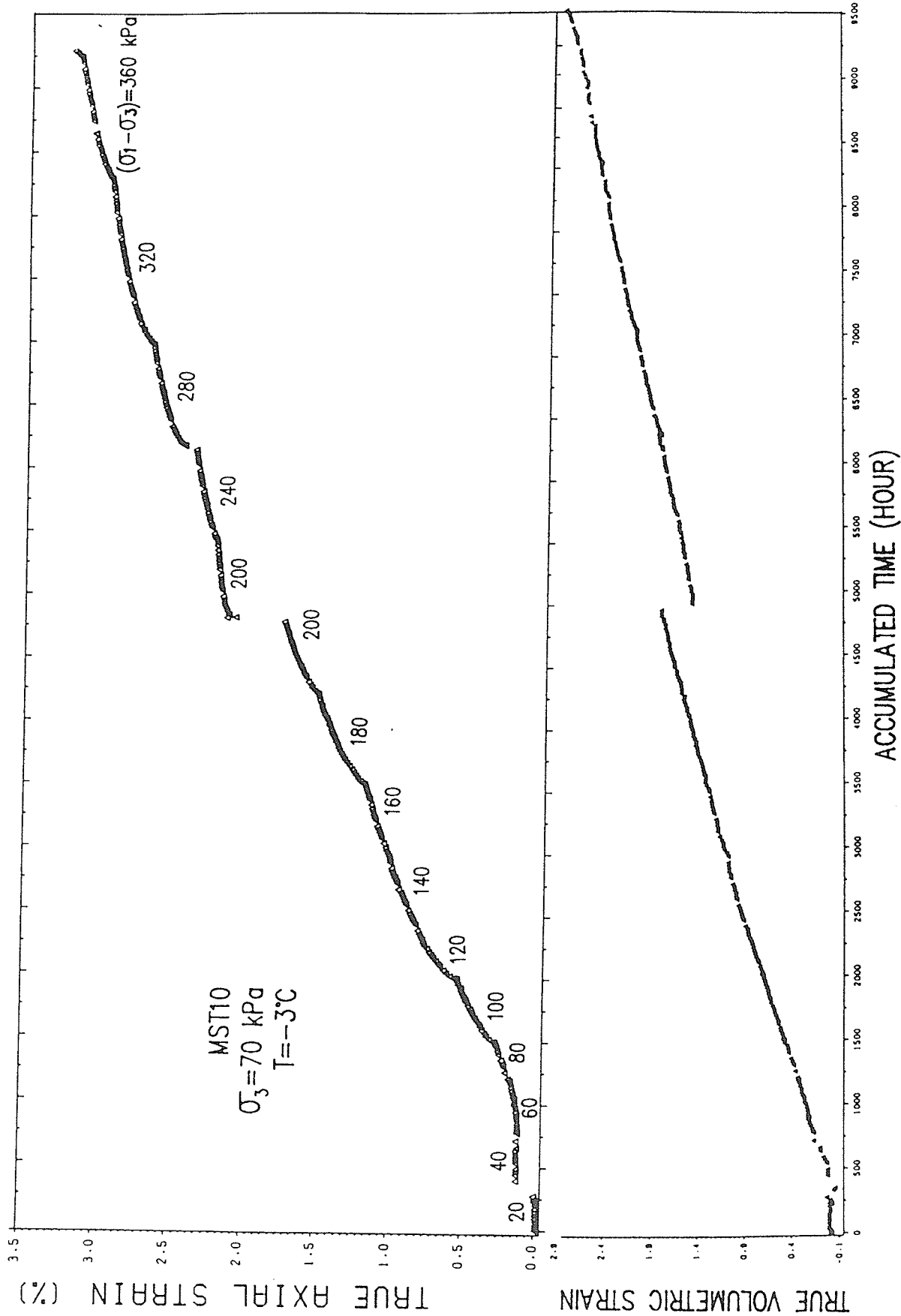


Figure 6.1 True volumetric and true axial strain versus accumulated time (MST10)

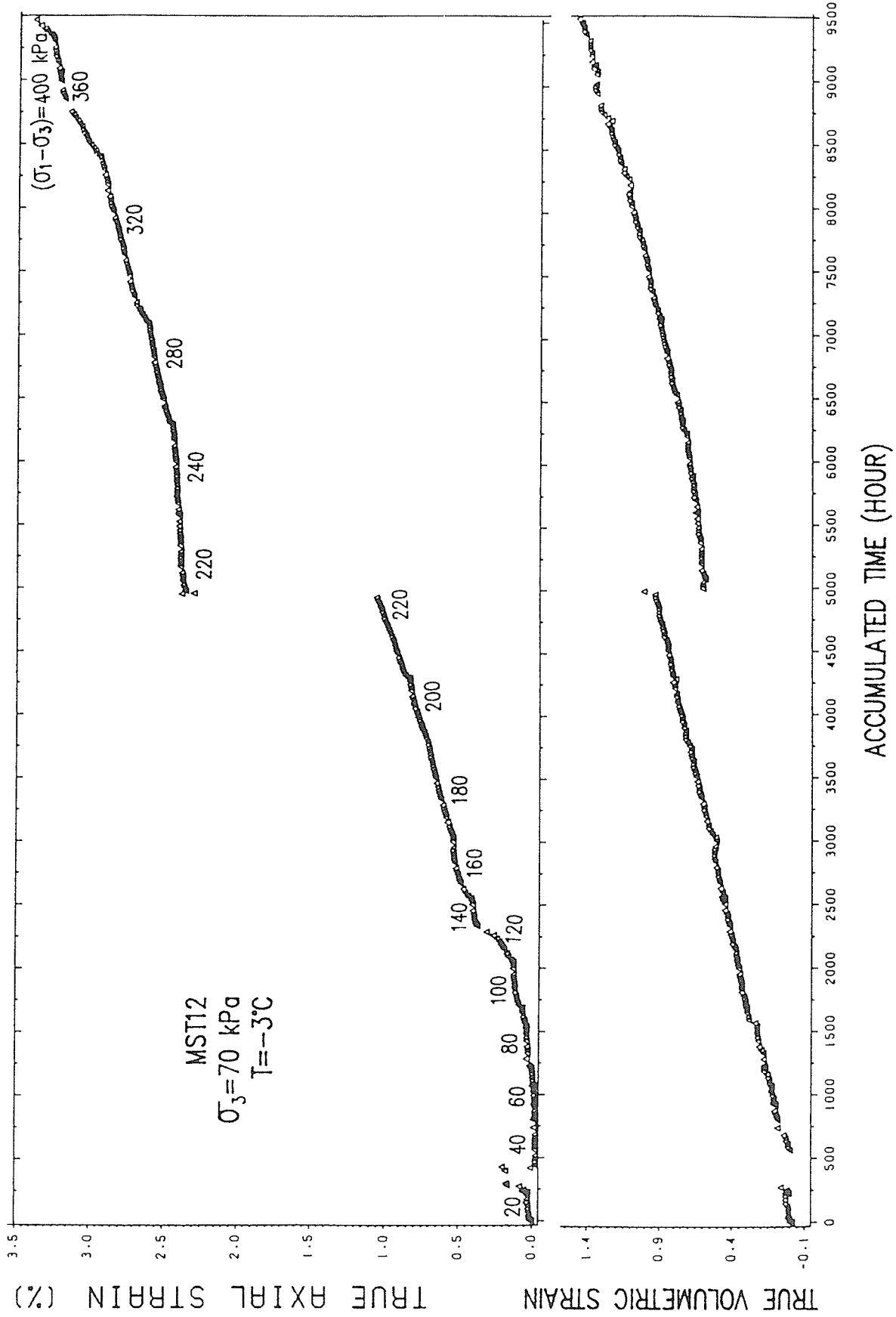


Figure 6.2 True volumetric and true axial strain versus accumulated time (MST12)

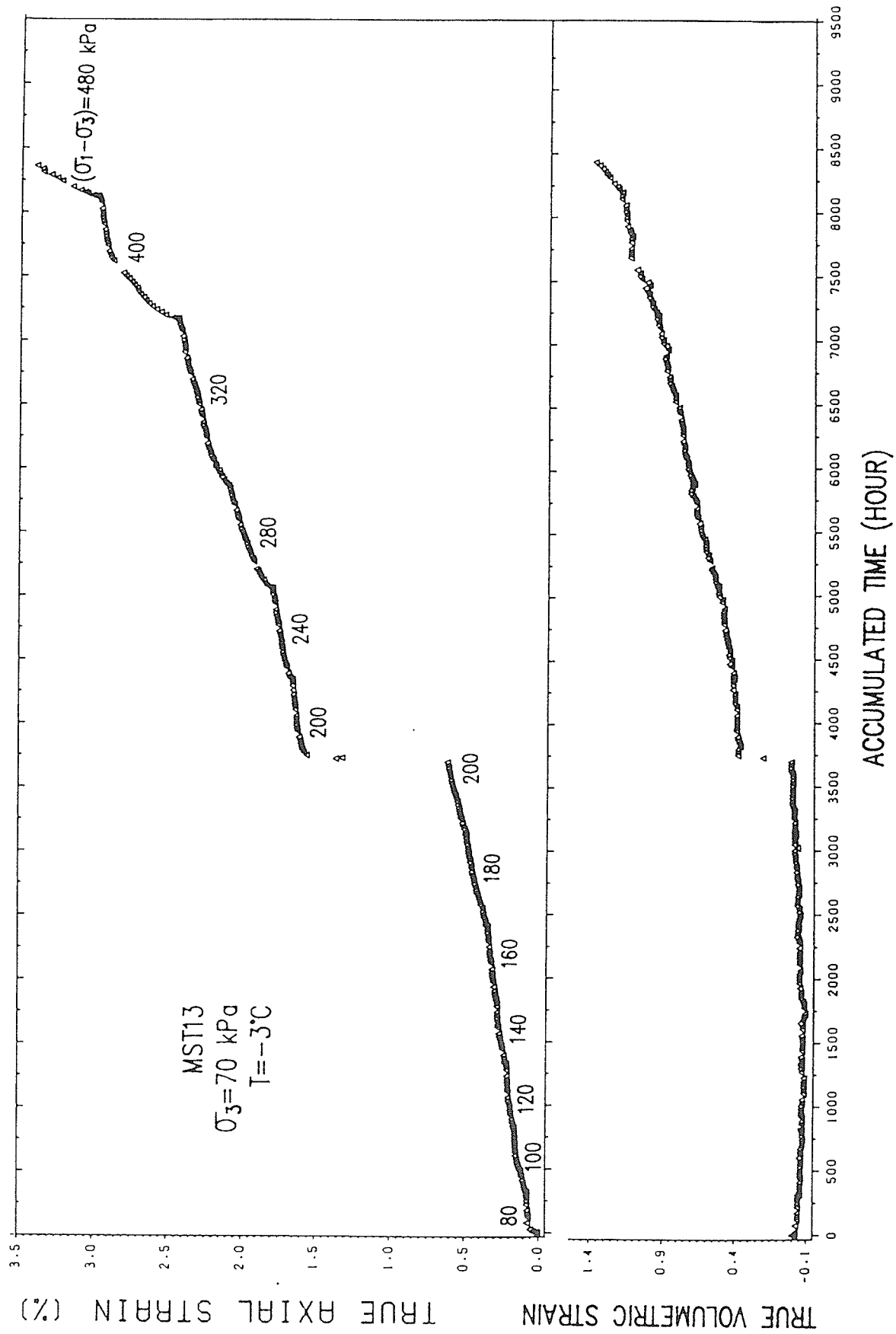


Figure 6.3 True volumetric and true axial strain versus accumulated time (MST13)

AXIAL CREEP STRAIN

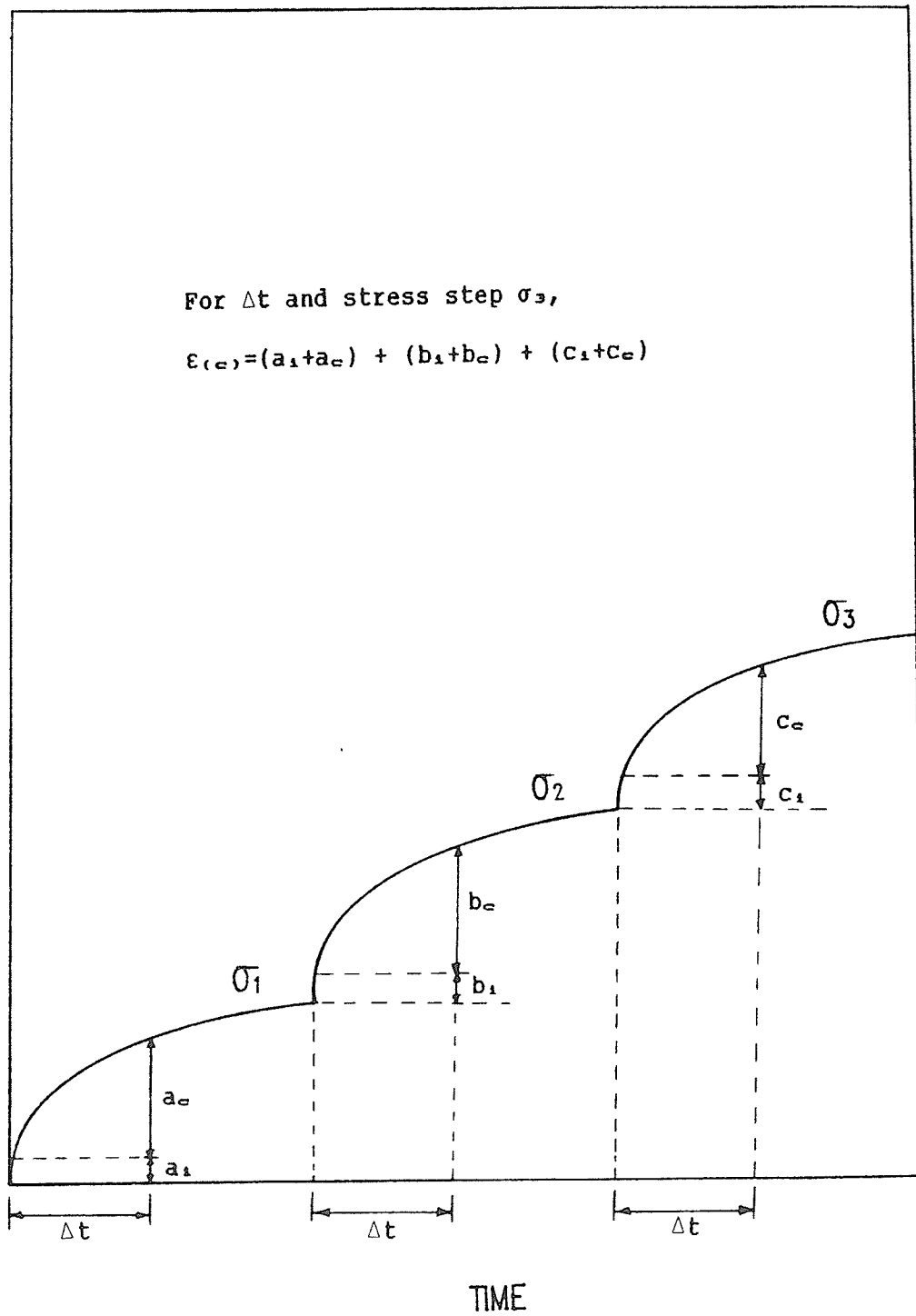


Figure 6.4 Axial creep strain versus time in a multi-stage test

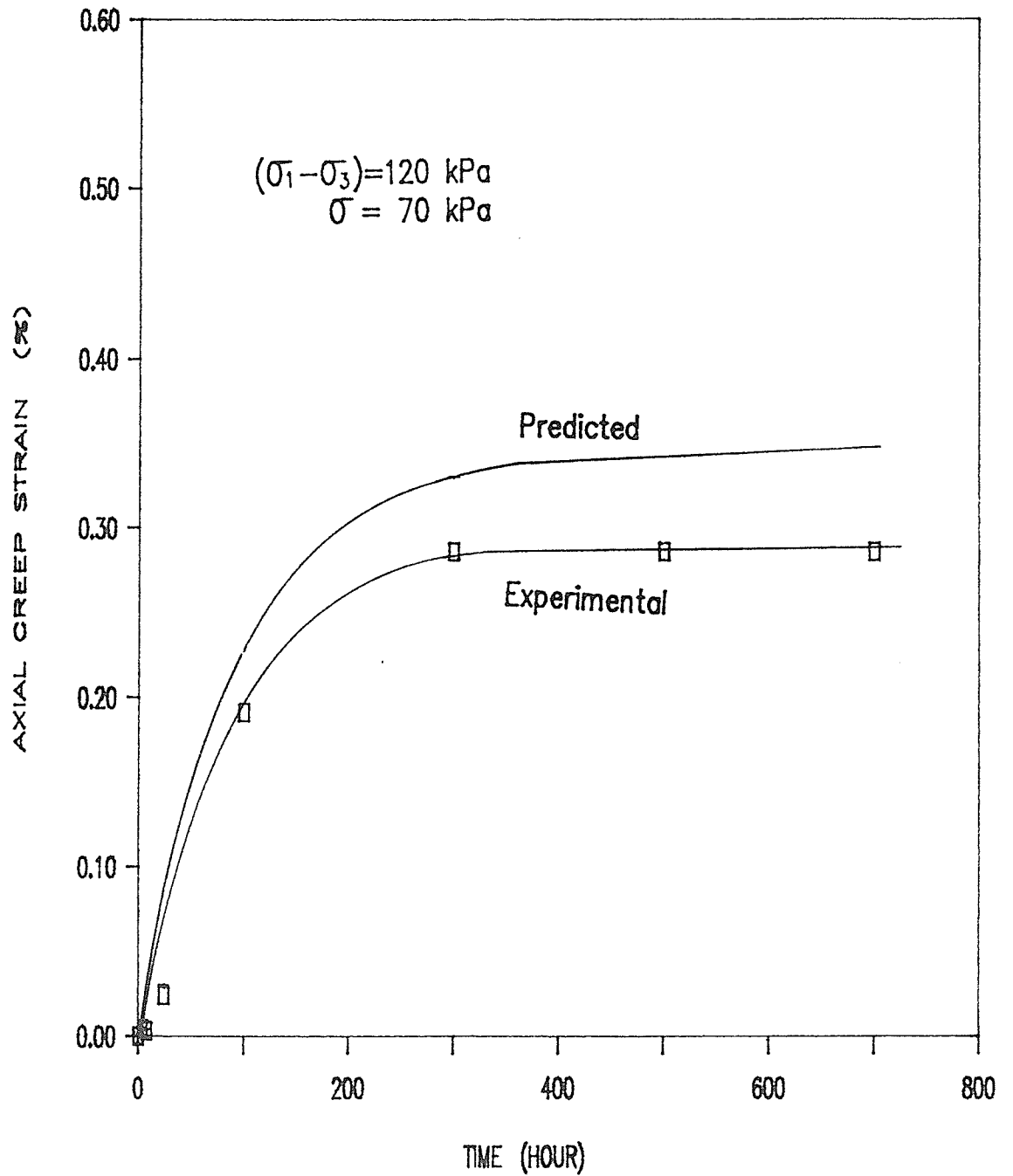


Figure 6.5 Axial creep strain versus time  $(\sigma_1 - \sigma_3) = 120 \text{ kPa}$

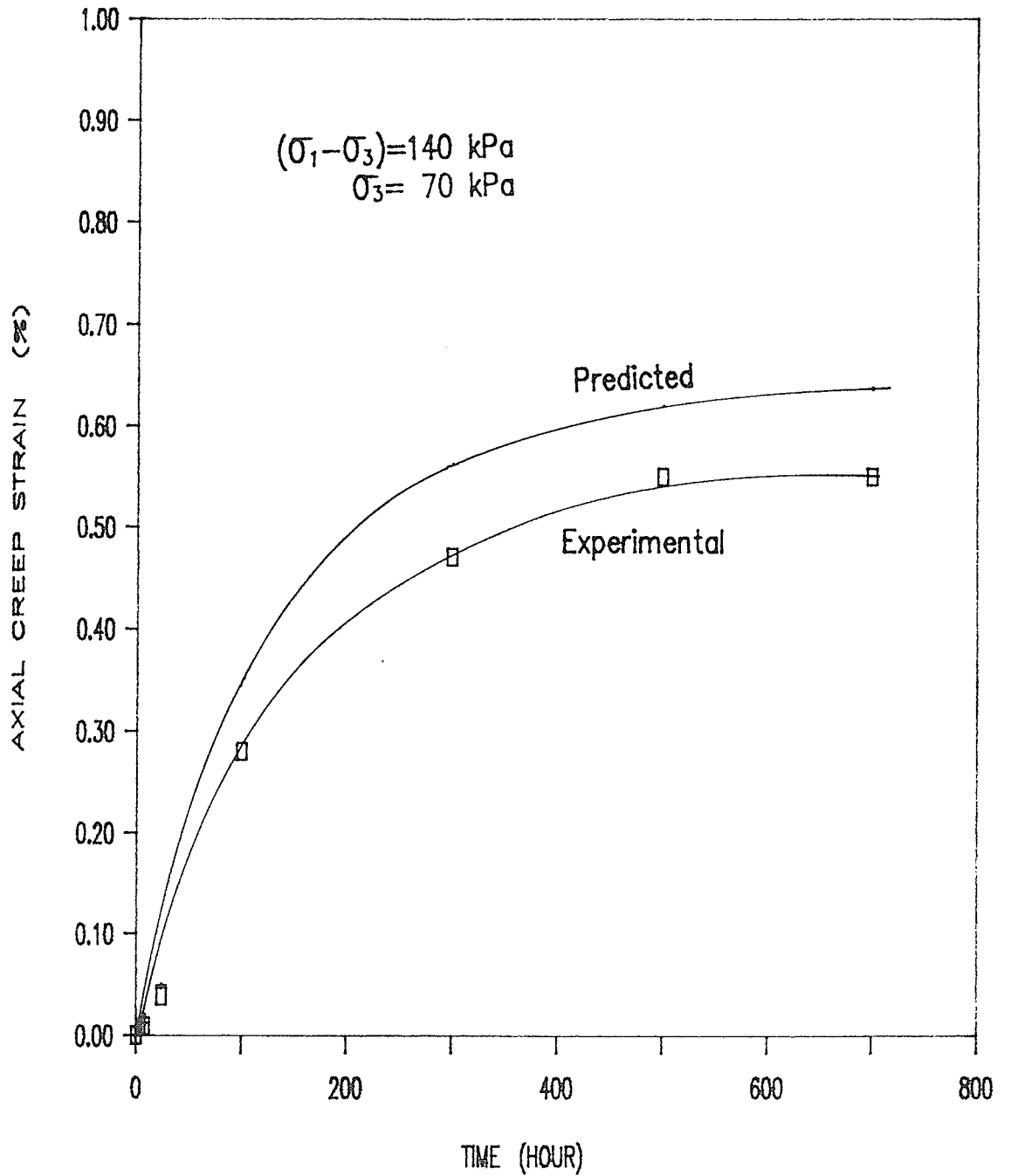


Figure 6.6 Axial creep strain versus time  $(\sigma_1 - \sigma_3) = 140 \text{ kPa}$

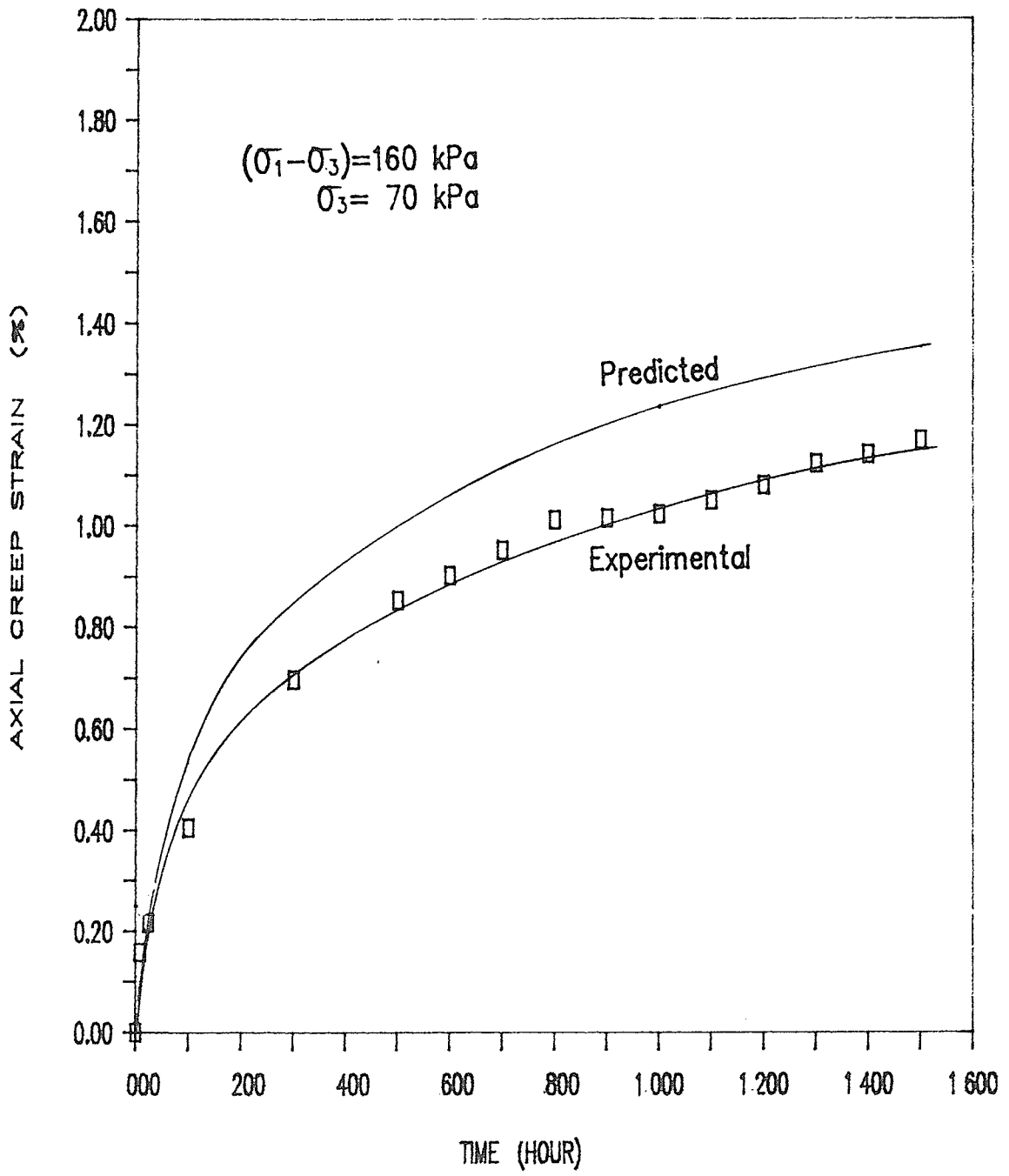


Figure 6.7 Axial creep strain versus time  $(\sigma_1 - \sigma_3) = 160 \text{ kPa}$



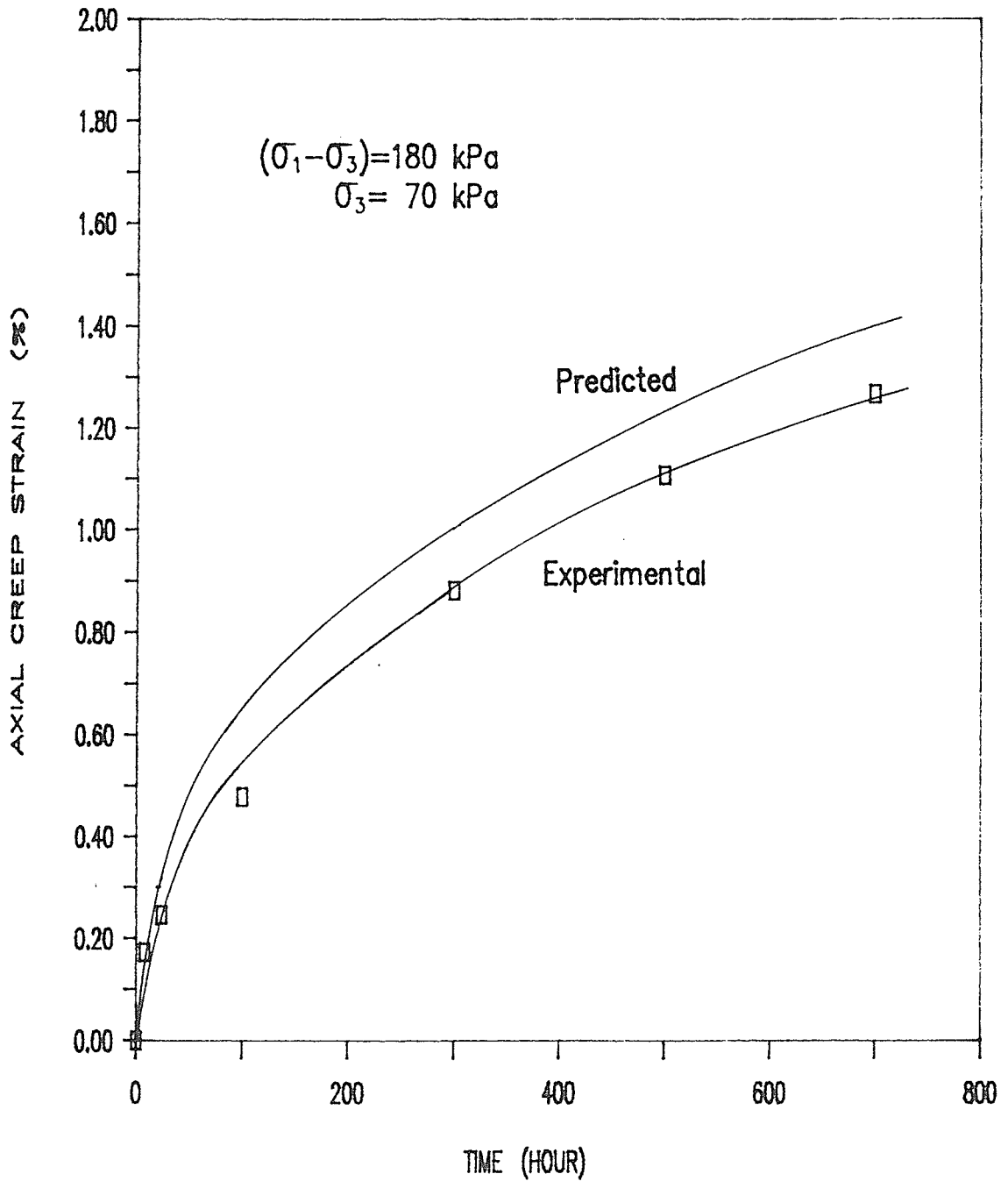


Figure 6.8 Axial creep strain versus time  $(\sigma_1 - \sigma_3) = 180 \text{ kPa}$

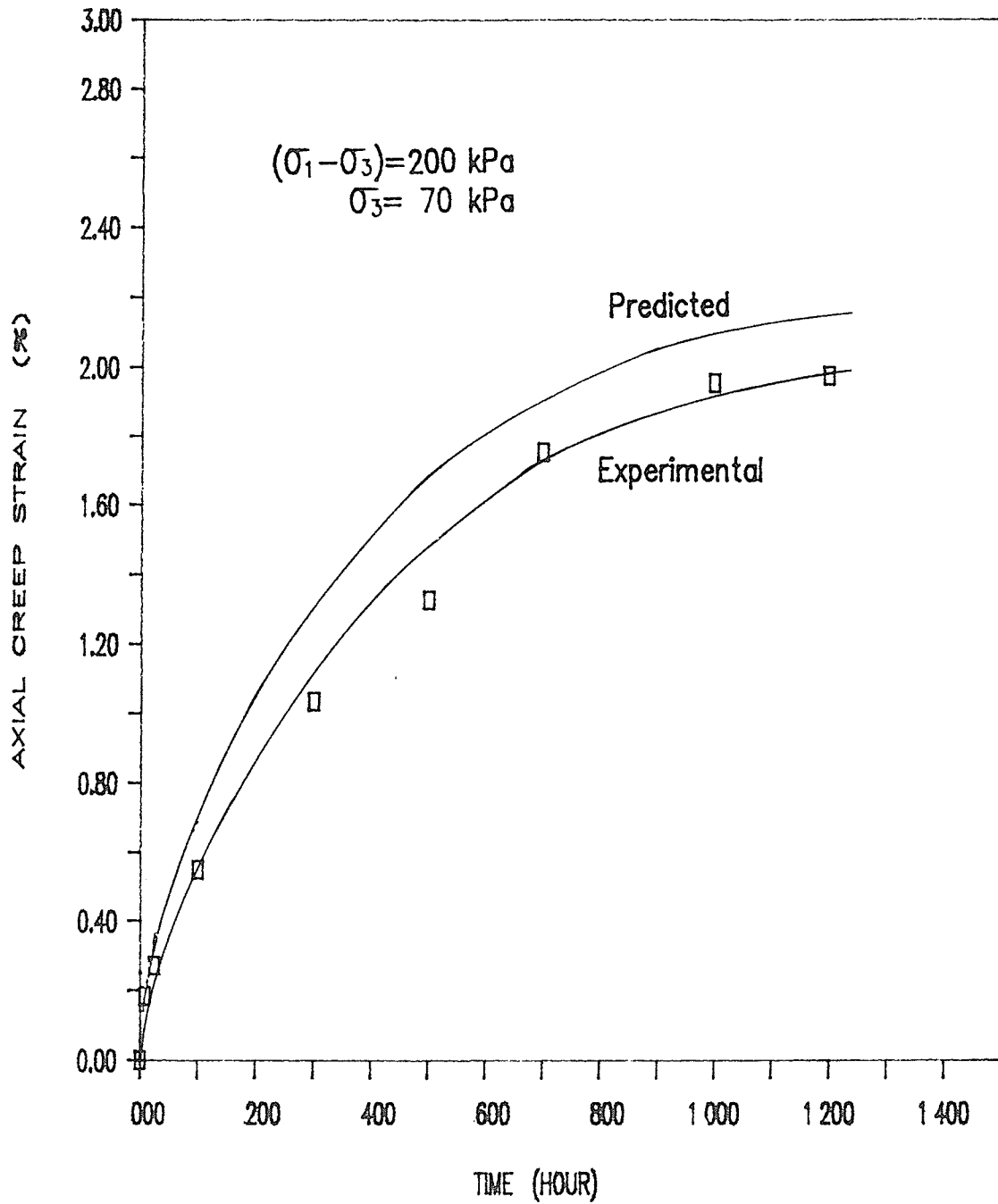


Figure 6.9 Axial creep strain versus time  $(\sigma_1 - \sigma_3) = 200 \text{ kPa}$

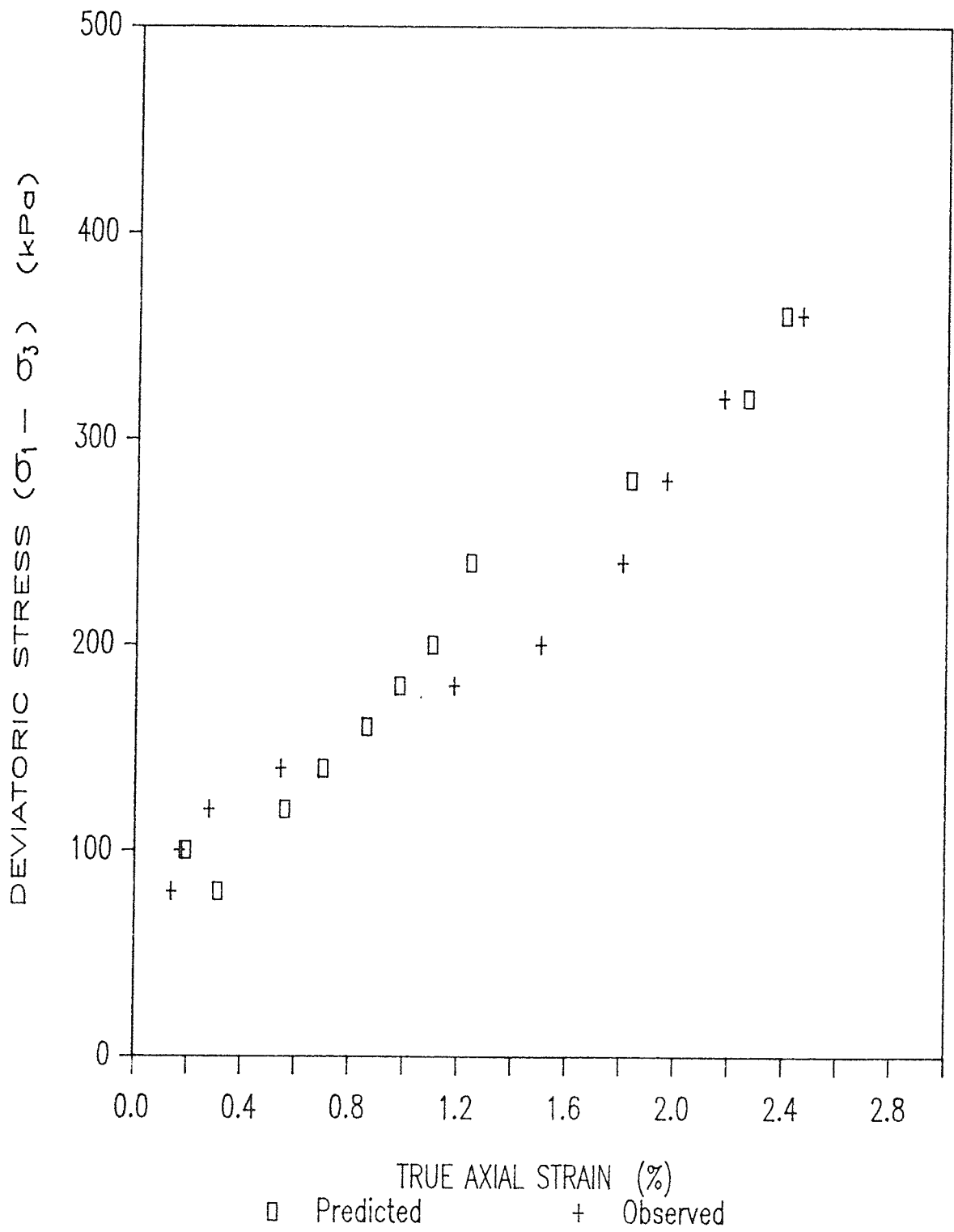


Figure 6.10 Deviatoric stress versus attenuated true axial stress (MST10)

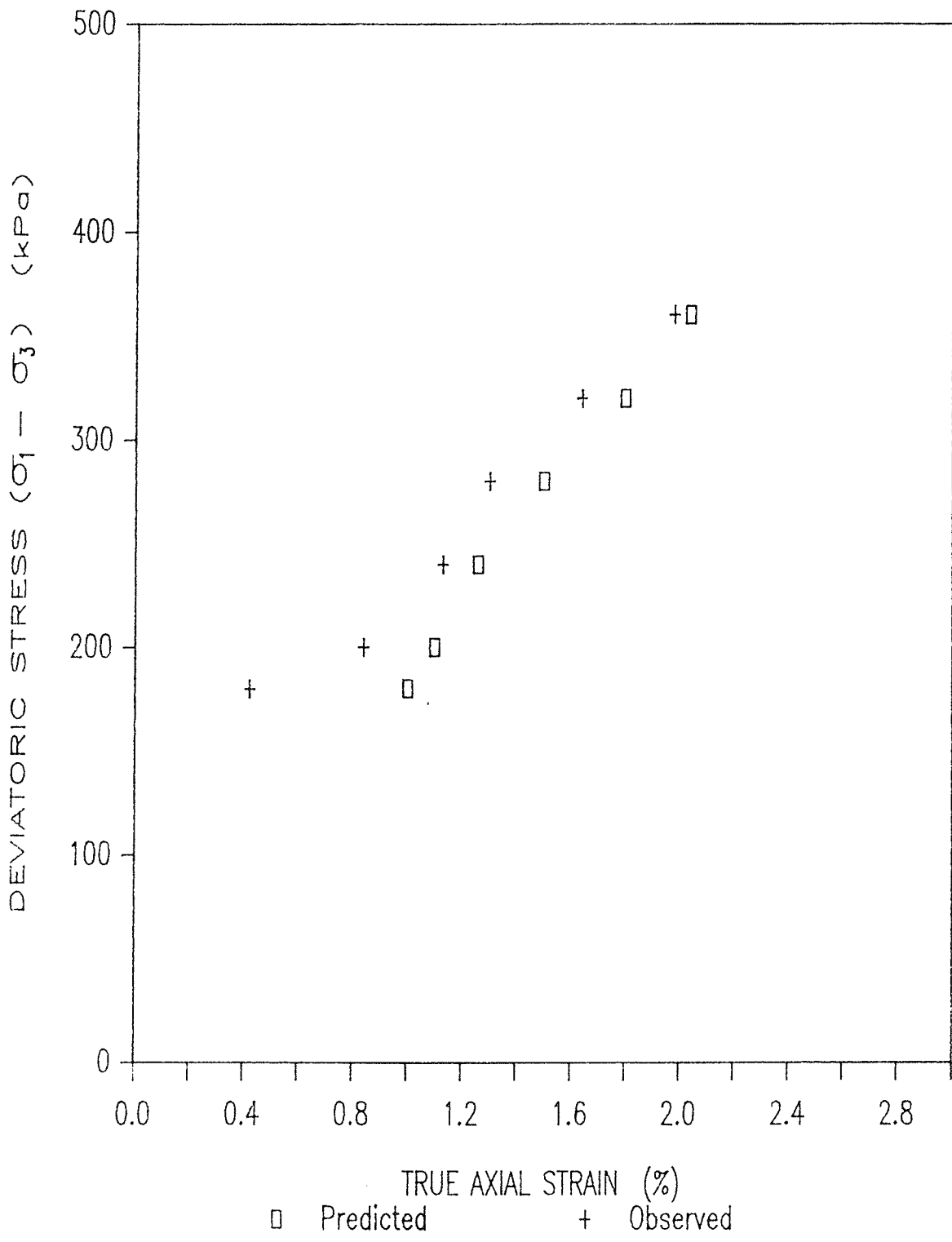


Figure 6.11 Deviatoric stress versus attenuated true axial stress (MST12)

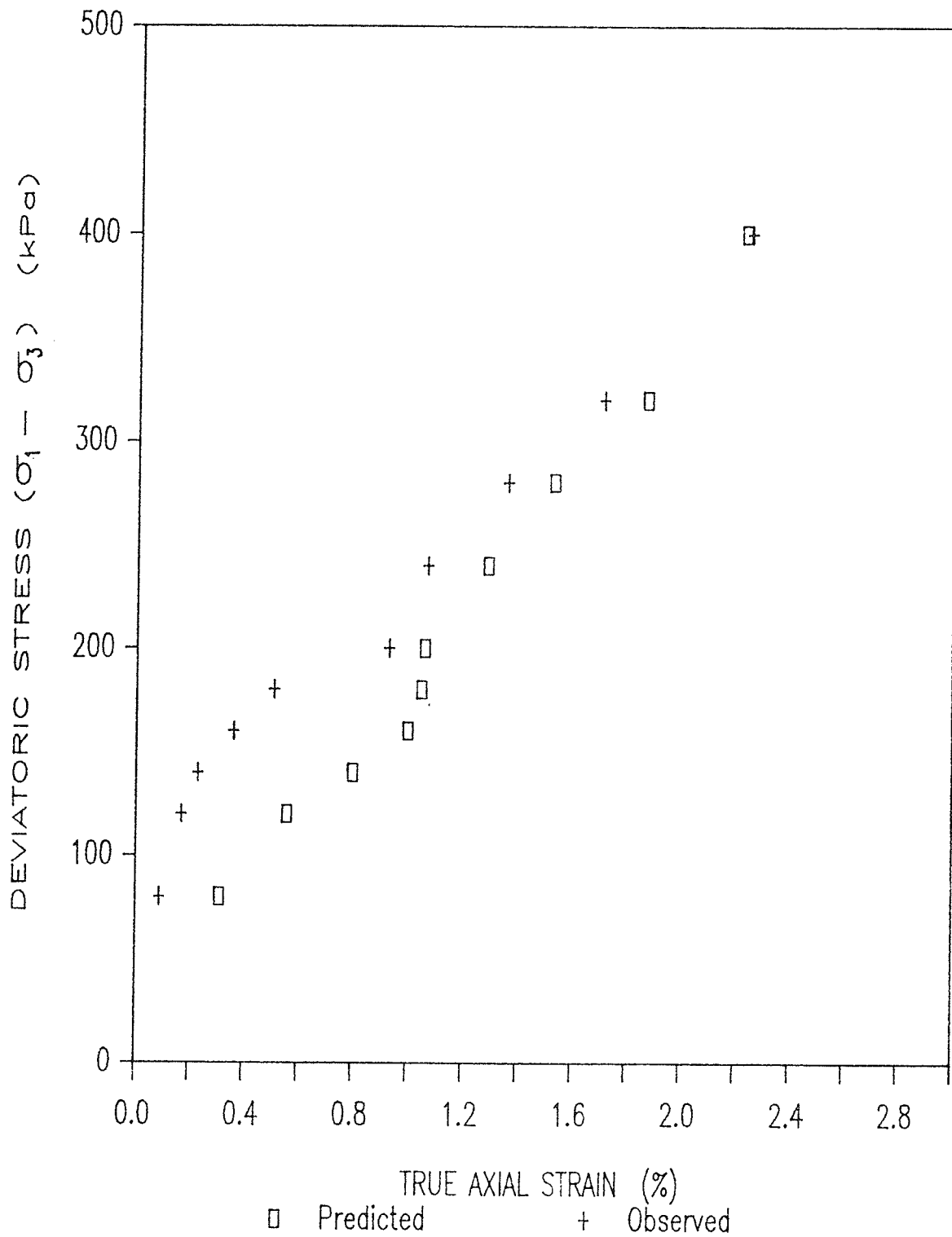


Figure 6.12 Deviatoric stress versus attenuated true axial strain (MST13)

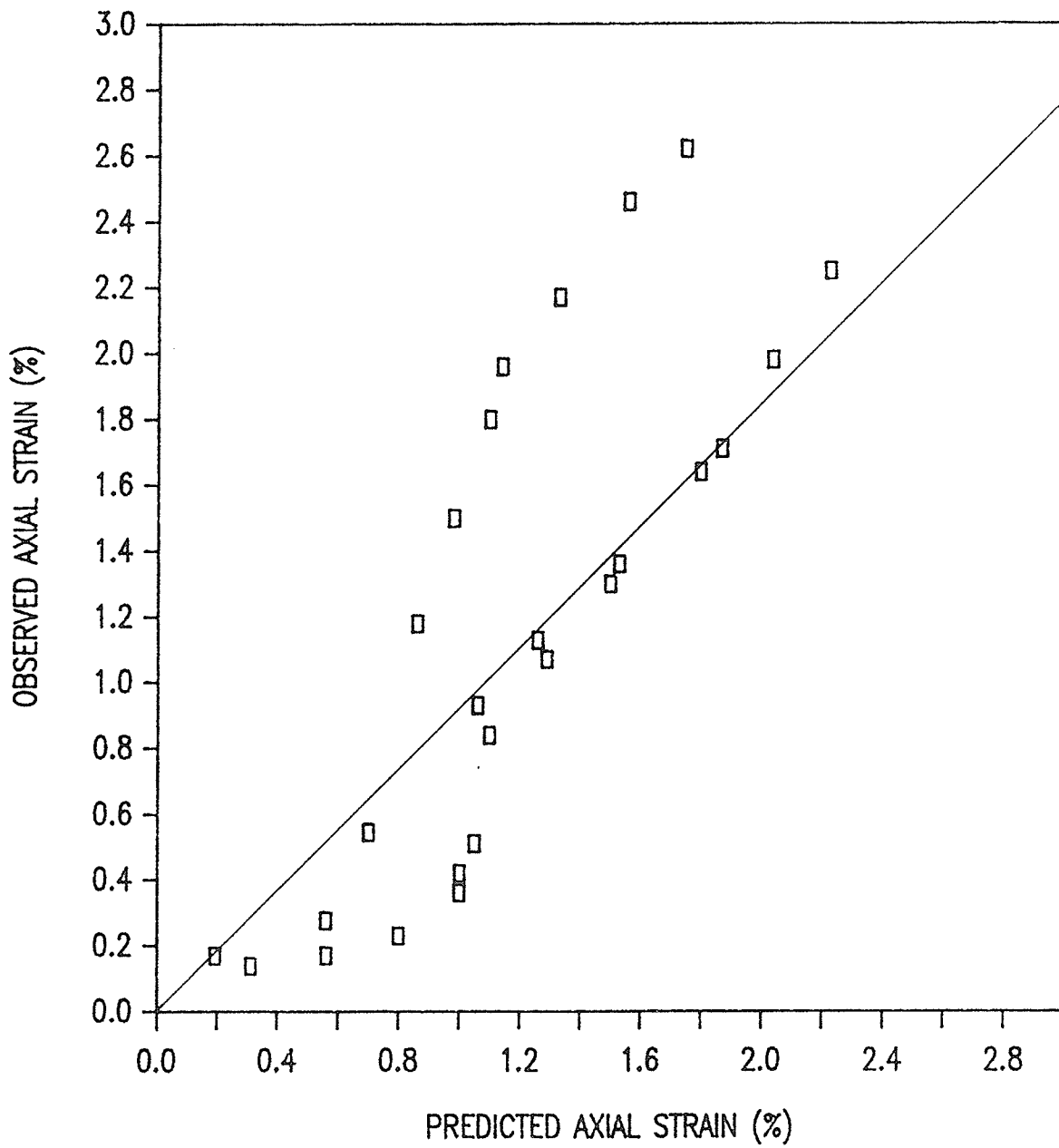


Figure 6.13 Observed axial strain versus predicted axial strain

# **CHAPTER SEVEN**

## **DILATION AND FAILURE**

## CHAPTER 7

### DILATION AND FAILURE

#### 7.1 INTRODUCTION

A variety of deformation mechanisms, such as, micro-cracking, closure and/or opening of existing cracks, movement of grain boundaries, recrystallization of ice etc occur in frozen soils. Some of the mechanisms tend to strengthen the soil through densification known as strain-hardening, while others tend to weaken the soil through dilation which constitutes in part at least, strain-softening. As mentioned previously, in the long-term tests reported herein, it was found that generally the onset of dilation coincided with the start of accelerating creep. Mechanistically, this makes sense since dilation is associated with opening of cracks and an increase in voids. Thus one could conceivably use the onset of dilation as a failure criterion. However this would require long-term tests, particularly at low stress levels. For this reason an investigation was carried out to determine if dilation occurred at approximately the same stress conditions irrespective of the duration of the test. The investigation was to determine if the start of dilation was governed primarily by the stress state or by the magnitude of accumulated strains. This was done by running a series of short-term, constant mean normal stress tests and



comparing the stress states at which dilation started, in the case of the long and short-term tests.

## 7.2 TEST PROCEDURE

### 7.2.1 Constant Mean Normal Stress Multi-stage Short-term Triaxial Tests

Four short-term constant mean normal stress multistage triaxial tests were performed. The sample preparation techniques and test procedures were those described in Sections 3.2 and 5.2.1 respectively. The physical properties of the samples are given in Table 7.1. The tests were conducted under similar stress condition to those presented in Chapter 5, but were short-term. The deviatoric stresses were increased in steps approximately every 24 hours irrespective of the creep state.

## 7.3 TEST RESULTS

### 7.3.1 MST6

In this test the mean normal stress was 70 kPa and the increment of resultant deviatoric stress component,  $S_d$ , was 24.5 kPa. Six stepwise increments of deviatoric stress were applied. Details of the stress applications are given in Table 7.2 and the axial and volumetric deformations are given in the Appendix.

The cumulative true axial and true volumetric strains versus time for the entire test are shown in Figure 7.1. The strain-time data indicated that dilation occurred at the stress step,  $S_a=147$  kPa. The volume change reversal was abrupt coinciding with the change in step. An abrupt increase in axial creep was also observed at the same stress step.

### 7.3.2 MST7

In this test the mean normal stress was 140 kPa and the increment of resultant deviatoric stress,  $S_d$ , was 49 kPa. Seven stepwise increments of deviatoric stress were applied. Details of the stress applications are given in Table 7.3 and the axial and volumetric deformations are given in the Appendix.

The cumulative true axial and true volumetric strains are shown plotted against time for the entire test in Figure 7.2. The dilation occurred at the stress step,  $S_d=294$  kPa, with an abrupt increase in volumetric strain. The axial creep accelerated at the same stress step.

### 5.3.8 MST8

In this test the mean normal stress was 280 kPa and the

incremental resultant deviatoric stress was 73.5 kPa. Eleven stepwise increments of deviatoric stress were applied. Details of the stress applications are given in Table 7.4 and the axial and volumetric deformations are given in the Appendix.

The cumulative true axial and true volumetric strains versus time for the entire test are shown in Figure 7.3. The strain-time data indicated that dilation occurred at the stress level,  $S_a=661$  kPa with an abrupt increase in volumetric strain. The axial creep accelerated at the same stress level.

#### 7.3.4 MST9

The mean normal stress, in this test, was 420 kPa and the incremental resultant deviatoric stress was 98 kPa. Eleven stepwise increments of deviatoric stress were applied. Details of the stress applications are given in Table 7.5 and the axial and volumetric deformations are given in the Appendix.

The cumulative true axial and true volumetric strains versus time for the entire test are shown in Figure 7.4. The strain-time data indicated that dilation occurred at the stress step,  $S_a=980$  kPa with an abrupt increase in volumetric strain. The axial creep accelerated at the same stress level.

## 7.4 DISCUSSION OF TEST RESULTS

#### 7.4.1 Failure Mechanisms

It was observed from the true axial and true volumetric strains versus cumulative time curves (Figures 7.1 through 7.4) that in the short-term tests the sample decreased in volume initially upon application of the deviatoric stresses. At successive increments of the deviatoric stresses, the samples continued to decrease in volume until a threshold stress was reached, at which time the samples started to dilate. The same phenomenon was observed in the long-term tests, as described in Section 5.3. In all of the long-term tests it was observed that the dilation was gradual while in all of the short-term tests an abrupt reversal in volume was observed. This may be attributed to the phenomenon that in the long-term tests the stresses were more evenly distributed between the ice matrix and the sand particles whereas in the short-term tests the time elapsed between increments was too short for even distribution, and most of the stresses were carried by the sand particles bearing on the ice matrix. Consequently, a greater portion of the stress was carried by the ice matrix and failed suddenly transferring the stress to grain to grain.

The resultant deviatoric stress at the beginning of dilation for both types of tests were plotted against mean normal stress in Figure 7.5. The resultant deviatoric stresses for the short-term tests were greater than those for the long-term tests beyond a stress of about 100 kPa. This plot can be used as failure criteria and has been discussed in sections 5.4.1 and 5.4.3. This plot also signifies that

the onset of dilation or failure is not strictly a stress phenomena.

The axial cumulative strains at the beginning of dilation were plotted against the mean normal stress in Figure 7.6. The axial strain at dilation increased approximately linearly with the mean normal stress in both test series. The increase in failure strain with increased mean normal stress can be explained by the concept of ductile fracture which generally occurs by the formation and subsequent growth of and coalescence of voids and cavities. If the cavity nucleation can be delayed or suppressed altogether, large increase in ductility can be achieved. By increasing the mean normal stress the dilation or the opening up of the cracks are suppressed and delayed, and thereby the axial strain at dilation increases. The cumulative strains at the start of dilation were greater for the long-term tests than for the short-term tests for a given mean normal stress which means that failure is not solely governed by the magnitude of the accumulated strain.

The cumulative axial strains at the beginning of dilation were plotted against the ratio of mean normal stress and resultant deviatoric stress in Figure 7.7. The ratios were found to lie within a narrow range of 0.41 to 0.71. This plot indicates that the ratio of mean normal stress to resultant deviatoric stress must be higher than 0.41 to occur any failure and below this attenuating creep will occur.

TABLE 7.1

## Physical Properties of Frozen Sand Sample

Sample	Dry Unit Weight (KN/m <sup>3</sup> )	Water Content (%)	Porosity (%)	Water Saturation (%)	Sample Test Temp. (°C)
MST6	16.0	22.8	40.6	87.0	-3
MST7	15.9	22.5	40.9	88.0	-3
MST8	16.0	23.2	40.7	91.0	-3
MST9	16.3	22.2	39.5	91.6	-3

TABLE 7.2

## Details of Stress Application

Test MST6  $\sigma_m=70$  kPa

$\sigma_1$ (kPa)	$\sigma_3$ (kPa)	$S_a$ (kPa)	Duration of Stress Application (Hour)
70	70	0	789
110	50	49.0	22
130	40	73.5	23
150	30	98.0	23
170	20	122.5	24
190	10	147.5	23
210	0	171.5	746

TABLE 7.3

## Details of Stress Application

Test MST7  $\sigma_m=140$  kPa

$\sigma_1$ (kPa)	$\sigma_3$ (kPa)	$S_d$ (kPa)	Duration of Stress Application (Hour)
140	140	0	791
180	120	49.0	22
220	100	98.0	23
260	80	147.0	23
300	60	196.0	24
340	40	245.0	23
380	20	294.0	23
420	0	343.0	719



TABLE 7.4

## Details of Stress Application

Test MST8  $\sigma_m=280$  kPa

$\sigma_1$ (kPa)	$\sigma_3$ (kPa)	$S_d$ (kPa)	Duration of Stress Application (Hour)
280	280	0	431
340	250	73.5	24
400	220	147.0	23
460	190	220.5	23
520	160	294.0	24
580	130	367.4	23
640	100	440.9	23
700	70	514.4	23
760	40	587.9	24
820	10	661.4	23
840	0	685.9	651

TABLE 7.5

## Details of Stress Application

Test MST9  $\sigma_m=420$  kPa

$\sigma_1$ (kPa)	$\sigma_3$ (kPa)	$S_a$ (kPa)	Duration of Stress Application (Hour)
420	420	0	454
500	380	98.0	24
580	340	196.0	23
660	300	294.0	23
740	260	392.0	24
820	220	490.0	23
900	180	588.0	25
980	140	686.9	24
1060	100	783.8	25
1140	60	881.8	23
1220	20	979.8	24
1260	0	1028.8	632

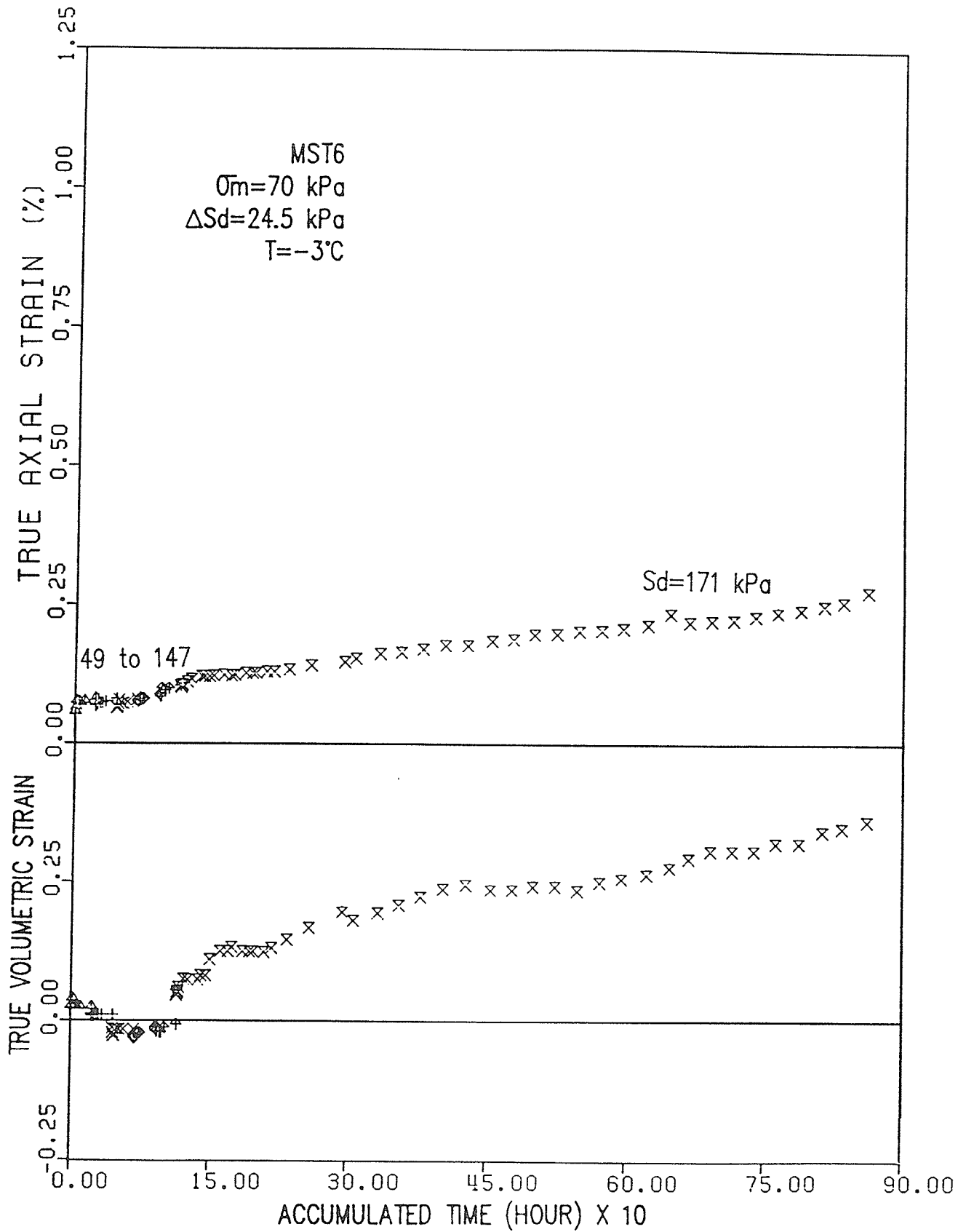


Figure 7.1 True volumetric and true axial strain versus accumulated time (MST6)

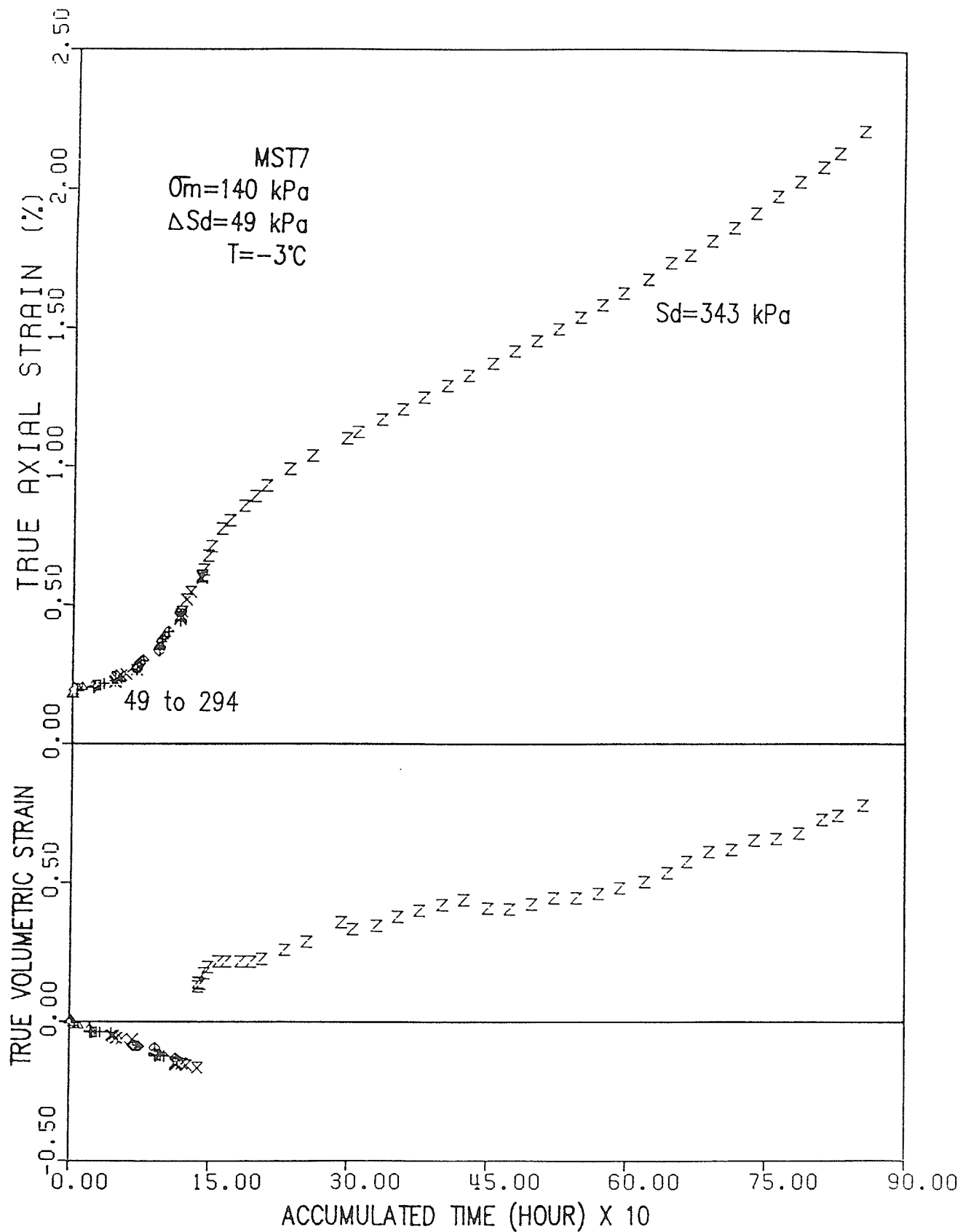


Figure 7.2 True volumetric and true axial strain versus accumulated time (MST7)

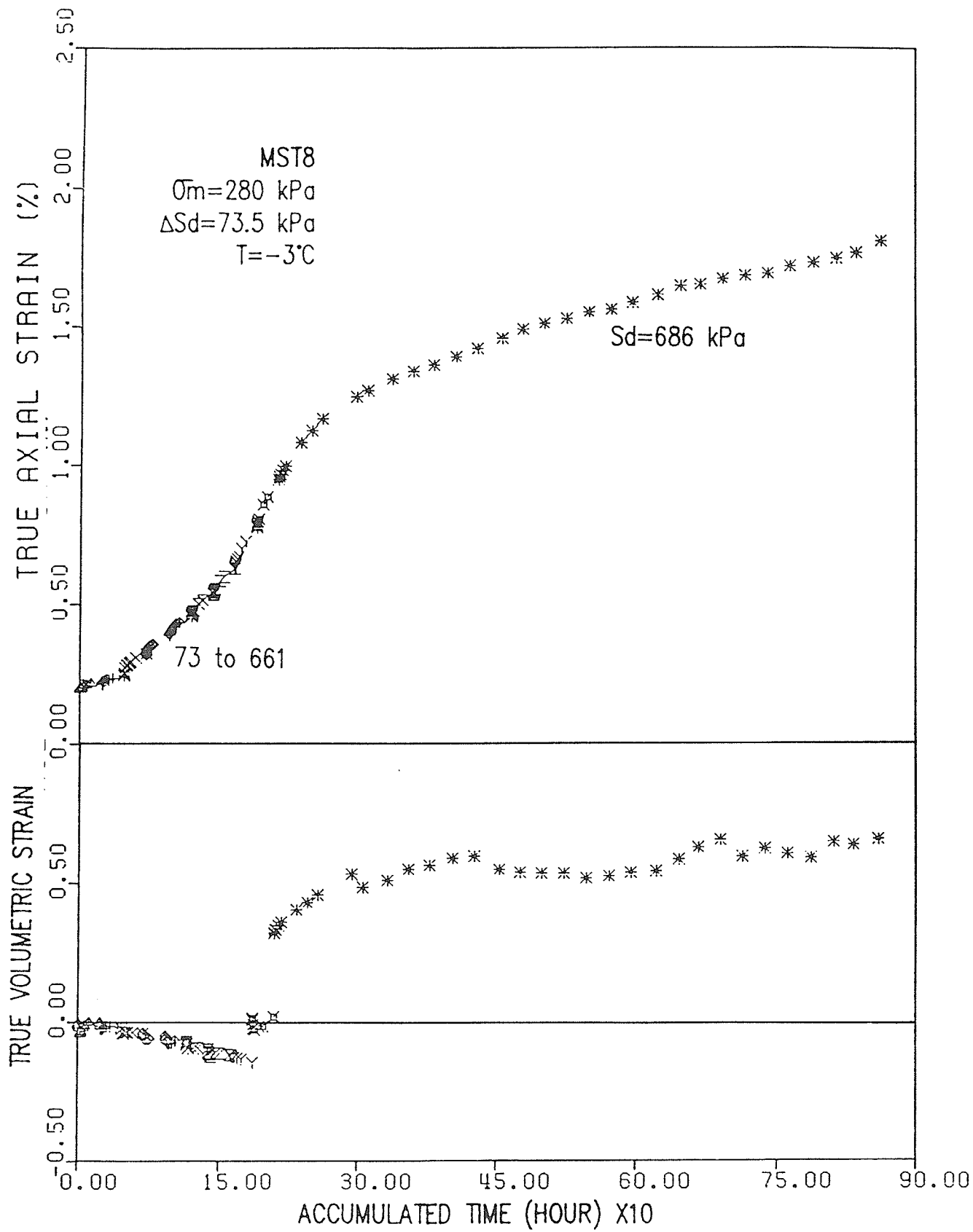


Figure 7.3 True volumetric and true axial strain versus accumulated time (MST8)

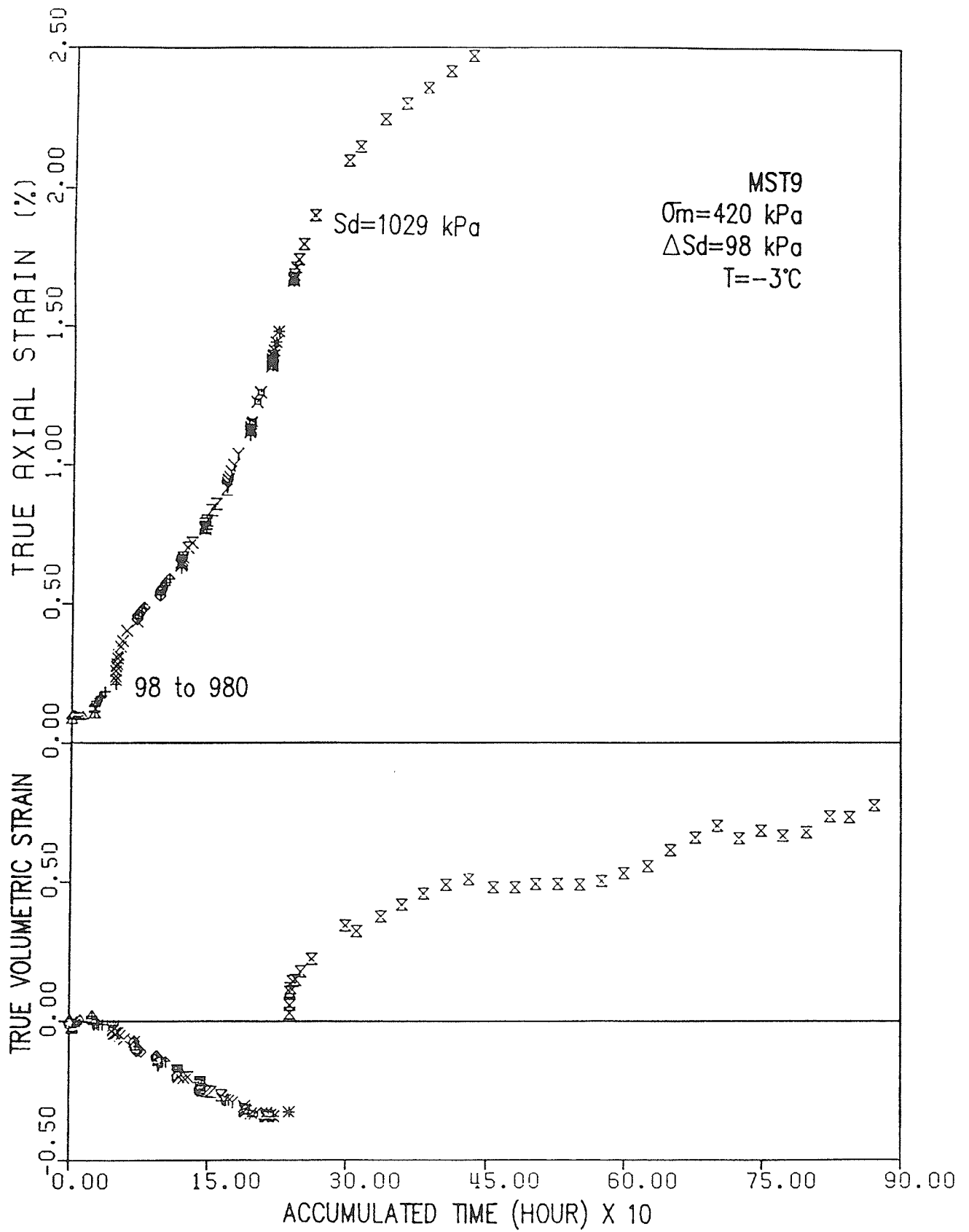


Figure 7.4 True volumetric and true axial strain versus accumulated time (MST9)

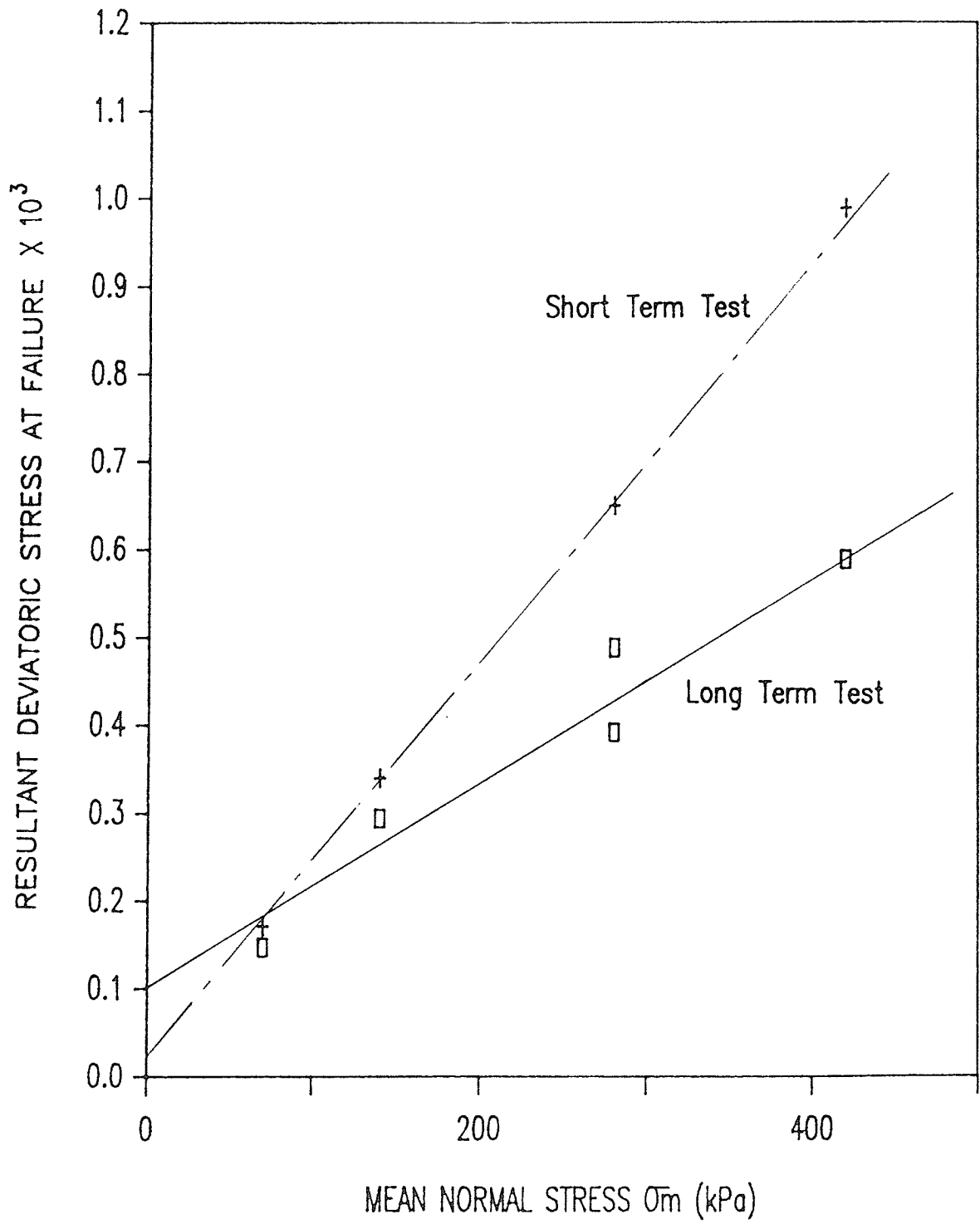


Figure 7.5 Resultant deviatoric stress at failure versus mean normal stress

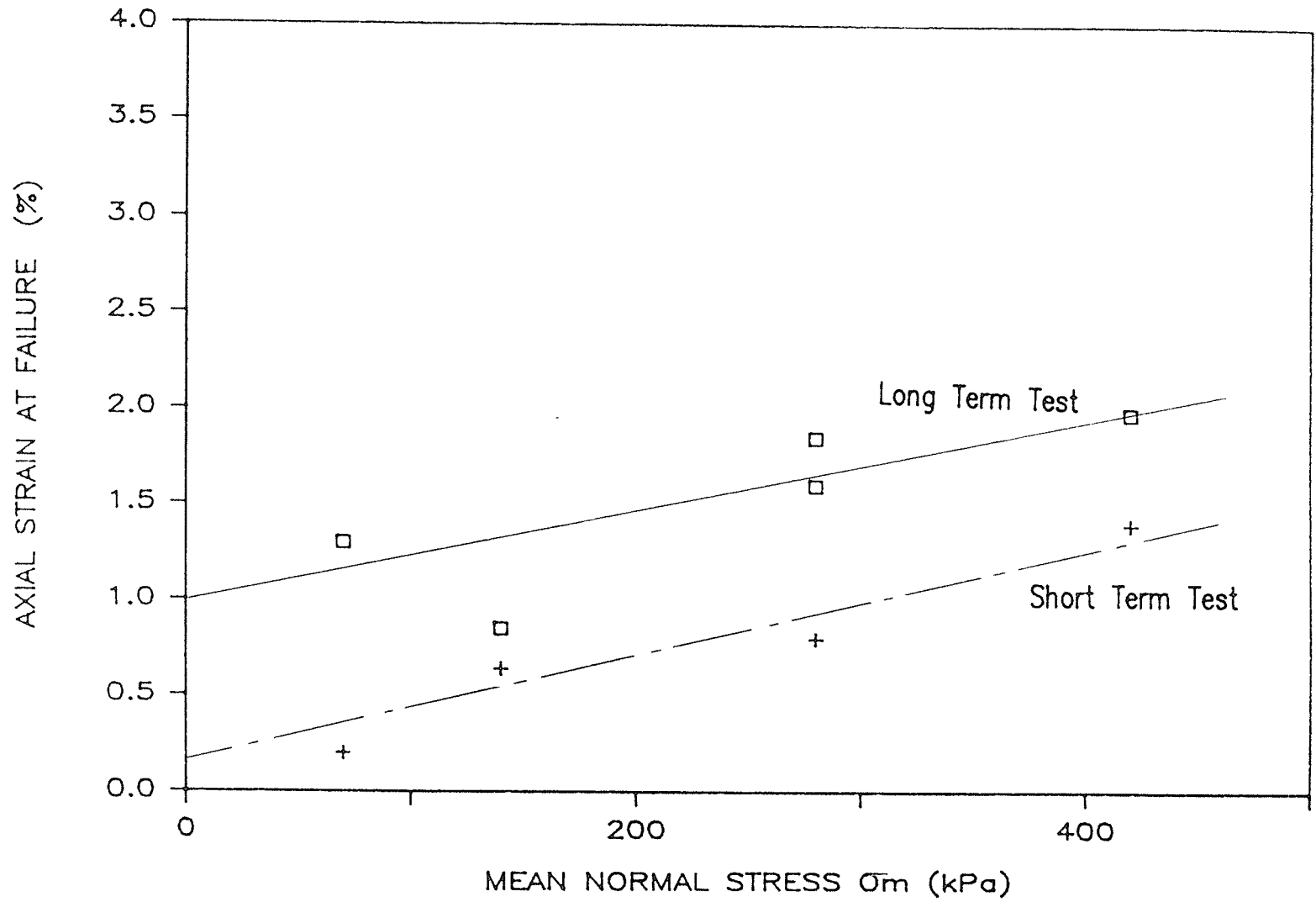


Figure 7.6 Axial strain at failure versus mean normal stress



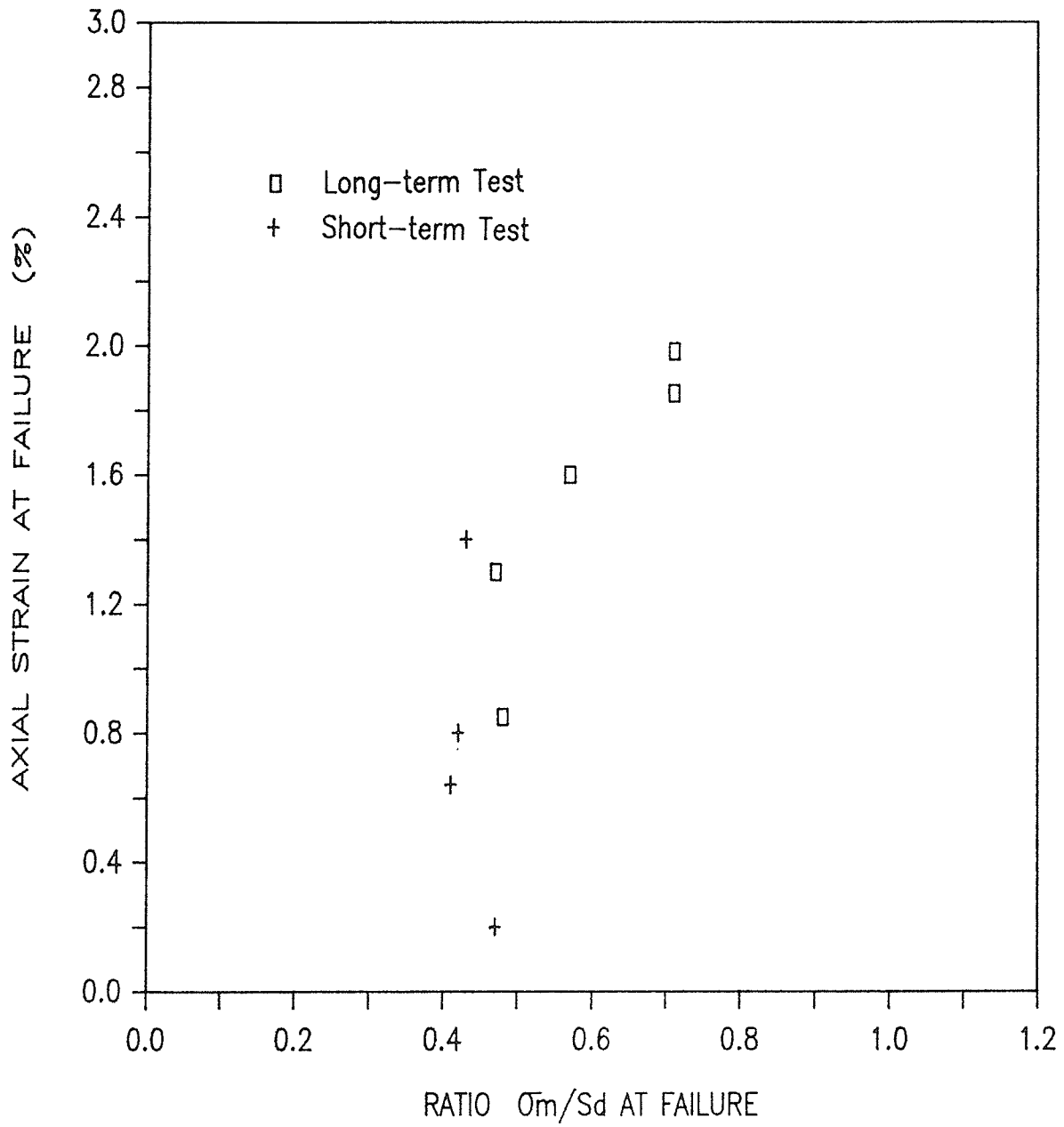


Figure 7.7 Axial strain at failure versus ratio  $\sigma_m/S_d$  at failure

**CHAPTER EIGHT**  
**INTERACTION OF RIGID PARTICLES**  
**AND ICE**

## CHAPTER 8

### INTERACTION OF RIGID PARTICLES AND ICE

#### 8.1 INTRODUCTION

Although the creep behaviour of ice and frozen soil has been studied extensively during the last decade, very little systematic information is available on the interaction of soil particles and their matrix material, namely ice. As described in chapter 2, the frozen soil is a composite mixture of soil particles, ice, unfrozen water and gases. The soil particles have the highest relative stiffness among its constituents. In an ice rich or fully ice saturated soil, the soil particles are surrounded by ice. When stressed, the soil particles, because of their high relative stiffness, penetrate or flow into the ice mass.

An attempt was made to simulate the interaction between soil particles and ice by loading rigid spheres which had been half-embedded into polycrystalline ice and monitoring the movement of the spheres with time.

#### 8.2 TEST PROGRAM

### 8.2.1 Ice Sample Preparation

Samples of polycrystalline ice were prepared in 108 mm diameter by 120 mm long plexiglass molds. The molds were half-filled with tap water and placed in a cold room at  $-3^{\circ}\text{C}$ . When the water was super-cooled to a temperature of 0 to  $-1^{\circ}\text{C}$ , ice chips were added to fill the mold to the top. The molds were then insulated with molded foam insulation leaving the bottom 25 mm and the base uninsulated. The molds were then placed on metal stands in a freezer at  $-20^{\circ}\text{C}$ . The samples were frozen unidirectionally upward. This procedure of unidirectional freezing resulted in upward expansion thus avoiding the build up of a large lateral stresses.

A steel spherical ball was placed at the centre of each sample during the latter stage of freezing when the top 6 mm was still unfrozen. The balls were held in place by a styrofoam cover with a hemispherical hole in its centre.

A schematic of the spherical ball and the ice sample is shown in Figure 8.1 to scale.

### 8.2.2 Loading Procedure

The samples were taken out of the freezer and placed in a cold room for about 24 hours to attain equilibrium at the room temperature

which was  $-30^{\circ}\text{C}$ . A dead weight hanger system was used to apply the load to the steel balls. The whole assembly was placed inside an insulated cabinet to minimize temperature variations during the defrosting cycle of the cold room.

The first test series consisted of loading spheres having a diameter of 11.57 mm to loads of 62.8 N, 85.1 N, 107.4 N and 129.6 N respectively. Dial gauges with an accuracy of 0.01 mm were used to monitor the penetration of the spheres with time. After 1100 hours of load application, the loads were removed, and rebound was allowed to reach equilibrium. The monitoring of the sphere movement was continued during unloading and rebound.

The spheres were then reloaded with higher loads of 151.8 N, 174.1 N, 196.0 N and 218.6 N. The monitoring of the movement of the spheres was continued.

In the second test series, spheres having diameters of 9.5 mm, 15.9 mm, 18.2 mm, and 23.7 mm respectively, were loaded with a constant hemispherical stress of 298.6 kPa. The monitoring of the movement of the spheres was carried out as before.

### 8.3 TEST RESULTS

#### 8.3.1 Constant Sphere Diameter Tests

The results of the tests in which spheres with a constant diameter were subjected to a variety of loads are shown in Figure 8.2. It can be seen that with the exception of the test in which the load was 129.6 N, there was no significant instantaneous penetration of the steel balls into the ice at the start of the load applications. Thus it would appear that the instantaneous penetration under the 129.6 N load was an aberration caused perhaps by imperfect contact between the sphere and the ice. As well there was no measurable rebound upon unloading, indicating that all of the penetration was due to plastic deformation of the ice.

The relationship between penetration and time was essentially linear for the range of load used. The rate of penetration increased with an increase in load. The relationship between the penetration rate and the average hemispherical stress acting on each sphere is shown in Figure 8.3. The rates increased with the applied stress at an increasing rate. This was to be expected, since at a very high stress, the resistance of ice to penetration approaches zero and the rate of penetration approaches infinity.

The plot of penetration rate versus hemispherical stress linearized on log-log plot as shown in Figure 8.4. The relationship may therefore be expressed as :

$$\dot{S} = \dot{S}_0 (\sigma/\sigma_0)^n \quad (8.1)$$

in which  $\dot{S}$  = penetration rate (mm/hour)

$\sigma$  = hemispherical stress (kPa)

$n$  = slope of the straight line defined as material parameter  
=2.4

$\dot{S}_o$  and  $\sigma_o$  = coordinates of any point on the straight line

For frozen sand under a deep circular load, Ladanyi and Paquin (1984) stated that a steady state penetration rate can be attained after a limited period of time varying from a minimum of about 1 day upto 5 days. They also stated that the penetration rate became essentially a function of applied stress. For the ice under investigation, steady rates were achieved after about 1 day in all load cases and the penetration rates increased exponentially with applied stress.

### 8.3.2 Constant Hemispherical Stress Tests

The results of the four tests in which sphere diameters of 9.5 mm, 15.9 mm, 18.2 mm and 23.7 mm were subjected to a constant hemispherical stress of 298.6 kPa are shown in Figure 8.5. It can be seen that there was very little instantaneous penetration of the steel balls into the ice at the start of the load applications. As well there was no measurable rebound upon unloading indicating that essentially all the penetration was due to plastic deformation of the ice.

The relationship between penetration and time was essentially

linear for the stress and the spheres used and therefore the rate of penetration was approximately constant for the applied hemispherical stress. This penetration rate is included in Figure 8.6 along with the results of the first test series. The rates fits in well with the results the from first test series.

### 8.3.3 Viscosity

From the tests results as presented in Figure 8.2 it was revealed that the deformation, under sustained loading, in the polycrystalline ice was almost entirely plastic, as no noticeable recovery was observed after removal of the load at the end of the tests. The polycrystalline ice may be considered to have behaved as a non-Newtonian fluid in the range of the stresses and the temperature used in the tests. The rate of penetration in a non-Newtonian fluid can be represented by :

$$\frac{du}{dt} = \frac{\sigma}{\eta} \quad (8.2)$$

in which  $du/dt$  = penetration rate

$\sigma$  = applied stress

$\eta$  = viscosity

For non-Newtonian fluid, the viscosity coefficient as defined in equation 8.2 is not a constant but varies with the applied stress. The viscosity coefficient computed for all the tests is shown plotted



against the applied stress in Figure 8.7. The viscosity coefficient varied nonlinearly with the applied stress and the relationship linearized on a semi-logarithmic plot with viscosity on the log scale as shown in Figure 8.8. Accordingly, the viscosity of the polycrystalline ice can be represented by the following equation :

$$\eta = ce^{-m\sigma} \quad (8.3)$$

in which  $\eta$  = viscosity (Pa Sec/m)

$c$  = constant dependent on temperature and ice type

=  $1.3 \cdot 10^{13}$  Pa sec/m at  $\sigma=0$

$m$  = slope of the straight dependent on temperature and ice type

$\eta = 1.0258 \cdot 10^{-3}$  for  $T=-3^{\circ}\text{C}$ .

$\sigma$  = applied hemispherical stress

The equation indicates that the viscosity coefficient of polycrystalline ice decreases exponentially with the applied hemispherical stress. Jellinek et al (1956) also observed that for polycrystalline ice, the viscosity coefficient decreased with applied stress.

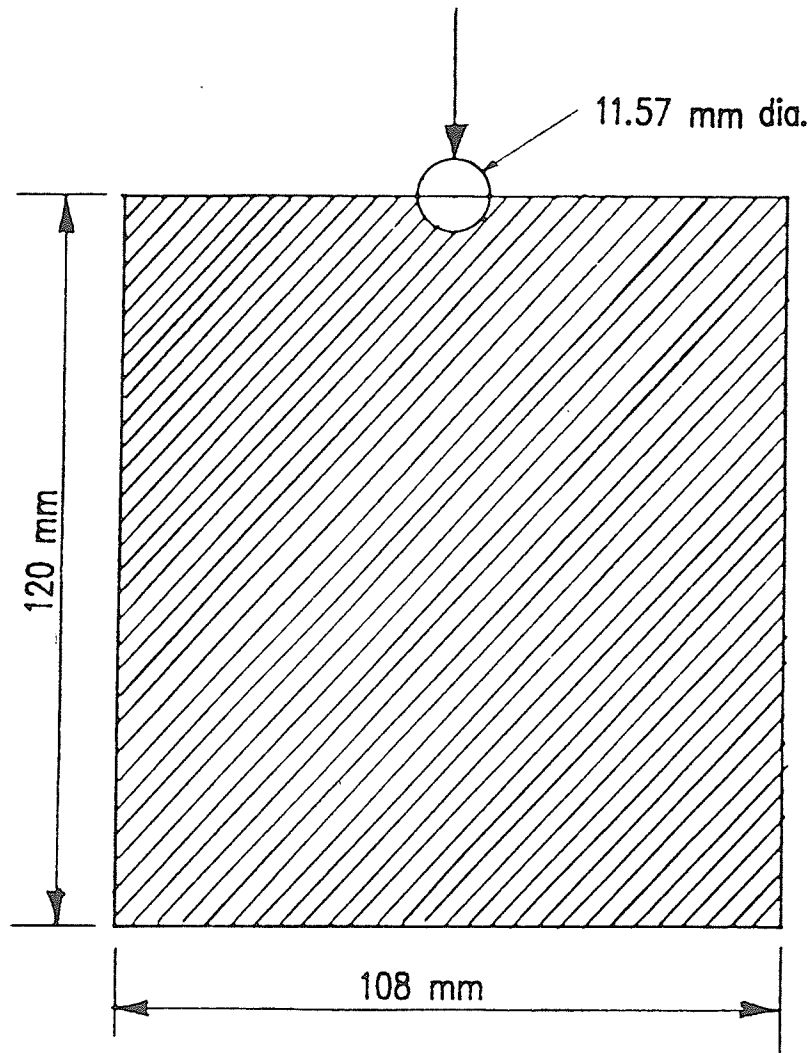


Figure 8.1 Ice sample with steel sphere at the centre

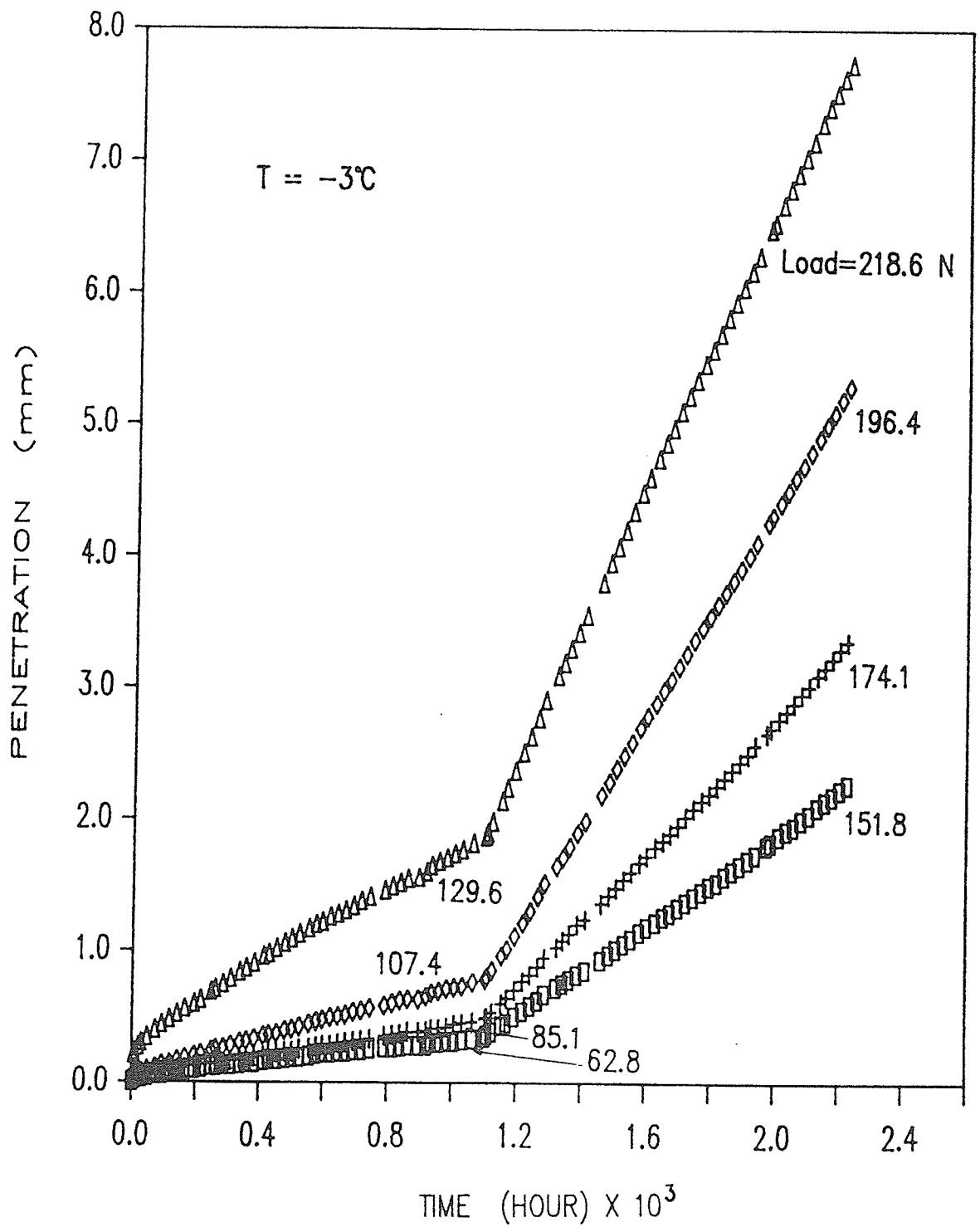


Figure 8.2 Penetration of steel spheres versus accumulated time  
(Tests—Phase 1 and Phase 2)

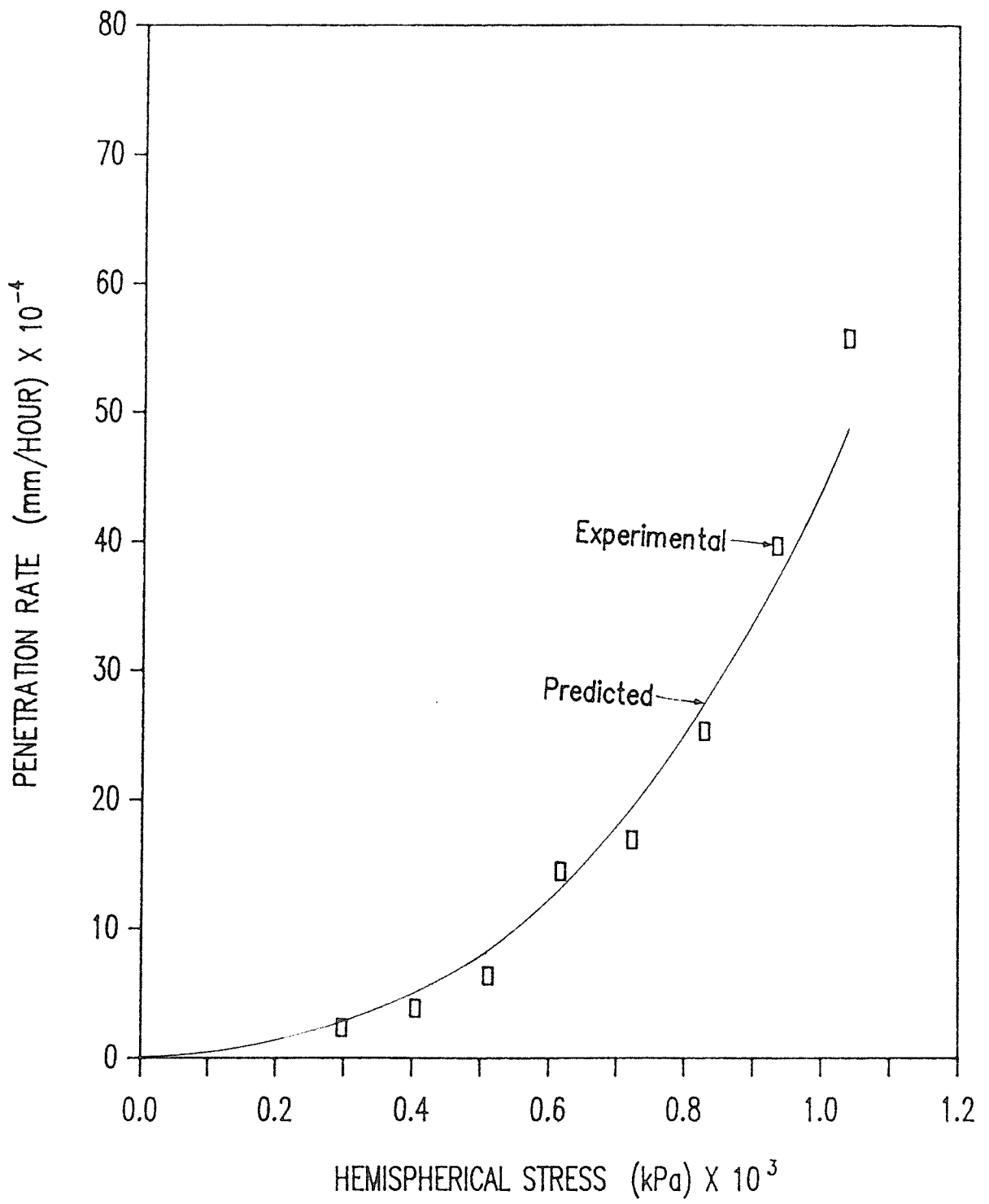


Figure 8.3 Penetration rate versus hemispherical stress

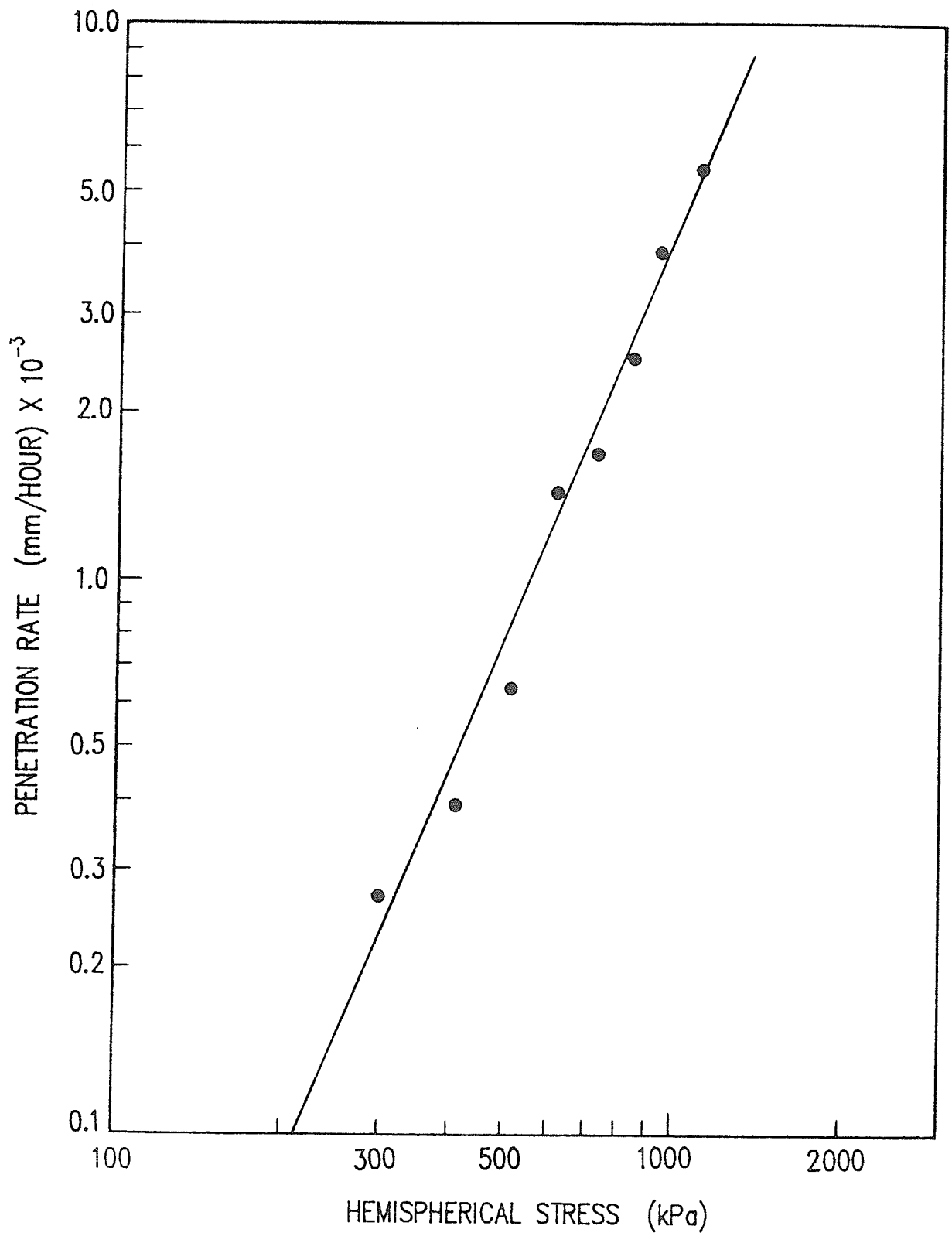


Figure 8.4 Penetration rate versus hemispherical stress

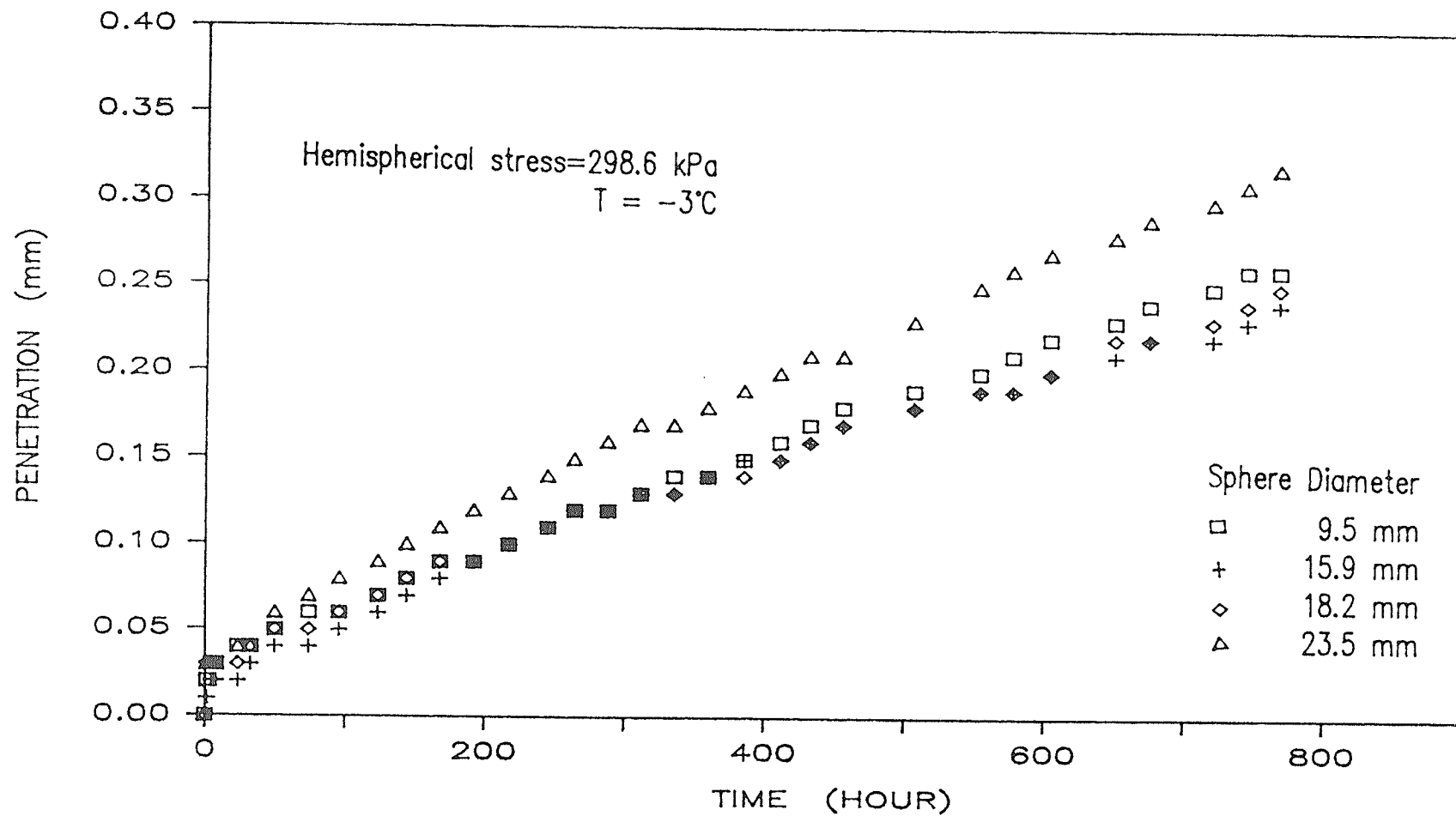


Figure 8.5 Penetration of steel spheres versus time (Tests - Series 2)

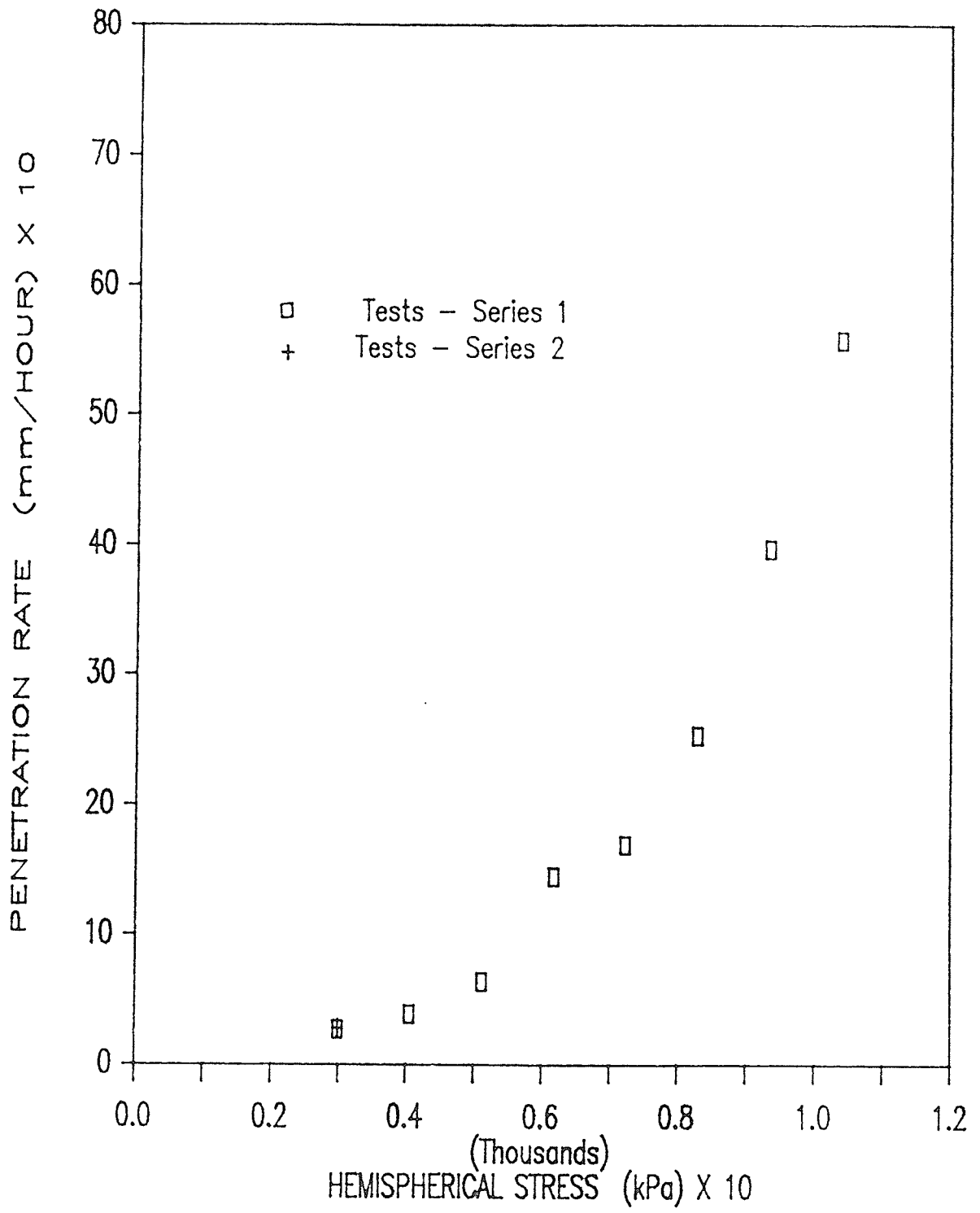


Figure 8.6 Penetration rate versus hemispherical stress (Tests - Series 1 and Series 2)

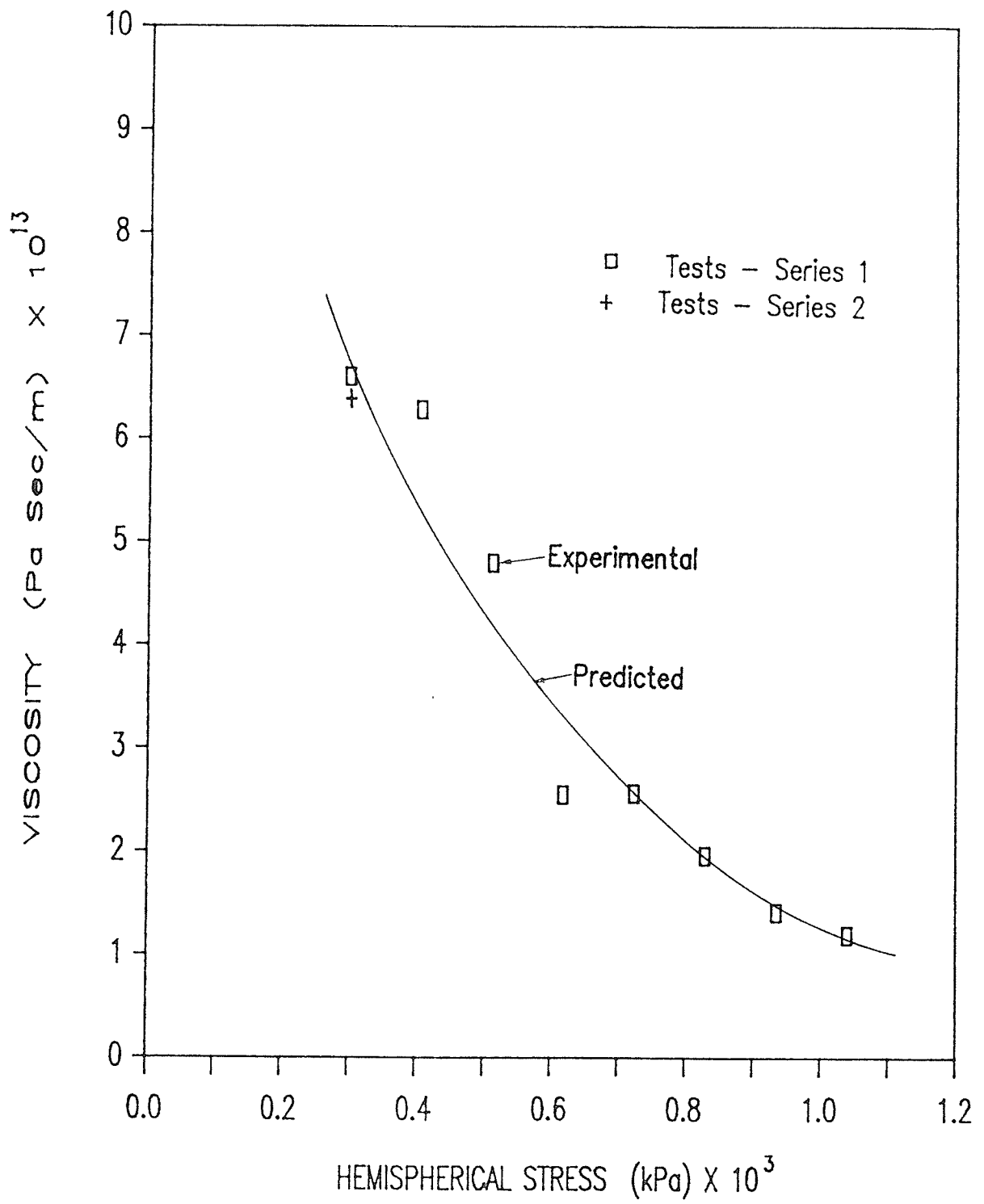


Figure 8.7 Viscosity of polycrystalline ice versus hemispherical stress



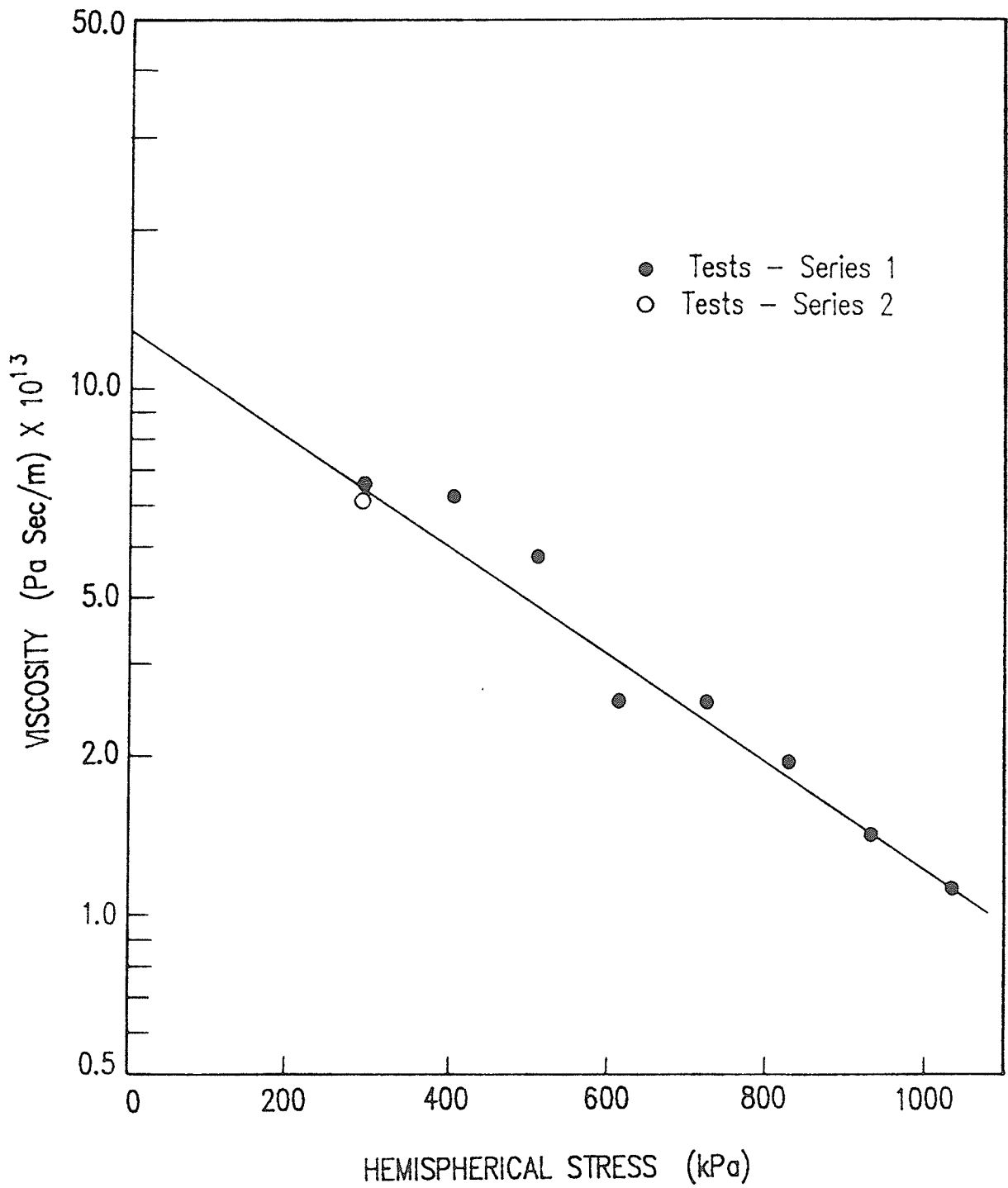


Figure 8.8 Viscosity of polycrystalline ice versus hemispherical stress (semi-log scale)

**CHAPTER NINE**  
**CONCLUSIONS AND**  
**RECOMMENDATIONS**

## CHAPTER 9

### CONCLUSIONS AND RECOMMENDATIONS

#### 9.1 CONCLUSIONS

The investigation was undertaken to study the creep behaviour of frozen sand subjected to a general state of stress. The study was divided into the following phases and the observations and conclusions are listed for each phase.

1. Creep behaviour under isotropic stress
2. Creep behaviour under deviatoric stress
3. Verification of proposed creep model
4. Comparison of long and short-term triaxial compression tests
5. Interaction of ice and rigid particles

##### 9.1.1 Creep Behaviour under Isotropic Stress

Multi-stage isotropic creep tests were undertaken to study the relationship between the volumetric stress, volumetric strain and time with the temperature kept constant. From the results of the investigation the following observations were drawn:

1. At each stress level there was an instantaneous volumetric

strain followed by time dependent volumetric strain, the rate of which decreased with time to a zero creep rate. Most of the instantaneous strain occurred during the first increment.

2. The time for complete attenuation increased exponentially with an increase in isotropic stress.
3. When the sample was unloaded at the end of isotropic compression, the recovery was immeasurable, indicating that all the strains were inelastic compression.
4. The relationship between the attenuated volumetric strain and the mean normal stress was approximately linear for the stress range investigated. The slope provided an ultimate bulk modulus which was 10,250 kPa for the frozen sand tested at a temperature of -30°C.
5. A model for bulk creep function was developed and expressed as a function of time and mean normal stress as follows:

$$K_e = K_o [1 + (1/K_o) e^{-mt} \sigma_m]^2$$

6. The bulk creep function,  $K_e$ , increased exponentially with an increase in mean normal stress and decreased hyperbolically with time.

### 9.1.2 Creep Behaviour under Deviatoric Stress

Constant mean normal stress multi-stage triaxial creep tests were performed to study the creep behaviour under changes in deviatoric stress. From the results of tests the following observations were drawn:

1. The samples underwent volume change during shear deformation, contrary to the belief that the creep deformation of frozen soil occurs at constant volume.
2. Up to a certain stress level the samples underwent attenuating creep and at higher stress levels the samples underwent accelerating creep.
3. The time for complete attenuation increased with an increase in mean normal stress.
4. For a given magnitude of deviatoric stress the volumetric strain decreased with an increase in mean normal stress.
5. The deviatoric stress at which samples began to dilate coincided with the stress at which accelerating creep first occurred. This stress was taken to be the failure stress.
6. The relationship between the deviatoric stress at failure and the mean normal stress was approximately linear and was expressed as follows:

$$S_{df} = S_o + m\sigma_m$$

7. The axial strain at which the failure occurred increased with an increase in mean normal stress.
8. A model for shear creep function expressed as a function of time, mean normal stress and deviatoric stress had the following form:

$$G_e = [m_1\sigma_m^{\beta} t^{\alpha} + ct^{\alpha} (S_d/\sigma_m)]^{-1}$$

9. The shear creep function,  $G_e$ , increased hyperbolically with an increase in mean normal stress, decreased exponentially with an increase in deviatoric stress, and decreased exponentially with time.

### 9.1.3 Verification of the Creep Models

Creep models were developed separately for hydrostatic and deviatoric stress changes. The validity of the models was examined by performing multi-stage constant cell pressure triaxial compression tests which involved concurrent changes in the hydrostatic and deviatoric components of stress. The assesment of the models was made by calculating the axial deformation based on the creep models and comparing the calculated values with the measured values. This was

done for time dependent strains and attenuated strains independently. The agreement between the predicted and experimental time dependent strains was quite good considering the scatter that was inherent in all test data. The theoretical attenuated axial deformations agreed well with the observed values. The correlation coefficient was found to be 0.85.

#### 9.1.4 Comparison of Long and Short-term Tests

A series of short-term (loading duration 24 hours or less) constant mean normal stress triaxial compression tests were performed to determine whether the onset of dilation was a stress or strain dependent phenomenon. The stresses were identical to those used in the long-term tests. The following observations were made:

1. The deviatoric stresses corresponding to the onset of dilation were higher in the short term tests than those in the long-term tests.
2. The axial strains at the onset of dilation were lower in the short-term tests than those in the long-term tests.
3. The results suggested that the onset of dilation was neither singly a strain nor a stress phenomena but was influenced by both.

### 9.1.5 Interaction of Ice and Rigid Particles

The interaction of ice and rigid particles was studied by observing the penetration of rigid steel spheres into ice. For a variety of loads the following observations were made:

1. The relationship between penetration and time was essentially linear for each hemispherical stress which was calculated on the basis of the hemispherical area and the applied load. The hemispherical stress ranged from 300 to 1000 kpa.

2. A relationship between the penetration rate and the hemispherical stress was represented by the following power law:

$$\dot{S} = \dot{S}_0 (\sigma/\sigma_0)^n$$

3. The penetration rate increased exponentially with an increase in hemispherical stress.

4. A relationship between the viscosity of the polycrystalline ice and the hemispherical stress was represented by the following exponential function.

$$\eta = me^{-n\sigma}$$



5. The viscosity of the polycrystalline ice decreased exponentially with an increase in hemispherical stress.
6. The penetration rate depended on the hemispherical stress and was independent of the size of the spheres.

## 9.2 RECOMMENDATIONS

The study was limited to quartz carbonate sand and a temperature of  $-30^{\circ}\text{C}$ . Thus the models developed for the bulk and shear creep functions did not include parameters representing material type and temperature. The following suggestions are made with regard to an extension of the work undertaken.

1. The study should include different material types and temperature variations to obtain a more general model.
2. Higher stresses should be used to obtain complete stress-strain curves for lower elapsed times.
3. The effect of single-step and multi-step loading on the creep behaviour should be investigated.
4. The interaction of soil particles and ice should be studied with rigid particles having shapes other than spheres to study the effects of particle shape.

## **REFERENCES**

## REFERENCES

- Alkire, B. D., and Andersland, O. B., 1973, "The Effect of Confining Pressure on the Mechanical Properties of Sand-Ice Material," *Journal of Glaciology*, Vol. 66, NO. 12, pp. 469-481.
- Andersland, O. B., and Akili, W., 1967, "Stress Effects on Creep Rates of a Frozen Clay Soil," *Geotechnique*, Vol. 17, No. 1, pp. 27-39.
- Andersland, O. B., and AlNouri, I., 1970, "Time Dependent Strength Behavior of Frozen Soils," *ASCE, Journal of Soil Mechanics and Foundation Division*, Vol. 96, No. 4, pp. 1249-1265.
- Andersland, O. B., and Anderson, D. M., 1978, "Geotechnical Engineering for Cold Region," McGraw-Hill, New York.
- Andersland, O. B., and Douglas, A. G., 1970, "Soil Deformation Rate and Activation Energies," *Geotechnique*, Vol. 20, No. 1, pp. 1-16.
- Anderson, D. M., and Morgenstern, N. R., 1973, "Physics, Chemistry and Mechanics of Frozen Ground: a Review," *Proceedings of Second International Conference on Permafrost, North American Contribution*, pp. 257-288.
- Anderson, D. M., and Tice, A. R., 1977, "Predicting Unfrozen Water Contents in Frozen Soils from Surface Area Measurements," *Highway Research Record*, No. 393, pp. 12-18.
- Andrade, E. N. da C., 1910, "The Viscous Flow in Metals and Allied Phenomena," *Proceedings Royal Society of London*, Vol. A84, pp. 1-12.
- Assur, A., 1979, "Some Promising Trends in Ice Mechanics," *Proceedings of International Union of Theoretical and Applied Mechanics, Physics and Mechanics of Ice, Copenhagen*, pp. 1-15.
- Baker, T. H. W., Jones, S. J., and Parameswaran, V. R., 1982, "Confined and Unconfined Compression Tests on Frozen Sands," *Proceedings Fourth Canadian Permafrost Conference, National Research Council of Canada, Ottawa*, pp. 387-393.
- Bailey, R. W., 1929, "Trans. World Power Conference, Tokyo", Vol. 13, pp. 1089
- Baker, T. H. W., 1979, "Strain Rate Effect on the Compressive Strength of Frozen Sand," *Proceedings First International Symposium on Ground Freezing, Bochum, Elsevier Sci. Pub. Co.*, pp. 223-231.
- Baker, T. H. W., 1978, "Effect of End Conditions on the Uniaxial Compressive Strength of Frozen Sand," *Proceedings of Third International Conference on Permafrost, Edmonton*, pp. 609-614.

- Barnes, P., Tabor, D., and Walker, J., 1971, "The Friction and Creep of Polycrystalline Ice," Proceedings Royal Society of London, Vol. A324, pp. 127-155.
- Brag, R. A., and Andersland, O. B., 1980, "Strain Rate, Temperature and Sample Size Effects on Compression and Tensile Properties of Frozen Sand," Second International Symposium on Ground Freezing, Trondheim, pp. 34-47.
- Chamberlain, E., 1973, "Mechanical Properties of Frozen Ground Under High Pressure," Proceedings Second International Conference on Permafrost, North American Contribution, pp. 295-305.
- Chamberlain, E., Groves, C., and Pertham, R., 1972, "The Mechanical Behaviour of Frozen Earth Materials Under High Pressure Triaxial Conditions," Geotechnique, Vol. 22, No. 3 pp. 469-483.
- Clough, G. W., and Duncan, J. M., 1971, "Finite Element Analysis of Retaining Wall Behaviour," Proceedings ASCE, Soil Mechanics and Foundation Division, Vol. 97, No. SM12, pp. 1657-1673.
- Clough, R. W., and Woodward, R. J., 1967, "Analysis of Embankment Stresses and Deformations," Proceedings ASCE, Soil Mechanics and Foundation Division, Vol. 93, No. SM4, pp. 529-549.
- Cole, D. M., 1983, "The Relationship Between Creep and Strength Behaviour of Ice at Failure," Cold Regions Science and Technology, Vol. 8, pp. 189-197.
- Cole, D. M., 1979, "Preparation of Polycrystalline Ice Specimens for Laboratory Experiments," Cold Regions Science and Technology, Vol.1, No. 1 pp. 153-159.
- Corte, J. B., 1962, "Vertical Migration of Particles in Front of Moving Freezing Plane," Journal of Geophysical Research, Vol. 67, No. 3, pp. 1085-1090.
- Domaschuk, L., Knutsson, S., Shields, D. H., and Rahman, M. G., 1984, "Creep of Frozen Sand Under Isotropic and Deviatoric Components of Stress," Proceedings ASME, Journal of Energy Resources Technology, Vol. 107, pp. 199-203.
- Domaschuk, L., Shields, D. H., Man, C-S., and Yong, E., 1983, "Creep Behaviour of Frozen Saline Silt Under Isotropic Compression", Proceedings Fourth International on Permafrost, National Academy Press, Washington D.C., pp. 238-343
- Domaschuk, L., and Valliappan, P., 1975, "Nonlinear Settlement Analysis by Finite Element," Proceedings ASCE, Journal of Geotechnical Engineering, Vol. 101., No. GT7, pp. 601-614.
- Domaschuk, L., and Wade, N. H., 1969, "A study of Bulk and Shear Moduli of Sand," Proceedings ASCE, Soil Mechanics and Foundation Division, Vol. 95, No. SM2, pp. 561-582.

- Duncan, J. M., and Chang, C-Y., 1970, "Nonlinear Analysis of Stress and Strain in Soils," Proceedings ASCE, Soil Mechanics and Foundation Division, Vol. 96, No. SM5, pp. 1629-1653.
- Eckardt, H., 1982, "Creep Tests With Frozen Soils Under Uniaxial Tension and Uniaxial Compression," Proceedings Fourth Canadian Permafrost Conference, National Research Council of Canada, Ottawa, pp. 394-405.
- Eyring, H., 1936, "Viscosity, Plasticity and Diffusion as Examples of Absolute Reaction Rates, Journal of Chemical Physics, Vol. 4, No. 4, pp. 283-291.
- Finnie, I., and Heller, W. R., 1959, "Creep of Engineering Materials," McGraw-Hill Book Company, Inc.
- Fish, A. M., and Assur, A., 1984, "Tertiary Creep Model for Frozen Sands," Discussion, Proceeding ASCE, Journal of Geotechnical Engineering, Vol. 110, No. GT9, pp. 1373-1376.
- Gardner, A. R., Jones, R. H., and Harris, J. S., 1984, "A New Creep Equation for Frozen Soils and Ice," Cold Regions Science and Technology, Vol. 9, pp. 271-275.
- Gilbert, P. A., Chamberlain, E. J. and Sayles, F. H., 1982, "Freezing of Triaxial Test Specimens of Cohesionless Soil to Determine Internal Density Variation," Proceedings Third International Symposium on Ground Freezing, pp. 113.
- Gill, J., 1969, "A Preliminary Investigation of the Bulk and Shear Moduli of Lake Agassiz Clay," M.Sc. Thesis, University of Manitoba, Winnipeg, Manitoba.
- Glen, J. W., 1955, "The Creep of Polycrystalline Ice," Proceedings Royal Society of London, Vol. A228, pp. 519-539.
- Gold, L. W., 1977, "Engineering Properties of Fresh Water Ice," Journal of Glaciology, Vol. 19, No. 8, pp. 197-211.
- Gold, L. W., 1973, "Activation Energy for Creep of Columnar Grained Ice," Physics and Chemistry of Ice, , pp. 362-364.
- Gold, L. W., 1970, "Process of Failure in Ice," Canadian Geotechnical Journal, Vol. 7, No. 4, pp.405-413.
- Gold, L. W., 1966(a), "Time to Formation of First Crack in Ice," Physics of Snow and Ice, pp. 359-370.
- Gold, L. W., 1966(b), "Dependence of Crack Formation on Crystallographic Orientation of Ice," Canadian Journal of Physics, Vol. 44, pp. 2757-2764.
- Gold, L. W., and Krausz, A. S., 1971, "Investigation of the Mechanical

- Properties of St. Lawrence River Ice," Canadian Geotechnical Journal, Vol. 23, NO. 8, pp. 163-169.
- Goughnour, R. R., and Andersland, O. B., 1968, "Mechanical Properties of a Sand-Ice System," ASCE, Journal of Soil Mechanics and Foundation Division, Vol. 94, No. 4, pp. 923-950.
- Hanrahan, E. T., 1985, "The Geotechnics of Real Materials : The  $\epsilon_v$ ,  $\epsilon_k$  Method," Elsevier Science Publishers.
- Hawkes, I., and Mellor, M., 1972, "Deformation and Fracture of Ice under Uniaxial Stress," Journal of Glaciology, Vol. 64, No. 11, pp. 103-131.
- Haynes, F. D., 1978, "Strength and Deformation of Frozen Silt," Proceedings Third International Conference on Permafrost, Edmonton, pp. 656-661.
- Haynes, F. D., and Mellor, M., "Measuring the Uniaxial Compressive Strength of Ice," Journal of Glaciology, Vol. 81, No. 19, pp. 213-222.
- Hooke, R. Leb., Dahlin, B. B., and Kauper, M. T., "Creep of Ice Containing Dispersed Fine Sand," Journal of Glaciology, Vol. 63, No. 11, pp. 327-336.
- Hult, J. A. H., 1966, "Creep in Engineering Structures," Blaisdell Publishing Company.
- Jacka, T. H., 1984a, "Laboratory Studies on Relationship Between Ice Crystal Size and Flow Rate," Cold Regions Science and Technology, Vol. 10, pp. 31-42.
- Jacka, T. H., 1984b, "Time and Strain Required for Development of Minimum Strain Rates in Ice," Cold Regions Science and Technology, Vol. 8, No. 3, pp. 261-268.
- Jellinek, . H. H. G., 1967, "Liquid-Like (Transition) Layer on Ice," Journal of Colloidal and Interface Science, Vol. 25, pp. 195-205.
- Jellinek, H. H. G., 1962, "Ice Adhesion," Canadian Journal of Physics, Vol. 40, No. 10, pp. 1294-1309.
- Jones, S. J., and Parameswaran, V. R., 1983, "Deformation Behaviour of Frozen Sand-Ice Materials Under Triaxial Compression," Proceedings Fourth International Conference on Permafrost, Fairbanks, Vol. 4, pp. 560-565.
- Jones, S. J., and Chew, H. A. M., 1981, "On the Grain-Size Dependence of Secondary Creep," Journal of Glaciology, Vol. 27, No. 97, pp. 517-518.
- Jones, S. J., 1978, "Triaxial Testing of Polycrystalline Ice," Proceedings Third International Conference on Permafrost,

- Edmonton, pp. 671-674.
- Kaplar, C. W., 1971, "Some Strength Properties of Frozen Soil and Effect of Loading Rate," USA CRREL, Spec. Rep. 159.
- Konder, R. L., and Zelasko, J. S., 1963, "A Hyperbolic Stress Strain Formulation for Sands," Proceedings Second Pan American Conference on Soil Mechanics and Foundation Engineering, Vol. 1, pp. 289-334.
- Ladanyi, B., 1985, "Stress Transfer Mechanism in Frozen Soils," Proceedings Tenth Canadian Congress of Applied Mechanics, The University of Western Ontario, London, pp. 11-23.
- Ladanyi, B., 1982, "Borehole Creep and Relaxation Tests in Ice-Rich Permafrost," Proceedings Fourth Canadian Permafrost Conference, Calgary, pp. 406-415.
- Ladanyi, B., 1981, "Mechanics of Structured Media," Proceedings of the International Symposium on the Mechanical Behaviour of Structured Media, Ottawa, pp. 205-245.
- Ladanyi, B., and Arteau, J., 1979, "Effect of Specimen Shape on Creep Responce of a Frozen Sand," Proceedings First International Symposium on Ground Freezing Bochum, pp. 207-222.
- Ladanyi, B., and Paquin, J., 1978, "Creep Behaviour of Frozen Sand under a Deep Circular Load," Proceedings Third International Conference on Permafrost, Edmonton, pp. 679-686.
- Ladanyi, B., 1972, "An Engineering Theory of Creep of Frozen Soils," Canadian Geotechnical Journal, Vol. 9, No. , pp. 63-80.
- Langdon, T. G., 1973, "Creep Mechanisms in Ice," Physics and Chemistry of Ice, pp. 356-361.
- Le Gac, H., and Duval, P., 1980, "Does the Permanent Creep Rate of Polycrystalline Ice Increase with Crystal Size ?," Journal of laciology, Vol. , pp. 153-158.
- Liu, V., 1970, "A Study of the Shear Modulus of a Lake Agassiz Clay," M.Sc. Thesis, University of Manitoba, Winnipeg, Manitoba.
- Man, C-S., 1984, "Ultimate Long Term Strength of Frozen Soil as the Phase Boundary of a Viscoelastic Solid-Fluid Transition," Proceedings Fourth International Conference on Permafrost, Fairbanks, pp. 798-803.
- Martin, R. T., Ting, J. M., and Ladd, C. C., 1979, "Creep Behaviour of Frozen Sand," Massachusetts Institute of Technology, Department of Civil Engineeinng, Research Report R81-19.
- Mellor, M., and Cole, D. M., 1983, "Stress/strain/Time Relations For Ice Under Uniaxial Compression," Cold Regions Science and Technology, Vol. 6, pp. 207-230.

- Mellor, M., and Cole, D. M., 1982, "Deformation and Failure of Ice Under Constant Stress or Constant Strain-Rate," Cold Regions Science and Technology, Vol. 5, pp. 201-219.
- Mellor, M., 1979, "Mechanical Properties of Polycrystalline Ice," Proceedings of International Union of Theoretical and Applied Mechanics, Physics and Mechanics of Ice, Copenhagen, pp. 217-245.
- Mellor, M., and Testa, R., 1969, "Effect of Temperature on the Creep of Ice," Journal of Glaciology, Vol. 8, pp. 131-145.
- Michel, B., 1978, "Ice Mechanics," Les Presses De L'Universite Laval, Quebec.
- Michel, B., 1978, "A Mechanical Model of Creep of Polycrystalline Ice," Canadian Geotechnical Journal, Vol. 15, pp. 155-170.
- Mugurama, J., 1969, "Effects of Surface Conditions on the Mechanical Properties of Ice Crystals," British Journal of Applied Physics, Series 2, Vol. 2, No. 11, pp. 1517-1525.
- Newmark, N. M., 1960, "Failure Hypothesis for Soils," Proceedings ASCE, Conference on Shear Strength of Cohesive Soils, University of Colorado, Boulder.
- Norton, F. H., 1929, "Creep of Steel at High Temperature," McGraw-Hill, New York.
- O'Connor, M. J. and Mitchel, R. J., 1978, "Measuring Total Volumetric Strain During Triaxial Tests on Frozen Soils," Canadian Geotechnical Journal, Vol. 15, No. 1, pp. 47-54.
- Odqvist, F. K. G., 1966, "Mathematical Theory of Creep and Creep Rupture," Oxford University Press.
- Parameswaran, V. R., and Jones, S. J., 1981, "Triaxial Testing of Frozen Sand," Journal of Glaciology, Vol. 27, No. 95, pp. 147-155.
- Parameswaran, V. R., 1980, "Deformation Behaviour and Strength of Frozen Sand," Canadian Geotechnical Journal, Vol. 17, No. , pp. 78-88.
- Phukan, A., 1983, "Long-Term Creep Deformation of Roadway Embankment of Ice-Rich Permafrost," Proceedings Fourth International Conference on Permafrost, Fairbanks, pp.994-999.
- Rein, R. G., Hathi, V. V., and Slipevich, C. M., 1975, "Creep of Sand-Ice System, ASCE, Journal of Geotechnical Engineering Division, Vol. 101, GT2, pp. 115-128.
- Roggensack, W. D., and Morgenstern, N. R., 1978, "Direct Shear Tests on Natural Fine Grained Permafrost Soils," Proceedings Third International Conference on Permafrost, Edmonton, pp. 729-735.



- Sayles, F. H., 1973, "Triaxial and Creep Tests on Frozen Ottawa Sand," Proceedings Second International Conference on Permafrost, North American Contribution, Yakutsk, pp. 384-391.
- Sayles, F. H., and Carbee, D. L., 1980, "Strength of Frozen Silt as a Function of Ice Content and Dry Unit Weight, Proceeding Second International Symposium on Ground Freezing, Trondheim, pp. 109-119.
- Sego, D. C., and Morgenstern, N. R., 1983, "Deformation of Ice Under Low Stresses," Canadian Geotechnical Journal, Vol. 20, pp. 587-602.
- Shoji, H. and Higashi, A., 1978, "A Deformation Mechanism Map of Ice," Journal of Glaciology, Vol. 85, No. 21, pp. 419-427.
- Simonsen, E. R., Jones, A. H., and Jones, S. J., 1975, "High Pressure Mechanical Properties of Three Frozen Materials, Proceedings Fourth International Conference on High Pressure, Kyoto, pp. 115-121.
- Skermer, N. A., 1973, "A Finite Element Analysis of El Infiernillo Dam," Canadian Geotechnical Journal, Vol. 10, No. 2, pp. 95-105.
- Smith, L. L. and Cheatham Jr., J. B., 1975, "Plasticity of Ice and Sand Ice System," Journal of Engineering for Industry, Vol. 97, No. 2, pp. 479-484.
- Ting, J. M., 1983a, "Tertiary Creep Model for Frozen Sands," Proceedings ASCE, Journal of Geotechnical Engineering, Vol. 109, No. 7, pp. 932-945.
- Ting, J. M., and Martin, T. R., and Ladd, C. C., 1983b, "Mechanics of Strength for Frozen Sand," Proceedings ASCE, Journal of Geotechnical Engineering, Vol. 109, No. 10, pp. 1286-1302.
- Ting, J. M., 1983c, "On the Nature of the Minimum Creep Rate-Time Correlation for Soil, Ice and Frozen Soil," Canadian Geotechnical Journal, Vol. 20, No. 1, pp. 176-182.
- Ting, J. M., and Martin, R. T., 1979, "Application of the Andrade Equation to Creep Data for Ice and Frozen Soil," Cold Regions Science and Technology, Vol. 1, No. 1, pp. 29-36.
- Tsyrovich, N. A., 1975, "Mechanics of Frozen Ground," McGraw-Hill, New York.
- Valliappan, P., 1974, "Nonlinear Stress-Deformation Analysis of Lake Agassiz Clays Using Finite Element Method," Ph.D. Thesis, University of Manitoba, Winnipeg, Manitoba.
- Vyalov, S. S., Zaretsky, and Gorodetsky, S. E., 1979, "Stability of Mine Workings in Frozen Soils," Proceedings First International

- Symposium on Ground Freezing, Bochum, pp. 339-351.
- Vyalov, S. S., 1973, "Long Term Failure of Frozen of Frozen Soil as a Thermally Activated Process, Proceedings Second International Conference on Permafrost, U. S. S. R. Contribution, Yakutsk, pp. 222-228.
- Vyalov, S. S., and Obruchev, V. A., 1966, "Rheology of Frozen Soils," In Permafrost : Proceedings of an International Conference, National Academy of Sciences, Washington, D.C., pp. 332-337.
- Vyalov, S. S., 1963, "Rheology of Frozen Soils," Proceedings First International Conference on Permafrost, pp. 332-342.
- Vyalov, S. S., 1962, "Strength and Creep of Frozen Soils and Calculations in Ice-Soil Retaining Structures," USA CRREL, Translation No. 76.
- Weaver, J. S., and Morgenstern, N. R., 1981, "Simple Shear Creep Tests on Frozen Soils," Canadian Geotechnical Journal, Vol. 18, No. 2, pp. 217-229.
- Weertman, J., 1973, "Creep of Ice," Physics and Chemistry of Ice, pp. 320-337.
- Yualin, Zhu, and Carbee, D. L., 1984, "Uniaxial Compressive Strength of Frozen Silt Under Constant Deformation Rates," Cold Regions Science and Technology, Vol. 9, 1984, pp. 3-15.
- Yualin, Zhu, and Carbee, D. L., 1983, "Creep Behaviour of Frozen Silt Under Constant Uniaxial Stress," Proceedings Fourth International Conference on Permafrost, Fairbanks, pp. 1507-1512.

# APPENDIX

GEOTECHNICAL LABORATORIES  
DEPARTMENT OF CIVIL ENGINEERING  
UNIVERSITY OF MANITOBA

ISOTROPIC CONSOLIDATION MULTI-STAGE  
TRIAXIAL CREEP TEST  
IC1 -  $\bar{\sigma}_m=50$  to 300 kPa

LOAD INCREMENT = 1

CONFINING PRESSURE = 50.0 KPA

TIME (HOURS)	VOL DISPL (CC)	AXIAL DISPL (MM)	STRAIN RATE (MM/HR)	TRUE AXIAL STRAIN %	VOLUMETRIC STRAIN %	LOG TIME HOUR	CUMULATIVE TIME (HRS)	VOL. STRAIN RATE/HR	LOGSTR RTE/HR
0.0	2.000	0.020	0.665E-02	0.013	0.212	-1.898	0.0		
0.2	2.200	0.030	0.370E-03	0.020	0.242	-0.888	0.2	0.106E+00	-0.874
0.5	2.300	0.030	0.0	0.020	0.258	-0.301	0.5	0.188E-02	-2.782
1.0	2.350	0.020	-0.133E-03	0.013	0.283	0.0	0.5	0.488E-03	-3.314
2.0	2.400	0.030	0.668E-04	0.020	0.271	0.301	1.0	0.138E-03	-3.871
5.0	2.600	0.030	0.0	0.020	0.300	0.775	2.0	0.788E-04	-4.105
24.0	3.200	0.030	0.0	0.020	0.388	1.360	5.0	0.728E-04	-4.137
48.0	3.700	0.040	0.277E-05	0.027	0.481	1.851	24.0	0.468E-04	-4.313
82.0	4.200	0.050	0.198E-05	0.033	0.535	1.914	48.0	0.308E-04	-4.514
89.0	4.400	0.050	0.0	0.033	0.554	1.966	82.0	0.218E-04	-4.885
121.0	4.700	0.050	0.0	0.033	0.608	2.083	89.0	0.172E-04	-4.764
145.0	4.800	0.050	0.0	0.033	0.622	2.181	121.0	0.199E-04	-4.701
189.8	4.950	0.050	0.280E-05	0.040	0.645	2.227	145.0	0.810E-05	-5.215
182.8	5.100	0.050	0.0	0.040	0.667	2.285	189.8	0.845E-05	-5.024
215.8	5.300	0.050	0.0	0.040	0.698	2.336	182.8	0.918E-05	-5.038
247.0	5.350	0.050	0.0	0.040	0.704	2.393	215.8	0.122E-04	-4.914
271.5	5.400	0.040	-0.543E-05	0.027	0.710	2.434	247.0	0.243E-05	-5.815
288.0	5.480	0.040	0.0	0.027	0.717	2.461	271.5	0.252E-05	-5.588
313.5	5.500	0.040	0.0	0.027	0.724	2.495	288.0	0.418E-05	-5.380
							313.5	0.288E-05	-5.524

LOAD INCREMENT = 2

CONFINING PRESSURE = 100.0 KPA

TIME (HOURS)	VOL DISPL (CC)	AXIAL DISPL (MM)	STRAIN RATE (MM/HR)	TRUE AXIAL STRAIN %	VOLUMETRIC STRAIN %	LOG TIME HOUR	CUMULATIVE TIME (HRS)	VOL. STRAIN RATE/HR	LOGSTR RTE/HR
0.0	5.800	0.220	0.732E-01	0.146	0.735	-1.898			
0.1	5.900	0.210	-0.111E-02	0.140	0.749	-1.087	313.5	0.367E+00	-0.435
0.3	5.900	0.210	0.0	0.140	0.748	-0.301	313.6	0.235E-02	-2.629
0.5	5.950	0.210	0.0	0.140	0.755	-0.301	313.7	0.0	-3.314
2.8	6.100	0.200	-0.298E-04	0.133	0.777	0.439	314.0	0.293E-03	-3.533
7.5	6.200	0.210	0.140E-04	0.140	0.783	0.875	318.2	0.950E-04	-4.022
23.5	6.350	0.210	0.0	0.140	0.815	1.371	321.0	0.321E-04	-4.494
47.0	6.550	0.210	0.0	0.140	0.844	1.872	321.0	0.137E-04	-4.862
71.5	6.700	0.210	0.0	0.140	0.866	1.854	337.0	0.125E-04	-4.904
103.5	7.000	0.210	0.0	0.140	0.910	2.015	385.0	0.898E-05	-5.047
124.5	7.100	0.210	0.0	0.140	0.924	2.095	417.0	0.137E-04	-4.862
187.5	7.200	0.200	-0.185E-05	0.133	0.938	2.224	438.0	0.897E-05	-5.156
191.5	7.450	0.200	0.0	0.133	0.975	2.282	481.0	0.328E-05	-5.484
215.0	7.400	0.200	0.0	0.133	0.968	2.285	505.0	0.153E-04	-4.816
218.5	7.400	0.210	0.444E-04	0.140	0.989	2.335	528.5	-0.313E-05	-5.038
							530.0	0.388E-05	-5.414





GEOTECHNICAL LABORATORIES  
DEPARTMENT OF CIVIL ENGINEERING  
UNIVERSITY OF MANITOBA

CONSTANT MEAN NORMAL STRESS MULTI-STAGE  
TRIAxIAL CREEP TEST  
MST1 -  $\bar{\sigma}_m=140$  kPa



LOAD INCREMENT # 1 S.D. : 0 KPA

TIME (HOURS)	VOL DISPL (CC)	AXIAL DISPL (MM)	STRAIN RATE (/HR)	TRUE AXIAL STRAIN %	TRUE VOL. STRAIN %	DEVIATORIC STRAIN %	CUMULATIVE TIME (HRS)	LOGSTRAIN RATE/HOUR	LOGTIME HOURS
0.4	-1.258	0.021	0.347E-03	0.014	-0.186	0.118	0.4	-3.459	-0.388
4.4	-1.715	0.033	0.218E-04	0.022	-0.253	0.162	4.4	-4.868	0.643
21.0	-2.114	0.031	-0.797E-06	0.021	-0.312	0.203	21.0	0.0	0.0

LOAD INCREMENT # 2 S.D. : 49 KPA

TIME (HOURS)	VOL DISPL (CC)	AXIAL DISPL (MM)	STRAIN RATE (/HR)	TRUE AXIAL STRAIN %	TRUE VOL. STRAIN %	DEVIATORIC STRAIN %	CUMULATIVE TIME (HRS)	LOGSTRAIN RATE/HOUR	LOGTIME HOURS
0.5	-0.562	0.005	0.720E-04	0.004	-0.082	0.058	0.5	-4.143	-0.301
1.8	-1.450	0.000	-0.264E-04	0.000	-0.215	0.175	1.8	-4.888	0.643
3.3	-2.000	0.000	0.0	0.000	-0.296	0.241	3.3	0.0	0.0

AVLIN EQUATION NUMBER 1  
 ERROR - INSUFFICIENT DATA POINTS FOR SUBROUTINE AVLIN - CALL IGNORED

LOAD INCREMENT # 3 S.D. : 98 KPA

TIME (HOURS)	VOL DISPL (CC)	AXIAL DISPL (MM)	STRAIN RATE (/HR)	TRUE AXIAL STRAIN %	TRUE VOL. STRAIN %	DEVIATORIC STRAIN %	CUMULATIVE TIME (HRS)	LOGSTRAIN RATE/HOUR	LOGTIME HOURS
0.3	-2.417	0.148	0.333E-02	0.100	-0.358	0.048	3.6	-2.478	-0.623
5.7	-2.632	0.182	0.417E-04	0.122	-0.390	0.019	9.0	-4.380	0.756
21.3	-2.555	0.234	0.225E-04	0.157	-0.379	0.076	24.6	-4.648	1.328
29.3	-2.901	0.226	-0.882E-05	0.152	-0.430	0.021	32.6	-2.000	0.0
45.2	-2.775	0.278	0.225E-04	0.188	-0.411	0.124	48.5	-4.648	1.855
69.3	-2.975	0.278	0.0	0.188	-0.441	0.100	72.6	0.0	0.0

AVLIN EQUATION NUMBER 2  
 Y = -1.157086 X - 1.221094 X^2 + 2.918693 X^3  
 T-VALUES ARE 0.8438 1.7886 1.7047  
 RSQUARE = 0.8421 STD. ERR. OF EST. = 1.178848

LOAD INCREMENT # 4 S.D. = 147 KPA

TIME (HOURS)	VOL DISPL (CC)	AXIAL DISPL (MM)	STRAIN RATE (/HR)	TRUE AXIAL STRAIN %	TRUE VOL. STRAIN %	DEVIATORIC STRAIN %	CUMULATIVE TIME (HRS)	LOGSTRAIN RATE/HOUR	LOGTIME HOURS
0.5	-3.114	0.255	0.344E-02	0.172	-0.462	0.044	73.1	-2.464	-0.301
7.3	-3.189	0.265	0.873E-05	0.178	-0.470	0.053	78.9	-5.012	0.863
23.2	-3.227	0.283	0.749E-05	0.190	-0.478	0.076	85.8	-5.126	1.386
31.3	-3.228	0.284	0.164E-05	0.192	-0.479	0.079	103.9	-5.786	1.496
51.8	-3.332	0.295	0.355E-05	0.199	-0.494	0.084	124.4	-5.448	1.714
73.8	-3.289	0.309	0.422E-05	0.208	-0.485	0.114	146.4	-5.375	1.868
95.2	-3.345	0.324	0.464E-05	0.218	-0.496	0.129	167.8	-5.334	1.979

AVLIN EQUATION NUMBER 3

Y = -3.272538 - 2.519612 X + .5598913 X\*\*2 + 9459503E-01 X\*\*3

T-VALUES ARE : 3.4643 0.4131 0.1927  
 RSQUARE = 0.9741 STD. ERR. OF EST. = .2541397

LOAD INCREMENT # 5 S.D. = 196 KPA

TIME (HOURS)	VOL DISPL (CC)	AXIAL DISPL (MM)	STRAIN RATE (/HR)	TRUE AXIAL STRAIN %	TRUE VOL. STRAIN %	DEVIATORIC STRAIN %	CUMULATIVE TIME (HRS)	LOGSTRAIN RATE/HOUR	LOGTIME HOURS
0.5	-3.344	0.322	0.433E-02	0.217	-0.496	0.126	168.3	-2.383	-0.301
6.5	-3.364	0.342	0.232E-04	0.231	-0.497	0.159	174.3	-4.635	0.813
23.4	-3.416	0.371	0.114E-04	0.260	-0.507	0.198	191.2	-4.944	1.369
31.1	-3.420	0.380	0.774E-05	0.256	-0.507	0.212	198.9	-5.111	1.493
47.0	-3.381	0.403	0.100E-04	0.272	-0.501	0.256	214.6	-5.000	1.672
54.0	-3.435	0.413	0.948E-05	0.278	-0.509	0.266	221.6	-5.024	1.732
70.0	-3.444	0.432	0.788E-05	0.291	-0.511	0.296	237.6	-5.104	1.845
78.0	-3.487	0.438	0.581E-05	0.296	-0.519	0.300	245.8	-5.236	1.892
94.0	-3.506	0.458	0.828E-05	0.309	-0.520	0.332	261.8	-5.082	1.973

AVLIN EQUATION NUMBER 4

Y = -3.268031 - 2.589321 X + 1.312916 X\*\*2 + .2435792 X\*\*3

T-VALUES ARE : 11.8404 3.3184 1.6901  
 RSQUARE = 0.9947 STD. ERR. OF EST. = .8326167E-01

LOAD INCREMENT # 6 S.D. = 245 KPA

TIME (HOURS)	VOL DISPL (CC)	AXIAL DISPL (MM)	STRAIN RATE (/HR)	TRUE AXIAL STRAIN %	TRUE VOL. STRAIN %	DEVIATORIC STRAIN %	CUMULATIVE TIME (HRS)	LOGSTRAIN RATE/HOUR	LOGTIME HOURS
0.7	-3.513	0.474	0.458E-02	0.319	-0.521	0.357	262.5	-2.341	-0.155
7.2	-3.538	0.523	0.510E-04	0.352	-0.524	0.436	269.0	-4.292	0.657
29.8	-3.515	0.591	0.205E-04	0.399	-0.521	0.551	291.6	-4.687	1.474
54.2	-3.506	0.683	0.253E-04	0.481	-0.520	0.704	316.0	-4.597	1.734
75.8	-3.435	0.746	0.197E-04	0.503	-0.509	0.817	337.6	-4.706	1.880
95.3	-3.505	0.792	0.160E-04	0.534	-0.520	0.884	357.1	-4.786	1.979

AVLIN EQUATION NUMBER 5

Y = -2.822820 - 2.885137 X + 1.600559 X\*\*2 + .3264927 X\*\*3

T-VALUES ARE : 7.8985 2.8240 1.6484  
 RSQUARE = 0.9967 STD. ERR. OF EST. = .8548972E-01

LOAD INCREMENT # 7 S.D. = 294 KPA

Table with 11 columns: TIME (HOURS), VOL DISPL (CC), AXIAL DISPL (MM), STRAIN RATE (/HR), TRUE AXIAL STRAIN %, TRUE VOL. STRAIN %, DEVIATORIC STRAIN %, CUMULATIVE TIME (HRS), LOGSTRAIN RATE/HOUR, LOGTIME HOURS. Contains 48 rows of data points.

AVLIN EQUATION NUMBER 6

Y = -2.651254 X + .5658468 X\*\*2 - .3755079E-01 X\*\*3

T-VALUES ARE : 12.7757 4.4892 1.4157
RSQUARE = 0.9313 STD. ERR. OF EST. = .1062342

LOAD INCREMENT # 8 S.D. = 343 KPA

Table with 11 columns: TIME (HOURS), VOL DISPL (CC), AXIAL DISPL (MM), STRAIN RATE (/HR), TRUE AXIAL STRAIN %, TRUE VOL. STRAIN %, DEVIATORIC STRAIN %, CUMULATIVE TIME (HRS), LOGSTRAIN RATE/HOUR, LOGTIME HOURS. Contains 48 rows of data points.

AVLIN EQUATION NUMBER 7

Y = -2.039707 X - 3.472120 X + 1.929217 X\*\*2 - .3327643 X\*\*3

T-VALUES ARE : 24.9921 16.3932 12.8933
RSQUARE = 0.9742 STD. ERR. OF EST. = .7907045E-01

\*\*\*PLOT 1, 671 UNPLOTTABLE POINTS\*\*\*

GEOTECHNICAL LABORATORIES  
DEPARTMENT OF CIVIL ENGINEERING  
UNIVERSITY OF MANITOBA

CONSTANT MEAN NORMAL STRESS MULTI-STAGE  
TRIAXIAL CREEP TEST  
MST2 -  $\bar{\sigma}_m = 280 \text{ kPa}$

LOAD INCREMENT # 1 S.D. : 0 KPA

TIME (HOURS)	VOL DISPL (CC)	AXIAL DISPL (MM)	STRAIN RATE (/HR)	TRUE AXIAL STRAIN %	TRUE VOL. STRAIN %	DEVIATORIC STRAIN %	CUMULATIVE TIME (HRS)	LOGSTRAIN RATE/HOUR	LOGTIME HOURS
0.5	-2.318	0.040	0.540E-03	0.027	-0.341	0.212	0.5	-3.267	-0.301
4.0	-2.356	0.125	0.161E-03	0.083	-0.346	0.078	4.0	-3.792	0.602
21.0	-3.165	0.145	0.782E-05	0.097	-0.485	0.143	21.0	-5.107	1.322
45.5	-6.206	0.237	0.252E-04	0.159	-0.915	0.358	45.5	-4.598	1.658
68.0	-2.972	0.272	0.103E-04	0.182	-0.437	0.089	68.0	-4.985	1.833
76.5	-4.192	0.316	0.352E-04	0.212	-0.817	0.015	76.5	-4.453	1.884
92.5	-3.692	0.316	0.0	0.212	-0.543	0.078	92.5	0.0	0.0
116.5	-3.748	0.329	0.361E-05	0.221	-0.551	0.090	116.5	-5.443	2.066
140.5	-3.912	0.362	0.915E-05	0.243	-0.576	0.124	140.5	-5.039	2.148
164.5	-4.386	0.414	0.147E-04	0.278	-0.846	0.153	164.5	-4.833	2.216
191.5	-4.049	0.444	0.740E-05	0.298	-0.596	0.243	191.5	-5.131	2.282
236.0	-3.905	0.456	0.180E-05	0.306	-0.574	0.280	236.0	-5.745	2.373
260.0	-4.518	0.486	0.833E-05	0.326	-0.665	0.255	260.0	-4.857	2.415
284.0	-4.140	0.536	0.139E-04	0.358	-0.609	0.382	284.0	-5.858	2.489
308.0	-4.843	0.541	0.139E-05	0.362	-0.713	0.306	308.0	-5.130	2.519
330.5	-4.554	0.565	0.741E-05	0.379	-0.670	0.381	330.5	-4.786	2.553
357.0	-5.083	0.630	0.164E-04	0.422	-0.748	0.424	357.0	0.0	0.0
404.0	-5.464	0.589	-0.582E-05	0.395	-0.805	0.311	404.0	-5.277	2.631
428.0	-5.573	0.606	0.528E-05	0.408	-0.821	0.329	428.0	-5.410	2.655
452.0	-5.029	0.622	0.389E-05	0.417	-0.741	0.417	452.0	-5.352	2.678
476.0	-5.836	0.638	0.444E-05	0.428	-0.830	0.370	476.0	0.0	0.0
500.0	-3.729	0.622	-0.444E-05	0.417	-0.549	0.574	500.0	-5.261	2.721
525.5	-3.686	0.643	0.549E-05	0.431	-0.543	0.613	525.5	0.0	0.0
572.0	-3.911	0.627	-0.229E-05	0.420	-0.575	0.560	572.0	-6.255	2.775
596.0	-3.782	0.629	0.556E-06	0.422	-0.556	0.579	596.0		

LOAD INCREMENT # 2 S.D. : 98 KPA

TIME (HOURS)	VOL DISPL (CC)	AXIAL DISPL (MM)	STRAIN RATE (/HR)	TRUE AXIAL STRAIN %	TRUE VOL. STRAIN %	DEVIATORIC STRAIN %	CUMULATIVE TIME (HRS)	LOGSTRAIN RATE/HOUR	LOGTIME HOURS
1.8	0.063	0.083	0.311E-03	0.056	0.009	0.145	1.8	-3.507	0.255
7.8	-0.044	0.098	0.167E-04	0.056	-0.007	0.156	7.8	-4.778	0.892
23.3	-0.149	0.110	0.517E-05	0.074	-0.022	0.183	23.3	-5.286	1.367
34.3	-0.108	0.130	0.121E-04	0.087	-0.016	0.201	34.3	-4.916	1.535
47.3	-0.218	0.151	0.108E-04	0.101	-0.032	0.222	47.3	-4.984	1.852
71.1	-0.334	0.187	0.104E-04	0.126	-0.049	0.289	71.1	-5.220	1.965
96.6	-0.494	0.210	0.602E-05	0.141	-0.073	0.277	96.6	-5.905	2.091
123.4	-0.647	0.215	0.125E-05	0.148	-0.095	0.277	123.4	-5.537	2.157
143.4	-0.748	0.218	0.100E-05	0.147	-0.110	0.289	143.4	-5.858	2.215
164.1	-0.852	0.227	0.290E-05	0.153	-0.126	0.272	164.1	-6.237	2.326
188.3	-0.904	0.232	0.138E-05	0.156	-0.133	0.273	188.3	-6.074	2.415
211.4	-1.005	0.234	0.578E-06	0.157	-0.148	0.265	211.4	-5.786	2.488
235.2	-1.106	0.237	0.843E-06	0.159	-0.183	0.257	235.2	-5.391	2.523
259.8	-1.081	0.293	0.152E-04	0.197	-0.160	0.352	259.8	-5.691	2.550
284.3	-1.234	0.299	0.164E-06	0.201	-0.182	0.343	284.3	-5.858	2.579
307.3	-1.437	0.306	0.204E-05	0.206	-0.212	0.330	307.3	-6.079	2.605
333.6	-1.944	0.321	0.407E-05	0.216	-0.287	0.295	333.6	-5.624	2.632
354.9	-1.847	0.328	0.220E-05	0.221	-0.273	0.318	354.9	0.0	0.0
378.0	-1.850	0.336	0.139E-05	0.224	-0.273	0.326	378.0	-5.858	2.678
403.0	-1.951	0.336	0.834E-06	0.226	-0.288	0.319	403.0	0.0	0.0
428.3	-1.955	0.345	0.238E-05	0.232	-0.289	0.333	428.3	-5.624	2.632
457.0	-2.052	0.338	-0.163E-05	0.228	-0.303	0.310	457.0	0.0	0.0
475.2	-2.103	0.340	0.732E-06	0.229	-0.311	0.307	475.2	-6.136	2.677

AVLIN EQUATION NUMBER 1

Y = -0.6789122 - 8.153956 X + 4.700424 X\*\*2 - 0.8998615 X\*\*3  
 T-VALUES ARE : 5.2958 3.5886 2.9817  
 RSQUARE : 0.8776 STD. ERR. OF EST. : 4883730



LOAD INCREMENT # 5 S.D. = 392 KPA

TIME (HOURS)	VOL DISPL (CC)	AXIAL DISPL (MM)	STRAIN RATE (/HR)	TRUE AXIAL STRAIN %	TRUE VOL. STRAIN %	DEVIATORIC STRAIN %	CUMULATIVE TIME (HRS)	LOGSTRAIN RATE/HOUR	LOGTIME HOURS
0.6	-13.206	3.646	0.413E-01	2.481	-1.967	4.471	1985.4	-1.384	-0.222
11.4	-13.202	3.683	0.234E-04	2.506	-1.967	4.533	1997.2	-4.630	1.057
24.0	-13.179	3.741	0.320E-04	2.547	-1.963	4.635	2009.8	-4.494	1.380
47.5	-13.226	3.736	-0.146E-05	2.543	-1.970	4.621	2033.3	-4.869	1.534
72.5	-13.342	3.771	0.958E-05	2.567	-1.988	4.665	2058.3	-5.019	1.850
96.5	-13.397	3.782	0.313E-05	2.576	-1.986	4.677	2082.3	-5.504	1.985
119.5	-13.446	3.779	-0.891E-06	2.573	-2.003	4.666	2105.3	-5.226	1.978
143.5	-13.499	3.786	0.200E-05	2.577	-2.011	4.671	2129.3	-5.700	2.157
168.5	-13.513	3.819	0.904E-05	2.800	-2.014	4.724	2154.3	-5.044	2.227
192.0	-13.634	3.865	0.137E-04	2.632	-2.032	4.788	2177.8	-4.864	2.283
216.5	-13.687	3.870	0.140E-05	2.636	-2.040	4.790	2202.3	-5.855	2.335
240.0	-13.794	3.886	0.467E-05	2.647	-2.056	4.804	2225.8	-5.331	2.380
264.0	-13.844	3.886	0.0	2.647	-2.063	4.798	2249.8	-5.437	2.381
288.0	-13.894	3.886	0.0	2.647	-2.071	4.792	2273.8	-6.082	2.423
312.0	-13.894	3.886	0.0	2.647	-2.071	4.792	2297.8	-5.314	2.468
336.0	-14.045	3.888	0.569E-06	2.848	-2.094	4.777	2321.8	-6.245	2.526
360.0	-14.105	3.911	0.656E-05	2.864	-2.103	4.808	2345.8	-5.183	2.556
384.0	-14.158	3.919	0.228E-05	2.869	-2.111	4.815	2369.8	-5.642	2.584
408.0	-14.206	3.913	-0.171E-05	2.865	-2.118	4.799	2393.8	-5.952	2.584
432.0	-14.207	3.917	0.114E-05	2.868	-2.125	4.805	2417.8	-5.943	2.635
457.0	-14.250	3.900	-0.466E-05	2.856	-2.132	4.767	2442.8	-6.077	2.635
479.5	-14.300	3.901	0.304E-06	2.857	-2.143	4.829	2465.3	-6.517	2.681
504.0	-14.369	3.943	0.117E-04	2.886	-2.150	4.832	2489.8	-4.930	2.702
528.0	-14.422	3.949	0.171E-05	2.890	-2.165	4.815	2513.8	-5.767	2.723
552.0	-14.520	3.946	-0.857E-06	2.888	-2.172	4.780	2537.8	-5.383	2.722
577.0	-14.562	3.928	-0.483E-05	2.875	-2.180	4.793	2562.8	-5.709	2.741
600.0	-14.618	3.940	0.358E-05	2.884	-2.179	4.785	2585.8	-5.446	2.778
624.5	-14.614	3.931	-0.252E-05	2.877	-2.187	4.779	2610.3	-5.051	2.778
648.5	-14.667	3.939	0.229E-05	2.883	-2.203	4.786	2634.3	-5.613	2.812
671.0	-14.771	3.947	0.244E-05	2.886	-2.219	4.766	2658.8	-5.699	2.827
696.5	-14.824	3.955	0.215E-05	2.894	-2.226	4.793	2682.3	-5.560	2.843
719.5	-14.920	3.945	-0.298E-05	2.887	-2.226	4.776	2705.3	-5.416	2.847
743.5	-14.923	3.952	0.200E-05	2.892	-2.219	4.805	2729.3	-5.699	2.871
768.5	-14.879	3.955	0.384E-05	2.701	-2.227	4.805	2754.3	-5.416	2.885
792.5	-14.927	3.960	-0.171E-05	2.697	-2.227	4.789	2778.3	-5.045	2.885
817.0	-14.979	3.964	0.140E-05	2.701	-2.235	4.791	2802.8	-5.855	2.912
843.0	-14.984	3.975	0.342E-05	2.708	-2.235	4.809	2824.8	-5.466	2.924
864.0	-15.118	4.052	0.211E-04	2.761	-2.255	4.921	2849.8	-4.675	2.937
887.0	-15.172	4.062	0.298E-05	2.788	-2.264	4.931	2872.8	-5.525	2.948
913.0	-15.222	4.061	-0.264E-06	2.787	-2.271	4.924	2898.8	0.0	0.0
935.0	-15.266	4.091	0.965E-05	2.788	-2.281	4.968	2920.8	-5.015	2.971
967.0	-15.421	4.068	-0.729E-05	2.755	-2.301	4.894	2952.8	0.0	0.0
986.0	-15.474	4.066	0.289E-05	2.771	-2.309	4.901	2971.8	-5.540	2.994
1006.5	-15.523	4.063	-0.100E-05	2.769	-2.317	4.890	2992.3	-5.341	3.003
1030.5	-15.569	4.055	0.229E-05	2.763	-2.324	4.871	3016.3	-2.000	0.0
1054.5	-15.668	4.062	-0.856E-06	2.761	-2.338	4.854	3040.3	0.600	0.700
1081.5	-15.785	4.045	-0.178E-05	2.756	-2.353	4.830	3067.3	0.0	0.0
1108.5	-15.865	4.046	0.254E-06	2.757	-2.368	4.819	3094.3	-6.595	3.045
1128.5	-15.914	4.044	-0.686E-06	2.755	-2.376	4.810	3114.3	0.0	0.0
1154.5	-15.965	4.046	0.528E-06	2.757	-2.383	4.807	3140.3	-6.278	3.062
1177.0	-15.968	4.052	0.183E-05	2.761	-2.384	4.817	3162.8	-5.738	3.071
1201.0	-16.064	4.043	-0.257E-05	2.755	-2.398	4.790	3186.8	0.0	0.0
1226.5	-16.086	4.048	0.134E-05	2.758	-2.399	4.798	3212.3	-5.872	3.089
1249.0	-16.061	4.037	-0.335E-05	2.751	-2.398	4.780	3234.8	0.0	0.0
1273.0	-16.110	4.034	-0.855E-06	2.749	-2.405	4.769	3258.8	0.0	0.0
1297.0	-16.026	4.071	0.106E-04	2.774	-2.393	4.841	3282.8	-4.976	3.113
1321.0	-15.827	4.072	0.286E-06	2.775	-2.363	4.868	3306.8	-6.543	3.121
1345.0	-15.885	4.091	0.543E-05	2.788	-2.371	4.892	3330.8	-5.265	3.129
1393.0	-15.988	4.096	0.857E-06	2.792	-2.387	4.890	3378.8	-6.067	3.144

AVLIN EQUATION NUMBER 4

Y = .3974371 -1.608702 X + .8720366 X\*\*2 + .2990469 X\*\*3

T-VALUES ARE : 1.9075 1.1548 1.9556  
RSQUARE = 0.8939 STD. ERR. OF EST. = .6887091

LOAD INCREMENT # 6 S.D. = 490 KPA

TIME (HOURS)	VOL DISPL (CC)	AXIAL DISPL (MM)	STRAIN RATE (/HR)	TRUE AXIAL STRAIN %	TRUE VOL. STRAIN %	DEVIATORIC STRAIN %	CUMULATIVE TIME (HRS)	LOGSTRAIN RATE/HOUR	LOGTIME HOURS
0.5	-16.132	4.127	0.563E-01	2.813	-2.409	4.924	3379.3	-1.260	-0.301
7.3	-16.130	4.233	0.108E-03	2.887	-2.408	5.104	3386.1	-3.987	0.863
24.0	-16.098	4.385	0.629E-04	2.992	-2.403	5.366	3402.8	-4.201	1.360
32.0	-15.979	4.455	0.601E-04	3.040	-2.385	5.498	3410.8	-4.221	1.505
48.0	-15.988	4.587	0.572E-04	3.131	-2.387	5.721	3426.8	-4.243	1.681
74.0	-15.929	4.789	0.540E-04	3.272	-2.378	6.073	3452.8	-4.267	1.869
120.0	-15.754	5.068	0.421E-04	3.466	-2.351	6.569	3498.8	-4.375	2.079
144.5	-15.706	5.184	0.330E-04	3.546	-2.344	6.773	3523.3	-4.482	2.160
166.5	-15.648	5.278	0.274E-04	3.612	-2.336	6.941	3547.3	-4.583	2.227
176.8	-15.574	5.335	0.475E-04	3.652	-2.324	7.047	3555.6	-4.323	2.247
192.5	-15.515	5.426	0.406E-04	3.715	-2.315	7.210	3571.3	-4.392	2.284
216.5	-15.485	5.583	0.456E-04	3.825	-2.311	7.481	3595.3	-4.341	2.335
242.0	-15.335	5.805	0.609E-04	3.980	-2.288	7.881	3620.8	-4.215	2.384
265.5	-15.086	6.030	0.668E-04	4.137	-2.251	8.296	3644.3	-4.175	2.424
288.5	-15.042	6.288	0.728E-04	4.304	-2.244	8.710	3667.3	-4.139	2.460
312.5	-14.837	6.478	0.616E-04	4.452	-2.213	9.097	3691.3	-4.211	2.495
336.5	-14.690	6.708	0.672E-04	4.613	-2.191	9.510	3715.3	-4.173	2.527
360.5	-14.683	6.804	0.282E-04	4.681	-2.190	9.677	3739.3	-4.549	2.557
384.5	-14.530	6.908	0.306E-04	4.754	-2.167	9.876	3763.3	-4.514	2.585
410.5	-14.365	6.987	0.215E-04	4.810	-2.142	10.033	3788.3	-4.667	2.613
441.5	-14.312	7.092	0.237E-04	4.884	-2.134	10.220	3820.3	-4.625	2.645
456.5	-14.238	7.149	0.271E-04	4.924	-2.123	10.329	3835.3	-4.567	2.659
480.5	-14.132	7.135	-0.409E-05	4.914	-2.107	10.318	3859.3	-4.930	2.702
504.5	-14.028	7.350	0.631E-04	5.066	-2.091	10.701	3883.3	-4.200	2.703
526.5	-13.836	7.480	0.383E-04	5.158	-2.062	10.950	3907.3	-4.417	2.723
552.5	-13.710	7.644	0.488E-04	5.274	-2.043	11.251	3931.3	-4.313	2.742
576.5	-13.711	7.758	0.308E-04	5.355	-2.043	11.448	3957.3	-4.511	2.762
603.5	-13.377	7.904	0.417E-04	5.459	-1.993	11.744	3982.3	-4.380	2.781
624.5	-13.124	8.121	0.732E-04	5.613	-1.955	12.152	4003.3	-4.136	2.796
648.5	-12.879	8.355	0.894E-04	5.779	-1.918	12.590	4027.3	-4.158	2.812
672.5	-12.545	8.613	0.756E-04	5.963	-1.888	13.081	4051.3	-4.116	2.828
696.0	-12.298	8.844	0.703E-04	6.128	-1.831	13.516	4074.8	-4.153	2.843
720.5	-12.009	9.091	0.721E-04	6.305	-1.788	13.984	4099.3	-4.142	2.858
748.5	-11.792	9.275	0.470E-04	6.436	-1.755	14.333	4127.3	-4.328	2.874
780.0	-11.564	9.436	0.366E-04	6.552	-1.721	14.644	4158.8	-4.437	2.892
816.0	-11.344	9.613	0.354E-04	6.679	-1.688	14.983	4194.8	-4.451	2.912
840.0	-11.152	9.744	0.392E-04	6.773	-1.659	15.237	4218.8	-4.406	2.924
864.0	-10.965	9.883	0.417E-04	6.873	-1.631	15.505	4242.8	-4.380	2.937
888.0	-10.831	10.032	0.447E-04	6.981	-1.611	15.784	4266.8	-4.350	2.948
916.0	-10.603	10.191	0.409E-04	7.095	-1.576	16.092	4294.8	-4.388	2.962
940.0	-10.418	10.337	0.439E-04	7.201	-1.549	16.373	4318.8	-4.358	2.973
960.0	-10.229	10.472	0.488E-04	7.298	-1.520	16.635	4338.8	-4.312	2.982
984.0	-10.062	10.657	0.559E-04	7.432	-1.495	16.984	4362.8	-4.252	2.993

AVLIN EQUATION NUMBER 5

$$Y = -2.198953 \quad -2.715420 \quad X + 1.107275 \quad X^{**2} \quad -1.1471249 \quad X^{**3}$$

T-VALUES ARE : 10.3393 4.9358 3.0221

RSQUARE = 0.8884 STD. ERR. OF EST. = .1747804

\*\*\*PLOT 1, 378 UNPLOTTABLE POINTS\*\*\*



GEOTECHNICAL LABORATORIES  
DEPARTMENT OF CIVIL ENGINEERING  
UNIVERSITY OF MANITOBA

CONSTANT MEAN NORMAL STRESS MULTI-STAGE  
TRIAxIAL CREEP TEST  
MST3 -  $\sigma_m=280$  kPa

LOAD INCREMENT # 1 S.D. : 0 KPA									
TIME (HOURS)	VOL DISPL (CC)	AXIAL DISPL (MM)	STRAIN RATE (/HR)	TRUE AXIAL STRAIN %	TRUE VOL. STRAIN %	DEVIATORIC STRAIN %	CUMULATIVE TIME (HRS)	LOGSTRAIN RATE/HOUR	LOGTIME HOURS
2.0	-5.051	-0.124	-0.410E-03	-0.082	-0.743	0.808	2.0	0.0	0.0
22.5	-6.553	-0.122	0.651E-05	-0.081	-0.966	0.986	22.5	-6.167	1.352
33.5	-6.966	-0.105	0.100E-04	-0.070	-1.027	1.009	33.5	-4.998	1.525
46.5	-7.483	-0.084	0.108E-04	-0.056	-1.103	1.038	46.5	-4.876	1.667
70.3	-8.293	-0.072	0.356E-05	-0.047	-1.224	1.115	70.3	-5.448	1.847
95.7	-8.854	-0.058	0.358E-05	-0.038	-1.307	1.161	95.7	-5.449	1.981
122.6	-9.413	-0.047	0.270E-05	-0.031	-1.390	1.211	122.6	-5.569	2.088
142.6	-9.713	-0.046	0.286E-06	-0.031	-1.435	1.246	142.6	-5.544	2.154
163.3	-10.227	-0.029	0.539E-05	-0.019	-1.511	1.281	163.3	-5.266	2.213
187.5	-10.481	-0.023	0.162E-05	-0.015	-1.549	1.303	187.5	-5.792	2.273
210.6	-10.740	-0.013	0.310E-05	-0.008	-1.587	1.316	210.6	-5.509	2.323
219.3	-10.842	-0.011	0.153E-05	-0.007	-1.603	1.326	219.3	-5.814	2.341
234.4	-11.044	-0.008	0.126E-05	-0.005	-1.633	1.345	234.4	-5.888	2.370
259.5	-11.265	0.019	0.899E-05	0.013	-1.666	1.329	259.5	-5.155	2.414
283.4	-11.567	0.022	0.818E-06	0.014	-1.711	1.361	283.4	-6.087	2.452
306.5	-11.963	0.017	-0.141E-05	0.011	-1.770	1.418	306.5	0.0	0.0
322.8	-12.389	0.049	0.819E-05	0.033	-1.833	1.417	322.8	-5.087	2.522
354.1	-12.586	0.045	-0.123E-05	0.030	-1.863	1.447	354.1	0.0	0.0
378.2	-12.735	0.043	-0.542E-06	0.029	-1.885	1.469	378.2	0.0	0.0
402.2	-12.935	0.043	0.0	0.029	-1.915	1.493	402.2	0.0	0.0
427.4	-13.088	0.047	0.104E-05	0.031	-1.938	1.505	427.4	-5.985	2.631
456.2	-13.367	0.046	-0.228E-06	0.031	-1.983	1.543	456.2	0.0	0.0
480.8	-13.588	0.048	0.531E-06	0.032	-2.013	1.565	480.8	-6.275	2.682
507.3	-13.786	0.045	-0.738E-06	0.030	-2.042	1.594	507.3	0.0	0.0
530.9	-13.989	0.049	0.111E-05	0.033	-2.073	1.612	530.9	-5.955	2.725
570.2	-14.392	0.052	0.498E-06	0.035	-2.133	1.657	570.2	-6.303	2.756

LOAD INCREMENT # 2 S.D. : 196 KPA									
TIME (HOURS)	VOL DISPL (CC)	AXIAL DISPL (MM)	STRAIN RATE (/HR)	TRUE AXIAL STRAIN %	TRUE VOL. STRAIN %	DEVIATORIC STRAIN %	CUMULATIVE TIME (HRS)	LOGSTRAIN RATE/HOUR	LOGTIME HOURS
7.4	-0.152	0.441	0.397E-03	0.294	-0.023	0.701	7.4	-3.401	0.869
25.3	-0.553	0.505	0.238E-04	0.336	-0.083	0.756	25.3	-4.624	1.403
56.4	-0.948	0.562	0.122E-04	0.374	-0.142	0.800	56.4	-4.913	1.751
72.1	-1.164	0.582	0.834E-05	0.387	-0.174	0.806	72.1	-5.079	1.858
96.0	-1.377	0.598	0.466E-05	0.398	-0.206	0.807	96.0	-5.332	1.982
120.0	-1.594	0.619	0.573E-05	0.412	-0.239	0.814	120.0	-5.242	2.079
143.9	-1.805	0.633	0.384E-05	0.421	-0.271	0.811	143.9	-5.416	2.158
167.7	-2.016	0.647	0.385E-05	0.430	-0.302	0.808	167.7	-5.414	2.225
199.2	-2.234	0.669	0.478E-05	0.446	-0.335	0.818	199.2	-5.321	2.299
221.4	-2.440	0.677	0.237E-05	0.451	-0.366	0.805	221.4	-5.626	2.345
240.0	-2.647	0.686	0.317E-05	0.457	-0.397	0.794	240.0	-5.489	2.380
263.0	-2.944	0.683	-0.854E-06	0.455	-0.442	0.753	263.0	-5.814	2.341
287.6	-3.245	0.684	0.263E-06	0.456	-0.487	0.718	287.6	-6.580	2.459
311.7	-3.446	0.685	0.271E-06	0.456	-0.517	0.695	311.7	-6.568	2.494
337.4	-3.648	0.688	0.767E-06	0.458	-0.533	0.687	337.4	-6.115	2.528
367.0	-3.851	0.688	0.0	0.458	-0.546	0.675	367.0	0.0	0.0
410.0	-3.851	0.691	0.457E-06	0.460	-0.578	0.654	410.0	-6.340	2.613

AVLIN EQUATION NUMBER 1

$$Y = .2937603E-01 - 6.457802 X + 3.249499 X^2 - .6621088 X^3$$

T-VALUES ARE : 7.1143 4.0088 3.4055  
 RSQUARE = 0.9760 STD. ERR. OF EST. = .2622861



GEOTECHNICAL LABORATORIES  
DEPARTMENT OF CIVIL ENGINEERING  
UNIVERSITY OF MANITOBA

CONSTANT MEAN NORMAL STRESS MULTI-STAGE  
TRIAXIAL CREEP TEST  
MST4 -  $\sigma_m=70$  kPa







GEOTECHNICAL LABORATORIES  
DEPARTMENT OF CIVIL ENGINEERING  
UNIVERSITY OF MANITOBA

CONSTANT MEAN NORMAL STRESS MULTI-STAGE  
TRIAXIAL CREEP TEST  
MST5 -  $\sigma_m=420$  kPa





LOAD INCREMENT # 3 S.D. = 392 KPA

TIME (HOURS)	VOL DISPL (CC)	AXIAL DISPL (MM)	STRAIN RATE (/HR)	TRUE AXIAL STRAIN %	TRUE VOL. STRAIN %	DEVIATORIC STRAIN %	CUMULATIVE TIME (HRS)	LOGSTRAIN RATE/HOUR	LOGTIME HOURS
0.1	-3.039	0.801	0.531E-01	0.531	-0.452	0.932	817.1	-1.275	-1.000
9.5	-3.263	1.120	0.226E-03	0.743	-0.485	1.425	826.5	-3.646	0.978
22.5	-3.410	1.266	0.750E-04	0.841	-0.507	1.646	839.5	-4.125	1.352
46.5	-3.629	1.416	0.415E-04	0.940	-0.540	1.863	853.5	-4.382	1.667
70.5	-3.752	1.508	0.257E-04	1.002	-0.558	1.998	867.5	-4.590	1.846
94.5	-3.858	1.578	0.194E-04	1.049	-0.574	2.100	881.5	-4.712	1.975
125.5	-3.916	1.650	0.157E-04	1.097	-0.583	2.212	892.5	-4.805	2.099
145.0	-3.939	1.680	0.101E-04	1.117	-0.586	2.257	902.0	-4.896	2.161
165.5	-4.016	1.713	0.108E-04	1.139	-0.598	2.303	912.6	-4.963	2.219
189.5	-4.040	1.743	0.848E-05	1.160	-0.601	2.349	922.6	-5.071	2.278
213.6	-4.109	1.767	0.857E-05	1.175	-0.612	2.380	930.5	-5.183	2.329
237.5	-4.127	1.790	0.630E-05	1.190	-0.614	2.414	938.5	-5.201	2.376
261.5	-4.143	1.810	0.575E-05	1.204	-0.617	2.446	947.5	-5.240	2.417
289.5	-4.180	1.831	0.493E-05	1.218	-0.619	2.478	956.5	-5.307	2.462
318.5	-4.179	1.854	0.526E-05	1.234	-0.622	2.514	965.5	-5.278	2.504
333.5	-4.205	1.882	0.375E-05	1.239	-0.626	2.524	975.5	-5.426	2.523
357.5	-4.209	1.867	0.137E-05	1.242	-0.627	2.532	982.5	-5.863	2.553
381.5	-4.227	1.890	0.630E-05	1.258	-0.629	2.567	992.5	-5.201	2.581
405.5	-4.237	1.903	0.356E-05	1.266	-0.631	2.586	1000.5	-5.448	2.608
429.5	-4.227	1.915	0.356E-05	1.275	-0.629	2.608	1008.5	-5.448	2.633
454.5	-4.236	1.926	0.289E-05	1.282	-0.631	2.625	1017.5	-5.539	2.658
482.0	-4.246	1.939	0.311E-05	1.290	-0.632	2.645	1029.0	-5.508	2.683
508.0	-4.254	1.949	0.253E-05	1.297	-0.633	2.660	1036.0	-5.597	2.706
534.0	-4.262	1.959	0.253E-05	1.304	-0.634	2.675	1043.0	-5.597	2.728
552.0	-4.272	1.971	0.475E-05	1.312	-0.636	2.695	1050.5	-5.323	2.742
578.0	-4.277	1.978	0.177E-05	1.317	-0.637	2.705	1058.5	-5.752	2.762
605.5	-4.283	1.986	0.191E-05	1.322	-0.638	2.717	1065.5	-5.716	2.782
630.5	-4.278	2.004	0.474E-05	1.334	-0.637	2.747	1072.5	-5.324	2.800
653.5	-4.301	2.009	0.143E-05	1.337	-0.640	2.752	1079.5	-5.844	2.815
677.5	-4.311	2.020	0.329E-05	1.345	-0.642	2.771	1086.5	-5.483	2.831
717.5	-4.324	2.037	0.240E-05	1.356	-0.674	2.772	1093.5	-5.553	2.856
741.5	-4.532	2.047	0.274E-05	1.363	-0.675	2.787	1098.5	-5.562	2.870
765.5	-4.538	2.056	0.220E-05	1.368	-0.676	2.799	1102.5	-5.658	2.884
796.5	-4.646	2.065	0.212E-05	1.375	-0.692	2.802	1108.5	-5.673	2.901
816.5	-4.652	2.072	0.263E-05	1.380	-0.693	2.814	1113.5	-5.580	2.912
837.5	-4.856	2.077	0.157E-05	1.383	-0.693	2.822	1118.5	-5.804	2.923
862.5	-4.861	2.083	0.158E-05	1.387	-0.694	2.831	1123.5	-5.801	2.936
885.5	-4.866	2.089	0.172E-05	1.391	-0.695	2.840	1128.5	-5.786	2.947
909.5	-4.870	2.095	0.185E-05	1.395	-0.695	2.849	1133.5	-5.783	2.959
933.5	-4.875	2.101	0.165E-05	1.399	-0.696	2.858	1138.5	-5.783	2.970
955.5	-4.887	2.111	0.208E-05	1.406	-0.697	2.873	1143.5	-5.687	2.985
985.5	-4.887	2.116	0.165E-05	1.409	-0.698	2.881	1148.5	-5.783	2.994
1006.5	-4.889	2.119	0.988E-06	1.411	-0.698	2.886	1152.5	-6.005	3.002
1029.5	-4.895	2.125	0.192E-05	1.415	-0.699	2.896	1156.5	-5.717	3.013

AVLIN EQUATION NUMBER 2

Y = -2.434335 - 1.200763 X - .2726175E-01 X\*\*2 + .1815100E-01 X\*\*3

T-VALUES ARE : 17.7362 0.2677 0.6815  
 RSQUARE = 0.9735 STD. ERR. OF EST. = .1326715



GEOTECHNICAL LABORATORIES  
DEPARTMENT OF CIVIL ENGINEERING  
UNIVERSITY OF MANITOBA

CONSTANT MEAN NORMAL STRESS MULTI-STAGE  
SHORT-TERM TRIAXIAL CREEP TEST  
MST6 -  $\sigma_m = 70 \text{ kPa}$

LOAD INCREMENT # 1 S.D.: 0 KPA									
TIME (HOURS)	VOL DISPL (CC)	AXIAL DISPL (MM)	STRAIN RATE (/HR)	TRUE AXIAL STRAIN %	TRUE VOL. STRAIN %	DEVIATORIC STRAIN %	CUMULATIVE TIME (HRS)	LOGSTRAIN RATE/HOUR	LOGTIME HOURS
0.0	0.880	0.0	0.0	0.0	0.144	0.117	0.0	0.0	0.0
0.1	-1.122	0.003	0.333E-03	0.002	-0.165	0.129	0.1	-3.478	-1.097
0.6	-1.324	0.009	0.698E-04	0.006	-0.195	0.145	0.6	-4.157	-0.237
2.6	-1.382	0.027	0.610E-04	0.018	-0.203	0.122	2.6	-4.215	0.412
6.1	-1.482	0.027	0.0	0.018	-0.218	0.134	6.1	0.0	0.0
21.6	-1.716	0.036	0.412E-05	0.024	-0.253	0.146	21.6	-5.385	1.334
45.6	-2.034	0.031	-0.145E-05	0.021	-0.289	0.183	45.6	0.0	0.0
71.1	-2.234	0.031	0.0	0.021	-0.329	0.217	71.1	0.0	0.0
88.1	-2.336	0.035	0.851E-06	0.023	-0.344	0.224	88.1	-6.065	1.992
117.6	-2.387	0.038	0.119E-05	0.026	-0.359	0.234	117.6	-5.926	2.070
141.6	-2.436	0.036	-0.482E-06	0.024	-0.359	0.234	141.6	0.0	0.0
165.6	-2.487	0.037	0.243E-06	0.025	-0.366	0.233	165.6	0.0	0.0
189.6	-2.488	0.040	0.725E-06	0.027	-0.365	0.238	189.6	-6.614	2.219
213.6	-2.539	0.042	0.725E-06	0.028	-0.374	0.236	213.6	-6.139	2.278
240.6	-2.639	0.043	0.212E-06	0.028	-0.388	0.246	240.6	-6.139	2.330
269.6	-2.690	0.044	0.201E-06	0.030	-0.396	0.251	269.6	-6.674	2.381
285.6	-2.691	0.046	0.727E-06	0.031	-0.396	0.248	285.6	-6.696	2.431
309.6	-2.741	0.047	0.243E-06	0.031	-0.404	0.253	309.6	-6.139	2.456
324.6	-2.736	0.036	-0.279E-05	0.024	-0.403	0.289	324.6	-6.614	2.481
357.6	-2.738	0.041	0.126E-05	0.027	-0.403	0.282	357.6	0.0	0.0
381.6	-2.738	0.041	0.0	0.027	-0.403	0.262	381.6	-5.800	2.553
407.6	-2.789	0.042	0.0	0.028	-0.411	0.266	407.6	0.0	0.0
438.6	-2.887	0.038	0.449E-06	0.026	-0.425	0.285	438.6	-6.347	2.610
457.6	-2.792	0.049	-0.939E-06	0.033	-0.411	0.255	457.6	0.0	0.0
477.6	-2.841	0.045	0.398E-05	0.031	-0.418	0.266	477.6	-5.401	2.660
501.6	-3.035	0.034	-0.116E-05	0.023	-0.447	0.310	501.6	0.0	0.0
527.1	-2.935	0.033	-0.339E-05	0.022	-0.432	0.299	527.1	0.0	0.0
550.1	-2.834	0.032	-0.229E-06	0.021	-0.418	0.288	550.1	0.0	0.0
575.6	-2.839	0.042	0.250E-05	0.028	-0.418	0.273	575.6	-5.602	2.760
599.6	-2.742	0.048	0.194E-05	0.033	-0.404	0.250	599.6	-5.713	2.778
621.6	-2.743	0.052	0.105E-05	0.035	-0.404	0.245	621.6	-5.977	2.794
645.6	-2.743	0.052	0.0	0.035	-0.404	0.245	645.6	0.0	0.0
669.6	-2.743	0.052	0.0	0.035	-0.404	0.245	669.6	0.0	0.0
695.6	-2.739	0.042	-0.268E-05	0.028	-0.403	0.261	695.6	0.0	0.0
717.6	-2.740	0.045	0.106E-05	0.030	-0.404	0.256	717.6	-5.976	2.856
744.6	-2.743	0.052	0.172E-05	0.035	-0.404	0.245	744.6	-5.764	2.872
767.6	-2.843	0.051	-0.249E-06	0.034	-0.419	0.258	767.6	0.0	0.0
789.6	-2.744	0.053	0.526E-06	0.035	-0.404	0.243	789.6	-6.279	2.897

LOAD INCREMENT # 2 S.D.: 49 KPA									
TIME (HOURS)	VOL DISPL (CC)	AXIAL DISPL (MM)	STRAIN RATE (/HR)	TRUE AXIAL STRAIN %	TRUE VOL. STRAIN %	DEVIATORIC STRAIN %	CUMULATIVE TIME (HRS)	LOGSTRAIN RATE/HOUR	LOGTIME HOURS
0.0	0.182	0.084	0.566E-01	0.057	0.027	0.181	0.0	-1.247	-2.000
0.1	0.182	0.085	0.835E-04	0.057	0.027	0.182	0.1	-4.078	-1.097
0.5	0.177	0.096	0.180E-03	0.055	0.026	0.180	0.5	-3.745	-0.201
1.5	0.269	0.114	0.115E-03	0.076	0.040	0.219	1.5	-3.935	0.176
3.5	0.170	0.112	-0.579E-05	0.075	0.025	0.205	3.5	0.0	0.0
5.5	0.171	0.108	-0.116E-04	0.073	0.025	0.199	5.5	-5.385	1.334
9.5	0.169	0.114	0.871E-05	0.076	0.025	0.207	9.5	-5.060	0.978
22.0	0.186	0.121	0.373E-05	0.081	0.024	0.218	22.0	-5.429	1.342

LOAD INCREMENT # 3 S.D.: 73 KPA									
TIME (HOURS)	VOL DISPL (CC)	AXIAL DISPL (MM)	STRAIN RATE (/HR)	TRUE AXIAL STRAIN %	TRUE VOL. STRAIN %	DEVIATORIC STRAIN %	CUMULATIVE TIME (HRS)	LOGSTRAIN RATE/HOUR	LOGTIME HOURS
0.0	0.073	0.104	0.699E-01	0.070	0.011	0.180	22.0	-1.155	-2.000
0.1	0.076	0.099	-0.317E-03	0.066	0.011	0.172	22.1	-4.078	-1.097
0.4	0.074	0.102	0.826E-04	0.089	0.011	0.177	22.4	-4.034	-0.432
0.6	0.054	0.103	0.234E-04	0.069	0.008	0.176	22.6	-4.631	-0.208
1.1	0.053	0.105	0.234E-04	0.070	0.008	0.179	23.1	-4.631	0.049
2.1	0.053	0.105	0.0	0.070	0.008	0.179	24.1	-5.385	1.334
3.1	0.067	0.118	0.872E-04	0.079	0.010	0.202	25.1	-4.059	0.494
5.1	0.071	0.108	-0.320E-04	0.073	0.010	0.187	27.1	-5.429	1.342
7.1	0.072	0.108	-0.286E-05	0.072	0.010	0.186	28.1	-6.065	1.992
11.1	0.070	0.111	0.579E-05	0.075	0.010	0.191	33.1	-5.238	1.046
23.1	0.066	0.120	0.485E-05	0.080	0.010	0.205	45.1	-5.315	1.364

LOAD INCREMENT # 4 S.D.: 98 KPA									
TIME (HOURS)	VOL DISPL (CC)	AXIAL DISPL (MM)	STRAIN RATE (/HR)	TRUE AXIAL STRAIN %	TRUE VOL. STRAIN %	DEVIATORIC STRAIN %	CUMULATIVE TIME (HRS)	LOGSTRAIN RATE/HOUR	LOGTIME HOURS
0.0	-0.103	0.095	0.641E-01	0.084	-0.015	0.145	45.1	-1.193	-2.000
0.1	-0.152	0.095	-0.818E-04	0.084	-0.023	0.137	45.2	-4.078	-1.097
0.3	-0.152	0.095	0.0	0.084	-0.023	0.137	45.4	-4.034	-0.432
0.6	-0.182	0.094	-0.234E-04	0.063	-0.027	0.132	45.7	-4.631	-0.208
1.1	-0.184	0.098	0.580E-04	0.066	-0.027	0.139	46.2	-4.237	0.033
2.1	-0.186	0.103	0.349E-04	0.069	-0.028	0.147	47.2	-4.457	0.316
3.1	-0.111	0.115	0.756E-04	0.077	-0.016	0.175	48.2	-4.122	0.469
5.1	-0.108	0.107	-0.282E-04	0.072	-0.016	0.163	50.2	-5.429	1.342
7.1	-0.108	0.107	0.0	0.072	-0.016	0.163	52.2	-6.065	1.992
12.1	-0.109	0.110	0.485E-05	0.074	-0.016	0.188	57.2	-5.332	1.082
23.1	-0.113	0.118	0.476E-05	0.079	-0.017	0.181	68.2	-5.323	1.363

LOAD INCREMENT # 5 S.D.# 122 KPA

TIME (HOURS)	VOL DISPL (CC)	AXIAL DISPL (MM)	STRAIN RATE (/HR)	TRUE AXIAL STRAIN %	TRUE VOL. STRAIN %	DEVIATORIC STRAIN %	CUMULATIVE TIME (HRS)	LOGSTRAIN RATE/HOUR	LOGTIME HOURS
0.0	-0.202	0.116	0.778E-01	0.078	-0.030	0.166	68.2	-1.110	-2.000
0.1	-0.200	0.111	-0.284E-03	0.075	-0.030	0.159	68.3	-4.078	-1.097
0.4	-0.200	0.111	0.0	0.075	-0.030	0.159	68.5	-4.034	-0.432
0.6	-0.220	0.111	0.0	0.075	-0.032	0.157	68.8	-4.831	-0.208
1.1	-0.200	0.112	0.117E-04	0.075	-0.030	0.160	69.3	-4.932	0.041
2.1	-0.200	0.112	0.0	0.075	-0.030	0.160	70.3	-4.457	0.318
3.1	-0.155	0.122	0.839E-04	0.082	-0.023	0.182	71.3	-4.195	0.491
5.1	-0.154	0.120	-0.579E-05	0.081	-0.023	0.179	73.3	-5.429	1.342
7.1	-0.154	0.120	0.0	0.081	-0.023	0.179	75.3	-6.065	1.892
24.1	-0.108	0.129	0.376E-05	0.087	-0.016	0.200	92.3	-5.425	1.362

LOAD INCREMENT # 6 S.D.# 147 KPA

TIME (HOURS)	VOL DISPL (CC)	AXIAL DISPL (MM)	STRAIN RATE (/HR)	TRUE AXIAL STRAIN %	TRUE VOL. STRAIN %	DEVIATORIC STRAIN %	CUMULATIVE TIME (HRS)	LOGSTRAIN RATE/HOUR	LOGTIME HOURS
0.0	-0.088	0.129	0.885E-01	0.088	-0.013	0.201	92.3	-1.063	-2.000
0.1	-0.088	0.130	0.650E-04	0.087	-0.013	0.203	92.4	-4.187	-1.000
0.3	-0.087	0.128	-0.888E-04	0.086	-0.013	0.200	92.6	-4.034	-0.432
0.5	-0.136	0.125	-0.897E-04	0.084	-0.020	0.190	92.8	-4.831	-0.208
0.8	-0.137	0.128	0.597E-04	0.086	-0.020	0.194	93.1	-4.157	-0.114
1.3	-0.137	0.128	0.0	0.086	-0.020	0.194	93.6	-4.457	0.318
2.3	-0.096	0.146	0.122E-03	0.098	-0.014	0.229	94.6	-3.913	0.356
4.3	-0.144	0.142	-0.146E-04	0.095	-0.021	0.216	96.6	-5.429	1.342
6.3	-0.143	0.141	-0.289E-05	0.095	-0.021	0.215	98.6	-6.065	1.892
9.8	-0.096	0.147	0.116E-04	0.099	-0.014	0.230	102.1	-4.835	0.890
22.8	-0.049	0.154	0.358E-05	0.103	-0.007	0.247	115.1	-5.446	1.357

LOAD INCREMENT # 7 S.D.# 171 KPA

TIME (HOURS)	VOL DISPL (CC)	AXIAL DISPL (MM)	STRAIN RATE (/HR)	TRUE AXIAL STRAIN %	TRUE VOL. STRAIN %	DEVIATORIC STRAIN %	CUMULATIVE TIME (HRS)	LOGSTRAIN RATE/HOUR	LOGTIME HOURS
0.0	0.301	0.153	0.103E+00	0.103	0.044	0.288	115.1	-0.988	-2.000
0.1	0.351	0.155	0.130E-03	0.104	0.052	0.297	115.2	-3.886	-1.000
0.4	0.333	0.149	-0.163E-03	0.100	0.048	0.285	115.4	-4.034	-0.432
0.6	0.332	0.151	0.463E-04	0.101	0.049	0.288	115.7	-4.334	-0.222
1.1	0.351	0.154	0.485E-04	0.103	0.052	0.296	116.2	-4.332	0.041
2.1	0.400	0.156	0.118E-04	0.105	0.059	0.304	117.2	-4.934	0.322
7.1	0.497	0.164	0.105E-04	0.110	0.073	0.329	126.7	-4.934	0.851
11.6	0.493	0.171	0.116E-04	0.115	0.073	0.341	127.2	-5.342	1.064
23.1	0.490	0.179	0.455E-05	0.120	0.072	0.354	136.2	-5.446	1.364
26.1	0.540	0.179	0.0	0.120	0.080	0.360	141.2	-5.886	0.990
31.1	0.540	0.179	0.0	0.120	0.080	0.360	146.2	-5.446	1.357
35.6	0.739	0.180	0.130E-05	0.121	0.109	0.385	150.7	-5.819	1.551
47.1	0.838	0.182	0.152E-05	0.123	0.124	0.401	162.2	-6.139	1.673
55.1	0.839	0.180	-0.218E-05	0.121	0.124	0.397	170.2	-5.361	2.330
59.1	0.888	0.182	0.436E-05	0.123	0.131	0.407	174.2	-5.537	1.772
71.1	0.836	0.188	0.290E-05	0.126	0.123	0.410	186.2	-6.139	2.330
78.1	0.836	0.188	0.0	0.126	0.123	0.410	193.2	-5.537	2.456
82.1	0.836	0.188	0.0	0.126	0.123	0.410	197.2	-6.139	2.491
94.1	0.834	0.191	0.193E-05	0.128	0.123	0.415	209.2	-5.713	1.874
102.1	0.884	0.191	0.0	0.128	0.130	0.421	217.2	-5.900	2.553
118.6	0.982	0.196	0.211E-05	0.132	0.145	0.441	233.7	-5.675	2.074
142.6	1.126	0.208	0.339E-05	0.140	0.166	0.479	257.7	-5.469	2.154
179.1	1.322	0.218	0.175E-05	0.147	0.195	0.518	294.2	-5.756	2.253
191.1	1.218	0.227	0.484E-05	0.152	0.180	0.520	306.2	-5.315	2.281
217.1	1.312	0.240	0.336E-05	0.161	0.194	0.553	332.2	-5.474	2.337
239.6	1.411	0.244	0.129E-05	0.164	0.208	0.571	354.7	-5.889	2.379
262.6	1.507	0.253	0.253E-05	0.170	0.222	0.597	377.7	-5.597	2.419
287.1	1.602	0.263	0.285E-05	0.177	0.236	0.626	402.2	-5.545	2.458
310.6	1.652	0.263	0.0	0.177	0.244	0.632	425.7	-5.602	2.760
337.1	1.597	0.275	0.307E-05	0.185	0.235	0.645	452.2	-5.513	2.528
380.1	1.595	0.279	0.101E-05	0.187	0.235	0.645	475.2	-5.995	2.556
383.1	1.639	0.282	0.379E-05	0.196	0.242	0.677	498.2	-5.421	2.583
407.1	1.638	0.294	0.729E-06	0.198	0.241	0.681	522.2	-5.137	2.811
431.1	1.585	0.301	0.194E-05	0.202	0.234	0.686	546.2	-5.714	2.880
455.1	1.684	0.303	0.485E-06	0.204	0.248	0.701	570.2	-5.314	2.835
478.1	1.731	0.309	0.177E-05	0.208	0.255	0.717	593.2	-5.752	2.858
505.1	1.777	0.318	0.237E-05	0.214	0.262	0.738	620.2	-5.625	2.703
530.1	1.864	0.348	0.792E-05	0.234	0.275	0.797	645.2	-5.101	2.724
551.1	1.974	0.326	-0.693E-05	0.219	0.291	0.775	666.2	0.0	0.0
575.1	2.072	0.329	0.727E-06	0.221	0.305	0.791	690.2	-6.139	2.760
599.1	2.072	0.330	0.463E-06	0.222	0.305	0.793	714.2	-6.316	2.777
623.1	2.067	0.340	0.267E-05	0.229	0.305	0.809	738.2	-5.574	2.795
647.1	2.183	0.349	0.267E-05	0.235	0.319	0.836	762.2	-5.573	2.811
672.6	2.180	0.349	0.205E-05	0.240	0.318	0.848	787.7	-5.687	2.828
697.6	2.305	0.368	0.303E-05	0.248	0.340	0.884	812.7	-5.519	2.844
719.1	2.350	0.378	0.288E-05	0.254	0.346	0.905	834.2	-5.526	2.857
746.1	2.434	0.406	0.690E-05	0.273	0.359	0.962	861.2	-5.161	2.873

GEOTECHNICAL LABORATORIES  
DEPARTMENT OF CIVIL ENGINEERING  
UNIVERSITY OF MANITOBA

CONSTANT MEAN NORMAL STRESS MULTI-STAGE  
SHORT-TERM TRIAXIAL CREEP TEST  
MST7 -  $\bar{\sigma}_m=140$  kPa

LOAD INCREMENT # 1 S.D.# 0 KPA									
TIME (HOURS)	VOL DISPL (CC)	AXIAL DISPL (MM)	STRAIN RATE (/HR)	TRUE AXIAL STRAIN %	TRUE VOL. STRAIN %	DEVIATORIC STRAIN %	CUMULATIVE TIME (HRS)	LOGSTRAIN RATE/HOUR	LOGTIME HOURS
0.0	-2.343	0.054	0.365E-01	0.037	-0.346	0.193	0.0	-1.438	-2.000
0.3	-2.543	0.054	0.0	0.037	-0.376	0.217	0.3	0.0	0.0
0.5	-2.648	0.060	0.154E-03	0.040	-0.391	0.221	0.5	-3.812	-0.276
1.3	-2.842	0.052	-0.713E-04	0.035	-0.420	0.257	1.3	0.0	0.0
2.3	-2.992	0.052	0.0	0.035	-0.442	0.275	2.3	0.0	0.0
7.8	-3.146	0.058	0.701E-05	0.039	-0.465	0.284	7.8	-5.154	0.889
23.3	-3.409	0.073	0.661E-05	0.049	-0.504	0.291	23.3	-5.180	1.385
47.3	-3.712	0.078	0.134E-05	0.053	-0.549	0.319	47.3	-5.874	1.674
72.8	-4.015	0.081	0.751E-06	0.054	-0.594	0.351	72.8	-6.125	1.852
100.3	-4.172	0.091	0.233E-05	0.061	-0.617	0.355	100.3	-5.633	2.001
119.2	-4.276	0.095	0.169E-05	0.064	-0.632	0.359	119.2	-5.772	2.076
143.2	-4.380	0.100	0.134E-05	0.067	-0.648	0.364	143.2	-5.874	2.156
167.2	-4.485	0.107	0.187E-05	0.072	-0.663	0.366	167.2	-5.729	2.233
191.2	-4.590	0.113	0.161E-05	0.078	-0.679	0.369	191.2	-5.794	2.262
215.2	-4.692	0.115	0.800E-06	0.080	-0.694	0.377	215.2	-6.097	2.333
242.2	-4.795	0.119	0.848E-06	0.080	-0.709	0.383	242.2	-6.023	2.384
271.2	-5.000	0.125	0.133E-05	0.084	-0.746	0.388	271.2	-5.877	2.433
287.2	-5.052	0.128	0.120E-05	0.086	-0.748	0.400	287.2	-5.919	2.458
311.2	-5.103	0.129	0.268E-06	0.087	-0.755	0.405	311.2	-6.571	2.493
336.2	-5.195	0.119	-0.257E-05	0.080	-0.769	0.432	336.2	0.0	0.0
359.2	-5.250	0.125	0.167E-05	0.084	-0.777	0.429	359.2	-5.777	2.555
383.2	-5.347	0.121	-0.107E-05	0.081	-0.791	0.447	383.2	0.0	0.0
408.2	-5.445	0.119	-0.513E-06	0.080	-0.806	0.462	408.2	0.0	0.0
440.2	-5.541	0.114	-0.989E-06	0.077	-0.820	0.481	440.2	0.0	0.0
459.2	-5.508	0.135	0.742E-05	0.091	-0.815	0.443	459.2	-5.130	2.862
479.2	-5.595	0.119	-0.545E-05	0.080	-0.828	0.460	479.2	0.0	0.0
503.2	-5.845	0.119	0.0	0.080	-0.866	0.511	503.2	0.0	0.0
528.7	-5.886	0.108	-0.302E-05	0.072	-0.842	0.510	528.7	0.0	0.0
551.7	-5.735	0.107	-0.280E-06	0.072	-0.849	0.518	551.7	0.0	0.0
577.2	-5.739	0.112	0.126E-05	0.075	-0.850	0.510	577.2	-5.900	2.761
601.2	-5.696	0.120	0.241E-05	0.081	-0.843	0.491	601.2	-5.619	2.779
623.2	-5.744	0.117	-0.878E-06	0.079	-0.850	0.501	623.2	0.0	0.0
647.2	-5.799	0.124	0.187E-05	0.083	-0.859	0.497	647.2	-5.728	2.811
671.2	-5.846	0.113	-0.107E-05	0.081	-0.866	0.509	671.2	0.0	0.0
697.2	-5.890	0.113	-0.197E-05	0.076	-0.872	0.527	697.2	0.0	0.0
719.2	-5.891	0.114	0.290E-06	0.076	-0.872	0.525	719.2	-6.537	2.857
746.2	-5.944	0.117	0.348E-06	0.079	-0.880	0.526	746.2	-6.023	2.873
769.2	-6.047	0.122	0.140E-05	0.082	-0.898	0.530	769.2	-5.855	2.886
791.2	-5.949	0.124	0.563E-06	0.083	-0.881	0.515	791.2	-6.234	2.898

LOAD INCREMENT # 2 S.D.# 49 KPA									
TIME (HOURS)	VOL DISPL (CC)	AXIAL DISPL (MM)	STRAIN RATE (/HR)	TRUE AXIAL STRAIN %	TRUE VOL. STRAIN %	DEVIATORIC STRAIN %	CUMULATIVE TIME (HRS)	LOGSTRAIN RATE/HOUR	LOGTIME HOURS
0.0	0.023	0.260	0.175E+00	0.175	0.003	0.432	0.0	-0.786	-2.000
0.1	0.021	0.262	0.183E-03	0.177	0.003	0.435	0.1	-3.737	-1.097
0.4	0.013	0.272	0.208E-03	0.184	0.002	0.451	0.4	-3.682	-0.377
1.4	0.042	0.298	0.174E-03	0.201	0.006	0.487	1.4	-3.760	0.152
3.4	-0.055	0.294	-0.129E-04	0.188	-0.008	0.479	3.4	0.0	0.0
5.4	-0.105	0.294	0.0	0.188	-0.016	0.473	5.4	-5.154	0.889
9.4	-0.109	0.300	0.966E-05	0.202	-0.016	0.482	9.4	-5.015	0.974
21.9	-0.169	0.313	0.669E-05	0.211	-0.025	0.485	21.9	-5.174	1.341

LOAD INCREMENT # 3 S.D.# 98 KPA									
TIME (HOURS)	VOL DISPL (CC)	AXIAL DISPL (MM)	STRAIN RATE (/HR)	TRUE AXIAL STRAIN %	TRUE VOL. STRAIN %	DEVIATORIC STRAIN %	CUMULATIVE TIME (HRS)	LOGSTRAIN RATE/HOUR	LOGTIME HOURS
0.0	-0.236	0.296	0.200E+00	0.200	-0.035	0.460	21.9	-0.700	-2.000
0.1	-0.244	0.306	0.919E-03	0.206	-0.036	0.475	22.0	-3.037	-1.097
0.3	-0.238	0.298	-0.303E-03	0.201	-0.035	0.463	22.2	-3.682	-0.377
0.5	-0.268	0.298	0.0	0.201	-0.040	0.459	22.4	-3.760	0.152
1.0	-0.272	0.304	0.772E-04	0.205	-0.041	0.468	22.9	-4.113	0.0
2.0	-0.275	0.308	0.257E-04	0.207	-0.041	0.474	23.9	-4.589	0.301
3.0	-0.250	0.313	0.386E-04	0.211	-0.037	0.487	24.9	-4.414	0.477
5.0	-0.249	0.312	-0.317E-05	0.211	-0.037	0.485	26.9	-5.174	1.341
7.0	-0.249	0.312	0.0	0.211	-0.037	0.485	28.9	-6.125	1.862
11.0	-0.255	0.320	0.129E-04	0.216	-0.038	0.497	32.9	-4.891	1.041
23.0	-0.267	0.334	0.805E-05	0.225	-0.040	0.520	44.9	-5.094	1.362

LOAD INCREMENT # 4 S.D.# 147 KPA									
TIME (HOURS)	VOL DISPL (CC)	AXIAL DISPL (MM)	STRAIN RATE (/HR)	TRUE AXIAL STRAIN %	TRUE VOL. STRAIN %	DEVIATORIC STRAIN %	CUMULATIVE TIME (HRS)	LOGSTRAIN RATE/HOUR	LOGTIME HOURS
0.0	-0.330	0.326	0.220E+00	0.220	-0.049	0.498	44.9	-0.658	-2.000
0.1	-0.330	0.326	0.0	0.220	-0.049	0.498	45.0	-3.037	-1.097
0.3	-0.331	0.328	0.516E-04	0.221	-0.048	0.501	45.2	-4.287	-0.481
0.6	-0.331	0.328	0.0	0.221	-0.049	0.501	45.5	-3.760	0.152
1.1	-0.337	0.335	0.989E-04	0.226	-0.050	0.513	46.0	-4.005	0.041
2.1	-0.345	0.345	0.644E-04	0.233	-0.051	0.528	47.0	-4.191	0.322
3.1	-0.355	0.357	0.837E-04	0.241	-0.053	0.547	48.0	-4.077	0.481
5.1	-0.403	0.355	-0.985E-05	0.249	-0.050	0.536	50.0	-5.174	1.341
7.1	-0.410	0.363	0.289E-04	0.245	-0.051	0.550	52.0	-4.538	0.851
12.1	-0.417	0.373	0.129E-04	0.251	-0.052	0.565	57.0	-4.890	1.083
23.1	-0.435	0.395	0.135E-04	0.266	-0.055	0.599	66.0	-4.871	1.364



## LOAD INCREMENT # 5 S.D. : 196 KPA

TIME (HOURS)	VOL DISPL (CC)	AXIAL DISPL (MM)	STRAIN RATE (/HR)	TRUE STRAIN %	AXIAL STRAIN %	TRUE VOL. STRAIN %	DEVIATORIC STRAIN %	CUMULATIVE TIME (HRS)	LOGSTRAIN RATE/HOUR	LOGTIME HOURS
0.0	-0.564	0.394	0.268E+00	0.255	-0.084	0.523	68.0	-0.575	-2.000	
0.1	-0.588	0.399	0.536E-03	0.269	-0.085	0.590	68.1	-3.271	-1.155	
0.3	-0.568	0.399	0.0	0.259	-0.085	0.590	68.3	-4.287	-0.481	
0.6	-0.570	0.401	0.514E-04	0.270	-0.086	0.593	68.6	-4.289	-0.244	
1.1	-0.576	0.408	0.103E-03	0.276	-0.086	0.605	69.1	-3.986	0.029	
2.1	-0.580	0.414	0.375E-04	0.279	-0.086	0.614	70.1	-4.428	0.322	
3.1	-0.592	0.429	0.888E-04	0.289	-0.088	0.636	71.1	-4.015	0.481	
5.1	-0.588	0.437	0.290E-04	0.295	-0.089	0.649	73.1	-4.538	0.708	
7.1	-0.605	0.445	0.258E-04	0.300	-0.090	0.661	75.1	-4.588	0.851	
24.1	-0.643	0.493	0.190E-04	0.332	-0.096	0.736	92.1	-4.722	1.382	

## LOAD INCREMENT # 6 S.D. : 245 KPA

TIME (HOURS)	VOL DISPL (CC)	AXIAL DISPL (MM)	STRAIN RATE (/HR)	TRUE STRAIN %	AXIAL STRAIN %	TRUE VOL. STRAIN %	DEVIATORIC STRAIN %	CUMULATIVE TIME (HRS)	LOGSTRAIN RATE/HOUR	LOGTIME HOURS
0.0	-0.768	0.499	0.337E+00	0.337	-0.114	0.731	82.1	-0.473	-2.000	
0.1	-0.789	0.501	0.184E-03	0.338	-0.115	0.734	82.2	-3.736	-1.097	
0.2	-0.771	0.503	0.144E-03	0.339	-0.115	0.737	82.3	-3.843	-0.770	
0.4	-0.821	0.503	0.0	0.339	-0.122	0.731	82.5	-4.289	-0.244	
0.7	-0.826	0.508	0.155E-03	0.343	-0.123	0.740	82.8	-3.811	-0.174	
1.2	-0.832	0.516	0.103E-03	0.348	-0.124	0.752	83.3	-3.967	0.068	
2.2	-0.802	0.542	0.189E-03	0.366	-0.119	0.798	84.3	-3.772	0.342	
4.2	-0.812	0.554	0.419E-04	0.374	-0.121	0.817	86.3	-4.378	0.623	
6.2	-0.826	0.572	0.580E-04	0.386	-0.123	0.844	88.3	-4.236	0.792	
9.7	-0.847	0.588	0.516E-04	0.404	-0.126	0.866	101.8	-4.288	0.987	
22.7	-0.894	0.658	0.308E-04	0.444	-0.133	0.878	114.8	-4.512	1.356	

## LOAD INCREMENT # 7 S.D. : 294 KPA

TIME (HOURS)	VOL DISPL (CC)	AXIAL DISPL (MM)	STRAIN RATE (/HR)	TRUE STRAIN %	AXIAL STRAIN %	TRUE VOL. STRAIN %	DEVIATORIC STRAIN %	CUMULATIVE TIME (HRS)	LOGSTRAIN RATE/HOUR	LOGTIME HOURS
0.0	-0.999	0.663	0.447E+00	0.447	-0.149	0.974	114.8	-0.348	-2.000	
0.1	-1.005	0.672	0.830E-03	0.453	-0.150	0.988	114.9	-3.081	-1.097	
0.3	-1.035	0.672	0.0	0.453	-0.154	0.984	115.1	-3.843	-0.770	
0.5	-1.039	0.675	0.103E-03	0.456	-0.155	0.990	115.3	-3.986	-0.301	
1.0	-1.048	0.687	0.155E-03	0.463	-0.156	1.008	115.8	-3.810	0.0	
2.0	-1.029	0.701	0.968E-04	0.473	-0.153	1.034	116.8	-4.014	0.301	
7.0	-1.030	0.765	0.865E-04	0.516	-0.153	1.140	121.6	-4.063	0.845	
11.5	-1.063	0.806	0.617E-04	0.544	-0.158	1.204	126.3	-4.210	1.061	
23.0	-1.120	0.878	0.421E-04	0.593	-0.167	1.315	137.8	-4.375	1.362	

## LOAD INCREMENT # 8 S.D. : 343 KPA

TIME (HOURS)	VOL DISPL (CC)	AXIAL DISPL (MM)	STRAIN RATE (/HR)	TRUE STRAIN %	AXIAL STRAIN %	TRUE VOL. STRAIN %	DEVIATORIC STRAIN %	CUMULATIVE TIME (HRS)	LOGSTRAIN RATE/HOUR	LOGTIME HOURS
0.0	0.842	0.888	0.800E+00	0.600	0.125	1.571	137.8	-0.222	-2.000	
0.3	0.941	0.889	0.267E+04	0.600	0.140	1.584	138.1	-4.573	-0.802	
0.5	0.935	0.897	0.207E+03	0.605	0.139	1.595	138.3	-3.685	-0.301	
2.3	0.913	0.924	0.107E+03	0.624	0.136	1.640	140.1	-3.970	0.352	
7.3	1.154	0.999	0.101E+03	0.675	0.171	1.792	145.1	-3.996	0.860	
10.8	1.313	1.050	0.998E-04	0.709	0.195	1.897	148.6	-4.001	1.031	
22.3	1.439	1.143	0.546E-04	0.772	0.214	2.066	160.1	-4.263	1.347	
30.3	1.455	1.186	0.364E-04	0.801	0.216	2.139	168.1	-4.439	1.481	
46.3	1.442	1.264	0.332E-04	0.854	0.214	2.268	184.1	-4.479	1.665	
58.3	1.450	1.316	0.297E-04	0.890	0.215	2.356	195.1	-4.527	1.785	
70.3	1.507	1.371	0.308E-04	0.927	0.224	2.454	208.1	-4.512	1.847	
94.8	1.737	1.458	0.244E-04	0.987	0.258	2.628	232.6	-4.613	1.977	
118.7	1.929	1.531	0.205E-04	1.036	0.287	2.772	256.6	-4.687	2.075	
155.2	2.407	1.622	0.169E-04	1.098	0.357	2.981	293.1	-4.772	2.191	
167.2	2.232	1.653	0.179E-04	1.119	0.332	3.012	305.1	-4.748	2.223	
193.2	2.327	1.722	0.180E-04	1.166	0.346	3.138	331.1	-4.745	2.286	
215.7	2.534	1.776	0.165E-04	1.203	0.376	3.254	353.6	-4.783	2.334	
228.7	2.685	1.836	0.178E-04	1.244	0.399	3.373	375.6	-4.749	2.378	
263.2	2.835	1.900	0.161E-04	1.287	0.421	3.497	401.1	-4.750	2.420	
286.7	2.941	1.956	0.165E-04	1.325	0.435	3.603	424.6	-4.794	2.458	
313.2	2.740	2.019	0.165E-04	1.369	0.407	3.685	451.1	-4.784	2.496	
336.2	2.735	2.088	0.204E-04	1.416	0.406	3.798	474.1	-4.891	2.527	
380.2	2.841	2.144	0.157E-04	1.454	0.422	3.905	496.1	-4.803	2.557	
384.2	2.893	2.204	0.171E-04	1.495	0.444	4.024	522.1	-4.767	2.585	
408.2	2.992	2.268	0.182E-04	1.538	0.444	4.131	546.1	-4.740	2.611	
432.2	3.091	2.331	0.182E-04	1.582	0.459	4.250	570.1	-4.740	2.636	
455.7	3.240	2.395	0.186E-04	1.626	0.481	4.375	593.6	-4.730	2.669	
482.2	3.384	2.466	0.182E-04	1.674	0.502	4.511	620.1	-4.739	2.683	
507.2	3.612	2.557	0.248E-04	1.736	0.536	4.690	645.1	-4.605	2.705	
528.2	3.880	2.596	0.128E-04	1.763	0.576	4.788	666.1	-4.894	2.723	
552.2	4.120	2.671	0.215E-04	1.815	0.611	4.944	690.1	-4.667	2.742	
576.2	4.185	2.741	0.199E-04	1.862	0.618	5.066	714.1	-4.701	2.761	
600.2	4.402	2.819	0.224E-04	1.916	0.653	5.226	738.1	-4.650	2.778	
624.2	4.434	2.905	0.246E-04	1.975	0.657	5.374	762.1	-4.610	2.795	
649.2	4.573	2.981	0.210E-04	2.027	0.678	5.520	787.1	-4.678	2.812	
674.7	4.912	3.058	0.206E-04	2.080	0.728	5.689	812.6	-4.687	2.829	
691.7	5.003	3.132	0.301E-04	2.131	0.742	5.825	829.6	-4.521	2.840	
718.7	5.262	3.246	0.292E-04	2.210	0.780	6.049	856.6	-4.535	2.857	

GEOTECHNICAL LABORATORIES  
DEPARTMENT OF CIVIL ENGINEERING  
UNIVERSITY OF MANITOBA

CONSTANT MEAN NORMAL STRESS MULTI-STAGE  
SHORT-TERM TRIAXIAL CREEP TEST  
MST8 -  $\bar{\sigma}_m = 280 \text{ kPa}$

LOAD INCREMENT # 1 S.D.: 0 KPA

TIME (HOURS)	VOL DISPL (CC)	AXIAL DISPL (MM)	STRAIN RATE (MM/HR)	TRUE AXIAL STRAIN %	TRUE VOL. STRAIN %	DEVIATORIC STRAIN %	CUMULATIVE TIME (HRS)	LOGSTRAIN RATE/HOUR	LOGTIME HOURS
0.0	-4.004	0.268	0.180E+00	0.180	-0.593	0.044	0.0	-0.746	-2.000
0.3	-4.154	0.011	-0.719E-02	0.007	-0.615	0.484	0.3	0.0	0.0
0.5	-4.197	-0.009	-0.517E-03	-0.006	-0.621	0.521	0.5	0.0	0.0
2.0	-4.282	-0.022	-0.579E-04	-0.014	-0.635	0.554	2.0	0.0	0.0
7.0	-4.309	-0.028	-0.892E-05	-0.015	-0.638	0.568	7.0	0.0	0.0
11.0	-4.341	-0.023	0.107E-04	-0.015	-0.643	0.562	11.0	-4.970	1.041
23.0	-4.447	-0.009	0.779E-05	-0.008	-0.658	0.552	23.0	-5.109	1.362
30.0	-4.444	-0.014	-0.531E-05	-0.009	-0.658	0.560	30.0	0.0	0.0
48.0	-4.597	-0.007	0.275E-05	-0.004	-0.681	0.567	48.0	-5.560	1.681
80.0	-4.869	0.048	0.114E-04	0.032	-0.721	0.510	80.0	-4.943	1.903
99.0	-4.755	0.013	-0.124E-04	0.008	-0.704	0.554	99.0	0.0	0.0
119.0	-4.810	0.026	0.465E-05	0.018	-0.712	0.422	119.0	-5.333	2.076
143.0	-5.302	0.134	0.300E-04	0.090	-0.785	0.422	143.0	-5.523	2.155
168.5	-4.994	0.087	-0.122E-04	0.059	-0.740	0.480	168.5	0.0	0.0
191.5	-5.020	0.181	0.272E-04	0.121	-0.744	0.310	191.5	-4.565	2.282
217.0	-4.973	0.168	0.195E-05	0.126	-0.737	0.292	217.0	-5.710	2.336
241.0	-4.977	0.197	0.258E-05	0.132	-0.737	0.277	241.0	-5.588	2.382
263.0	-4.977	0.198	0.285E-06	0.133	-0.737	0.276	263.0	-6.545	2.420
311.0	-4.976	0.196	-0.778E-06	0.131	-0.737	0.280	311.0	0.0	0.0
337.0	-4.977	0.199	0.103E-05	0.134	-0.737	0.274	337.0	-5.985	2.493
359.0	-5.027	0.197	-0.477E-06	0.132	-0.744	0.283	359.0	0.0	0.0
386.0	-5.026	0.196	-0.564E-06	0.131	-0.744	0.285	386.0	0.0	0.0
408.0	-4.877	0.198	0.692E-06	0.133	-0.737	0.276	408.0	-6.160	2.587
431.0	-5.179	0.203	0.135E-05	0.136	-0.767	0.293	431.0	-5.871	2.612
	-4.980	0.206	0.846E-06	0.138	-0.738	0.264		-6.072	2.634

LOAD INCREMENT # 3 S.D.: 147 KPA

TIME (HOURS)	VOL DISPL (CC)	AXIAL DISPL (MM)	STRAIN RATE (MM/HR)	TRUE AXIAL STRAIN %	TRUE VOL. STRAIN %	DEVIATORIC STRAIN %	CUMULATIVE TIME (HRS)	LOGSTRAIN RATE/HOUR	LOGTIME HOURS
0.0	0.007	0.316	0.213E+00	0.213	0.001	0.522	23.5	-0.672	-2.000
0.1	0.007	0.318	0.177E-03	0.214	0.001	0.525	23.6	-3.751	-1.097
0.3	-0.041	0.313	-0.149E-03	0.210	-0.006	0.510	23.8	-3.534	-0.602
0.6	-0.094	0.320	0.199E-03	0.215	-0.014	0.515	24.1	-3.702	-0.237
0.8	-0.145	0.323	0.748E-04	0.217	-0.022	0.514	24.3	-4.126	-0.081
1.3	-0.169	0.332	0.124E-03	0.223	-0.025	0.526	24.8	-3.906	0.124
2.3	-0.170	0.335	0.187E-04	0.225	-0.025	0.531	25.8	-4.728	0.367
3.3	-0.152	0.339	0.311E-04	0.228	-0.023	0.540	26.8	-4.507	0.522
5.3	-0.103	0.343	0.124E-04	0.231	-0.015	0.552	28.8	-4.806	0.727
7.3	-0.101	0.338	-0.156E-04	0.228	-0.015	0.545	30.8	-4.963	1.041
11.3	-0.103	0.344	0.935E-05	0.231	-0.015	0.554	34.8	-5.029	1.054
23.3	-0.110	0.362	0.984E-05	0.243	-0.016	0.582	46.8	-5.007	1.368

AVLIN EQUATION NUMBER 2  
 Y = -4.210072 - .5408115 X + .1322600 X\*\*2 - .2246729 X\*\*3  
 T-VALUES ARE . 2.1124 0.8927 1.8553  
 RSQUARE = 0.9382 STD. ERR. OF EST. = .3517765

LOAD INCREMENT # 2 S.D.: 73 KPA

TIME (HOURS)	VOL DISPL (CC)	AXIAL DISPL (MM)	STRAIN RATE (MM/HR)	TRUE AXIAL STRAIN %	TRUE VOL. STRAIN %	DEVIATORIC STRAIN %	CUMULATIVE TIME (HRS)	LOGSTRAIN RATE/HOUR	LOGTIME HOURS
0.0	-0.031	0.286	0.192E+00	0.192	-0.005	0.467	0.0	-0.716	-2.000
0.1	-0.061	0.286	0.0	0.192	-0.008	0.464	0.1	0.0	0.0
0.3	-0.084	0.293	0.292E-03	0.197	-0.012	0.473	0.3	-3.534	-0.602
0.5	-0.087	0.303	0.249E-03	0.203	-0.013	0.488	0.5	-3.604	-0.301
1.0	-0.131	0.285	-0.236E-03	0.192	-0.018	0.454	1.0	0.0	0.0
2.0	-0.245	0.295	0.684E-04	0.198	-0.042	0.452	2.0	-4.165	0.301
3.0	-0.140	0.315	0.131E-03	0.212	-0.036	0.489	3.0	-3.884	0.477
5.0	-0.091	0.310	-0.158E-04	0.208	-0.021	0.493	5.0	0.0	0.0
7.0	-0.091	0.312	0.621E-05	0.210	-0.014	0.503	7.0	-5.207	0.845
11.0	0.007	0.318	0.108E-04	0.214	0.001	0.525	11.0	-4.963	1.041
23.5	0.001	0.331	0.697E-05	0.223	0.000	0.546	23.5	-5.157	1.371

AVLIN EQUATION NUMBER 1  
 Y = -2.180993 - 1.026749 X - .8716336 X\*\*2 + .3392593 X\*\*3  
 T-VALUES ARE : 0.5191 0.9569 0.3984  
 RSQUARE = 0.4523 STD. ERR. OF EST. = 1.939934

LOAD INCREMENT # 4 S.D. = 220 KPA

TIME (HOURS)	VOL DISPL (CC)	AXIAL DISPL (MM)	STRAIN RATE (MM/HR)	TRUE AXIAL STRAIN %	TRUE VOL. STRAIN %	DEVIATORIC STRAIN %	CUMULATIVE TIME (HRS)	LOGSTRAIN RATE/HOUR	LOGTIME HOURS
0.0	-0.120	0.360	0.242E+00	0.242	-0.018	0.579	46.8	-0.616	-2.000
0.1	-0.172	0.366	0.748E-03	0.246	-0.026	0.582	46.9	-3.126	-1.222
0.4	-0.175	0.374	0.165E-03	0.252	-0.026	0.595	47.2	-3.783	-0.398
1.4	-0.266	0.402	0.187E-03	0.270	-0.040	0.630	48.2	-3.729	0.146
2.4	-0.290	0.411	0.623E-04	0.277	-0.043	0.642	49.2	-4.206	0.380
3.4	-0.243	0.421	0.884E-04	0.283	-0.036	0.685	50.2	-4.185	0.531
5.4	-0.246	0.428	0.218E-04	0.288	-0.037	0.675	52.2	-4.662	0.732
7.4	-0.249	0.436	0.280E-04	0.293	-0.037	0.688	54.2	-4.553	0.869
12.4	-0.258	0.458	0.299E-04	0.308	-0.038	0.724	59.2	-4.525	1.093
23.4	-0.265	0.478	0.119E-04	0.321	-0.039	0.755	70.2	-4.925	1.369

AVLIN EQUATION NUMBER 3

$$Y = -4.021373 - .3324787 X + .1027710 X^{**2} - .2837694 X^{**3}$$

T-VALUES ARE : 1.8400 1.0421 3.4725  
 RSQUARE = 0.9774 STD. ERR. OF EST. = .2295523

LOAD INCREMENT # 5 S.D. = 294 KPA

TIME (HOURS)	VOL DISPL (CC)	AXIAL DISPL (MM)	STRAIN RATE (MM/HR)	TRUE AXIAL STRAIN %	TRUE VOL. STRAIN %	DEVIATORIC STRAIN %	CUMULATIVE TIME (HRS)	LOGSTRAIN RATE/HOUR	LOGTIME HOURS
0.0	-0.263	0.473	0.318E+00	0.318	-0.039	0.747	70.2	-0.498	-2.000
0.1	-0.264	0.474	0.179E-03	0.319	-0.039	0.750	70.3	-3.746	-1.097
0.3	-0.289	0.487	0.348E-03	0.328	-0.043	0.768	70.6	-3.458	-0.481
0.6	-0.290	0.491	0.995E-04	0.330	-0.043	0.774	70.8	-4.002	-0.237
0.8	-0.312	0.496	0.125E-03	0.333	-0.046	0.779	71.1	-3.904	-0.124
1.3	-0.344	0.501	0.749E-04	0.337	-0.051	0.784	71.6	-4.126	-0.081
2.3	-0.397	0.507	0.373E-04	0.341	-0.059	0.787	72.6	-4.428	0.167
3.3	-0.401	0.517	0.685E-04	0.348	-0.060	0.803	73.6	-4.164	0.522
5.3	-0.403	0.524	0.249E-04	0.353	-0.060	0.815	75.6	-4.603	0.727
7.3	-0.404	0.526	0.622E-05	0.354	-0.060	0.818	77.6	-5.206	0.865
24.3	-0.426	0.582	0.220E-04	0.391	-0.063	0.907	94.6	-4.658	1.386

AVLIN EQUATION NUMBER 4

$$Y = -4.181327 - .4472888 X + .2214018 X^{**2} - .2203997 X^{**3}$$

T-VALUES ARE : 1.4031 1.2497 1.5265  
 RSQUARE = 0.9159 STD. ERR. OF EST. = .4242845

LOAD INCREMENT # 6 S.D. = 387 KPA

TIME (HOURS)	VOL DISPL (CC)	AXIAL DISPL (MM)	STRAIN RATE (MM/HR)	TRUE AXIAL STRAIN %	TRUE VOL. STRAIN %	DEVIATORIC STRAIN %	CUMULATIVE TIME (HRS)	LOGSTRAIN RATE/HOUR	LOGTIME HOURS
0.0	-0.334	0.577	0.388E+00	0.388	-0.050	0.910	94.6	-0.411	-2.000
0.1	-0.334	0.577	0.0	0.388	-0.050	0.910	94.6	-3.746	-1.097
0.3	-0.387	0.585	0.224E-03	0.394	-0.058	0.917	94.9	-3.649	-0.481
0.6	-0.387	0.585	0.0	0.394	-0.058	0.917	95.1	-4.002	-0.237
0.8	-0.428	0.588	0.749E-04	0.395	-0.065	0.915	95.4	-4.125	-0.081
1.1	-0.489	0.591	0.922E-04	0.398	-0.073	0.915	95.7	-4.035	0.041
1.6	-0.491	0.596	0.624E-04	0.401	-0.073	0.923	96.2	-4.205	0.204
2.6	-0.517	0.611	0.997E-04	0.411	-0.074	0.944	97.2	-4.001	0.415
4.6	-0.500	0.619	0.280E-04	0.417	-0.075	0.960	99.2	-4.552	0.863
6.6	-0.506	0.635	0.529E-04	0.427	-0.075	0.985	101.2	-4.276	0.820
10.1	-0.459	0.641	0.125E-04	0.432	-0.068	1.001	104.7	-4.904	1.004
23.1	-0.522	0.675	0.177E-04	0.455	-0.078	1.050	117.7	-4.751	1.364

AVLIN EQUATION NUMBER 5

$$Y = -4.126232 - .1542941 X + .1232253 X^{**2} - .3529629 X^{**3}$$

T-VALUES ARE : 0.7268 1.0220 3.5463  
 RSQUARE = 0.9568 STD. ERR. OF EST. = .2821130

LOAD INCREMENT # 7 S.D. = 441 KPA

TIME (HOURS)	VOL DISPL (CC)	AXIAL DISPL (MM)	STRAIN RATE (MM/HR)	TRUE AXIAL STRAIN %	TRUE VOL. STRAIN %	DEVIATORIC STRAIN %	CUMULATIVE TIME (HRS)	LOGSTRAIN RATE/HOUR	LOGTIME HOURS
0.0	-0.562	0.676	0.455E+00	0.465	-0.084	1.047	117.7	-0.342	-2.000
0.1	-0.464	0.661	0.446E-03	0.458	-0.069	1.066	117.7	-3.351	-1.097
0.3	-0.515	0.684	0.110E-03	0.460	-0.077	1.065	117.8	-3.959	-0.602
0.5	-0.516	0.685	0.249E-04	0.461	-0.077	1.066	118.2	-4.604	-0.301
0.8	-0.539	0.694	0.248E-03	0.467	-0.080	1.078	118.4	-3.603	-0.125
1.3	-0.621	0.698	0.624E-04	0.470	-0.092	1.076	118.9	-4.205	0.097
2.3	-0.624	0.707	0.561E-04	0.476	-0.093	1.090	119.8	-4.251	0.352
7.3	-0.637	0.741	0.461E-04	0.489	-0.095	1.144	124.8	-4.336	0.860
11.8	-0.625	0.761	0.305E-04	0.513	-0.093	1.179	128.4	-4.516	1.070
23.3	-0.660	0.798	0.217E-04	0.537	-0.098	1.236	140.9	-4.664	1.366

AVLIN EQUATION NUMBER 6

Y = -4.184645 - .8811235E-01 X + .2349831 X\*\*2 - .3400687 X\*\*3  
 T-VALUES ARE : 0.3587 1.6604 2.8572  
 RSQUARE = 0.9618 STD. ERR. OF EST. = .3066781

LOAD INCREMENT # 8 S.D. = 514 KPA

TIME (HOURS)	VOL DISPL (CC)	AXIAL DISPL (MM)	STRAIN RATE (MM/HR)	TRUE AXIAL STRAIN %	TRUE VOL. STRAIN %	DEVIATORIC STRAIN %	CUMULATIVE TIME (HRS)	LOGSTRAIN RATE/HOUR	LOGTIME HOURS
0.0	-0.727	0.790	0.532E+00	0.532	-0.108	1.216	140.8	-0.274	-2.000
0.1	-0.727	0.790	0.0	0.532	-0.108	1.216	141.0	-3.351	-1.097
0.3	-0.728	0.794	0.147E-03	0.535	-0.108	1.222	141.2	-3.832	-0.602
0.4	-0.728	0.795	0.363E-04	0.535	-0.108	1.223	141.3	-4.440	-0.377
0.7	-0.742	0.805	0.274E-03	0.542	-0.110	1.238	141.5	-3.562	-0.174
0.9	-0.755	0.813	0.200E-03	0.547	-0.112	1.249	141.8	-3.699	-0.036
1.4	-0.767	0.816	0.489E-04	0.550	-0.114	1.254	142.3	-4.302	0.152
2.4	-0.840	0.825	0.562E-04	0.555	-0.125	1.258	143.3	-4.251	0.384
7.4	-0.755	0.863	0.524E-04	0.582	-0.112	1.333	146.3	-4.281	0.870
11.9	-0.765	0.868	0.375E-04	0.598	-0.114	1.373	152.8	-4.427	1.076
23.4	-0.782	0.933	0.261E-04	0.626	-0.116	1.444	164.3	-4.584	1.370

AVLIN EQUATION NUMBER 7

Y = -4.078146 - .9819311E-01 X + .2164536 X\*\*2 - .3390687 X\*\*3  
 T-VALUES ARE : 0.4046 1.5672 2.9860  
 RSQUARE = 0.9541 STD. ERR. OF EST. = .3109382

LOAD INCREMENT # 9 S.D. = 588 KPA

TIME (HOURS)	VOL DISPL (CC)	AXIAL DISPL (MM)	STRAIN RATE (MM/HR)	TRUE AXIAL STRAIN %	TRUE VOL. STRAIN %	DEVIATORIC STRAIN %	CUMULATIVE TIME (HRS)	LOGSTRAIN RATE/HOUR	LOGTIME HOURS
0.0	-0.782	0.933	0.628E+00	0.628	-0.116	1.444	164.3	-0.202	-2.000
0.1	-0.784	0.939	0.625E-03	0.633	-0.117	1.454	164.4	-3.204	-1.097
0.3	-0.786	0.943	0.998E-04	0.635	-0.117	1.460	164.7	-4.001	-0.602
0.6	-0.790	0.954	0.300E-03	0.643	-0.118	1.478	164.9	-3.523	-0.237
1.1	-0.814	0.964	0.132E-03	0.650	-0.121	1.492	165.4	-3.679	0.041
1.6	-0.847	0.970	0.875E-04	0.654	-0.126	1.499	165.9	-4.058	0.204
2.6	-0.851	0.982	0.749E-04	0.661	-0.127	1.517	166.9	-4.126	0.415
4.6	-0.858	0.999	0.594E-04	0.673	-0.128	1.545	168.9	-4.226	0.663
7.6	-0.873	1.038	0.875E-04	0.700	-0.130	1.607	171.9	-4.058	0.881
11.6	-0.888	1.077	0.656E-04	0.726	-0.132	1.670	175.9	-4.183	1.064
23.6	-0.986	1.151	0.417E-04	0.776	-0.144	1.783	187.9	-4.380	1.373

AVLIN EQUATION NUMBER 8

Y = -3.982222 - .1608195 X + .2785617 X\*\*2 - .2889426 X\*\*3  
 T-VALUES ARE : 1.0657 3.2927 4.1366  
 RSQUARE = 0.9804 STD. ERR. OF EST. = .1978319

LOAD INCREMENT #10 S.D. = 661 KPA

TIME (HOURS)	VOL DISPL (CC)	AXIAL DISPL (MM)	STRAIN RATE (MM/HR)	TRUE AXIAL STRAIN %	TRUE VOL. STRAIN %	DEVIATORIC STRAIN %	CUMULATIVE TIME (HRS)	LOGSTRAIN RATE/HOUR	LOGTIME HOURS
0.0	0.105	1.148	0.774E+00	0.774	0.016	1.808	187.9	-0.111	-2.000
0.1	0.104	1.150	0.180E-03	0.775	0.015	1.911	188.0	-3.744	-1.097
0.3	0.082	1.155	0.220E-03	0.779	0.012	1.917	188.2	-3.657	-0.602
0.4	0.049	1.163	0.331E-03	0.784	0.007	1.927	188.4	-3.480	-0.377
0.9	-0.055	1.174	0.138E-03	0.791	-0.008	1.931	188.9	-3.861	-0.036
1.4	-0.159	1.183	0.125E-03	0.798	-0.024	1.934	189.4	-3.902	0.152
2.4	-0.182	1.192	0.625E-04	0.804	-0.027	1.947	190.4	-4.204	0.384
7.4	-0.093	1.271	0.106E-03	0.857	-0.014	2.088	195.4	-3.973	0.870
11.4	-0.108	1.310	0.673E-04	0.884	-0.016	2.152	199.4	-4.172	1.058
23.4	0.135	1.404	0.527E-04	0.947	0.020	2.336	211.4	-4.278	1.370

AVLIN EQUATION NUMBER 9

$$Y = -3.931531 + .850093E-01 X + .2067547 X^{**2} + .3836039 X^{**3}$$

T-VALUES ARE : 0.3500 1.4560 3.3888  
 RSQUARE = 0.9571 STD. ERR. OF EST. = .3121578

LOAD INCREMENT #11 S.D. = 886 KPA

TIME (HOURS)	VOL DISPL (CC)	AXIAL DISPL (MM)	STRAIN RATE (MM/HR)	TRUE AXIAL STRAIN %	TRUE VOL. STRAIN %	DEVIATORIC STRAIN %	CUMULATIVE TIME (HRS)	LOGSTRAIN RATE/HOUR	LOGTIME HOURS
0.0	2.175	1.404	0.947E+00	0.947	0.323	2.584	211.4	-0.024	-2.000
0.2	2.156	1.403	-0.295E-04	0.947	0.320	2.580	211.6	-3.744	-1.097
1.2	2.249	1.419	0.113E-03	0.958	0.334	2.619	212.6	-3.946	0.066
2.7	2.245	1.431	0.550E-04	0.966	0.333	2.638	214.1	-4.259	0.431
4.7	2.337	1.451	0.658E-04	0.979	0.347	2.881	216.1	-4.182	0.672
7.7	2.429	1.473	0.501E-04	0.994	0.360	2.729	219.1	-4.300	0.886
24.2	2.729	1.600	0.524E-04	1.081	0.405	2.978	235.6	-4.280	1.384
35.9	2.905	1.662	0.358E-04	1.123	0.421	3.102	247.3	-4.446	1.556
47.7	3.080	1.726	0.389E-04	1.166	0.457	3.229	259.0	-4.433	1.679
84.2	3.585	1.843	0.217E-04	1.245	0.531	3.484	295.5	-4.664	1.925
96.2	3.273	1.875	0.183E-04	1.267	0.485	3.500	307.5	-4.737	1.983
122.2	3.448	1.940	0.169E-04	1.311	0.511	3.629	333.5	-4.771	2.087
144.7	3.713	1.977	0.112E-04	1.336	0.550	3.723	355.0	-4.952	2.160
167.7	3.820	2.011	0.101E-04	1.360	0.566	3.792	379.0	-4.995	2.225
192.7	3.983	2.055	0.123E-04	1.390	0.590	3.886	403.5	-4.909	2.284
242.2	4.036	2.089	0.129E-04	1.420	0.598	3.966	427.0	-4.891	2.384
285.2	3.714	2.154	0.140E-04	1.457	0.551	4.018	453.5	-4.853	2.424
288.2	3.845	2.203	0.145E-04	1.490	0.540	4.092	476.5	-4.836	2.460
312.2	3.835	2.231	0.822E-05	1.509	0.539	4.137	489.5	-5.085	2.494
336.2	3.512	2.256	0.709E-05	1.526	0.537	4.178	523.5	-5.149	2.527
380.2	3.556	2.280	0.971E-05	1.550	0.520	4.221	547.5	-5.013	2.557
383.7	3.642	2.341	0.420E-05	1.560	0.527	4.251	571.5	-4.969	2.584
410.2	3.676	2.382	0.107E-04	1.585	0.540	4.323	595.0	-4.980	2.613
435.2	3.957	2.431	0.134E-04	1.613	0.545	4.395	621.5	-4.874	2.639
456.2	4.254	2.439	0.240E-05	1.651	0.586	4.511	667.5	-5.620	2.659
480.2	4.443	2.466	0.789E-05	1.670	0.630	4.559	691.5	-5.103	2.703
504.2	4.036	2.485	0.528E-05	1.683	0.658	4.628	715.5	-5.501	2.723
528.2	4.232	2.496	0.315E-05	1.690	0.598	4.610	738.5	-5.000	2.742
552.2	4.118	2.531	0.100E-04	1.714	0.627	4.652	763.5	-5.305	2.762
577.7	4.011	2.549	0.495E-05	1.727	0.610	4.697	814.0	-5.200	2.780
602.7	4.402	2.572	0.631E-05	1.743	0.652	4.715	835.5	-5.055	2.795
624.2	4.341	2.600	0.881E-05	1.762	0.643	4.840	862.5	-4.786	2.814
651.2	4.466	2.685	0.164E-04	1.806	0.662	4.964			

AVLIN EQUATION NUMBER 10

$$Y = -4.226858 + .5060314 X + .4360352 X^{**2} + .1415045 X^{**3}$$

T-VALUES ARE : 4.7898 8.0085 5.7273  
 RSQUARE = 0.9249 STD. ERR. OF EST. = .2689781  
 \*\*\*PLOT 1, 1425 UNPLOTTABLE POINTS\*\*\*

GEOTECHNICAL LABORATORIES  
DEPARTMENT OF CIVIL ENGINEERING  
UNIVERSITY OF MANITOBA

CONSTANT MEAN NORMAL STRESS MULTI-STAGE  
SHORT-TERM TRIAXIAL CREEP TEST  
MST9 -  $\bar{\sigma}_m = 420$  kPa

LOAD INCREMENT # 1 S.D. : 0 KPA

TIME (HOURS)	VOL DISPL (CC)	AXIAL DISPL (MM)	STRAIN RATE (MM/HR)	TRUE AXIAL STRAIN %	TRUE VOL. STRAIN %	DEVIATORIC STRAIN %	CUMULATIVE TIME (HRS)	LOGSTRAIN RATE/HOUR	LOGTIME HOURS
0.0	-4.073	0.008	0.574E-02	0.005	-0.618	0.491	0.0	-2.241	-2.000
0.1	-4.073	0.008	0.0	0.005	-0.619	0.491	0.1	0.0	0.0
0.6	-4.223	0.008	0.0	0.006	-0.642	0.510	0.6	0.0	0.0
1.3	-4.373	0.008	0.0	0.006	-0.664	0.528	1.3	0.0	0.0
4.3	-4.522	0.008	0.0	0.006	-0.664	0.528	4.3	0.0	0.0
10.3	-4.522	0.006	-0.310E-05	0.004	-0.687	0.552	10.3	0.0	0.0
22.3	-4.774	0.011	-0.310E-05	0.008	-0.726	0.574	22.3	-5.509	1.348
30.3	-4.889	-0.002	-0.115E-04	-0.002	-0.743	0.611	30.3	0.0	0.0
46.3	-5.024	0.010	-0.538E-05	0.007	-0.784	0.606	46.3	-5.270	1.866
71.3	-5.172	0.004	-0.174E-05	0.003	-0.786	0.635	71.3	0.0	0.0
103.3	-5.473	0.008	0.889E-06	0.006	-0.832	0.655	103.3	-6.014	2.014
122.3	-5.475	0.012	0.131E-05	0.008	-0.832	0.650	122.3	-5.884	2.067
142.3	-5.524	0.011	-0.310E-06	0.008	-0.840	0.667	142.3	0.0	0.0
165.3	-5.873	0.007	-0.103E-05	0.005	-0.893	0.717	165.3	0.0	0.0
191.8	-5.671	0.002	-0.146E-05	0.001	-0.852	0.701	191.8	0.0	0.0
214.8	-5.671	0.002	0.0	0.001	-0.862	0.701	214.8	0.0	0.0
240.3	-5.673	0.007	0.146E-05	0.005	-0.840	0.692	240.3	-5.836	2.381
286.3	-5.677	0.019	0.175E-05	0.013	-0.853	0.673	286.3	-5.756	2.457
310.3	-5.675	0.012	-0.207E-05	0.008	-0.863	0.684	310.3	0.0	0.0
334.3	-5.727	0.018	0.181E-05	0.013	-0.871	0.680	334.3	-5.743	2.524
360.3	-5.774	0.010	-0.215E-05	0.007	-0.878	0.700	360.3	0.0	0.0
382.3	-5.775	0.013	0.845E-06	0.009	-0.878	0.695	382.3	-6.073	2.582
409.3	-5.773	0.007	-0.181E-05	0.005	-0.878	0.706	409.3	0.0	0.0
432.3	-5.877	0.019	0.377E-05	0.013	-0.894	0.698	432.3	-5.423	2.636
454.3	-5.777	0.019	0.0	0.013	-0.879	0.685	454.3	0.0	0.0

LOAD INCREMENT # 2 S.D. : 98 KPA

TIME (HOURS)	VOL DISPL (CC)	AXIAL DISPL (MM)	STRAIN RATE (MM/HR)	TRUE AXIAL STRAIN %	TRUE VOL. STRAIN %	DEVIATORIC STRAIN %	CUMULATIVE TIME (HRS)	LOGSTRAIN RATE/HOUR	LOGTIME HOURS
0.0	0.035	0.115	0.794E-01	0.079	0.005	0.199	0.0	-1.100	-2.000
0.1	0.025	0.142	0.155E-02	0.098	0.004	0.243	0.1	-2.809	-0.886
0.3	0.025	0.142	0.0	0.098	0.004	0.243	0.3	0.0	0.0
0.6	-0.024	0.139	-0.993E-04	0.095	-0.004	0.231	0.6	0.0	0.0
0.8	-0.055	0.140	0.496E-04	0.097	-0.008	0.230	0.8	-4.304	-0.097
1.3	-0.095	0.140	0.0	0.097	-0.015	0.225	1.3	0.0	0.0
2.3	-0.224	0.138	-0.186E-04	0.095	-0.034	0.205	2.3	-5.509	1.348
3.3	-0.175	0.140	0.186E-04	0.097	-0.027	0.215	3.3	-4.730	0.519
5.3	-0.073	0.136	-0.155E-04	0.094	-0.011	0.220	5.3	-5.270	1.866
7.3	-0.023	0.136	0.0	0.094	-0.004	0.227	7.3	0.0	0.0
11.3	0.027	0.137	0.155E-05	0.094	0.004	0.234	11.3	-5.809	1.053
23.8	0.123	0.145	0.447E-05	0.100	0.019	0.260	23.8	-5.349	1.377

AYLIN EQUATION NUMBER 1  
 $Y = -1.760999 - 1.833156 X - 0.6711310 X^2 + .9098876E-01 X^3$   
 T-VALUES ARE : 1.0352 1.2370 0.1436  
 RSQUARE : 0.5522 STD. ERR. OF EST. : 1.986680

LOAD INCREMENT # 3 S.D. : 196 KPA

TIME (HOURS)	VOL DISPL (CC)	AXIAL DISPL (MM)	STRAIN RATE (MM/HR)	TRUE AXIAL STRAIN %	TRUE VOL. STRAIN %	DEVIATORIC STRAIN %	CUMULATIVE TIME (HRS)	LOGSTRAIN RATE/HOUR	LOGTIME HOURS
0.0	0.108	0.160	0.110E+00	0.110	0.016	0.283	23.8	-0.858	-2.000
0.1	0.055	0.167	0.414E-03	0.115	0.008	0.289	23.9	-3.383	-0.886
0.4	0.047	0.188	0.596E-03	0.130	0.007	0.324	24.2	-3.225	-0.420
0.6	-0.003	0.188	0.0	0.130	-0.001	0.316	24.4	0.0	0.0
0.9	-0.056	0.195	0.174E-03	0.134	-0.009	0.322	24.7	-3.780	-0.056
1.4	-0.060	0.205	0.136E-03	0.141	-0.009	0.336	25.2	-3.885	0.140
2.4	-0.084	0.215	0.745E-04	0.149	-0.013	0.353	26.2	-4.128	0.377
3.4	-0.085	0.219	0.248E-04	0.151	-0.010	0.362	27.2	-4.605	0.529
5.4	-0.071	0.233	0.465E-04	0.160	-0.011	0.384	29.2	-4.332	0.731
7.4	-0.075	0.242	0.342E-04	0.167	-0.011	0.400	31.2	-4.466	0.868
11.4	-0.084	0.266	0.403E-04	0.183	-0.013	0.439	35.2	-4.394	1.056
23.4	-0.099	0.305	0.228E-04	0.211	-0.015	0.504	47.2	-4.843	1.369

AYLIN EQUATION NUMBER 2  
 $Y = -3.301862 - 0.8215630 X - 0.1279252 X^2 - 0.1333860 X^3$   
 T-VALUES ARE : 0.8007 0.2316 0.2852  
 RSQUARE : 0.4539 STD. ERR. OF EST. : 1.249029



LOAD INCREMENT # 4 S.D.: 294 KPA

TIME (HOURS)	VOL DISPL (CC)	AXIAL DISPL (MM)	STRAIN RATE (MM/HR)	TRUE AXIAL STRAIN %	TRUE VOL. STRAIN %	DEVIATORIC STRAIN %	CUMULATIVE TIME (HRS)	LOGSTRAIN RATE/HOUR	LOGTIME HOURS
0.0	-0.118	0.328	0.228E+00	0.228	-0.018	0.539	47.2	-0.846	-2.000
0.1	-0.175	0.345	0.189E+02	0.228	-0.027	0.561	47.3	-2.773	-1.097
0.4	-0.235	0.373	0.566E-03	0.257	-0.036	0.601	47.6	-3.247	-0.377
0.9	-0.293	0.394	0.286E-03	0.272	-0.045	0.628	48.1	-3.544	-0.036
1.4	-0.299	0.408	0.189E-03	0.281	-0.046	0.652	48.6	-3.702	0.152
2.4	-0.311	0.439	0.211E-03	0.303	-0.048	0.702	49.6	-3.675	0.384
3.4	-0.268	0.458	0.131E-03	0.316	-0.041	0.740	50.6	-3.884	0.534
5.4	-0.285	0.501	0.149E-03	0.345	-0.044	0.811	52.6	-3.826	0.734
7.4	-0.346	0.529	0.995E-04	0.365	-0.053	0.852	54.6	-4.002	0.870
12.4	-0.417	0.583	0.747E-04	0.403	-0.084	0.934	59.6	-4.127	1.094
23.4	-0.485	0.629	0.288E-04	0.434	-0.074	1.004	70.6	-4.540	1.370

AVLIN EQUATION NUMBER 3

Y = -3.553347 - .4077806 X + .8500344E-01 X\*\*2 + .2178743 X\*\*3  
T-VALUES ARE : 6.2648 2.4260 7.3886  
RSQUARE : 0.9955 STD. ERR. OF EST. : .8331382E-01

LOAD INCREMENT # 5 S.D.: 392 KPA

TIME (HOURS)	VOL DISPL (CC)	AXIAL DISPL (MM)	STRAIN RATE (MM/HR)	TRUE AXIAL STRAIN %	TRUE VOL. STRAIN %	DEVIATORIC STRAIN %	CUMULATIVE TIME (HRS)	LOGSTRAIN RATE/HOUR	LOGTIME HOURS
0.0	-0.469	0.640	0.442E+00	0.442	-0.072	1.023	70.6	-0.355	-2.000
0.1	-0.521	0.645	0.534E-03	0.445	-0.080	1.026	70.7	-3.273	-1.097
0.3	-0.576	0.657	0.324E-03	0.453	-0.088	1.039	70.9	-3.490	-0.461
0.6	-0.577	0.680	0.996E-04	0.456	-0.088	1.045	71.2	-4.002	-0.237
0.8	-0.599	0.685	0.124E-03	0.459	-0.092	1.050	71.4	-3.906	-0.061
1.3	-0.679	0.685	0.0	0.459	-0.104	1.040	71.9	-3.675	0.384
2.3	-0.703	0.675	0.685E-04	0.466	-0.107	1.053	72.9	-4.164	0.367
3.3	-0.707	0.686	0.748E-04	0.473	-0.108	1.071	73.9	-4.126	0.522
5.3	-0.690	0.692	0.217E-04	0.478	-0.105	1.084	75.9	-4.663	0.727
7.3	-0.714	0.702	0.343E-04	0.485	-0.109	1.098	77.9	-4.465	0.865
24.3	-0.818	0.764	0.253E-04	0.528	-0.125	1.190	94.9	-4.597	1.386

AVLIN EQUATION NUMBER 4

Y = -3.995064 - .3612718 X + .2145858 X\*\*2 - .2497985 X\*\*3  
T-VALUES ARE : 1.7140 1.7956 2.6103  
RSQUARE : 0.9596 STD. ERR. OF EST. : .2868983

LOAD INCREMENT # 6 S.D.: 490 KPA

TIME (HOURS)	VOL DISPL (CC)	AXIAL DISPL (MM)	STRAIN RATE (MM/HR)	TRUE AXIAL STRAIN %	TRUE VOL. STRAIN %	DEVIATORIC STRAIN %	CUMULATIVE TIME (HRS)	LOGSTRAIN RATE/HOUR	LOGTIME HOURS
0.0	-0.839	0.768	0.530E+00	0.530	-0.128	1.194	94.9	-0.275	-2.000
0.1	-0.840	0.770	0.139E-03	0.532	-0.128	1.197	95.0	-3.856	-1.000
0.4	-0.845	0.781	0.324E-03	0.540	-0.129	1.216	95.3	-3.490	-0.456
0.6	-0.897	0.787	0.150E-03	0.543	-0.137	1.219	95.5	-3.825	-0.222
0.9	-0.947	0.789	0.501E-04	0.545	-0.145	1.216	95.8	-4.300	-0.071
1.1	-0.970	0.795	0.175E-03	0.549	-0.148	1.224	96.0	-3.758	0.041
1.6	-1.051	0.798	0.374E-04	0.551	-0.161	1.218	96.5	-4.427	0.204
2.6	-1.005	0.808	0.748E-04	0.558	-0.154	1.242	97.5	-4.126	0.415
4.6	-0.959	0.818	0.343E-04	0.565	-0.147	1.265	99.5	-4.465	0.663
6.6	-0.965	0.834	0.530E-04	0.576	-0.148	1.290	101.5	-4.276	0.820
10.1	-0.972	0.852	0.356E-04	0.586	-0.149	1.320	105.0	-4.449	1.004
23.1	-1.144	0.907	0.297E-04	0.627	-0.175	1.393	118.0	-4.527	1.364

AVLIN EQUATION NUMBER 5

Y = -4.112198 - .1980265 X + .2486756 X\*\*2 - .2957316 X\*\*3  
T-VALUES ARE : 0.7935 1.7694 2.5449  
RSQUARE : 0.9434 STD. ERR. OF EST. : .3245508

LOAD INCREMENT # 7 S.D. = 588 KPA

TIME (HOURS)	VOL DISPL (CC)	AXIAL DISPL (MM)	STRAIN RATE (MM/HR)	TRUE AXIAL STRAIN %	TRUE VOL. STRAIN %	DEVIATORIC STRAIN %	CUMULATIVE TIME (HRS)	LOGSTRAIN RATE/HOUR	LOGTIME HOURS
0.0	-1.158	0.918	0.634E+00	0.634	-0.177	1.409	118.0	-0.188	-2.000
0.1	-1.160	0.924	0.625E-03	0.639	-0.177	1.419	118.1	-3.204	-1.097
0.3	-1.162	0.928	0.147E-03	0.641	-0.178	1.425	118.3	-3.833	-0.602
0.5	-1.213	0.931	0.988E-04	0.644	-0.186	1.425	118.5	-4.001	-0.301
0.8	-1.265	0.938	0.198E-03	0.649	-0.194	1.430	118.8	-3.701	-0.125
1.3	-1.290	0.949	0.180E-03	0.656	-0.197	1.446	119.3	-3.824	0.097
2.3	-1.325	0.963	0.935E-04	0.655	-0.203	1.464	120.3	-4.029	0.352
7.3	-1.345	1.013	0.688E-04	0.700	-0.206	1.547	125.3	-4.156	0.860
11.8	-1.325	1.039	0.402E-04	0.718	-0.203	1.594	129.8	-4.396	1.070
24.9	-1.431	1.106	0.351E-04	0.765	-0.219	1.694	142.9	-4.454	1.396

AVLIN EQUATION NUMBER 6

Y = -3.954831 + .9347880E-01 X + .2134890 X\*\*2 - .3365144 X\*\*3  
 T-VALUES ARE : 0.7407 3.0556 5.8384  
 RSQUARE = 0.9891 STD. ERR. OF EST. = .1588062

LOAD INCREMENT # 8 S.D. = 687 KPA

TIME (HOURS)	VOL DISPL (CC)	AXIAL DISPL (MM)	STRAIN RATE (MM/HR)	TRUE AXIAL STRAIN %	TRUE VOL. STRAIN %	DEVIATORIC STRAIN %	CUMULATIVE TIME (HRS)	LOGSTRAIN RATE/HOUR	LOGTIME HOURS
0.0	-1.464	1.113	0.789E+00	0.759	-0.224	1.702	142.9	-0.114	-2.000
0.1	-1.494	1.114	0.692E-04	0.770	-0.229	1.699	143.0	-4.049	-1.097
0.3	-1.515	1.116	0.110E-03	0.772	-0.232	1.701	143.2	-3.958	-0.602
0.4	-1.517	1.122	0.220E-03	0.776	-0.232	1.710	143.4	-3.657	-0.377
0.7	-1.572	1.134	0.350E-03	0.784	-0.240	1.725	143.6	-3.456	-0.174
1.2	-1.623	1.136	0.250E-04	0.786	-0.248	1.722	144.1	-4.602	0.086
1.7	-1.624	1.139	0.375E-04	0.787	-0.248	1.726	144.6	-4.426	0.223
2.7	-1.629	1.152	0.938E-04	0.797	-0.249	1.748	145.6	-4.028	0.427
7.7	-1.650	1.206	0.750E-04	0.834	-0.252	1.838	150.6	-4.125	0.865
12.2	-1.664	1.241	0.542E-04	0.859	-0.255	1.896	155.1	-4.266	1.085
23.7	-1.742	1.314	0.440E-04	0.909	-0.267	2.010	166.6	-4.356	1.374

AVLIN EQUATION NUMBER 7

Y = -4.129566 + .1596953 X + .2463465 X\*\*2 - .4042735 X\*\*3  
 T-VALUES ARE : 0.4617 1.2538 2.5090  
 RSQUARE = 0.9072 STD. ERR. OF EST. = .4529850

LOAD INCREMENT # 9 S.D. = 784 KPA

TIME (HOURS)	VOL DISPL (CC)	AXIAL DISPL (MM)	STRAIN RATE (MM/HR)	TRUE AXIAL STRAIN %	TRUE VOL. STRAIN %	DEVIATORIC STRAIN %	CUMULATIVE TIME (HRS)	LOGSTRAIN RATE/HOUR	LOGTIME HOURS
0.0	-1.757	1.327	0.918E+00	0.918	-0.269	2.029	166.6	-0.037	-2.000
0.1	-1.789	1.330	0.358E-03	0.920	-0.274	2.031	166.7	-3.446	-1.097
0.3	-1.841	1.337	0.200E-03	0.925	-0.282	2.037	166.9	-3.899	-0.481
0.6	-1.845	1.346	0.250E-03	0.932	-0.282	2.052	167.2	-3.602	-0.237
1.1	-1.851	1.362	0.213E-03	0.942	-0.283	2.077	167.7	-3.672	0.033
1.6	-1.853	1.367	0.751E-04	0.946	-0.283	2.086	168.2	-4.124	0.199
2.6	-1.878	1.381	0.939E-04	0.956	-0.287	2.106	169.2	-4.027	0.412
4.6	-1.889	1.408	0.970E-04	0.975	-0.286	2.155	171.2	-4.013	0.661
7.6	-1.882	1.443	0.793E-04	0.999	-0.286	2.211	174.2	-4.101	0.880
11.6	-1.904	1.498	0.971E-04	1.038	-0.291	2.303	178.2	-4.013	1.064
24.9	-1.992	1.597	0.515E-04	1.106	-0.305	2.460	191.5	-4.289	1.395

AVLIN EQUATION NUMBER 8

Y = -3.920307 + .2659363E-01 X + .2604466 X\*\*2 - .3396515 X\*\*3  
 T-VALUES ARE : 0.1553 2.7954 4.3644  
 RSQUARE = 0.9750 STD. ERR. OF EST. = .2254757

LOAD INCREMENT #10 S.D.: 882 KPA

TIME (HOURS)	VOL DISPL (CC)	AXIAL DISPL (MM)	STRAIN RATE (MM/HR)	TRUE AXIAL STRAIN %	TRUE VOL. STRAIN %	DEVIATORIC STRAIN %	CUMULATIVE TIME (HRS)	LOGSTRAIN RATE/HOUR	LOGTIME HOURS
0.0	-2.006	1.808	0.111E+01	1.112	-0.307	2.474	191.5	0.046	-2.000
0.1	-2.009	1.812	0.628E-03	1.117	-0.307	2.485	191.5	-3.202	-1.097
0.3	-2.061	1.820	0.295E-03	1.122	-0.315	2.490	191.7	-3.530	-0.802
0.4	-2.115	1.828	0.332E-03	1.128	-0.324	2.498	191.9	-3.479	-0.377
0.9	-2.118	1.836	0.113E-03	1.133	-0.324	2.511	192.4	-3.948	-0.036
1.4	-2.124	1.851	0.213E-03	1.144	-0.325	2.536	192.9	-3.871	0.152
2.4	-2.129	1.865	0.940E-04	1.153	-0.326	2.559	193.9	-4.027	0.384
7.4	-2.168	1.764	0.138E-03	1.222	-0.332	2.723	198.9	-3.880	0.870
11.4	-2.188	1.815	0.894E-04	1.258	-0.335	2.808	202.9	-4.049	1.058
23.4	-2.240	1.948	0.774E-04	1.351	-0.343	3.029	214.9	-4.111	1.370

AVLIN EQUATION NUMBER 9

Y = -3.827833 - .8327949E-01 X + .2942041 X\*\*2 - .3106521 X\*\*3

T-VALUES ARE : 0.5589 3.3645 4.4303  
RSQUARE = 0.9840 STD. ERR. OF EST. = .1922255

LOAD INCREMENT #11 S.D.: 880 KPA

TIME (HOURS)	VOL DISPL (CC)	AXIAL DISPL (MM)	STRAIN RATE (MM/HR)	TRUE AXIAL STRAIN %	TRUE VOL. STRAIN %	DEVIATORIC STRAIN %	CUMULATIVE TIME (HRS)	LOGSTRAIN RATE/HOUR	LOGTIME HOURS
0.0	-2.162	1.954	0.136E+01	1.355	-0.331	3.049	214.9	0.132	-2.000
0.1	-2.165	1.961	0.718E-03	1.360	-0.331	3.061	214.9	-3.144	-1.097
0.3	-2.167	1.989	0.285E-03	1.365	-0.332	3.073	215.1	-3.530	-0.802
0.5	-2.171	1.977	0.226E-03	1.371	-0.332	3.087	215.4	-3.645	-0.301
0.8	-2.175	1.987	0.302E-03	1.378	-0.333	3.105	215.6	-3.520	-0.125
1.3	-2.230	2.007	0.188E-03	1.388	-0.341	3.121	216.1	-3.725	0.097
1.8	-2.243	2.007	0.880E-04	1.392	-0.342	3.131	216.6	-4.055	0.243
2.8	-2.209	2.076	0.182E-03	1.410	-0.343	3.175	217.6	-3.739	0.439
4.8	-2.209	2.076	0.148E-03	1.440	-0.348	3.251	219.6	-3.830	0.677
7.8	-2.232	2.133	0.134E-03	1.480	-0.342	3.347	222.6	-3.872	0.869
24.3	-2.134	2.386	0.111E-03	1.664	-0.327	3.810	239.1	-3.953	1.385

AVLIN EQUATION NUMBER 10

Y = -3.793068 - .5589550E-01 X + .3371367 X\*\*2 - .3020164 X\*\*3

T-VALUES ARE : 0.4272 4.5611 5.0721  
RSQUARE = 0.9843 STD. ERR. OF EST. = .1771756

LOAD INCREMENT #12 S.D.: 1028 KPA

TIME (HOURS)	VOL DISPL (CC)	AXIAL DISPL (MM)	STRAIN RATE (MM/HR)	TRUE AXIAL STRAIN %	TRUE VOL. STRAIN %	DEVIATORIC STRAIN %	CUMULATIVE TIME (HRS)	LOGSTRAIN RATE/HOUR	LOGTIME HOURS
0.0	0.182	2.406	0.167E+01	1.671	0.028	4.116	239.1	0.223	-2.000
0.1	0.382	2.406	0.0	1.671	0.058	4.141	239.2	-3.144	-1.097
0.4	0.680	2.410	0.929E-04	1.674	0.104	4.185	239.5	-4.032	-0.377
1.2	0.773	2.428	0.188E-03	1.687	0.116	4.228	240.3	-3.775	0.058
3.2	0.940	2.483	0.121E-03	1.711	0.143	4.309	242.3	-3.917	0.505
6.2	0.962	2.508	0.105E-03	1.743	0.147	4.389	245.3	-3.878	0.792
11.4	1.161	2.588	0.106E-03	1.798	0.177	4.550	250.6	-3.876	1.059
23.2	1.455	2.731	0.860E-04	1.899	0.222	4.834	262.3	-4.086	1.365
59.7	2.247	3.009	0.534E-04	2.094	0.343	5.409	298.8	-4.273	1.776
71.7	2.119	3.080	0.417E-04	2.144	0.323	5.516	310.8	-4.380	1.856
97.7	2.485	3.219	0.378E-04	2.242	0.376	5.799	336.8	-4.423	1.990
120.2	2.734	3.299	0.251E-04	2.299	0.417	5.971	359.3	-4.601	2.080
143.2	3.004	3.376	0.234E-04	2.353	0.458	6.137	382.3	-4.630	2.156
167.7	3.221	3.461	0.246E-04	2.413	0.491	6.311	406.8	-4.609	2.225
191.2	3.341	3.538	0.230E-04	2.467	0.509	6.458	430.3	-4.639	2.281
217.7	3.154	3.631	0.249E-04	2.533	0.481	6.597	456.8	-4.603	2.338
240.7	3.151	3.715	0.260E-04	2.593	0.480	6.743	479.8	-4.585	2.381
263.7	3.230	3.772	0.172E-04	2.632	0.492	6.849	502.8	-4.766	2.421
287.7	3.232	3.817	0.133E-04	2.664	0.493	6.928	526.8	-4.878	2.459
311.7	3.209	3.876	0.175E-04	2.706	0.489	7.028	550.8	-4.767	2.494
335.7	3.295	3.911	0.104E-04	2.731	0.502	7.099	574.8	-4.985	2.526
359.2	3.475	3.962	0.154E-04	2.767	0.529	7.211	598.3	-4.765	2.555
385.7	3.651	4.024	0.164E-04	2.811	0.556	7.339	624.8	-4.765	2.586
410.7	4.030	4.078	0.153E-04	2.849	0.614	7.479	649.8	-4.815	2.614
437.7	4.319	4.106	0.756E-05	2.869	0.658	7.565	676.8	-5.122	2.641
461.7	4.602	4.151	0.133E-04	2.901	0.700	7.678	700.8	-4.877	2.684
485.7	4.298	4.161	0.293E-05	2.908	0.654	7.658	724.8	-5.534	2.686
508.7	4.478	4.213	0.152E-04	2.945	0.682	7.769	748.8	-4.819	2.707
533.7	4.361	4.256	0.128E-04	2.975	0.664	7.830	772.8	-4.894	2.727
559.2	4.447	4.291	0.977E-05	3.000	0.677	7.901	798.3	-5.010	2.748
584.2	4.833	4.328	0.105E-04	3.026	0.736	8.013	823.3	-4.980	2.767
605.7	4.817	4.368	0.134E-04	3.055	0.733	8.082	844.8	-4.874	2.782
632.7	5.093	4.429	0.161E-04	3.088	0.775	8.222	871.8	-4.793	2.801

AVLIN EQUATION NUMBER 11

Y = -4.002481 - .4761460 X + .4588840 X\*\*2 - .1547353 X\*\*3

T-VALUES ARE : 5.8735 11.2593 8.3183  
RSQUARE = 0.9653 STD. ERR. OF EST. = .2125106

\*\*\*PLOT 1. 1670 UNPLOTTABLE POINTS\*\*\*

GEOTECHNICAL LABORATORIES  
DEPARTMENT OF CIVIL ENGINEERING  
UNIVERSITY OF MANITOBA

CONSTANT CELL PRESSURE MULTI-STAGE  
TRIAXIAL CREEP TEST  
MST10 -  $\sigma_3 = 70 \text{ kPa}$

LOAD INCREMENT # 1 S.D. : 0 KPA									
TIME (HOURS)	VOL DISPL (CC)	AXIAL DISPL (MM)	STRAIN RATE (/HR)	TRUE AXIAL STRAIN %	TRUE VOL. STRAIN %	DEVIATORIC STRAIN %	CUMULATIVE TIME (HRS)	LOGSTRAIN RATE/HOUR	LOGTIME HOURS
0.0	-1.020	0.0	0.0	0.0	-0.149	0.122	0.0	0.0	0.0
0.5	-1.220	0.0	0.0	0.0	-0.179	0.146	0.5	0.0	0.0
2.3	-1.323	0.008	0.308E-04	0.005	-0.194	0.146	2.3	-4.512	0.352
6.3	-1.222	0.006	-0.300E-05	0.004	-0.179	0.136	6.3	0.0	0.0
23.8	-1.422	0.006	0.0	0.004	-0.206	0.160	23.8	0.0	0.0
48.8	-1.622	0.006	0.0	0.004	-0.223	0.172	48.8	0.0	0.0
70.8	-1.573	0.007	0.274E-06	0.005	-0.230	0.176	70.8	-5.563	1.850
95.3	-1.671	0.002	-0.147E-05	0.001	-0.245	0.197	95.3	0.0	0.0
118.7	-1.821	0.003	0.257E-06	0.002	-0.267	0.213	118.7	-6.591	2.074
142.7	-1.821	0.003	0.0	0.002	-0.267	0.213	142.7	0.0	0.0
166.7	-1.872	0.006	0.996E-06	0.004	-0.274	0.214	166.7	-6.002	2.222
191.7	-1.921	0.004	-0.718E-06	0.002	-0.281	0.224	191.7	0.0	0.0
221.2	-2.172	0.006	0.808E-06	0.004	-0.318	0.250	221.2	-6.216	2.345
238.2	-2.174	0.009	0.106E-05	0.006	-0.318	0.245	238.2	-5.977	2.377
262.0	-2.123	0.007	-0.501E-06	0.005	-0.311	0.242	262.0	0.0	0.0
286.0	-2.223	0.007	0.0	0.005	-0.326	0.254	286.0	0.0	0.0
310.0	-2.325	0.013	0.150E-05	0.008	-0.341	0.258	310.0	-5.825	2.491
334.0	-2.324	0.009	-0.998E-06	0.006	-0.340	0.263	334.0	0.0	0.0
359.5	-2.225	0.012	0.706E-06	0.008	-0.328	0.247	359.5	-6.151	2.556
388.0	-2.324	0.011	-0.211E-05	0.007	-0.341	0.260	388.0	0.0	0.0
407.0	-2.376	0.016	0.189E-05	0.011	-0.348	0.258	407.0	-5.723	2.610

LOAD INCREMENT # 2 S.D. : 16 KPA									
TIME (HOURS)	VOL DISPL (CC)	AXIAL DISPL (MM)	STRAIN RATE (/HR)	TRUE AXIAL STRAIN %	TRUE VOL. STRAIN %	DEVIATORIC STRAIN %	CUMULATIVE TIME (HRS)	LOGSTRAIN RATE/HOUR	LOGTIME HOURS
0.0	-0.043	-0.018	-0.127E-01	-0.013	-0.006	0.036	0.0	0.0	0.0
0.5	-0.092	-0.020	-0.117E-04	-0.013	-0.014	0.044	0.5	0.0	0.0
1.0	-0.143	-0.019	0.114E-04	-0.013	-0.021	0.048	1.0	-4.941	0.0
2.0	-0.144	-0.016	0.181E-04	-0.011	-0.021	0.044	2.0	-4.742	0.301
4.0	-0.042	-0.022	-0.176E-04	-0.014	-0.006	0.040	4.0	0.0	0.0
17.0	-0.041	-0.024	-0.954E-06	-0.016	-0.006	0.043	17.0	0.0	0.0
23.0	0.059	-0.023	0.954E-06	-0.015	0.009	0.030	23.0	-6.021	1.362
31.0	0.059	-0.023	0.0	-0.015	0.009	0.030	31.0	0.0	0.0
46.0	0.057	-0.019	0.159E-05	-0.013	0.008	0.024	46.0	-5.799	1.663
71.5	0.057	-0.019	0.0	-0.013	0.008	0.024	71.5	0.0	0.0
95.0	0.057	-0.017	0.527E-06	-0.011	0.008	0.021	95.0	-6.276	1.978
121.0	0.057	-0.017	0.0	-0.011	0.008	0.021	121.0	0.0	0.0
146.0	0.055	-0.014	0.954E-06	-0.009	0.008	0.016	146.0	-6.021	2.164
173.0	0.005	-0.014	0.0	-0.009	0.001	0.022	173.0	-5.977	2.377
202.0	0.057	-0.018	-0.102E-05	-0.012	0.008	0.023	202.0	0.0	0.0
226.5	0.057	-0.019	-0.272E-06	-0.013	0.008	0.024	226.5	0.0	0.0

LOAD INCREMENT # 3 S.D. : 33 KPA									
TIME (HOURS)	VOL DISPL (CC)	AXIAL DISPL (MM)	STRAIN RATE (/HR)	TRUE AXIAL STRAIN %	TRUE VOL. STRAIN %	DEVIATORIC STRAIN %	CUMULATIVE TIME (HRS)	LOGSTRAIN RATE/HOUR	LOGTIME HOURS
0.0	0.040	-0.026	-0.169E-01	-0.017	0.006	0.037	0.0	0.0	0.0
0.5	-0.040	-0.026	0.0	-0.017	-0.006	0.046	0.5	0.0	0.0
1.3	-0.144	-0.016	0.877E-04	-0.010	-0.021	0.042	1.3	0.0	0.0
2.3	-0.146	-0.011	0.295E-04	-0.007	-0.021	0.042	2.3	-4.057	0.097
4.3	-0.095	-0.013	-0.572E-05	-0.006	-0.014	0.035	4.3	-4.529	0.352
7.3	-0.047	-0.008	0.118E-04	-0.005	-0.007	0.032	7.3	0.0	0.0
24.0	0.003	-0.008	-0.342E-06	-0.006	0.000	0.018	24.0	-4.930	0.860
47.5	0.248	0.004	0.354E-05	0.003	0.036	0.037	250.5	-6.021	1.362
							274.0	-5.451	1.677

LOAD INCREMENT # 4 S.D. : 33 KPA									
TIME (HOURS)	VOL DISPL (CC)	AXIAL DISPL (MM)	STRAIN RATE (/HR)	TRUE AXIAL STRAIN %	TRUE VOL. STRAIN %	DEVIATORIC STRAIN %	CUMULATIVE TIME (HRS)	LOGSTRAIN RATE/HOUR	LOGTIME HOURS
55.5	-0.232	-0.560	-0.669E-04	-0.372	-0.034	0.938	329.5	0.0	0.0
73.5	-0.384	-0.425	0.497E-04	-0.282	-0.056	0.737	347.5	-4.304	1.866
120.0	-1.222	0.185	0.871E-04	0.123	-0.180	0.155	394.0	-4.060	2.079
187.0	0.178	0.185	0.0	0.123	0.026	0.323	441.0	-4.529	0.352
191.0	0.179	0.183	-0.500E-06	0.122	0.026	0.320	466.0	0.0	0.0
215.0	0.179	0.181	-0.500E-06	0.121	0.026	0.317	489.0	-4.930	0.860
264.0	0.229	0.183	0.245E-06	0.122	0.033	0.328	538.0	-6.811	2.422
287.0	0.378	0.185	0.522E-06	0.123	0.055	0.347	561.0	-6.283	2.458
311.0	0.477	0.188	0.748E-06	0.125	0.070	0.363	585.0	-6.126	2.483
335.0	0.577	0.188	0.0	0.125	0.085	0.375	609.0	0.0	0.0
359.0	0.675	0.191	0.100E-05	0.127	0.099	0.393	633.0	-6.000	2.555
383.0	0.730	0.179	-0.350E-05	0.119	0.107	0.379	657.0	0.0	0.0
439.0	1.179	0.189	0.118E-05	0.125	0.172	0.448	713.0	-5.929	2.642
503.0	1.179	0.181	-0.749E-06	0.121	0.173	0.437	777.0	-5.977	2.377

## LOAD INCREMENT # 5 S.D.: 49 KPA

TIME (HOURS)	VOL DISPL (CC)	AXIAL DISPL (MM)	STRAIN RATE (/HR)	TRUE AXIAL STRAIN %	TRUE VOL. STRAIN %	DEVIATORIC STRAIN %	CUMULATIVE TIME (HRS)	LOGSTRAIN RATE/HOUR	LOGTIME HOURS
0.0	1.201	0.176	0.117E+00	0.117	0.176	0.431	777.0	-0.931	-2.000
0.3	1.231	0.177	0.251E-04	0.118	0.180	0.436	777.2	-4.800	-0.602
0.8	1.203	0.172	-0.720E-04	0.114	0.176	0.424	777.7	-4.060	2.079
2.3	1.203	0.172	0.0	0.114	0.176	0.424	779.2	-4.529	0.352
4.8	1.203	0.172	0.0	0.114	0.176	0.424	781.7	0.0	0.0
23.0	1.282	0.175	0.131E-05	0.117	0.188	0.439	800.0	-5.881	1.362
47.0	1.381	0.176	0.249E-06	0.117	0.202	0.452	824.0	-6.804	1.672
89.0	1.480	0.179	0.819E-06	0.119	0.217	0.489	848.0	-6.087	1.839
96.5	1.580	0.179	0.0	0.119	0.232	0.481	873.5	-8.126	2.493
117.0	1.579	0.183	0.146E-05	0.122	0.231	0.488	894.0	-5.837	2.068

## LOAD INCREMENT # 6 S.D.: 85 KPA

TIME (HOURS)	VOL DISPL (CC)	AXIAL DISPL (MM)	STRAIN RATE (/HR)	TRUE AXIAL STRAIN %	TRUE VOL. STRAIN %	DEVIATORIC STRAIN %	CUMULATIVE TIME (HRS)	LOGSTRAIN RATE/HOUR	LOGTIME HOURS
0.0	1.579	0.181	0.120E+00	0.120	0.231	0.484	894.0	-0.819	-2.000
0.3	1.580	0.179	-0.500E-04	0.119	0.232	0.481	894.2	-4.800	-0.802
0.8	1.481	0.178	-0.119E-04	0.118	0.217	0.468	894.7	-4.060	2.079
2.3	1.579	0.182	0.180E-04	0.121	0.231	0.485	898.2	-4.797	0.352
9.3	1.579	0.181	-0.853E-06	0.120	0.231	0.484	903.2	0.0	0.0
24.0	1.579	0.181	0.0	0.120	0.231	0.484	918.0	-5.881	1.362
48.0	1.626	0.191	0.275E-05	0.127	0.238	0.505	942.0	-8.561	1.881
73.5	1.675	0.194	0.707E-06	0.129	0.245	0.516	967.5	-8.151	1.868
101.0	1.770	0.204	0.281E-05	0.136	0.259	0.545	985.0	-5.583	2.004
120.0	1.870	0.204	0.0	0.136	0.274	0.557	1014.0	-6.837	2.068
144.0	1.869	0.208	0.997E-06	0.138	0.274	0.562	1038.0	-6.001	2.158

## LOAD INCREMENT # 7 S.D.: 82 KPA

TIME (HOURS)	VOL DISPL (CC)	AXIAL DISPL (MM)	STRAIN RATE (/HR)	TRUE AXIAL STRAIN %	TRUE VOL. STRAIN %	DEVIATORIC STRAIN %	CUMULATIVE TIME (HRS)	LOGSTRAIN RATE/HOUR	LOGTIME HOURS
0.0	1.871	0.204	0.136E+00	0.136	0.274	0.556	1038.0	-0.868	-2.000
0.5	1.871	0.203	-0.122E-04	0.135	0.274	0.554	1038.5	-4.800	-0.802
1.0	1.870	0.206	0.359E-04	0.137	0.274	0.559	1039.0	-4.445	0.0
2.5	1.867	0.214	0.360E-04	0.142	0.274	0.571	1040.5	-4.444	0.398
4.5	1.870	0.205	-0.300E-04	0.136	0.274	0.557	1042.5	0.0	0.0
7.5	1.870	0.205	0.0	0.136	0.274	0.557	1045.5	-5.881	1.362
23.5	1.984	0.221	0.673E-05	0.147	0.288	0.595	1061.5	-5.172	1.371
47.5	2.062	0.225	0.125E-05	0.150	0.302	0.614	1085.5	-5.903	1.677
71.5	2.058	0.236	0.299E-05	0.157	0.301	0.631	1109.5	-5.524	1.854
97.5	2.157	0.239	0.893E-06	0.159	0.316	0.647	1135.5	-6.159	1.889
123.5	2.253	0.248	0.230E-05	0.165	0.330	0.673	1161.5	-5.638	2.092
144.0	2.301	0.253	0.176E-05	0.168	0.337	0.688	1182.0	-5.755	2.158

## LOAD INCREMENT # 8 S.D.: 98 KPA

TIME (HOURS)	VOL DISPL (CC)	AXIAL DISPL (MM)	STRAIN RATE (/HR)	TRUE AXIAL STRAIN %	TRUE VOL. STRAIN %	DEVIATORIC STRAIN %	CUMULATIVE TIME (HRS)	LOGSTRAIN RATE/HOUR	LOGTIME HOURS
0.0	2.300	0.257	0.171E+00	0.171	0.337	0.693	1182.0	-0.788	-2.000
0.5	2.251	0.255	-0.245E-04	0.169	0.330	0.684	1182.5	-4.800	-0.802
1.0	2.249	0.258	0.480E-04	0.172	0.330	0.690	1183.0	-4.319	0.0
2.0	2.249	0.260	0.120E-04	0.173	0.329	0.693	1184.0	-4.821	0.301
4.5	2.299	0.260	0.0	0.173	0.337	0.699	1186.5	0.0	0.0
7.0	2.248	0.261	0.239E-05	0.174	0.329	0.694	1189.0	-5.822	0.845
23.0	2.342	0.277	0.675E-05	0.184	0.343	0.732	1205.0	-5.171	1.372
74.0	2.628	0.312	0.458E-05	0.208	0.370	0.811	1256.0	-5.339	1.869
121.0	2.824	0.324	0.188E-05	0.218	0.384	0.842	1303.0	-5.740	2.083
144.5	2.720	0.334	0.281E-05	0.222	0.398	0.870	1326.5	-5.551	2.160
171.5	2.814	0.349	0.377E-05	0.232	0.412	0.906	1353.5	-5.423	2.234
218.0	3.004	0.376	0.374E-05	0.250	0.440	0.971	1400.0	-5.427	2.338
243.5	3.050	0.384	0.238E-05	0.256	0.447	0.991	1425.5	-5.628	2.386
270.0	3.096	0.384	0.249E-05	0.262	0.453	1.013	1452.0	-5.804	2.431
289.5	3.281	0.407	0.430E-05	0.271	0.482	1.057	1471.5	-5.366	2.462
312.5	3.338	0.416	0.261E-05	0.277	0.489	1.077	1494.5	-5.584	2.495







LOAD INCREMENT #13 S.D.# 186 KPA

TIME (HOURS)	VOL DISPL (CC)	AXIAL DISPL (MM)	STRAIN RATE (/HR)	TRUE AXIAL STRAIN %	TRUE VOL. STRAIN %	DEVIATORIC STRAIN %	CUMULATIVE TIME (HRS)	LOGSTRAIN RATE/HR	LOGTIME HOURS
0.0	10.984	3.299	0.222E+01	2.218	1.596	6.735	5491.0	0.348	-2.000
0.5	10.983	3.302	0.374E-04	2.218	1.596	6.740	5491.5	-4.427	-0.301
8.5	10.981	3.307	0.459E-05	2.223	1.596	6.748	5499.5	-5.339	0.929
23.5	10.958	3.314	0.327E-05	2.228	1.595	6.760	5514.5	-5.486	1.371
47.5	11.054	3.323	0.254E-05	2.234	1.609	6.786	5538.5	-5.584	1.877
87.5	11.148	3.344	0.281E-06	2.248	1.623	6.832	5588.5	-5.551	2.077
119.5	11.242	3.366	0.334E-05	2.268	1.636	6.861	5610.5	-5.477	2.188
146.8	11.337	3.367	0.295E-05	2.284	1.650	6.892	5637.5	-5.631	2.224
167.5	11.386	3.389	0.874E-06	2.271	1.657	6.902	5658.5	-6.069	2.282
191.5	11.433	3.377	0.229E-05	2.276	1.664	6.924	5682.5	-5.639	2.333
215.5	11.430	3.386	0.230E-05	2.282	1.677	6.981	5735.5	-5.876	2.368
244.5	11.527	3.395	0.211E-05	2.290	1.691	6.978	5759.5	-5.991	2.428
268.5	11.625	3.398	0.102E-05	2.285	1.691	6.980	5778.5	-5.589	2.459
287.5	11.622	3.405	0.258E-05	2.290	1.705	7.008	5802.5	-5.748	2.493
311.5	11.670	3.412	0.178E-05	2.284	1.712	7.026	5826.5	-5.593	2.526
335.5	11.716	3.421	0.265E-05	2.300	1.719	7.041	5850.5	-5.815	2.566
359.5	11.784	3.426	0.153E-05	2.304	1.732	7.057	5874.5	-5.748	2.584
383.5	11.812	3.432	0.178E-06	2.308	1.739	7.066	5892.5	-5.825	2.636
432.5	11.908	3.443	0.150E-05	2.316	1.739	7.101	5946.5	-5.777	2.858
455.5	11.956	3.448	0.180E-05	2.319	1.746	7.117	5970.5	-5.748	2.881
479.5	12.003	3.455	0.128E-05	2.324	1.763	7.130	5994.5	-5.894	2.702
503.5	12.051	3.459	0.204E-05	2.331	1.760	7.148	6018.5	-5.891	2.722
527.5	12.099	3.472	0.153E-05	2.335	1.774	7.167	6042.5	-5.833	2.742
551.5	12.096	3.481	0.117E-05	2.341	1.780	7.188	6095.0	-5.724	2.781
604.0	12.193	3.486	0.189E-05	2.345	1.802	7.224	6138.5	-5.815	2.811
623.5	12.241	3.488	0.153E-05	2.349	1.808	7.236	6162.5	-5.816	2.827
647.5	12.289	3.497	0.153E-05	2.352	1.809	7.242	6186.5	-6.282	2.842
671.5	12.417	3.499	0.511E-06	2.354	1.816	7.256	6210.5	-5.894	2.867
695.5	12.436	3.503	0.128E-05	2.357					
719.5	12.484								

LOAD INCREMENT #14 S.D.# 229 KPA

TIME (HOURS)	VOL DISPL (CC)	AXIAL DISPL (MM)	STRAIN RATE (/HR)	TRUE AXIAL STRAIN %	TRUE VOL. STRAIN %	DEVIATORIC STRAIN %	CUMULATIVE TIME (HRS)	LOGSTRAIN RATE/HR	LOGTIME HOURS
0.0	12.266	4.063	0.274E+01	2.738	1.784	8.164	6210.5	0.437	-2.000
1.0	12.264	4.069	0.373E-04	2.742	1.784	8.173	6211.5	-4.428	0.0
3.0	12.261	4.076	0.248E-04	2.747	1.783	8.185	6213.5	-4.609	0.477
9.0	12.257	4.085	0.102E-04	2.753	1.783	8.199	6219.5	-4.990	0.854
19.0	12.399	4.105	0.141E-04	2.776	1.803	8.251	6229.5	-4.849	1.279
39.5	12.443	4.122	0.540E-05	2.778	1.810	8.283	6250.0	-5.268	1.597
63.0	12.536	4.139	0.497E-05	2.790	1.823	8.323	6273.5	-5.303	1.798
87.0	12.629	4.159	0.564E-05	2.803	1.836	8.367	6297.5	-5.249	1.940
111.0	12.643	4.173	0.410E-05	2.813	1.839	8.392	6321.5	-5.387	2.045
135.0	12.718	4.186	0.385E-05	2.823	1.849	8.424	6345.5	-5.415	2.130
153.0	12.813	4.198	0.445E-05	2.831	1.863	8.455	6363.5	-5.352	2.185
209.5	12.906	4.216	0.218E-05	2.843	1.876	8.496	6420.0	-5.562	2.321
231.5	13.002	4.226	0.308E-05	2.850	1.890	8.524	6442.0	-5.512	2.365
255.0	13.050	4.233	0.209E-05	2.855	1.897	8.541	6465.5	-5.878	2.407
279.0	13.095	4.245	0.334E-05	2.863	1.904	8.566	6489.5	-5.477	2.446
303.0	13.122	4.254	0.257E-05	2.869	1.907	8.584	6513.5	-5.591	2.481
327.0	13.188	4.262	0.231E-05	2.874	1.917	8.606	6537.5	-5.637	2.515
351.0	13.216	4.268	0.180E-05	2.879	1.921	8.620	6551.5	-5.745	2.545
377.5	13.283	4.276	0.186E-05	2.883	1.931	8.639	6588.0	-5.731	2.577
399.0	13.381	4.282	0.201E-05	2.888	1.945	8.662	6609.5	-5.698	2.601
423.0	13.378	4.289	0.205E-05	2.893	1.944	8.673	6633.5	-5.888	2.626
447.0	13.424	4.300	0.308E-05	2.900	1.951	8.697	6657.5	-5.511	2.650
471.0	13.472	4.305	0.154E-05	2.904	1.958	8.711	6681.5	-5.813	2.673
499.0	13.569	4.311	0.132E-05	2.908	1.972	8.732	6709.5	-5.880	2.698
544.5	13.664	4.325	0.218E-05	2.917	1.985	8.767	6755.0	-5.717	2.736
567.0	13.661	4.331	0.192E-05	2.922	1.985	8.777	6777.5	-5.745	2.754
591.0	13.739	4.338	0.180E-05	2.926	1.996	8.797	6801.5	-5.892	2.772
615.0	13.757	4.342	0.128E-05	2.928	1.999	8.807	6825.5	-5.688	2.789
663.0	13.852	4.356	0.205E-05	2.939	2.012	8.842	6873.5	-5.891	2.822
687.0	13.930	4.361	0.128E-05	2.946	2.024	8.859	6897.5	-5.813	2.837
711.0	13.998	4.366	0.154E-05	2.946	2.033	8.876	6921.5	-5.812	2.852
735.0	14.047	4.369	0.772E-06	2.948	2.041	8.886	6945.5	-5.814	2.866
759.0	14.045	4.374	0.153E-05	2.951	2.040	8.895	6969.5	-5.888	2.880
783.0	14.043	4.378	0.103E-05	2.954	2.040	8.901	6993.5	-5.988	2.894
807.0	14.042	4.382	0.103E-05	2.956	2.040	8.907	7017.5	-5.988	2.907



GEOTECHNICAL LABORATORIES  
DEPARTMENT OF CIVIL ENGINEERING  
UNIVERSITY OF MANITOBA

CONSTANT CELL PRESSURE MULTI-STAGE  
TRIAxIAL CREEP TEST  
MST11 -  $\sigma_3 = 70 \text{ kPa}$

LOAD INCREMENT # 1 S.D. : 0 KPA

TIME (HOURS)	VOL DISPL (CC)	AXIAL DISPL (MM)	STRAIN RATE (/HR)	TRUE AXIAL STRAIN %	TRUE VOL. STRAIN %	DEVIATORIC STRAIN %	CUMULATIVE TIME (HRS)	LOGSTRAIN RATE/HOUR	LOGTIME HOURS
0.0	0.980	0.0	0.0	0.0	0.144	0.117	0.0	0.0	0.0
0.0	-1.721	0.002	0.125E-02	0.001	-0.253	0.203	0.0	-2.905	-1.899
0.5	-2.074	0.010	0.115E-03	0.007	-0.305	0.232	0.5	-3.938	-0.301
1.3	-2.129	0.024	0.123E-03	0.018	-0.313	0.216	1.3	-3.910	0.097
4.3	-2.031	0.029	0.103E-04	0.019	-0.299	0.197	4.3	-4.868	0.828
24.0	-2.134	0.042	0.281E-05	0.025	-0.314	0.196	24.0	-5.652	1.360
49.0	-2.136	0.045	0.123E-05	0.028	-0.314	0.189	49.0	-5.911	1.890
71.0	-2.138	0.047	0.112E-05	0.030	-0.314	0.183	71.0	-5.949	1.851
95.0	-2.240	0.052	0.512E-06	0.031	-0.329	0.192	95.0	-6.291	1.878
119.0	-2.240	0.052	0.128E-06	0.034	-0.329	0.184	119.0	-5.891	2.076
143.0	-2.240	0.053	0.253E-06	0.035	-0.329	0.183	143.0	-6.596	2.155
167.0	-2.242	0.056	0.103E-05	0.038	-0.330	0.177	167.0	-5.989	2.223
192.0	-2.242	0.056	0.0	0.038	-0.330	0.177	192.0	0.0	0.0
221.0	-2.389	0.049	-0.170E-05	0.033	-0.351	0.207	221.0	0.0	0.0
238.0	-2.392	0.055	0.254E-05	0.037	-0.352	0.189	238.0	-5.595	2.377
262.0	-2.342	0.056	0.253E-06	0.038	-0.344	0.189	262.0	-6.596	2.418
286.0	-2.393	0.059	0.773E-06	0.039	-0.352	0.191	286.0	-6.112	2.456
310.0	-2.444	0.061	0.512E-06	0.041	-0.359	0.194	310.0	-6.291	2.491
334.0	-2.344	0.062	0.254E-06	0.041	-0.345	0.180	334.0	-6.588	2.524
359.0	-2.345	0.064	0.491E-06	0.043	-0.345	0.177	359.0	-6.309	2.555
388.0	-2.343	0.060	-0.847E-06	0.040	-0.345	0.183	388.0	0.0	0.0
407.0	-2.393	0.060	0.0	0.040	-0.352	0.189	407.0	0.0	0.0

LOAD INCREMENT # 2 S.D. : 16 KPA

TIME (HOURS)	VOL DISPL (CC)	AXIAL DISPL (MM)	STRAIN RATE (/HR)	TRUE AXIAL STRAIN %	TRUE VOL. STRAIN %	DEVIATORIC STRAIN %	CUMULATIVE TIME (HRS)	LOGSTRAIN RATE/HOUR	LOGTIME HOURS
0.0	0.005	-0.012	-0.772E-02	-0.008	0.001	0.018	0.0	0.0	0.0
0.5	-0.085	-0.013	-0.138E-04	-0.008	-0.010	0.028	0.5	-2.905	-1.899
1.0	-0.146	-0.010	0.381E-04	-0.006	-0.022	0.033	1.0	-4.419	0.0
3.0	-0.127	-0.007	0.906E-05	-0.005	-0.019	0.027	3.0	-5.043	0.477
7.0	-0.047	-0.008	-0.143E-05	-0.005	-0.007	0.018	7.0	-4.988	0.626
23.0	0.051	-0.003	0.191E-05	-0.002	0.008	0.001	23.0	-5.720	1.362
31.0	0.050	-0.001	0.228E-05	-0.000	0.007	0.005	31.0	-5.645	1.491
46.0	0.099	0.002	0.123E-05	0.001	0.015	0.015	46.0	-5.911	1.663
71.5	0.098	0.004	0.482E-06	0.003	0.014	0.018	71.5	-6.317	1.854
95.0	0.098	0.005	0.264E-06	0.003	0.014	0.020	95.0	-6.579	1.878
121.0	0.097	0.009	0.947E-06	0.006	0.014	0.028	121.0	-6.024	2.083
146.0	0.140	0.025	0.444E-05	0.017	0.021	0.058	146.0	-5.353	2.164
173.0	0.143	0.018	-0.182E-05	0.012	0.021	0.046	173.0	0.0	0.0
202.5	0.142	0.022	0.835E-06	0.014	0.021	0.052	202.5	-6.079	2.306
226.5	0.142	0.021	-0.258E-06	0.014	0.021	0.051	226.5	-5.595	2.377

LOAD INCREMENT # 3 S.D. : 33 KPA

TIME (HOURS)	VOL DISPL (CC)	AXIAL DISPL (MM)	STRAIN RATE (/HR)	TRUE AXIAL STRAIN %	TRUE VOL. STRAIN %	DEVIATORIC STRAIN %	CUMULATIVE TIME (HRS)	LOGSTRAIN RATE/HOUR	LOGTIME HOURS
0.0	0.145	0.013	0.834E-02	0.008	0.021	0.038	226.5	-2.079	-2.000
0.5	0.097	0.009	-0.502E-04	0.005	0.014	0.025	227.0	-2.905	-1.899
1.3	-0.002	0.005	-0.330E-04	0.003	-0.000	0.008	227.7	-4.419	0.0
4.3	0.042	0.020	0.329E-04	0.013	0.006	0.038	230.7	-4.483	0.628
7.3	0.085	0.038	0.411E-04	0.026	0.012	0.073	233.7	-4.386	0.860
24.0	0.139	0.027	-0.441E-05	0.018	0.021	0.061	250.5	-5.720	1.362
47.5	0.346	0.011	-0.472E-05	0.007	0.051	0.059	274.0	-5.645	1.491
55.5	-0.308	0.149	0.118E-03	0.100	-0.045	0.207	282.0	-3.937	1.744
73.5	-0.461	0.157	0.274E-05	0.104	-0.088	0.200	300.0	-3.757	1.856
97.0	-0.700	0.772	0.175E-03	0.516	-0.103	1.180	323.5	-6.024	2.083
120.0	2.240	0.541	-0.672E-04	0.381	0.329	1.154	346.5	-3.834	2.112
129.5	2.359	0.749	0.147E-03	0.501	0.347	1.509	356.0	0.0	0.0
142.5	1.671	0.589	-0.823E-04	0.393	0.246	1.165	369.0	0.0	0.0
167.0	4.750	0.516	-0.199E-04	0.345	0.697	1.414	393.5	-6.079	2.306
191.0	4.650	0.516	0.0	0.345	0.683	1.402	417.5	-5.595	2.377
215.0	4.653	0.509	-0.208E-05	0.340	0.883	1.390	441.5	-6.596	2.418
264.0	4.652	0.511	0.378E-06	0.342	0.883	1.394	490.5	-6.422	2.422
287.0	4.650	0.514	0.107E-05	0.344	0.883	1.400	513.5	-5.969	2.458
311.0	4.751	0.515	-0.254E-06	0.343	0.697	1.411	537.5	-6.588	2.524
335.0	4.850	0.514	0.254E-06	0.344	0.712	1.424	561.5	-6.595	2.525
359.0	4.851	0.514	-0.254E-06	0.343	0.712	1.422	585.5	0.0	0.0
383.0	4.951	0.512	-0.518E-06	0.342	0.727	1.432	609.5	0.0	0.0
439.0	5.245	0.528	0.188E-05	0.353	0.770	1.492	665.5	-5.727	2.642

GEOTECHNICAL LABORATORIES  
DEPARTMENT OF CIVIL ENGINEERING  
UNIVERSITY OF MANITOBA

CONSTANT CELL PRESSURE MULTI-STAGE  
TRIAXIAL CREEP TEST  
MST12 -  $\sigma_3 = 70 \text{ kPa}$

LOAD INCREMENT # 1 S.D.: 0 KPA

TIME (HOURS)	VOL DISPL (CC)	AXIAL DISPL (MM)	STRAIN RATE (/HR)	TRUE AXIAL STRAIN %	TRUE VOL. STRAIN %	DEVIATORIC STRAIN %	CUMULATIVE TIME (HRS)	LOGSTRAIN RATE/HOUR	LOGTIME HOURS
0.0	-2.473	-0.080	-0.397E-01	-0.040	-0.363	0.383	0.0	0.0	0.0
0.8	-2.873	0.008	0.533E-03	0.004	-0.436	0.348	0.8	-3.273	-0.081
5.8	-2.778	0.020	0.187E-04	0.013	-0.408	0.300	5.8	-4.727	0.780
23.2	-2.880	0.022	0.887E-06	0.015	-0.423	0.308	23.2	-6.006	1.385
48.2	-2.880	0.023	0.234E-06	0.016	-0.437	0.319	48.2	-6.631	1.883
70.2	-2.880	0.023	0.0	0.018	-0.437	0.319	70.2	0.0	0.0
94.7	-2.880	0.022	-0.474E-06	0.014	-0.437	0.322	94.7	0.0	0.0
118.2	-2.880	0.022	-0.248E-06	0.015	-0.437	0.320	118.2	-6.609	2.073
142.2	-2.880	0.023	0.243E-06	0.015	-0.437	0.319	142.2	-6.614	2.163
166.2	-2.882	0.027	0.961E-06	0.018	-0.423	0.301	166.2	-6.017	2.221
191.2	-2.882	0.027	0.0	0.018	-0.423	0.301	191.2	0.0	0.0
221.0	-3.030	0.023	-0.774E-06	0.015	-0.445	0.325	221.0	0.0	0.0
238.0	-3.032	0.027	0.136E-06	0.018	-0.445	0.319	238.0	-5.867	2.377
262.0	-2.982	0.026	-0.243E-06	0.017	-0.437	0.315	262.0	0.0	0.0
286.0	-2.982	0.026	0.0	0.017	-0.437	0.315	286.0	0.0	0.0
310.0	-2.982	0.026	0.0	0.017	-0.437	0.315	310.0	0.0	0.0
334.0	-2.982	0.026	0.0	0.017	-0.437	0.315	334.0	0.0	0.0
359.5	-3.032	0.028	0.451E-06	0.018	-0.445	0.318	359.5	-6.346	2.556
388.0	-2.982	0.026	-0.404E-06	0.017	-0.437	0.315	388.0	0.0	0.0
407.0	-2.982	0.027	0.307E-06	0.018	-0.438	0.313	407.0	-6.512	2.610

LOAD INCREMENT # 2 S.D.: 16 KPA

TIME (HOURS)	VOL DISPL (CC)	AXIAL DISPL (MM)	STRAIN RATE (/HR)	TRUE AXIAL STRAIN %	TRUE VOL. STRAIN %	DEVIATORIC STRAIN %	CUMULATIVE TIME (HRS)	LOGSTRAIN RATE/HOUR	LOGTIME HOURS
0.0	-0.002	0.004	0.282E-02	0.003	-0.000	0.007	0.0	-2.550	-2.000
0.5	-0.106	0.013	0.118E-03	0.009	-0.015	0.008	0.5	-3.929	-0.301
2.5	-0.062	0.028	0.489E-04	0.018	-0.009	0.037	2.5	-4.310	0.398
6.5	-0.012	0.027	-0.145E-05	0.018	-0.002	0.042	6.5	-6.006	1.365
22.5	0.036	0.030	0.144E-05	0.020	0.005	0.054	22.5	-5.841	1.352
30.5	0.085	0.033	0.216E-05	0.022	0.012	0.064	30.5	-5.667	1.484
45.5	0.084	0.036	0.154E-05	0.024	0.012	0.069	45.5	-5.812	1.658
71.0	0.082	0.041	0.113E-05	0.027	0.012	0.076	71.0	-5.948	1.851
94.5	0.081	0.043	0.736E-06	0.029	0.012	0.080	94.5	-6.133	1.975
120.5	0.130	0.044	0.222E-06	0.029	0.019	0.087	120.5	-6.653	2.081
145.5	0.224	0.058	0.369E-05	0.039	0.033	0.121	145.5	-5.433	2.163
172.5	0.227	0.051	-0.171E-05	0.034	0.033	0.110	172.5	0.0	0.0
202.0	0.228	0.050	-0.194E-06	0.033	0.033	0.109	202.0	-5.867	2.377
226.0	0.227	0.051	0.239E-06	0.034	0.033	0.110	226.0	-6.623	2.354

LOAD INCREMENT # 3 S.D.: 33 KPA

TIME (HOURS)	VOL DISPL (CC)	AXIAL DISPL (MM)	STRAIN RATE (/HR)	TRUE AXIAL STRAIN %	TRUE VOL. STRAIN %	DEVIATORIC STRAIN %	CUMULATIVE TIME (HRS)	LOGSTRAIN RATE/HOUR	LOGTIME HOURS
0.0	0.180	0.044	0.286E-01	0.030	0.026	0.084	226.0	-1.529	-2.000
1.0	0.071	0.085	0.140E-03	0.043	0.010	0.115	227.0	-3.855	0.0
4.0	0.165	0.079	0.307E-04	0.053	0.024	0.149	230.0	-4.512	0.802
7.0	0.154	0.103	0.538E-04	0.069	0.023	0.187	233.0	-4.289	0.845
23.5	0.160	0.089	-0.559E-05	0.060	0.023	0.165	249.5	-5.841	1.672
47.0	0.442	0.130	0.115E-04	0.087	0.065	0.285	273.0	-3.978	1.740
55.0	-1.115	0.266	0.105E-03	0.171	-0.164	0.285	281.0	-3.978	1.740
73.0	-1.168	0.264	0.289E-05	0.176	-0.172	0.291	299.0	-5.540	1.863

LOAD INCREMENT # 4 S.D.: 33 KPA

TIME (HOURS)	VOL DISPL (CC)	AXIAL DISPL (MM)	STRAIN RATE (/HR)	TRUE AXIAL STRAIN %	TRUE VOL. STRAIN %	DEVIATORIC STRAIN %	CUMULATIVE TIME (HRS)	LOGSTRAIN RATE/HOUR	LOGTIME HOURS
96.5	-4.123	0.274	0.190E-04	0.183	-0.608	0.048	395.5	-4.722	1.985
119.5	-1.809	0.020	-0.737E-04	0.013	-0.266	0.185	418.5	-3.855	0.0
129.0	-3.837	0.306	0.200E-03	0.204	-0.536	0.061	428.0	-3.898	2.111
142.0	-1.035	-0.033	-0.173E-03	-0.022	-0.152	0.177	441.0	-4.269	0.845
166.5	-1.088	-0.026	0.187E-05	-0.017	-0.160	0.173	465.5	-5.728	2.221
190.5	-1.086	-0.031	-0.143E-05	-0.021	-0.160	0.161	489.5	-4.938	1.672
214.5	-1.087	-0.030	0.238E-06	-0.020	-0.160	0.179	513.5	-6.623	2.331
263.5	0.012	-0.027	0.467E-06	-0.018	-0.002	0.042	562.5	-6.331	2.421
286.5	0.112	-0.026	0.249E-06	-0.017	0.016	0.028	585.5	-6.604	2.457
310.5	0.112	-0.028	0.0	-0.017	0.016	0.028	609.5	-6.653	2.081
334.5	0.211	-0.024	0.477E-06	-0.016	0.031	0.014	633.5	-6.322	2.524
358.5	0.211	-0.025	-0.238E-06	-0.016	0.031	0.015	657.5	0.0	0.0
382.5	0.311	-0.025	0.0	-0.016	0.046	0.003	681.5	-5.867	2.377
438.5	0.806	-0.013	0.145E-05	-0.008	0.089	0.052	737.5	-5.838	2.642
502.5	0.806	-0.014	-0.179E-06	-0.010	0.089	0.049	801.5	0.0	0.0

LOAD INCREMENT # 5 S.D. : 49 KPA

TIME (HOURS)	VOL DISPL (CC)	AXIAL DISPL (MM)	STRAIN RATE (/HR)	TRUE AXIAL STRAIN %	TRUE VOL. STRAIN %	DEVIATORIC STRAIN %	CUMULATIVE TIME (HRS)	LOGSTRAIN RATE/HOUR	LOGTIME HOURS
0.0	0.802	-0.005	-0.334E-02	-0.003	0.088	0.084	801.5	-4.722	1.885
0.8	0.609	-0.021	-0.140E-03	-0.014	0.080	0.039	802.2	-3.855	0.0
2.3	0.809	-0.020	0.381E-05	-0.013	0.088	0.041	803.7	-5.419	0.352
4.8	0.609	-0.021	-0.229E-05	-0.014	0.090	0.039	806.2	-4.289	0.845
23.0	0.660	-0.022	-0.313E-06	-0.014	0.097	0.044	824.5	-5.729	2.221
47.0	0.710	-0.022	0.0	-0.014	0.104	0.050	848.5	-4.938	1.672
69.0	0.759	-0.019	0.780E-06	-0.013	0.111	0.060	870.5	-6.108	1.839
96.5	10.809	-0.019	0.0	-0.013	1.577	1.256	898.0	-6.331	2.421
117.0	0.757	-0.016	0.112E-05	-0.010	0.111	0.066	918.5	-5.952	2.068

LOAD INCREMENT # 6 S.D. : 65 KPA

TIME (HOURS)	VOL DISPL (CC)	AXIAL DISPL (MM)	STRAIN RATE (/HR)	TRUE AXIAL STRAIN %	TRUE VOL. STRAIN %	DEVIATORIC STRAIN %	CUMULATIVE TIME (HRS)	LOGSTRAIN RATE/HOUR	LOGTIME HOURS
0.0	0.758	-0.019	-0.126E-01	-0.013	0.111	0.060	918.5	-4.722	1.985
0.8	0.709	-0.020	-0.773E-05	-0.013	0.104	0.053	919.2	-3.855	0.0
2.3	0.754	-0.009	0.464E-04	-0.006	0.111	0.075	920.7	-4.333	0.352
5.3	0.806	-0.014	-0.409E-05	-0.009	0.118	0.074	927.7	-4.269	0.845
24.0	0.806	-0.014	0.0	-0.009	0.118	0.074	942.5	-5.729	2.221
48.0	0.807	-0.015	-0.238E-06	-0.010	0.118	0.073	966.5	-4.938	1.672
73.5	0.856	-0.013	0.449E-06	-0.008	0.126	0.082	992.0	-6.348	1.866
101.0	0.904	-0.009	0.832E-06	-0.006	0.133	0.093	1018.5	-6.080	2.004
120.0	0.904	-0.009	0.0	-0.006	0.133	0.093	1038.5	-5.952	2.068
144.0	0.905	-0.010	-0.238E-06	-0.007	0.133	0.092	1062.5	-6.653	2.081

LOAD INCREMENT # 7 S.D. : 82 KPA

TIME (HOURS)	VOL DISPL (CC)	AXIAL DISPL (MM)	STRAIN RATE (/HR)	TRUE AXIAL STRAIN %	TRUE VOL. STRAIN %	DEVIATORIC STRAIN %	CUMULATIVE TIME (HRS)	LOGSTRAIN RATE/HOUR	LOGTIME HOURS
0.0	0.907	-0.015	-0.102E-01	-0.010	0.133	0.084	1062.5	-4.722	1.885
0.8	0.907	-0.015	0.0	-0.010	0.133	0.084	1063.2	-3.855	0.0
2.3	0.896	0.010	0.111E-03	0.006	0.132	0.123	1064.7	-3.954	0.352
7.3	0.905	-0.012	-0.287E-04	-0.008	0.133	0.089	1069.7	-4.269	0.845
23.0	1.001	-0.002	0.442E-06	-0.001	0.147	0.118	1085.5	-5.355	1.382
47.0	1.000	0.000	0.485E-06	0.000	0.147	0.120	1109.5	-6.352	1.672
71.0	1.048	0.002	0.479E-06	0.001	0.154	0.129	1133.5	-6.318	1.851
97.0	1.099	0.003	0.222E-06	0.002	0.161	0.136	1159.5	-6.653	1.987
123.0	1.246	0.008	0.133E-06	0.005	0.183	0.162	1185.5	-5.876	2.090
144.0	1.243	0.015	0.220E-05	0.010	0.183	0.173	1206.5	-5.658	2.158

LOAD INCREMENT # 8 S.D. : 98 KPA

TIME (HOURS)	VOL DISPL (CC)	AXIAL DISPL (MM)	STRAIN RATE (/HR)	TRUE AXIAL STRAIN %	TRUE VOL. STRAIN %	DEVIATORIC STRAIN %	CUMULATIVE TIME (HRS)	LOGSTRAIN RATE/HOUR	LOGTIME HOURS
0.0	1.195	0.010	0.676E-02	0.007	0.176	0.160	1206.5	-2.170	-2.000
1.0	1.193	0.016	0.407E-04	0.011	0.175	0.159	1207.5	-4.390	0.0
4.5	1.240	0.022	0.115E-04	0.015	0.182	0.185	1211.0	-4.938	0.653
7.0	1.190	0.021	-0.229E-05	0.014	0.175	0.178	1213.5	-4.269	0.845
23.0	1.234	0.035	0.576E-05	0.023	0.181	0.205	1229.5	-5.240	1.362
74.0	1.272	0.063	0.362E-05	0.042	0.187	0.255	1280.5	-6.442	1.869
121.0	1.278	0.050	-0.184E-05	0.033	0.188	0.235	1327.5	-6.319	1.851
144.5	1.377	0.051	0.246E-06	0.034	0.202	0.248	1351.0	-6.608	2.160
171.5	1.474	0.058	0.170E-05	0.038	0.216	0.271	1378.0	-6.758	2.234
218.0	1.522	0.063	0.744E-06	0.042	0.223	0.285	1424.5	-6.128	2.338
243.5	1.551	0.065	0.456E-06	0.043	0.228	0.291	1450.0	-6.341	2.386
270.0	1.571	0.065	0.0	0.043	0.231	0.294	1476.5	0.0	0.0
289.5	1.571	0.064	-0.300E-06	0.042	0.231	0.292	1496.0	-5.867	2.377
312.5	1.572	0.063	-0.251E-06	0.042	0.231	0.291	1519.0	-5.639	2.642

LOAD INCREMENT # 9 S.D.: 114 KPA

TIME (HOURS)	VOL DISPL (CC)	AXIAL DISPL (MM)	STRAIN RATE (/HR)	TRUE AXIAL STRAIN %	TRUE VOL. STRAIN %	DEVIATORIC STRAIN %	CUMULATIVE TIME (HRS)	LOGSTRAIN RATE/HOUR	LOGTIME HOURS
0.0	1.572	0.062	0.415E-01	0.042	0.231	0.280	1518.0	-1.381	-2.000
1.0	1.572	0.063	0.578E-05	0.042	0.231	0.282	1520.0	-5.238	0.0
4.0	1.589	0.068	0.115E-04	0.046	0.230	0.300	1523.0	-4.937	0.802
23.0	1.570	0.067	-0.808E-06	0.044	0.231	0.297	1542.0	-4.269	0.845
47.0	1.685	0.078	0.336E-05	0.053	0.244	0.328	1566.0	-5.473	1.672
71.0	1.982	0.086	0.182E-05	0.057	0.288	0.375	1590.0	-6.717	1.851
95.0	1.986	0.089	0.360E-05	0.066	0.399	0.416	1614.0	-5.443	1.978
126.5	2.053	0.104	0.110E-05	0.068	0.301	0.418	1645.5	-5.980	2.102
145.0	2.053	0.106	0.629E-06	0.070	0.301	0.418	1684.0	-6.202	2.161
167.0	2.101	0.108	0.786E-06	0.072	0.308	0.428	1686.0	-6.104	2.223

LOAD INCREMENT #10 S.D.: 131 KPA

TIME (HOURS)	VOL DISPL (CC)	AXIAL DISPL (MM)	STRAIN RATE (/HR)	TRUE AXIAL STRAIN %	TRUE VOL. STRAIN %	DEVIATORIC STRAIN %	CUMULATIVE TIME (HRS)	LOGSTRAIN RATE/HOUR	LOGTIME HOURS
0.0	2.103	0.105	0.701E-01	0.070	0.308	0.424	1686.0	-1.154	-2.000
1.0	2.050	0.110	0.349E-04	0.074	0.301	0.426	1687.0	-4.457	0.0
4.0	2.126	0.120	0.212E-04	0.080	0.312	0.450	1690.0	-4.675	0.602
23.0	2.135	0.145	0.880E-05	0.097	0.313	0.493	1709.0	-5.055	1.362
47.0	2.130	0.156	0.312E-05	0.104	0.313	0.510	1733.0	-5.506	1.672
71.0	2.177	0.162	0.168E-05	0.108	0.320	0.526	1757.0	-5.774	1.851
95.0	2.224	0.169	0.182E-05	0.113	0.326	0.577	1808.0	-5.467	2.086
122.0	2.318	0.183	0.341E-05	0.122	0.340	0.543	1837.0	-5.716	1.978
151.0	2.318	0.182	-0.198E-06	0.121	0.340	0.575	1853.0	-6.202	2.161
167.0	2.317	0.185	0.108E-05	0.123	0.340	0.579	1837.0	-6.202	2.161
191.0	2.316	0.188	0.952E-06	0.125	0.340	0.585	1877.0	-5.966	2.223
215.0	2.384	0.193	0.120E-05	0.128	0.347	0.588	1901.0	-6.017	2.281
239.0	2.412	0.195	0.721E-06	0.130	0.354	0.608	1925.0	-5.820	2.332
263.0	2.412	0.196	0.241E-06	0.131	0.354	0.609	1949.0	-6.618	2.378
312.5	2.461	0.199	0.464E-06	0.133	0.361	0.620	1998.5	-6.142	2.495
336.5	2.510	0.201	0.485E-06	0.134	0.368	0.629	2022.5	-6.314	2.527
359.0	2.510	0.201	0.0	0.134	0.368	0.629	2046.0	0.0	0.0

LOAD INCREMENT #11 S.D.: 147 KPA

TIME (HOURS)	VOL DISPL (CC)	AXIAL DISPL (MM)	STRAIN RATE (/HR)	TRUE AXIAL STRAIN %	TRUE VOL. STRAIN %	DEVIATORIC STRAIN %	CUMULATIVE TIME (HRS)	LOGSTRAIN RATE/HOUR	LOGTIME HOURS
0.0	2.511	0.199	0.133E+00	0.133	0.368	0.626	2045.0	-0.877	-2.000
1.5	2.509	0.203	0.155E-04	0.135	0.368	0.632	2046.5	-4.811	0.176
4.5	2.538	0.204	0.386E-05	0.138	0.372	0.638	2049.5	-5.413	0.653
7.5	2.508	0.206	0.384E-05	0.137	0.368	0.637	2052.5	-5.416	0.875
23.5	2.551	0.222	0.648E-05	0.148	0.374	0.867	2068.5	-5.188	1.371
47.5	2.587	0.252	0.842E-05	0.168	0.380	0.721	2092.5	-5.075	1.677
71.5	2.580	0.267	0.409E-05	0.178	0.379	0.745	2116.5	-5.388	1.854
103.5	2.620	0.290	0.487E-05	0.193	0.384	0.788	2148.5	-5.313	2.015
121.0	2.662	0.306	0.593E-05	0.204	0.381	0.818	2166.0	-5.227	2.083
143.5	2.755	0.323	0.513E-05	0.215	0.404	0.857	2188.5	-5.290	2.157
167.5	2.748	0.339	0.457E-05	0.226	0.403	0.883	2212.5	-5.340	2.224
191.5	2.785	0.367	0.770E-05	0.245	0.409	0.933	2236.5	-5.114	2.282
215.5	2.819	0.402	0.987E-05	0.268	0.414	0.995	2260.5	-5.006	2.333
242.5	2.868	0.472	0.173E-04	0.315	0.424	1.118	2287.5	-4.761	2.385
289.5	2.895	0.569	0.138E-04	0.380	0.425	1.277	2334.5	-4.861	2.462
311.5	2.938	0.584	0.447E-05	0.390	0.431	1.307	2356.5	-5.350	2.493
336.5	2.983	0.595	0.301E-05	0.397	0.438	1.330	2381.5	-5.522	2.527
359.5	3.031	0.595	0.0	0.397	0.438	1.330	2404.5	-6.346	2.556
410.5	3.126	0.600	0.145E-05	0.401	0.445	1.345	2428.5	-5.840	2.584
460.0	3.125	0.611	0.257E-06	0.408	0.458	1.373	2455.5	-5.590	2.613
487.5	3.220	0.623	0.233E-06	0.408	0.458	1.376	2505.0	-6.632	2.663
506.5	3.219	0.627	0.252E-05	0.416	0.472	1.404	2532.5	-5.598	2.688
			0.153E-05	0.419	0.472	1.411	2551.5	-5.816	2.705



LOAD INCREMENT #12 S.D. = 163 KPA

TIME (HOURS)	VOL DISPL (CC)	AXIAL DISPL (MM)	STRAIN RATE (/HR)	TRUE STRAIN %	AXIAL STRAIN %	TRUE VOL. STRAIN %	DEVIATORIC STRAIN %	CUMULATIVE TIME (HRS)	LOGSTRAIN RATE/HOUR	LOGTIME HOURS
0.0	3.220	0.624	0.417E+00	0.417	0.472	1.406	2551.5	-0.380	-2.000	
1.5	3.118	0.629	0.194E-04	0.420	0.457	1.401	2553.0	-4.713	0.176	
3.5	3.216	0.634	0.174E-04	0.423	0.472	1.421	2555.0	-4.761	0.544	
8.5	3.286	0.655	0.278E-04	0.437	0.482	1.464	2560.0	-4.556	0.929	
23.5	3.202	0.663	0.386E-05	0.443	0.470	1.468	2575.0	-5.413	1.371	
47.5	3.240	0.690	0.747E-05	0.461	0.475	1.516	2599.0	-5.126	1.672	
74.5	3.332	0.709	0.472E-05	0.473	0.489	1.559	2626.0	-5.325	1.872	
121.0	3.369	0.737	0.398E-05	0.492	0.494	1.608	2672.5	-5.400	2.083	
143.5	3.414	0.750	0.386E-05	0.501	0.501	1.635	2695.0	-5.413	2.157	
167.5	3.460	0.757	0.217E-05	0.506	0.507	1.653	2719.0	-5.413	2.224	
191.5	3.457	0.765	0.217E-05	0.511	0.507	1.666	2743.0	-5.663	2.262	
215.5	3.451	0.777	0.338E-05	0.519	0.506	1.685	2767.0	-5.472	2.333	
239.5	3.548	0.784	0.193E-05	0.524	0.520	1.708	2791.0	-5.714	2.379	
266.0	3.593	0.796	0.174E-05	0.532	0.527	1.733	2837.5	-5.759	2.456	
308.5	3.639	0.805	0.258E-05	0.538	0.533	1.753	2860.0	-5.589	2.488	
332.5	3.637	0.809	0.986E-06	0.540	0.533	1.758	2884.0	-6.015	2.522	
356.5	3.637	0.809	0.242E-06	0.541	0.533	1.760	2908.0	-6.616	2.562	
380.5	3.635	0.814	0.121E-05	0.543	0.533	1.786	2932.0	-5.919	2.580	
404.5	3.585	0.813	-0.242E-06	0.543	0.526	1.759	2956.0	-5.840	2.584	
452.5	3.534	0.815	0.242E-06	0.544	0.518	1.766	3004.0	-6.616	2.656	
476.5	3.584	0.815	0.0	0.548	0.526	1.762	3028.0	-6.632	2.663	
500.5	3.732	0.821	0.169E-05	0.557	0.547	1.789	3052.0	-5.773	2.699	
524.5	3.826	0.834	0.386E-05	0.557	0.561	1.823	3076.0	-5.413	2.720	
548.5	3.920	0.847	0.338E-05	0.565	0.575	1.854	3100.0	-5.471	2.739	
572.5	3.917	0.853	0.193E-05	0.570	0.574	1.885	3124.0	-5.715	2.758	
605.5	4.010	0.869	0.316E-05	0.581	0.588	1.902	3157.0	-5.500	2.782	
844.5	4.053	0.885	0.268E-05	0.591	0.594	1.933	3186.0	-5.572	2.809	
868.5	4.099	0.893	0.242E-05	0.597	0.601	1.952	3220.0	-5.617	2.825	
892.5	4.145	0.903	0.266E-05	0.603	0.608	1.973	3244.0	-5.715	2.840	
916.5	4.142	0.910	0.193E-05	0.608	0.607	1.984	3268.0	-5.617	2.855	
940.5	4.188	0.918	0.242E-05	0.614	0.614	2.004	3292.0	-5.617	2.870	
964.5	4.280	0.937	0.246E-05	0.626	0.627	2.045	3341.5	-5.609	2.898	
988.5	4.324	0.948	0.360E-05	0.634	0.634	2.070	3364.0	-5.443	2.910	
1012.5	4.370	0.957	0.242E-05	0.640	0.640	2.090	3388.0	-5.617	2.922	
1036.5	4.367	0.964	0.193E-05	0.644	0.640	2.101	3412.0	-5.715	2.935	
1060.5	4.415	0.969	0.145E-05	0.648	0.647	2.115	3436.0	-5.839	2.947	
1084.5	4.459	0.983	0.290E-05	0.657	0.653	2.143	3468.0	-5.538	2.962	
1108.5	4.505	0.991	0.128E-05	0.662	0.660	2.161	3509.5	-5.900	2.981	
1132.5	4.551	1.000	0.258E-05	0.668	0.667	2.181	3532.0	-5.689	2.991	
1156.5	4.598	1.008	0.242E-05	0.674	0.674	2.201	3556.0	-5.617	3.002	
1180.5	4.644	1.017	0.242E-05	0.680	0.680	2.220	3680.0	-5.617	3.012	
1204.5	4.661	1.023	0.169E-05	0.684	0.683	2.232	3804.0	-5.772	3.022	
1228.5	4.639	1.027	0.121E-05	0.687	0.680	2.237	3828.0	-5.918	3.032	
1252.5	4.714	1.038	0.278E-05	0.694	0.691	2.263	3853.0	-5.555	3.042	
1276.5	4.731	1.045	0.211E-05	0.698	0.693	2.276	3878.0	-5.675	3.051	
1300.5	4.779	1.051	0.162E-05	0.702	0.700	2.292	3700.0	-5.790	3.060	
1324.5	4.727	1.054	0.968E-06	0.705	0.693	2.291	3724.0	-6.014	3.069	
1348.5	4.825	1.059	0.145E-05	0.708	0.707	2.312	3748.0	-5.838	3.078	
1372.5	4.920	1.070	0.258E-06	0.715	0.721	2.340	3775.0	-5.589	3.088	
1396.5	5.017	1.077	0.218E-05	0.720	0.735	2.364	3799.0	-5.662	3.096	
1420.5	5.010	1.091	0.404E-05	0.730	0.734	2.385	3822.0	-5.394	3.104	
1444.5	5.008	1.097	0.173E-05	0.734	0.734	2.388	3845.5	-5.762	3.112	
1468.5	5.001	1.111	0.404E-05	0.743	0.733	2.418	3868.5	-5.394	3.120	
1492.5	5.094	1.129	0.494E-05	0.755	0.746	2.457	3892.0	-5.306	3.127	
1516.5	5.090	1.137	0.241E-05	0.760	0.745	2.471	3916.0	-5.617	3.135	
1540.5	5.185	1.147	0.268E-05	0.767	0.759	2.498	3940.0	-5.576	3.143	
1564.5	5.180	1.160	0.355E-05	0.775	0.759	2.519	3964.5	-5.449	3.150	
1588.5	5.226	1.168	0.228E-05	0.781	0.765	2.539	3990.0	-5.642	3.158	
1612.5	5.270	1.180	0.348E-05	0.789	0.772	2.564	4013.5	-5.461	3.165	
1636.5	5.317	1.187	0.207E-05	0.794	0.779	2.581	4036.0	-5.886	3.172	
1660.5	5.361	1.202	0.411E-05	0.804	0.785	2.610	4060.0	-5.366	3.179	
1684.5	5.407	1.211	0.194E-05	0.810	0.782	2.630	4090.0	-5.713	3.187	
1708.5	5.405	1.215	0.162E-05	0.813	0.791	2.637	4108.0	-5.792	3.192	
1732.5	5.451	1.224	0.207E-05	0.818	0.788	2.656	4136.0	-5.683	3.200	
1756.5	5.447	1.232	0.264E-05	0.824	0.796	2.670	4158.0	-5.579	3.206	
1780.5	5.543	1.241	0.126E-05	0.830	0.812	2.696	4204.0	-5.898	3.218	
1804.5	5.542	1.243	0.483E-06	0.831	0.812	2.699	4228.0	-6.316	3.224	
1828.5	5.638	1.252	0.268E-05	0.838	0.826	2.726	4252.0	-5.574	3.231	
1852.5	5.489	1.251	-0.238E-06	0.837	0.804	2.706	4276.5	0.0	0.0	
1876.5	5.627	1.255	0.969E-06	0.839	0.826	2.730	4300.5	-6.014	3.243	





## LOAD INCREMENT #17 S.D.: 294 KPA

TIME (HOURS)	VOL DISPL (CC)	AXIAL DISPL (MM)	STRAIN RATE (/HR)	TRUE STRAIN %	AXIAL STRAIN %	TRUE VOL. STRAIN %	DEVIATORIC STRAIN %	CUMULATIVE TIME (HRS)	LOGSTRAIN RATE/HOUR	LOGTIME HOURS
0.0	8.338	4.373	0.296E+01	2.956	1.218	8.236	8439.5	0.471	-2.000	
1.0	8.336	4.376	0.180E-04	2.958	1.218	8.240	8440.5	-4.745	0.0	
2.0	8.335	4.380	0.296E-04	2.961	1.218	8.248	8441.5	-4.529	0.301	
8.0	8.328	4.394	0.158E-04	2.971	1.217	8.270	8447.5	-4.800	0.903	
27.0	8.418	4.418	0.843E-05	2.987	1.230	8.320	8466.5	-5.074	1.431	
50.0	8.513	4.429	0.336E-05	2.994	1.244	8.350	8489.5	-5.474	1.699	
72.5	8.503	4.450	0.633E-05	3.009	1.242	8.384	8512.0	-5.199	1.850	
95.5	8.592	4.475	0.749E-05	3.026	1.255	8.437	8535.0	-5.126	1.980	
119.5	8.632	4.497	0.643E-05	3.041	1.261	8.479	8559.0	-5.192	2.077	
143.5	8.676	4.511	0.396E-05	3.051	1.267	8.508	8583.0	-5.402	2.157	
167.5	8.671	4.523	0.346E-05	3.059	1.267	8.527	8607.0	-5.461	2.224	
191.5	8.761	4.544	0.594E-05	3.073	1.280	8.573	8631.0	-5.226	2.282	
216.5	8.854	4.560	0.451E-05	3.085	1.293	8.612	8655.0	-5.345	2.335	
240.5	8.851	4.565	0.149E-05	3.088	1.264	8.586	8680.0	-5.828	2.381	
263.5	8.841	4.589	0.697E-05	3.104	1.291	8.658	8703.0	-5.157	2.421	
287.5	9.032	4.608	0.545E-05	3.117	1.319	8.713	8727.0	-5.264	2.459	
311.5	9.172	4.631	0.669E-05	3.133	1.339	8.769	8751.0	-5.175	2.493	
335.5	9.213	4.652	0.595E-05	3.148	1.345	8.808	8775.0	-5.226	2.526	
359.5	9.203	4.674	0.619E-05	3.162	1.344	8.844	8799.0	-5.208	2.556	
455.5	9.377	4.731	0.415E-05	3.202	1.369	8.962	8895.0	-5.430	2.658	
479.5	9.471	4.744	0.372E-05	3.211	1.383	8.995	8919.0	-5.429	2.681	
503.5	9.465	4.757	0.372E-05	3.220	1.382	9.016	8943.0	-5.852	2.722	
527.5	9.412	4.765	0.223E-05	3.225	1.374	9.023	8967.0	-6.357	2.830	
576.5	9.458	4.775	0.439E-06	3.232	1.381	9.044	9040.5	-5.732	2.795	
601.0	9.406	4.778	-0.316E-06	3.234	1.373	9.044	9063.0	-6.307	2.811	
623.5	9.353	4.784	0.185E-05	3.239	1.366	9.048	9087.0	-5.760	2.827	
647.5	9.553	4.786	0.493E-06	3.240	1.395	9.074	9111.0	-5.631	2.845	
671.5	9.550	4.792	0.174E-05	3.244	1.394	9.084	9139.0	-5.825	2.872	
695.5	9.846	4.802	0.234E-05	3.250	1.408	9.112	9207.1	-5.559	2.899	
744.5	9.842	4.809	0.119E-05	3.256	1.408	9.124	9233.0	-5.827	2.924	
767.8	9.836	4.819	0.284E-05	3.262	1.407	9.140	9303.0	-6.071	2.936	
793.5	9.733	4.829	0.276E-05	3.269	1.421	9.169	9352.0	-5.742	2.971	
815.5	9.733	4.829	0.0	3.269	1.421	9.169	9375.0	-5.402	2.982	
839.5	9.730	4.835	0.174E-05	3.274	1.420	9.179	9399.0			
863.5	9.728	4.840	0.149E-05	3.277	1.420	9.187				
912.5	9.925	4.847	0.850E-06	3.281	1.449	9.221				
935.5	10.023	4.853	0.181E-05	3.286	1.463	9.242				
959.5	10.016	4.866	0.397E-05	3.295	1.462	9.265				

## LOAD INCREMENT #18 S.D.: 327 KPA

TIME (HOURS)	VOL DISPL (CC)	AXIAL DISPL (MM)	STRAIN RATE (/HR)	TRUE STRAIN %	AXIAL STRAIN %	TRUE VOL. STRAIN %	DEVIATORIC STRAIN %	CUMULATIVE TIME (HRS)	LOGSTRAIN RATE/HOUR	LOGTIME HOURS
0.0	10.016	4.867	0.330E+01	3.296	1.462	9.266	9399.0	0.516	-2.000	
0.5	10.014	4.872	0.729E-04	3.299	1.462	9.274	9399.5	-4.137	-0.301	
2.0	10.010	4.882	0.437E-04	3.306	1.461	9.290	9401.0	-4.360	0.301	
7.5	10.006	4.890	0.108E-04	3.312	1.473	9.304	9406.5	-4.866	0.875	
23.5	10.095	4.915	0.104E-04	3.328	1.473	9.355	9422.5	-4.982	1.371	
33.0	10.091	4.923	0.627E-05	3.334	1.473	9.370	9432.0	-5.203	1.519	
47.5	10.134	4.940	0.780E-05	3.346	1.479	9.402	9446.6	-5.108	1.677	
75.0	10.267	4.977	0.932E-05	3.371	1.498	9.461	9474.0	-5.031	1.875	
120.5	10.344	5.029	0.786E-05	3.407	1.509	9.576	9519.5	-5.105	2.081	
143.5	10.432	5.055	0.777E-05	3.425	1.522	9.632	9542.5	-5.109	2.157	
167.5	10.518	5.085	0.870E-05	3.446	1.535	9.693	9566.6	-5.061	2.224	
181.5	10.509	5.106	0.596E-05	3.460	1.533	9.727	9590.5	-5.225	2.282	
215.5	10.648	5.131	0.721E-05	3.477	1.553	9.786	9614.5	-5.142	2.333	
240.5	10.684	5.161	0.835E-05	3.498	1.559	9.841	9639.5	-5.078	2.381	

GEOTECHNICAL LABORATORIES  
DEPARTMENT OF CIVIL ENGINEERING  
UNIVERSITY OF MANITOBA

CONSTANT CELL PRESSURE MULTI-STAGE  
TRIAXIAL CREEP TEST  
MST13 -  $\sigma_3 = 70$  kPa

LOAD INCREMENT # 1 S.D. : 0 KPA									
TIME (HOURS)	VOL DISPL (CC)	AXIAL DISPL (MM)	STRAIN RATE (/HR)	TRUE AXIAL STRAIN %	TRUE VOL. STRAIN %	DEVIATORIC STRAIN %	CUMULATIVE TIME (HRS)	LOGSTRAIN RATE/HOUR	LOGTIME HOURS
0.0	-2.080	-0.025	-0.188E-01	-0.017	-0.302	0.287	0.0	0.0	0.0
0.5	-2.131	-0.023	0.253E-04	-0.015	-0.312	0.293	0.5	-4.597	-0.301
2.0	-2.216	-0.010	0.578E-04	-0.007	-0.325	0.282	2.0	-4.238	0.301
4.0	-2.266	-0.011	-0.334E-05	-0.007	-0.332	0.289	4.0	0.0	0.0
10.0	-2.317	-0.007	0.413E-05	-0.005	-0.340	0.289	10.0	-5.384	1.000
27.0	-2.421	0.004	0.432E-05	0.002	-0.355	0.284	27.0	-5.388	1.431
47.5	-2.542	0.005	0.287E-06	0.003	-0.373	0.287	47.5	-5.528	1.877
71.5	-2.622	0.005	0.0	0.003	-0.384	0.306	71.5	0.0	0.0
95.5	-2.672	0.005	0.0	0.003	-0.392	0.312	95.5	0.0	0.0
121.0	-2.723	0.006	0.484E-06	0.004	-0.399	0.315	121.0	-6.315	2.083
148.5	-2.723	0.006	0.0	0.004	-0.399	0.315	148.5	0.0	0.0
167.5	-2.723	0.006	0.0	0.004	-0.399	0.315	167.5	0.0	0.0
191.5	-2.773	0.006	0.0	0.004	-0.407	0.321	191.5	0.0	0.0
215.0	-2.823	0.007	0.264E-06	0.005	-0.414	0.326	215.0	-6.578	2.332
239.0	-2.873	0.006	-0.258E-06	0.004	-0.421	0.333	239.0	0.0	0.0
263.0	-2.923	0.006	0.0	0.004	-0.429	0.339	263.0	0.0	0.0
289.0	-2.942	0.006	-0.238E-06	0.004	-0.432	0.343	289.0	0.0	0.0
315.0	-2.923	0.006	0.238E-06	0.004	-0.429	0.339	315.0	-6.627	2.498
335.5	-2.923	0.006	0.0	0.004	-0.429	0.339	335.5	0.0	0.0

LOAD INCREMENT # 2 S.D. : 85 KPA									
TIME (HOURS)	VOL DISPL (CC)	AXIAL DISPL (MM)	STRAIN RATE (/HR)	TRUE AXIAL STRAIN %	TRUE VOL. STRAIN %	DEVIATORIC STRAIN %	CUMULATIVE TIME (HRS)	LOGSTRAIN RATE/HOUR	LOGTIME HOURS
0.0	-0.004	0.011	0.783E-02	0.008	-0.001	0.018	0.0	-2.117	-2.000
0.5	-0.089	0.023	0.151E-03	0.015	-0.013	0.026	0.5	-3.821	-0.301
2.0	-0.119	0.048	0.115E-03	0.032	-0.017	0.065	2.0	-3.940	0.301
4.5	-0.121	0.055	0.173E-04	0.037	-0.018	0.075	4.5	-4.763	0.853
7.0	-0.123	0.059	0.123E-04	0.040	-0.018	0.082	7.0	-4.910	0.845
23.0	-0.152	0.082	0.924E-05	0.054	-0.022	0.115	23.0	-5.035	1.362
74.0	-0.165	0.116	0.447E-05	0.077	-0.024	0.169	74.0	-5.350	1.869
121.0	-0.241	0.107	-0.131E-05	0.071	-0.038	0.145	121.0	0.0	0.0
144.5	-0.243	0.111	0.131E-05	0.074	-0.036	0.152	144.5	-5.882	2.180
171.5	-0.245	0.117	0.137E-05	0.078	-0.036	0.161	171.5	-5.863	2.234
218.0	-0.248	0.123	0.925E-06	0.082	-0.036	0.171	218.0	-6.034	2.338
243.5	-0.248	0.122	-0.239E-06	0.082	-0.036	0.170	243.5	0.0	0.0
270.0	-0.248	0.122	0.0	0.082	-0.036	0.170	270.0	0.0	0.0
289.5	-0.249	0.125	0.948E-06	0.083	-0.037	0.174	289.5	-6.023	2.462
312.5	-0.249	0.127	0.537E-06	0.085	-0.037	0.177	312.5	-6.270	2.485

LOAD INCREMENT # 3 S.D. : 82 KPA									
TIME (HOURS)	VOL DISPL (CC)	AXIAL DISPL (MM)	STRAIN RATE (/HR)	TRUE AXIAL STRAIN %	TRUE VOL. STRAIN %	DEVIATORIC STRAIN %	CUMULATIVE TIME (HRS)	LOGSTRAIN RATE/HOUR	LOGTIME HOURS
0.0	-0.248	0.125	0.831E-01	0.083	-0.037	0.174	312.5	-1.080	-2.000
0.5	-0.347	0.122	-0.377E-04	0.081	-0.051	0.157	313.0	-3.821	-0.301
2.0	-0.351	0.132	0.451E-04	0.088	-0.052	0.173	314.5	-4.345	0.301
4.0	-0.301	0.131	-0.304E-06	0.087	-0.044	0.178	316.5	-4.763	0.853
6.5	-0.301	0.132	0.243E-05	0.088	-0.044	0.179	319.0	-5.614	0.813
23.0	-0.355	0.142	0.411E-05	0.095	-0.052	0.189	335.5	-5.386	1.362
47.0	-0.360	0.153	0.308E-05	0.102	-0.053	0.207	359.5	-5.511	1.872
71.5	-0.362	0.158	0.151E-05	0.105	-0.053	0.216	384.0	-5.822	1.854
95.0	-0.365	0.167	0.238E-05	0.111	-0.054	0.229	407.5	-5.627	1.978
126.5	-0.389	0.176	0.186E-05	0.118	-0.057	0.241	439.0	-5.708	2.102
145.0	-0.371	0.182	0.200E-05	0.121	-0.055	0.253	457.5	-5.899	2.161
167.0	-0.371	0.184	0.559E-06	0.123	-0.055	0.255	479.5	-6.253	2.223

LOAD INCREMENT # 4 S.D. : 98 KPA									
TIME (HOURS)	VOL DISPL (CC)	AXIAL DISPL (MM)	STRAIN RATE (/HR)	TRUE AXIAL STRAIN %	TRUE VOL. STRAIN %	DEVIATORIC STRAIN %	CUMULATIVE TIME (HRS)	LOGSTRAIN RATE/HOUR	LOGTIME HOURS
0.0	-0.371	0.183	0.122E+00	0.122	-0.055	0.254	479.5	-0.915	-2.000
0.5	-0.371	0.183	0.0	0.122	-0.055	0.254	480.0	-3.821	-0.301
2.0	-0.374	0.189	0.288E-04	0.126	-0.055	0.264	481.5	-4.541	0.301
4.0	-0.375	0.193	0.123E-04	0.129	-0.055	0.270	483.5	-4.909	0.802
6.5	-0.374	0.191	-0.494E-05	0.127	-0.055	0.267	485.0	-5.814	0.813
23.0	-0.380	0.206	0.598E-05	0.137	-0.056	0.290	502.5	-5.223	1.362
47.0	-0.384	0.215	0.257E-05	0.143	-0.056	0.305	526.5	-5.591	1.672
71.0	-0.387	0.224	0.257E-05	0.149	-0.057	0.320	550.5	-5.590	1.851
95.0	-0.389	0.229	0.128E-05	0.153	-0.057	0.327	574.5	-5.892	1.978
122.0	-0.344	0.241	0.297E-05	0.161	-0.051	0.352	601.5	-5.527	2.086
151.0	-0.393	0.240	-0.214E-06	0.160	-0.058	0.345	630.5	-5.699	2.161
167.0	-0.394	0.241	0.388E-06	0.161	-0.058	0.346	646.5	-6.411	2.223
191.0	-0.395	0.245	0.768E-06	0.162	-0.058	0.350	670.5	-6.116	2.281
215.0	-0.445	0.249	0.517E-06	0.164	-0.066	0.347	694.5	-5.286	2.332
239.0	-0.477	0.249	0.103E-05	0.165	-0.070	0.350	718.5	-5.988	2.376
263.0	-0.477	0.250	0.254E-06	0.167	-0.070	0.351	742.5	-6.596	2.420
288.5	-0.448	0.253	0.728E-06	0.169	-0.066	0.359	768.0	-6.138	2.460
312.5	-0.450	0.257	0.129E-05	0.172	-0.066	0.366	792.0	-5.891	2.495
335.0	-0.401	0.259	0.547E-06	0.173	-0.059	0.375	814.5	-6.262	2.525

## LOAD INCREMENT # 5 S.D.: 114 KPA

TIME (HOURS)	VOL DISPL (CC)	AXIAL DISPL (MM)	STRAIN RATE (/HR)	TRUE AXIAL STRAIN %	TRUE VOL. STRAIN %	DEVIATORIC STRAIN %	CUMULATIVE TIME (HRS)	LOGSTRAIN RATE/HOUR	LOGTIME HOURS
0.0	-0.448	0.255	0.170E+00	0.170	-0.086	0.383	814.5	-0.788	-2.000
0.5	-0.449	0.285	0.0	0.170	-0.069	0.381	815.0	-3.821	-0.301
2.5	-0.452	0.282	0.218E-04	0.175	-0.086	0.373	817.0	-4.866	0.388
4.5	-0.401	0.280	-0.821E-06	0.173	-0.058	0.378	819.0	-4.809	0.802
7.5	-0.401	0.289	-0.203E-06	0.173	-0.059	0.376	822.0	-5.614	0.813
23.5	-0.403	0.285	0.270E-06	0.177	-0.059	0.385	838.0	-5.569	1.371
47.5	-0.427	0.278	0.283E-06	0.184	-0.063	0.399	862.0	-5.549	1.677
71.5	-0.459	0.280	0.129E-06	0.187	-0.067	0.403	886.0	-5.881	1.854
103.5	-0.463	0.290	0.212E-06	0.194	-0.064	0.419	918.0	-5.674	2.015
121.0	-0.414	0.294	0.141E-06	0.186	-0.061	0.431	935.5	-5.852	2.083
143.5	-0.416	0.299	0.137E-05	0.199	-0.061	0.438	958.0	-5.863	2.167
167.5	-0.416	0.298	0.0	0.199	-0.061	0.438	982.0	-6.411	2.223
191.5	-0.419	0.307	0.231E-06	0.205	-0.062	0.451	1006.0	-5.636	2.282
215.5	-0.473	0.317	0.282E-06	0.212	-0.070	0.461	1030.0	-5.549	2.333
242.5	-0.444	0.320	0.688E-06	0.213	-0.065	0.469	1057.0	-6.162	2.385
289.5	-0.525	0.323	0.393E-06	0.215	-0.077	0.464	1104.0	-6.406	2.462
311.5	-0.527	0.326	0.842E-06	0.217	-0.077	0.469	1126.0	-6.075	2.493
336.5	-0.527	0.326	0.0	0.217	-0.077	0.469	1151.0	-5.891	2.495
359.5	-0.528	0.328	0.805E-06	0.219	-0.078	0.473	1174.0	-6.094	2.556
383.5	-0.528	0.331	0.789E-06	0.221	-0.078	0.477	1198.0	-6.114	2.584
410.5	-0.529	0.333	0.456E-06	0.222	-0.078	0.480	1225.0	-6.341	2.613
457.0	-0.429	0.333	0.0	0.222	-0.063	0.492	1271.5	0.0	0.0
484.5	-0.381	0.338	0.112E-06	0.225	-0.056	0.506	1299.0	-5.950	2.685
503.5	-0.431	0.338	0.0	0.225	-0.063	0.500	1318.0	0.0	0.0

## LOAD INCREMENT # 6 S.D.: 130 KPA

TIME (HOURS)	VOL DISPL (CC)	AXIAL DISPL (MM)	STRAIN RATE (/HR)	TRUE AXIAL STRAIN %	TRUE VOL. STRAIN %	DEVIATORIC STRAIN %	CUMULATIVE TIME (HRS)	LOGSTRAIN RATE/HOUR	LOGTIME HOURS
0.0	-0.431	0.338	0.224E+00	0.224	-0.063	0.498	1318.0	-0.649	-2.000
0.5	-0.450	0.335	-0.127E-04	0.224	-0.066	0.494	1318.5	-3.821	-0.301
3.5	-0.433	0.343	0.185E-04	0.229	-0.064	0.508	1321.5	-4.783	0.544
8.5	-0.388	0.354	0.148E-04	0.236	-0.067	0.532	1326.5	-4.830	0.929
23.5	-0.388	0.354	0.0	0.236	-0.067	0.532	1341.5	-5.614	0.813
47.5	-0.440	0.359	0.154E-05	0.240	-0.065	0.535	1365.5	-5.812	1.677
71.5	-0.392	0.366	0.180E-05	0.244	-0.066	0.551	1369.5	-5.745	1.854
121.0	-0.448	0.380	0.187E-05	0.253	-0.066	0.567	1439.0	-5.728	2.083
143.5	-0.449	0.384	0.137E-05	0.256	-0.066	0.574	1461.5	-5.862	2.157
167.5	-0.453	0.394	0.267E-05	0.263	-0.067	0.589	1485.5	-5.590	2.224
191.5	-0.455	0.389	0.155E-05	0.266	-0.067	0.598	1509.5	-5.811	2.282
215.5	-0.458	0.406	0.180E-05	0.271	-0.067	0.608	1533.5	-5.746	2.333
238.5	-0.410	0.411	0.155E-05	0.274	-0.060	0.623	1557.5	-5.811	2.379
289.0	-0.463	0.420	0.125E-05	0.281	-0.068	0.632	1607.0	-5.904	2.461
311.5	-0.465	0.425	0.137E-05	0.284	-0.068	0.639	1629.5	-5.862	2.493
335.5	-0.387	0.429	0.103E-05	0.286	-0.054	0.657	1653.5	-5.989	2.526
359.5	-0.467	0.431	0.516E-06	0.287	-0.089	0.648	1677.5	-6.288	2.556
407.5	-0.519	0.433	0.772E-06	0.289	-0.076	0.646	1701.5	-6.112	2.584
455.5	-0.519	0.434	0.259E-06	0.290	-0.084	0.642	1725.5	-6.587	2.610
478.5	-0.519	0.434	0.0	0.290	-0.076	0.648	1773.5	-6.114	2.584
503.5	-0.471	0.433	-0.259E-06	0.289	-0.076	0.646	1797.5	-6.341	2.613
527.5	-0.375	0.440	0.180E-05	0.294	-0.089	0.652	1821.5	-5.745	2.702
551.5	-0.377	0.455	0.258E-05	0.300	-0.055	0.689	1845.5	-5.589	2.722
575.5	-0.378	0.458	0.154E-05	0.303	-0.055	0.698	1889.5	-5.812	2.742
608.5	-0.331	0.465	0.103E-05	0.306	-0.056	0.704	1893.5	-5.988	2.760
647.5	-0.284	0.473	0.142E-05	0.316	-0.049	0.720	1926.5	-5.883	2.784
671.5	-0.286	0.478	0.129E-05	0.319	-0.042	0.739	1965.5	-5.846	2.811
695.5	-0.287	0.481	0.103E-05	0.321	-0.042	0.747	1989.5	-5.890	2.827
719.5	-0.289	0.485	0.103E-05	0.324	-0.042	0.752	2013.5	-5.988	2.842
746.5	-0.339	0.486	0.230E-06	0.324	-0.050	0.758	2037.5	-5.988	2.857
786.0	-0.291	0.492	0.748E-06	0.328	-0.043	0.754	2084.5	-6.638	2.873
818.5	-0.294	0.499	0.220E-05	0.333	-0.043	0.769	2114.0	-6.126	2.901
842.5	-0.296	0.508	0.257E-05	0.339	-0.044	0.785	2136.5	-5.858	2.912
886.5	-0.299	0.511	0.773E-06	0.341	-0.044	0.800	2180.5	-5.590	2.926
890.5	-0.299	0.513	0.513E-06	0.342	-0.044	0.802	2208.5	-6.112	2.938
922.5	-0.301	0.518	0.966E-06	0.345	-0.044	0.810	2240.5	-6.015	2.950
984.0	-0.303	0.522	0.742E-06	0.348	-0.045	0.817	2282.0	-6.127	2.984
886.5	-0.303	0.524	0.553E-06	0.350	-0.037	0.826	2304.5	-6.259	2.994
1010.5	-0.155	0.527	0.770E-06	0.352	-0.023	0.843	2328.5	-5.113	3.005
1034.5	-0.208	0.534	0.206E-05	0.356	-0.031	0.848	2352.5	-5.646	3.015
1058.5	-0.208	0.536	0.516E-06	0.358	-0.031	0.851	2376.5	-6.287	3.025
1082.5	-0.259	0.538	0.513E-06	0.359	-0.038	0.848	2400.5	-6.290	3.034





LOAD INCREMENT # 9 S.D.: 196 KPA

TIME (HOURS)	VOL DISPL (CC)	AXIAL DISPL (MM)	STRAIN RATE (/HR)	TRUE AXIAL STRAIN %	TRUE VOL. STRAIN %	DEVIATORIC STRAIN %	CUMULATIVE TIME (HRS)	LOGSTRAIN RATE/HOUR	LOGTIME HOURS
0.0	2.829	2.487	0.168E+01	1.677	0.430	4.480	4344.5	0.225	-2.000
1.5	2.908	2.500	0.126E+04	1.679	0.427	4.462	4346.0	-4.898	0.176
8.5	2.873	2.514	0.134E+04	1.689	0.421	4.481	4353.0	-4.873	0.929
23.5	2.920	2.522	0.378E+05	1.684	0.428	4.500	4368.0	-5.425	1.371
47.5	2.916	2.532	0.287E+05	1.701	0.428	4.516	4392.0	-5.542	1.677
97.5	3.009	2.548	0.225E+06	1.713	0.441	4.555	4442.0	-5.847	1.988
119.5	3.104	2.562	0.389E+05	1.721	0.455	4.588	4484.0	-5.400	2.077
146.5	3.000	2.572	0.255E+05	1.728	0.440	4.592	4491.0	-5.593	2.166
167.5	3.098	2.576	0.149E+05	1.731	0.454	4.612	4512.0	-5.828	2.224
191.5	3.144	2.587	0.287E+05	1.738	0.461	4.634	4536.0	-5.542	2.282
215.5	3.094	2.587	0.258E+06	1.739	0.454	4.630	4560.0	-5.589	2.333
244.5	3.142	2.592	0.108E+05	1.742	0.461	4.642	4589.0	-5.986	2.388
268.5	3.190	2.597	0.130E+05	1.745	0.468	4.657	4613.0	-5.885	2.429
287.5	3.190	2.598	0.661E+06	1.746	0.468	4.680	4622.0	-5.180	2.459
311.5	3.237	2.605	0.183E+05	1.751	0.475	4.676	4656.0	-5.738	2.493
335.5	3.285	2.611	0.156E+05	1.755	0.482	4.691	4680.0	-5.806	2.564
359.5	3.283	2.615	0.131E+05	1.758	0.481	4.698	4704.0	-5.884	2.556
383.5	3.330	2.623	0.236E+05	1.763	0.488	4.718	4728.0	-5.629	2.584
432.5	3.376	2.633	0.128E+05	1.770	0.495	4.739	4777.0	-5.893	2.636
455.5	3.374	2.639	0.191E+05	1.774	0.495	4.749	4800.0	-5.720	2.658
479.5	3.402	2.645	0.156E+05	1.778	0.499	4.762	4824.0	-5.806	2.881
503.5	3.399	2.651	0.183E+05	1.782	0.498	4.772	4848.0	-5.738	2.702
527.5	3.397	2.656	0.131E+05	1.785	0.498	4.780	4872.0	-5.864	2.722
551.5	3.386	2.659	0.781E+06	1.787	0.494	4.780	4896.0	-5.107	2.742
604.0	3.485	2.683	0.598E+06	1.790	0.508	4.800	4948.5	-6.224	2.781
623.5	3.482	2.670	0.225E+05	1.795	0.507	4.810	4968.0	-5.648	2.795
647.5	3.610	2.676	0.183E+05	1.799	0.529	4.839	4992.0	-5.738	2.811
671.5	3.656	2.685	0.261E+05	1.805	0.536	4.860	5016.0	-5.583	2.827
695.5	3.654	2.690	0.130E+05	1.808	0.536	4.867	5040.0	-5.884	2.842
719.5	3.704	2.690	0.0	1.808	0.543	4.873	5064.0	-5.988	2.857

LOAD INCREMENT #10 S.D.: 229 KPA

TIME (HOURS)	VOL DISPL (CC)	AXIAL DISPL (MM)	STRAIN RATE (/HR)	TRUE AXIAL STRAIN %	TRUE VOL. STRAIN %	DEVIATORIC STRAIN %	CUMULATIVE TIME (HRS)	LOGSTRAIN RATE/HOUR	LOGTIME HOURS
0.0	3.700	2.701	0.182E+01	1.816	0.542	4.890	5084.0	0.259	-2.000
1.0	3.648	2.705	0.316E+04	1.819	0.535	4.892	5085.0	-4.500	0.0
3.0	3.647	2.708	0.938E+05	1.821	0.535	4.896	5067.0	-5.028	0.477
9.0	3.642	2.720	0.136E+04	1.829	0.534	4.916	5073.0	-4.867	0.954
19.0	3.733	2.745	0.169E+04	1.846	0.547	4.968	5083.0	-4.771	1.279
39.5	3.805	2.764	0.642E+05	1.859	0.558	5.009	5103.5	-5.193	1.597
63.0	3.818	2.782	0.507E+05	1.871	0.560	5.040	5127.0	-5.295	1.799
87.0	3.830	2.804	0.827E+05	1.886	0.561	5.078	5151.0	-5.203	1.940
111.0	3.904	2.820	0.444E+05	1.897	0.572	5.113	5175.0	-5.352	2.045
135.0	3.998	2.836	0.444E+05	1.907	0.586	5.150	5199.0	-5.352	2.130
153.0	3.991	2.851	0.592E+05	1.918	0.585	5.175	5217.0	-5.227	2.185
209.5	4.082	2.875	0.289E+05	1.934	0.598	5.226	5273.6	-5.539	2.321
231.0	4.157	2.888	0.409E+05	1.943	0.609	5.257	5295.0	-5.388	2.384
255.0	4.151	2.904	0.444E+05	1.954	0.608	5.282	5319.0	-5.489	2.446
279.0	4.266	2.916	0.340E+05	1.962	0.625	5.316	5343.0	-5.541	2.481
303.0	4.262	2.926	0.288E+05	1.989	0.625	5.332	5367.0	-5.489	2.446
327.0	4.277	2.940	0.393E+05	1.978	0.627	5.357	5391.0	-5.406	2.515
351.0	4.284	2.947	0.163E+05	1.983	0.628	5.368	5415.0	-5.737	2.577
377.5	4.349	2.951	0.379E+05	1.993	0.637	5.401	5441.5	-5.421	2.545
399.0	4.444	2.972	0.350E+05	2.000	0.651	5.431	5463.0	-5.456	2.601
423.0	4.490	2.983	0.314E+05	2.008	0.658	5.455	5487.0	-5.503	2.628
447.0	4.515	2.995	0.340E+05	2.016	0.661	5.478	5511.0	-5.468	2.650
471.0	4.531	3.006	0.288E+05	2.023	0.664	5.497	5535.0	-5.541	2.673
499.0	4.577	3.016	0.247E+05	2.030	0.671	5.519	5563.0	-5.608	2.698
544.5	4.672	3.029	0.183E+05	2.044	0.684	5.552	5608.5	-5.714	2.736
567.0	4.719	3.037	0.251E+05	2.050	0.681	5.571	5631.0	-5.800	2.764
591.0	4.716	3.045	0.236E+05	2.057	0.691	5.585	5655.0	-5.628	2.772
615.0	4.712	3.056	0.268E+05	2.068	0.690	5.601	5679.0	-5.541	2.789
663.0	4.726	3.072	0.236E+05	2.078	0.692	5.631	5727.0	-5.628	2.822
687.0	4.800	3.087	0.419E+05	2.083	0.703	5.664	5751.0	-5.378	2.837
711.0	4.887	3.094	0.210E+05	2.083	0.717	5.888	5775.0	-5.678	2.862
735.0	4.994	3.101	0.183E+05	2.087	0.731	5.710	5799.0	-5.737	2.866
759.0	4.992	3.107	0.183E+05	2.092	0.731	5.721	5823.0	-5.737	2.860
783.0	4.939	3.115	0.210E+05	2.097	0.723	5.727	5847.0	-5.678	2.894
807.0	4.936	3.122	0.209E+05	2.102	0.723	5.739	5871.0	-5.679	2.907



LOAD INCREMENT #13 S.D.F. 382 KPA

TIME [HOURS]	VOL DISPL [CC]	AXIAL DISPL [MM]	STRAIN RATE [1/HR]	TRUE AXIAL STRAIN %	TRUE VOL. STRAIN %	DEVIATORIC STRAIN %	CUMULATIVE TIME [HRS]	LOGSTRAIN RATE/HOUR	LOGTIME HOURS
0.0	8.372	4.445	0.301E+01	3.006	1.223	8.362	8150.0	0.478	-2.000
0.5	8.368	4.456	0.155E-03	3.014	1.222	8.380	8150.5	-3.808	-0.301
2.0	8.382	4.470	0.634E-04	3.023	1.222	8.403	8152.0	-4.198	0.301
7.5	8.353	4.494	0.300E-04	3.040	1.220	8.442	8157.5	-4.523	0.875
23.5	8.533	4.545	0.218E-04	3.075	1.248	8.548	8173.5	-4.861	1.371
33.0	8.523	4.570	0.180E-04	3.092	1.245	8.590	8183.0	-4.744	1.519
47.5	8.606	4.614	0.210E-04	3.122	1.257	8.674	8197.5	-4.677	1.677
75.0	8.778	4.887	0.182E-04	3.172	1.282	8.817	8226.0	-4.739	1.875
120.5	8.886	4.793	0.161E-04	3.245	1.312	9.021	8270.5	-4.794	2.081
143.5	9.118	4.840	0.141E-04	3.278	1.331	9.116	8293.5	-4.851	2.157
167.5	9.196	4.898	0.164E-04	3.317	1.343	9.222	8317.5	-4.784	2.224
191.5	9.315	4.976	0.225E-04	3.371	1.360	9.369	8341.5	-4.647	2.282
215.5	9.462	4.985	0.239E-05	3.377	1.381	9.400	8365.5	-5.622	2.333
240.5	9.641	5.040	0.153E-04	3.415	1.407	9.515	8390.5	-4.816	2.381